Clarification on Metric ID: 3.3.1

Index

Query No. 02: **Kindly note that calendar year should be considered in this metric, as paper published in year 2018 should comes under 2018-19 so on and paper in 2023 comes under 2023-24, Please check and provide correct revise data for all years.**

Response:

Institution have revised the data to ensure that the calendar year is considered in this metric. Papers published in the year 2018 have been included under 2018-19, and papers published in 2023 have been excluded because that are coming under 2023-24 which is out of assessment period.

Dr. Yashwant Moreshwar Donde Sarwajanik Shaikshanik Trust's

INDIRA MAHAVIDYALAYA

KALAMB, DIST. YAVATMAL, MAHARASHTRA 445401

Principal: 9422867658 **IQAC Co-Ordinator:** 8668564641

NAAC Accredited with 'B+' Grade, Under UGC Section 2(f) and 12 (B)

College Code-414 **AISHE: C-42925**

E mail - imvkalamb@yahoo.co.in **Website** – www.indiramahavidyalaya.com

Certificate

This is to certify that, in response to Query No. 02, the institution has revised the data to ensure that the calendar year is considered in the relevant metrics. Specifically, papers published in the year 2018 have been included under the period 2018-19, and papers published in 2023 have been excluded because that are coming under 2023-24 which is out of assessment period.

The revised data has been thoroughly reviewed and is now accurate and compliant with the specified requirements.

Co-ordinator
IQAC
Indira Mahavidyalaya
Kalamb

Indira Mahavidyalaya Code No. 414 Kalamb

PRINCIPAL
Indira Mahavidyalaya
Kalamb Dist.Yavatmal

SUMMARY OF RESEARCH PAPERS PUBLISHED IN JOURNAL NOTIFIED ON UGC CARE YEAR WISE DURING THE LAST FIVE YEARS

(Total: 42)

Year	2022-23	2021-22	2020-21	2019-20	2018-19
Number	04	07	02	12	17

List of Research Papers Published in UGC CARE Listed and Link of These Papers on Institutional Website
(Year-wise: 2022-23, 2021-22, 2020-21, 2019-20, 2018-19)

S.No	Title of Paper	Name of the Author/s	Department of the Teacher	Name of Journal	Calendar Year of Publication	ISSN Number	Is it listed in UGC Care List	Link of These Papers on Institutional Website
1	Optimization of supercapacitive properties of polyindole by dispersion of MnO2 nanoparticles	K.R. Nemade	Physics	Chemical Physics Impact, 5, 100-105	2022	2667-0224	Yes	https://www.indiramahavidyalaya.com/pdfpage.php?unum=543
2	Alumina tunnel contact based lateral spin-Field effect transistor	K.R. Nemade	Physics	Materials Science and Engineering: B, 286, 115977	2022	0921-5107	Yes	https://www.indiramahavidyalaya.com/pdfpage.php?unum=544
3	Investigation of optical properties of sodium superoxide loaded polyaniline in uv and visible region	K.R. Nemade	Physics	Songklanakarin J. of Sci. & Tech., 44, 54-60	2022	0125-3395	Yes	https://www.indiramahavidyalaya.com/pdfpage.php?unum=545
4	Complex Optical Investigation of Sodium Superoxide	K.R. Nemade	Physics	Trends in Sciences, 19, 2077-2081	2022	2774-0226	Yes	https://www.indiramahavidyalaya.com/pdfpage.php?unum=546

	Loaded Phosphovanadate Glass System in Ultra-Violet and Visible Region							
5	The Comprehensive study of Titanium oxide doped Conducting polymers nanocomposites for Photovoltaic applications	K.R. Nemade,	Physics	Polymer-Plastics Technology and Materials, 60, 1775-1784	2021	2574-0881	Yes	https://www.indiramahavidyalaya.com/pdfpage.php?unum=548
6	Graphene based nano-composites for efficient energy conversion and storage in Solar cells and Supercapacitors: A Review	K.R. Nemade	Physics	Polymer-Plastics Technology and Materials, 60, 784-797	2021	2574-0881	Yes	https://www.indiramahavidyalaya.com/pdfpage.php?unum=548
7	Comprehensive study of spin field effect transistors with co-graphene ferromagnetic contacts	K.R. Nemade	Physics	Journal of Magnetism and Magnetic Materials, 517, 167410	2021	0304-8853	Yes	https://www.indiramahavidyalaya.com/pdfpage.php?unum=549
8	Communal Riot and Social Integration in Mahesh Dattani	Prof. P.S. Jawade	English	Infokara Research	2021	1021-9056	Yes	https://www.indiramahavidyalaya.com/pdfpage.php?unum=810

	‘s Final Solution282-285							
9	Impedance spectroscopy study of the AC conductivity of sodium superoxide nanoparticles doped vanadate-based glasses	K.R. Nemade	Physics	Materials Science for Energy Technologies, 4, 202-207	2021	2589-2991	Yes	https://www.indiramahavidyalaya.com/pdfpage.php?unum=550
10	Comprehensive study to ascertain the effect of MnO2 loading on supercapacitive properties of conducting polymers	K.R. Nemade	Physics	Int. J. of Polymer Analysis and Characterization, 26, 593-603	2021	1563-5341	Yes	https://www.indiramahavidyalaya.com/pdfpage.php?unum=551
11	Hawaman badal an jalstrot : ek Abhyas (**English Title:** Climate Change and Water Resources: A Study)	N.V.Narule	Geography	Vidyawarta International Multilingual Research Journal	2021	2319 - 9320	Yes	https://www.indiramahavidyalaya.com/pdfpage.php?unum=313
12	Job Categories, Mental Health and Jobsatisfaction	P.B. Ingle	Psychology	Ajanta	2020	2279-4089	Yes	https://www.indiramahavidyalaya.com/pdfpage.php?unum=382

13	Preparation of spintronically active ferromagnetic contacts based on Fe, Co and Ni Graphene nanosheets for Spin-Field Effect Transistor	K.R. Nemade	Physics	Materials Science and Engineering: B, 261, 114772	2020	0921-5107	Yes	https://www.indiramahavidyalaya.com/pdfpage.php?unum=552
14	Preparation of nanorefrigerants using mono-, bi- and tri-layer graphene nanosheets in R134a refrigerant	K.R. Nemade	Physics	AIP Conference Proceedings, 2104, 20017	2019	1551-7616	Yes	https://www.indiramahavidyalaya.com/pdfpage.php?unum=270
15	Recent advancements in the field of ballistic and non-ballistic spin-based field-effect transistors	K.R. Nemade	Physics	AIP Conference Proceedings, 2104, 15-18	2019	1551-7616	Yes	https://indiramahavidyalaya.com/profile/pdf_show.php?unum=269
16	Role of nanoparticle shape in enhancing the thermal conductivity of nanofluids	K.R. Nemade	Physics	Materials Today: Proceedings, 28, 873-878	2019	2214-7853	Yes	https://www.indiramahavidyalaya.com/pdfpage.php?unum=554
17	Contribution of Psychology in Physical, Mental and Occupational	P.B. Ingle	Psychology	Ajanta Journal	2019	2277-5730	Yes	https://www.indiramahavidyalaya.com/pdfpage.php?unum=190

	Health.							
18	Anna-dhanya Suraksha Yojanechya Amalbajavanitil Shasanachi Bhumika (**English Title**: The Role of Government in the Implementation of the Food Security Scheme)	Prof. R.M. Wath	Commerce	Ajanta Journal	2019	2277-5730	Yes	https://www.indiramahavidyalaya.com/pdfpage.php?unum=781
19	GST palanache tantradyan vastu v seva kar network: labh ani samasya (English Title: The Technology of GST Compliance and the Goods and Services Tax Network: Benefits and Challenges)	Prof. R.M. Wath	Commerce	Ajanta Journal	2019	2277-5730	Yes	https://www.indiramahavidyalaya.com/pdfpage.php?unum=782
20	Maharastra Rajyachya Arthasankalpat Mahilanvishayi Tartudi va yojan: Ek Drustikshep (**English Title** :	R.M. Wath	Commerce	Gurukul international Multidisciplinary Research Journal	2019	2394-8426	Yes	https://www.indiramahavidyalaya.com/pdfpage.php?unum=783

	Budgetary Allocations and Schemes for Women in the State Budget of Maharashtra: An Overview)							
21	Junglacha Vinash aani Hawamanbadal: Ek Abbhyas (**English Title:** Deforestation and Climate Change: A Study)	N.V.Narule	Geography	Gurukul international Multidisciplinary Research Journal	2019	2394-8426	Yes	https://www.indiramahavidyalaya.com/pdfpage.php?unum=784
22	Vidyarthyanchi Sarvangin Surakhshata Palak va Shikshkachi Jababdari (**English Title:** The Comprehensive Safety of Students: Responsibilities of Parents and Teachers.)	S. Y. Lakhdive	Home economics	Gurukul international Multidisciplinary Research Journal	2019	2394-8426	Yes	https://www.indiramahavidyalaya.com/pdfpage.php?unum=785
23	Samajik shastra Sanshodhanat Shaikshnik granthalaychi Bhumika (	Dr. G.P. Urkunde	Library	Gurukul international Multidisciplinary Research Journal	2019	2394-8426	Yes	https://www.indiramahavidyalaya.com/pdfpage.php?unum=786

	English Title: The Role of Academic Libraries in Social Science Research.")							
24	Strijanivecha Hunkar : Kamal Desai Aani Vijaya Rajadhyksha (**English Title:** The Roar of Women's Writing: Kamal Desai and Vijaya Rajadhyaksha.)	Dr. V.P. Mandavkar	Marathi	Gurukul international Multidisciplinary Research Journal	2019	2394-8426	Yes	https://www.indiramahavidyalaya.com/pdfpage.php?unum=797
25	Swatantryottar Sathpurva Vaidharbiya kadambaritil Samajik Janiva **(English title**: Social Consciousness in Post-Independence Mid-20th Century Novels from Vidarbha.)	Dr. P. Mandavkar	Marathi	Gurukul international Multidisciplinary Research Journal	2019	2394-8426	Yes	https://www.indiramahavidyalaya.com/pdfpage.php?unum=795
26	Teaching Methodology in Geography at College level	N.V.Narule	Geography	Vidyawarta International Multilingual Research Journal	2018	2319 - 9318	Yes	https://www.indiramahavidyalaya.com/pdfpage.php?unum=315

27	Jagtik Tpman Ani Prayawarn Pradushan: ek abhyas (**English Title:** Global Temperature and Environmental Pollution: A Study)	N.V.Narule	Geography	Vidyawarta International Multilingual Research Journal	2018	2319 - 9319	Yes	https://www.indiramahavidyalaya.com/pdfpage.php?unum=314
28	A chief, industrial waste, activated red mud for subtraction of methylene blue dye from environment	Dr. P R Bonde (Pal)	Chemistry	Material Today: Proceeding	2018	2214-7853	Yes	https://www.indiramahavidyalaya.com/pdfpage.php?unum=809
29	Strengthening of photovoltaic and supercapacitive properties of graphene oxide-polyaniline composite by dispersion of α-Al2O3 nanoparticles	K.R. Nemade	Physics	Chemical Physics Letters, 706, 647-651	2018	0009-2614	Yes	https://www.indiramahavidyalaya.com/pdfpage.php?unum=224
30	Effect of Shape on Thermophysical and Heat Transfer Properties of ZnO/R-134a Nanorefrigerant	K.R. Nemade	Physics	Materials Today: Proceedings, 5, 1635-1639	2018	2214-7853	Yes	https://www.indiramahavidyalaya.com/pdfpage.php?unum=553

31	Mindfulness and Life satisfaction: A review	P.B. Ingle	Psychology	Ajanta Journal	2018	2277-5730		https://indiramahavidyalaya.com/profile/pdf_show.php?unum=189
32	Enhancement of photovoltaic performance of polyaniline/graphene composite-based dye-sensitized solar cells by adding TiO2 nanoparticles	K.R. Nemade	Physics	Solid State Sciences, 83, 99-106	2018	1873-3085	Yes	https://www.indiramahavidyalaya.com/pdfpage.php?unum=268
33	Synthesis and charctrerization of cycloruthenation of cycloruthenated complexes	S.R. Khandekar	Chemistry	Gurukul international Multidisciplinary Research Journal	2018	2394-8426	Yes	https://www.indiramahavidyalaya.com/pdfpage.php?unum=796
34	Inferiority of Women in Shashi Deshpande's Novel the binding wine	P.S.Jawade	English	Gurukul international Multidisciplinary Research Journal	2018	2394-8426	Yes	https://www.indiramahavidyalaya.com/pdfpage.php?unum=273
35	Prakrutik Sansadhno ke Sanrkashan me Vyakti ki bhumika (**English Title:** The Role of Individuals in	N.V.Narule	Geography	Gurukul international Multidisciplinary Research Journal	2018	2394-8426	Yes	https://www.indiramahavidyalaya.com/pdfpage.php?unum=792

	Conservation of Natural Resources)							
36	Mogalkalin Bhartacha Jama Kharcha (**English Title:** The Public Expenditure of Ancient India)	N.R.Thavale	History	Gurukul international Multidisciplinary Research Journal	2018	2394-8426	Yes	https://www.indiramahavidyalaya.com/pdfpage.php?unum=787
37	Mahavidyalyan Granthalay Aani Mahiti Sakhshrata (**English Title:** University Libraries and Information Literacy)	G.P. Urkunde	Library	Gurukul international Multidisciplinary Research Journal	2018	2394-8426	Yes	https://www.indiramahavidyalaya.com/pdfpage.php?unum=793
38	Shramyogi Baba Amate (**English Title:** Worker Saint Baba Amte)	R.T.Aade	Marathi	Gurukul international Multidisciplinary Research Journal	2018	2394-8426	Yes	https://www.indiramahavidyalaya.com/pdfpage.php?unum=794
39	Kishor Awastet mahiti wa tantradhyananach a Honara Parinam ek manasshastriy abbhyas (**English Title:** Psychological Study of the Impact of	P.B.Ingale	Psychology	Gurukul international Multidisciplinary Research Journal	2018	2394-8426	Yes	https://www.indiramahavidyalaya.com/pdfpage.php?unum=791

	Adolescent Information and Technology Exposure)							
40	Strengthening of photovoltaic and supercapacitive properties of graphene oxide-polyaniline composite by dispersion of a-Al2O3 nanoparticles	Kailash Nemade , Pradip Tekade, Priyanka Dudhe	Physics	Chemical Physics Letters	2018	0009-2614	Yes	https://indiramahavidyalaya.com/profile/pdf_show.php?unum=1222
41	Enhancement of photovoltaic performance of polyaniline/graphene composite-based dye-sensitized solar cells by adding TiO2 nanoparticles	Kailash Nemade , Pradip Tekade, Priyanka Dudhe	Physics	Solid State Sciences	2018	1293-2558	Yes	https://indiramahavidyalaya.com/profile/pdf_show.php?unum=1223
42	Effect of Shape on Thermophysical and Heat Transfer Properties of ZnO/R-134a Nanorefrigerant	P.B. Maheshwarya, C.Handa, K.R. Nemadec	Physics	Materials Today: Proceedings	2018	1635–1639	Yes	https://indiramahavidyalaya.com/profile/pdf_show.php?unum=1224

List of Research Papers Published in UGC CARE Listed and Link of their Journal Home Page
(Year-wise: 2022-23, 2021-22, 2020-21, 2019-20, 2018-19)

S.No.	Title of paper	Name of the author/s	Department of the Teacher	Name of Journal & ISSN Number	Calendar Year of Publication	Link of Journal Home Page
1.	Optimization of supercapacitive properties of polyindole by dispersion of MnO2 nanoparticles	K.R. Nemade	Physics	Chemical Physics Impact, 5, 100-105	2022	https://www.sciencedirect.com/journal/chemical-physics-impact
2.	Alumina tunnel contact based lateral spin-Field effect transistor	K.R. Nemade	Physics	Materials Science and Engineering: B, 286, 115977	2022	https://www.sciencedirect.com/journal/materials-science-and-engineering-b
3.	Investigation of optical properties of sodium superoxide loaded polyaniline in uv and visible region	K.R. Nemade	Physics	Songklanakarin J. of Sci. & Tech., 44, 54-60	2022	https://sjst.psu.ac.th/
4.	Complex Optical Investigation of Sodium Superoxide Loaded Phosphovanadate Glass System in Ultra-Violet and Visible Region	K.R. Nemade	Physics	Trends in Sciences, 19, 2077-2081	2022	https://tis.wu.ac.th/index.php/tis/

5.	The Comprehensive study of Titanium oxide doped Conducting polymers nanocomposites for Photovoltaic applications	K.R. Nemade,	Physics	Polymer-Plastics Technology and Materials, 60, 1775-1784	2021	https://www.tandfonline.com/journals/lpte21
6.	Graphene based nano-composites for efficient energy conversion and storage in Solar cells and Supercapacitors: A Review	K.R. Nemade	Physics	Polymer-Plastics Technology and Materials, 60, 784-797	2021	https://www.tandfonline.com/journals/lpte21
7.	Comprehensive study of spin field effect transistors with co-graphene ferromagnetic contacts	K.R. Nemade	Physics	Journal of Magnetism and Magnetic Materials, 517, 167410	2021	https://www.sciencedirect.com/journal/journal-of-magnetism-and-magnetic-materials
8.	Communal Riot and Social Integration in Mahesh Dattani ‘s Final Solution282-285	Prof. P.S. Jawade	English	Infokara Research	2021	https://infokara.com/
9.	Impedance spectroscopy study of the AC conductivity of sodium superoxide nanoparticles	K.R. Nemade	Physics	Materials Science for Energy Technologies, 4, 202-207	2021	https://www.sciencedirect.com/journal/materials-science-for-energy-technologies

	doped vanadate-based glasses					
10.	Comprehensive study to ascertain the effect of MnO2 loading on supercapacitive properties of conducting polymers	K.R. Nemade	Physics	Int. J. of Polymer Analysis and Characterizatio n, 26, 593-603	2021	https://www.tandfonline.com/journals/gpac20
11.	Hawaman badal an jalstrot : ek Abhyas (**English Title:** Climate Change and Water Resources: A Study)	N.V.Narule	Geography	Vidyawarta International Multilingual Research Journal	2021	https://www.vidyawarta.com/
12.	Job Categories, Mental Health and Jobsatisfaction	P.B. Ingle	Psychology	Ajanta	2020	https://www.ajantaprakashan.in/ajanta_journal.html
13.	Preparation of spintronically active ferromagnetic contacts based on Fe, Co and Ni Graphene nanosheets for Spin-Field Effect Transistor	K.R. Nemade	Physics	Materials Science and Engineering: B, 261, 114772	2020	https://www.sciencedirect.com/journal/materials-science-and-engineering-b
14.	Preparation of nanorefrigerants using mono-, bi- and tri-layer	K.R. Nemade	Physics	AIP Conference Proceedings, 2104, 20017	2019	https://pubs.aip.org/aip/acp

	graphene nanosheets in R134a refrigerant					
15.	Recent advancements in the field of ballistic and non-ballistic spin-based field-effect transistors	K.R. Nemade	Physics	AIP Conference Proceedings, 2104, 15-18	2019	https://pubs.aip.org/aip/acp
16.	Role of nanoparticle shape in enhancing the thermal conductivity of nanofluids	K.R. Nemade	Physics	Materials Today: Proceedings, 28, 873-878	2019	https://www.sciencedirect.com/journal/materials-today-proceedings
17.	Contribution of Psychology in Physical, Mental and Occupational Health.	P.B. Ingle	Psychology	Ajanta Journal	2019	https://www.ajantaprakashan.in/ajanta_journal.html
18.	Anna-dhanya Suraksha Yojanechya Amalbajavanitil Shasanachi Bhumika (**English Title**: The Role of Government in the Implementation of the Food Security Scheme)	Prof. R.M. wath	Commerce	Ajanta Journal	2019	https://www.ajantaprakashan.in/ajanta_journal.html
19.	GST palanache tantradyan vastu v seva kar network: labh ani samasya	Prof. R.M. wath	Commerce	Ajanta Journal	2019	https://www.ajantaprakashan.in/ajanta_journal.html

	(English Title: The Technology of GST Compliance and the Goods and Services Tax Network: Benefits and Challenges)					
20.	Maharastra Rajyachya Arthasankalpat Mahilanvishayi Tartudi va yojan: Ek Drustikshep (**English Title** : Budgetary Allocations and Schemes for Women in the State Budget of Maharashtra: An Overview)	R.M. Wath	Commerce	Gurukul international Multidisciplinary Research Journal	2019	https://gurukuljournal.com/
21.	Junglacha Vinash aani Hawamanbadal: Ek Abbhyas (**English Title:** Deforestation and Climate Change: A Study)	N.V.Narule	Geography	Gurukul international Multidisciplinary Research Journal	2019	https://gurukuljournal.com/
22.	Vidyarthyanchi Sarvangin Surakhshata Palak va Shikshkachi Jababdari (**English Title:** The	S. Y. Lakhdive	Home economics	Gurukul international Multidisciplinary Research Journal	2019	https://gurukuljournal.com/

	Comprehensive Safety of Students: Responsibilities of Parents and Teachers.)					
23.	Samajik shastra Sanshodhanat Shaikshnik granthalaychi Bhumika (**English Title:** The Role of Academic Libraries in Social Science Research.")	Dr. G.P. Urkunde	Library	Gurukul international Multidisciplinary Research Journal	2019	https://gurukuljournal.com/
24.	Strijanivecha Hunkar : Kamal Desai Aani Vijaya Rajadhyksha (**English Title:** The Roar of Women's Writing: Kamal Desai and Vijaya Rajadhyaksha.)	Dr. V.P. Mandavkar	Marathi	Gurukul international Multidisciplinary Research Journal	2019	https://gurukuljournal.com/
25.	Swatantryottar Sathpurva Vaidharbiya kadambaritil Samajik Janiva **(English title**: Social Consciousness in Post-Independence Mid-20th Century Novels from	Dr. P. Mandavkar	Marathi	Gurukul international Multidisciplinary Research Journal	2019	https://gurukuljournal.com/

	Vidarbha.)					
26.	Teaching Methodology in Geography at College level	N.V.Narule	Geography	Vidyawarta International Multilingual Research Journal	2018	https://www.vidyawarta.com/
27.	Jagtik Tpman Ani Prayawarn Pradushan: ek abhyas (**English Title:** Global Temperature and Environmental Pollution: A Study)	N.V.Narule	Geography	Vidyawarta International Multilingual Research Journal	2018	https://www.vidyawarta.com/
28.	A chief, industrial waste, activated red mud for subtraction of methylene blue dye from environment	Dr. P R Bonde (Pal)	Chemistry	Material Today: Proceeding	2018	www.elsevier.com/locate/matpr
29.	Strengthening of photovoltaic and supercapacitive properties of graphene oxide-polyaniline composite by dispersion of α-Al2O3 nanoparticles	K.R. Nemade	Physics	Chemical Physics Letters, 706, 647-651	2018	https://www.sciencedirect.com/journal/chemical-physics-letters

30.	Effect of Shape on Thermophysical and Heat Transfer Properties of ZnO/R-134a Nanorefrigerant	K.R. Nemade	Physics	Materials Today: Proceedings, 5, 1635-1639	2018	https://www.sciencedirect.com/journal/materials-today-proceedings
31.	Mindfulness and Life satisfaction: A review	P.B. Ingle	Psychology	Ajanta Journal	2018	https://www.ajantaprakashan.in/ajanta_journal.html
32.	Enhancement of photovoltaic performance of polyaniline/graphene composite-based dye-sensitized solar cells by adding TiO2 nanoparticles	K.R. Nemade	Physics	Solid State Sciences, 83, 99-106	2018	https://www.sciencedirect.com/journal/solid-state-sciences
33.	Synthesis and charctrerization of cycloruthenation of cycloruthenated complexes	S.R. Khandekar	Chemistry	Gurukul international Multidisciplinary Research Journal	2018	https://gurukuljournal.com/
34.	Inferiority of Women in Shashi Deshpande's Novel the binding wine	P.S.Jawade	English	Gurukul international Multidisciplinary Research Journal	2018	https://gurukuljournal.com/
35.	Prakrutik Sansadhno ke Sanrkashan me Vyakti ki bhumika (**English Title:** The Role of Individuals in	N.V.Narule	Geography	Gurukul international Multidisciplinary Research Journal	2018	https://gurukuljournal.com/

	Conservation of Natural Resources)					
36.	Mogalkalin Bhartacha Jama Kharcha (**English Title:** The Public Expenditure of Ancient India)	N.R.Thavale	History	Gurukul international Multidisciplinary Research Journal	2018	https://gurukuljournal.com/
37.	Mahavidyalyan Granthalay Aani Mahiti Sakhshrata (**English Title:** University Libraries and Information Literacy)	G.P. Urkunde	Library	Gurukul international Multidisciplinary Research Journal	2018	https://gurukuljournal.com/
38.	Shramyogi Baba Amate (**English Title:** Worker Saint Baba Amte)	R.T.Aade	Marathi	Gurukul international Multidisciplinary Research Journal	2018	https://gurukuljournal.com/
39.	Kishor Awastet mahiti wa tantradhyananacha Honara Parinam ek manasshastriy abbhyas (**English Title:** Psychological Study of the Impact of Adolescent Information and Technology	P.B.Ingale	Psychology	Gurukul international Multidisciplinary Research Journal	2018	https://gurukuljournal.com/

	Exposure)					
40.	Strengthening of photovoltaic and supercapacitive properties of graphene oxide-polyaniline composite by dispersion of a-Al2O3 nanoparticles	Kailash Nemade , Pradip Tekade, Priyanka Dudhe	Physics	Chemical Physics Letters	2018	https://www.sciencedirect.com/journal/chemical-physics-letters
41.	Enhancement of photovoltaic performance of polyaniline/graphene composite-based dye-sensitized solar cells by adding TiO2 nanoparticles	Kailash Nemade , Pradip Tekade, Priyanka Dudhe	Physics	Solid State Sciences	2018	https://www.sciencedirect.com/journal/solid-state-sciences
42.	Effect of Shape on Thermophysical and Heat Transfer Properties of ZnO/R-134a Nanorefrigerant	P.B. Maheshwary a, C.Handa, K.R. Nemadec	Physics	Materials Today: Proceedings	2018	https://www.sciencedirect.com/science/article/abs/pii/S2214785317325257

List of Research Papers Published in UGC CARE Listed and Exact Link of Research Papers

(Year-wise: 2022-23, 2021-22, 2020-21, 2019-20, 2018-19)

S.No.	Title of paper	Name of the author/s	Department of the teacher	Name of journal & ISSN Number	Calendar Year of publication	Link of Research paper on Journal Page
1.	Optimization of supercapacitive properties of polyindole by dispersion of MnO2 nanoparticles	K.R. Nemade	Physics	Chemical Physics Impact, 5, 100-105	2022	https://www.sciencedirect.com/science/article/pii/S266702242200038X#:~:text=As%20expected%2C%20the%20supercapacitive%20properties,rate%20of%2050%20mVs%E2%88%921.
2.	Alumina tunnel contact based lateral spin-Field effect transistor	K.R. Nemade	Physics	Materials Science and Engineering: B, 286, 115977	2022	https://www.sciencedirect.com/science/article/abs/pii/S0921510722003658
3.	Investigation of optical properties of sodium superoxide loaded polyaniline in uv and visible region	K.R. Nemade	Physics	Songklanakarin J. of Sci. & Tech., 44, 54-60	2022	https://sjst.psu.ac.th/journal/44-6/10.pdf

4.	Complex Optical Investigation of Sodium Superoxide Loaded Phosphovanadate Glass System in Ultra-Violet and Visible Region	K.R. Nemade	Physics	Trends in Sciences, 19, 2077-2081	2022	https://tis.wu.ac.th/index.php/tis/article/view/2077
5.	The Comprehensive study of Titanium oxide doped Conducting polymers nanocomposites for Photovoltaic applications	K.R. Nemade,	Physics	Polymer-Plastics Technology and Materials, 60, 1775-1784	2021	https://www.tandfonline.com/doi/full/10.1080/25740881.2021.1930047
6.	Graphene based nano-composites for efficient energy conversion and storage in Solar cells and Supercapacitors: A Review	K.R. Nemade	Physics	Polymer-Plastics Technology and Materials, 60, 784-797	2021	https://www.tandfonline.com/doi/abs/10.1080/25740881.2020.1851378#:~:text=ABSTRACT,rate%20and%20long%2Dtime%20stability.
7.	Comprehensive study of spin field effect transistors with co-graphene	K.R. Nemade	Physics	Journal of Magnetism and Magnetic Materials, 517, 167410	2021	https://www.sciencedirect.com/science/article/abs/pii/S0304885320323775

	ferromagnetic contacts					
8.	Communal Riot and Social Integration in Mahesh Dattani ‘s Final Solution282-285	Prof. P.S. Jawade	English	Infokara Research	2021	https://drive.google.com/file/d/123prCOtWxUVI48zxcXEXSpjbvvq-558Y/view
9.	Impedance spectroscopy study of the AC conductivity of sodium superoxide nanoparticles doped vanadate-based glasses	K.R. Nemade	Physics	Materials Science for Energy Technologies , 4, 202-207	2021	https://www.sciencedirect.com/science/article/pii/S2589299121000197
10.	Comprehensive study to ascertain the effect of MnO2 loading on supercapacitive properties of conducting polymers	K.R. Nemade	Physics	Int. J. of Polymer Analysis and Characterization, 26, 593-603	2021	https://www.tandfonline.com/doi/full/10.1080/1023666X.2021.1933853
11.	Hawaman badal an jalstrot : ek Abhyas (**English Title:** Climate Change and Water Resources: A Study)	N.V.Narule	Geography	Vidyawarta International Multilingual Research Journal	2021	https://www.indiramahavidyalaya.com/pdfpage.php?unum=313

12.	Job Categories, Mental Health and Jobsatisfaction	P.B. Ingle	Psychology	Ajanta	2020	https://www.indiramahavidyalaya.com/pdfpage.php?unum=382
13.	Preparation of spintronically active ferromagnetic contacts based on Fe, Co and Ni Graphene nanosheets for Spin-Field Effect Transistor	K.R. Nemade	Physics	Materials Science and Engineering: B, 261, 114772	2020	https://www.sciencedirect.com/science/article/abs/pii/S0921510720302798
14.	Preparation of nanorefrigerants using mono-, bi- and tri-layer graphene nanosheets in R134a refrigerant	K.R. Nemade	Physics	AIP Conference Proceedings, 2104, 20017	2019	https://pubs.aip.org/aip/acp/article-abstract/2104/1/020017/888592/Preparation-of-nanorefrigerants-using-mono-bi-and?redirectedFrom=fulltext
15.	Recent advancements in the field of ballistic and non-ballistic spin-based field-effect transistors	K.R. Nemade	Physics	AIP Conference Proceedings, 2104, 15-18	2019	https://pubs.aip.org/aip/acp/article-abstract/2104/1/020018/888692/Recent-advancements-in-the-field-of-ballistic-and?redirectedFrom=fulltext
16.	Role of nanoparticle shape in enhancing the thermal conductivity of	K.R. Nemade	Physics	Materials Today: Proceedings, 28, 873-878	2019	https://www.sciencedirect.com/science/article/abs/pii/S2214785319343457#:~:text=Conclusion&text=During%20this%20investigation%20results%20indicated,area%20of%20cubic%20shaped%20nanoparticles.

	nanofluids					
17.	Contribution of Psychology in Physical, Mental and Occupational Health.	P.B. Ingle	Psychology	Ajanta Journal	2019	https://www.indiramahavidyalaya.com/pdfpage.php?unum=190
18.	Anna-dhanya Suraksha Yojanechya Amalbajavanitil Shasanachi Bhumika (**English Title**: The Role of Government in the Implementation of the Food Security Scheme)	Prof. R.M. Wath	Commerce	Ajanta Journal	2019	https://www.indiramahavidyalaya.com/pdfpage.php?unum=781
19.	GST palanache tantradyan vastu v seva kar network: labh ani samasya (English Title: The Technology of GST Compliance and the Goods and Services Tax Network:	Prof. R.M. Wath	Commerce	Ajanta Journal	2019	https://www.indiramahavidyalaya.com/pdfpage.php?unum=782

	Benefits and Challenges)					
20.	Maharastra Rajyachya Arthasankalpat Mahilanvishayi Tartudi va yojan: Ek Drustikshep (**English Title** : Budgetary Allocations and Schemes for Women in the State Budget of Maharashtra: An Overview)	R.M. Wath	Commerce	Gurukul international Multidisciplinary Research Journal	2019	https://www.indiramahavidyalaya.com/pdfpage.php?unum=783
21.	Junglacha Vinash aani Hawamanbadal: Ek Abbhyas (**English Title:** Deforestation and Climate Change: A Study)	N.V.Narule	Geography	Gurukul international Multidisciplinary Research Journal	2019	https://www.indiramahavidyalaya.com/pdfpage.php?unum=784
22.	Vidyarthyanchi Sarvangin Surakhshata Palak va Shikshkachi Jababdari (**English Title:** The	S. Y. Lakhdive	Home economics	Gurukul international Multidisciplinary Research Journal	2019	https://www.indiramahavidyalaya.com/pdfpage.php?unum=785

	Comprehensive Safety of Students: Responsibilities of Parents and Teachers.)					
23.	Samajik shastra Sanshodhanat Shaikshnik granthalaychi Bhumika (**English Title:** The Role of Academic Libraries in Social Science Research.")	Dr. G.P. Urkunde	Library	Gurukul international Multidisciplinary Research Journal	2019	https://www.indiramahavidyalaya.com/pdfpage.php?unum=786
24.	Strijanivecha Hunkar : Kamal Desai Aani Vijaya Rajadhyksha (**English Title:** The Roar of Women's Writing: Kamal Desai and Vijaya Rajadhyaksha.)	Dr. V.P. Mandavkar	Marathi	Gurukul international Multidisciplinary Research Journal	2019	https://www.indiramahavidyalaya.com/pdfpage.php?unum=797
25.	Swatantryottar Sathpurva Vaidharbiya kadambaritil Samajik Janiva **(English title**:	Dr. P.B. Mandavkar	Marathi	Gurukul international Multidisciplinary Research Journal	2019	https://www.indiramahavidyalaya.com/pdfpage.php?unum=795

	Social Consciousness in Post-Independence Mid-20th Century Novels from Vidarbha.)					
26.	Teaching Methodology in Geography at College level	N.V.Narule	Geography	Vidyawarta International Multilingual Research Journal	2018	https://www.indiramahavidyalaya.com/pdfpage.php?unum=315
27.	Jagtik Tpman Ani Prayawarn Pradushan: ek abhyas (**English Title:** Global Temperature and Environmental Pollution: A Study)	N.V.Narule	Geography	Vidyawarta International Multilingual Research Journal	2018	https://www.indiramahavidyalaya.com/pdfpage.php?unum=314
28.	A chief, industrial waste, activated red mud for subtraction of methylene blue dye from environment	Dr. P R Bonde (Pal)	Chemistry	Material Today: Proceeding	2018	https://www.sciencedirect.com/science/article/pii/S2214785320334076#:~:text=ARM%20is%20industrial%20waste%20and,subtraction%20of%20methylene%20blue%20dye
29.	Strengthening of photovoltaic and supercapacitive properties of graphene oxide-	K.R. Nemade	Physics	Chemical Physics Letters, 706, 647-651	2018	https://www.sciencedirect.com/science/article/abs/pii/S0009261418305633

	polyaniline composite by dispersion of α-Al2O3 nanoparticles					
30.	Effect of Shape on Thermophysical and Heat Transfer Properties of ZnO/R-134a Nanorefrigerant	K.R. Nemade	Physics	Materials Today: Proceedings, 5, 1635-1639	2018	https://www.sciencedirect.com/science/article/abs/pii/S2214785317325257
31.	Mindfulness and Life satisfaction: A review	P.B. Ingle	Psychology	Ajanta Journal	2018	https://indiramahavidyalaya.com/profile/pdf_show.php?unum=189
32.	Enhancement of photovoltaic performance of polyaniline/graphene composite-based dye-sensitized solar cells by adding TiO2 nanoparticles	K.R. Nemade	Physics	Solid State Sciences, 83, 99-106	2018	https://www.sciencedirect.com/science/article/abs/pii/S1293255818305405
33.	Synthesis and charctrerization of cycloruthenation of cycloruthenated complexes	S.R. Khandekar	Chemistry	Gurukul international Multidisciplinary Research Journal	2018	https://www.indiramahavidyalaya.com/pdfpage.php?unum=796

34.	Inferiority of Women in Shashi Deshpande's Novel the binding wine	P.S.Jawade	English	Gurukul international Multidisciplinary Research Journal	2018	https://www.indiramahavidyalaya.com/pdfpage.php?unum=273
35.	Prakrutik Sansadhno ke Sanrkashan me Vyakti ki bhumika (**English Title:** The Role of Individuals in Conservation of Natural Resources)	N.V.Narule	Geography	Gurukul international Multidisciplinary Research Journal	2018	https://www.indiramahavidyalaya.com/pdfpage.php?unum=792
36.	Mogalkalin Bhartacha Jama Kharcha (**English Title:** The Public Expenditure of Ancient India)	N.R.Thavale	History	Gurukul international Multidisciplinary Research Journal	2018	https://www.indiramahavidyalaya.com/pdfpage.php?unum=787
37.	Mahavidyalyan Granthalay Aani Mahiti Sakhshrata (**English Title:** University Libraries and Information Literacy)	G.P. Urkunde	Library	Gurukul international Multidisciplinary Research Journal	2018	https://www.indiramahavidyalaya.com/pdfpage.php?unum=793

38.	Shramyogi Baba Amate (**English Title:** Worker Saint Baba Amte)	R.T.Aade	Marathi	Gurukul international Multidisciplinary Research Journal	2018	https://www.indiramahavidyalaya.com/pdfpage.php?unum=794
39.	Kishor Awastet mahiti wa tantradhyananacha Honara Parinam ek manasshastriy abbhyas (**English Title:** Psychological Study of the Impact of Adolescent Information and Technology Exposure)	P.B.Ingale	Psychology	Gurukul international Multidisciplinary Research Journal	2018	https://www.indiramahavidyalaya.com/pdfpage.php?unum=791
40.	Strengthening of photovoltaic and supercapacitive properties of graphene oxide-polyaniline composite by dispersion of a-Al2O3 nanoparticles	Kailash Nemade , Pradip Tekade, Priyanka Dudhe	Physics	Chemical Physics Letters	2018	https://indiramahavidyalaya.com/profile/pdf_show.php?unum=1222

41.	Enhancement of photovoltaic performance of polyaniline/graphene composite-based dye-sensitized solar cells by adding TiO2 nanoparticles	Kailash Nemade , Pradip Tekade, Priyanka Dudhe	Physics	Solid State Sciences	2018	https://www.sciencedirect.com/science/article/abs/pii/S1293255818305405
42.	Effect of Shape on Thermophysical and Heat Transfer Properties of ZnO/R-134a Nanorefrigerant	P.B. Maheshwarya, C.Handa, K.R. Nemadec	Physics	Materials Today: Proceedings	2018	https://www.sciencedirect.com/science/article/abs/pii/S2214785317325257

Photocopies of Research Papers (All Pages) Published in UGC CARE (Year-wise: 2022-23, 2021-22, 2020-21, 2019-20, 2018-19)

1 Optimization of supercapacitive properties of polyindole by dispersion of MnO2 nanoparticles

Chemical Physics Impact 5 (2022) 100100

Contents lists available at ScienceDirect

Chemical Physics Impact

journal homepage: www.sciencedirect.com/journal/chemical-physics-impact

Optimization of supercapacitive properties of polyindole by dispersion of MnO_2 nanoparticles

R.V. Barde [a,*], K.R. Nemade [b], S.A. Waghuley [c]

[a] Department of Physics, Government Vidarbha Institute of Science and Humanities, Amravati 444 604, India
[b] Department of Physics, Indira Mahavidyalaya, Kalamb, India
[c] Department of Physics, Sant Gadge Baba Amravati University, Amravati 444 602, India

ARTICLE INFO

Keywords:
Supercapacitive properties
Polyindole
MnO_2 nanoparticles
Optical band gap

ABSTRACT

This study demonstrates the dispersion of MnO_2 nanoparticles in Polyindole (PIn) to optimize the supercapacitive properties of MnO_2-PIn composites. As expected, the supercapacitive properties of MnO_2-PIn composites influenced by the addition of MnO_2 nanoparticles and it is optimized for 1 wt.% of MnO_2 concentration. The 1 Wt.% MnO_2 loaded PIn composite shows specific capacitance of the order 1558 Fg^{-1} at a scan rate of 50 mVs^{-1}. The main accomplishment of present work is that the 1 Wt.% MnO_2 loaded PIn composite shows long-term stability that is capacitance retention up to 6000 cycles. Galvanostatic charge/discharge curves of 1 Wt.% MnO_2 loaded PIn composite shows long nearly symmetric behavior which is suitable for range of practical applications.

Introduction

Globally, we are facing a huge problem about energy shortage due to rapid development of economy and increasing depletion of fossil fuels [1]. Hence, there is a crucial need for development new energy sources. Now a days, supercapacitors as high-performance energy storage devices offer a great promise in the field of energy storing technology because of its remarkable properties that is high charging and discharging rates, excellent power density, good stability and excellent long-term cyclability [2–4]. Nevertheless, to meet the requirement of budding applications like electric vehicles, energy density of supercapacitor still need some improvement. Increasing the window working potential, which primarily related with the employed electrolyte is a cogent way to increase energy density of supercapacitor as energy density of it is proportional to the square of operating potential window and specific capacitance. In supercapacitors, active materials play a vital role in an electrochemical performance [5]. Recently, more devotion has been given on the growth of electrode materials of supercapacitor and it is a crucial component which determines the performance of supercapacitor. The carbon materials, metal oxides and conducting polymers have been most commonly used for the growth of electrode as they exhibit such supercapacitor behavior [6–7].

Among these metal oxide MnO_2, is considered to be the most auspicious one because of its characteristics like higher specific capacitance, environmentally friendly, natural abundance and economical [8–9]. Despite of this, it has some drawbacks like poor ionic and electronic conductivity, less specific surface area and partial dissolution in the electrolyte during cycling which limiting the practical applications of MnO_2 in supercapacitors [10]. Hence for researcher it is a significant task to overcome these disadvantages of MnO_2. Dai et al reported nanobelt-structured MnO_2 films which were prepared by the electrochemical deposition method under various deposition time to explore the effects of electrodeposition time change on the microstructure and electrochemical properties of this material. Result show that the optimum sample deposited for 50 s has a specific capacitance of 291.9 F g^{-1} at the current density of 1 A g^{-1} [11]. In addition, Zhanga et al reported the structure and electrochemical performance of MnO_2 and MnO_2/reduced graphene oxide electrode materials which shows the capacitance of 467 F g^{-1} [12].

Conducting polymers are fascinating materials for fundamental and applied researches due to their 1D intrinsic properties and remarkable applications such as field effect transistor (FET), displays, rechargeable batteries, etc. [13]. Among various conducting polymers, comparatively polyindole has been less studied as it has low polymerization efficiency. Recently polyindol (PIn) has received enormous attention because of its good environmental stability and electrical conductivity [14]. As it is

* Corresponding author.
E-mail address: rajeshbarde1976@gmail.com (R.V. Barde).

https://doi.org/10.1016/j.chphi.2022.100100
Received 6 April 2022; Received in revised form 21 May 2022; Accepted 21 July 2022
Available online 23 July 2022

well known that Polyindole has benzine and pyrrol ring, also these polymers have good thermal stability, low degradation rate and high storage capacity [15]. Due good electrocatalytic activity of Polyindole it has been reported in mediated based biofuel cell [14]. Polymer-metal oxide nanocomposite synthesis is incipient research as it has a remarkable technological applications like rechargeable batteries, fuel cells, and super capacitors [16]. Polyindole and its derivatives attract the researcher to take curiosity in the field of nanocomposites due to interesting properties. Nanoparticles of metal oxide such as copper and silver when doped in polyindole shows good antibacterial activity [17].

In the light of above discussion, we planned to investigate the supercapacitive properties of MnO_2-PIn composites. In this work, we studied the supercapacitive properties such, cyclic voltammetry (CV) curve, cycle stability performance and galvanostatic charge/discharge curves of composite materials. The main accomplishment of present work is that we achieved considerable values of specific capacitance, cycle stability and charging/discharging time.

Experimental

Materials

Indole, manganese dioxide, ferric chloride and ethanol (AR grade, 99% purity, SD Fine) were procured from local chemical supplier. Throughout the synthesis double distilled (DD) water was used to prepare the solution.

Synthesis of polyindole (PIn)

Oxidative polymerization method was preferred for the synthesis of polyindole (PIn) from indole in which ferric chloride used as oxidizing agent in aqueous medium. The aqueous solution (1M) was taken in a beaker and kept for continuously stirred on magnetic stirrer at normal temperature for 45 min. The ferric chloride solution (1M) was added dropwise manner to indole solution and stirred for 180 min. and then kept this mixture for overnight. The mixture was turn into dark brown which confirms formation of PIn. This mixture was filtered and to remove the impurities, precipitate was repeatedly washed with double distilled water. The obtained PIn was dried out at 60°C for 4 h and by using mortar and pestle the product was crushed.

Synthesis of MnO_2 nanoparticle

The nanoparticle of MnO_2 was prepared by sonication. A horn type 20 kHz Sonics sonifier with a tip diameter of 13 mm was used. Typically, 5 gm of MnO_2 was dissolved in 100 ml of double distilled water and kept for continuous stirring for 20 min. and then this mixture was ultrasonicated for 30 min. a brown color precipitate was formed. This precipitate was filtered, washed in double distilled water and then wash by ethanol and dried out in an air oven at 100° C for 4 h.

Synthesis of PIn/MnO_2 composites and characterizations

PIn doped with MnO_2 nanoparticles was synthesized by using an ethanolic solution of PIn and MnO_2 by varying concentration of MnO_2 with fixed PIn using Ex-situ technique in wt.% stichometry with the interval of 0.25 wt.% [18]. The composites preparation range was fixed from 0.25 to 1 wt.%. The as such prepared composites were nomenclature as 0.25 wt.% MnO_2 as (PM1), 0.5 wt.% MnO_2 as (PM2), 0.75 wt. % MnO_2 as (PM3) and 1 wt.% MnO_2 as (PM4). This prepared samples were used for further study of supercapacitor and ultraviolet-visible spectro-photometer.

By using Bruker D8 advance with Cu Kα radiation the phase purity and structure of as prepared samples were confirmed in which the pattern recorded with step height of 0.02° with scan rate 6.00 in the range 10°–80°. Morphologies of all samples were studied by using JEOL-6390LV scanning electron microscope. Ultraviolet-visible spectrophotometer was used to record the complex optical properties of all prepared samples, from which the values of optical band gap was calculated. The FTIR was taken in the KBr medium at room temperature in the region 4000–500 cm^{-1} at scan rate 16. Supercapacitor property measurements such as cyclic voltammetry (CV) curve, cycle stability performance and galvanostatic charge/discharge curves were carried out using three-electrode cell systems (CHI 660 D, CH Instruments). The composites systems under study were used as the working electrode, platinum wire as counter electrode and Ag/AgCl as the reference electrode.

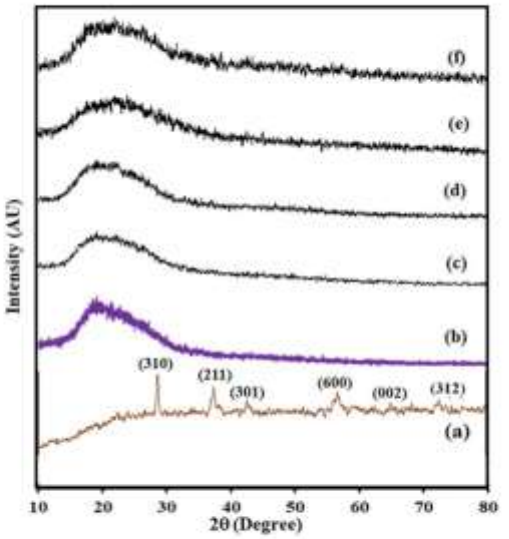

Fig. 1. XRD pattern of (a) MnO_2 nanoparticle material, (b) Pure PIn, (c) PM1, (d) PM2, (e) PM3 and (f) PM4 composites.

Results and discussion

XRD analysis

XRD patterns of MnO_2 nanoparticles, Pure PIn and PIn/MnO_2 composites were recorded at normal temperature in two theta range 10°–80°. Fig. 1 depicts the diffractogram of MnO_2 nanoparticles (Fig. 1 a), Pure PIn (Fig. 1 b) and PIn/MnO_2 composites (Fig. 1 c, d, e and f). All diffraction peaks of undoped MnO_2 nanoparticles corresponded well to tetragonal crystal symmetry of MnO_2 (ICDD: 44–0141). Diffraction peaks observed at 28.81°, 37.45°, 42.95°, 56.73°, 65.36° and 72.70° and these values corresponds to (310), (211), (301), (600), (002) and (312) planes [19–20]. The mean crystallite size of MnO_2 was found to be 23.45 nm calculated by using Debye-scherrer formula:

$$D = \frac{k\lambda}{\beta\cos\theta}$$

where k is Scherrer constant, λ is wavelength of X-ray, β is full width half maxima and θ is the Bragg's angle.

In Fig. 1(b), the broad peak appears in between 15° to 30° is the characteristic peak of the amorphous PIn, indicating the presence of PIn [21]. No evident peaks for MnO_2 were observed in XRD patterns of MnO_2/PIn composite. This could be a part of distortion in crystal structure of MnO_2 and also may be that MnO_2 particles were covered by

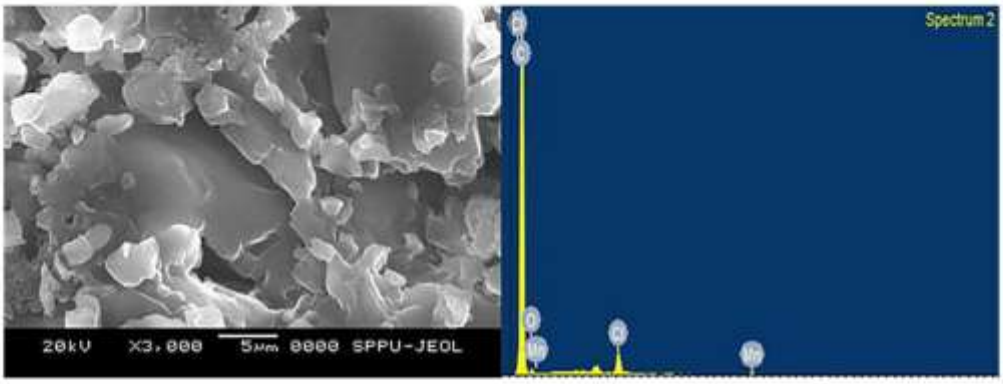

Fig. 2. SEM and EDAX image of PM4 composite.

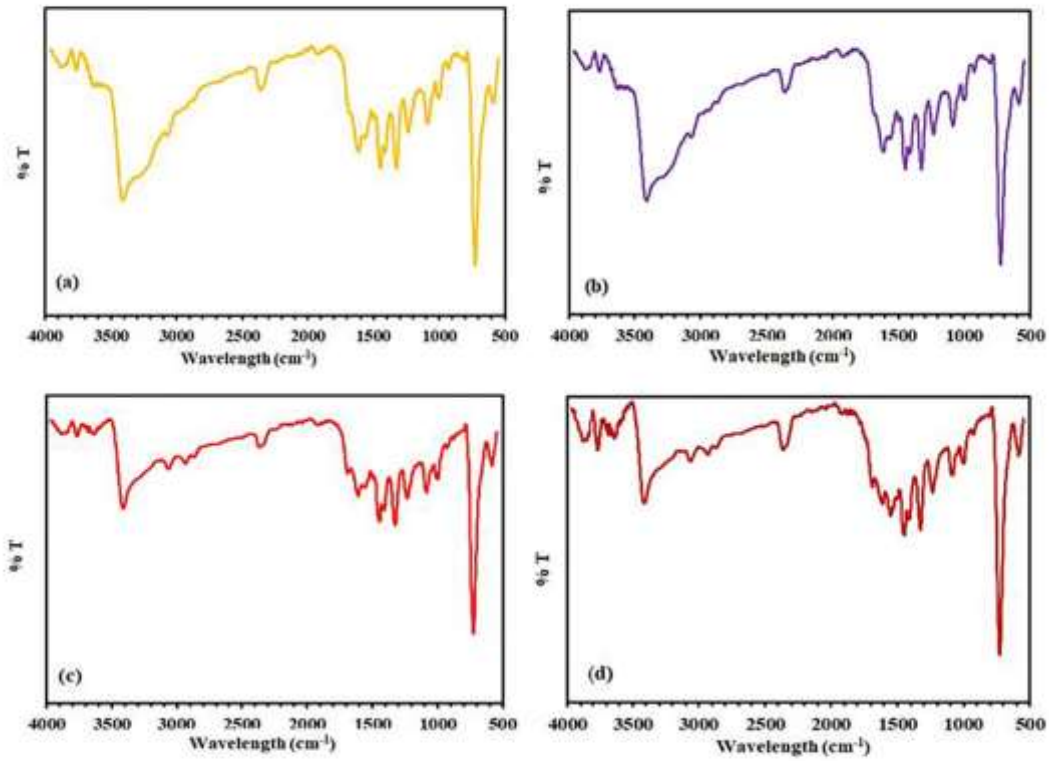

Fig. 3. FTIR spectra of (a) PM1, (b) PM2, (c) PM3 and (d) PM4 composites.

Pln.

SEM and EDAX study

The SEM proposed an external morphology of prepared samples. Fig. 2 shows the SEM and EDAX image of PM4 composite. SEM shows that composites have an irregular shape particle [22]. The EDAX spectrum of PM4 composite gives the confirmation about the presence of Manganese (Mn) and oxygen (O). Also, some impurities found during the preparation of composites which was removed by annealing process.

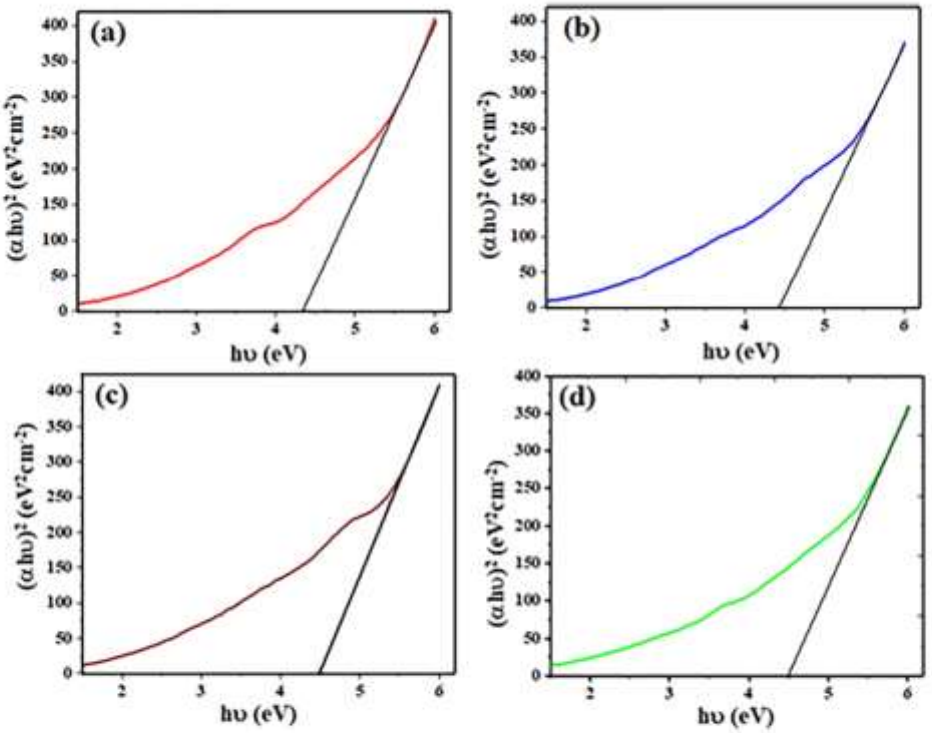

Fig. 4. Tauc plots of (a) PM_1, (b) PM_2, (c) PM_3 and (d) PM_4 composites.

The peak due to oxygen in EDAX confirms the oxygen storage capacity of prepared composites. As EDAX shows the existence of small amount of Mn and due to this reason MnO_2 was not detected by XRD.

FTIR study

Fig. 3 depict the FTIR spectrum of Pln/MnO_2 for all composites. A small peak at 530 cm^{-1} was assigned with Mn–O stretching [23]. Also, the peak at 600 cm^{-1} indicates the characteristic stretching collision of O–Mn–O, which confirmed the existence of the MnO_2 in the sample [24–25]. A strong peak observed at 742 and 1467 cm^{-1} are corresponding to the benzene ring, which indicates that the benzene ring did not involve in the polymerization [26–27]. The peak located at 1100 cm^{-1} is induced by different stretching frequencies of aromatic ring in the polymer chain, which corresponds to the stretching mode of C=N bond [28]. The peaks observed at 1336 and 1010 cm^{-1} shows the stretching mode of pyrrole ring and vibration mode of C–N bond [27]. The peak near 1236 cm^{-1} shows the surface OH groups of Mn–OH [24]. The peak 1559 cm^{-1} together with 3436 cm^{-1} can be ascribed to N–H bond stretching and deformation vibrations shows that nitrogen species are not the polymerization sites, hence the possibility of polymerization is through 2 and 3 position of indole monomer [29–30]. The peaks appear at 1630 cm^{-1} can be attributed C=O stretching vibrations [31].

Optical properties

The optical band gap gives idea about the energy to excite the electrons from outermost band to conduction band. The optical band gap of all Pln/MnO_2 composite was calculated from UV–visible spectroscopy ranging from 200 to 800 nm are shown in Fig. 4 (a, b, c and d). The Tauc plots were drawn to calculate band gap from following relation [32]:

$$\alpha h\vartheta = A\left(h\vartheta - E_g\right)^m$$

where A is an energy dependent constant, Eg is optical band gap of material, m is constant that depends on the semiconducting materials, which can be expected to have values of 1/2, 3/2, 2 and 3 depending on the nature of the electronic transition responsible for absorption; 1/2 for allowed direct transitions, 3/2 for direct forbidden transitions, 2 for allowed indirect transitions and 3 for indirect forbidden transitions [33]. Bandgap value of all samples was estimated by drawing $(\alpha h\upsilon)^2$ on y-axis and ($h\upsilon$) on x-axis. $h\upsilon$ was calculated simply using the relation;

$$h\vartheta = \frac{1240}{\lambda(nm)}\ eV$$

The band gap was found out by extra plotting the straight line of graph. The point where extra plotting intersects the $h\upsilon$ axis (x-axis) gives band gap value. The highest band gap value was observed to be 4.50 eV for PM4 composite where as lowest band gap value was observed to be 4.33 eV for PM1 composite. The highest band gap was probably due to quantum confinement [34–35].

Supercapacitive study

Electrochemical energy storage capacitance of PM1, PM2, PM3 and PM4 composite as electrode of electrochemical capacitor was evaluated

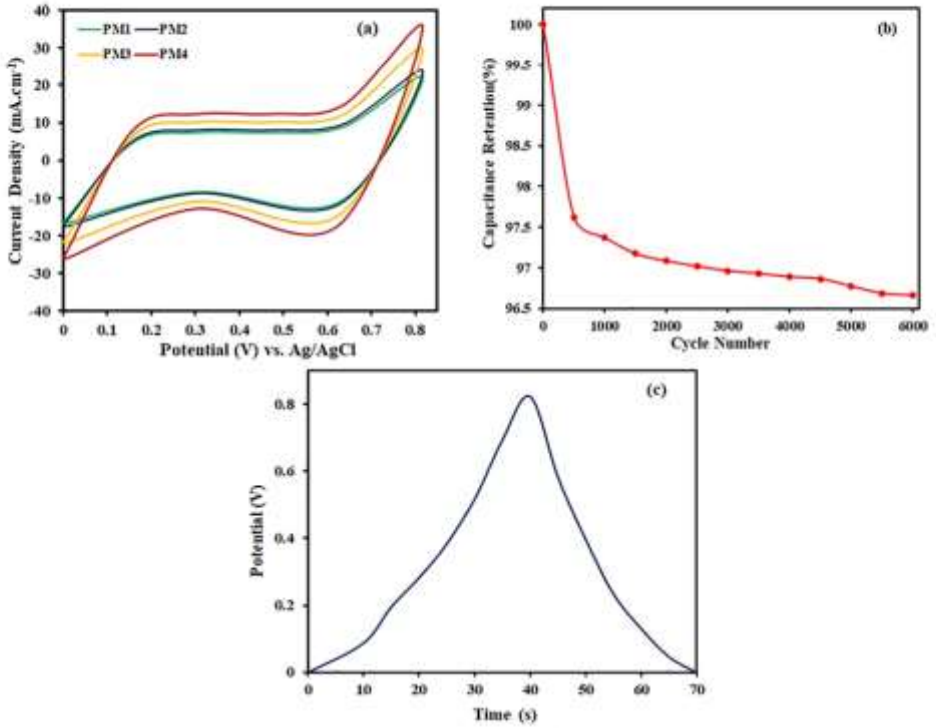

Fig. 5. (a) CV curves of PM1, PM2, PM3 and PM4 composites recorded at a scan rate of 50 mVs^{-1}, (b) Cycle performance of the PM4 composite 6000 cycles and (c) Galvanostatic charge/discharge curves of the PM4 composite recorded at a current density of 10 μAcm^{-2}.

from cyclic voltametric (CV) curves. Fig. 5 (a) illustrates the cyclic voltametric (CV) curves of PM1, PM2, PM3 and PM4 composite recorded at a scan rate of 50 mVs^{-1} in potential range of 0 to 0.8 V, which shows quasi-rectangular graphs indicating a pseudo-capacitive behavior and reversible doping/dedoping reactions [36]. The CV plots clearly shows the doping of MnO_2 nanoparticles in PIn influence supercapacitive properties composite. The superior supercapacitive properties of PIn/MnO_2 composite can be attributed to oxidation/reduction of surface hydroxyl groups [37]. The curve shape of PIn/MnO_2 composites are more rectangular, which shows a good capacitive behavior. Specific capacitance has been estimated using the relation [38]:

$$Cs = \frac{I}{m \times v}\left(Fg^{-1}\right)$$

where I is the average current during anodic and cathodic scan (A), m is the mass of the electrode (g) and v is the scan rate (V). In our case, the highest value of specific capacitance was found to be 1558 Fg^{-1} at a scan rate of 50 mVs^{-1} for PM4 composite which may be due to the porous structure of PIn/MnO_2 composites enhances specific capacitance.

Fig. 5(b) shows the PM4 composite exhibits considerable long-term stability that is capacitance retention up to 6000 cycles. The decent capacitance capability of PM4 composite is recognized to boosted electrical conductivity and vastly stable surface redox reaction and it is more suitable for electrode applications.

Fig. 5(c) shows the galvanostatic charge/discharge (GCD) curves of PM4 composite at current density 10 μAcm^{-2} within potential window 0 to 0.8 V. GCD curves of PM4 composite is nearly symmetric and considerably lengthy for practical application. The characteristic pseudocapacitive performance was indicated by nonlinear GCD curves, which may be due to the reversible redox reaction with insignificant loss of voltage and it suggest that electrolyte has excellent electrical conductivity between the current collector and active materials.

Conclusions

In summary, we have successfully demonstrated and concludes that concentration of MnO_2 nanoparticles in PIn composite have significant influence. The PM4 composite have specific capacitance of the order 1558 Fg^{-1} at a scan rate of 50 mVs^{-1} and also shows long-term stability that is capacitance retention up to 6000 cycles. The galvanostatic charge/discharge curves depicts that PM4 composite also have long and nearly symmetric behavior which is suitable for range of practical applications. The obtained results in this work attributed to the porous structure of PIn/MnO_2 composites.

Compliance with ethical standards

The submitted work is original and not submitted/published elsewhere in any form or in any other language.

Research data policy and data availability statements

The raw/processed data required to reproduce these findings cannot be shared at this time as the data also forms part of an ongoing study.

Author contribution

All authors contributed to the study conception and design. Material preparation, data collection and analysis were performed by Rajesh Barde. The first draft of the manuscript was written by Rajesh Barde, Sandeep Waghuley and Kailash Nemade and all authors commented on previous versions of the manuscript. All authors read and approved the final manuscript.

Author statement

We hereby declare that the submitted work is outcome of our original lab work and not published elsewhere also all the authors have given permissions for the submission. If present work found published elsewhere in any other language, I will be considered as a responsible person for the further actions.

The authors whose names are listed immediately below certify that they have NO affiliations with or involvement in any organization or entity with any financial interest (such as honoraria; educational grants; participation in speakers' bureaus; membership, employment, consultancies, stock ownership, or other equity interest; and expert testimony or patent-licensing arrangements), or non-financial interest (such as personal or professional relationships, affiliations, knowledge or beliefs) in the subject matter or materials discussed in this manuscript.

Declaration of Competing Interests

The authors have no relevant financial or non-financial interests to disclose.

Acknowledgements

The author acknowledges Director, Govt. Vidarbha institute of Science and Humanities, Amravati, Head, Department of Physics, Govt. Vidarbha institute of Science and Humanities, Amravati, and Head, Department of Physics, Sant Gadge Baba Amravati University, Amravati for providing necessary facilities for the work.

References

[1] Y. Zhang, Y. Mo, Preparation of MnO_2 electrodes coated by Sb-doped SnO_2 and their effect on electrochemical performance for supercapacitor, Electrochimica Acta 142 (2014) 76–83.
[2] C. Poochai, C. Sriprachuabwong, J. Sodtipinta, J. Lohitkarn, P. Pasakon, V. Primpray, N. Maeboonruan, T. Lomas, A. Wisitsoraat, A. Tuantranont, Alpha-MnO_2 nanofibers/nitrogen and sulfur-co-doped reduced graphene oxide for 4.5 V quasi-solid-state supercapacitors using ionic liquid-based polymer electrolyte, J. Coll. and Interf. Sci. 583 (2021) 734–745.
[3] A. Tyagi, K.M. Tripathi, R.K. Gupta, Recent progress in micro-scale energy storage devices and future aspects, J. Mate. Chem. A 3 (2015) 22507–22541.
[4] L. Chen, Z. Song, G. Liu, J. Qiu, C. Yu, J. Qin, L. Ma, F. Tian, W. Liu, Synthesis and electrochemical performance of polyaniline–MnO_2 nanowire composites for supercapacitors, J. Phys. and Chem. of Sol. 74 (2013) 360–365.
[5] M. Winter, R.J. Brodd, What Are Batteries, Fuel Cells, and Supercapacitors? Chem. Revi. 104 (2004) 4245–4269.
[6] C.B. Diaz-Arriaga, J.M. Baas-Lopez, D.E. Pacheco-Catalan, J. Uribe-Calderon, Uribe-Calderon, Symmetric electrochemical capacitor based on PPy obtained via MnO_2 reactive template synthesis, Synth. Met. 269 (2020), 116541.
[7] M. Ho, P. Khiew, D. Isa, T. Tan, W. Chiu, C.H. Chia, A review of metal oxide composite electrode materials for electrochemical capacitors, Nano 9 (2014), 1430002.
[8] X. Lu, T. Zhai, X. Zhang, Y. Shen, L. Yuan, B. Hu, L. Gong, J. Chen, Y. Gao, J. Zhou, Y. Tong, Z.L. Wang, WO3–x@Au@MnO_2 core-shell nanowires on carbon fabric for high-performance flexible supercapacitors, Adv. Mater. 24 (2012) 938–944.
[9] L. Bao, J. Zang, X. Li, Flexible Zn_2SnO_4/MnO_2 core/shell nanocable-carbon microfiber hybrid composites for high-performance supercapacitor electrodes, Nano Lett 11 (2011) 1215–1220.
[10] Z. Chen, V. Augustyn, J. Wen, Y. Zhang, M. Shen, B. Dunn, Y. Lu, High-performance supercapacitors based on intertwined CNT/V_2O_5 nanowire nanocomposites, Adv. Mater. 23 (2011) 791–795.
[11] X. Dai, M. Zhang, J. Li, D. Yang, Effects of electrodeposition time on a manganese dioxide supercapacitor, RSC Adv. 10 (2020) 15860.
[12] M. Zhang, D. Yang, J. Li, Effective improvement of electrochemical performance of electrodeposited MnO_2 and MnO_2/reduced graphene oxide supercapacitor materials by alcohol pretreatment, J. Ener. Stora. 30 (2020), 101511.
[13] S.P. Koiry, V. Saxena, D. Sutar, S. Bhattacharya, D.K. Aswal, S.K. Gupta, J. V. Yakhmi, Interfacial synthesis of long polyindole fibers, J. Appl. Poly. Sci. 103 (2007) 595–599.
[14] R. Perveen, S.Haque Inamuddin, A. Nasar, A.M. Asiri, G.M. Ashraf, Electrocatalytic performance of chemically synthesized PIn-Au-SGO composite toward mediated biofuel cell anode, Sci. Rep. 7 (2017) 13353.
[15] S.Mehtab Rim, M.O.H. Zaidi, K. Singha, R. Arya, T.I. Siddiqui, Polyindole based nanocomposites and their applications: A review, Mater. Sci. Res. India 16 (2019) 97–102.
[16] G. Rajasudha, A.P. Nancy, T. Paramasivam, N. Boukos, N. Vangidasamy, S. Arumainathan, Synthesis and Characterization of Polyindole-NiO-Based Composite Polymer Electrolyte with $LiClO_4$, Int. J. Polym. Mater. 60 (2011) 877–892.
[17] V. Kumar, C. Jolivalt, J. Pulpytel, R. Jafari, F. Arefi-Khonsari, Development of Silver Nanoparticle Loaded Antibacterial Polymer Mesh Using Plasma Polymerization Process, J. Biomed. Mater. Res., Part A 101 (2013) 1121–1132.
[18] R.V. Barde, Preparation, characterization and CO_2 gas sensitivity of Polyaniline doped with Sodium Superoxide (NaO_2), Mate. Res. Bul. 73 (2016) 70–76.
[19] L. Feng, Z. Xuan, H. Zhao, Y. Bai, J. Guo, C. Su, X. Chen, MnO_2 prepared by hydrothermal method and electrochemical performance as anode for lithium-ion battery, Nano. Res. Lett. 9 (2014) 290–298.
[20] S. Sivakumar, L.N. Prabu, Synthesis and Characterization of α-MnO_2 nanoparticles for Supercapacitor application, Mate. Sci., Eng. Mate. Today: Proc. 47 (2021) 52–55.
[21] L. Yuan, C. Wan, L. Zhao, Facial In-situ Synthesis of MnO_2/PPy composite for supercapacitor, Int. J. Electrochem. Sci. 10 (2015) 9456–9465.
[22] K.S. Shaker, A.H. Abd Alsalm, Synthesis and characterization nano structure of MnO_2 via chemical method, Eng. and Techn. Jou. 36 (9) (2018) 946–950.
[23] Y. Kumar, S. Chopra, A. Gupta, Y. Kumar, S.J. Uke, S.P. Mardikar, Low temperature synthesis of MnO_2 nanostructures for supercapacitor application, Mat. Sci. for Ener. Tech. 3 (2020) 566–574.
[24] D. Jaganyi, M. Altaf, I. Wekesa, Synthesis and characterization of whisker-shaped MnO_2 nanostructure at room temperature, Appl Nano sci 3 (2013) 329–333.
[25] M. Peng, G. Long, S. Jiang, Y. Ji, W. Han, B. Wang, X. Liu, Y. Xi, Rapid synthesis of graphene/amorphous α-MnO_2 composite with enhanced electrochemical performance for electrochemical capacitor, Mater. Sci. Eng., B 194 (2015) 41–47.
[26] N.Shaheel Inamuddin, M.I. Ahamed, S. Kanchi, H.A. Kashmery, Green synthesis of ZnO nanoparticles decorated on polyindole functionalized-MCNTs and used as anode material for enzymatic biofuel cell applications, Scient. Rep. 10 (2020) 5052.
[27] M. Elango, M. Deepa, R. Subramanian, A.M. Musthafa, Synthesis, characterization, and antibacterial activity of Polyindole/Ag–Cuo nanocomposites by reflux condensation method, Poly. Plast. Tech. and Eng. 57 (2018) 1440–1451.
[28] K. Girihabu, R. Murugavelan, R. Suresh, L. Vijayalakshmi, A. Stephen, V. Narayanan, Polyindole nanowires: Synthesis, characterization and electrochemical sensing property, Chem Sci Trans. 2 (2013) 13–16.
[29] H. Talbi, D. Billaud, G. Monard, M. Loos, Theoretical investigation of the monomer reactivity in polyindole derivatives, Synth. Met. 101 (1999) 115.
[30] J. Xu, G. Nie, S. Zhang, X. Han, J. Hou, S. Pu, Electrosyntheses of freestanding polyindole films in boron trifluoride diethyl etherate, J. Poly. Sci., Part A: Poly. Chem. 43 (2005) 1444–1453.
[31] T.L. Montanheiro, F.H. Cristovan, J.P.B. Machado, D.B. Tada, N. Duran, A. P. Lemes, Effect of MWCNT functionalization on thermal and electrical properties of PHBV/MWCNT nanocomposites, J. Mater. Res. 30 (2015) 55–65.
[32] Y. Hu, B. Hu, B. Wu, Z. Wei, J. Li, Hydrothermal preparation of ZnS:Mn quantum dots and the effects of reaction temperature on its structural and optical properties, J. Mater. Sci.: Mater. in Elect. 29 (2018) 16715–16720.
[33] R.V. Barde, Influence of CeO_2 content on complex optical parameters of phosphovanadate glass system, Spect. Acta Part A: Mol. and Bio. Spect. 153 (2016) 160–164.
[34] M.U. Khalid, M.F. Warsi, I. Shakir, M.F. Aly Aboud, M. Shahid, S.S. Ilias, S. Zulfiqar, Zulfiqar, Al^{3+}/Ag^{1+} induced phase transformation of MnO2 nanoparticles from α to β and their enhanced electrical and photocatalytic properties, Ceram. Int. 7 (2020) 9913–9921.
[35] N. Rajamanickam, P. Ganesan, S. Rajashabala, K. Ramachandran, Structural and optical properties of α − MnO_2 nanowires and β − MnO_2 nanorods, AIP Conf. Proc. 1591 (1) (2014) 267–269.
[36] J.G. Wang, Y. Yang, Z.H. Huang, F. Kang, MnO_2/polypyrrole nanotubular composites: Reactive template synthesis, characterization and application as superior electrode materials for high-performance supercapacitors, Electrochim. Acta 130 (2014) 642–649.
[37] D. Choi, G.E. Blomgren, P.N. Kumta, Fast and reversible surface redox reaction in nanocrystalline vanadium nitride supercapacitors, Adv. Mater. 18 (2006) 1178–1182.
[38] B. Sethuraman, K.K. Purushothaman, G. Muralidharan, Synthesis of mesh-like Fe_2O_3/C nanocomposite via greener route for high performance supercapacitors, RSC Adv. 4 (2014) 4631–4636.

2 Alumina tunnel contact based lateral spin-Field effect transistor

Materials Science and Engineering B 286 (2022) 115977

Contents lists available at ScienceDirect

Materials Science & Engineering B

journal homepage: www.elsevier.com/locate/mseb

Alumina tunnel contact based lateral spin-Field effect transistor

Neetu Gyanchandani [a], Prashant Maheshwary [b], Kailash Nemade [c,*]

[a] JD College of Engineering and Management, Nagpur 441501, India
[b] Dean (Science and Technology), RTM Nagpur University, Nagpur 440033, India
[c] Department of Physics, Indira Mahavidyalaya, Kalamb 445401, India

ARTICLE INFO

Keywords:
Alumina
Tunnel contacts
Spin-field effect transistor, spintronics

ABSTRACT

In the present work, modified Datta and Das Type silicon based lateral spin-Field Effect Transistor (MDD Type s-FET) is presented with alumina as tunnel contact. The insertion of alumina enhances the spin injection ability of Co-Graphene nanosheets based ferromagnetic electrode (FM) and also resolves the conductivity mismatch problem. The main accomplishment of present work is that fabricated MDD Type s-FET with alumina as tunnel contact exhibits the non-rectifying current-voltage characteristic with sufficiently large value of MR which is an indispensable requirement of spintronics devices. Also, in present work 2-dimensional electron gas was used as a channel which can control MR through gate voltage. Similarly, the control on MR through gate voltage enables the switching action in s-FET.

1. Introduction

For the fabrication of spintronics devices, electrical spin injection and its detection have extraordinary importance [1]. Recently, few reports have explored that the insertion of tunnel barrier between ferromagnet and semiconducting channel increases the spin injection efficiency of electrode [2–4].

In case of spin-Field Effect Transistor (s-FET) the important thing is that spin-orbit coupling must be large enough for the transfer of spin and small enough to maintain spin relaxation between source and drain. In s-FET, transistor action can be achieved by two approaches, (i) first is the electrical control of the spin injection process [5] and (ii) second is the spin transport efficiency along the channel [6].

The major challenge in the realization of s-FET are,

1. Efficient spin injection from ferromagnetic source electrode into semiconductor channel.
2. Transfer of spin-polarized signal without changing spin through semiconductor channel.
3. Detection of spin-polarized signal by ferromagnetic drain electrode.

To resolve these challenges, sufficient knowledge of charge transfer process from ferromagnetic materials to semiconductor is needed. It is well known fact that ferromagnetic materials comprise an excess of electrons having one sided spin, which gives the magnetization direction.

By simply applying the potential difference to FM material, it is not possible to inject quality spin-polarized signal into semiconductor. This difficulty arises due to the huge difference in conductivity of FM material and semiconductor which is also known as conductivity mismatch. To overcome the conductivity mismatch problems, many reports in literature suggest that the insertion of thin layer of insulator between FM and semiconductor enables the spin-dependent tunnel resistance [7–9]. This results in efficient spin injection into the semiconductor.

In the literature, few reports support to the fabrication device with tunnel contact for efficient spin injection and detection. Erve et al demonstrated graphene as tunnel barrier to resolve the conductivity mismatch problem. Study of Hanle model, this study shows that spin lifetime does not depend on the tunnel barrier material. The main accomplishment of this work is using graphene as tunnel contact stopping metal ion diffusion from the FM electrode [10]. Schmidt et al suggested that in the diffusive transport region strictly use small polarization current from FM to 2DEG, which results in long spin-flip length [11]. Cubukcu et al reported significant spin transport in graphene-based lateral spin valves using FM contacts. This study shows that insertion of alumina as tunnel barrier improves spin transfer efficiency by many folds [12].

Min et al reported that spin injection from ferromagnet to silicon characteristics using Al_2O_3 as tunnel contacts. This study concluded that thickness of tunnel contact that is Al_2O_3 and doping concentration of

* Corresponding author.
E-mail address: kmemade@gmail.com (K. Nemade).

https://doi.org/10.1016/j.mseb.2022.115977
Received 22 November 2021; Received in revised form 24 July 2022; Accepted 21 August 2022
Available online 6 September 2022

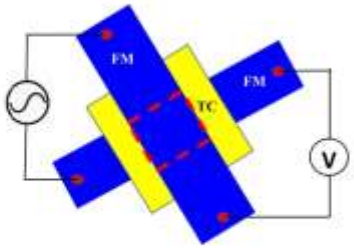

Fig. 1. Typical structure of spin valve with Co-Graphene nanosheets based FM electrodes separated bytunnel contacts (TC). Dotted red color line indicates active region of device. (For interpretation of the references to color in this figure legend, the reader is referred to the web version of this article.)

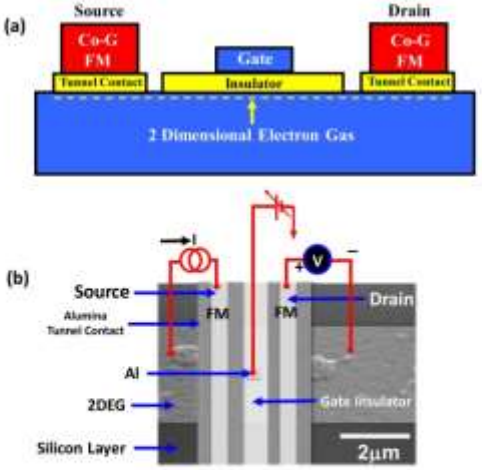

Fig. 2. (a) Schematics of MDD Type silicon based lateral s-FET with tunnel contact and (b) Scanning electron micrograph of MDD Type s-FET.

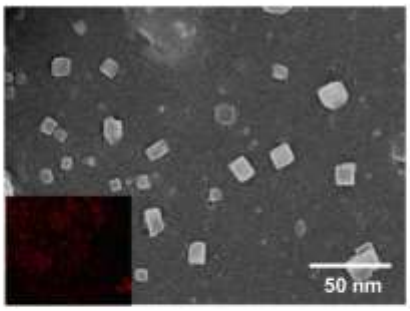

Fig. 3. SEM image of Co-Graphene nanosheets with elemental X-ray mapping of elements (inset).

silicon plays a very crucial role [13]. Dankert et al validated the production of large spin polarizations in *n*-type and p-type oxidized silicon as a tunnel barrier. In this paper, author explained the role of Schottky barrier in the process of spin injection and detection. Study concluded that width of the Schottky barrier resulted in nondegenerate silicon, which produces an anomalous sign change of spin signal [14].Svintsov et al reported the tunnel field effect transistors based on graphene channels. The proposed transistor shows that tunnel gap in the channel operated by gate, which shows ON and OFF state current in semiconductor channels [15].

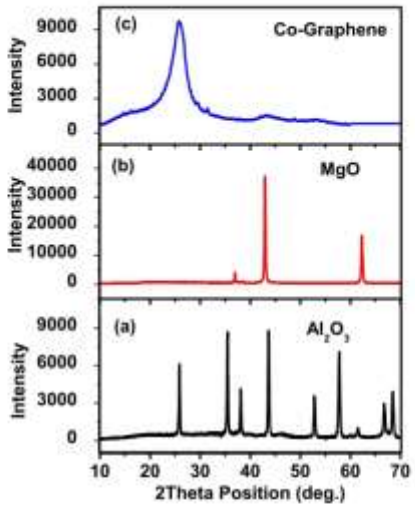

Fig. 4. XRD pattern of (a) alumina, (b) MgO and (c) Co loaded Graphene nanosheets.

Motivated by the above findings, this paper modified Datta and Das Type silicon based lateral spin-Field Effect Transistor (MDD Type s-FET) is presented with tunnel contact that enhances the spin injection ability of Co-Graphene nanosheets based ferromagnetic electrode (FM). The main accomplishment of present work is that both the key requirements of good s-FET that is non-linear/non-rectifying I–V characteristic and large MR value satisfied by the fabricated device. In spin-transistor technology, high value of MR is an indispensable requirement [16]. In this work, *n*-type silicon was used as a channel which can control on MR through gate voltage. This is the beauty of present work that MR can be tunable using gate voltage, which enables the switching action in s-FET.

2. Experimentation

2.1. Materials preparation and characterisation

In the present study, cobalt anchored graphene nanosheets (Co-Graphene nanoshhets) were prepared by ex-situ approach. In the process of preparation of nanosheets the graphene was used as previously reported method [17]. To prepare the Co-Graphene nanoshhets, 15 g of graphene sheets were dissolved in 100 ml of acetic acid under constant magnetic stirring for 15 min.

Then solution was subjected to probe-sonication for 30 min. simultaneously, the separate solution of 0.5 g of $Co(NO_3)_3$ was prepared with 20 ml of acetic acid. The second solution of $Co(NO_3)_3$ was added in graphene solution under magnetic stirring at room temperature for 60 min. Lastly, the solution was filtered and washed two times by deionized water. So obtained final product is dried at 100 °C in oven. Next, the dried product was kept for heating from 100 to 500 °C with an interval of 100 °C for 60 min. Then the sample was permitted to cool at 400, 300, 200 and 100 °C each for 60 min.

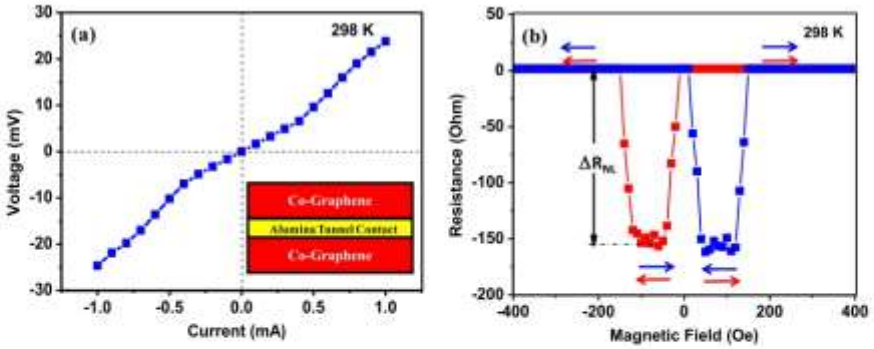

Fig. 5. (a) Non-linear current–voltage curve of Co-Graphene/Alumina/Co-Graphene junction indicating alumina works like a tunnel contact in charge transport. Inset shows general schematic of Co-Graphene/Alumina/Co-Graphene junction. (b) Negative magnetoresistance of Co-Graphene/Alumina/Co-Graphene junction.

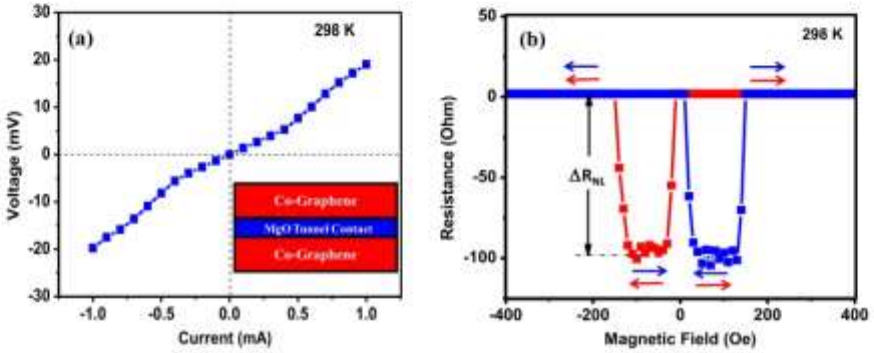

Fig. 6. (a) Non-linear current–voltage curve of Co-Graphene/MgO/Co-Graphene junction indicating MgO works like a tunnel contact in charge transport. Inset shows general schematic of Co-Graphene/MgO/Co-Graphene junction. (b) Negative magnetoresistance of Co-Graphene/MgO/Co-Graphene junction.

The X-ray diffraction (XRD) (Rigaku Miniflex-XRD; Wavelength = 1.5406 Å) technique was employed to study structural properties of prepared sample. To analyze the morphology of sample was subjected to field emission scanning electron microscopy on SEM instrument, Model: ZEISS SIGMA. Elemental analysis was completed using an energy dispersive X-ray analysis instrument (Model: EAG AN461).

2.2. Device fabrication and measurements

In this fabrication process, the Co-Graphene/Alumina/Co-Graphene junction and Co-graphene/MgO/Co-Graphene junction were prepared on Si/SiO_2 substrate by e-beam evaporation technique. The Co-Graphene nanosheets were used as top and bottom ferromagnetic electrode with thickness of 50 nm by sandwiching the tunnel contacts (in the present work Al_2O_3 and MgO) having thickness of the order of 5 nm. Fig. 1 depicts the schematics of complete spin valve device.

To fabricate the modified Datta and Das Type silicon based lateralspin field effect transistor (MDD Type s-FET), all necessary components like heavily doped *n*-type silicon wafer and insulator were procured from India-Mart. The *n*-type silicon wafer used for MDD Type s-FET fabrication have thickness of the order of 500 μm.The details of *n*-type silicon waferare resistivity = 10 Ω.m, conductivity = 0.1 S/m, dopant concentration = $4.48 \times 10^{6} m^{-3}$ and mobility = $0.1351 m^{2}V^{-1}s^{-1}$. Firstly, the *n*-type silicon wafer was cleaned to remove the grease, adsorbed water molecule and air borne dust using mild-detergent solution (Labolene) and then with distilled water. After cleaning step, using atomic layer deposition technique the two layers of alumina with separation of ~ 0.8 μm was transferred on *n*-type silicon wafer having thickness ~ 5 nm. The alumina was transferred on *n*-type silicon wafer, to resolve the issue of conductivity mismatch between ferromagnetic electrode and semiconductor.

In deposition process, the substrate temperature was maintained at 120 °C. The remaining area of substrate was masked with Kapton tape (as it withstands temperatures up to 260 °C). Subsequent to this step, Co-Graphene nanosheets based ferromagnetic (FM) electrodes were also deposited on both alumina tunnel contacts. After removal of masking tape, the area between the channel of FM electrodes was coated with polyvinyl acetate using spin-coating technique. The aluminum of thickness 5 nm was transferred as gate on the top of insulating layer of polyvinyl acetate.

As fabricated MDD Type s-FET has channel length of the order of ~ 1.8 μm and channel width ~ 2.3 μm. Fig. 2 (a) shows the schematic drawing of MDD Type silicon based lateral-FET with tunnel contact and Fig. 2(b) shows the scanning electron micrograph of MDD Type silicon based lateral-FET with alumina as tunnel contact and all components of device displayed on SEM image with circuitry arrangement. In the fabrication of MDD Type s-FET with MgO as tunnel barrier, the same process was adopted.

The transport measurements of MDD Type s-FETs with tunnel contact alumina and MgO tested on Physical Properties Measurements

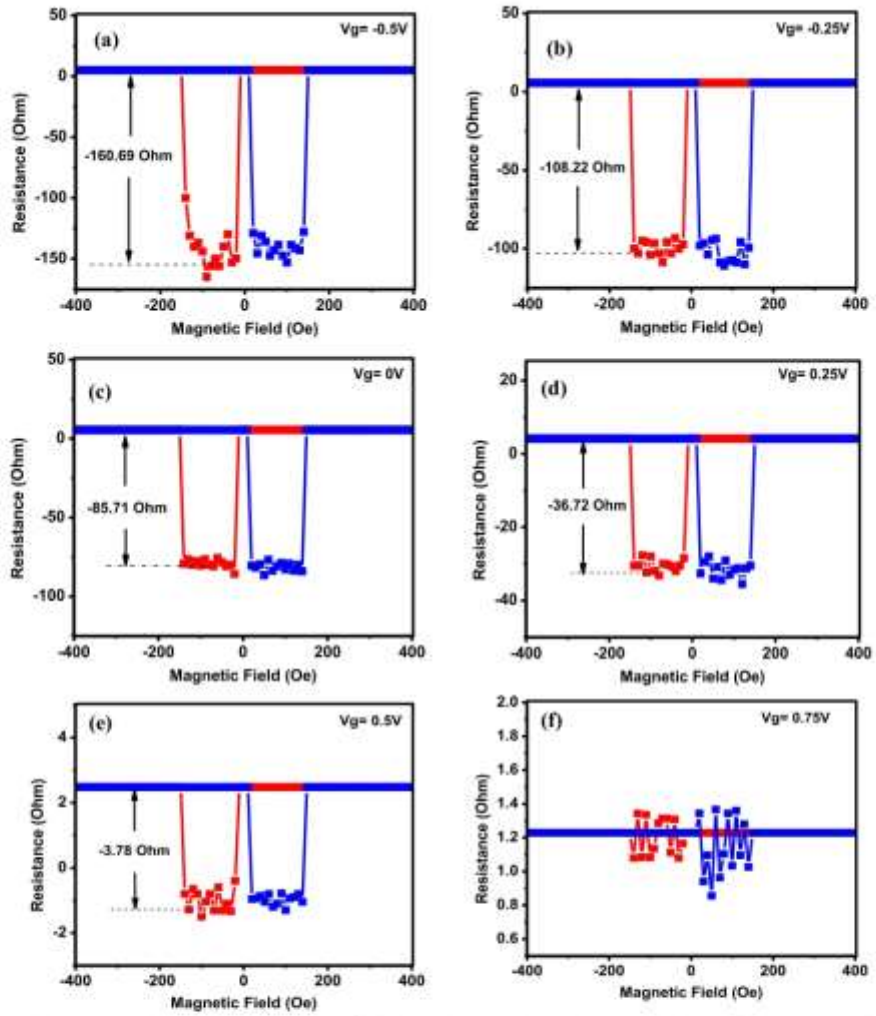

Fig. 7. Gate controlled magnetoresistance in MDD Type silicon based lateral-FET with alumina as tunnel contact at (a) −0.5 V, (b) −0.25 V, (c) 0 V, (d) 0.25 V, (e) 0.5 V and (f) 0.75 V.

System (PPMS) made by Quantum Design. The current–voltage curves of both junctions Co-Graphene/Alumina/Co-Graphene junction and Co-graphene/MgO/Co-Graphene junction were recorded to study the tunneling behavior of junction. The performance of both MDD Type s-FETs with tunnel contact was analyzed by measuring the magnetoresistance (MR) as a function of magnetic field. Similarly, the switching action in MDD Type s-FETs with tunnel contact alumina was revealed in the form of change in amplitude of MR (ΔR_{Rp}). MR curves were recorded at 298 K for different values of gate voltages. Magnetoresistance (MR) is defined as, MR%=[(Rap-Rp)/Rp] × 100, where Rap is magnetization vectors of two electrodes are antiparallel and Rp is the magnetization vectors of two electrodes are parallel.

3. Results and discussion

The surface morphology of Co loaded graphene nanosheets prepared by ex-situ approach was investigated. The SEM image of Co loaded graphene nanosheets with elemental X-ray mapping of cobalt (inset) is shown in Fig. 3. SEM image shows smooth and flat surface with islands of cobalt nanocrystals. The temperature conditioning of Co loaded graphene nanosheets between 100 and 500 °C, results in diffusion of Co and O atom [18]. This diffusion with limited number of crystal seeds available on graphene surface results in the formation of islands. Hence, the SEM image of Co loaded graphene nanosheets have coarse surface due to the presence of islands on graphene. Inset image shows that Co was detected in elemental X-ray mapping.

The quality of the tunnel barrier is very crucial, as the present study

5. Data availability

The raw/processed data required to reproduce these findings cannot be shared at this time as the data also forms part of an ongoing study.

Declaration of Competing Interest

The authors declare that they have no known competing financial interests or personal relationships that could have appeared to influence the work reported in this paper.

Data availability

No data was used for the research described in the article.

Acknowledgments

Prof. (Mrs.) Neetu Gyanchandani is very much thankful to the management and Principal of JD College of Engineering and Management, Nagpur for providing necessary academic help.

References

[1] X. Lou, C. Adelmann, S.A. Crooker, E.S. Garlid, J. Zhang, K.S.M. Reddy, S. D. Flexner, C.J. Palmstrøm, P.A. Crowell, Electrical detection of spin transport in lateral ferromagnet–semiconductor devices, Nat. Phys. 3 (2007) 197–202.
[2] R. Jansen, Silicon spintronics, Nat. Mater. 11 (5) (2012) 400–408.
[3] M. Ghosher, M. Ciorga, M. Utz, D. Schuh, D. Bougeard, D. Weiss, Electrical spin injection into high mobility 2D systems, Phys. Rev. Lett. 113 (2014), 236602.
[4] S.P. Dash, S. Sharma, R.S. Patel, M.P. de Jong, R. Jansen, Electrical creation of spin polarization in silicon at room temperature, Nature 462 (7272) (2009) 491–494.
[5] R. Jansen, B.-C. Min, S.P. Dash, Oscillatory spin-polarized tunnelling from silicon quantum wells controlled by electric field, Nat. Mater. 9 (2) (2010) 133–138.
[6] C. Betthausen, T. Dollinger, H. Saarikoski, V. Kolkovsky, G. Karczewski, T. Wojtowicz, K. Richter, D. Weiss, Spin-transistor action via tunable Landau-Zener transitions, Science 337 (6092) (2012) 324–327.
[7] E.I. Rashba, Theory of electrical spin injection: tunnel contacts as a solution of the conductivity mismatch problem, Phys. Rev. B 62 (2000) 16267.
[8] A.M. Roy, D.E. Nikonov, K.C. Saraswat, Conductivity mismatch and voltage dependence of magnetoresistance in a semiconductor spin injection device, J. Appl. Phys. 107 (2010), 064504.
[9] S.A. Crooker, M. Furis, X. Lou, C. Adelmann, D.L. Smith, C.J. Palmstrøm, P. A. Crowell, Imaging spin transport in lateral ferromagnet/semiconductor structures, Science 309 (2005) 2191.
[10] O.M.J. van 't Erve, A.L. Friedman, E. Cobas, C.H. Li, A.T. Hanbicki, K.M. McCreary, J.T. Robinson, B.T. Jonker, A graphene solution to conductivity mismatch: Spin injection from ferromagnetic metal/graphene tunnel contacts into silicon, J. Appl. Phys. 113 (2013) 17C502.
[11] G. Schmidt, D. Ferrand, L.W. Molenkamp, Fundamental obstacle for electrical spin injection from a ferromagnetic metal into a diffusive semiconductor, Phys. Rev. B 62 (2000) 1–4.
[12] M. Cobaken, M.B. Martin, P. Laczkowski, C. Vergnaud, A. Marty, J.-P. Attane, P. Seneor, A. Anane, C. Deranlot, A. Fert, S. Auffret, C. Ducruet, L. Notin, L. Vila, M. Jamet, Ferromagnetic tunnel contacts to graphene: Contact resistance and spin signal, J. Appl. Phys. 117 (2015), 093909.
[13] B.C. Min, J.C. Lodder, R. Jansen, Cobalt-Al2O3-silicon tunnel contacts for electrical spin injection into silicon, J. Appl. Phys. 99 (2006) 093701–13.
[14] A. Dankert, R.S. Dulal, S.P. Dash, Efficient Spin Injection into Silicon and the Role of the Schottky Barrier, Sci. Rep. 3196 (2013) 1–8.
[15] D.A. Svintsov, V.V. Vyurkov, V.P. Lukichev, A.A. Orlikovsky, A. Burenkov, R. Oechsner, Tunnel Field Effect Transistors with Graphene Channels, Semiconductors 47 (2) (2013) 279–284.
[16] S. Sugahara, M.A. Tanaka, A spin metal–oxide–semiconductor field-effect transistor using half-metallic-ferromagnet contacts for the source and drain, Appl. Phys. Lett. 84 (2004) 2307.
[17] K.R. Nemade, S.A. Waghuley, Chemiresistive gas sensing by few-layered graphene, J. Electron. Mater. 42 (10) (2013) 2857–2866.
[18] S.I. Park, Y. Tchoe, H. Baek, J. Heo, J.K. Hyun, J. Jo, M. Kim, N.-J. Kim, G.-C. Yi, Growth and optical characteristics of high-quality ZnO thin films on graphene layers, APL Mater. 3 (1) (2015) 016103, https://doi.org/10.1063/1.4905488.
[19] K.R. Nemade, S.A. Waghuley, Low temperature synthesis of semiconducting α-Al2O3 quantum dots, Ceram. Int. 40 (4) (2014) 6109–6113.
[20] K.R. Nemade, B.V. Bonde, S.A. Waghuley, Photocatalytic study of alumina-zirconia ceramic nanocomposite synthesized by spray pyrolysis, Ceram. Int. 41 (3) (2015) 4836–4840.
[21] H.S. Kim, N. Park, T.J. Lee, M. Um, M. Kang, Preparation of Nanosized α-Al2O3 Particles Using a Microwave Pretreatment at Mild Temperature, Adv. Mater. Sci. Eng. 2012 (2012) Article ID 920105 (6 pages).
[22] S. Cava, S.M. Tebcherani, I.A. Souza, S.A. Pianaro, C.A. Paskocimas, E. Longo, J. A. Varela, Structural characterization of phase transition of Al2O3 nanopowders obtained by polymeric precursor method, Mater. Chem. Phys. 103 (2-3) (2007) 394–399.
[23] M. Mehra, M. Mukhopadhyay, R. Christian, N. Mistry, Synthesis and characterization of MgO nanocrystals using strong and weak bases, Powder Technol. 226 (2012) 213–221.
[24] K.R. Nemade, S.A. Waghuley, Synthesis of MgO Nanoparticles by Solvent Mixed Spray Pyrolysis Technique for Optical Investigation, Int. J. Metals 2014 (2014) 1–4.
[25] X. Wang, L. Song, H. Yang, W. Xing, H. Lu, Y. Hu, Cobalt oxide/graphene composite for highly efficient CO oxidation and its application in reducing the fire hazards of aliphatic polyesters, J. Mater. Chem. 22 (2012) 3426–3431.
[26] M.Z. Iqbal, G. Hussain, S. Siddique, M.W. Iqbal, Interlayer-reliant magnetotransport in graphene spin valve, J. Magnet. Magn. Mater. 441 (2017) 38–42.
[27] B. Dlubak, M.-B. Martin, R.S. Weatherup, H. Yang, C. Deranlot, R. Blume, R. Schlogl, A. Fert, A. Anane, S. Hofmann, P. Seneor, J. Robertson, Graphene-passivated nickel as an oxidation resistant electrode for spintronics, ACS Nano 6 (12) (2012) 10930–10934.
[28] P. Laczkowski, L. Vila, V.D. Nguyen, A. Marty, J.P. Attane, H. Jaffres, J.M. George, A. Fert, Enhancement of the spin signal in permalloy/gold multiterminal nanodevices by lateral confinement, Phys. Rev. B 85 (2012), 220404.
[29] T.A. Peterson, S.J. Patel, C.C. Geppert, K.D. Christie, A. Rath, Spin injection and detection up to room temperature in Heusler alloy/n-GaAs spin valves, Phys. Rev. B 94 (2016), 235309.
[30] M. Johnson, R.H. Silsbee, Coupling of electronic charge and spin at a ferromagnetic-paramagnetic metal interface, Phys. Rev. B 37 (10) (1988) 5312–5325.

3 Investigation of optical properties of sodium superoxide loaded polyaniline in uv and visible region

Songklanakarin J. Sci. Technol.
44 (6), 1467-1472, Nov. – Dec. 2022

http://www.sjst.psu.ac.th

Original Article

Investigation of optical properties of sodium superoxide loaded polyaniline in uv and visible region

Rajesh Barde[1*], Kailash Nemade[2], and Sandeep Waghuley[3]

[1] *Department of Physics, Government Vidarbha Institute of Science and Humanities, Amravati, 444604 India*

[2] *Department of Physics, Indira Mahavidyalaya, Kalamb, India*

[3] *Department of Physics, Sant Gadge Baba Amravati University, Amravati 444602, India*

Received: 5 November 2021; Revised: 19 January 2022; Accepted: 30 October 2022

Abstract

The PANi/NaO_2 composites were prepared using an ex-situ technique in 5–20 wt.% range. The NaO_2 was prepared in a single step by heating sodium nitrate in oxygen rich environment. Ultraviolet-visible spectroscopy was employed to extract optical parameters like direct band gap, refractive index, complex dielectric constant and optical conductivity. The refractive index increased with NaO_2 content for 5 and 10 wt. %, and then decreased possibly due to non-bridging oxygen (NBO) atoms. The composite with 10 wt. % NaO_2 showed the largest refractive index. On increasing the concentration of NaO_2, the band gap decreased from 2.538 to 2.307 eV and became narrower. Beyond 225 nm wavelength the extinction coefficient increased linearly, indicating that light trapping was proportional to wavelength. Both parts of the dielectrics follow the same pattern and the real dielectric constant is higher than the imaginary dielectric constant. The optical conductivity increased with hυ due to a change in density of localized states in the band gap, and also possibly due to the electrons excited by photon energy.

Keywords: chemical synthesis, sodium superoxide, optical conductivity, direct band gap, dielectric constant

1. Introduction

Conducting polymers are pursued with a view to applications. With long-conjugated structures, these polymers have exclusive properties such as flexibility, thermal and electrical stability, ease of synthesis, and durability (Cabuka & Gunduz, 2017). With the help of a series of simple anionic or cationic species, the conductivity of such polymers is approached through chemical oxidation or reduction reactions (Chen, 2003). The conducting polymers behave like semiconductors with small charge carrier mobility, and their conductivity approaches the range of metals on doping with suitable dopants (Khairy, & Gouda, 2015). The transport, optical and mechanical properties of these polymers can changed with the addition of dopant agents (Vadukumpully, Paul, Mahanta, & Valiyaveettil, 2011). The most common conducting polymer is polyaniline (PANi) because it is environmentally stable, easy to synthesize, has variable conductivity, and remarkable chemical, electrical and optical properties (Mini, Archana, Raghu, Sharanappa, & Devendrappa, 2016). It has industrial applications in electrochromic devices, sensors, conductive paints, drug delivery, rechargeable battery electrolytes, and solar cells (Stenicka *et al*., 2008; Yılmaz, Akgoz, Cabuk, & Karagac., 2011). The PANi can be synthesized from acidic aqueous solutions chemically or electrochemically. The chemical method is useful for large scale production of PANi, as it is very affordable. Oxidative polymerization is widely used for the preparation of PANi with an oxidant like ammonium persulfate ($(NH_4)_2S_2O_8$) (Mathew, Yang, & Mattes, 2002).

Nowadays, sodium-ion batteries appear to be most promising for electrical energy storage, to address the energy crisis and the pollution from fossil fuels (Li *et al.*, 2019; Xu,

*Corresponding author
Email address: rajeshbarde1976@gmail.com

Hui, Dinh, Hui, & Wang, 2019). The NaO_2 battery that takes advantage of superoxide chemistry differentiates itself from current energy-storage techniques (Ren, & Wu, 2013). Sodium superoxide has more feasible cell chemistry than lithium oxide, due to the discharge products (Hartmann *et al.*, 2013). The preparation of stable superoxide is a complicated task for researchers. Nemade *et al.* reported a novel synthesis approach for stable NaO_2. The nanoparticles of NaO_2 are synthesized by spray pyrolysis while maintaining high-density oxygen environment, so that a higher purity of the superoxide phase is achieved. These batteries can be cycled forming sodium superoxide as the lone discharge product with improved cycle life (He *et al.*, 2016). Peled *et al.* reported that on using sodium as the anode and oxygen as the cathode, these batteries ran several cycles at the temperature of 105°C (Peled, Golodnitsky, Mazor, Goor, & Avshalomov, 2011). The 0.2 V charge polarization of sodium superoxide battery makes it a potential competitor to lithium-oxygen batteries. These results show the formation of NaO_2 crystals in a one-electron allocation step as a solid discharge. This suggests replacing lithium-ions by sodium in batteries, with an unexpected outcome of metal-air batteries (Hartmann *et al.*, 2013). These batteries have garnered lots of attention because they exhibit the highest theoretical energy density and also offer the benefits of using abundant rare earth elements and potential cost efficiency (Park *et al.*, 2018).

In this study, we plan to examine the optical properties of NaO_2 doped polyaniline in UV and visible regions at room temperature. Several parameters like band gap, refractive index, complex dielectric constant, and optical conductivity were investigated.

2. Materials and Methods

2.1 Materials

AR grade chemicals (99% purity, SD Fine) were used to prepare PANi/NaO_2 Composites. Sodium nitrate was used for the synthesis of sodium superoxide (NaO_2). For the synthesis of polyaniline (PANi) aniline monomer and ammonium persulfate was used. As such synthesized PANi was washed with hydrochloric acid. Doubled distilled (De-ionized) water was used in all experiments.

2.2 Methods

2.2.1 Synthesis of PANi

By using oxidative polymerization, PANi was chemically synthesized at room temperature. Ammonium persulfate ($(NH_4)_2S_2O_8$) (45.34 gm) was dissolved in doubly distilled water (100 ml) and mixed with magnetic stirring for 90 min. Again, with constant stirring for 90 min, aniline monomer (18 ml, for better yield) was added drop by drop from a burette, in an ammonium persulfate solution. The resultant product appears greenish black and was kept for 12 h at room temperature. To wash the product, 1M hydrochloric acid solution was used. The product was filtered and washed until the filtrate become colorless, and then dried at 45 °C overnight (Ibrahim, 2017).

2.2.2 Synthesis of NaO_2

The sodium superoxide (NaO_2) was prepared using spray pyrolysis in an oxygen rich environment at a temperature of 673 K. Sodium nitrate and hydrogen peroxide were used as precursors in the preparation of NaO_2. The suspension for spray pyrolysis was prepared by adding 1 M sodium nitrate in 20 ml H_2O_2 under strong magnetic stirring. Subsequently, this suspension was employed for spraying under constant oxygen flow on SiO_2 heating substrate. The structure and phase purity of NaO_2 were confirmed through XRD analysis that was published in our previous work (Barde, 2016).

2.2.3 Preparation of PANi/NaO_2 composites

The PANi/NaO_2 composites were synthesized in organic medium for good dispersion of NaO_2 in the polymeric matrix, using an ex-situ technique with the quantity of NaO_2 varied in 5 wt.% steps in the range from 5 to 20 wt.%. The composites were labeled for pure PANi as (P_0), 5 wt.% NaO_2 as (P_1), 10 wt.% NaO_2 as (P_2), 15 wt.% NaO_2 as (P_3) and 20 wt.% NaO_2 as (P_4). The samples were subjected to an optical study using ultraviolet–visible spectro-photometer on samples of equal thickness (2 ± 0.1 mm) to record the optical properties of all prepared composites. The samples were also tested by XRD, SEM and FTIR as published in our previous work (Barde, 2016).

3. Results and Discussion

The optical absorption spectrum allows estimating the optical energy band gap of crystalline and amorphous materials. The absorption corresponds to electron excitation from the valance band to the conduction band, and is used to verify the character and value of the optical band gap (Cabuk, & Gunduz, 2017). The absorption spectra of PANi/NaO_2 composites were obtained over the range 200-700 nm. The absorption coefficient (α) was calculated using (Fox, 2001):

$$\alpha(\vartheta) = \frac{2.303\,A}{l}$$

where l is the sample thickness in cm and A is defined by A = log (Io/I) where Io is the intensity of the incident beam and I is the intensity of transmitted beam.

Figure 1 shows a penetrating absorption dip in the region from 210 to 220 nm and a broad hump in the region 300–600 nm. The absorption bands in the regions 200- 400 nm and 400–600 nm are attributed to the ligand-to-metal charge transfer (Lian *et al.*, 2009; Li *et al.*, 2008) and to the pair excitation processes (Wang *et al.*, 2014) respectively. The wide absorption band in 250-600 nm may be a charge transfer transition from O_2^- to Na^+ in NaO_2.

The refractive index (n) is another significant parameter in opto-electronic parameters. Refractive index (n) and extinction coefficient (k) are the real and imaginary components of the complex refractive index $N=n-ik$. These components represent the optical properties of the prepared composites. The refractive index has a substantial role in optical communication as well in designing antireflection coatings (Chopra, & Kaur, 1969). The refractive index is calculated by using the relation:

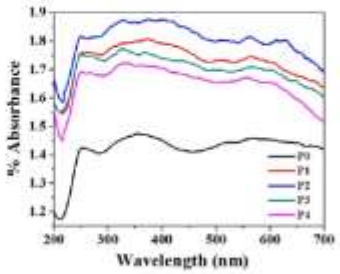

Figure 1. Absorption spectra of pure PANi and PANi/ NaO_2 composites

$$n = \frac{1}{\%T} + \sqrt{\frac{1}{\%T} - 1}$$

where % T is transmission through the sample.

Figure 2 shows the plot of refractive index vs wavelength. Due to the intense absorption by composites in the ultraviolet region, there is a sharp decrease in refractive index around 215 nm. Also, on the lower wavelength side the PANi/ NaO_2 composites have a low refractive index, whereas its value increases up to 370 nm, and beyond this decreases gradually. Initially, the refractive index also increases for 5 and 10 wt. % NaO_2, and then decreases possibly due to non-bridging oxygen (NBO) atoms. The composites with 10 wt. % NaO_2 show the largest refractive index.

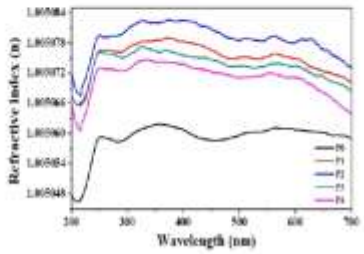

Figure 2. Variation of the refractive index as a function of wavelength

Extinction coefficient can be estimated by (Gedia *et al.*, 2015)

$$k = \frac{\alpha\lambda}{4\pi}$$

where α is % absorption and λ is the wavelength.

Figure 3 shows that beyond the wavelength 225 nm, the extinction coefficient of undoped PANi and all PANi/ NaO_2 composites increases linearly, indicating light trapping. From this, we conclude that light trapping is proportional to wavelength (Barde, 2016; Barde, Nemade, & Waghuley, 2015). On other hand, the wavelengths between 200 and 225 nm are not trapped by the samples as the extinction coefficient is nearly constant between 200 and 225 nm. The largest extinction coefficient was found for the 10 wt. % case of PANi/NaO_2 composite.

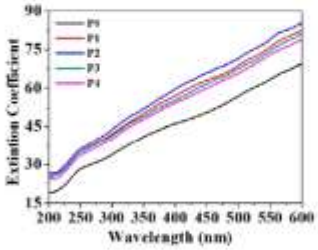

Figure 3. Variation of extinction coefficient as a function of wavelength

Analysis of absorption spectra is the most valuable means for explaining the optical transition and electronic band structure of materials. The band gap is also a very important property for photovoltaic device applications. The basic principle is that an electromagnetic wave interacts with the electron in the valance band and a photon having higher energy than the band gap will be absorbed as the electron is transferred across the fundamental gap to the conduction band. The expression of the absorption coefficient, (α), to determine direct band gap (Eg) was given by (Song, Wang, Yuan, Yao, & Jing, 2015):

$$\alpha h\vartheta = A\left(h\vartheta - E_g\right)^m$$

where A is an energy dependent constant, Eg is the band gap of the material, and the index m is a constant with discrete values 1/2, 3/2, 2 or more, depending on whether the transition is direct or indirect and allowed or forbidden, respectively (Shaimaila *et al.*, (2011)).

Figure 4 shows the Tauc plots between $(\alpha h\vartheta)^2$ and $h\vartheta$ for all compositions of PANi/NaO_2 composites. By extrapolation of the linear part of the plot, the band gap energy was estimated. It was found that on increasing NaO_2, Eg decreased from 2.538 to 2.307 eV and became narrower. The doping of NaO_2 may increase localized electrons due to an increase of the donor centers, which decreases the band gap, and this is responsible for the red shift of the absorption edge (Shailajha, Geetha, Vasantharani, & Sheik Abdul Kadhar, 2015). This band gap narrowing is predictable and important to applications in photocatalysis.

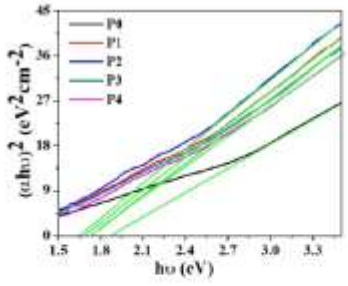

Figure 4. Tauc plot of $(\alpha h\upsilon)^2$ versus photon energy

The dielectric function comprises (i) its real part (ε_r), which signifies the capability of materials to decrease the speed of light; and (ii) its imaginary part (ε_i), which represents absorption of energy from an electric field due to dipole motion. Both these parts have direct relations with refractive index and extinction coefficient (Equations (3) and (4)) (Abdullah, 2013; Barde, Nemade, & Waghuley, 2015).

$$\varepsilon_r = n^2 - k^2$$

$$\varepsilon_i = 2nk$$

where k is the extinction coefficient and n the refractive index.

It was found that the real dielectric constant (ε_r) mostly depended on refractive index (n^2) because of low values of extinction coefficient (k), while the imaginary dielectric constant (ε_i) mostly depended on extinction coefficient (k) which is related to the variation of absorption coefficient. Figure 5 shows the variation of the real dielectric constant with wavelength. The real dielectric constant increased linearly with wavelength. The 10 wt. % of NaO_2 sample shows the largest real dielectric constant, hence this sample exhibits the highest ability to slow down light (Sharma, & Katyal, 2007).

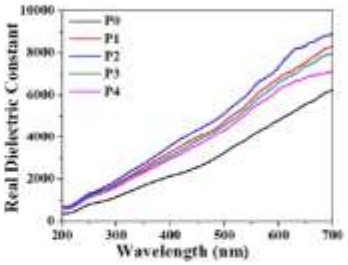

Figure 5. Variation of real dielectric constant

The plots of the imaginary dielectric constant against wavelength are shown in Figure 6. The imaginary dielectric constant increased linearly with wavelength, and the 10 wt. % case of NaO_2 in sample had the largest energy absorption from an electric field due to dipole motion (Bakr *et al.*, 2011). Both the real and imaginary parts show the same pattern and the real dielectric constant was larger than the imaginary dielectric constant.

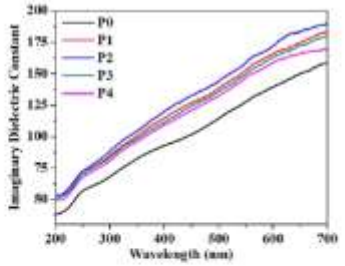

Figure 6. Variation of imaginary dielectric constant.

Optical response is explained by optical conductivity (σ_{opt}) and its dimension is similar to frequency, which is valid only in a Gaussian system of units. It is calculated by using following relation (Barde, Nemade, & Waghuley, 2015).

$$\sigma_{opt} = \frac{\alpha c n}{4\pi}$$

where c is velocity of light, α is absorption coefficient, and n the refractive index.

The plot of σ_{opt} verses $h\upsilon$ is shown in Figure 7. In it σ_{opt} increased with photon energy. Initially as NaO_2 content increases, the optical conductivity first increases and then decreases. The increase in optical conductivity is due to increases in both absorption coefficient and refractive index with NaO_2, and may be due to the change in density of localized states in the band gap (Yakuphanoglu, Cukurovali, & Yilmaz, 2005) and also may be due to the electron excitation by photon energy.

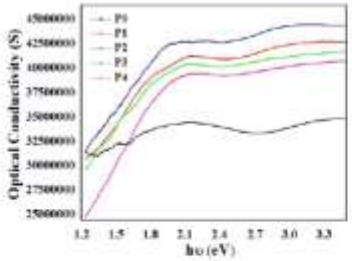

Figure 7. Variation of optical conductivity as a function of photon energy

The optical study of Sodium Superoxide Loaded Polyaniline composites indicates that this material system potentially has applications in terahertz devices, flexible and thin screens, electromagnetic shielding, and electronic components. The characteristics, such as being lightweight, resistant, and stable, enable these composites to be used in electromagnetic shielding applications. Easy control of the electrical conductivity of these composites makes them an important research domain for reliable industrial development.

In the context of environmental impact, polyaniline-based composites exhibit high water dispersibility. In addition to this, polyaniline is considered most promising due to its easy synthesis, environmental stability, low toxicity, and thermal and radiation stability.

4. Conclusions

This work successfully demonstrated PANi/NaO_2 composites prepared by using an ex-situ technique. The NaO_2 was prepared in a single step by heating sodium nitrate in an oxygen rich environment. The optical absorption spectra of PANi/NaO_2 composites show an intense absorption dip in the region from 210 to 220 nm and a broad hump in the region 300–700 nm. The prepared composites show trapping of light with extinction coefficient proportional to wavelength. These composites have a low refractive index on the shorter

wavelength side, whereas on the longer wavelength side it increases up to 360 nm; and beyond this the refractive index decreases gradually. The direct band gap was estimated for sodium superoxide loaded polyaniline composites. The dielectric constant measurements show linear behavior as a function of wavelength. Optical conductivity increases with an increase of photon energy due to the change in density of localized states in the band gap.

Acknowledgements

The author acknowledges Director, Govt. Vidarbha Institute of Science and Humanities, Amravati, Head, Department of Physics, Govt. Vidarbha Institute of Science and Humanities, Amravati, and Head, Department of Physics, Sant Gadge Baba Amravati University, Amravati for providing necessary facilities for the work.

References

Abdullah, A. Q. (2013). Surface and volume energy loss, optical conductivity of rhodamine 6G dye (R6G). *Chemistry and Materials Research, 3*(10), 56-63.

Bakr, N. A., Funde, A. M., Waman, V. S., Kamble, M. M., Hawaldar, R. R., Amalnerkar, D. P., & Jadkar, S. R. (2011). Determination of the optical parameters of a-Si: H thin films deposited by hot wire–chemical vapour deposition technique using transmission spectrum only. *Pramana Journal of Physics, 76*, 519–531.

Barde, R. V. (2016). Influence of CeO_2 content on complex optical parameters of phosphovanadate glass system. *Spectrochimica Acta, part A: Molecular and Biomolecular Spectroscopy, 153*, 160 –164.

Barde, R. V. (2016). Preparation, characterization and CO_2 gas sensitivity of polyaniline doped with sodium superoxide (NaO_2). *Material Research Bulletin, 73*, 70–76.

Barde, R. V., Nemade, K. R., & Waghuley, S. A. (2015). Complex optical study of V_2O_5–P_2O_5–B_2O_3–Dy_2O_3 glass systems. *Journal of Taibah University for Science's, 10*(3), 340-344.

Barde, R. V., Nemade, K. R., & Waghuley, S. A. (2015). Complex optical study of V_2O_5-P_2O_5–B_2O_3–GO glass systems by ultraviolet–visible spectroscopy. *Optical Materials, 40*, 118–121.

Cabuka, M., & Gunduz B. (2017). Controlling the optical properties of polyaniline doped by boric acid particles by changing their doping agent and initiator concentration. *Applied Surface Science, 424*(3), 345-351

Chen, C. H. (2003). Thermal and morphological studies of chemically prepared emeraldine-base-form polyaniline powder. *Journal of Applied Polymer Science, 89*, 2142–2148.

Chopra, K. L., & Kaur, I. (1969). Thin film phenomena. New York, NY: McGraw-Hill.

Fox, M. (2001). Optical properties of solids. New York, NY: Oxford University Press.

Gedia, S., Reddy, V., Reddya, M., Parkb, C., Wookb, J. C., & Reddy, K. T. R. (2015). Comprehensive optical studies on SnS layers synthesized by chemical bath deposition. *Optical Materials, 42*, 468-475.

Hartmann, P., Bender, C. L., Vracar, M., Garsuch, A., Durr, A. K., Janek, J., & Adelhelm, P. (2013). Rechargeable room-temperature sodium superoxide (NaO_2) battery. *Nature Materials, 12*, 228-232.

He, M., Lau, K. C., Ren, X., Xiao, N., McCulloch, W. D., Curtiss, L. A., & Wu, Y. (2016). Concentrated electrolyte for the sodium–oxygen battery: Solvation structure and improved cycle life. *Angewandte Chemie International Edition, 55*, 1–6.

Ibrahim K. A. (2017). Synthesis and characterization of polyaniline and poly (aniline-co-o-nitroaniline) using vibrational spectroscopy. *Arabian Journal of Chemistry, 10*, S2668–S2674

Khairy, M., & Gouda, M. E. (2015). Electrical and optical properties of nickel ferrite/polyaniline nano composite. *Journal of Advanced Research, 6*, 555-562.

Li, F., Wei, Z., Manthiram, A., Feng, Y., Mao, J., & Maid, L. (2019). Sodium-based batteries: From critical materials to battery systems. *Journal of Materials Chemistry A, 7*, 9406-9431.

Li, X. G., Li, A., & Huang, M. R. (2008). Facile high-yield synthesis of polyaniline nanosticks with intrinsic stability and electrical conductivity. *Chemistry - A European Journal, 14*(33), 10309-10317.

Lian, J. B., Duan, X. C., Ma, J. M., Peng, P., Kim, T., & Zheng, W. J. (2009), Hematite (alpha-Fe2O3) with various morphologies: ionic liquid-assisted synthesis, formation mechanism, and properties. *ACS Nano, 3*(11), 3749–3761.

Mathew, R. J., Yang, D. L., & Mattes, B. R. (2002). Effect of elevated temperature on the reactivity and structure of polyaniline. *Macromolecules, 35*, 7575–81.

Mini, V., Archana, K., Raghu, S., Sharanappa, C., & Devendrappa, H. (2016). Nanostructured multifunctional core/shell ternary composite of polyaniline-chitosan-cobalt oxide: preparation, electrical and optical properties. *Materials Chemistry and Physics, 170*, 90–98.

Park, H., Kim, J., Lee, M. H., Park, S. K., Do-Hoon Kim, Bae, Y., . . . Kang, K. (2018). Highly durable and stable sodium superoxide in concentrated electrolytes for sodium–oxygen batteries. *Advanced Energy Materials, 8*(34), 1801760.

Peled, E., Golodnitsky, D., Mazor, H., Goor, M., & Avshalomov, S. (2011). Parameter analysis of a practical lithium- and sodium-air electric vehicle battery. *Journal of Power Sources, 196*(16), 6835-6840.

Ren, X., & Wu, Y. (2013). A low-overpotential potassium–oxygen battery based on potassium superoxide. *Journal of the American Chemical Society, 135*(8), 2923–2926.

Shailajha, S., Geetha, K., Vasantharani, P., & Sheik Abdul Kadhar, S. P. (2015). Effects of copper on the preparation and characterization of Na–Ca–P borate glasses. *Spectrochimica Acta Part A: Molecular and Biomolecular Spectroscopy, 138*, 846–856.

Sharma, P., & Katyal, S. C. (2007). Determination of optical parameters of a-(As2Se3)90Ge10 thin film. *Journal of Physics D: Applied Physics, 40*, 2115–2120.

Shumaila, Lakshmi, G. B. V. S., Alam, M., Siddiqui, A. M., Zulfequar, M., & Husain, M. (2011). Synthesis and characterization of Se doped polyaniline. *Current Applied Physics, 11*, 217-222.

Song, S., Wang, Y., Yuan, X., Yao, W., & Jing, W. (2015). Characterization and preparation of Sn-doped CuGaS2 thin films by paste coating. *Materials Letters, 148*, 41–44.

Stenicka, M., Pavlinek, V., Saha, P., Blinova, N. V., Stejskal, J., & Quadrat, O. (2008). Conductivity of flowing polyaniline suspensions in electric field. *Colloid and Polymer Science, 286*, 1403–1409.

Vadukumpully, S., Paul, J., Mahanta, N., & Valiyaveettil, S. (2011). Flexible conductive graphene/polyvinyl chloride) composite thin films with high mechanical strength and thermal stability. *Carbon, 49*, 198–205.

Wang, T., Zhou, S., Zhang, C., Lian, J., Liang Y., & Yuan, W. (2014). Facile synthesis of hematite nanoparticles and nanocubes and their shape-dependent optical properties. *Journal of Chemistry, 38*, 46-49.

Xu, X., Hui, K. S., Dinh, D. A., Hui, K.N., & Wang, H. (2019). Recent advances in hybrid sodium-air batteries. *Materials Horizons, 6*, 1306-1335.

Yakuphanoglu, F., Cukurovali, A., & Yilmaz, I. (2005). Refractive index and optical absorption properties of the complexes of a cyclobutane containing thiazolylhydrazone ligand. *Optical Materials, 27*, 1363–1368.

Yılmaz, K., Akgoz, A., Cabuk, M., & Karaagac, H. (2011). Electrical transport, optical and thermal properties of polyaniline-pumice composites. *Materials Chemistry and Physics, 130*, 956–961.

4 Complex Optical Investigation of Sodium Superoxide Loaded Phosphovanadate Glass System in Ultra-Violet and Visible Region

TRENDS IN SCIENCES 2022; 19(23): 2077 RESEARCH ARTICLE
https://doi.org/10.48048/tis.2022.2077

Complex Optical Investigation of Sodium Superoxide Loaded Phosphovanadate Glass System in Ultra-Violet and Visible Region

Rajesh Barde[1,*], Kailash Nemade[2] and Sandeep Waghuley[3]

[1]*Department of Physics, Government Vidarbha Institute of Science and Humanities, Amravati 444604, India*
[2]*Department of Physics, Indira Mahavidyalaya, Kalamb, India*
[3]*Department of Physics, Sant Gadge Baba Amravati University, Amravati 444602, India*

(*Corresponding author's e-mail: rajeshbarde1976@gmail.com)

Received: 18 January 2022, Revised: 2 March 2022, Accepted: 18 March 2022, Published: 10 November 2022

Abstract

Sodium superoxide loaded phosphovanadate based glass systems were prepared from a mixture of vanadium pentoxide (V_2O_5), phosphorus pentoxide (P_2O_5) boric acid (H_3BO_3) and sodium superoxide (NaO_2) using a melt-quenching method. Amorphous phase of as-prepared glass system confirmed using XRD technique. Surface morphology of glass system studied using scanning electron microscope. Ultraviolet-visible spectroscopy was employed to extract complex optical parameters like direct and indirect optical band gap, Urbach energy, refractive index, complex dielectric constant and optical conductivity. The absorption bands in the region 200 - 400 nm are recognized to the ligand-to-metal charge transfer. The region of 400 - 600 nm is ascribed to the pair excitation processes. The refractive index increases initially and then decreases for 15 and 20 mol % of NaO_2 due non bridging oxygen (NBO) atoms. The 25 mol % of NaO_2 sample shows maximum value of extinction coefficient and refractive index. The direct and indirect band gap energies vary in between 2.067 to 1.824 eV and 1.869 to 1.495 eV, respectively. With increase in concentration of NaO_2, the effective band gap of NaO_2 decreases because band edge shifted into forbidden gap due to increase in defect levels below the conduction. This primary report on sodium superoxide loaded phosphovanadate based glass systems opens wide avenue for battery and supercapacitor applications. Tailing in the bandgap was observed and found to obey Urbach rule.

Keywords: Optical properties, Sodium superoxide, Phosphovanadate glass, Optical conductivity, Urbach energy, Direct band gap, Dielectric constant

Introduction

Conducting glasses are potential candidate for solid state batteries due their admirable conductivity and chemical stability against atmospheric changes. In this category, V_2O_5 glasses has a great potential due to its advantages like generating various structural groups [1,2], showing electrical and optical properties and mostly its competence as a host for different metallic ions [3]. These properties usually used in fabrication of electrochemical batteries [4], memory switching devices [5] and supercapacitor [6]. The electrical properties of vanadate glasses are determined by the transition metal ions which existing in V^{4+} and V^{5+} states and the conduction mechanism is conquered by small polaron hopping between them [7,8]. One of the greatest imperative glass forms is Borate glass as it is often appropriate, optical and dielectric, it also insulates materials that are extremely transparent, have a low melting point and have a high thermal stability. It can also be utilized in many applications [9,10]. The B_2O_3-P_2O_5 glasses are more popular for their low refractive index and extraordinary optical properties [11]. These glasses exhibit excellent chemical durability when doped with transition metals due to formation of BO_4 tetrahedral, which transforms metaphosphate chain into 3-dimensional network [12]. Hence, they are useful as tune able solid-state lasers [13], optical materials [14], memories [15], luminescence materials [16], converters for solar energy [17] and fiber optic communication devices [18].

Now a days, sodium-ion batteries have been explored as the most promising power sources for electrical energy storage due to energy crisis and pollution from fossil fuels. [19,20]. The NaO_2 battery that takes advantage of the superoxide chemistry differentiates itself among current energy-storage techniques [21]. The sodium superoxide is feasible to the cell chemistry than lithium oxide cells, due to easily noticeable discharge products [22]. The preparation of stable superoxide is a complicated task for the researchers. Nemade *et al.* reported the novel synthesis approach for stable NaO_2. The spray pyrolysis technique is employed for preparation of NaO_2 nanoparticles in which high density oxygen environment is

maintain to achieve higher degree of purity in superoxide phase [23]. These batteries can be cycled forming sodium superoxide as the lone discharge product with improved cycle life [24]. Peled *et al.* reported that using sodium as the anode and oxygen as the cathode, these batteries ran several cycles at the temperature of 105 °C [25]. Hartmann *et al.* reported that a sodium superoxide battery with 0.2 V voltage polarizations upon charge, which makes this technology as optimistic competitor to lithium oxygen batteries. The results of the study show that sodium superoxide crystals forms in a one-electron allocation step as a solid discharge. This work opens the way for the replacement of lithium-ion by sodium for batteries, which offer an unpredicted outcome as metal-air batteries [22]. These batteries have engrossed great attention because they exhibit the highest theoretical energy density while also offering the advantages of elemental earth abundance and potential cost efficiency [26]. The photochromic effect enticed many researchers. The main defect found in the glasses arenNegative electron-centers (EC) and positive hole. This defect was investigated by optical spectroscopy to inspect their electronic transitions that cause high absorbance in the UV-VIS region [27]. Thakur *et al.* studied the optical, structural, and dielectric spectroscopic properties of B2O3-Bi2O3 glasses glasses doped with ZrO2, and SeO2 which confirms the ionic character of the studied glass samples [28].

In this we plan to investigate the complex optical properties of sodium superoxide doped vanadate glass system in UV and visible region. Several parameters like as optical band gap, Urbach energy, refractive index, complex dielectric constant and optical conductivity were investigated at room temperature.

Materials and methods

NaO_2 was synthesis from AR grade, SD fine sodium nitrate ($NaNO_3$) by heating in oxygen rich surrounding [29]. For the preparation of glasses 99 % Purity, SD fine vanadium pentoxide (V_2O_5), phosphorus pentoxide (P_2O_5) and boric acid (H_3BO_3) along with a prepared NaO_2 was used. The samples of compositions $60V_2O_5$–$5P_2O_5$–(35-x) B_2O_3–xNaO_2, x = 5, 10, 15, 20 and 25 mol % were prepared by usual melt-quenching method as described in our previous work [30]. By using Bruker D8 advance with Cu Kα radiation the phase purity and structure of as prepared NaO_2 and glasses were confirmed with scan rate 6.00 in the range 20° - 80°. Morphologies of all prepared samples were studied by using JEOL-6390LV SEM. Ultraviolet-visible spectro-photometer was used to record the optical properties of all prepared glasses, from which the optical band gap, Urbach energy, refractive index, Complex dielectric constant and optical conductivity were calculated.

Results and discussion

XRD pattern of NaO_2 is shown in **Figure 1**. The peaks (200), (220), (311) and (222) appear in XRD accurately index to NaO_2 according to JCPDS reference card No. 01-077-0207, which confirms the formation of NaO_2 [22, 29]. In XRD pattern of prepared glass samples depicts in **Figure 2**, there was no characteristic peak which corresponds to any crystalline phase pointed out the formation of glasses.

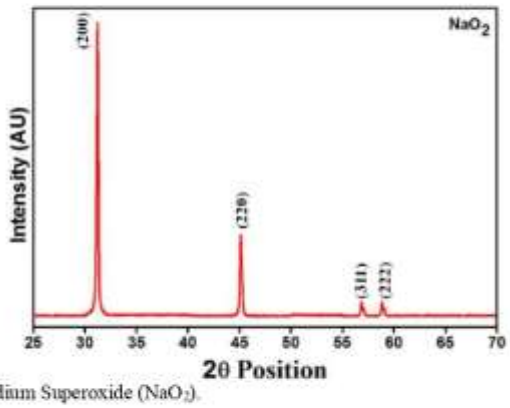

Figure 1 XRD of Sodium Superoxide (NaO_2).

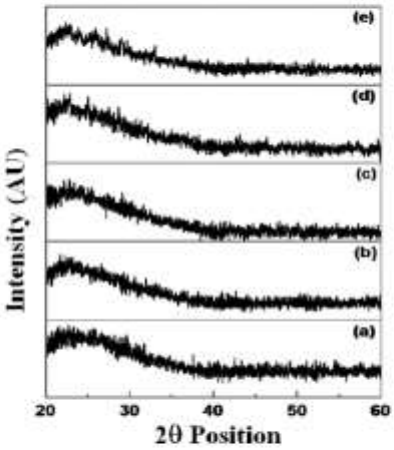

Figure 2 XRD of $60V_2O_5$–$5P_2O_5$–$(35\text{-}x)B_2O_3$–$xNaO_2$ for (a) 5 mol %, (b) 10 mol %, (c) 15 mol %, (d) 20 mol % and (e) 25 mol % of NaO_2.

From **Figure 3** it is shows that, the grains are high agglomerated having good interconnectivity between the particles, which helps the transportation of charge particles [31]. From the image it is clear that sample exhibit an irregular granular morphology.

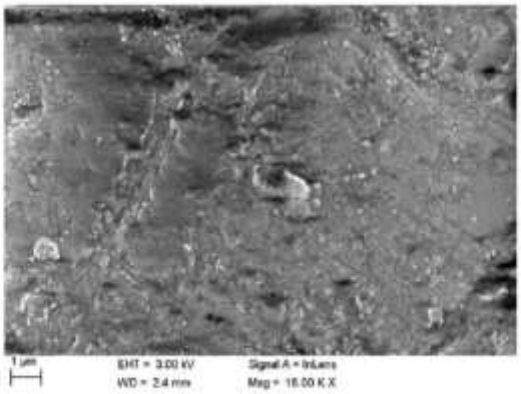

Figure 3 SEM image of 20 mol % of NaO_2 doped glass sample.

The absorption spectra were recorded at room temperature by using UV-Visible spectrophotometer in range of 200 - 600 nm. From the absorbance, the optical absorption coefficient (α) was calculated. After correction for reflection losses, α may be find out by using the relation [32]:

$$\alpha(\theta) = \frac{2.303\,A}{l} \quad (1)$$

where l is the sample thickness in cm and A is defined by A = log (Io/I) where Io and I are the intensity of the incident and transmitted beams.

From these spectra, displayed in **Figure 4**, shows an intense absorption dip in the wavelength region 220 to 230 nm and a broad hump in the wavelength region of 300 - 450 nm. The absorption bands in the region 200 - 400 nm are recognized to the ligand-to-metal charge transfer [33]. The region of 400 - 600 nm is ascribed to the pair excitation processes [34]. The broad absorption band between 250 - 450 nm may be due to the charge transfer transition from O_2^- to Na^+ in NaO_2.

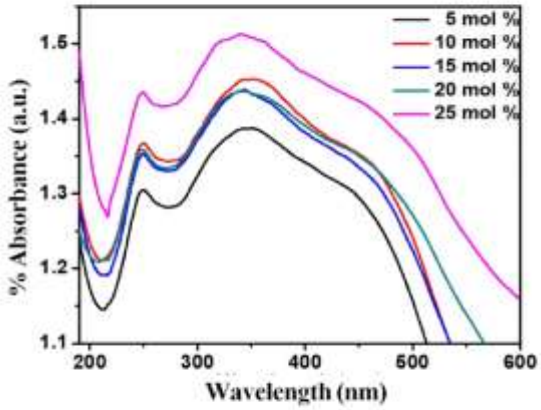

Figure 4 Absorption spectra of the glass systems.

The optical properties of as such prepared glass system may be represented by the refractive index (n) and extinction coefficient (k), which are the real and imaginary components of the complex refractive index $N = n - ik$, respectively. The extinction coefficient can be estimated by using the relation [35];

$$k = \frac{\alpha\lambda}{4\pi} \tag{2}$$

where, α is % absorption and λ is wavelength.

From **Figure 5(a)** shows that, in the region 225 - 500 nm, extinction coefficient of all glasses increases linearly and it is measure of capturing of light, which concluded that light trapping is proportional to wavelength. The extinction coefficient curve becomes almost linear beyond 525 nm. [36,37]. Which is favourable with absorption behavior of glass system. The 25 mol % of NaO_2 sample shows maximum value of extinction coefficient.

Refractive index has an important role in the search for optical materials, in optical communication and in designing antireflection coating [38]. The refractive index was estimated using the formula Eq. (3) [36];

$$n = \frac{1}{\%T} + \sqrt{\frac{1}{\%T} - 1} \tag{3}$$

where %T is transmission through sample.

Figure 5(b) shows the plot of refractive index with wavelength, which shows that samples have jagged reduction in refractive index around 225 nm due to strong absorption in UV region. Also, samples have small value of refractive index on shorter wavelength side, whereas on longer wavelength side its value increases up to 340 nm and beyond it, refractive index decreases gradually. With the concentration of NaO_2, refractive index also increases initially and then decreases for 15 and 20 mol % of NaO_2 due non bridging oxygen (NBO) atoms. The maximum value of refractive index is detected for 25 mol % of NaO_2.

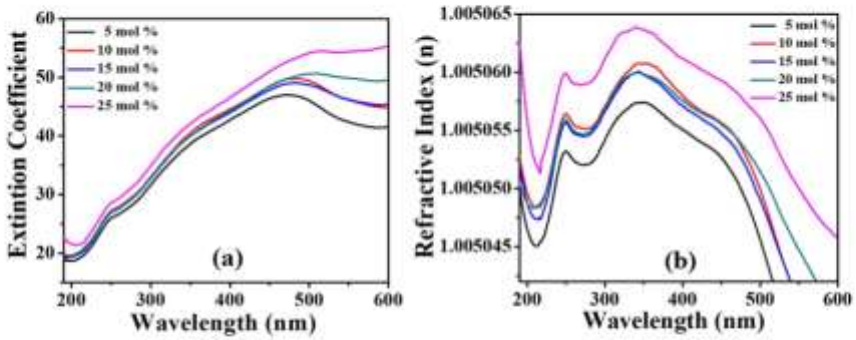

Figure 5 (a) Variation of extinction coefficient and (b) Variation of refractive index of the glass system as a function of wavelength.

Analysis of absorption spectra is one of the most valuable means for explaining the optical transition and electronic band structure materials. The band gap is also very important properties for photovoltaic device application. The basic principle is that, electromagnetic wave interacts with the electron in valance band and photon having higher energy than the band gap will be absorbed. There are 2 categories of optical transitions direct and indirect and in both cases, due to interaction of electromagnetic waves with electrons in the valence band, it raised across the fundamental gap and goes to the conduction band. The expression of the absorption co-efficient, (α) to determine direct and indirect band gap (Eg) was given by Davis and Mott [39]:

$$\alpha h\vartheta = A\left(h\vartheta - E_g\right)^m \quad (4)$$

where A is an energy dependent constant, Eg is the optical band gap of the material, m is a constant that depends on the semiconducting materials, which can be expected to have values of 1/2, 3/2, 2 and 3. The value of m depends on the type of the electronic transition responsible for absorption; 1/2 for allowed direct transitions, for direct forbidden transitions it is 3/2, for allowed indirect transitions it is 2 and for indirect forbidden transitions it is 3 [23]. For glassy materials indirect transitions (m = 2) are valid according to the Tauc's relations. The indirect optical energy band gaps (Eg') of samples can be found by plotting $(\alpha h\upsilon)^{1/n}$ verses $h\upsilon$ and extrapolating it to $(\alpha h\upsilon)^{1/n} = 0$.

Figures 6(a) and **6(b)** shows the Tauc plots for indirect and direct band gap energy of different composition of NaO_2 loaded glass system, respectively. The direct and indirect band gap energies vary in between 2.067 to 1.824 eV and 1.869 to 1.495 eV respectively. The band gap of the glasses became more and more narrower along with the concentration of NaO_2. Also, due to increase in NaO_2 in the glasses creates a large number of donor centers and growth of new polaronic can lead to a considerable reduction in the band gap which suggests the conversion of the bridging oxygen (BO) atoms in to non-bridging oxygen (NBO) in the glasses. The band gap of glasses are effectively impacts as NBOs have higher energies than the BOs. The addition of NaO_2 may increases localized electrons due to increase of donor center in the which decreases the band gap and it is accountable for the red shift of the absorption edge [40]. It indicated that NaO_2 doping successfully extended their solar response spectra.

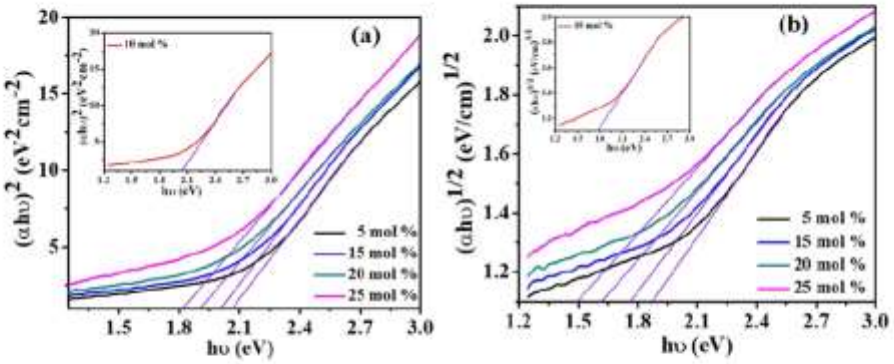

Figure 6 (a). Tauc plot of $(\alpha h\upsilon)^2$ versus photon energy and (b) Tauc plot of $(\alpha h\upsilon)^{1/2}$ versus photon energy of various glass samples.

The width of the defect bands formed in the band gap of NaO_2 as an intermediate state which create a band tail known as the Urbach tail on both sides of the top of the valence band and bottom of the conduction band and the energy associated with this tail is referred as Urbach energy explained by following equation:

$$\alpha(\theta) = \alpha_0 exp\left(\frac{h\theta}{E_U}\right) \quad (5)$$

where α_0 is a constant, hυ is the photon energy and E_U is the Urbach's energy [41,42].

The E_U is calculated from the plot of Ln α vs. hυ, i.e., from the slopes of the linear portion, below the band gap and the source of it is considered as thermal vibrations in the lattice. Urbach energy for each glass samples are as shown in **Figure 7** which varies in between 0.433 to 0.574 eV. The defect energy increases with decrease in band gap, which obviously supports the creation of sub-band states in between the valence and conduction bands consequence in the reduction of the band gap. With increase in concentration of NaO_2, the effective band gap of NaO_2 decreases because band edge shifted into forbidden gap due to increase in defect levels below the conduction [43, 44]. The relationship of the band gap with Urbach energy for different samples are shown in **Figure 8(a)**. The pictorial representation of formation of Urbach tail in NaO_2 doped V_2O_5–P_2O_5–B_2O_3 glass is shown in **Figure 8(b)**. **Table 1** displays the estimated values of direct, indirect band gap and Urbach energies for various NaO_2 contents.

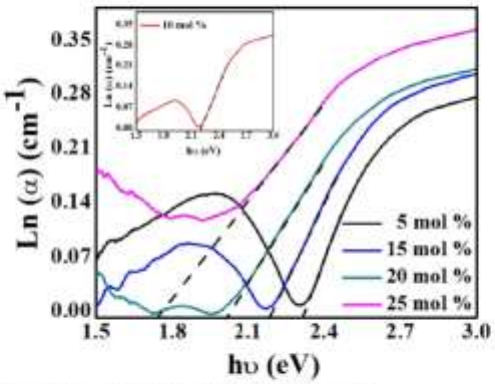

Figure 7 Plot of Ln(α) vs. hυ for the determination of Urbach energy.

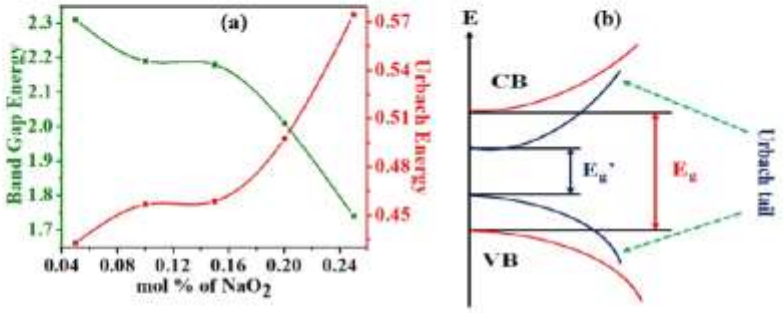

Figure 8 (a) Variation of band gap and Urbach energy for different mol % of NaO_2. and (b) Formation of Urbach tail for NaO_2 doped V_2O_5–P_2O_5–B_2O_3 glass.

Table 1 Direct, indirect band gap values and the Urbach energies for various NaO_2 contents.

Sample	Direct band gap Energy (E_g) (eV)	Indirect band gap Energy (E_g') (eV)	Urbach Energy (E_U) (eV)
5 mol %	2.067	1.869	0.433
10 mol %	2.407	1.771	0.456
15 mol %	2.008	1.762	0.459
20 mol %	1.912	1.618	0.497
25 mol %	1.824	1.495	0.575

The optical dielectric function is complex quantity which consists of real part (ε_r) which represents the ability of materials to reduce speed of light and imaginary part (ε_i) represents absorption of energy from an electric field respectively. Both part of dielectric constant shows direct relation with refractive index (n) and extinction coefficient (k) [45,46].

$$\varepsilon_r = n^2 - k^2 \quad (6)$$

$$\varepsilon_i = 2nk \quad (7)$$

It is found that ε_r mostly depended on n^2 because of insignificant values of k^2, while ε_i mostly depends on k values which are related to the change of absorption coefficients.

The plots of real and imaginary part of dielectric constant verses wavelength at room temperature are shown in **Figure 9(a)** and **9(b)**, respectively. The value of ε_r increases linearly with wavelength from 225 nm up to 490 nm. The 25 mol % of NaO_2 sample shows uppermost value of ε_r, hence it exhibits highest ability to slowdown light, as real dielectric constant is measure of slowdown of speed of light [47]. The curve of ε_i increases linearly from 225 nm upto 500 nm. In this, due to dipole motion, 25 mol % of NaO_2 sample have the highest strength to absorb energy from an electric field. [48]. In this both real and imaginary parts follow the same pattern and ε_r are higher than the ε_i.

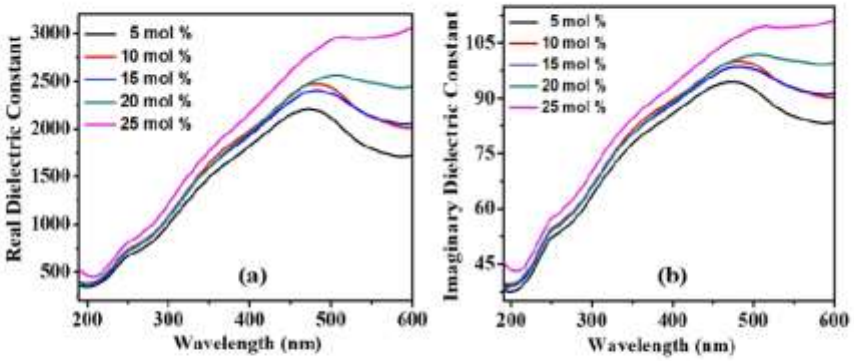

Figure 9 (a) Variation of real dielectric constant and (b) Variation of imaginary dielectric constant as a function of wavelength.

Optical conductivity denotes the optical response of a material and the dimension is same as that of frequency which is valid solitary in a Gaussian system. The optical conductivity (σ_{opt}) has been calculated by using the relation [37],

$$\sigma_{opt} = \frac{\alpha c n}{4\pi} \quad (8)$$

where c, α and n are speed of light, absorption coefficient and the refractive index respectively. The plot of σ_{opt} with photon energy is shown in **Figure 10**. It shows that σ_{opt} increases with photon energy as well as NaO_2, which may be due to the increase of both absorption coefficient and refractive index with NaO_2 also due to the change in density of localized states in band gap [49,50], and electron excited by photon energy.

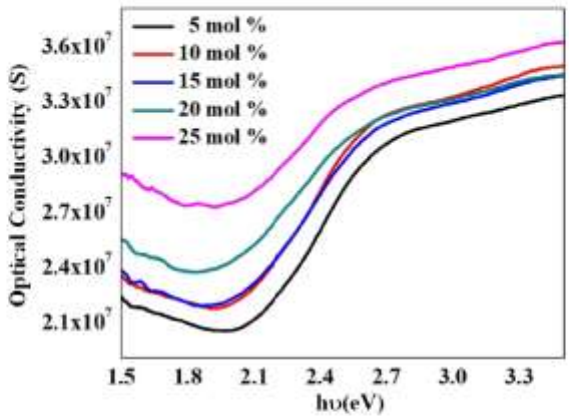

Figure 10 Variation of optical conductivity of glass samples as a function of photon energy.

Conclusions

The present work successfully reports the preparation of sodium superoxide loaded phosphovanadate glass system by melt-quenching method. The prepared glass system has good quality amorphous phase, confirmed through XRD study. The absorption spectra show intense absorption dip in the wavelength region 220 to 230 nm and a broad hump in the wavelength region of 300 - 450 nm. The prepared glass system shows capturing of light that is extinction coefficient is proportional to wavelength in range 225 - 500 nm. Prepared samples have small value of refractive index on shorter wavelength side, whereas on longer wavelength side its value increases up to 340 nm and beyond it, refractive index decreases gradually. The values of direct and indirect band gap, and Urbach energy were successfully estimated for the prepared glass system. The dielectric constant measurements show linear behavior with wavelength. The defect energy increases with decrease in band gap, which obviously supports the creation of sub-band states in between the valence and conduction bands consequence in the reduction of the band gap. With increase in concentration of NaO_2, the effective band gap of NaO_2 decreases because band edge shifted into forbidden gap due to increase in defect levels below the conduction.

Acknowledgements

The author acknowledges Director, Government Vidarbha Institute of Science and Humanities, Amravati, Head, Department of Physics, Government Vidarbha Institute of Science and Humanities, Amravati, and Head, Department of Physics, Sant Gadge Baba Amravati University, Amravati for providing necessary facilities for the work.

References

[1] GI Petrov, VV Yakovlev and J Squier. Raman microscopy analysis of phase transformation mechanisms in vanadium dioxide. *Appl. Phys. Lett.* 2002; **81**, 1023-5.
[2] MM El-Desoky and MS Al-Assiri. Structural and polaronic transport properties of semiconducting $CuO–V_2O_5–TeO$ glasses. *Mater. Sci. Eng. B* 2007; **137**, 237-46.
[3] GM Clark and AN Pick. DTA study of the reactions of V_2O_5 with metal (II) oxides. *J. Therm. Anal.* 1975; **7**, 289-300.
[4] H Liu and D Tang. Synthesis of ZnV_2O_6 powder and its cathodic performance for lithium secondary battery. *Mater. Chem. Phys.* 2009; **114**, 656-9.
[5] E Mansour, YM Moustafa, GM El-Damrawi, SA El-Maksoud and H Doweidar. Memory switching of $Fe_2O_3–BaO–V_2O_5$ glasses. *Physica B* 2001; **305**, 242-9.
[6] K Jeyalakshmi, S Vijayakumar, S Nagamuthu and G Muralidharan. Effect of annealing temperature on the supercapacitor behaviour of β-V_2O_5 thin films, Mater. *Res. Bull.* 2013; **48**, 760-6.
[7] L Murawski. Electrical conductivity in iron-containing oxide glasses. *J. Mater. Sci.* 1982; **17**, 2155-63.
[8] NF Mott. Conduction in glasses containing transition metal ions. *J. Non-Cryst. Solids* 1968; **1**, 1-17.
[9] MA Hassan, FM Ebrahim, MG Moustafa, ZMA El-Fattah and MM El-Okr. Unraveling the hidden Urbach edge and Cr^{6+} optical transitions in borate glasses. *J. Non Cryst. Solids* 2019; **515**, 157.
[10] AI Ismail, A Samir, F Ahmad, LI Soliman and A Abdelghany. Spectroscopic studies and the effect of radiation of alkali borate glasses containing chromium ions. *J. Non Cryst. Solids* 2021; **565**, 120743.
[11] S Yusub and D Krishna Rao. The role of chromium ions on dielectric and spectroscopic properties of $Li_2O–PbO–B_2O_3–P_2O_5$ glasses. *J. Non-Cryst. Solids* 2014; **398**-**399**, 1-9.
[12] RK Brow and DR Tallant. Structural design of sealing glasses, J. Non-Cryst. *Solids* 1997; **222**, 396-406.
[13] TO Hardwell. *Solid-state lasers: Properties and applications*. Nova Science Pub Inc, New York, 2008, p. 227.
[14] B Denker, B Galagan, V Osiko, S Sverchkov and E Dianov. Luminescent properties of Bi-doped boro-alumino-phosphate glasses. *Appl. Phys. B* 2007; **87**, 135-7.
[15] O Mao, RL Turner, IA Courtney, BD Fredericksen, MI Buckett, LJ Krause and JR Dahn. Active/inactive nanocomposites as anodes for Li-Ion batteries. *Electrochem. Solid-State Lett.* 1999; **2**, 3-5.
[16] CR Kesavulu, RPS Chakradhar, RS Muralidhara, JL Rao and RV Anavekar. EPR, optical absorption and photoluminescence properties of Cr^{3+} ions in lithium borophosphate glasses. *J. Alloys Compd.* 2010; **496**, 75-80.

[17] JT Tsai, CY Huang and ST Lin. The development of conductive pastes for solar cells. *Adv. Mater. Res.* 2012; **557- 559**, 1201-4.
[18] JW Yu and K Oh. New in-line fiber band pass filters using high silica dispersive optical fibers. *Opt. Commu.* 2002; **204**, 111–8.
[19] F Li, Z Wei, A Manthiram, Y Feng, J Maa and L Maid. Sodium-based batteries: From critical materials to battery systems. *J. Mater. Chem. A* 2019; **7**, 9406-31.
[20] X Xu, KS Hui, DA Dinh, KN Hui and H Wang. Recent advances in hybrid sodium-air batteries, *Mater. Horiz.* 2019; **6**, 1306-35.
[21] X Ren and Y Wu. A low-overpotential potassium-oxygen battery based on potassium superoxide. *J. Am. Chem. Soc.* 2013; **135**, 2923-6.
[22] P Hartmann, CL Bender, M Vracar, A Garsuch, AK Durr, J Janek and P Adelhelm. A rechargeable room-temperature sodium superoxide (NaO2) battery. *Nat. Mater.* 2012; **12**, 228-32.
[23] KR Nemade and SA Waghuley. Novel synthesis approach for stable sodium superoxide (NaO_2) nanoparticles for LPG sensing application. *Int. Nano Lett.* 2017; **7**, 233-6.
[24] M He, KC Lau, X Ren, N Xiao, WD McCulloch, LA Curtiss and Y Wu. Concentrated electrolyte for the sodium-oxygen battery: Solvation structure and improved cycle life. *Angew. Chem. Int. Ed.* 2016; **55**, 1-6.
[25] E Peled, D Golodnitsky, H Mazor, M Goor and S Avshalomov. Parameter analysis of a practical lithium- and sodium-air electric vehicle battery. *J. Powe. Sour.* 2011; **196**, 6835-40.
[26] H Park, J Kim, MH Lee, SK Park, D Kim, Y Bae, Y Ko, B Lee and K Kang. Highly durable and stable sodium superoxide in concentrated electrolytes for sodium-oxygen batteries. *Adv. Energy Mater.* 2018; **8**, 1801760.
[27] MS Sadeq and MA Abdo. Effect of iron oxide on the structural and optical properties of alumino-borate glasses. *Ceram. Int.* 2021; **47**, 2043-9.
[28] S Thakur, A Kaur and L Singh. Mixed valence effect of Se^{6+} and Zr^{4+} on structural, thermal, physical, and optical properties of B_2O_3–Bi_2O_3–SeO_2–ZrO_2 glasses. *Opt. Mat.* 2019; **96**, 109338.
[29] RV Barde. Preparation, characterization and CO_2 gas sensitivity of polyaniline doped with sodium superoxide. *Mater. Res. Bull.* 2016; **73**, 70-6.
[30] RV Barde and SA Waghuley. Preparation and electrical conductivity of novel vanadate borate glass system containing graphene oxide. *J. Non-Cryst. Solids* 2013; **376**, 117-25.
[31] RV Barde and SA Waghuley. Transport properties of rare earth CeO_2 doped phospho-vanadate glass systems. *J. Chin. Adv. Mater. Soc.* 2014; **2**, 273-83.
[32] M Fox. *Optical properties of solids*. Oxford University Press, New York, 2001, p. 274.
[33] JB Lian, XC Duan, JM Ma, P Peng, T Kim and WJ Zheng. Hematite (alpha-Fe_2O_3) with various morphologies: Ionic liquid-assisted synthesis, formation mechanism, and properties. *ACS Nano* 2009; **3**, 3749-61.
[34] T Wang, S Zhou, C Zhang, J Lian, Y Liang and W Yuan. Facile synthesis of hematite nanoparticles and nanocubes and their shape-dependent optical properties. *J. Chem.* 2014; **38**, 46-9.
[35] S Gedia, V Reddy, M Reddya, C Parkb, JC Wookb and KTR Reddy. Comprehensive optical studies on SnS layers synthesized by chemical bath deposition. *Opti. Mate.* 2015; **42**, 468-75.
[36] RV Barde. Influence of CeO_2 content on complex optical parameters of phosphovanadate glass system, Spectroch *Spectrochim. Acta A Mol. Biomol. Spectrosc.* 2016; **153**, 160-4.
[37] RV Barde, KR Nemade and SA Waghuley. Complex optical study of V_2O_5–P_2O_5–B_2O_3–GO glass systems by ultraviolet-visible spectroscopy. *Opti. Mate.* 2015; **40**, 118-21.
[38] KL Chopra and I Kaur. *Thin film phenomena*. McGraw-Hill, New York, 1969, p. 736.
[39] S Song, Y Wang, X Yuan, W Yao, W Jing. Characterization and preparation of Sn-doped CuGaS2 thin films by paste coating. *Mater. Lett.* 2015; **148**, 41-4.
[40] S Shailajha, K Geetha, P Vasantharani and SPSA Kadhar. *Spectrochi. Acta Part A: Mole. and Biomol. Spectro.* 2015; **138**, 846-56.
[41] K Boubaker. A physical explanation to the controversial Urbach tailing universality. *Eur. Phys. J. Plus* 2011; **126**, 10.
[42] B Choudhur, B Borah and A Choudhury. Extending photocatalytic activity of TiO_2 nanoparticles to visible region of illumination by doping of cerium. *Photochem. Photobiol.* 2012; **88**, 257-64.
[43] B Choudhury, M Dey and A Choudhury. Defect generation, d-d transition, and band gap reduction in Cu-doped TiO2 nanoparticles. *Int. Nano Lett*, 2013; **3**, 1-8.
[44] CO Ayieko1, RJ Musembi, SM Waita, BO Aduda and PK Jain. Structural and optical characterization of nitrogen-doped TiO_2 thin films deposited by spray pyrolysis on fluorine doped tin oxide (FTO) coated glass slides. *Int. J. Ene. Eng.* 2012; **2**, 67-72.

[45] AQ Abdullah. Surface and volume energy loss, optical conductivity of rhodamine 6G dye (R6G). *Chem. and Mat. Res.* 2013; **3**, 56-63.
[46] RV Barde, KR Nemade and SA Waghuley. Complex optical study of V_2O_5–P_2O_5–B_2O_3–Dy_2O glass systems. *J. Taib. Uni. Sci.* 2015; **10**, 340-4.
[47] P Sharma and SC Katyal. Determination of optical parameters of a-(As2Se3)90Ge10 thin film. *J. Phys. D: Appl. Phys.* 2007; **40**, 2115-20.
[48] NA Bakr, AM Funde, VS Waman, MM Kamble, RR Hawaldar, DP Amalnerkar and SR Jadkar, Determination of the optical parameters of a-Si: H thin films deposited by hot wire-chemical vapour deposition technique using transmission spectrum only. *Pramana J. Phys.* 2011; **76**, 519-31.
[49] NF Mott and EA Davis. Conduction in non-crystalline systems V conductivity, optical absorption and photoconductivity in amorphous semiconductors. *Philos. Mag.* 1970; **22**, 0903-22.
[50] F Yakuphanoglu, A Cukurovali and I Yilmaz. Refractive index and optical absorption properties of the complexes of a cyclobutane containing thiazolylhydrazone ligand. *Opt. Mater.* 2005; **27**, 1363-8.

5 The Comprehensive study of Titanium oxide doped Conducting polymers nanocomposites for Photovoltaic applications

POLYMER-PLASTICS TECHNOLOGY AND MATERIALS
https://doi.org/10.1080/25740881.2021.1930047

Taylor & Francis
Taylor & Francis Group

The Comprehensive study of Titanium oxide doped Conducting polymers nanocomposites for Photovoltaic applications

Bhagyashri U. Tale[a], K. R. Nemade[b], and P. V. Tekade[a]

[a]Department of Chemistry, Bajaj College of Science, Wardha, India; [b]Department of Physics, Indira Mahavidyalaya, Kalamb, India

ABSTRACT

To make the effective use of renewable energy, high performance, low-cost, and eco-friendly energy conversion devices are topic of intense research. Effect of addition of TiO_2 on photovoltaic performance of polymers was studied. The significant enhancement in % η was observed after addition of TiO_2 in Polyaniline. The Titanium dioxide (TiO_2) is n-type semiconductor with mechanical flexibility, and its conductivity can be modified by doping with PANi (*p*-type) to obtain high current by exciton separation at TiO_2/PANi interface. The value of % η (10.47%) for TiO_2-Polyaniline composite is found to be highest.

ARTICLE HISTORY
Received 14 April 2021
Revised 3 May 2021
Accepted 11 May 2021

KEYWORDS
Nano-composites; solar cells; supercapacitors

1. Introduction

The energy requirement of world is rising day by day and it is estimated that energy requirement will be double by 2050.[1] A photovoltaic or solar cell is used to convert the light energy into electrical energy. The electric power generation from renewable energy sources is the need of time. Among renewable energy resources used for generation of electricity, solar photovoltaic technology is rapidly growing.[2,3]

The interesting characteristics for the replacement of traditional energy sources by photovoltaic technology are

- Fossil fuels are limited and their cost is increasing day by day on the other hand solar energy is abundant & free.
- Fossil-fuels pollute the environment & solar PV's does not release pollutants.
- Fossil-fuels create global warming & solar PV's does not.
- As compared to other renewable energy sources, solar PV's provide the highest power density.
- Solar PV's has low operational costs & maintenance.
- There are more than 100 countries in the world where the work on solar PV technology is topic of intense research.[4–10]

1.1. Metal oxide/polymer composites

Polymer solar cells work in the following four stages for photocurrent generation:

(1) Excitons formation by absorption of light by the activated layer.

(2) Free charges formation by excitons at electron donor/acceptor interface.

(3) Transfer of the charged species in presence of electric field.

(4) Collection of charge by electrodes.[11]

One of the popular methods for charge separation in organic films is the addition of electron acceptors like TiO_2nanomaterial.[12,13]Polymer/inorganic composite is topic of interest in research due to the synergetic effects which lead to better electrical properties. The direct interfacial interaction of the polymers &inorganic component in composite improves electronic properties. In composite, the polymeric material acts as donors and inorganic component are acceptors.

In this study, Titanium dioxide (TiO_2) is n-type semiconductor with mechanical flexibility, and its conductivity can be modified by doping with PANi (*p*-type) to obtain high current by exciton separation at TiO_2 /PANiinterface.[14–17] Polyaniline is one of the most studied material because of its eco-friendliness, good electrical conductivity, low cost, rigidity, unique reversible protonic dupability etc. PANI is widely used in nanoelectronic devices.

The high efficiency of composites of PANi&TiO_2in photovoltaic devices can be explained on the basis of following:

1. The band-gap energies of PANI (2.8 eV) &TiO_2 (3.2 eV) are nearly same which facilitates the separation of charges and the transfer of electrons.

CONTACT Bhagyashri U. Tale bhagyashritale@gmail.com Department of Chemistry, Bajaj College of Science, Wardha, Maharashtra, India

2. The photo-generated electrons get excited by light which increases the conductivity as well as photoelectrochemical response.

Another reason for enhanced photosensitivity of PANI/TiO_2 film depends on energy level. When PANI/TiO_2film irradiates withlight, boththeTiO_2 and PANI shows absorption of photons & charge separation. As the conduction band of TiO_2 and the LUMO level of the PANI are nearer to each other, it facilitates the charge transfer.[18,19]

2. Experimental

In present work, Polyaniline (PANi) was prepared by Chemical oxidative method by Ammonium persulfate as oxidant. Both aniline and oxidant in stoichiometric ratio were dissolved in aqueous medium. The greenish black ppt was obtained and it was kept for 24 hours at room temperature to achieve complete polymerization. The product was washed with distilled water and then dried in an oven.[20] For preparation of Polypyrrole(PPy), $FeCl_3$ was used as oxidizing agent. The suspension was kept at room temperature for 24 hours to get complete polymerization. Finally, the black ppt. of polypyrrole was washed with Acetone and dried in an oven.[21]

Polyindole(PIn) was synthesized by Chemical oxidative method using $FeCl_3$ as an oxidizing agent and 0.1 M Hydrogen peroxide was added to enhance the rate of reaction. The reaction mixture was stirred for 12 hours at 30°C.[22] Polythiophene (PTh) was obtained by mixing thiophene with ferric chloride. Hydrogen peroxide was added to increase the rate of reaction. The complete polymerization was obtained by constant stirring for 24 hours at 30°C. Then, concentrated sodium hydroxide solution was added to get the product. The product was washed with distilled water and dried in oven.[23]

The Titanium dioxide (TiO_2) was obtained using 10% titanium chloride ($TiCl_3$), 15% HCl and ammonia solution in aqueous solution at alkaline pH. 3% $H_2O_2$was added to increase oxidation rate. The resulting solution was kept at room temperature for 24 hours and probe sonicated. The product was washed with distilled water and dried in oven.[24]The Polymer/Metal oxide composites were prepared by ex-situ approach. During preparation of composite, Polymer (1 g) and Metal oxide (0.1 g) were added to the organic media.

The X-ray diffraction (XRD) patterns of as prepared materials were recorded on Rigaku Miniflex-II X-Ray Diffractometer. The morphology of samples was investigated using scanning electron microscope (SEM) images obtained from JEOL JSM-7500 F. The ultraviolet–visible (UV–VIS) absorption spectra of composites were acquired using Agilent Cary 60 UV–VIS spectrophotometer. The Bruker RFS 27 Raman spectrometer was used for Raman analysis. Electrochemical study of prepared samples was carried out using three-electrode cell systems (CHI 660 D, CH Instruments). As-prepared materials were used as the working electrode, platinum wire as counter electrode and Ag/AgCl as the reference electrode. Photoluminescence (PL) spectra recorded using fluorescence spectroscopy (FL spectrophotometer model F-7000; Hitachi).

Figure 1. Side face of fabricated PV cell.

2.1. Fabrication of photovoltaic cell

The PV cells were prepared by doctor blade technique. The composite material was present as sandwich between ITO layer of plate and aluminum (Figure 1). The foil of aluminum acts as metallic electrode. The temporary binder was used to deposit the composite material on ITO coated plate and on that layer aluminum foil was kept. Then, it was dried at 40°C in order to remove the volatile organic components. The thickness of deposited layer was controlled by using transparency in doctor blade technique.

The current-voltage, that is, I–Vstudy of Photovoltaic cell was done by using an incandescent light bulb having power 0.2956 Watt/m^2. The parameters like short circuit current (I_{SC}), fill factor (FF), power conversion efficiency (η) & open-circuit voltage (V_{OC}) were measured using these conditions. The Fill Factor of Photovoltaic cell was measured using following equation,

$$FF = \frac{I_{MAX} \times V_{MAX}}{I_{SC} \times V_{OC}}$$

The power conversion efficiency, that is, %η of Photovoltaic cell was calculated by following relation,

$$\%\eta = \left(\frac{I_{SC} \times V_{OC} \times FF}{P_{in}}\right) \times 100$$

The FF and %η are the very important parameters for study of any PV cell. By using these parameters, it is possible to study any photovoltaic cell and its performance.

3. Result & discussion

3.1. XRD

Figure 2 indicates XRD pattern of (a) TiO_2, (b) Polyaniline (PANi), (c) Polythiophene (PTh), (d) Polypyrrole (PPy), (e) Polyindole (Pin), (f) TiO_2-Polyaniline composite (Ti-PANi), (g) TiO_2-Polythiophene composite (Ti-PTh), (h) TiO_2-Polypyrrole composite (Ti-PPy) and (i) TiO_2-Polyindole composite (Ti-Pin).

The experimental XRD pattern of TiO_2matches with the JCPDS card no. 21–1272 (anatase TiO_2). Strong diffraction peaks at 25°,38°, 48°, and 54° indicates TiO_2 in the anatase phase. The intensity of XRDpeaks indicates that the formed nanoparticles are crystalline.[25,26] X-ray diffraction of PANI shows peaks in the 2θ range 15° to 30°. The sharp and well-defined peaks indicate semi-crystalline nature of PANI. The crystalline nature of PANI is because of its nano fibrous nature and planarity of Benzenoid and Quinoid functional groups.[27]

XRD spectra of Polythiophene with only one broad peak centered at near 2θ value of 35°. This diffraction peak is due to π-π stacking structure in polythiophene chains. Thus, spectrum indicates the semi-crystalline nature of polythiophene.[28] The XRD pattern of Polyindole (PIn) shows a broad hump which indicates an amorphous structure which is the characteristic of Polyindole.[22] It is observed from the XRD of polypyrrole indicates its amorphous nature, as there is no sharp peak in the diffraction pattern. But a broad peak at about 24° of 2θ value is the characteristics peak of amorphous PPy polymer.[29]

Further the absence of broad diffraction peak of PANi at 2θ = 25° in the PANi/TiO_2 composite is due to the presence of PANi in the polymerization system which strongly affects the degree of crystallinity of TiO_2.[30] Similarly, crystalline behavior is found to be decrease with composite formation. Thus, the XRD pattern of TiO_2-Polyaniline composite (Ti-PANi), TiO_2-Polyindole composite(Ti-PIn), TiO_2-Polypyrrole

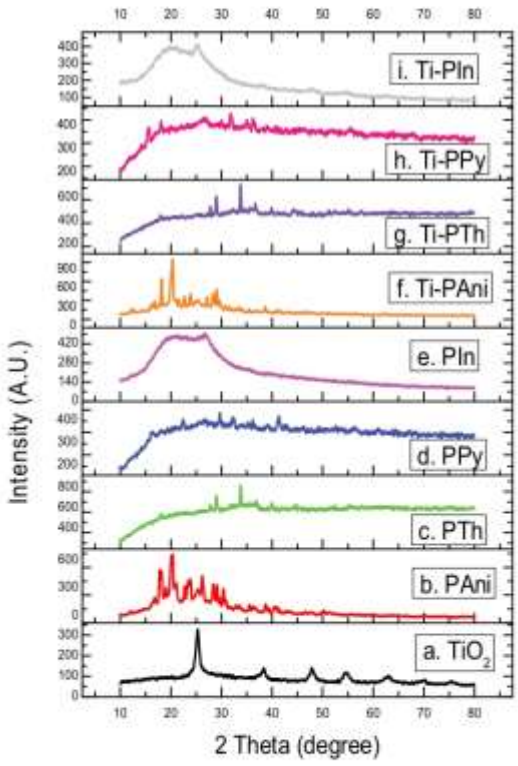

Figure 2. XRD pattern of (a) TiO_2, (b) Polyaniline (PANi), (c) Polythiophene (PTh), (d) Polypyrrole (PPy), (e) Polyindole (Pin), (f) TiO_2-Polyaniline composite (Ti-PANi), (g) TiO_2-Polythiophene composite (Ti-PTh), (h) TiO_2-Polypyrrole composite (Ti-PPy) and (i) TiO_2-Polyindole composite (Ti-PIn).

composite(Ti-PPy) and TiO_2-Polythiophene composite (Ti-PTh) indicates amorphous nature as there is no sharp peak.

Particle size of TiO_2, Polymers and their composites calculated by Scherrer equation are shown in Table 1.

Table 1. Particle size of TiO_2, polymers and their composites.

Compound	Observed particle size calculated by Scherrer equation D(nm) = Kλ/βCosθ[31]
1. TiO_2,	92.74
2. Polyaniline(PANi),	84
3. Polythiophene(PTh),	108.51
4. Polypyrrole (PPy),	108.13
5. Polyindole(Pin),	10.28
6. TiO_2-Polyaniline composite(Ti-PANi),	165
7. TiO_2-Polythiophene composite(Ti-PTh),	90.67
8. TiO_2-Polypyrrole composite(Ti-PPy) and	50.67
9. TiO_2-Polyindole composite(Ti-Pin).	8

3.2. SEM

SEM images of (a) TiO_2, (b) Polyaniline (PANi), (c) Polythiophene (PTh), (d) Polypyrrole (PPy), (e) Polyindole (Pin), (f) TiO_2-Polyaniline composite (Ti-PANi), (g) TiO_2-Polythiophene composite (Ti-PTh), (h) TiO_2-Polypyrrole composite (Ti-PPy) and (i) TiO_2-Polyindole composite (Ti-Pin) are shown in Figure 3.

3.3. Raman spectroscopy

Raman Spectra of(a) TiO_2, (b) Polyaniline (PANi), (c) Polythiophene (PTh), (d) Polypyrrole (PPy), (e) Polyindole (Pin), (f) TiO_2-Polyaniline composite (Ti-PANi), (g) TiO_2-Polythiophene composite (Ti-PTh), (h) TiO_2-Polypyrrole composite (Ti-PPy) and (i) TiO_2-Polyindole composite (Ti-PIn) are shown in Figure 4.

TiO_2 peak at 235 is due to rutile phase.[32,33] Raman spectra of Polyaniline indicates signal at 1140, 1230,1500 and 1582 cm^{-1}. 1100–1210 cm^{-1} region is due to C–H bending vibrations of benzene or quinone type rings. 1210–1520 cm^{-1} region indicates C-N stretching vibrations and 1520–1650 cm^{-1} region denotes C–C stretching vibration of benzene and quinone type rings.[34]

Polythiophene shows sharp signal at 1209,1379 and 1651 cm^{-1}. Peak near 1600 cm^{-1} indicates unquestionably frequency dispersion with increasing chain length. Signal

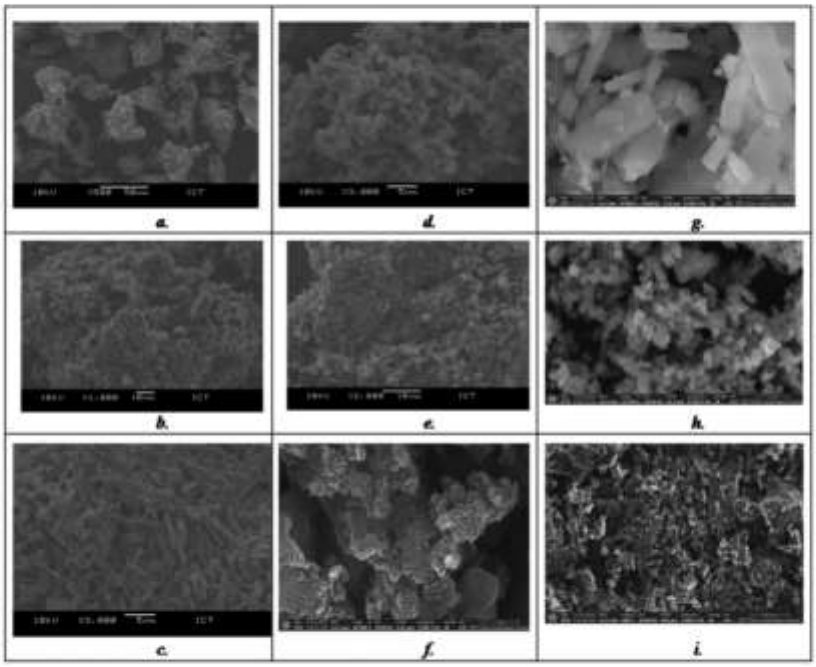

Figure 3. SEM images of(a) TiO_2, (b) Polyaniline(PANi), (c) Polythiophene (PTh), (d) Polypyrrole (PPy), (e) Polyindole (Pin), (f) TiO_2-Polyaniline composite (Ti-PANi), (g) TiO_2-Polythiophene composite (Ti-PTh), (h) TiO_2-Polypyrrole composite (Ti-PPy) and (i) TiO_2-Polyindole composite (Ti-Pin).

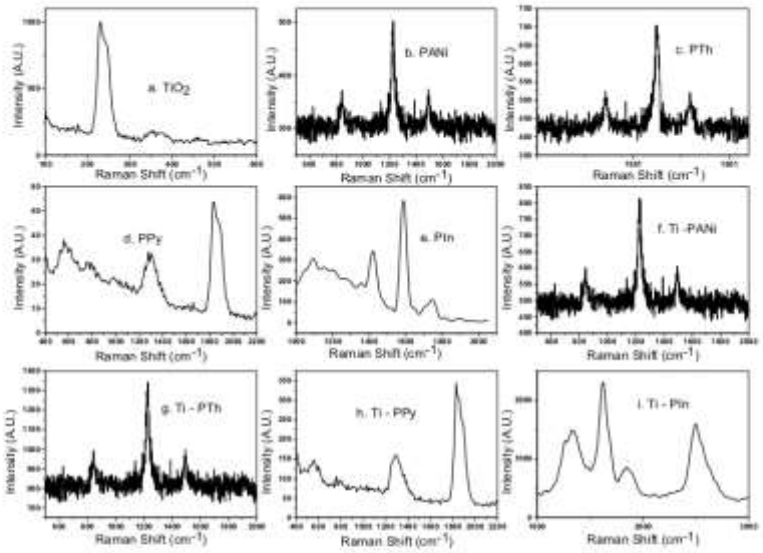

Figure 4. Raman Spectra of (a) TiO_2, (b) Polyaniline(PANi), (c) Polythiophene (PTh), (d) Polypyrrole (PPy), (e) Polyindole (Pin), (f) TiO_2-Polyaniline composite (Ti-PANi), (g) TiO_2-Polythiophene composite (Ti-PTh), (h) TiO_2-Polypyrrole composite (Ti-PPy) and (i) TiO_2-Polyindole composite (Ti-PIn).

near 1500 cm^{-1} is a characteristic feature of the Raman spectra of aromatic and heteroaromatic systems. It is reported as very strong and dominating in the whole Raman spectrum. While it shifts toward lower frequencies with an increase in chain length. It shows somewhat variation in frequencies from one chemical series to another within the class of oligo and polythiophenes, but within individual class it is almost invariably strong and unshifted. Some signals appearing at the lower frequency side shows intensity enhancement with increase in chain length.[35]

Polypyrrole signal at 1330 cm^{-1} corresponds to C–C stretching in ring and antisymmetric C–N stretching.[36] Polyindole signal 1102 is due to out-of-plane as well as in-plane deformation of N-H, peak near 1594 is because of C = C backbone stretching and peak at 1414 correspond to ring stretching.[37,38] Ti-PANi and Ti-PPy composites show the same peak as polymer. Ti-PIn and Ti-PTh show shifting of peaks. Peaks observed in composites indicate strong interaction between TiO_2 and polymers.

3.4. UV spectroscopy

Figure 5 shows UV-Visible spectra of (a) TiO_2, (b) Polyaniline (PANi), (c) Polythiophene (PTh), (d) Polypyrrole (PPy), (e) Polyindole (Pin), (f) TiO_2-Polyaniline composite (Ti-PANi), (g) TiO_2-Polythiophene composite (Ti-PTh), (h) TiO_2-Polypyrrole composite (Ti-PPy) and (i) TiO_2-Polyindole composite (Ti-Pin). Band gap and absorption peak values for TiO_2, Polymers and their composites are shown in Table 2.

In the present work, UV-VIS technique was used to study the absorption wavelengths of materials and band gap. The absorption study of samples under study was recorded using Agilent Cary 60 UV–VIS spectrophotometer.

The energy band gap of sample can be calculated using relations: $E = hc/\lambda$[39]

Where Energy (E) = Band gap, Planks constant (h) = 6.626×10^{-34} Joules sec,

Velocity of Light (c) = 2.99×10^{8} meter/sec and Wavelength (λ) = Absorption peak value. Also, 1 eV = 1.6×10^{-19} Joules (Conversion factor)

3.5. Photo luminescence

Figure 6 shows Photoluminescence (PL) spectra of (a) TiO_2, (b) Polyaniline(PANi), (c) Polythiophene (PTh), (d) Polypyrrole (PPy), (e) Polyindole (Pin), (f) TiO_2-Polyaniline composite (Ti-PANi), (g) TiO_2-Polythiophene composite (Ti-PTh), (h) TiO_2-Polypyrrole composite (Ti-PPy) and (i) TiO_2-Polyindole composite (Ti-Pin).

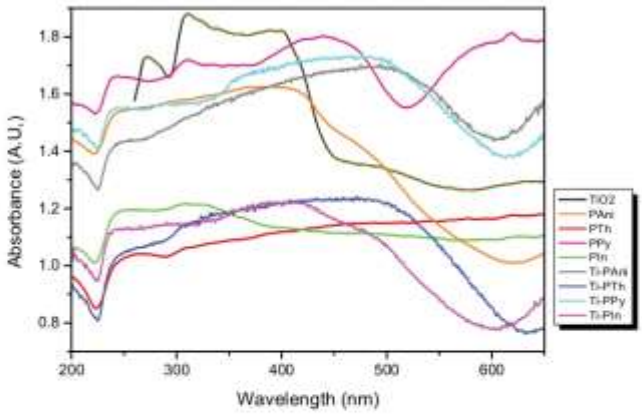

Figure 5. UV-Visible spectra of (a) TiO_2, (b) Polyaniline(PANi), (c) Polythiophene (PTh), (d) Polypyrrole (PPy), (e) Polyindole (Pin), (f) TiO_2-Polyaniline composite (Ti-PANi), (g) TiO_2-Polythiophene composite (Ti-PTh), (h) TiO_2-Polypyrrole composite (Ti-PPy) and (i) TiO_2-Polyindole composite (Ti-Pin).

Table 2. Band gap and absorption peak values for TiO_2, polymers and their composites.

Compound	Absorption peak value (Wavelength in nm)	Band gap (eV)
1. TiO_2	350	3.54
2. Polyaniline(PANI)	310	3.99
4. Polythiophene(PTh)	265	4.67
3. Polypyrrole (PPy)	440	2.82
5. Polyindole(Pin)	249	4.98
6. TiO_2-Polyaniline composite(Ti-PANi)	450	2.8
8. TiO_2-Polythiophene composite(Ti-PTh)	400	3.1
7. TiO_2-Polypyrrole composite(Ti-PPy)	450	2.8
9. TiO_2-Polyindole composite(Ti-Pin)	400	3.1

TiO_2 shows PL signal near 490 nm.[40–42] Polyaniline shows peak at 367 nm, due to $\pi \rightarrow \pi^*$ transition.[43] Polythiophene shows absorption peak near excitation wavelength 325 nm.[44] PL signal for polyindole comes from the recombination of electron in singly occupied oxygen vacancies with photo excited holes.[45,46] Polypyrrole shows PL emission peaks near 400 nm. However, agglomeration affects the PL intensity of the polymer.[47] This PL emission characteristics indicate the promise of the synthesized materials for practical applications in ultraviolet and visible light emission devices.

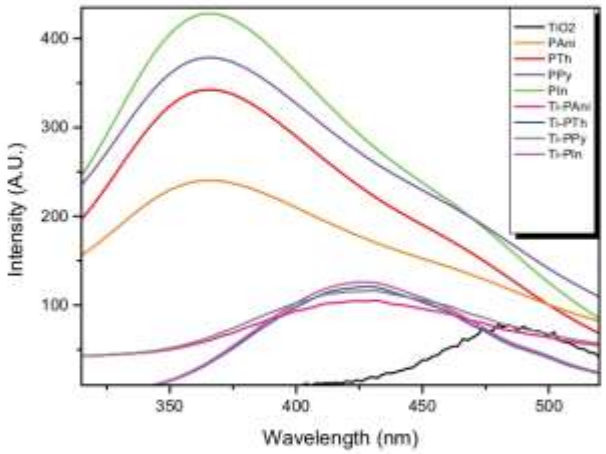

Figure 6. Photoluminescence(PL) spectra of (a) TiO_2, (b) Polyaniline(PANi), (c) Polythiophene (PTh), (d) Polypyrrole (PPy), (e) Polyindole (Pin), (f) TiO_2-Polyaniline composite (Ti-PANi), (g) TiO_2-Polythiophene composite (Ti-PTh), (h) TiO_2-Polypyrrole composite (Ti-PPy) and (i) TiO_2-Polyindole composite (Ti-Pin).

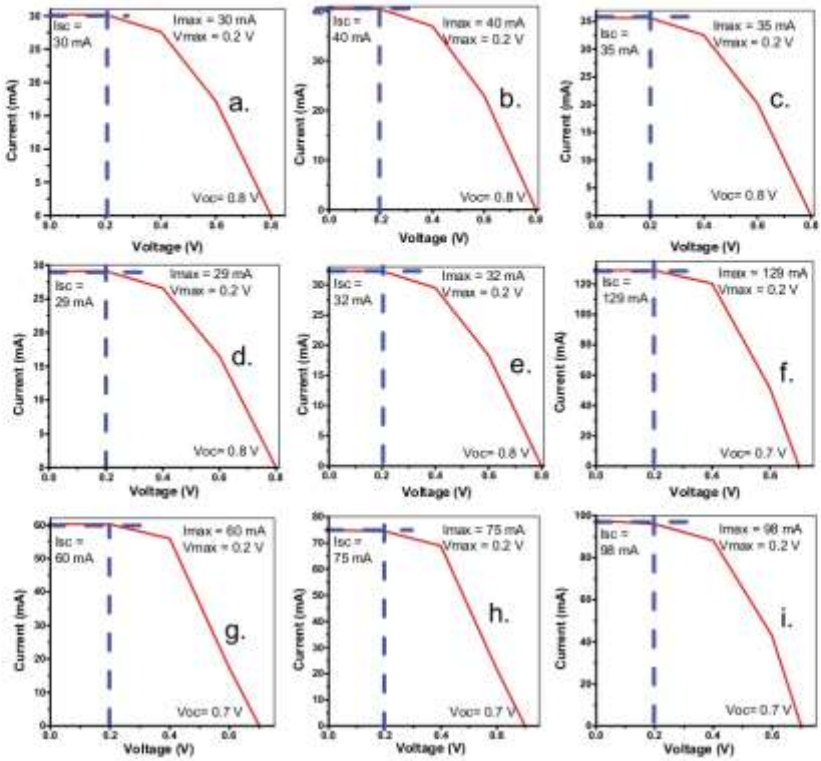

Figure 7. PV response of (a) TiO_2, (b) Polyaniline(PANi), (c) Polythiophene (PTh), (d) Polypyrrole (PPy), (e) Polyindole (PIn), (f) TiO_2-Polyaniline composite (Ti-PANi), (g) TiO_2-Polythiophene composite (Ti-PTh), (h) TiO_2-Polypyrrole composite (Ti-PPy) and (i) TiO_2-Polyindole composite (Ti-PIn).

Table 3. PV parameters (where Pin = 0.25 W/m^2).

Compound	Imax (mA)	Vmax (V)	Isc (mA)	Voc (V)	$FF = \frac{I_{max} \times V_{max}}{I_{sc} \times V_{oc}}$	$\%\eta = \left(\frac{I_{sc} \times V_{oc} \times FF}{P_{in}}\right) \times 100$
(a) TiO_2	30	0.2	30	0.8	0.25	2.4
(b) Polyaniline(PANi)	40	0.2	40	0.8	0.25	3.2
(c) Polythiophene (PTh)	35	0.2	35	0.8	0.25	2.8
(d) Polypyrrole (PPy)	29	0.2	29	0.8	0.25	2.32
(e) Polyindole (PIn)	32	0.2	32	0.8	0.25	2.56
(f) TiO_2-Polyaniline composite (Ti-PANi)	129	0.2	129	0.7	0.29	10.47
(g) TiO_2-Polythiophene composite (Ti-PTh)	60	0.2	60	0.7	0.29	4.872
(h) TiO_2-Polypyrrole composite (Ti-PPy)	75	0.2	75	0.7	0.29	6.09
(i) TiO_2-Polyindole composite (Ti-PIn)	98	0.2	98	0.7	0.29	7.957

3.6. Measurements of photovoltaic characteristics

Figure 7a–i represents Current-Voltage (IV) characteristics of fabricated photovoltaic cell (a) TiO_2, (b) Polyaniline(PANi), (c) Polythiophene (PTh), (d) Polypyrrole (PPy), (e) Polyindole (PIn), (f) TiO_2 Polyaniline composite (Ti-PANi), (g) TiO2-Polythiophene composite (Ti-PTh), (h) TiO2-Polypyrrole composite (Ti-PPy) and (i) TiO2-Polyindole composite (Ti-PIn) respectively. The photovoltaic parameters of these materials are listed in Table 3. It is observed that TiO2-Polyaniline composite (Ti-PANi) shows higher short

circuit current (Isc) ascompared to all other mentioned materials.

The Current-Voltage (I–V) characteristics of PANI-TiO2 heterostructure diode show a nonlinear behavior. It indicates that a *p*–n heterostructure at PANI-TiO2 interface has been generated. The doping of TiO2 nanoparticles which facilitates the formation of a more efficient network for charge transport. Consequently, the conductivity of nanocomposites also increases with the addition of TiO2. It also facilitates interchain conduction due to the formation of conducting pathways between the chains. Thus, by the addition of TiO2, there becomes a more efficient network for charge transport in the PANI matrix which leads to higher conductivities. As a result, dispersion capacity of TiO2-Polyaniline composite (Ti-PANi) and charge transfer phenomenon are significantly enhancing due to synergistic effects in composite which leads to higher values of Isc.[48–51] The significant enhancement in the value of % η is due to the addition of TiO2 in PANi in composite. The maximum value of % η is found to be 10.47% for TiO2-Polyaniline composite (Ti-PANi).

4. Conclusion

In summary, TiO_2, four Polymers (Polyaniline, Polythiophene, Polypyrrole, Polyindole) and their four composites (TiO_2-Polyaniline composite, TiO_2-Polythiophene composite, TiO_2-Polypyrrole composite, TiO_2-Polyindole composite) were prepared. PV performance of all above compounds were studied. The significant enhancement in value of % η takes place by the addition of TiO_2 in PANi during preparation of composite. The value of % η is found to be highest for TiO_2-Polyaniline composite (Ti-PANi)i.e.10.47%.

Notes on contributors

Ms. Bhagyashri U.Tale is Ph.D. student, at department of chemistry, Bajaj College of Science, Dist.Wardha, Maharashtra, India.

Dr. K.R. Nemade is Assistant Professor, at department of physics, Indira Mahavidyalaya, Kalamb,Dist. yavatmal, Maharashtra, India.

Dr. P.V. Tekade is Associate Professor, at department of chemistry, Bajaj College of Science, Dist.Wardha, Maharashtra, India.

References

[1] Mahmood, N.; Zhang, C.; Yin, H.; Hou, Y. Graphene-based Nanocomposites for Energy Storage and Conversion in Lithium Batteries, Supercapacitors and Fuel Cells. *J. Mater. Chem. A* 2014, *2*(1), 15–32. DOI: 10.1039/C3TA13033A.

[2] Jordehi, A. R. Parameter Estimation of Solar Photovoltaic (PV) Cells: A Review. *Renewable Sustainable Energy Rev.* 2016, *61*, 354–371. DOI: 10.1016/j.rser.2016.03.049.

[3] Bai, J.; Liu, S.; Hao, Y.; Zhang, Z.; Jiang, M.; Zhang, Y. Development of a New Compound Method to Extract the Five Parameters of PV Modules. *Energy Conversion Manage.* 2014, *79*, 294–303. DOI: 10.1016/j.enconman.2013.12.041.

[4] Shafiee, S.; Topal, E. When Will Fossil Fuel Reserves Be Diminished? *Energy Policy*. 2009, *37*(1), 181–189. DOI: 10.1016/j.enpol.2008.08.016.

[5] Apergis, N.; Payne, J. E. Renewable Energy, Output, CO2 Emissions, and Fossil Fuel Prices in Central America: Evidence from a Nonlinear Panel Smooth Transition Vector Error Correction Model. *Energy Econ.* 2014, *42*, 226–232. DOI: 10.1016/j.eneco.2014.01.003.

[6] Shivalkar, R. S.; Jadhav, H. T.; Deo, P. Feasibility Study for the Net Metering Implementation in Rooftop Solar PV Installations across Reliance Energy Consumers. 2015 International Conference on Circuits, Power and Computing Technologies [ICCPCT-2015], IEEE: Nagercoil, India, Mar, 2015, pp 1–6.

[7] Wang, Y.; Zhou, S.; Huo, H. Cost and CO2 Reductions of Solar Photovoltaic Power Generation in China: Perspectives for 2020. *Renewable Sustainable Energy Rev.* 2014, *39*, 370–380. DOI: 10.1016/j.rser.2014.07.027.

[8] Sundareswaran, K.; Sankar, P.; Nayak, P. S. R.; Simon, S. P.; Palani, S. Enhanced Energy Output from a PV System under Partial Shaded Conditions through Artificial Bee Colony. *IEEE Trans. Sustainable Energy*. 2014, *6*(1), 198–209. DOI: 10.1109/TSTE.2014.2363521.

[9] Trifunović, M. Energy at the Crossroads. Synthesis 2015-International Scientific Conference of IT and Business-Related Research. Singidunum University: Serbia, 2015, pp 186–190.

[10] Hunt, T. *The Solar Singularity Is Nigh*; Greentech Media, (accessed 29, 2015).

[11] Liu, Z.; Zhou, J.; Xue, H.; Shen, L.; Zang, H.; Chen, W. Polyaniline/TiO2 Solar Cells. *Synth. Met.* 2006, *156*(9–10), 721–723. DOI: 10.1016/j.synthmet.2006.04.001.

[12] Breeze, A. J.; Schlesinger, Z.; Carter, S. A.; Brock, P. J. Charge Transport in TiO 2/M E H– P P V Polymer Photovoltaics. *Phys. Rev. B.* 2001, *64*(12), 125205. DOI: 10.1103/PhysRevB.64.125205.

[13] Arango, A. C.; Johnson, L. R.; Bliznyuk, V. N.; Schlesinger, Z.; Carter, S. A.; Hörhold, H. H. Efficient Titanium Oxide/conjugated Polymer Photovoltaics for Solar Energy Conversion. *Adv.Mate.* 2000, *12*(22), 1689–1692. DOI: 10.1002/1521-4095(200011)12:22<1689::AID-ADMA1689>3.0.CO;2-9.

[14] Kawata, K.; Gan, S. N.; Ang, D. T. C.; Sambasevam, K. P.; Phang, S. W.; Kuramoto, N. Preparation of polyaniline/TiO2 Nanocomposite Film with Good Adhesion Behavior for Dye-sensitized Solar Cell Application. *Polym. Compos.* 2013, *34*(11), 1884–1891. DOI: 10.1002/pc.22595.

[15] Bouclé, J.; Ravirajan, P.; Nelson, J. Hybrid Polymer–metal Oxide Thin Films for Photovoltaic Applications.

J. Mater. Chem. 2007, *17*(30), 3141–3153. DOI: 10.1039/b706547g.

[16] Çetin, H.; Boyarbay, B.; Akkaya, A.; Uygun, A.; andAyyildiz, E. N. İ. S. E. Electrical Characterization of Heterojunction between Polyaniline Titanium Dioxide Tetradecyltrimethylammonium Bromide and N-silicon. *Synth. Met.* 2011, *161*(21–22), 2384–2389. DOI: 10.1016/j.synthmet.2011.09.005.

[17] Ameen, S.; Akhtar, M. S.; Kim, Y. S.; Shin, H. S. *Fabrication, Doping and Characterization of Polyaniline and Metal Oxides: Dye Sensitized Solar Cells*; Solar cells-dye-sensitized devices, 2011.

[18] Bahramian, A.; Vashaee, D. In-situ Fabricated Transparent Conducting Nanofiber-shape Polyaniline/coral-like TiO2 Thin Film: Application in Bifacial Dye-sensitized Solar Cells. *Solar Energy Mater. Solar Cells.* 2015, *143*, 284–295. DOI: 10.1016/j.solmat.2015.07.011.

[19] Chung, I.; Lee, B.; He, J.; Chang, R. P.; Kanatzidis, M. G. All-solid-state Dye-sensitized Solar Cells with High Efficiency. *Nature.* 2012, *485*, 486. DOI: 10.1038/nature11067.

[20] Jing, X.; Wang, Y.; Wu, D.; Qiang, J. Sonochemical Synthesis of Polyaniline Nanofibers. *Ultrason. Sonochem.* 2007, *14*(1), 75–80. DOI: 10.1016/j.ultsonch.2006.02.001.

[21] Tat'yana, V. V.; Efimov, O. N. Polypyrrole: A Conducting Polymer; Its Synthesis, Properties and Applications. *Russ. Chem. Rev.* 1997, *66*(5), 443. DOI: 10.1070/RC1997v066n05ABEH000261.

[22] Wadatkar, N. S.; Waghuley, S. A. Complex Optical Studies on Conducting Polyindole As-synthesized through Chemical Route. *Egypt. J. Basic Appl. Sci.* 2015, *2*(1), 19–24. DOI: 10.1016/j.ejbas.2014.12.006.

[23] Wadatkar, N. S.; Waghuley, S. A. Studies on Properties of As-synthesized Conducting Polythiophene through Aqueous Chemical Route. *J. Mater. Sci.: Mater. Electron.* 2016, *27*(10), 10573–10581.

[24] Molea, A.; Popescu, V. The Obtaining of Titanium Dioxide Nanocrystalline Powders. *Optoelectron. Adv. Mater. Rapid Commun.* 2011, *5*(3–4), 242–246.

[25] Theivasanthi, T.; Alagar, M. Titanium Dioxide (Tio2) Nanoparticles XRD Analyses: An Insight. *arXiv preprint arXiv:1307.1091.* 2013.

[26] Rajakani, P.; Vedhi, C. Electrocatalytic Properties of polyaniline–TiO2 Nanocomposites. *Int. J. Ind. Chem.* 2015, *6*(4), 247–259. DOI: 10.1007/s40090-015-0046-8.

[27] Bhagwat, A. D.; Sawant, S. S.; Mahajan, C. M. *Facile Rapid Synthesis of Polyaniline (Pani) Nanofibers*, 2016.

[28] Sakthivel, S.; Boopathi, A. Synthesis and Preparation of Polythiophene Thin Film by Spin Coating Method. *Int. J. Sci. Res. Sec.* 2014, *141*, 97–100.

[29] Ma, C.; Sg, P.; Pr, G.; Shashwati, S. Synthesis and Characterization of Polypyrrole (Ppy) Thin Films. *Soft Nanosci. Lett.* 2011, *2011*,6–10.

[30] Sathiyanarayanan, S.; Azim, S. S.; Venkatachari, G. Preparation of polyaniline–TiO2 Composite and Its Comparative Corrosion Protection Performance with Polyaniline. *Synth. Met.* 2007, *157*(4–5), 205–213. DOI: 10.1016/j.synthmet.2007.01.012.

[31] Nemade, K. R.; Waghuley, S. A. Low Temperature Synthesis of Semiconducting α-Al2O3 Quantum Dots. *Ceram. Int.* 2014, *40*(4), 6109–6113. DOI: 10.1016/j.ceramint.2013.11.062.

[32] Balachandran, U. G. E. N.; Eror, N. G. Raman Spectra of Titanium Dioxide. *J. Solid State Chem.* 1982, *42*(3), 276–282. DOI: 10.1016/0022-4596(82)90006-8.

[33] Frank, O.; Zukalova, M.; Laskova, B.; Kürti, J.; Koltai, J.; Kavan, L. Raman Spectra of Titanium Dioxide (Anatase, Rutile) with Identified Oxygen Isotopes (16, 17, 18). *Phys. Chem. Chem. Phys.* 2012, *14*(42), 14567–14572. DOI: 10.1039/c2cp42763j.

[34] Mažeikienė, R.; Tomkutė, V.; Kuodis, Z.; Niaura, G.; Malinauskas, A. Raman Spectroelectrochemical Study of Polyaniline and Sulfonated Polyaniline in Solutions of Different pH. *Vib. Spectrosc.* 2007, *44*(2), 201–208. DOI: 10.1016/j.vibspec.2006.09.005.

[35] Agosti, E.; Rivola, M.; Hernandez, V.; Del Zoppo, M.; Zerbi, G. Electronic and Dynamical Effects from the Unusual Features of the Raman Spectra of Oligo and Polythiophenes. *Synth. Met.* 1999, *100*(1), 101–112. DOI: 10.1016/S0379-6779(98)00167-2.

[36] Šetka, M.; Calavia, R.; Vojkůvka, L.; Llobet, E.; Drbohlavová, J.; Vallejos, S. Raman and XPS Studies of Ammonia Sensitive Polypyrrole Nanorods and Nanoparticles. *Sci. Rep.* 2019, *9*(1), 1–10. DOI: 10.1038/s41598-019-44900-1.

[37] Raj, R. P.; Ragupathy, P.; Mohan, S. Remarkable Capacitive Behavior of a Co3O 4–polyindole Composite as Electrode Material for Supercapacitor Applications. *J. Mater. Chem. A.* 2015, *3*(48), 24338–24348. DOI: 10.1039/C5TA07046E.

[38] Liu, Y. C.; Hwang, B. J.; Jian, W. J.; Santhanam, R. In Situ Cyclic Voltammetry-surface-enhanced Raman Spectroscopy: Studies on the Doping–undoping of Polypyrrole Film. *Thin Solid Films.* 2000, *374*(1), 85–91. DOI: 10.1016/S0040-6090(00)01061-0.

[39] Nemade, K. R.; Waghuley, S. A. UV–VIS Spectroscopic Study of One Pot Synthesized Strontium Oxide Quantum Dots. *Results Phys.* 2013, *3*, 52–54. DOI: 10.1016/j.rinp.2013.03.001.

[40] Brüninghoff, R.; Wenderich, K.; Korterik, J. P.; Mei, B. T.; Mul, G.; Huijser, A. Time-Dependent Photoluminescence of Nanostructured Anatase TiO2 and the Role of Bulk and Surface Processes. *J. Phys. Chem. C.* 2019, *123*(43), 26653–26661. DOI: 10.1021/acs.jpcc.9b06890.

[41] Xiao, Q.; Si, Z.; Yu, Z.; Qiu, G. Sol–gel Auto-combustion Synthesis of Samarium-doped TiO2 Nanoparticles and Their Photocatalytic Activity under Visible Light Irradiation. *Mater. Sci. Eng.* 2007, *137*(1–3), 189–194. DOI: 10.1016/j.mseb.2006.11.011.

[42] Haque, F. Z.; Nandanwar, R.; Singh, P. Evaluating Photodegradation Properties of Anatase and Rutile TiO2 Nanoparticles for Organic Compounds. *Optik.* 2017, *128*, 191–200. DOI: 10.1016/j.ijleo.2016.10.025.

[43] Chatterjee, M. J.; Ghosh, A.; Mondal, A.; Banerjee, D. Polyaniline–single Walled Carbon Nanotube Composite–a Photocatalyst to Degrade Rose Bengal and Methyl Orange Dyes under Visible-light Illumination. *RSC Adv.* 2017, *7*(58), 36403–36415. DOI: 10.1039/C7RA03855K.

[44] Tripathi, A.; Mishra, S. K.; Bahadur, I.; Shukla, R. K. Optical Properties of Regiorandom polythiophene/

Al2O3 Nanocomposites and Their Application to Ammonia Gas Sensing. *J. Mater. Sci.: Mater. Electron.* 2015, *26*(10), 7421–7430.

[45] Vanheusden, K.; Warren, W. L.; Seager, C. H.; Tallant, D. R.; Voigt, J. A.; Gnade, B. E. Mechanisms behind Green Photoluminescence in ZnO Phosphor Powders. *J. Appl. Phys.* 1996, *79*(10), 7983–7990. DOI: 10.1063/1.362349.

[46] Vanheusden, K.; Seager, C. H.; Warren, W. T.; Tallant, D. R.; Voigt, J. A. Correlation between Photoluminescence and Oxygen Vacancies in ZnO Phosphors. *Appl. Phys. Lett.* 1996, *68*(3), 403–405. DOI: 10.1063/1.116699.

[47] Dey, S.; Kar, A. K. Morphological and Optical Properties of Polypyrrole Nanoparticles Synthesized by Variation of Monomer to Oxidant Ratio. *Mater. Today Proc.* 2019, *18*, 1072–1076.

[48] Nemade, K.; Dudhe, P.; Tekade, P. Enhancement of Photovoltaic Performance of Polyaniline/graphene Composite-based Dye-sensitized Solar Cells by Adding TiO2 Nanoparticles. *Solid State Sci.* 2018, *83*, 99–106. DOI: 10.1016/j.solidstatesciences.2018.07.009.

[49] Zhang, X.; Yan, G.; Ding, H.; Shan, Y. Fabrication and Photovoltaic Properties of Self-assembled Sulfonated polyaniline/TiO2 Nanocomposite Ultrathin Films. *Mater. Chem. Phys.* 2007, *102*(2–3), 249–254. DOI: 10.1016/j.matchemphys.2006.12.013.

[50] Abaci, S.; Nessark, B.; Riahi, F. Preparation and Characterization of Polyaniline+ TiO 2 Composite Films. *Ionics.* 2014, *20*(12), 1693–1702. DOI: 10.1007/s11581-014-1129-9.

[51] Deivanayaki, S.; Ponnuswamy, V.; Ashokan, S.; Jayamurugan, P.; Mariappan, R. Synthesis and Characterization of TiO2-doped Polyaniline Nanocomposites by Chemical Oxidation Method. *Mater. Sci. Semicond. Process.* 2013, *16*(2), 554–559. DOI: 10.1016/j.mssp.2012.07.004.

6 Graphene based nano-composites for efficient energy conversion and storage in Solar cells and Supercapacitors: A Review

POLYMER-PLASTICS TECHNOLOGY AND MATERIALS
https://doi.org/10.1080/25740881.2020.1851378

Taylor & Francis
Taylor & Francis Group

Graphene based nano-composites for efficient energy conversion and storage in Solar cells and Supercapacitors : A Review.

Bhagyashri Tale[a], K. R. Nemade[b], and P. V. Tekade[a]

[a]Department of Chemistry, J. B. College of Science, Wardha, Maharashtra, India; [b]Department of Physics, Indira Mahavidyalaya Kalamb, District: Yavatmal, Maharashtra, India

ABSTRACT

Due to unique properties, ease of synthesis and functionalization, graphene-based nanocomposites show great potential in energy storage and conversion. These hybrid materials have excellent characteristics like high carrier mobility, faster recombination rate and long-time stability. In this review, the recent progresses in the synthesis and applications of graphene and its composites in the fields of energy storage (supercapacitors) and conversion (Solar cells) are summarized. This article highlights the challenges of the practical applications of graphene-based materials in supercapacitors and solar cells. Future research to develop new methodologies for the design and the synthesis of graphene-based nanocomposite are also proposed.

ARTICLE HISTORY
Received 23 August 2020
Revised 15 October 2020
Accepted 11 November 2020

KEYWORDS
Graphene; nano-composites; solar cells; supercapacitors

1. Introduction

The energy requirement of world is rising day by day and it is estimated that energy requirement will be double by 2050. Besides that, the energy production from conventional ways creates pollution of environment. So, renewable energy storage and conversion materials as well as their devices are topics of intense research.[1] To make the effective use of renewable energy, it is necessary to develop high-performance, low-cost and eco-friendly energy conversion and storage devices. Carbon materials are of great interest in research related to electrochemical devices due to their abundance, stability and eco-friendliness. Among different allotropes of carbon, graphene, is emerged as an excellent candidate for energy conversion and storage applications because of its unique properties, including high specific surface area (2630 m^2/g), good chemical stability and excellent electrical conductivity.[2]

2. History of graphene

Graphene appears frequently in our day to day life and it is topic of intense research for more than six decades, but the pioneer efforts were of two scientists from the University of Manchester, Prof. Andre Geim and Prof. Kostya Novoselov who successfully carried out the cleavage of one atom thick single layer of graphene from graphite. This was a milestone discovery in history of nanotechnology as it practically demonstrates the concept of single atom components from theory closer to reality. The various events in the discovery of single-layer graphene are as follows[3]:

- Simonio and Lyndiana Bernacotti developed the first pencil in 1560.
- John Desmond Bernal described the layered structure of graphite in 1924.
- The theoretical study of electronic properties of a single graphite layer was initiated by Philip Wallace in 1947.

3. J. W. McClure proposed the equation of wave function for single graphite layer in 1956

- In 1987, S. Mouras used the term graphene for the first time as a virtual expression of unit structure in graphite instead of a realistic form of carbon nanomaterials.

In 2004, Andre Geim and Konstantin Novoselov published very first article about the synthesis of graphene by mechanical exfoliation method in the Science magazine. For their groundbreaking experiments in the synthesis and characterization of this two-dimensional material Graphene, they received the Nobel Prize in Physics 2010.

CONTACT Bhagyashri Tale bhagyashritale@gmail.com Bajaj College of Science, Wardha 442001, India.

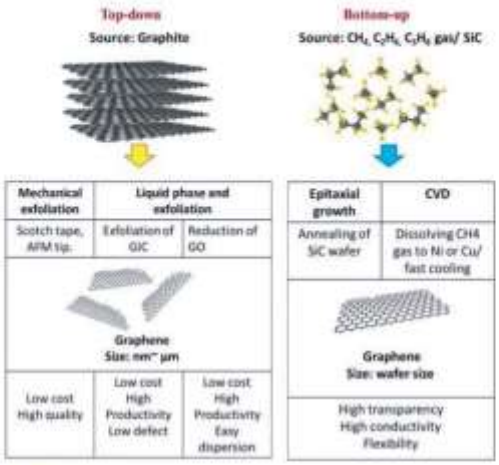

Figure 1. Top-down and bottom-up graphene synthesis approaches[96] (Adopted from Mahmoudi, T., Wang, Y., and Hahn, Y. B. (2018). Graphene and its derivatives for solar cells application. Nano Energy, 47, 51–65).

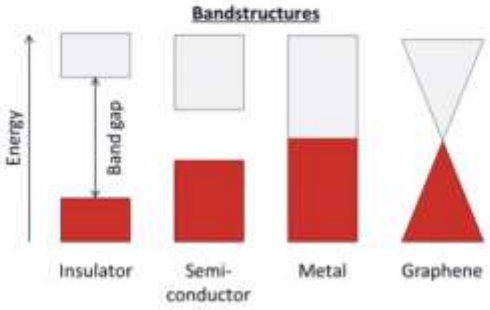

Figure 2. Band structure of different materials (Adopted from https://whitenoise.kinja.com/graphene-miracle-material-1575961841[97].

4. Synthesis of graphene

The amazing properties of graphene are mainly due to the defect of less pristine graphene. structural defects occur during growth and processing steps of graphene which alters their properties. Several scientists reported innovations in the mass and low-cost production of graphene with minimal defects for various applications. The approach for the synthesis of graphene is classified into two types:

(1) In top-down approach, the stack of graphene precursor (graphite) dissociates into individual atomic layer graphene sheet by overcoming Vander Waals forces of attraction.

(2) In bottom-up approach, carbon molecules obtained from various resources are used to develop the honeycomb structure of graphene sheet.

Various methods reported worldwide by many researchers for synthesis of graphene are given below:

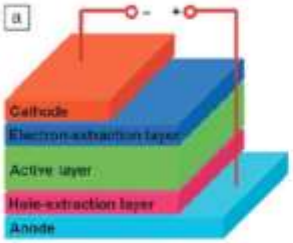

Figure 3. Device structure of polymer solar cell[73].

4.1. Mechanical exfoliation

This is top-down approach to produce high-quality graphene with minimal defects and high electron mobility. It is a repeated peeling process used to break weak Vander Waals forces present between the stacked layers of graphite to produce individual graphene sheets.[4–7]

4.2. Chemical exfoliation

Using this technique, good quality graphene suspension can be obtained from graphite by using aqueous electrolyteThis technique can be used for the production of conductive inks, transparent conducting oxides and electrodes for batteries and supercapacitors but cannot be used to generate large sheets of graphene required for device applications.[8–10]

4.3. Hummer's method

Synthesis of graphene oxide is reported by placing graphite in concentrated acid in the presence of an oxidizing agent. In this process, potassium permanganate is used in a solution of graphite, sodium nitrate, and sulfuric acid to generate graphene oxide and the reaction is terminated with the help of hydrogen peroxide. Many modifications are reported to make it more efficient and environmentally friendly.[11–13]

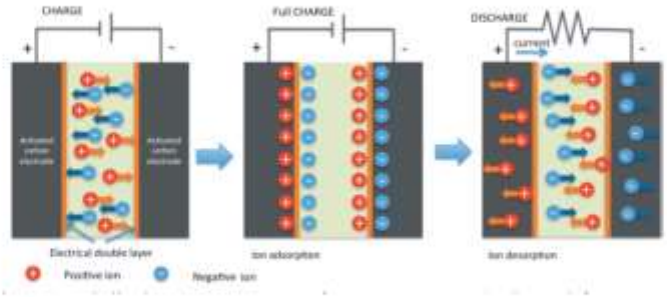

Figure 4. Charge and discharge processes of an EDLC.[98] (Adopted from Notarianni, M., Liu, J., Vernon, K., and Motta, N. (2016). Synthesis and applications of carbon nanomaterials for energy generation and storage. *Beilstein journal of nanotechnology*, *7*(1), 149–196.).

4.4. Chemical vapor deposition(CVD)

It involves pyrolysis of the precursor material to form carbon which is used to form the structure of graphene. This process is carried out in an inert environment by passing the gases like N_2/Ar.[14,15]

5. Properties of graphene

Major properties of graphene are as follows.[3,16,17]

- Graphene is considered as the first two dimensional crystalline material developed in lab.
- Graphene is a zero-gap semiconductor and it shows conductivity higher than copper.
- Graphene is a highly transparent material with great flexibility and stretchability.
- Graphene can be stretch up to 120% of its length and can recover its original shape.
- At room temperature, the thermal conductivity of Graphene is found to be more than diamond, graphite and any other known material.

This is a thinnest material **and** it can transmit up to 98% of light.

- Graphene is very strong. Graphene is 200 times stronger as compared to steel.

Graphene is a two-dimensional atomic sheet with sp^2-hybridized carbon atoms arranged in a Hexagonal manner. The s, p_x and p_y orbitals involve in σ-bond formation with neighbouring carbon atoms while p_z orbital forms π-bond . This makes one electron free. The C-C bond length is reported as 0.142 nm and the thickness of single layer of graphene is found to be 0.35 nm. The graphene is stable due to strong interatomic bonds present in the material which helps to overcome the thermal fluctuations and does not create dislocations or other crystal defects even at high temperatures

5.1. Electrical and thermal properties of graphene

Graphene is a zero-gap semiconductor or semi-metal. Its conduction band and valence band are same as semiconductor with no band gap. Here, holes and electrons act as charge carrier which leads to a very high electrical conductivity (more than copper). The π-bonds have high mobile pi (π) electrons that overlap together to form bonding π (valence) and antibonding π* (conduction) bands. The free moving electrons show high mobility and hence travel sub-micrometer distances without any scattering (ballistic transport). The electron mobility in graphene is found to be 15,000 $cm^2 \cdot V^{-1} \cdot s^{-1}$and its theoretical potential limits are 200,000 $cm^2 \cdot V^{-1} \cdot s^{-1}$ mainly due to the quality of graphene and the substrate. Graphene also shows the highest value of thermal conductivity because of the highly stable sp^2 bonding pattern and a two-dimensional nature. The experimental values are found to be in the range of 3000– 5000 $Wm^{-1}K^{-1}$.

5.2. Thermal and mechanical properties of graphene

The study of mechanical properties of single-layer graphene was done by atomic force microscopy technique and it is reported as strongest material ever tested. Thermal conductivity was found in the range of 3000–5000 $Wm^{-1}K^{-1}$. Graphene shows an extraordinary tensile strength, i.e.,130 GPa which is found to be higher than 0.4 GPa of A36 steel and 0.375 GPa of Kevlar (Aramid) fibers. The values of Spring constant and Young's modulus values were reported to be 1–5 Nm^{-1} and 1TPa respectively.

Table 1. Summary of Supercapacitor work based on graphene-based composite.

Material	Capacitance	Reference
Fluorographene	7 $F g^{-1}$	[98]
Cyanographene	97 $F g^{-1}$	[100]
Graphene acid	86 $F g^{-1}$	[100]
5-Ethynylpyrimidinegraphene	188 $F g^{-1}$	[101]
Graphene-dicarboxylic acid	326 $F g^{-1}$	[98]
Graphene-dicarboxylic acid conjugated with tetraaminophthalocyanine	936 $F g^{-1}$	[102]
Inkjet-printed graphene/PANI	82 Fg^{-1} @ 10 mVs1	[103]
PANI–GO	475 Fg^{-1} @ 0.4 Ag^{-1}	[104]
PANIGRAPHENE (PG100:1)	25 mF cm^{-2} @ 5 m Vs^{-1}	[105]
PANI–GO	25 mF cm^{-2} @ 5mVs^{-1}	[106]
PANI-GO	355 Fg^{-1} @ 0.5 Ag^{-1}	[107,108]
Graphene/PANI	408 Fg^{-1} from CV at a scan rate of 5 mVs^{-1}	[109]
Graphene/PANI	233 Fg^{-1}	[31]
GO/PANI	GO/PANI: 827 Fg^{-1} from CV at a scan	[110]
RGO/PANI	rate of 1 mVs^{-1} RGO/PANI: 1129 Fg^{-1} from CV at a scan rate of 1 mVs^{-1}	
GO/PANI	320 Fg^{-1} at 0.1 Ag^{-1}	[111]
RGO/PANI	480 Fg^{-1} at 0.1 Ag^{-1}	
Graphene/PANI	1046 Fg^{-1} from CV at a scan rate of 1 mVs^{-1}	[112]
RGO/PANI	361 Fg^{-1} at 0.3 Ag^{-1}	[113]
Graphene/PANI Paper	763 Fg^{-1} at 1 Ag^{-1}	[114]
RGO/PANI	257 Fg^{-1} at 0.1 Ag^{-1}	[115]
GO/PANI	448 Fg^{-1} at 0.5 Ag^{-1}	[116]
Crumpled graphene/ CNT/PANI	456 Fg^{-1} at 0.1 Ag^{-1}	[117]
RGO/PANI	438.8 Fg^{-1} at 0.5 Ag^{-1}	[118]
Graphene/PPy	165 Fg^{-1} at 1 Ag^{-1} at end of 1000th cycle	[119]
GO/PPy	417 Fg^{-1} from CV (scan rate: 100 mVs^{-1}) 267 Fg^{-1} from CV (scan rate: 100 mVs^{-1})	[119]
RGO/PPy	249 Fg^{-1} at 0.3 Ag^{-1}	[120]
RGO/PPy	420 Fg^{-1} at 0.1 Ag^{-1} 240 Fg^{-1} at 5 Ag^{-1}	[121]
RGO/PPy nanowire	728 Fg^{-1} at 0.5 Ag^{-1} 675 Fg^{-1} at 2.5 Ag^{-1}	[122]
Exfoliated graphene/ PPy	351 Fg^{-1} at 1 Ag^{-1}	[123]
Graphene/PPy Nanotubes	514 Fg^{-1} at 0.2 Ag^{-1} 420 Fg^{-1} at 1 Ag^{-1}	[124]
RGO/PPy	440 $mFcm^{-2}$ at 0.5 $mAcm^{-2}$	[125]
Sulfonated graphene/PPy	310 Fg^{-1} at 0.3 Ag^{-1}	[111]
Graphene/PEDOT	HCl: 304 Fg^{-1} from CV at a scan rate of 10 mVs^{-1} H_2SO_4: 261 Fg^{-1} from CV at a scan rate of 10 mVs^{-1}	[126]
RGO/PEDOT	108 Fg^{-1} at 0.3 Ag^{-1}	[127]
Graphene/PEDOT	270 Fg^{-1} at 1 Ag^{-1}	[128]
RGO/PEDOT	213 Fg^{-1} at 0.5 Ag^{-1}	[129]
Hallow RGO/PEDOT	304.5 $mFcm^{-2}$ at 0.08 $mAcm^{-2}$	[130]
RGO/PEDOT:PSS	367 Fg^{-1} at 1 Ag^{-1}	[131]

5.3. Optical properties of graphene

In Graphene, there is no gap between the conduction and valence band and it touches each other at Dirac point which leads to strong interaction of Dirac Fermions with electromagnetic radiation. Pristine graphene layer has thickness equal to only one atom and it can absorb 2.3% of the white light. The wide range of spectral absorption of pristine graphene is due to the

Table 2. Performance summary of solar cells studied by different research groups.

Cell structure	Eff (%)	Reference
TiO_2– graphene	6.49%	[132]
TiO_2– graphene	6.49%	[133]
TiO_2– graphene	15.6%	[134]
TiO_2– graphene sulfide	1.68%	[135]
Silicon	17%	[136]
Organic molecules or polymers	5%	[136]
Hybrid solar cell	22–23%	[136]
Graphene nanoplatelets	5%	[137]
rGO–PANI	6.15%	[138]
TiO2/RGO	7.46	[81]
Dye-sensitized solar cells based on TiO_2 nanoparticles	4.81%	[139]
Dye-sensitized solar cells based on PANI/graphene	7.70	[140]
Dye-sensitized solar cells based on PANI-RGO	7.84	[141]
Dye-sensitized solar cells based on Ppy/RGO	6.45	[142]
Dye-sensitized solar cells based on PANI/graphene	6.09	[143]
dye-sensitized solar cells (DSSC) were fabricated using graphene-TiO2composite	4.28%	[144]
2D graphene	6.97%	[145]
Dye-Sensitized Solar Cells by using GrapheneTiO_2 Composites	6.86%	[146]
A dye-sensitized solar cell (DSSC) based on graphene–TiO_2composite photoelectrode	4.28%	[147]
DSSC based on pure TiO_2 photoelectrode	3.11%	[147]
Dye-sensitized Solar Cell using Graphene-TiO_2	7.1%	[148]
. DSSCs based on TiO2@RGO hybrid photoanodes with a graphene content of 1.6 wt %	7.68%	[82]
DSSC based on Polyaniline/graphene (1 wt%) complex	6.71	[149]
DSSC based on Polyaniline/graphene (8 wt%) complex	7.78	[149]
DSSC based on Polyaniline/graphene (15 wt%) complex	6.89	[149]
DSSC based on Polyaniline-graphene (10 wt%)/GO) n (n = 10)	7.88	[150]
DSSC based on Polyaniline-graphene (10 wt%)/GO) n (n = 5)	6.61	[150]
DSSC based on Polyaniline-graphene (8 wt%)/GO) n (n = 10)	7.83	[150]
DSSC based on Polyaniline-graphene (8 wt%)/GO) n (n = 5)	6.03	[150]
DSSC based on Polyaniline-graphene (4 wt%)/GO) n (n = 10)	6.38	[150]
DSSC based on Polyaniline-graphene (4 wt%)/GO) n (n = 5)	4.21	[150]
DSSC based on Graphene/TiO_2	9.2	[151]
DSSC based on TiO_2/graphene nanocomposite (0.5 wt%)	5.41	[152]
DSSC based on TiO_2 only	4.11	[152]
DSSC based on TiO_2/graphene nanocomposite (1.6 wt%)	3.69	[152]
DSSC based on TiO_2/graphene nanocomposite (0.4 wt%)	2.82	[152]
DSSC based on TiO_2 only	2.49	[152]
DSSC based on Graphene (1.5 wt%)/TiO_2	4.20	[153]
DSSC based on TiO_2 only	3.17	[153]
JDSSC based on TiO_2/graphene composite	3.98	[153]
DSSC based on TiO_2 only	1.45	[153]

contribution from both interband and intraband optical transitions. The optical absorption of single-layer graphene in visible region takes place mainly due to interband transitions which are independent of frequency. The optical absorption in the far-infrared region is mainly due to intraband transitions or free carrier absorption.

Hence, graphene shows excellent thermal management applications especially in micro- and nano-electronics.

6. Solar cells

A solar cell, or photovoltaic cell, is an electrical device which is used to converts the energy of light into electricity. In electric power generation by use of renewable energy resources instead of conventional fossil-fuels is rapidly increasing. Among renewable energy resources which are used for electric power generation, solar photovoltaics (PVs) are the fastest growing resource.[18] After hydro and wind energy, solar energy is the third largest renewable energy resource of electric power generation in the world.[19]

The motivating factors for the replacement of conventional fossil-fuels by solar PVs for electric power generation are

> Price of fossil fuels is increasing day by day and they are limited while the source of solar energy is free and abundant.[20,21]

> Use of Fossil-fuels pollutes the environment while solar PV's does not release any pollutant.[22,23]

> Use of fossil-fuels contribute to global warming while solar PV's mitigate this issue.

> Solar PV's requires less maintenance and operational costs.[24]

> Among renewable energy sources, solar PVs provide the highest power density.[25,26]

> More than100 countries in the world are using solar PVs.[24]

> In order to encourage investments, governments declared financial assistance for solar electricity generation.[27–31] PV cell is the basic component of PV systems. Basically, PV cell is a semiconductor diode in which P–N junction is exposed to the light.[32]

Despite all the above advantages of solar PV systems, there are some challenges.

> PV systems do not create emissions during their operation, but these technologies are not completely emission-free. A lifecycle assessment (LCA) of solar PV cells is found to be divided into three phases; manufacturing, operation and recycling. It is observed that, Manufacturing phase is responsible for most of GHG emissions (around 90 percent) while recycling phase lowers GHG emissions[33]

> Currently, the efficiency of solar PV cells is low, hence cost of electricity produced from them is high. Hence, researchers are taking effort to increase the efficiency of solar cells so as to reduce the cost of produced electricity .[19–22]

Because of such drawbacks, they are generally combined with carbon materials which are known as hybrid supercapacitors.[54,55] In study the electrical properties of a supercapacitor, three electrochemical measurement techniques are generally used: cyclic voltammetry (CV), galvanostatic charging/discharging and electrochemical impedance measurements.[56]

Some important characteristics of an EDLC which should be considered to maximize the performance of the device are:

- The appropriate specific surface area of the electrodes so as to increase the capacitance
- The conductivity of the electrodes to minimize the power density losses
- The resistance to any oxidation/reduction at the surface of the electrode to achieve good stability and performance
- Sufficient size distribution of the pores so that it should match with the size of the electrolyte ions
- Good electrochemical stability of the electrolyte material in the voltage operating range of the device
- Low interconnected resistance of the electrolyte material
- Good wettability of the electrolyte material on the electrode.[52]

8. Challenges associated with manufacture and use of graphene

(i) Graphene is expensive and it is difficult to manufacture.
(ii) It is difficult to obtain monolayer graphene every time during synthesis of Graphene. If thickness of graphene is more than 10 layers of graphene, the properties resemble graphite more than graphene.
(iii) Because of above reasons, results of graphene synthesis are not very reproducible.
(iv) Graphene is not suitable for its application as a transistor since it does not have an off state and it cannot be switched off completely.
(v) Graphene is a hydrophobic material and hence it cannot be used in water-oriented applications like in humidity sensor, water filters.

9. Applications of graphene

Graphene has wide range of applications. During the last decade, graphene is a topic of interest in the field of research due to their exceptional electrical, optical and mechanical properties. Graphene can significantly improve the properties of existing products and to develop new materials with novel functionalities. Some of the applications are[3, 57–59].

9.1. Graphene – metal oxide/graphene – polymer composites for supercapacitor study

Energy storage is the major topic of interest for researchers and scientists. Graphene has extremely high surface area of ~2600 m^2g^{-1} and it is an ideal material for electrostatic charge storage such as in supercapacitors. Supercapacitors are different from capacitors as charge storage is not done by the insulator material which is present in between the electrodes but by the electrodes which are dipped in the electrolytic solution. Graphene with high surface area and high porosity can store more ions as compared to activated carbon. The specific capacitance of a Graphene-based supercapacitor is found to be five times more than of the activated carbon-based supercapacitor. Researchers are working for lightweight, low-cost, elastic with high mechanical strength graphene-based supercapacitors to reduce and ultimately replace the use of fossil fuels for energy.

The performance of hybrid structures is found to be better than those of pure graphene, GO, rGO, or pure metal oxides due to synergistic effects of both graphene and Metal-oxides. The graphene in the hybrid-structure has various advantages such as high surface area, ultra-thin thickness, excellent electrical and thermal conductivity, mechanical flexibility, while metal oxides have high chemical functionality, and other electrochemical properties. Consequently, graphene can be an ideal 2D membrane for growing tiny nanoparticles with very distinct structures and precious morphologies for constituting a three-dimensional interconnected conductive porous network, with enhanced the electrical conductivity and the charge transport. The other advantages of using hybrid structures are:

It can prevent the volume change and particle agglomeration of metal-oxides during the process of charging-discharging;

2) Oxygen-containing functional groups on GO, rGO imparts good interfacial bonding and electrical contacts between graphene and metal oxides; and

3) Metal-oxide nanoparticles suppress the re-stacking of graphene layers to get continuous, porous, interconnected network structure is with highest achievable power density and capacitance in supercapacitors. Thus, graphene-metal oxide hybrid-materials with all remarkable

properties turn it into a more efficient material for supercapacitor electrode applications.[58]

Hybrid nanocomposites obtained from graphene and polymers also show excellent mechanical, electrical properties and large specific surface areas are particularly suitable for supercapacitor applications. Polymers with a good electrical conductivity and a high pseudo-capacitance are required to prepare such nanocomposites. Such hybrid materials show enhanced electrochemical performance in supercapacitor devices due to the synergetic effects of graphene and polymers which combines the unique properties of the individual components.[60,61]Thus Along with energy conversion, energy storage (as in supercapacitors and batteries) is also important and for many practical applications, high energy-storage capability, high power-delivery capability, and long cycle life are necessary. Due to the unique characteristics of graphene, much effort has been taken to study the applications of graphene in high-performance supercapacitors and batteries.[46,62–66] Metal oxide shows high specific capacitance and low resistance makes it simpler to construct supercapacitors with high energy and power. A special attention was toward manganese dioxide MnO_2 as an electrode material for supercapacitors because of their low cost, excellent capacitive performance in aqueous electrolytes and environmental benignity. Different conducting polymers are widely used as supercapacitor electrode material due to its ease of production and low cost. Conducting polymers shows a relatively high conductivity, capacitance and equivalent series resistance as compared to carbon-based electrode materials. In conducting polymers reduction-oxidation process stores and releases charge.[67] So, graphene – metal oxide/graphene – polymer composites are topic of interest for supercapacitor study.

Researchers have been working on a pathway to improve the performance of supercapacitors, and meet that demand for increased storage capacity. Recently, Mojtaba et al suggested a new path to develop further miniaturized on-chip energy storage systems, which are compatible with silicon electronics and can support the power demand to operate integrated smart systems.[68]

9.2. Graphene-metal oxide/graphene-polymer composites for photovoltaic study

Inorganic semiconductor materials, such as amorphous silicon, gallium arsenide, and sulfide salts, have been widely used in conventional photovoltaic cells, where free electrons and holes are generated directly upon photon absorption. Although a power conversion efficiency (PCE) of more than 40% is achieved by using inorganic semiconductor materials in solar cells, the widespread use of inorganic solar cells is still limited due to difficulties in modifying the bandgap of inorganic semiconductors and high costs associated with the elaborate fabrication processes including elevated temperature and high vacuum. These inorganic solar cells are very much expensive than the conventional grid electricity. Alternative approaches with organic or polymer materials have gained considerable attention due to their low cost, light weight, flexibility, and solution processability.[61, 69–74]

9.3. Dye-sensitized solar cells (DSSCs)

As compared to other types of solar cells, DSSCs are different. They consist of a semiconducting material (e.g. TiO_2) with a photosensitive dye as the anode which is coupled with an electrolyte solution and a pure metal cathode (e.g. Platinum). Graphene has a number of favorable properties so that the loading efficiency of the dye molecules can be increased by increasing the interfacial area and enhancing the conductivity of the electrons. The proper ratio of graphene and TiO_2 is necessary for achieving an efficient system. The valence electrons from graphene get excited to the TiO_2 conduction band through the Graphene-TiO_2 interface, so as to separate the holes and the electrons. So, about 1% graphene is needed for this separation and the introduction of higher graphene concentrations into the matrix reduces the transmittance. The use of graphene in DSSCs increases the light scattering phenomenon at the photoanode, provides an efficiency that is 39% greater than that of pure TiO_2 electrodes and efficiently disperses the dye molecules.[74] In the photovoltaic study done by Morais et_al, the influence of different amounts of RGO in the TiO_2 film was investigated and it was compared to pristine TiO_2 films. The best solar cells made up of TiO_2/RGO films were obtained with 2.0 wt % RGO.[75] At the national level, several national laboratories and universities have been working on PV cell based on graphene-metal oxide nanocomposites.[76–86]

Thus, Dye-sensitized solar cells have gained attention in field of research because of their low production costs, ease of fabrication, lighter weight property, eco-friendliness and recyclable advantages, optical properties regardless of its low-efficiency output as compared to conventional silicon solar cell.[87] Dye-sensitized solar cells containing TiO2 are found to be more efficient. It consists of a dye-sensitized nanocrystalline TiO_2 film, an electrolyte with an I-/I3-redox couple and a Pt counter-

properties turn it into a more efficient material for supercapacitor electrode applications.[58]

Hybrid nanocomposites obtained from graphene and polymers also show excellent mechanical, electrical properties and large specific surface areas are particularly suitable for supercapacitor applications. Polymers with a good electrical conductivity and a high pseudo-capacitance are required to prepare such nanocomposites. Such hybrid materials show enhanced electrochemical performance in supercapacitor devices due to the synergetic effects of graphene and polymers which combines the unique properties of the individual components.[60,61]Thus Along with energy conversion, energy storage (as in supercapacitors and batteries) is also important and for many practical applications, high energy-storage capability, high power-delivery capability, and long cycle life are necessary. Due to the unique characteristics of graphene, much effort has been taken to study the applications of graphene in high-performance supercapacitors and batteries.[46,62–66] Metal oxide shows high specific capacitance and low resistance makes it simpler to construct supercapacitors with high energy and power. A special attention was toward manganese dioxide MnO_2 as an electrode material for supercapacitors because of their low cost, excellent capacitive performance in aqueous electrolytes and environmental benignity. Different conducting polymers are widely used as supercapacitor electrode material due to its ease of production and low cost. Conducting polymers shows a relatively high conductivity, capacitance and equivalent series resistance as compared to carbon-based electrode materials. In conducting polymers reduction-oxidation process stores and releases charge.[67] So, graphene – metal oxide/graphene – polymer composites are topic of interest for supercapacitor study.

Researchers have been working on a pathway to improve the performance of supercapacitors, and meet that demand for increased storage capacity. Recently, Mojtaba et al suggested a new path to develop further miniaturized on-chip energy storage systems, which are compatible with silicon electronics and can support the power demand to operate integrated smart systems.[68]

9.2. Graphene-metal oxide/graphene-polymer composites for photovoltaic study

Inorganic semiconductor materials, such as amorphous silicon, gallium arsenide, and sulfide salts, have been widely used in conventional photovoltaic cells, where free electrons and holes are generated directly upon photon absorption. Although a power conversion efficiency (PCE) of more than 40% is achieved by using inorganic semiconductor materials in solar cells, the widespread use of inorganic solar cells is still limited due to difficulties in modifying the bandgap of inorganic semiconductors and high costs associated with the elaborate fabrication processes including elevated temperature and high vacuum. These inorganic solar cells are very much expensive than the conventional grid electricity. Alternative approaches with organic or polymer materials have gained considerable attention due to their low cost, light weight, flexibility, and solution processability.[61, 69–74]

9.3. Dye-sensitized solar cells (DSSCs)

As compared to other types of solar cells, DSSCs are different. They consist of a semiconducting material (e.g. TiO_2) with a photosensitive dye as the anode which is coupled with an electrolyte solution and a pure metal cathode (e.g. Platinum). Graphene has a number of favorable properties so that the loading efficiency of the dye molecules can be increased by increasing the interfacial area and enhancing the conductivity of the electrons. The proper ratio of graphene and TiO_2 is necessary for achieving an efficient system. The valence electrons from graphene get excited to the TiO_2 conduction band through the Graphene-TiO_2 interface, so as to separate the holes and the electrons. So, about 1% graphene is needed for this separation and the introduction of higher graphene concentrations into the matrix reduces the transmittance. The use of graphene in DSSCs increases the light scattering phenomenon at the photoanode, provides an efficiency that is 39% greater than that of pure TiO_2 electrodes and efficiently disperses the dye molecules.[74] In the photovoltaic study done by Morais et_al, the influence of different amounts of RGO in the TiO_2 film was investigated and it was compared to pristine TiO_2 films. The best solar cells made up of TiO_2/RGO films were obtained with 2.0 wt % RGO.[75] At the national level, several national laboratories and universities have been working on PV cell based on graphene-metal oxide nanocomposites.[76–86]

Thus, Dye-sensitized solar cells have gained attention in field of research because of their low production costs, ease of fabrication, lighter weight property, eco-friendliness and recyclable advantages, optical properties regardless of its low-efficiency output as compared to conventional silicon solar cell.[87] Dye-sensitized solar cells containing TiO2 are found to be more efficient. It consists of a dye-sensitized nanocrystalline TiO_2 film, an electrolyte with an I-/I3-redox couple and a Pt counter-

electrode. In addition to practical applications as an alternative energy source, these devices are also useful from a scientific point of view, as it converts light in to electrical energy through complex energy and charge transfer processes. The overall energy conversion efficiency depends on the individual properties of the constituents of the cell. To enhance their performance requires better understanding of processes in energy conversion and controlling the properties of each component.[88] ICPs are organic polymers which conduct electricity. It may have metallic conductivity or can be semiconductors. The advantage of ICPs is their processability, mainly by dispersion.[53, 89–94] So, Graphene – metal oxide/Graphene – Polymer composites are topic of interest for Photovoltaic study.

Typical efficiency of Polycrystalline silicon solar cells is 13% to 16%. Thin-Film solar cells (TFSC), are made by depositing one or several thin layers of photovoltaic material onto a substrate. Different types of TFSCs are categorized by which photovoltaic material is deposited onto the substrate: Amorphous silicon (a-Si), cadmium telluride (CdTe), copper indium gallium selenide (CIS/CIGS), polymer solar panels and organic photovoltaic cells (OPC). Thin-film modules have reached efficiencies of 7–13%. Recently, researchers have used graphene to develop a perovskite-silicon solar cell – a promising new solar technology – with an impressive conversion efficiency of 26.3%.[95]

10. Conclusion

As discussed herein, the extensive study of graphene-based nanocomposite with unique structure and properties offer a great opportunity to deal with challenges of energy conversion and storage. Many of fundamental properties of graphene are discovered, but there are still much new discoveries to be made in properties of graphene-based materials and in their applications. Due to unique properties, ease of synthesis and functionalization, graphene-based nanocomposites show great potential in energy storage and conversion. These hybrid materials have excellent characteristics like excellent mechanical, electrical properties and large specific surface areas and long-time stability. So, it is interesting to study the graphene to open up new possibilities to produce graphene-based nanocomposites and to better understand their properties as well as related phenomenon.

Disclosure statement

No potential conflict of interest was reported by the authors.

References

[1] Mahmood, N.; Zhang, C.; Yin, H.; Hou, Y. Graphene-based Nanocomposites for Energy Storage and Conversion in Lithium Batteries, Supercapacitors and Fuel Cells. *J. Mater. Chem. A.* 2014, *2*(1), 15–32.

[2] Choi, H. J.; Jung, S. M.; Seo, J. M.; Chang, D. W.; Dai, L.; Baek, J. B. Graphene for Energy Conversion and Storage in Fuel Cells and Supercapacitors. *Nano Energy*. 2012, *1* (4), 534–551.

[3] Module 29: ChemApplications: Graphene and Its Applications, Online Refresher Course in Chemistry for Higher Education Faculty. (2018). @swayam.gov.in

[4] Lee, X. J.; Hiew, B. Y. Z.; Lai, K. C.; Lee, L. Y.; Gan, S.; Thangalazhy-Gopakumar, S.; Rigby, S. Review on Graphene and Its Derivatives: Synthesis Methods and Potential Industrial Implementation. *J. Taiwan Inst. Chem. Eng.* 2019, *98*, 163–180.

[5] Shams, S. S.; Zhang, R.; Zhu, J. Graphene Synthesis: A Review. *Mater. Science-Poland*. 2015, *33*(3), 566–578.

[6] Choi, W.; Lahiri, I.; Seelaboyina, R.; Kang, Y. S. Synthesis of Graphene and Its Applications: A Review. *Crit. Rev. Solid State Mater. Sci.* 2010, *35*(1), 52–71.

[7] Yi, M.; Shen, Z. A Review on Mechanical Exfoliation for the Scalable Production of Graphene. *J. Mater. Chem. A.* 2015, *3*(22), 11700–11715.

[8] Jibrael, R. L.; Mohammed, M. K. Structural and the Optical Properties of Graphene Prepared by Electrochemical Exfoliation Technique. *Al-Nahrain J. Sci.* 2016, *19*(4), 71–77.

[9] Tripathi, P.; Patel, C.; Prakash, R.; Shaz, M. A.; Srivastava, O. N., 2013. Synthesis of High-quality Graphene through Electrochemical Exfoliation of Graphite in Alkaline Electrolyte. arXiv preprint arXiv:1310.7371.

[10] Parvez, K.; Yang, S.; Feng, X.; Müllen, K. Exfoliation of Graphene via Wet Chemical Routes. *Synth. Met.* 2015, *210*, 123–132.

[11] Narasimharao, K.; Venkata Ramana, G.; Sreedhar, D.; Vasudevarao, V. Synthesis of Graphene Oxide by Modified Hummers Method and Hydrothermal Synthesis of graphene-NiO Nano Composite for Supercapacitor Application. *J. Mater. Sci. Eng.* 2016, *5* (284), 2169–0022.

[12] Alam, S. N.; Sharma, N.; Kumar, L. Synthesis of Graphene Oxide (GO) by Modified Hummers Method and Its Thermal Reduction to Obtain Reduced Graphene Oxide (Rgo). *Graphene*. 2017, *6*(1), 1–18.

[13] Krane, N.;. *Preparation of Graphene*; Physics of Nanoscale Carbon: Selected Topics in Physics. 2011.

[14] Colombo, L.; Li, X.; Ruoff, R. S. *U.S. Patent No. 8,470,400*; U.S. Patent and Trademark Office: Washington, DC. 2013.

[15] https://investorintel.com/sectors/technology-metals/technology-metals-intel/understanding-graphene-part-3/

[16] Atif, R.; Shyha, I.; Inam, F. Mechanical, Thermal, and Electrical Properties of Graphene-epoxy nanocomposites—A Review. *Polymers*. 2016, *8*(8), 281.

[17] Gong, J. R.; ed., *Graphene: Synthesis, Characterization, Properties and Applications*; BoD–Books on Demand, 2011.

[18] Jordehi, A. R.;. Parameter Estimation of Solar Photovoltaic (PV) Cells: A Review. *Renewable Sustainable Energy Rev.* 2016, *61*, 354–371.
[19] Bai, J.; Liu, S.; Hao, Y.; Zhang, Z.; Jiang, M.; Zhang, Y. Development of a New Compound Method to Extract the Five Parameters of PV Modules. *Energy Conversion Manage.* 2014, *79*, 294–303.
[20] Shafiee, S.; Topal, E. When Will Fossil Fuel Reserves Be Diminished? *Energy Policy.* 2009, *37*(1), 181–189.
[21] Apergis, N.; Payne, J. E. Renewable Energy, Output, CO2 Emissions, and Fossil Fuel Prices in Central America: Evidence from a Nonlinear Panel Smooth Transition Vector Error Correction Model. *Energy Econ.* 2014, *42*, 226–232.
[22] Shivalkar, R. S.; Jadhav, H. T.; Deo, P.; Feasibility Study for the Net Metering Implementation in Rooftop Solar PV Installations across Reliance Energy Consumers. In 2015 International Conference on Circuits, Power and Computing Technologies [ICCPCT-2015] 2015 March (pp. 1–6). IEEE.
[23] Wang, Y.; Zhou, S.; Huo, H. Cost and CO2 Reductions of Solar Photovoltaic Power Generation in China: Perspectives for 2020. *Renewable Sustainable Energy Rev.* 2014, *39*, 370–380.
[24] The Solar Singularity Is Nigh. 2015. http://www.greentechmedia.com/ articles.
[25] Sundareswaran, K.; Sankar, P.; Nayak, P. S. R.; Simon, S. P.; Palani, S. Enhanced Energy Output from a PV System under Partial Shaded Conditions through Artificial Bee Colony. *IEEE Trans. Sustainable Energy.* 2014, *6*(1), 198–209.
[26] Energyatthecrossroads;2015. http://home.cc.umanitoba.ca/_vsmil/pdf_pubs/oecd.pdf
[27] Dusonchet, L.; Telaretti, E. Economic Analysis of Different Supporting Policies for the Production of Electrical Energy by Solar Photovoltaics in Western European Union Countries. *Energy Policy.* 2010, *38*(7), 3297–3308.
[28] Solangi, K. H.; Islam, M. R.; Saidur, R.; Rahim, N. A.; Fayaz, H. A Review on Global Solar Energy Policy. *Renewable Sustainable Energy Rev.* 2011, *15*(4), 2149–2163.
[29] Branker, K.; Pearce, J. M. Financial Return for Government Support of Large-scale Thin-film Solar Photovoltaic Manufacturing in Canada. *Energy Policy.* 2010, *38*(8), 4291–4303.
[30] Campoccia, A.; Dusonchet, L.; Telaretti, E.; Zizzo, G. Comparative Analysis of Different Supporting Measures for the Production of Electrical Energy by Solar PV and Wind Systems: Four Representative European Cases. *Solar Energy.* 2009, *83*(3), 287–297.
[31] Timilsina, G. R.; Kurdgelashvili, L.; Narbel, P. A. Solar Energy: Markets, Economics and Policies. *Renewable Sustainable Energy Rev.* 2012, *16*(1), 449–465.
[32] Iwan, A.; Chuchmała, A. Perspectives of Applied Graphene: Polymer Solar Cells. *Prog. Polym. Sci.* 2012, *37*(12), 1805–1828.
[33] Where-is-solar-power-used-the-most. 2015. http://energyinformative.org
[34] Karaveli, A. B.; Soytas, U.; Akinoglu, B. G. Comparison of Large Scale Solar PV (Photovoltaic) and Nuclear Power Plant Investments in an Emerging Market. *Energy.* 2015, *84*, 656–665.
[35] Clò, S.; D'Adamo, G. The Dark Side of the Sun: How Solar Power Production Affects the Market Value of Solar and Gas Sources. *Energy Econ.* 2015, *49*, 523–530.
[36] Köberle, A. C.; Gernaat, D. E.; van Vuuren, D. P. Assessing Current and Future Techno-economic Potential of Concentrated Solar Power and Photovoltaic Electricity Generation. *Energy.* 2015, *89*, 739–756.
[37] Lungenschmied, C.; Dennler, G.; Neugebauer, H.; Sariciftci, S. N.; Glatthaar, M.; Meyer, T.; Meyer, A. Flexible, Long-lived, Large-area, Organic Solar Cells. *Solar Energy Mater. Solar Cells.* 2007, *91*(5), 379–384.
[38] Parida, B.; Iniyan, S.; Goic, R. A Review of Solar Photovoltaic Technologies. *Renewable Sustainable Energy Rev.* 2011, *15*(3), 1625–1636.
[39] Jannat, A.; Rahman, M. F.; Khan, M. S. H. A Review Study of Organic Photovoltaic Cell. *Int. J. Sci. Eng. Res.* 2013, *4*(1), 1–6.
[40] Savinije, T. J.;, Delf ChemTech, Organic Solar Cells, Faculty of Applied sciencesDelf University of Technology.
[41] Lu, M.;. *Supercapacitors: Materials, Systems, and Applications*; John Wiley and Sons, 2013.
[42] Becker, H. I.; General Electric Co, 1957. Low Voltage Electrolytic Capacitor. U.S. Patent 2,800,616.
[43] Boos, D. L.; Standard Oil Co. 1970. Electrolytic Capacitor Having Carbon Paste Electrodes. U.S. Patent 3,536,963.
[44] Murphy, T. C.; Wright, R. B.; Sutula, R. A., 1997. US Department of Energy Electrochemical Capacitor Development and Testing Activities. In Proceedings of the Symposium on Electrochemical Capacitors II, (Vol.96, pp. 258–267). The Electrochemical Society, Inc.: Pennington, NJ.
[45] Notarianni, M.; Liu, J.; Vernon, K.; Motta, N. Synthesis and Applications of Carbon Nanomaterials for Energy Generation and Storage. *Beilstein J. Nanotechnol.* 2016, *7*(1), 149–196.
[46] Zhang, L. L.; Zhao, X. S. Carbon-based Materials as Supercapacitor Electrodes. *Chem. Soc. Rev.* 2009, *38* (9), 2520–2531.
[47] Birss, V. I.; Conway, B. E.; Wojtowicz, J.; 1997. The Role and Utilization of Pseudocapacitance for Energy Storage by Supercapacitors.
[48] Frackowiak, E.; Beguin, F.; Carbon Materials for the Electrochemical Storage of Energy in Capacitors. *Carbon.* 2001, *39*(6), 937–950.
[49] Zheng, J. P.; Cygan, P. J.; Jow, T. R.; Hydrous Ruthenium Oxide as an Electrode Material for Electrochemical Capacitors. *J. Electrochem. Soc.* 1995, *142*(8), 2699.
[50] Timperman, L.; Béguin, F.; Frackowiak, E.; Anouti, M. Comparative Study of Two Protic Ionic Liquids as Electrolyte for Electrical Double-layer Capacitors. *J. Electrochem. Soc.* 2013, *161*(3), A228.
[51] Elcap Supercapacitor. Wikipedia http://en.wikipedia.org/wiki/Supercapacitor (accessed Dec 12, 2015).
[52] McEvoy, A.; Castaner, L.; Markvart, T.; *Solar Cells: Materials, Manufacture and Operation*; Academic Press, 2012.
[53] Zhang, K.; Zhang, L. L.; Zhao, X. S.; Wu, J.; Graphene/polyaniline Nanofiber Composites as Supercapacitor Electrodes. *Chem. Mater.* 2010, *22*(4), 1392–1401.

[54] Sugimoto, W.; Yokoshima, K.; Murakami, Y.; Takasu, Y.; Charge Storage Mechanism of Nanostructured Anhydrous and Hydrous Ruthenium-based Oxides. *Electrochim. Acta.* 2006, *52*(4), 1742–1748.
[55] Wang, J.; Controlled-potential Techniques. In *Analytical Electrochemistry*, 2006; pp 67–114.
[56] Coroş, M.; Pogăcean, F.; Măgeruşan, L.; Socaci, C.; Pruneanu, S.; A Brief Overview on Synthesis and Applications of Graphene and Graphene-based Nanomaterials. *Front. Mater. Sci.* 2019, *13*(1), 23–32.
[57] Geim, A. K.; Novoselov, K. S. The Rise of Graphene, Nanoscience and Technology: A Collection of Reviews from Nature Journals. *World Sci.* 2010, 11–19.
[58] Mattevi, C.; Colléaux, F.; Kim, H.; Lin, Y. H.; Park, K. T.; Chhowalla, M.; Anthopoulos, T. D. Solution-processable Organic Dielectrics for Graphene Electronics. *Nanotechnology.* 2012, *23*(34), 344017.
[59] Khedekar, V. V.; Zaeem, S. M.; Das, S. Graphene-metal Oxide Nanocomposites for Supercapacitors: A Perspective Review. *Adv. Mater. Lett.* 2018, *9*, 02–19.
[60] Zhang, X.; Samori, P.; Graphene/polymer Nanocomposites for Supercapacitors. *ChemNanoMat.* 2017, *3*(6), 362–372.
[61] Liu, J.; Xue, Y.; Zhang, M.; Dai, L.; Graphene-based Materials for Energy Applications. *Mrs Bull.* 2012, *37* (12), 1265–1272.
[62] Stoller, M. D.; Park, S.; Zhu, Y.; An, J.; Ruoff, R. S.; Graphene-based Ultracapacitors. *Nano Lett.* 2008, *8* (10), 3498–3502.
[63] Zhu, Y.; Murali, S.; Stoller, M. D.; Velamakanni, A.; Piner, R. D.; Ruoff, R. S.; Microwave Assisted Exfoliation and Reduction of Graphite Oxide for Ultracapacitors. *Carbon.* 2010, *48*(7), 2118–2122.
[64] Zhu, Y.; Stoller, M. D.; Cai, W.; Velamakanni, A.; Piner, R. D.; Chen, D.; Ruoff, R. S. Exfoliation of Graphite Oxide in Propylene Carbonate and Thermal Reduction of the Resulting Graphene Oxide Platelets. *ACS Nano.* 2010, *4*(2), 1227–1233.
[65] Wang, Y.; Shi, Z.; Huang, Y.; Ma, Y.; Wang, C.; Chen, M.; Chen, Y. Supercapacitor Devices Based on Graphene Materials. *J. Phys. Chem. C.* 2009, *113*(30), 13103–13107.
[66] Iro, Z. S.; Subramani, C.; Dash, S. S. A Brief Review on Electrode Materials for Supercapacitor. *Int. J. Electrochem. Sci.* 2016, *11*(12), 10628–10643.
[67] Seelajaroen, H.; Bakandritsos, A.; Otyepka, M.; Zbořil, R.; Sariciftci, N. S. Immobilized Enzymes on Graphene as Nanobiocatalyst. *ACS Appl. Mater. Interfaces.* 2019, *12*(1), 250–259.
[68] https://www.sciencedaily.com/releases/2020/08/200803092131.htm.
[69] Swanson, R. M.; *Photovoltaics Res. Appl.*. 2006, *14*, 443–453.
[70] Johnson, J.; *Chem. Eng. News*. 2004, *82*, 13.
[71] Krebs, F. C.; *Polymer Photovoltaics: A Practical Approach*; SPIE-International Society for Optical Engineering, 2008.
[72] Sariciftci, N. S.; Sun, S. S. *Organic Photovoltaics: Mechanism, Materials, and Devices*. Taylor and Francis: New York, 2005.
[73] Morais, A.; Alves, J. P. C.; Lima, F. A. S.; Lira-Cantu, M.; Nogueira, A. F. Enhanced Photovoltaic Performance of Inverted Hybrid Bulk-heterojunction Solar Cells Using TiO2/reduced Graphene Oxide Films as Electron Transport Layers. *J. Photonics Energy*. 2015, *5*(1), 057408.
[74] Using Graphene Based Solar Cells for Solar Applications Saved from URL. https://www.azonano.com/article.aspx?ArticleID=4565
[75] Dutta, M.; Sarkar, S.; Ghosh, T.; Basak, D.; ZnO/graphene Quantum Dot Solid-state Solar Cell. *J. Phys. Chem. C.* 2012, *116*(38), 20127–20131.
[76] Chen, J.; Li, C.; Eda, G.; Zhang, Y.; Lei, W.; Chhowalla, M.; Milne, W. I.; Deng, W. Q.; Incorporation of Graphene in Quantum Dot Sensitized Solar Cells Based on ZnO Nanorods. *Chem. Commun.* 2011, *47*(21), 6084–6086.
[77] Hsu, Y. C.; Chen, G. L.; Lee, R. H.; Graphene Oxide Sheet-polyaniline Nanocomposite Prepared through In-situ Polymerization/deposition Method for Counter Electrode of Dye-sensitized Solar Cell. *J. Polym. Res.* 2014, *21*(5), 440.
[78] Wan, L.; Wang, B.; Wang, S.; Wang, X.; Guo, Z.; Xiong, H.; Dong, B.; Zhao, L.; Lu, H.; Xu, Z.; et al. Water-soluble Polyaniline/graphene Prepared by in Situ Polymerization in Graphene Dispersions and Use as Counter-electrode Materials for Dye-sensitized Solar Cells. *React. Funct. Polym.* 2014, *79*, 47–53.
[79] Jung, J. W.; Jo, J. W.; Jung, E. H.; Jo, W. H.; Recent Progress in High Efficiency Polymer Solar Cells by Rational Design and Energy Level Tuning of Low Bandgap Copolymers with Various Electron-withdrawing Units. *Org. Electron.* 2016, *31*, 149–170.
[80] Cong, H. P.; Chen, J. F.; Yu, S. H.; Graphene-based Macroscopic Assemblies and Architectures: An Emerging Material System. *Chem. Soc. Rev.* 2014, *43* (21), 7295–7325.
[81] He, B.; Tang, Q.; Wang, M.; Ma, C.; Yuan, S.; Complexation of Polyaniline and Graphene for Efficient Counter Electrodes in Dye-sensitized Solar Cells: Enhanced Charge Transfer Ability. *J. Power Sources.* 2014, *256*, 8–13.
[82] Wang, M.; Tang, Q.; Xu, P.; He, B.; Lin, L.; Chen, H.; Counter Electrodes from Polyaniline– Graphene Complex/graphene Oxide Multilayers for Dye–Sensitized Solar Cells. *Electrochim. Acta.* 2014, *137*, 175–182.
[83] Wang, M.; Tang, Q.; Chen, H.; He, B.; Counter Electrodes from Polyaniline– Carbon Nanotube Complex/graphene Oxide Multilayers for Dye-sensitized Solar Cell Application. *Electrochim. Acta.* 2014, *125*, 510–515.
[84] Cai, H.; Tang, Q.; He, B.; Wang, M.; Yuan, S.; Chen, H.; Self-assembly of Graphene Oxide/polyaniline Multilayer Counter Electrodes for Efficient Dye-sensitized Solar Cells. *Electrochim. Acta.* 2014, *121*, 136–142.
[85] Gong, J.; Sumathy, K.; Qiao, Q.; Zhou, Z.; Review on Dye-sensitized Solar Cells (Dsscs): Advanced Techniques and Research Trends. *Renewable Sustainable Energy Rev.* 2017, *68*, 234–246.
[86] Longo, C.; De Paoli, M. A.; Dye-sensitized Solar Cells: A Successful Combination of Materials. *J. Braz. Chem. Soc.* 2003, *14*(6), 898–901.

[87] Bavane, R. G.; 2014. Synthesis and Characterization of Thin Films of Conducting Polymers for Gas Sensing Applications.
[88] Tan, S.; Zhai, J.; Wan, M.; Meng, Q.; Li, Y.; Jiang, L.; Zhu, D.; Influence of Small Molecules in Conducting Polyaniline on the Photovoltaic Properties of Solid-state Dye-sensitized Solar Cells. *J. Phys. Chem. B.* 2004, *108* (48), 18693–18697.
[89] Tan, S.; Zhai, J.; Xue, B.; Wan, M.; Meng, Q.; Li, Y.; Jiang, L.; Zhu, D.; Property Influence of Polyanilines on Photovoltaic Behaviors of Dye-sensitized Solar Cells. *Langmuir.* 2004, *20*(7), 2934–2937.
[90] Wu, Q.; Xu, Y.; Yao, Z.; Liu, A.; Shi, G.; Supercapacitors Based on Flexible Graphene/polyaniline Nanofiber Composite Films. *ACS Nano.* 2010, *4*(4), 1963–1970.
[91] Inoue, M.; Navarro, R. E.; Inoue, M. B.; New Soluble Polyaniline: Synthesis, Electrical Properties and Solution Electronic Spectrum. *Synth. Met.* 1989, *30*(2), 199–207.
[92] Tahir, Z. M.; Alocilja, E. C.; Grooms, D. L.; Polyaniline Synthesis and Its Biosensor Application. *Biosens. Bioelectron.* 2005, *20*(8), 1690–1695.
[93] Zhu, P.; Nair, A. S.; Shengjie, P.; Shengyuan, Y.; Ramakrishna, S.; Facile Fabrication of TiO2–graphene Composite with Enhanced Photovoltaic and Photocatalytic Properties by Electrospinning. *ACS Appl. Mater. Interfaces.* 2012, *4*(2), 581–585.
[94] Zhang, H.; Wang, W.; Liu, H.; Wang, R.; Chen, Y.; Wang, Z.; Effects of TiO2 Film Thickness on Photovoltaic Properties of Dye-sensitized Solar Cell and Its Enhanced Performance by Graphene Combination. *Mater. Res. Bull.* 2014, *49*, 126–131.
[95] https://www.graphene-info.com/graphene-solar-panels
[96] Mahmoudi, T.; Wang, Y.; Hahn, Y. B.; Graphene and Its Derivatives for Solar Cells Application. *Nano Energy.* 2018, *47*, 51–65.
[97] https://whitenoise.kinja.com/graphene-miracle-material-1575961841
[98] Kötz, R.; Carlen, M. J. E. A. Principles and Applications of Electrochemical Capacitors. *Electrochim. Acta.* 2000, *45(15-16)*, 2483–2498.
[99] Chronopoulos, D. D.; Błoński, P.; Nováček, Z.; Jakubec, P.; Tomanec, O.; Bakandritsos, A.; Novotná, V.; Zbořil, R.; Otyepka, M.; Alkynylation of Graphene via the Sonogashira C–C Cross-coupling Reaction on Fluorographene. *Chem. Commun.* 2019, *55*(8), 1088–1091.
[100] Bakandritsos, A.; Jakubec, P.; Pykal, M.; Otyepka, M. Covalently Functionalized Graphene as a Supercapacitor Electrode Material. *FlatChem.* 2019, *13*, 25–33.
[101] Wang, Q.; Yan, J.; Fan, Z.; Wei, T.; Zhang, M.; Jing, X.; Mesoporous Polyaniline Film on Ultra-thin Graphene Sheets for High Performance Supercapacitors. *J. Power Sources.* 2014, *247*, 197–203.
[102] Zhang, Q.; Li, Y.; Feng, Y.; Feng, W.; Electropolymerization of Graphene Oxide/polyaniline Composite for High-performance Supercapacitor. *Electrochim. Acta.* 2013, *90*, 95–100.
[103] Channu, V. S. R.; Holze, R.; Rambabu, B.; Kalluru, R. R.; Synthesis and Characterization of PANI Nanostructures for Supercapacitors and Photoluminescence. *Iran. Polym. J.* 2012, *21*(7), 457–462.
[104] Luo, Z.; Zhu, L.; Zhang, H.; Tang, H.; Polyaniline Uniformly Coated on Graphene Oxide Sheets as Supercapacitor Material with Improved Capacitive Properties. *Mater. Chem. Phys.* 2013, *139*(2–3), 572–579.
[105] Liu, H.; Xu, B.; Jia, M.; Zhang, M.; Cao, B.; Zhao, X.; Wang, Y.; Polyaniline Nanofiber/large Mesoporous Carbon Composites as Electrode Materials for Supercapacitors. *Appl. Surf. Sci.* 2015, *332*, 40–46.
[106] Majumdar, D.; Functionalized-graphene/polyaniline Nanocomposites as Proficient Energy Storage Material: An Overview. *Innov. Ener. Res.* 2016, *5*(145), 2.
[107] Murugan, A. V.; Muraliganth, T.; Manthiram, A.; Rapid, Facile Microwave-solvothermal Synthesis of Graphene Nanosheets and Their Polyaniline Nanocomposites for Energy Storage. *Chem. Mater.* 2009, *21*(21), 5004–5006.
[108] Wang, D. W.; Li, F.; Zhao, J.; Ren, W.; Chen, Z. G.; Tan, J.; Wu, Z. S.; Gentle, I.; Lu, G. Q.; Cheng, H. M.; Fabrication of Graphene/polyaniline Composite Paper via in Situ Anodic Electropolymerization for High-performance Flexible Electrode. *ACS Nano.* 2009, *3*(7), 1745–1752.
[109] Wang, H.; Hao, Q.; Yang, X.; Lu, L.; Wang, X.; A Nanostructured Graphene/polyaniline Hybrid Material for Supercapacitors. *Nanoscale.* 2010, *2*(10), 2164–2170.
[110] Yan, J.; Wei, T.; Shao, B.; Fan, Z.; Qian, W.; Zhang, M.; Wei, F.; Preparation of a Graphene Nanosheet/polyaniline Composite with High Specific Capacitance. *Carbon.* 2010, *48*(2), 487–493.
[111] Zhang, J.; Zhao, X. S. Conducting Polymers Directly Coated on Reduced Graphene Oxide Sheets as High-performance Supercapacitor Electrodes. *J. Phys. Chem. C.* 2012, *116*(9), 5420–5426.
[112] Cong, H. P.; Ren, X. C.; Wang, P.; Yu, S. H.; Flexible Graphene–polyaniline Composite Paper for High-performance Supercapacitor. *Energy Environ. Sci.* 2013, *6*(4), 1185–1191.
[113] Li, Z. F.; Zhang, H.; Liu, Q.; Sun, L.; Stanciu, L.; Xie, J.; Fabrication of High-surface-area Graphene/polyaniline Nanocomposites and Their Application in Supercapacitors. *ACS Appl. Mater. Interfaces.* 2013, *5* (7), 2685–2691.
[114] Hassan, M.; Reddy, K. R.; Haque, E.; Faisal, S. N.; Ghasemi, S.; Minett, A. I.; Gomes, V. G.; Hierarchical Assembly of Graphene/polyaniline Nanostructures to Synthesize Free-standing Supercapacitor Electrode. *Compos. Sci. Technol.* 2014, *98*, 1–8.
[115] Jo, E. H.; Jang, H. D.; Chang, H.; Kim, S. K.; Choi, J. H.; Lee, C. M.; 3 D Network-Structured Crumpled Graphene/Carbon Nanotube/Polyaniline Composites for Supercapacitors. *ChemSusChem.* 2017, *10*(10), 2210–2217.
[116] Hong, X.; Zhang, B.; Murphy, E.; Zou, J.; Kim, F.; Three-dimensional Reduced Graphene Oxide/polyaniline Nanocomposite Film Prepared by Diffusion Driven Layer-by-layer Assembly for High-performance Supercapacitors. *J. Power Sources.* 2017, *343*, 60–66.

[117] Biswas, S.; Drzal, L. T.; Multilayered Nanoarchitecture of Graphene Nanosheets and Polypyrrole Nanowires for High Performance Supercapacitor Electrodes. *Chem. Mater.* 2010, *22*(20), 5667–5671.
[118] Bose, S.; Kim, N. H.; Kuila, T.; Lau, K. T.; Lee, J. H.; Electrochemical Performance of a Graphene–polypyrrole Nanocomposite as a Supercapacitor Electrode. *Nanotechnology.* 2011, *22*(29), 295202.
[119] Liu, Y.; Zhang, Y.; Ma, G.; Wang, Z.; Liu, K.; Liu, H. Ethylene Glycol Reduced Graphene Oxide/polypyrrole Composite for Supercapacitor. *Electrochim. Acta.* 2013, *88*, 519–525.
[120] Li, J.; Xie, H.; Li, Y.; Fabrication of Graphene Oxide/polypyrrole Nanowire Composite for High Performance Supercapacitor Electrodes. *J. Power Sources.* 2013, *241*, 388–395.
[121] Song, Y.; Xu, J. L.; Liu, X. X.; Electrochemical Anchoring of Dual Doping Polypyrrole on Graphene Sheets Partially Exfoliated from Graphite Foil for High-performance Supercapacitor Electrode. *J. Power Sources.* 2014, *249*, 48–58.
[122] Kashani, H.; Chen, L.; Ito, Y.; Han, J.; Hirata, A.; Chen, M.; Bicontinuous Nanotubular Graphene–polypyrrole Hybrid for High Performance Flexible Supercapacitors. *Nano Energy.* 2016, *19*, 391–400.
[123] Shu, K.; Wang, C.; Zhao, C.; Ge, Y.; Wallace, G. G.; A Free-standing Graphene-polypyrrole Hybrid Paper via Electropolymerization with an Enhanced Areal Capacitance. *Electrochim. Acta.* 2016, *212*, 561–571.
[124] Zuo, X.; Zhang, Y.; Si, L.; Zhou, B.; Zhao, B.; Zhu, L.; Jiang, X.; One-step Electrochemical Preparation of Sulfonated Graphene/polypyrrole Composite and Its Application to Supercapacitor. *J. Alloys Compd.* 2016, 688, 140–148.
[125] Alvi, F.; Ram, M. K.; Basnayaka, P. A.; Stefanakos, E.; Goswami, Y.; Kumar, A.; Graphene–polyethylenedioxythiophene Conducting Polymer Nanocomposite Based Supercapacitor. *Electrochim. Acta.* 2011, *56*(25), 9406–9412.
[126] Sun, D.; Jin, L.; Chen, Y.; Zhang, J. R.; Zhu, J. J.; Microwave-Assisted in Situ Synthesis of Graphene/PEDOT Hybrid and Its Application in Supercapacitors. *ChemPlusChem.* 2013, *78*(3), 227–234.
[127] Wen, J.; Jiang, Y.; Yang, Y.; Li, S.; Conducting Polymer and Reduced Graphene Oxide Langmuir–Blodgett Films: A Hybrid Nanostructure for High Performance Electrode Applications. *J. Mater. Sci.: Mater. Electron.* 2014, *25*(2), 1063–1071.
[128] Qu, G.; Cheng, J.; Li, X.; Yuan, D.; Chen, P.; Chen, X.; Wang, B.; Peng, H.; A Fiber Supercapacitor with High Energy Density Based on Hollow Graphene/conducting Polymer Fiber Electrode. *Adv.Mate.* 2016, *28*(19), 3646–3652.
[129] Islam, M. M.; Subramaniyam, C. M.; Akhter, T.; Faisal, S. N.; Minett, A. I.; Liu, H. K.; Konstantinov, K.; Dou, S. X.; Three Dimensional Cellular Architecture of Sulfur Doped Graphene: Self-standing Electrode for Flexible Supercapacitors, Lithium Ion and Sodium Ion Batteries. *J. Mater. Chem. A.* 2017, *5*(11), 5290–5302.
[130] Gao, Y.; Graphene and Polymer Composites for Supercapacitor Applications: A Review. *Nanoscale Res. Lett.* 2017, *12*(1), 387.
[131] Bube, R. H.; *Photoelectronic Properties of Semiconductors*; Cambridge University Press, 1992.
[132] Wang, J. T. W.; Ball, J. M.; Barea, E. M.; Abate, A.; Alexander-Webber, J. A.; Huang, J.; Saliba, M.; Mora-Sero, I.; Bisquert, J.; Snaith, H. J.; et al. Low-temperature Processed Electron Collection Layers of graphene/TiO2 Nanocomposites in Thin Film Perovskite Solar Cells. *Nano Lett.* 2014, *14*(2), 724–730.
[133] Tang, Y. B.; Lee, C. S.; Xu, J.; Liu, Z. T.; Chen, Z. H.; He, Z.; Cao, Y. L.; Yuan, G.; Song, H.; Chen, L.; et al. Incorporation of Graphenes in Nanostructured TiO2 Films via Molecular Grafting for Dye-sensitized Solar Cell Application. *ACS Nano.* 2010, *4*(6), 3482–3488.
[134] Orgil, K. 2018. Comparison of Organic and Inorganic Solar Photovoltaic Systems.
[135] Kavan, L.; Yum, J. H.; Grätzel, M. Optically Transparent Cathode for Dye-sensitized Solar Cells Based on Graphene Nanoplatelets. *Acs Nano.* 2011, *5*(1), 165–172.
[136] Das, S.; Sudhagar, P.; Kang, Y. S.; Choi, W. Graphene Synthesis and Application for Solar Cells. *J. Mater. Res.* 2014, *29*(3), 299–319.
[137] Zi, M.; Zhu, M.; Chen, L.; Wei, H.; Yang, X.; Cao, B. ZnO Photoanodes with Different Morphologies Grown by Electrochemical Deposition and Their Dye-sensitized Solar Cell Properties. *Ceram. Int.* 2014, *40*(6), 7965–7970.
[138] Sugathan, V.; John, E.; Sudhakar, K. Recent Improvements in Dye Sensitized Solar Cells: A Review. *Renewable Sustainable Energy Rev.* 2015, *52*, 54–64.
[139] Wang, Y. S.; Li, S. M.; Hsiao, S. T.; Yang, S. Y.; Tien, H. W.; Ma, C. C. M.; Hu, C. C. Thickness-self-controlled Synthesis of Porous Transparent Polyaniline-reduced Graphene Oxide Composites Towards Advanced Bifacial Dye-sensitized Solar Cells. *J. Power Sources.* 2014, *260*, 326–337.
[140] Liu, W.; Fang, Y.; Xu, P.; Lin, Y.; Yin, X.; Tang, G.; He, M. Two-step Electrochemical Synthesis of Polypyrrole/reduced Graphene Oxide Composites as Efficient Pt-free Counter Electrode for Plastic Dye-sensitized Solar Cells. *ACS Appl. Mater. Interfaces.* 2014, *6*(18), 16249–16256.
[141] Wang, G.; Xing, W.; Zhuo, S. The Production of Polyaniline/graphene Hybrids for Use as a Counter Electrode in Dye-sensitized Solar Cells. *Electrochim. Acta.* 2012, *66*, 151–157.
[142] Sun, S.; Gao, L.; Liu, Y. Enhanced Dye-sensitized Solar Cell Using graphene-TiO 2 Photoanode Prepared by Heterogeneous Coagulation. *Appl. Phys. Lett.* 2010, *96*(8), 083113.
[143] Yang, N.; Zhai, J.; Wang, D.; Chen, Y.; Jiang, L. Two-dimensional Graphene Bridges Enhanced Photoinduced Charge Transport in Dye-sensitized Solar Cells. *ACS Nano.* 2010, *4*(2), 887–894.
[144] Tsai, T. H.; Chiou, S. C.; Chen, S. M. Enhancement of Dye-sensitized Solar Cells by Using graphene-TiO2 Composites as Photoelectrochemical Working Electrode. *Int. J. Electrochem. Sci.* 2011, *6*(8), 3333–3343.
[145] Zhu, M.; Li, X.; Liu, W.; Cui, Y. An Investigation on the Photoelectrochemical Properties of Dye-sensitized

Solar Cells Based on graphene–TiO2 Composite Photoanodes. *J. Power Sources.* 2014, *262*, 349–355.

[146] Tu, W.; Zhou, Y.; Liu, Q.; Yan, S.; Bao, S.; Wang, X.; Xiao, M.; Zou, Z. An in Situ Simultaneous Reduction-hydrolysis Technique for Fabrication of TiO2-graphene 2D Sandwich-like Hybrid Nanosheets: Graphene-promoted Selectivity of Photocatalytic-driven Hydrogenation and Coupling of CO2 into Methane and Ethane. *Adv. Funct. Mater.* 2013, *23* (14), 1743–1749.

[147] Cheng, G.; Akhtar, M. S.; Yang, O. B.; Stadler, F. J. *ACS Appl. Mater. Interfaces.* 2013, *5*, 6635.

[148] He, B.; Tang, Q.; Wang, M.; Chen, H.; Yuan, S. Robust Polyaniline–graphene Complex Counter Electrodes for Efficient Dye-sensitized Solar Cells. *ACS Appl. Mater. Interfaces.* 2014, *6*(11), 8230–8236.

[149] Lee, D. H.; Song, D.; Kang, Y. S.; Park, W. I. Three-dimensional Monolayer Graphene and TiO2 Hybrid Architectures for High-efficiency Electrochemical Photovoltaic Cells. *J. Phys. Chem. C.* 2015, *119*(12), 6880–6885.

[150] Madhavan, A. A.; Ranjusha, R.; Daya, K. C.; Arun, T. A.; Praveen, P.; Sanosh, K. P.; Subramanian, K. R. V.; Nair, S. K. V.; Nair, A. S.; Balakrishnan, A. Molten Salt Synthesized TiO2-graphene Composites for Dye Sensitized Solar Cells Applications. *Sci. Adv. Mater.* 2014, *6*(4), 828–834.

[151] Zhu, G.; Pan, L.; Sun, H.; Liu, X.; Lv, T.; Zhou, N.; Sun, Z. Enhanced Performance of Dye-sensitized Solar Cells by Graphene-incorporated Nanocrystalline TiO2 Films. *Nanosci. Nanotech. Lett.* 2013, *5*(2), 154–158.

[152] Zhu, Y.; Meng, X.; Cui, H.; Jia, S.; Dong, J.; Zheng, J.; Zhao, J.; Wang, Z.; Li, L.; Zhang, L.; et al. Graphene Frameworks Promoted Electron Transport in Quantum Dot-sensitized Solar Cells. *ACS Appl. Mater. Interfaces.* 2014, *6*(16), 13833–13840.

[153] Zabihi, F.; Tebyetekerwa, M.; Xu, Z.; Ali, A.; Kumi, A. K.; Zhang, H.; Jose, R.; Ramakrishna, S.; Yang, S. Perovskite Solar Cell-hybrid Devices: Thermoelectrically, Electrochemically, and Piezoelectrically Connected Power Packs. *J. Mater. Chem. A.* 2019, *7*(47), 26661–26692.

7 Comprehensive study of spin field effect transistors with co-graphene ferromagnetic contacts

Journal of Magnetism and Magnetic Materials 517 (2021) 167410

Contents lists available at ScienceDirect

Journal of Magnetism and Magnetic Materials

journal homepage: www.elsevier.com/locate/jmmm

Comprehensive study of spin field effect transistors with co-graphene ferromagnetic contacts

Neetu Gyanchandani[a], Santosh Pawar[b], Prashant Maheshwary[a], Kailash Nemade[c,*]

[a] JD College of Engineering and Management, Nagpur 441501, India
[b] School of Engineering, Dr. A.P.J. Abdul Kalam University, Indore 452016, India
[c] Department of Physics, Indira Mahavidyalaya, Kalamb 445401, India

ARTICLE INFO

Keywords:
Ferromagnetic contacts
Spintronics
Graphene
Spin field effect transistor

ABSTRACT

Two-dimensional graphene is considered potent candidate for the development of spintronics technology. Present work reports study of graphene-based spin-Field Effect Transistors.

(s-FET) of two types namely, Top-Gated s-FET and Back-Gated s-FET. The Ohmic contact behavior was analyzed as Co-Graphene nanosheets (CGNs) used as ferromagnetic electrode for both types of s-FETs. The magnetoresistance (MR) study is conducted for both devices as a function of temperature and gate voltage. Study shows that MR monotonically reduces as temperature increases. For greater insight into about the functioning of device, spin-polarization values were estimated at different temperatures. Switching action in both the devices was analyzed and finally it is found that Top-Gated Type s-FET shows appropriate switching action.

1. Introduction

Spin-field effect transistor (s-FET) is the new type of electronic device, which comes with additional feature of spin-based magnetoresistance. In s-FET, switching action can be achieved by spin precession or dephasing of spin-polarized carriers injected into the channel. The concept of s-FET was first time coined by Datta and Das [1]. After this wide range of s-FETs were proposed by many researchers on the basis of their operating principles [2,3]. In semiconductor spintronics, various phenomenon such as spin–orbit interaction, coupling of electron spin to external electric fields, spin transport through semiconductor channel with spin-orbit coupling and spin-Hall effect plays very crucial role [4]. By employing magnetic field and controlling gate bias, the parallel and antiparallel spin-state of electron and subsequently magnetization of the ferromagnetic contacts can be achieved. In this way, output currents depend on spin-state of electron and magnetization. The high current state is associated with parallel spin state of electron, however low current is associated with anti- parallel spin state [5,6].

For s-FET operation, three major conditions must be satisfied. First requirement is the injection of spin-polarized electrons from ferromagnetic source into 2-dimensional electron gas channel. Second requirement is the transport of electrons through 2-dimensional electron gas channel without losing spin state. Third requirement is the detection of spin-state electron by ferromagnetic drain [7]. Besides these requirements, two main challenges are associated with s-FET, first is the leakage current in the off-state and second is the spin relaxation in the channel. But these issues can be resolved by two approaches, by choosing materials with a long spin de-phasing length and strong spin–orbit coupling [8].

The performance of s-FET is also affected by conductivity mismatch problem between ferromagnetic electrode and semiconductor channel. To resolve the issue of conductivity mismatch, few reports suggested that the use of graphene as tunnel barrier is appropriate option, because the significant lateral transport and low out of-plane conductivity of graphene [9–12].

Another reason for graphene appropriateness for spintronics application is that it has unique characteristics related to spin-polarized electrons. The spin-polarized electron in graphene can travel tens of microns without losing spin orientation at room temperature. This characteristic of graphene makes it enable for long-distance spin communication in future spintronic technologies [13–15].

In the present study, Cobalt-Graphene nanosheets are chosen as ferromagnetic material for source and drain contacts due to long spin relaxation distances of graphene than any other traditional metals and semiconductors [16–18]. In addition to this, another feature of graphene is that, it can conduct spin current up to macroscopic distances due to weak spin-orbit and hyperfine couplings in carbon materials [19].

Here, two types of s-FET namely Top-Gated s-FET and Back-Gated s-FET are reported. In this study, Co-Graphene nanosheets (CGNs) were

* Corresponding author.
E-mail address: krnemade@gmail.com (K. Nemade).

https://doi.org/10.1016/j.jmmm.2020.167410
Received 7 April 2020; Received in revised form 23 August 2020; Accepted 16 September 2020
Available online 22 September 2020
0304-8853/

used as ferromagnetic contact for source and drain purpose. The Ohmic nature of contacts are also discussed in this work. The magnetoresistance curves were recorded as the function of temperature and gate voltage. Switching action for both the types of devices is also studied.

2. Experimentation

2.1. Preparation of Co-Graphene nanosheets

The necessary amount of Co-Graphene nanosheets (CGNs) were prepared by ex-situ approach. The graphene for preparation was obtained by using previously reported method [20]. To prepare the CGNs, 10 g of graphene sheets were dissolved in 50 ml acetic acid under rigorous magnetic stirring for 30 min. After magnetic stirring, solution was kept under probe-sonication for 1 h. During this step, separate solution of 0.5 g of $Co(NO_3)_3$ was dissolved in 10 ml of acetic acid and kept for 30 min under magnetic stirring. This solution was added in former solution in drop-wise manner under constant magnetic stirring. Final solution was then filtered and washed several times by deionized water. The black colored precipitate was collected and dried at 100 °C in oven.

To form homogeneous magnetic system, CGNs were kept for heating in the temperature range of 100 to 500 °C in stepwise manner with an interval of 100 °C. At each temperature value, sample was heated for 60 min. Similarly, the sample was allowed to cool at 400, 300, 200 and 100 °C each for 60 min.

2.2. Materials characterization techniques

The structural study of CGNs was completed using X-ray diffraction (XRD) technique (Rigaku Miniflex-XRD; Wavelength = 1.5406 Å). The surface study of CGNs was performed by field emission scanning electron microscopy (FESEM) on SEM instrument, Model: ZEISS SIGMA operating at 5 kV ETH voltage. The elemental analysis was done using an energy dispersive X-ray analysis (EDAX) instrument, Model: EAG AN461. The magnetic behavior of CGNs was studied using Vibrating Sample Magnetometer technique (Quantum Design Model- PAR 155) having specifications as Range: 0.00001 to 10,000 emu and Magnetic field: −10 to +10 kOe.

2.3. Device fabrication and measurements

2.3.1. Top-Gated s-FET

For the fabrication of Top-Gated s-FET, required heavily doped n-type silicon wafer was procured from India-Mart of thickness 500 μm. Before starting the device fabrication process, n-type silicon wafer was kept for cleaning process to break the bonds between substrate and contaminants present on substrate in the form of grease, adsorbed water molecule and air borne dust.

In the cleaning process of substrate, firstly the substrate was washed with mild-detergent solution (Labolene) and then with distilled water. Subsequent to this step, substrate was kept in NaOH solution for the removal of acidic contaminations and then again washed with distilled water. Finally, the substrate was kept in alcohol vapors. After completion of cleaning process, the substrate was kept for etching to pattern Co-Graphene based ferromagnetic electrodes. In this process, buffered hydrofluoric acid was used as etchants. The remaining area of substrate was masked with kapton tape. The Co-Graphene based ferromagnetic material was used as source and drain contacts on substrate.

The electrode material that is Co-Graphene and gate were deposited by using photolithography technique. The electrode material Co-Graphene was achieved by depositing cobalt on previously deposited graphene. After deposition of FM contacts as source and drain, polyvinyl acetate was deposited on the channel between FM electrodes using spin-coating technique. The fabricated device has channel length of the order of 1.21 μm and channel width 14.25 μm. Fig. 1(a) depicts the schematic drawing of Top-Gated s-FET structure and Fig. 1(b) shows the scanning electron micrograph of s-FET, with all necessary components displayed on SEM image with circuitry arrangement.

2.3.2. Back Gated s-FET

All necessary components required for the s-FET fabrication procured from India-Mart. Before the fabrication of device, substrate was cleaned according to the process discussed in the earlier section. To fabricate the back-gate configuration type s-FET [21], the heavily doped n-type silicon having 1 μm thick thermally oxidized SiO_2 layer on the surface was used as the substrate. For the formation of 2-dimensional electron gas condition, heavily doped n-type semiconducting layer was fixed on thermally oxidized SiO_2 layer. The thermally oxidized SiO_2 layer of substrate was used as gate insulator, whereas the heavily doped n-type silicon part of substrate was used as gate electrode. The Co-Graphene based ferromagnetic electrodes as source and drain were designed on 2-dimensional electron gas layer by photolithography. The fabricated device has channel length of the order 1.2 μm and channel width 12.1 μm. Fig. 2(a) depicts the schematic drawing of back-gated type s-FET structure and Fig. 2(b) shows the scanning electron micrograph of s-FET, with all necessary components of s-FET displayed on SEM image with circuitry arrangement.

2.3.3. Device characterization and measurements

The transport measurements for Top-Gated s-FET and Back-Gated s-FET were performed using Physical Properties Measurements System (PPMS) made by Quantum Design.

The Ohmic contact characteristics of devices were studied using current-voltage (IV) curves. The performance of s-FET was analyzed by measuring the electrical resistance as a function of magnetic field. It is well known that electrical resistance can be tuned into the high and low-resistance state by sweeping the magnetic field.

Magnetoresistance (MR) is defined as, $MR\% = [(R_{ap} - R_p)/R_p] \times 100$, where R_{ap} is magnetization vectors of two electrodes are antiparallel and R_p is the magnetization vectors of two electrodes are parallel. MR curves were recorded for different values of temperature and gate voltage.

3. Results and discussion

3.1. XRD, SEM and VSM study

Fig. 3(a) shows the XRD pattern of CGNs, comprised of two broad peaks at 26.3° and 44.2° with Miller indices (0 0 2) and (1 0 0), respectively. These peaks are signature peaks of graphene [22]. No separate peak was obtained for Co, which indicates that the orientation of graphene layers is unchanged. Fig. 3(b) depicts the SEM images and elemental X-ray mapping of CGNs. The SEM image confirmed that Co nanocrystals are uniformly spread on graphene surface and elemental analysis also confirmed that Co nanocrystals are distributed over the graphene surface. Actually, the pure graphene is a diamagnetic material due to sp^2 hybridization. The graphene used in this study was synthesized using electrochemical exfoliation of graphite, which certainly contains defects, which imprint magnetic features into graphene [23]. Many reports demonstrated that magnetic properties can be instilled in graphene, by adding ferromagnetic metal in graphene [24–26]. In present study, magnetic properties imprinted in graphene by decorating its surface with Co particles. Fig. 3(c) shows the hysteresis loops of CGNs recorded at room temperature (298 K). The good quality hysteresis loops of CGNs indicates that prepared CGNs comprises of good ferromagnetic ordering. The values of coercivity, remanant magnetization and saturation magnetization estimated from hysteresis loop were 537 Gauss, 0.2002 emu/gm and 0.761 emu/g, respectively. It shows that Co-graphene system comprise the ferromagnetic-like behavior, which characteristically correlate with the existence of interaction between graphene and Co Also, electronic structure modifications and

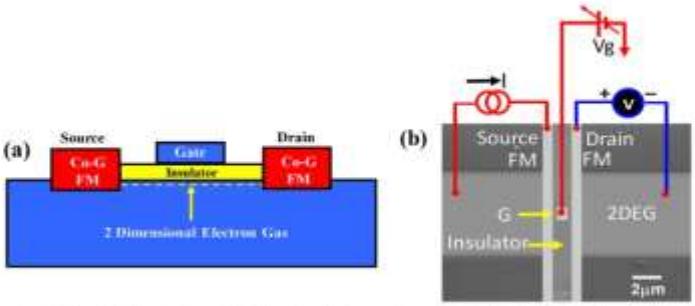

Fig. 1. (a) Schematic drawing of Top-Gated s-FET structure and (b) Scanning electron micrograph of s-FET. For better understanding, all necessary components of s-FET are displayed on SEM image with circuitry arrangement.

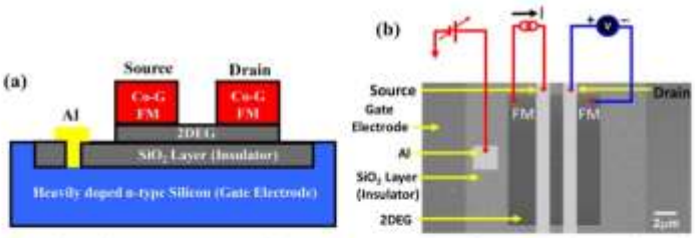

Fig. 2. (a) Schematic drawing of Back-Gated Type s-FET structure and (b) Scanning electron micrograph of s-FET. For better understanding, all necessary components of s-FET were displayed on SEM image with circuitry arrangement.

symmetry breaking in Co-graphene system improves the magnetic properties of system [27].

Fig. 3(d) shows the magnetoconductance curve of CGNs as a function of the magnetic field at different temperatures. The magnetoconductance in CGNs is attributed to weak spin-orbit coupling. Magnetoconductance gives insight to study microscopic behavior of ferromagnetic materials. This parameter also helps to identify scattering centers in ferromagnetic materials [28]. The positive value of magnetoconductance was obtained on entire scale of magnetic field for all temperatures. Similarly, the magnetoresistance curve did not exhibit

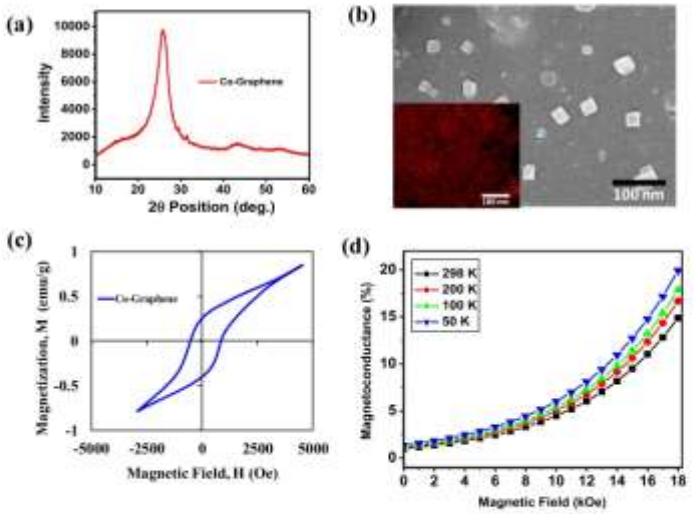

Fig. 3. (a) XRD pattern, (b) SEM images with elemental X-ray mapping of elements (inset), (c) VSM hysteresis loop and (d) Magnetoconductance as a function of magnetic field at different temperature of CGNs.

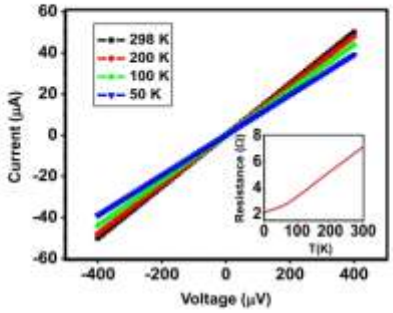

Fig. 4. Current-voltage curves of device at different temperature and inset shows variation of resistance curve with temperature at zero magnetic field.

any peak in low magnetic field. This indicates intrinsic impurities or defects have negligible contribution in magnetoconductance [29]. The magnetoconductance curve with no peak reflects that good quality interfaces formed between graphene and cobalt.

3.2. Ohmic contact study

Fig. 4 displays the current-voltage (I-V) curves of the device recorded at different temperatures (50, 100, 200 and 298 K) to study the behavior of contacts between CGNs and 2-dimensional electron gas. The linear nature of curve indicates that contact used in fabrication of Top-Gated s-FET device has Ohmic nature. Inset of Fig. 4 shows that the resistance increases with increasing temperature, indicates that 2-dimensional electron gas in device behaves like metal. The behavior of curve also suggests that 2-dimensional electron gas channel works like conducting thin film between two CGNs based FM electrodes [30]. The results obtained for Ohmic study have good agreement with other reports in literature. The researcher's team of Samsung Advanced Institute of Technology studied critically the effect of graphene insertion on the behavior of Ohmic contacts in metal-semiconductor. This work concluded that metal deposited graphene has reduced the work

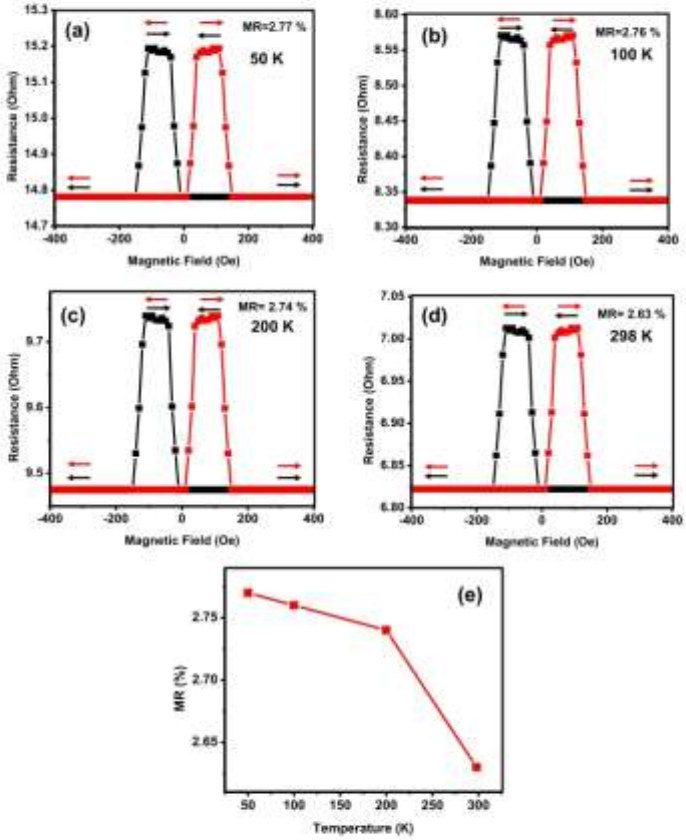

Fig. 5. Magnetoresistance ratio of device (Top-Gated s-FET) as a function of magnetic field at temperature (a) 50 K, (b) 100 K, (c) 200 K and (d) 298 K. Magnetoresistance ratio is high for the antiparallel magnetization configuration and low for parallel magnetization configuration. (e) Variation of magnetoresistance ratio with temperature.

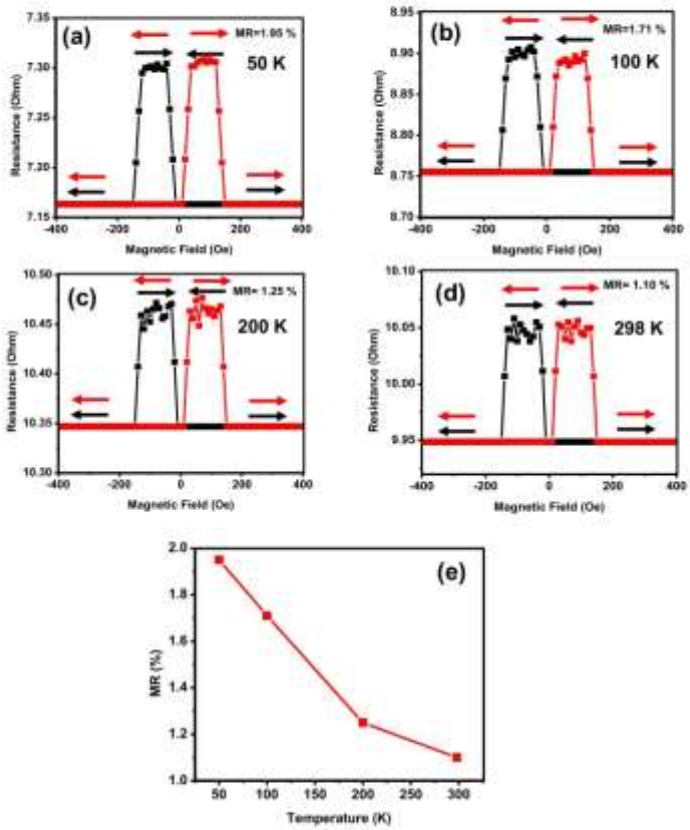

Fig. 6. Magnetoresistance ratio of device (Back-Gated s-FET) as a function of magnetic field at temperature (a) 50 K, (b) 100 K, (c) 200 K and (d) 298 K. (e) Variation of magnetoresistance ratio with temperature.

Table 1
MR and spin-polarization values of CGNs based ferromagnetic electrodes used for fabrication of Top-Gated s-FET and Back-Gated s-FET.

Temperature (K)	MR %	Amplitude of MR curve (Ω)	Spin-Polarization
Top-Gated s-FET			
50	2.77	0.42	0.374
100	2.76	0.23	0.276
200	2.74	0.26	0.294
298	2.63	0.18	0.244
Back-Gated s-FET			
50	1.95	0.14	0.216
100	1.71	0.15	0.223
200	1.25	0.13	0.208
298	1.10	0.11	0.191

function of graphene. In other words, it reduces the height of Schottky barrier at the metal-semiconductor junction [31]. Another report on graphene based Ohmic contact at metal–semiconductor junctions supports that insertion of graphene between metal-semiconductor reduces the Schottky barrier height and enhances the Ohmic characteristics [32].

3.3. Variation of magnetoresistance with temperature

Fig. 5(a–d) shows a series of MR curves for Top-Gated s-FET at different temperatures ranging from 50 K to 298 K. The highest value of MR% was found to be 2.77% at 50 K. Fig. 5(e) shows the variation of MR% with temperature. Similarly, Fig. 6(a–d) shows the MR curves for Back-Gated s-FET recorded at different temperatures ranging from 50 K to 298 K. For Back Gated s-FET, the highest value of MR% was found to be 1.95% at 50 K. Fig. 6(e) shows the variation of MR% with temperature.

In both type of s-FETs, magnitude of the MR monotonically decreases as the temperature increases. This behavior of MR curve attributed to inelastic scattering with phonons, surface states, and thermal smearing of energy distribution in the ferromagnetic material [33,34].

Whereas the highest value of MR for both devices at 50 K, attributed to the higher value of spin-polarization. For Top-Gated s-FET, the value of spin-polarization was found to be 0.374 and for Back-Gated s-FET, its value was 0.216. This study also discloses that spin-polarization in ferromagnetic materials reduces by increasing temperature.

In spintronics technology, spin polarization of ferromagnetic material plays a very crucial role. Because, ferromagnetic materials are the ideal foundation for spin polarized carriers because of their intrinsic

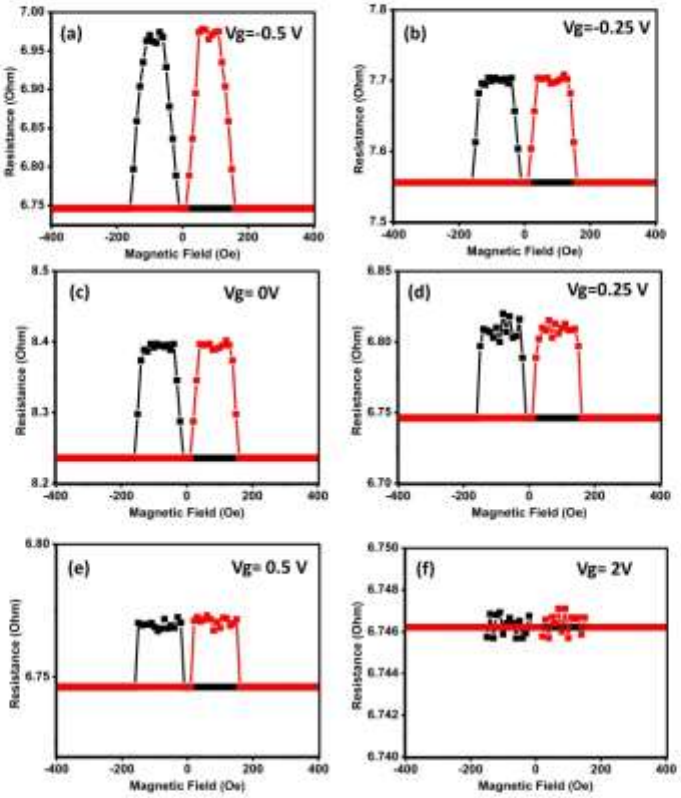

Fig. 7. Gate-controlled MR measurements in Top-Gated s-FET at gate voltage (a) −0.5 V, (b) 0.25 V, (c) 0 V, (d) 0.25 V, (e) 0.5 V and (f) 2 V at room temperature 298 K.

spin polarization. Ferromagnetic materials have an imbalance among the number of charges having particular spin orientation at the Fermi level. This imbalance in spin orientation at the Fermi level results in net spin polarization of the conduction electrons. The spin polarization P of a material is defined by (Eq. (1)),

$$P = \frac{n_\uparrow - n_\downarrow}{n_\uparrow + n_\downarrow} \quad (1)$$

where, n↑ and n↓ are spin orientation of charges in material.

The relation between the MR and polarization of ferromagnetic electrode can be approximated as (Eq. (2)),

$$MR = \frac{2P_1P_2e^{\frac{-d}{\lambda_s}}}{1 - P_1P_2e^{\frac{-d}{\lambda_s}}} \quad (2)$$

where d is the length of the trajectories of the electrons. λs is spin diffusion length. Assuming efficient spin transport, we could say surviving probability factor $\{\exp(-d/\lambda_s)\} \sim 1$.

In the present study, both contacts materials that is CGNs based FM electrodes have been used, hence their spin-polarization value is assumed as same (P1 = P2 = P). Thus, by using Eqs. (1) and (2), the spin-polarization values at different temperatures were estimated as listed in Table 1. To the best of our knowledge, this is one of the first reports which speaks about the spin-polarization of Co-graphene system for spin-field effect transistor application. Dayen et al recently published detailed report on two-dimensional van der Waals spin-interfaces and magnetic-interfaces. This report discussed some 2D ferromagnets and graphene-based materials with considerable value of spin-polarization for efficient spin transmission and dynamic control through exotic heterostructures [35].

Therefore, comparison of these reports with other studies is not appropriate. The study reported by Zhou et al and co-workers shows that graphene-passivated cobalt as a spin-polarized electrode with positive spin polarization properties [36].

3.4. Gate controlled magnetoresistance

Fig. 7(a–f) shows the series of MR variation with gate voltage ranging from −0.5 V to 2 V for Top-Gated s-FET. The results reveal that by increasing gate voltage the magnetoresistance monotonically reduces. This trend indicates that MR can be controlled by gate voltage. The decrease in MR by increasing gate voltage ascribed to the localized trap states in the interlayers [37].

Similarly, the Fig. 8(a–f) shows the series of MR variation with gate voltage ranging from −0.5 V to 2 V for Back-Gated s-FET. Here also, the amplitude of MR decreases with increasing value of gate voltage. In the case of both devices, around the gate voltage value of 2 V, amplitude of MR disappears and MR curve shows noisy behavior. At the large

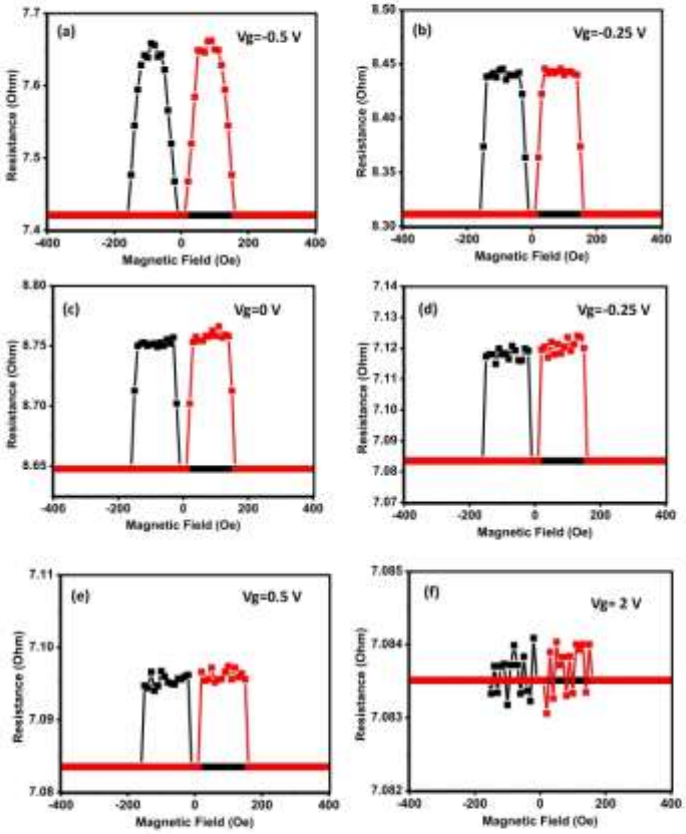

Fig. 8. Gate-controlled MR measurements in Back-Gated s-FET at gate voltage (a) −0.5 V, (b) 0.25 V, (c) 0 V, (d) 0.25 V, (e) 0.5 V and (f) 2 V at room temperature 298 K.

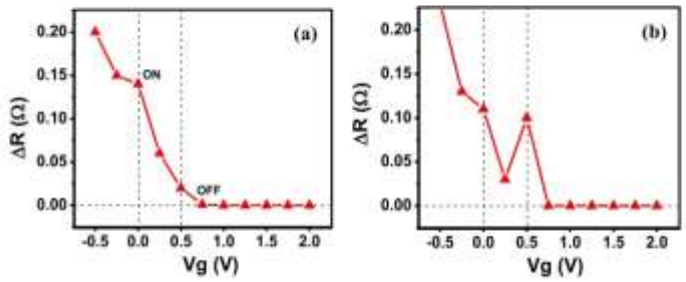

Fig. 9. Switching (ON/OFF state) of (a) Top-Gated s-FET and (b) Back-Gated s-FET based on ΔR of MR curve at room temperature 298 K.

value of gate voltage, the spin excitations localized at the interfaces between FM electrodes. Unfortunately, we did not understand the reason behind flat nature of the parallel state of the magnetization.

3.5. Switching of s-FETs

Finally, we investigated the switching action in Top-Gated s-FET (Fig. 9(a)) and Back-Gated s-FET (Fig. 9(b)) based on amplitude modulation of MR curve at room temperature 298 K. Here, the switching action in both the devices is presented in the form of amplitude

modulation of MR curve (Amplitude of MR curve $|\Delta R = Rap - Rp|$). Through this approach, we successfully archive switching action in Top-Gated s-FET in the gate voltage range −0.5 to 2 V, but unfortunately, appropriate switching action for Back-Gated Type s-FET is not witnessed. To maintain the reproducibility of results, the value of ΔR used in this study is the average of five sets of results.

The considerable variation and vanishing MR by the application of gate voltage operates devices from ON to OFF state, indicates that CGNs based ferromagnetic electrodes have an efficient electrical spin-control operation at room temperature. This spin-control operation at room temperature using gate voltage is attributed to efficient variation of magnetoresistance in the semiconductor channel due to the on/off state of the channel. This is the indication of healthier spin transport [38].

In our case, Top-Gated s-FET and Back-Gated s-FET shows different sets of MR data for same temperature values. In filed effect transistors, contact resistance and mobility in transistors is sensitive to gate voltage and operating temperature. Urban et al demonstrated that increasing the temperature lowers the carrier mobility and exhibits considerable influence on the contact resistance as a function of applied gate voltage [39]. Therefore, device with different architecture behaves differently. In our case, it may be due to the modifications in the graphene density of states due to the coupling of graphene to Co d-states, which results in formation of electron-hole puddles [40,41].

4. Conclusions

In conclusion, we have demonstrated Top-Gated s-FET and Back-Gated s-FET with CGNs based ferromagnetic electrodes. The ohmic contact study of both the devices that is Top-Gated s-FET and Back-Gated s-FET shows that the contacts between CGNs based ferromagnetic electrodes and 2-dimensional electron gas are Ohmic in nature. Similarly, the electrical resistance increases with increasing temperature, which indicates that 2-dimensional electron gas behaves like metal.

The MR study at different temperature reveals that MR decreases monotonically by increasing the temperature for both devices. The highest value of MR was obtained at 50 K, for both devices. This higher value of MR ascribed to the greater value of spin-polarization found in CGNs based ferromagnetic electrodes at lower temperature. The main accomplishment of present work is that the MR of both devices shows good dependence on gate voltage. In addition to this, switching action found appropriate for Top-Gated s-FET. These results motivate and provide a possible avenue for future spintronics applications such as magnetic memory, spin-oscillators and logic devices.

Declaration of Competing Interest

The authors declare that they not have conflict of interest in term financial interests or personal relationships that could have appeared to influence the work reported in this paper.

Acknowledgements

Prof. (Mrs.) Neetu Gyanchandani is very much thankful to the management and Principal of JD College of Engineering and Management, Nagpur for providing necessary academic help.

Data availability

The raw/processed data required to reproduce these findings cannot be shared at this time as the data also forms part of an ongoing study.

References

[1] S. Datta, B. Das, Electronic analog of the electro-optic modulator, Appl. Phys. Lett. 56 (7) (1990) 665–667.
[2] S. Sundyopadhyay, M. Cahay, Reexamination of some spintronic field-effect device concepts, Appl. Phys. Lett. 85 (8) (2004) 1433–1435.
[3] S. Sugahara, J. Nitta, Spin-transistor electronics: an overview and outlook, Proc. IEEE 98 (2010) 2124–2154.
[4] E.I. Rashba, Spin-orbit coupling and spin transport, Physica E 34 (1-2) (2006) 31–35.
[5] D.E. Nikonov, G.I. Bourianoff, Operation and modeling of semiconductor spintronics computing devices, J. Supercond. Nov. Magn. 21 (8) (2008) 479–493.
[6] J. Fabian, A. Matos-Abiaguea, C. Ertlera, P. Stano, I. Zutic, Semiconductor spintronics, Acta Phys. Slovaca 57 (2007) 565–907.
[7] J.C. Egues, G. Burkard, D. Loss, Datta-Das transistor with enhanced spin control, Appl. Phys. Lett. 82 (2003) 2658–2660.
[8] Y. Tian, S.R. Bakaul, T. Wu, Oxide nanowires for spintronics: materials and devices, Nanoscale 4 (2012) 1529–1540.
[9] B. Dlubak, M.-B. Martin, R.S. Weatherup, H. Yang, C. Deranlot, R. Blume, R. Schloegl, A. Fert, A. Anane, S. Hofmann, P. Seneor, J. Robertson, Graphene-Passivated nickel as an oxidation-resistant electrode for spintronics, ACS Nano 6 (12) (2012) 10930–10934.
[10] F. Godel, M.V. Kamalakar, B. Dlubak, V. Henry, D. Halley, J.-F. Dayen, Voltage-controlled inversion of tunnel magnetoresistance in epitaxial nickel/graphene/MgO/cobalt junctions, Appl. Phys. Lett. 105 (20) (4) 152407.
[11] V.M. Karpan, G. Giovannetti, P.A. Khomyakov, M. Talanana, A.A. Starikov, M. Zwierzycki, J. van den Brink, G. Brocks, P.J. Kelly, Graphite and graphene as perfect spin filters, Phys. Rev. Lett. 99 (2007) 176602.
[12] E. Cobos, A.L. Friedman, O.M.J. van't Erve, J.T. Robinson, B.T. Jonker, Graphene as a tunnel barrier: graphene-based magnetic tunnel junctions, Nano Lett. 12 (2012) 3000–3004.
[13] I.O. Serrano, J. Panda, Fernand Demoet, Örjan Vallin, Dibya Phuyal, Olof Karis, M. Venkata Kamalakar, Two-dimensional flexible high diffusive spin circuits, Nano Lett. 19 (2) (2019) 666–673.
[14] M.V. Kamalakar, C. Groenveld, A. Dankert, S.P. Dash, Long distance spin communication in chemical vapour deposited graphene, Nat. Commun. 6 (2015) 6766.
[15] Z.M. Gebeyehu, S. Parui, J.F. Sierra, M. Timmermans, M.J. Esplandiu, S. Brems, C. Huyghebaert, K. Garello, M.V. Costache, S.O. Valenzuela, Spin communication over 30 μm long channels of chemical vapor deposited graphene on SiO2, 2D Mater. 6 (2019) 1–20.
[16] N. Theodoropoulou, A.F. Hebard, M.E. Overberg, C.R. Abernathy, S.J. Pearton, S.N.G. Chu, R.G. Wilson, Unconventional carrier-mediated ferromagnetism above room temperature in ion-implanted (Ga, Mn)P:C, Phys. Rev. Lett. 89 (10) (2002).
[17] X. Cartoixa, Z.Y. Ting, Y.C. Chang, A resonant spin lifetime transistor, Appl. Phys. Lett. 82 (2003) 1462–1464.
[18] C. Peng, Z. Yu, Carbon-based spintronics, Sci. China 56 (2013) 207–221.
[19] D. Huertas-Hernando, F. Guinea, A. Brataas, Spin-orbit coupling in curved graphene, fullerenes, nanotubes, and nanotube, Phys. Rev. B 74 (2006) 155426.
[20] K.R. Nemade, S.A. Waghuley, Chemiresistive gas sensing by few-layered graphene, J. Electr. Mater. 42 (10) (2013) 2857–2866.
[21] M.A. Mohamed, N. Inami, E. Shikoh, Y. Yamamoto, H. Hori, A. Fujiwara, Fabrication of spintronics device by direct synthesis of single-walled carbon nanotubes from ferromagnetic electrodes, Sci. Technol. Adv. Mater. 9 (2008) 025019–025028.
[22] F.T. Johra, J. Lee, W. Jung, Facile and safe graphene preparation on solution-based platform, J. Ind. Eng. Chem. 20 (2014) 2883–2887.
[23] J. Tuček, P. Błoński, J. Ugolotti, A.K. Swain, T. Enoki, R. Zbořil, Emerging chemical strategies for imprinting magnetism in graphene and related 2D materials for spintronic and biomedical applications, Chem. Soc. Rev. 47 (2018) 3899–3990.
[24] M. Weser, Y. Rehder, K. Horn, M. Sicot, M. Fonin, A.B. Preobrajenski, E.N. Voloshina, E. Goering, Yu.S. Dedkov, Induced magnetism of carbon atoms at the graphene/Ni(111) interface, Appl. Phys. Lett. 96 (2010) 012504.
[25] M. Weser, E.N. Voloshina, K. Horn, Y.S. Dedkov, Electronic structure and magnetic properties of the graphene/Fe/Ni(111) intercalation-like system, PCCP 13 (2011) 7534–7539.
[26] H. Vita, St. Bottcher, P. Leicht, K. Horn, A.B. Shick, F. Maca, Electronic structure and magnetic properties of cobalt intercalated in graphene on Ir(111), Phys. Rev. B 90 (2014) 165432.
[27] Z. Ji, X. Shen, Y. Song, G. Zhu, In situ synthesis of graphene/cobalt nanocomposites and their magnetic properties, Mater. Sci. Eng. B 176 (2011) 711–715.
[28] P. Hou, A.J. Akhtar, S. Bhattacharya, M. Miah, S.K. Saha, Ferromagnetism in graphene due to charge transfer from atomic Co to graphene, Appl. Phys. Lett. 111 (2017) 042402.
[29] S.V. Morozov, K.S. Novoselov, M.I. Katsnelson, F. Schedin, L.A. Ponomarenko, D. Jiang, A.K. Geim, Strong suppression of weak localization in graphene, Phys. Rev. Lett. 97 (2006) 016801.
[30] W. Wang, A. Narayan, L. Tang, K. Dolui, Y. Liu, X. Yuan, Y. Jia, Y. Wu, I. Rungger, S. Sanvito, F. Xiu, Spin-valve effect in NiFe/MoS2/NiFe junctions, Nano Lett. 15 (2015) 5261–5267.
[31] K. Byun, S. Park, H. Yang, H. Chung, H. Song, J. Lee, D.H. Seo, J. Heo, D. Lee, H. Jin, Y.S. Woo, Graphene for Metal-semiconductor Ohmic Contacts, Nanotechnology Material and Devices Conference, Hawaii, USA October 16-19, 2012.
[32] K. Byun, H. Chung, J. Lee, H. Yang, H.J. Song, J. Heo, D.H. Seo, S. Park, S.W. Hwang, I. Yoo, K. Kim, Graphene for true ohmic contact at metal-semiconductor junctions, Nano Lett. 13 (2013) 4001–4005.
[33] J.J. Akerman, I.V. Roshchin, J.M. Slaughter, R.W. Dave, I.K. Schuller, Origin of temperature dependence in tunneling magnetoresistance, Europhys. Lett. 63 (2003) 104–110.
[34] C.H. Shang, J. Nowak, R. Jansen, J.S. Moodera, Temperature dependence of magnetoresistance and surface magnetization in ferromagnetic tunnel junctions, Phys.

Rev. B 58 (6) (1998) R2917–R2920.
[35] J.-F. Dayen, S.J. Ray, O. Karis, I.J. Vera-Marun, M.V. Kamalakar, Two-dimensional van der Waals spinterfaces and magnetic-interfaces, Appl. Phys. Rev. 7 (2020) 011303.
[36] G. Zhou, G. Tang, T. Li, G. Pan, Z. Deng, P. Zhang, Graphene-passivated cobalt as a spin-polarized electrode: growth and application to organic spinterfaces, J. Phys. D Appl. Phys. 50 (2017) 095001.
[37] E.Y. Tsymbal, O.N. Mryasov, P.R. LeClair, Spin-dependent tunnelling in magnetic tunnel junctions, J. Phys.: Condens. Matter 15 (4) (2003) R109–R142.
[38] A. Dankert, S.P. Dash, Electrical gate control of spin current in van der Waals heterostructures at room temperature, Nat. Commun. 8 (1) (2017).
[39] F. Urban, G. Lupina, A. Grillo, N. Martucciello, A.D. Bartolomeo, Contact resistance and mobility in back-gate graphene transistors, Nano Express 1 (2020) 010001.
[40] A. Di Bartolomeo, S. Santandrea, F. Giubileo, F. Romeo, M. Petrosino, R. Citro, P. Barbara, G. Lupina, T. Schroeder, A. Rubino, Effect of back gate on contact resistance and on channel conductance in graphene-based field-effect transistors, Diam. Relat. Mater. 58 (2015) 19–23.
[41] J. Martin, N. Akerman, G. Ulbricht, T. Lohmann, J.H. Smet, K. von Klitzing, A. Yacoby, Observation of electron–hole puddles in graphene using a scanning single-electron transistor, Nat. Phys. 4 (2) (2008) 144–148.

8 Communal Riot and Social Integration in Mahesh Dattani 's Final Solution

Communal Riot & Social Disintegration in Mahesh Dattani's Final Solutions

Asst. Prof. D.D. Ghodekar

Indira Mahavidyalaya, Kalamb

Email: dipakghodekar44@gmail.com

Asso. Prof. P.S. Jawade

Indira Mahavidyalaya, Kalamb

Email: bhaktijawade@gmail.com

Abstract:

The plays of Mahesh Dattani touched the burning issues of the contemporary Indian society. The India is land of varied cultures traditions, religions and customs. The disharmony between the religion the major problem occurred in the society which disturbs the national unity, economic strength, and image of state/ nation. This issue is rendered from the independence. The mutual understanding in such diversities is only the way to enjoy the resources for the progress of nation. The crisis or communal tension, the challenge like this has placed unique place in the Indian theatre/ drama. Such issues found the path in the plays of Mahesh Dattani. The play '*Final Solution*' [1992] throws light on communalism simultaneously inhuman behavior discrimination based on the caste/ religion conventionally formed the prejudices which can creates social distances among the society. The final solution depicted community riot between Hindu and Muslim, its effects on the peace of society during the period of post partition. The psychological changes, feeling of enemy causes the brotherhood of nation. Mahesh Dattani pictured the communal unrest by family of three generations happened with it. The present research paper evaluates the conditions of middle urban life and communal stress in the *Final Solution*.

Key –words: riot, marginalized, vegetarianism, communalism, and demonization.

Introduction:

Drama is such an art form which deal with social subjects. It mirrored the social problems and made attempt to create future society which has base of existing society. This form of literature enlightened the audience but gives number of thought/ concept to think. So drama is partially sociological and literary.

Mahesh Dattani is well known dramatist In Indian drama In English. He has been awarded by '*Sahitya Academy Award*' for the significant contribution in the world of drama, with his dramatic writings. He was fond of Gujarati and Kannad plays which inspired him to the dramatic writings. His interest in drama, pave the way to found 'Playpen' a theatre company in 1984. Before that he performed in numerous plays as leading role in Indian English plays and British plays. His prolong experience of acting provokes him for direction of plays. In his writings he dealt with current issues, marginalized sections of society and handled the crying circumstances of society like child abuse homosexuality, the problems of underestimation of Hijada community social frame. The outstanding works of Dattani's final solution was first performed at Bangalore in 1993. The play mainly highlighted the communal violence. The religious scratches between communities took wild fire in the hearts of people of both sides. So the attacks, fighting's happened in the corners of nation for religious existence. Dattani had written his plays in the post colonial period the play has recorded the Indian society with its sorrow sufferings dreams and aspirations incidents of violence happened for the sake of religious feelings. He is not only actor, writer or director but he played as active role of social activist. He strongly believed the people who lived in Indian society were living in unexpected fear and anxiety. So Dattani tried to cover the unanswered concerns through his commentaries and plays about the undirected laws which affect the urban middle class families with their habits of living and equalizing the conditions they have. His imaginative power captured the deep rooted issues of society which was totally voiceless.

The play Final Solution opens with the diary writing, Diksha or Hardika Newly married girl was writing her experiences with new people and house she had not in good tune in laws house. After the India's Independence she was also free from the four walls of her house. Now she has her own views and choices. She was fond of music especially she loves to listen Shamshad Begum and Noor Jahan songs. She wanted to be a singer but her family did not allow and support her to fulfill her dream. She planned to take the visit of Zarin her good friend, their relation tighten the bond of friendship. The scene is now shifted to forty years forward and Diksha's granddaughter Smita was taking phone call of Tasneem. Smita was collecting the information regarding the bomb blast in her hostel. There was tension and fearful atmosphere outside in Moholla. So Diksha advised her daughter-in-law Anna to be sure to close the doors and windows. At this moment Javed and Bobby was running on the street and Hindus were following them to kill as they belongs to Muslim community. At last they knocked the door of Ramnik, Javed and Bobby entered and requested to save their lives.

The mob threatened the family of Ramnik to hand over the Javed but Ramnik refused to do so.

Communal Riot

The differences of two communities were shown as Javed and Bobby was from Muslim community. Before that, they attacked on the chariot and wanted to kill the temple's Pujari [worshipper of Temple]. This is the reason that, the people from Hindu community got hurt and decided to take revenge of Muslim people. Javed committed this act on the name of Jihad. It was the poison of caste/ community to prepare the young minds for the fighting on the name of religion. Ramnik asked Javed about his involvement in terrorism. Javed released all the incidents happened with him in his teenage and hoe his family was abused. Bobby was good nature boy; he told all truth which was only the cause of religion. Smita was very familiar with these two boys appeared in the family of Ramnik. She behaved friendly with two boys, Ramnik was so kind person and gave good treatment to them. He asked Javed about his job. Diksha was watching all the discussion and incidents and memorizing that she was beaten by her husband for the friendship with Zarin. Ramnik also did not forget the incident the burning of shop for the purpose to take at low price. The final Solution ends with undefined solution.

The play final Solution handled the issue of communal crisis in the different context. It talked about the sufferings of Hindu and Muslims mutually. The character of Hardika, Diksha and Jawed suffered in the set-up of Indian community. This all disturbed the normal social life and day to day affairs, need, working etc. It directly affected the empowerment and progress of nation. The scene of play took place inside and outside of Ramnik Gandhi's house. Though the ashes of partition are not destroyed, the dispute between land and nationalism is unsolved; even after the Indian society is celebrating the fifty six years of independence. The required solution is based on establishment of communal harmony in the nation which depends on the communities of nation.

The whole play is full of memories, dialogues, images sudden shifts etc. In the communal tension the youngster like Jawed and Bobby were used to spread communal violence. Such young people were not able to lead normal life in society. Society do not support such persons to lead in better way and ready to look them as criminal of it, either they end their lives or police department encountered them. In such circumstances some

talented minds are diverted from their aims which shall useful to develop the recourses for national development.

Conclusion

Mahesh Dattani was keen observer of the society. He found that Indian society and its culture has impact of religions and other religious customs. Due to caste the marginalization of some sections of society had been occurred, and the dominance of some sections of society has been the different issue, he highlighted the hurdles which stood in the welfare of society and break down to the progress of nation. Secondly he was sensitive about the human relationship and its vital role in development of society. Conflicts, ego, clashes in families shows that male centered norms brought suffocation to the other members living in the family /society and it is done by the leaders of particular groups or community. Such conditions leads to communal tension aroused and the fellowmen might suffer in this disputes. Dattani's play are suitable examples to justify the actual documentation of society in the post partition period of India. Once in interview he claimed that 'Theater is reflection of what you observe'. At the same time Dattani's dramatic writing projected the rapid changes and alterations in the existed system more than that he offered the most challenging scenario of Indian Society, which was not changed after the independence of India, with his own style of description and narrative technique. On this basis Rakesh Sharma made documentary entitled as **FINAL SOLUTION**, on the aftermath of the 2002 Gujarat riots — that left 2,000 dead, hundreds raped, and more than 2,00,000 people got homeless or displaced.

References:

Dattani, Mahesh. *Final Solutions In Final Solutions*: Text and Criticism. Edited by Anjali Multani. New Delhi: Pencraft International, 2009.

Dattani, Mahesh. *"Final Solutions"*, Collected Plays, vol. 1. New Delhi: Penguin, 2000..

Balram, Ajay. *"Final Solutions*- Play on Harmony. The Statesman, April 1, 1994.

9 Impedance spectroscopy study of the AC conductivity of sodium superoxide nanoparticles doped vanadate-based glasses

Materials Science for Energy Technologies 4 (2021) 202–207

Contents lists available at ScienceDirect

Materials Science for Energy Technologies

journal homepage: www.keaipublishing.com/en/journals/materials-science-for-energy-technologies

Impedance spectroscopy study of the AC conductivity of sodium superoxide nanoparticles doped vanadate based glasses

R.V. Barde [a,*], K.R. Nemade [b], S.A. Waghuley [c]

[a] Department of Physics, Govt. Vidarbha Institute of Science and Humanities, Amravati, India
[b] Department of Physics, Indira Mahavidyalaya, Kalamb, India
[c] Department of Physics, Sant Gadge Baba Amravati University, Amravati, India

ARTICLE INFO

Article history:
Received 25 April 2021
Revised 17 June 2021
Accepted 19 June 2021
Available online 24 June 2021

Keywords:
Sodium superoxide
Nyquist plots
Electrical conductivity
Impedance spectroscopy
Hopping distance

ABSTRACT

In the present work, we successfully prepared sodium superoxide (NaO_2) doped vanadium phosphate borate glasses using normal melt quenching technique of composition $60V_2O_5$–$5P_2O_5$–$(35\text{-}x)$ B_2O_3–$xNaO_2$, x = 0, 10, 15 and 20 mol %. The foremost objective of this work is to explore the transport properties of sodium superoxide doped vanadium phosphate borate glasses. The impedance spectroscopy was employed to investigate transport properties of all glass systems under study. The AC conductivity for all glass systems were investigated in temperature range 308–473 K. The Jonscher's power law found to be fit with conductivity data, which decrease with temperature and satisfies the criteria of the correlated hopping model. The activation energy (E_a) estimated from the Arrhenius plot and it is observed to be 0.12 eV.

1. Introduction

Conducting glasses with superionic electrochemistry are potential candidate for solid state batteries due their excellent conductivity and chemical stability against atmospheric changes. In this category of conducting glasses, V_2O_5 glasses has an inordinate potential due to its practical advantages like generating various structural groups [1], providing wide range of structure [2], showing optical as well as electrical properties and mainly its capability as a host for different metallic ions [3]. These properties generally used in fabrication of electrochemical batteries [4], memory switching devices [5] and supercapacitor [6]. The electrical properties of glasses containing large amount of transition metal oxide such as V_2O_5 are determine by the transition metal ions present in two different valence states V^{4+} and V^{5+} [7]. The conduction mechanism is such glasses is dominated by small polaron hopping amongst such ions [8].

Since long time, much attention is attracted by B_2O_3–P_2O_5 glasses for their low refractive index and extraordinary optical properties [9]. These glasses show excellent chemical durability when doped with transition metals than that of phosphate glasses due to boron oxide in the glass network in the form of BO_4 tetrahedral and it transforms metaphosphate chain into 3D network [10] which useful as tuneable solid-state lasers [11], optical [12] and luminescence materials [13], memory devices [14], solar energy converters [15] and fiber optic communication devices [16].

The better formation of NaO_2 at the oxygen side is mainly due to the transport limitation of gaseous oxygen through the electrolyte-filled cathode structure. It is recognized that, NaO_2 can be formed as a stable and solid compound which is the discharge product in a NaO_2 cell with a diglyme based electrolyte and it provides easier access to the study of the cell chemistry as compared to LiO_2 cells, because discharge products are easily noticeable due to the stronger interaction of sodium with spectroscopic probes [17].

For researchers it is very difficult task to prepared stable superoxide. The spray pyrolysis technique is employed for preparation of sodium superoxide nanoparticles in which oxygen rich environment is maintain to achieve higher degree of purity in superoxide phase [18]. As discussed earlier, preparation of stable NaO_2 is the key barrier in the realization of sodium-air batteries. This instability is attributed to discharge product of sodium superoxide is reversibly oxidized toward oxygen as compared to peroxide and oxide [19]. The rechargeable room-temperature battery application of NaO_2 was demonstrated by Hartmann et al. The results of the study show that sodium superoxide crystals forms as a solid discharge in a one-electron transfer step. This work opens the possibility of the substitution of Li-ion batteries by sodium, which offers an unexpected result as metal–air batteries [20].

* Corresponding author.
E-mail address: rajeshbarde1976@gmail.com (R.V. Barde).

https://doi.org/10.1016/j.mset.2021.06.004
2589-2991/

Some recent reports suggest that vanadates glass system is appropriate for high temperature battery applications. Khan et al reported the Li doped vanadates glass system useful for battery/-solid oxide fuel cell due to their good conductivity. The results of the study shows that DC conductivity of the present samples is increased from 0.08 to 0.12 Scm^{-1} at 450 °C with Li_2O doping. Also, the optical band gap decreases from 2.2 to 2.08 eV and Urbach energy increases from 0.31 to 0.41 eV with the addition of Li_2O. These aspects make Li doped vanadates system useful for battery application at higher temperature [21].

Hailemariam et al studied the impedance spectroscopic of lithium substituted niobo vanadate glasses using Nyquist plots and electrical conductivity analysis. In this work, the DC part of the electrical conductivity was studied using alkali ion distance and alkali-oxygen distance method. The activation energy shows the variation with lithium content, it decreases from 0.54 to 0.39 eV as lithium content increases. The mobility study of lithium ions depicts that the decrease in lithium content increases mobility [22].

Alves et al reported the bismuth-vanadate glass system based a novel photochemiresistor sensor for the determination of chemical oxygen demand. The thin film of bismuth-vanadate glass system shows the monoclinic phase deposited on an FTO glass surface. The thin film works efficiently and shows a good correlation between the charge transfer resistance and chemical oxygen demand concentration in the electrolyte solution [23].

Sujatha et al reported the microwave based novel approach for the preparation of Li-vanadate based glasses. This study concludes that microwave-based preparation approach offers advantage of efficient transformation of energy throughout the volume in an effectively short time. Impedance and electron paramagnetic resonance spectroscopic studies of as prepared Li-vanadate based glass system shows the explicate the nature of conduction mechanism [24].

Inspiring from above discussion and research gap identified from literature of materials science, we plan to report first time the transport properties of sodium superoxide loaded vanadate glasses. The main accomplishment of present work is that we successfully prepared the superoxide based stable glasses for transport properties measurement. Typically, the study of conducting glass comprising parameters like frequency exponent and scaling to modulus. The purpose of this work is to analyse the effect of NaO_2 addition in glasses on temperature and frequency of the polarization by means of electrical conductivity, dielectric constant and modulus in the frequency and temperature range 20 Hz to 1 MHz and 308 to 473 K respectively. The structural, physical and topographical study of prepared glass samples were completed using X-ray diffraction (XRD).

2. Experimental

2.1. Materials

NaO_2 was prepared by using AR grade sodium nitrate (SD fine). Glass samples were prepared by using vanadium pentoxide (V_2O_5), phosphorus pentoxide (P_2O_5) and boric acid (H_3BO_3) along with a prepared NaO_2.

2.2. Preparation of NaO_2 and glass samples

For the present work, sodium superoxide (NaO_2) was prepared using spray pyrolysis executed with oxygen rich environment at temperature 673 K. The sodium nitrate and hydrogen peroxide were used as precursors for the preparation of NaO_2. The suspension for spray pyrolysis was prepared by adding 1 M of sodium nitrate in 20 ml H2O under strong magnetic stirring. Subsequently, this suspension was employed for spraying under constant oxygen flow on SiO_2 heating substrate. Its phase purity and structure of as-prepared NaO_2 was confirmed through XRD study. The usual melt-quenching method was used for the preparation of glass samples of compositions $60V_2O_5$–$5P_2O_5$–(35-x) B_2O_3–xNaO_2, x = 0, 10, 15 and 20 mol %. The were weighed and mixed together. This mixture was homogenized and melted in silica crucible in a furnace at 900 °C for 3 h. After melting, the mixture was poured out onto a nonmagnetic stainless-steel plate maintained at temperature 15 °C and pressed with another stainless-steel substrate so that the sheet sample had a circular Shape and a thickness of about 4 mm. To avoid internal strains, the sample was annealed at 200 °C for 1 h and then cooled slowly to room temperature. [25–27]. The melts were three time stirred during heating to attain homogeneous glasses and lastly poured on an aluminum plate and pressed immediately by another aluminum plate.

2.3. Characterizations

The powder samples were characterized at room temperature by using Bruker D8 advance with Cu Kα radiation with scan rate 6.00 in the range 10°–80° to studied morphologies of all samples.

2.4. Impedance study

The LCR meter, Agilent Technology, Singapore was used for impedance study which directly gives the impedance (Z), phase angle (θ), capacitance (C) and the resistance (R) in a frequency and temperature region of 20 Hz to 1 MHz and 308–473 K respectively. For these measurements, the samples were cut into circular discs, polished and conducting silver paste was deposited on both sides. The sample area was taken to be the area exposed to the electrode surface. A firm contact was confirmed at the boundaries of the sample/electrode interfaces. By using above parameter AC conductivity was obtained. From the Z and θ data the values of Z' and Z'' computed from $|Z| \cos\theta$ and $|Z| \sin\theta$, respectively. The results presented in this work are average of three trials of reading to avoid errors measurement. During trials no significant deviation was observed in reading.

3. Result and discussion

3.1. XRD analysis

XRD pattern of sodium superoxide (NaO_2) is shown in Fig. 1 (i). The four peaks positions (200), (220), (311) and (222) appear in pattern exactly index to NaO_2 according to JCPDS reference card No. 01–077–0207, which confirms the formation of NaO_2 [17]. XRD pattern of prepared samples (Fig. 1(ii)), confirms the formation of glasses (amorphous nature), as there was no distinguishing peak corresponds to any crystalline phase. [26].

3.2. Impedance study

The experimental impedance data for 20 mol % of NaO_2 glass sample at different temperatures as Nyquist plots is shown in Fig. 2 (a), (b) and (c). It is observed that, with increase in temperature, the inclined straight line disappears with the formation of semicircle. It is observed that, the center of completely formed depressed semicircle and partially formed semicircle is positioned below the real impedance axis, which reveals a non-Debye relaxation behavior with distributed relaxation time and the intercept of semicircle with the real axis shift towards lower frequency at distinct temperature. At higher temperatures this intercept shifted

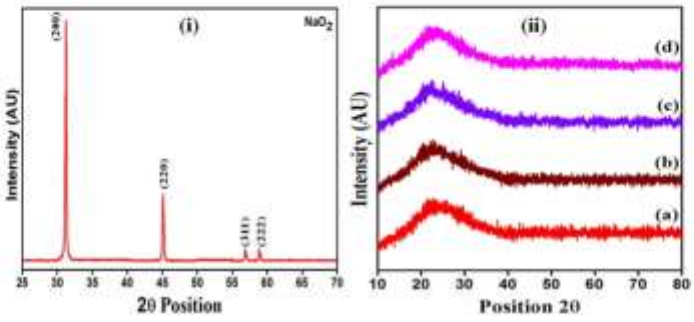

Fig. 1. (i) XRD of Sodium Superoxide (NaO_2) and (ii) XRD of $60V_2O_5$–$5P_2O_5$–$(35-x)B_2O_3$–$xNaO_2$ for (a) 0 mol%, (b) 10 mol%, (c) 15 mol% and (d) 20 mol% of NaO_2.

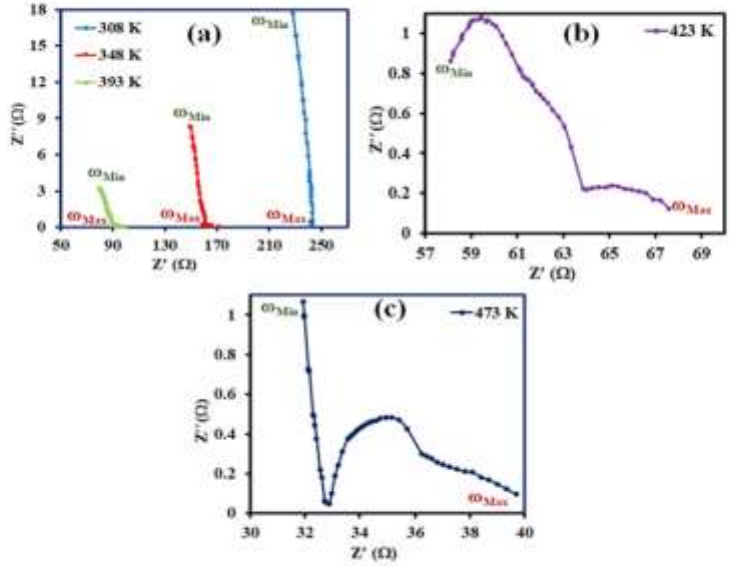

Fig. 2. Nyquist plots of 20 mol % of NaO_2 at different temperature.

towards origin and it gives the bulk resistance of the sample at various temperatures. In these glasses, the electrical relaxation is purely a bulk phenomenon which is mainly due to the absence of a low frequency electrode spike [28,29]. The double layer capacitance of these glasses confirms from the equivalent circuit of dejected semicircle which is the parallel combination of bulk resistance and constant phase element (CPE). The similar behaviour is also observing for other glass samples. From the intercepts of the semicircle of low frequency with real impedance axis, the DC conductivity (σ_{dc}) is calculated using sample dimensions at various temperatures [30]. Its value thus shows a gradual enhancement with the increase in temperature that is with the increase in temperature, bulk resistance of the sample decreases, which is activated conduction mechanism. The dc conductivity plot shown in Fig. 3 fitted to Arrhenius equation

The activation energy, E_{dc} was calculated from the least square straight-line fitting of plot. The lowest value of activation energy was found to be 0.12 eV for 20 mol % of NaO_2. It is observed that conductivity increases with increase in mol % of NaO_2. The maximum in conductivity corresponds with minimum of activation energy. The explanation for enhancement in conductivity is given on the basis of the Anderson and Stuart model. According to this model, as one of the glass former ion is substituted by another glass former ion, the average interionic bond distance changes. It becomes larger/smaller depending on substituting ion is larger/smaller. Thus, with the addition of NaO_2 content, the structure becomes loose and hence conductivity increases [31–33].

3.3. AC conductivity

The frequency dependence of AC. conductivity for 20 mol % of NaO_2 glass sample at different temperatures is shown in Fig. 4. These figures shows that AC conductivity increases linearly with frequency. The temperature dependence of AC. conductivity in glasses is studied in the glass transition regime. From Fig. 4, suggest two thermally activated phenomena for conduction i.e. this

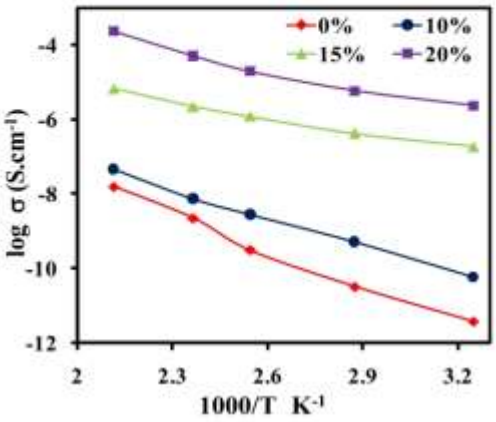

Fig. 3. dc conductivity Plot of all glass samples with varying temperature.

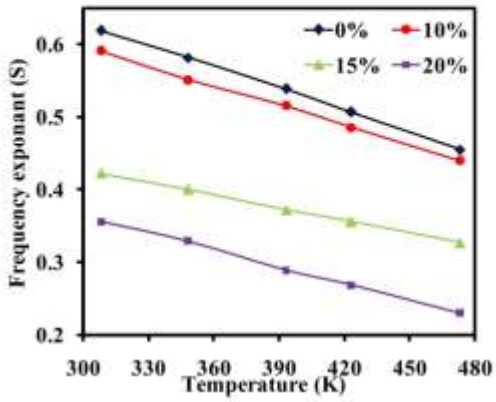

Fig. 5. Variation of frequency exponent (s) with temperature for all samples.

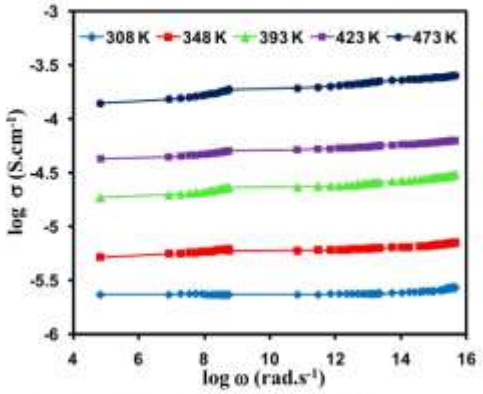

Fig. 4. Variation of Conductivity of 20 mol % NaO_2 of with temperature.

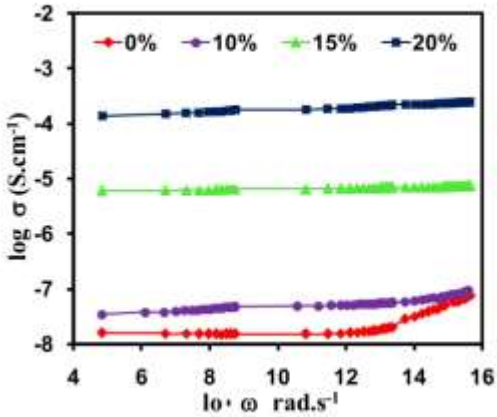

Fig. 6. Variation of Conductivity with mol % of NaO_2 in temperature range 308 – 473 K.

plot consists of two distinct regions low frequency plateau region and high frequency dispersion region. In plateau region the conductivity is observed to be almost independent of frequency suggesting that the ionic diffusion is random less via activated hopping process and by extrapolating the conductivity value to zero limit frequency the dc conductivity obtained which shows good agreement with the dc conductivity obtained from impedance plot indicating the thermally induced process due to the increase in the energy of charge carriers [34]. In high frequency region dispersion is predominant at low temperature and becomes prominent with increase in temperature (linear behavior) and it shift to higher frequency region, which was analysed by Jonscher's Universal Power law [35,36]. Comparable nature is also observed in other glasses.

$$\sigma(\omega) = \sigma(0) + A\omega^{S} \quad (2)$$

$\sigma(0)$ is the direct current conductivity of the sample, $A\omega^{S}$ is the pure dispersive component of AC conductivity having a characteristic of power law in terms of angular frequency ω and exponent S ($0 \leq S \leq 1$) that represents the degree of interaction between

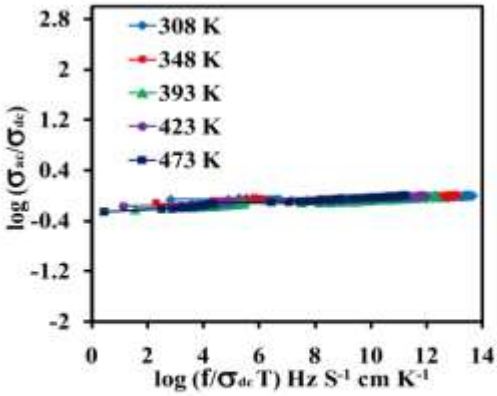

Fig. 7. Conductivity scaling data of 20 mol% NaO_2 glass sample with different temperatures.

Table 1
Activation energy (E_a), Feequency exponant (s) and Hopping distance (R).

Sample mol %	E_a (eV)	Frequency exponent (s)					Hopping distance (R)				
		308 K	348 K	393 K	423 K	473 K	308 K	348 K	393 K	423 K	473 K
0	0.28	0.62	0.58	0.54	0.51	0.46	0.42	0.43	0.44	0.44	0.45
10	0.21	0.60	0.55	0.52	0.49	0.44	0.39	0.40	0.42	0.42	0.44
15	0.15	0.42	0.40	0.37	0.36	0.33	0.28	0.30	0.32	0.34	0.36
20	0.12	0.36	0.33	0.29	0.27	0.22	0.25	0.27	0.29	0.30	0.32

mobile ions and the lattices around them, and A is a constant which determines the strength of polarizability. It is clear that conductivity is dependent on ω^S in high frequency regime. The frequency exponent (S) lies in between 0.3 and 0.6. The temperature dependence of the frequency exponent, for the investigated glass samples is shown in Fig. 5 [37,38].

It is notable that, from the temperature dependent behaviour of s, the conduction mechanism in any material can be explained. From figure it is clear that, correlated barrier hopping {CBH} conduction mechanism is predominant for all glasses as, s decreases with increase in temperature [29]. With the addition of NaO_2 the transition probability in between valance state V^{5+} and V^{6+} increases, which results in enhancement of conductivity.

From Fig. 6 it is observed that, conductivity increases with increasing frequency and mol % of NaO_2 in the temperature range 308 to 473 K. The result of normalised plot of conduction at different temperature is shown in Fig. 7. It is observed that data for different temperature overlap on single curve which indicates that, conduction mechanism is independent of temperature i.e. dynamic processes occurring at various frequencies needs nearly the same thermal activation energy. [39,40].

The maximum barrier height (R) was calculated by using Eq. (3) as [41,42]:

$$R = \frac{6kT}{1-S} \tag{3}$$

where k is the Boltzmann constant, and T is the absolute temperature. The values of R for all samples were listed in Table 1. The maximum barrier height (R) increases with temperature whereas decreases with increasing NaO_2 content as shown in Fig. 8.

The comparison of results of this work with recent works reported by Khan et al [21] and Hailemariam et al [22], our NaO_2-vanadate based glass system shows good and stable Impedance and AC conductivity properties.

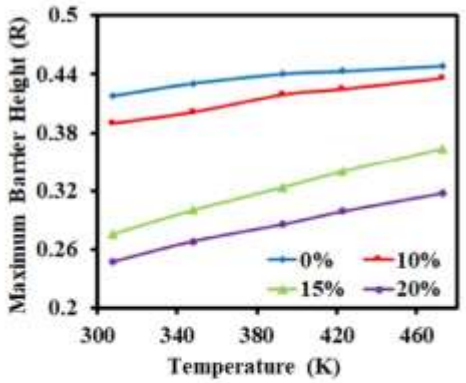

Fig. 8. Variation of maximum barrier height (R) with temperature for all samples.

4. Conclusions

The formation of NaO_2 was confirms by using XRD analysis. Similarly, the amorphous nature of all glass systems was confirmed from XRD analysis. The addition of NaO_2 increases significantly the conductivity of glasses. In the summery of present work, it is concluded that sodium superoxide is a potential dopant to improve transport characteristics of conducting glasses. The universal power law was employed to investigate variation of AC conductivity. Results shows that temperature increases and frequency exponent (s) decreases during AC conduction. The results of the study found fit with Elliot's correlated barrier hopping model (CBH). The scaling study confirms that conduction mechanism shows direct dependency on composition of glass system and temperature independent.

In summary, we first time successfully explored the impedance spectroscopy and AC conductivity study of sodium superoxide nanoparticles doped vanadates-based glasses. The major accomplishment of present study is that we succeed in preparation of stable superoxide-based glasses, which shows good transport characteristics over the wide range of temperature. This virtue make glass useful for wide variety of applications such as high temperature battery application, supercapacitor application.

Declaration of Competing Interest

The authors declare that they have no known competing financial interests or personal relationships that could have appeared to influence the work reported in this paper.

Acknowledgements

Authors are thankful to Head Department of physics, Director, Government Vidarbha Institute of Science and Humanities, Amravati and Head, Department of Physics Sant Gadge Baba Amravati University, Amravati for providing necessary facilities.

References

[1] G.I. Petrov, V.V. Yakovlev, J. Squier, Raman microscopy analysis of phase transformation mechanisms in vanadium dioxide, Appl. Phys. Lett. 81 (6) (2002) 1023–1025.
[2] M.M. El-Desoky, M.S. Al-Assiri, Structural and Polaronic transport properties of semiconducting CuO–V_2O_5–TeO glasses, Mater. Sci. Eng. B 137 (2007) 237–246.
[3] G.M. Clark, A.N. Pick, DTA study of the reactions of V_2O_5 with metal (II) oxides, J. Therm. Anal. 7 (2) (1975) 289–300.
[4] H. Liu, D. Tang, Synthesis of ZnV_2O_6 powder and its cathodic performance for lithium secondary battery, Mater. Chem. Phys. 114 (2-3) (2009) 656–659.
[5] E. Mansour, Y.M. Moustafa, G.M. El-Damrawi, S. Abd El-Maksoud, H. Doweidar, Memory switching of Fe_2O_3–BaO–V_2O_5 glasses, Physica B 305 (2001) 242–249.
[6] K. Jeyalakshmi, S. Vijayakumar, S. Nagamuthu, G. Muralidharan, Effect of annealing tempetature on the supercapacitor behaviour of β-V_2O_5 thin films, Mater. Res. Bull. 48 (2) (2013) 760–766.
[7] L. Musawski, Electrical conductivity in iron-containing oxide glasses, J. Mater. Sci. 17 (1982) 2155–2163.
[8] N.F. Mott, Conduction in glasses containing transition metal ions, J. Non-Cryst. Solids 1 (1) (1968) 1–17.
[9] S. Yusub, D. Krishna Rao, The role of chromium ions on dielectric and spectroscopic properties of Li_2O–PbO–B_2O_3–P_2O_5 glasses, J. Non-Cryst. Solids 398–399 (2014) 1–9.

[10] R.K. Brow, D.R. Tallant, Structural design of sealing glasses, J. Non-Cryst. Solids 222 (1997) 396–406.
[11] T.O. Hardwell, Solid-state lasers: properties and applications, Nova Science (2008).
[12] B. Denker, B. Galagan, V. Osiko, S. Svetchkov, E. Dianov, Luminescent properties of Bi-doped boro-alumino-phosphate glasses, App. Phys. B 87 (2007) 135–137.
[13] C.R. Kesavulu, R.P.S. Chakradhar, R.S. Muralidhara, J. Lakshmana Rao, K.V. Anavekar, EPR, optical absorption and photoluminescence properties of Cr^{3+} ions in lithium borophosphate glasses, J. Alloys Compd. 496 (2010) 75–80.
[14] O. Mao, R.L. Turner, I.A. Courtney, B.D. Fredericksen, M.I. Buckett, L.J. Krause, J. R. Dahn, Active/inactive nanocomposites as anodes for Li-ion batteries, Electrochem. Solid-State Lett. 2 (1) (1998) 3–5.
[15] J.T. Tsai, C.Y. Huang, S.T. Lin, The development of conductive pastes for solar cells, Adv. Mater. Res. 557–559 (2012) 1201–1204.
[16] J.W. Yu, K. Oh, New in-line fiber band pass filters using high silica dispersive optical fibers, Optics Commun. 204 (1-6) (2002) 111–118.
[17] Pascal Hartmann, Conrad L. Bender, Joachim Sann, Anna Katharina Dürr, Martin Jansen, Jürgen Janek, Philipp Adelhelm, A comprehensive study on the cell chemistry of the sodium superoxide (NaO2) battery, Phys. Chem. Chem. Phys. 15 (28) (2013) 11661, https://doi.org/10.1039/c3cp50430c.
[18] Kailash Nemade, Sandeep Waghuley, Novel synthesis approach for stable sodium superoxide (NaO_2) nanoparticles for LPG sensing application, Int. Nano Lett. 7 (3) (2017) 233–236.
[19] V.S. Dilimon, C. Hwang, Y. Cho, J. Yang, H. Lim, K. Kang, S.J. Kang, H. Song, Superoxide stability for reversible Na-O_2 electrochemistry, Scie. Rep. 7 (2017) 17635–17642.
[20] Pascal Hartmann, Conrad L. Bender, Miloš Vračar, Anna Katharina Dürr, Arnd Garsuch, Jürgen Janek, Philipp Adelhelm, A rechargeable room-temperature sodium superoxide (NaO_2) battery, Natu. Mate. 12 (3) (2013) 228–232.
[21] S. Khan, K. Singh, Structural, optical, thermal and conducting properties of V2−xLixO5−δ (0.15 ≤ x ≤ 0.30) systems, Sci. Rep. 10 (2020) 1–11.
[22] B.G. Hademariam, G.V. Honnavar, M. Irfan, R. Keralapura, Structural and electrical properties of lithium substituted niobo vanadate glasses doped with nickel ferrite, AIP Adv. 11 (2021) 210–220.
[23] N.A. Alves, A. Olean-Oliveira, C.X. Cardoso, M.F.S. Teixeira, Photochemiresistor sensor development based on a bismuth vanadate type semiconductor for determination of chemical oxygen demand, ACS Appl. Mater. Interfaces 12 (2020) 18723–18729.
[24] Basareddy Sujatha, Ramarao Viswanatha, Hanumathappa Nagabushana, Chinnappa Narayana Reddy, Electronic and ionic conductivity studies on microwave synthesized glasses containing transition metal ions, J. Mater. Res. Technol. 6 (1) (2017) 7–12.
[25] R.V. Barde, S.A. Waghuley, Preparation and electrical conductivity of novel vanadate borate glass system containing graphene oxide, J. Non-Cryst. Solids 376 (2013) 117–125.
[26] Rajesh Barde, Sandeep Waghuley, Transport properties of rare earth CeO_2 doped phospho-vanadate glass systems, J. Chin. Adv. Mater. Soc. 2 (4) (2014) 273–283.
[27] A. V. Sekhar, L. Pavic, A. Mogus-Milankovic, V. R. Kumar, A. S. Sesha Reddy, G. N. Raju, and N. Veeraiah, Dielectric dispersion and impedance spectroscopy of NiO doped Li2SO4eMgOeP2O5 glass system, J. of Allo. and Comp., 824 (2020) 153907.
[28] S. Jayaseelan, P. Muralidharan, M. Venkateshwarlu, N. Satyanarayana, Ion transport and relaxation studies of silver vanado tellurite glasses at low temperature, Mate. Chem. and phys. 87 (2004) 370–377.
[29] Saroj Rani, Sujata Sanghi, Neetu Ahlawat, Ashish Agarwal, Influence of Bi_2O_3 on physical, electrical and thermal properties of Li_2O-ZnO-Bi_2O_3-SiO_2 glasses, J. Alloys Comp. 619 (2015) 659–666.
[30] R.V. Barde, S.A. Waghuley, Study of AC electrical properties of V_2O_5–P_2O_5–B_2O_3–Dy_2O_3 glasses, Ceram. Inter. 39 (6) (2013) 6303–6311.
[31] C.R. Mariappan, G. Govindaraj, S. Vinoth Rathan, G. Vijaya Prakash, Preparation, characterization, AC conductivity and permittivity studies on vitreous $M_2AlCdP_3O_{12}$ (M = Li, Na, K) system, Mater. Sci. Eng. B 121 (1-2) (2005) 2–8.
[32] R.S. Gedam, V.K. Deshpande, An anomalous enhancement in the electrical conductivity of Li2O : B2O3: Al2O3 glasses, Solid State Ionics 177 (26-32) (2006) 2589–2592.
[33] R.V. Barde, S.A. Waghuley, Thermal and electrical properties of $60V_2O_5$–$5P_2O_5$–$[35-x]B_2O_3$–$xCeO_2$ ($1 \le x \le 5$) glasses, Bull. Mater. Sci. 38 (2) (2015) 557–563.
[34] P. Jaiswal, P.K. Singh, P. Lohia, D.K. Dwivedi, Study of ac conductivity mechanism and impedance spectroscopy in CNT-added $Cu_5Se_5Te_{15}In_{75}$ chalcogenide system, Bull. Mater. Sci. 43 (2020) 216.
[35] B. Saravanakumar, G. Ravi, V. Ganesh, R.K. Guduru, R. Yuvakkumar, $MnCo_2O_4$ nanosphere synthesis for electrochemical application, Mater. Sci. Ener. Techn. 2 (2019) 130–138.
[36] P.M. Anjana, M.R. Bindhu, R.B. Rakhi, Green synthesized gold nanoparticle dispersed porous carbon composites for electrochemical energy storage, Mater. Sci. for Ene. Tech. 2 (3) (2019) 389–395.
[37] C. Dobare, M.M.A. Imran, N. Mehta, Study of dielectric relaxation and thermally activated a.c. conduction in glassy $Se_{70}Te_{30}$ and Se70Te28M2 (M =Ag Zn and Cd) alloys, J. Asi. Ceram. Soc. 4 (2016) 252–258.
[38] Ali Dhahri, E. Dhahri, E.K. Hlil, Electrical conductivity and dielectric behaviour of nanocrystalline $La_{0.6}Gd_{0.1}Sr_{0.3}Mn_{0.95}Si_{0.05}O_3$, RSC Adv. 8 (17) (2018) 9103–9111.
[39] B. Roling, A. Happe, K. Funke, M.D. Ingram, Carrier concentrations and relaxation spectroscopy: new information from scaling properties of conductivity spectra in ionically conducting glasses, Phys. Rev. Lett. 78 (11) (1997) 2160–2163.
[40] Somyia El-Sayed, Optical properties and dielectric relaxation of polyvinylidene fluoride thin films doped with gadolinium chloride, Physica B 454 (2014) 197–203.
[41] R.V. Barde, K.R. Nemade, S.A. Waghuley, AC conductivity and dielectric relaxation in V_2O_5–P_2O_5–B_2O_3 glasses, J. Asian Ceram. Soc. 3 (1) (2015) 116–122.
[42] H. Bouaamlat, N. Hadi, N. Belghiti, H. Sadki, M. N. Bennani, F. Abdi, T. Lamcharfi, M. Bouachrine, and M. Abarkan, Dielectric Properties, AC Conductivity, and Electric Modulus Analysis of Bulk Ethylcarbazole-Terphenyl, Adv. Mate. Sc. and Eng., (2020), Article ID 8689150, 8 pages. doi:10.1155/2020/8689150.

10 Comprehensive study to ascertain the effect of MnO2 loading on supercapacitive properties of conducting polymers

International Journal of Polymer Analysis and Characterization

ISSN: (Print) (Online) Journal homepage: https://www.tandfonline.com/loi/gpac20

Comprehensive study to ascertain the effect of MnO_2 loading on supercapacitive properties of conducting polymers

Bhagyashri Tale, Kailash Nemade & Pradip Tekade

To cite this article: Bhagyashri Tale, Kailash Nemade & Pradip Tekade (2021): Comprehensive study to ascertain the effect of MnO_2 loading on supercapacitive properties of conducting polymers, International Journal of Polymer Analysis and Characterization, DOI: 10.1080/1023666X.2021.1933853

To link to this article: https://doi.org/10.1080/1023666X.2021.1933853

INTERNATIONAL JOURNAL OF POLYMER ANALYSIS AND CHARACTERIZATION
https://doi.org/10.1080/1023666X.2021.1933853

Taylor & Francis
Taylor & Francis Group

Comprehensive study to ascertain the effect of MnO_2 loading on supercapacitive properties of conducting polymers

Bhagyashri Tale[a], Kailash Nemade[b], and Pradip Tekade[a]

[a]Department of Chemistry, Bajaj College of Science, Wardha, India; [b]Department of Physics, Indira Mahavidyalaya, Kalamb, India

ABSTRACT

This study reports the electrochemical properties of Manganese dioxide (MnO_2) with four types of conducting polymers such as polyaniline (PANi), polythiophene (PTh), polypyyrole, and polyindole (PIn) by preparing their composites. All four conducting polymers were prepared by chemical oxidative polymerization approach. The prepared composites were characterized by X-ray diffraction (XRD), scanning electron microscope (SEM), Raman spectroscopy, ultra–violate visible (UV–VIS) spectroscopy, and photoluminance (PL). Similarly, the supercapacitive properties such, cyclic voltammetry (CV) curve, capacitance retention and cycle stability of composite materials were investigated. The highest value of specific capacitance was obtained for MnO_2-PANi (Mn-PANi) composite, which was found to be 633.75 Fg^{-1}.

ARTICLE HISTORY
Received 2 December 2020
Accepted 19 May 2021

KEYWORDS
Conducting polymers; MnO_2; supercapacitor

Introduction

Global demand of energy is increasing day by day. As demand of high energy storage system is increased globally, study of electrode material for supercapacitor application became topic of intense research. Climate changes and the limited availability of fossil fuels create a need of sustainable and renewable energy sources. Thus, renewable energy production from sun and wind, as well as the development of electric/hybrid electric vehicles with low CO_2 emissions has started. As the sun does not shine during the night and wind does not blow on demand, energy storage systems play a major role and electrical energy storage systems, such as batteries, electrochemical capacitors (ECs) are need to be developed. The performance of energy storage systems has to be increased substantially to meet the higher requirements of future systems. ECs (also known as supercapacitors or ultracapacitors) store energy by ion adsorption (electrochemical double-layer capacitors) or fast surface redox reactions (pseudo-capacitors). These can be more efficient than batteries used in electrical energy storage, when high power delivery or uptake is needed. Numerous efforts have been taken to increase the specific capacitance value of the electrode materials. The electrode materials with high capacity and cyclic stability found to possess great supercapacitor performance.[1–3]

Over the past decades, various types of electrode materials are studied for high-performance supercapacitor application and many approaches are employed to fabricate various composites prepared using different types of electroactive materials. As lithium-ion batteries has some disadvantages such as slow power delivery or uptake, faster and higher power energy storage systems are needed and for this, supercapacitor are considered as good alternative. ECs are power devices

CONTACT Bhagyashri Tale bhagyashritale@gmail.com Department of Chemistry, Bajaj College of Science, Wardha, Maharashtra, India.

which can be fully charged or discharged in seconds. Their energy density (about 5 Wh kg^{-1}) is lower as compared to batteries, but it shows much higher power delivery or uptake (10 kW kg^{-1}) for shorter times (a few seconds). They can replace batteries in the energy storage field for uninterruptible power supplies (back-up supplies used to protect against power disruption) and load-leveling.[4–6]

Transition metal oxides and conducting polymers are pseudo-capacitive active materials. Addition of metal oxides to conducting polymers is called composites. Composite formation improves electrochemical properties. Among transition metal oxides, manganese dioxide (MnO_2) shows best EC properties than others. PANi/MnO_2 composite has been studied by Chen et al who reported the specific capacitance value of 80 F g^{-1} and its stable columbic efficiency of about 98% up to 1000 cycles.[2]

Transition metal oxides such as RuO_2,[7] NiO,[8,9] CoOx, and MnO_2[10] are studied and implemented as electrode materials for SCs.[11–15] Metal oxides have wide charge/discharge potential range, but most of the transition metal oxides shows relatively low capacitance.[11,14] Conducting polymers such as polyaniline (PANi) are reported as another promising material in the redox SCs. Polymers shows advantages such as high capacitance, high conductivity, low cost, and ease of fabrication.[16] But they suffer from disadvantages such as the relatively low mechanical stability and cycle life which are major limitations for applications. In recent years, considerable efforts have been made to couple the unique advantages of these capacitive materials for SCs by formation of composites.[17–22] Thus, the composites of PANi and MnO_2 have attracted much attention because of their low cost and eco-friendliness. The PANi-MnO_2 composite can be prepared using different chemical methods.[18,23–28] The PANi serves as an electroactive material for energy storage and it is also a good coating layer to protect MnO_2 from dissolution in acidic electrolytes.[23] It is reported that the composite prepared by intercalation of PANi into layers of MnO_2 shows an enhanced specific capacitance of 330 $F.g^{-1}$ by the synergistic effects.[24]

Motivating from above discussion, we planned to investigate the electrochemical properties of MnO_2 with four types of conducting polymers such as PANi, polythiophene (PTh), polypyyrole, and polyindole (PIn) by preparing their composites. In this work, we studied the supercapacitive properties such, cyclic voltammetry (CV) curve, capacitance retention, and cycle stability performance of composite materials. Prime novelty of present work is that out of four type of composites system of MnO_2 with conducting polymer, we successfully optimized MnO_2-PANi (Mn-PANi) composite system as active electrode material for supercapacitor application.

Experimental

In this work, chemicals of analytical grade procured from SD Fine, India of purity 99.8% were used without further purification. PANi was synthesized with chemical oxidative method using ammonium persulfate as oxidizing agent. Both aniline and oxidant in 1:1 ratio were dissolved in aqueous medium. The greenish black ppt was observed and it was kept for 24 h at room temperature in order to get complete polymerization. The obtained product was washed with distilled water and dried in an oven.[29] For polymerization of pyrrole, $FeCl_3$ was used as oxidant and ethanol as solvent. The suspension was kept at room temperature for 24 h for polymerization. Finally, solution was filtered and washed with acetone and distilled water to remove unreacted pyrrole and excess ferric chloride. A black ppt of polypyrrole (PPy) was dried in an oven.[30]

PIn was prepared *via* chemical oxidative technique using $FeCl_3$ as an oxidant. In this technique, monomer and oxidant in stoichiometric ratio were dissolved in distilled water. To that reaction mixture, 0.1 M hydrogen peroxide was added to enhance the rate of reaction. The reaction mixture was continuously stirred for 12 h with magnetic stirrer at 30 °C.[31] PTh was synthesized at room temperature by mixing thiophene with ferric chloride in distilled water. Hydrogen peroxide was added dropwise to reaction mixture to enhance the rate of reaction. The

polymerization was allowed to take place with constant stirring for 24 h with magnetic stirring at 30°. Then concentrate sodium hydroxide solution was added to generate precipitate. The precipitate was washed with distilled water and dried in oven.[32]

MnO_2 was synthesized using co-precipitation method using manganese sulfate monohydrate ($MnSO_4.H_2O$) and potassium permanganate ($KMnO_4$). The solution was further stirred for 20 min and kept at room temp. for 24 h. The solution was probe sonicated using sonicator (PCi, 750-F, PCI analytics Pvt. Ltd) to split the MnO_2 particles to nano dimensions. The black-brown product was obtained which is washed with deionized water and dried in oven.[33] The *ex-situ* approach was adopted for preparation of polymer/metal oxide composite. The weight % stoichiometry was adopted for preparation of composite. During preparation of composite, polymer (1 g) and metal oxide (0.1 g) was added in organic media.

The X-ray diffraction (XRD) patterns of as prepared materials were recorded on Rigaku Miniflex-II X-ray diffractometer. The morphology of samples was investigated using scanning electron microscope (SEM) images obtained from JEOL JSM-7500F. The ultraviolet–visible (UV–VIS) absorption spectra of composites were acquired using Agilent Cary 60 UV–VIS spectrophotometer. The Bruker RFS 27 Raman spectrometer was used for Raman analysis. Electrochemical study of prepared samples was carried out using three-electrode cell systems (CHI 660D, CHInstruments). As-prepared materials were used as the working electrode, platinum wire as counter electrode and Ag/AgCl as the reference electrode. In this work, the working electrodes were prepared by mixing 85 wt.% sample that is Mn-PANi composite, 10 wt.% activated carbon, and 5 wt% polytetrafluoroethylene with acetone. Then the mixture of sample was coated onto a nickel foam using spin coating technique. Photoluminescence (PL) spectra recorded using fluorescence spectroscopy (FL spectrophotometer model F-7000; Hitachi).

Results and discussion

The XRD patterns of the MnO_2 micromaterials are shown in Figure 1(a–i). The diffraction peak which appeared at $2\theta = 18°$, 28°, 37°, 42°, 56° matched well with the diffraction peak of α- MnO_2 standard data (JCPDS card PDF file no. 44-0141).[34] XRD of PANi recorded at room temperature with several diffraction peaks in the 2θ range 15–30°. The pattern shows sharp and well-defined peaks, which indicate semi-crystalline nature of PANi. The crystalline nature of PANi is due to its nano fibrous form and planer nature of benzenoid and quinoid functional groups.[35]

XRD spectra of PTh shows only one broad peak centered at near 2θ value of 35°. This diffraction peak strongly associated with the π-π stacking structure in PTh chains. Thus, spectrum shows that the semi-crystalline nature of PTh.[36] The XRD pattern of PIn showing a broad hump which suggests an amorphous structure which is the characteristic of PIn.[31] It is observed from the XRD of PPy that the polymer is in an amorphous state, and hence there are no sharp peaks observed in the diffraction pattern. But a broad peak at about 24° of 2θ value is observed, which incidentally is the characteristics peak of amorphous PPy polymer.[37]

The XRD pattern of Mn-PANi composite clearly shows the crystalline phase with shape peaks. The XRD patterns of MnO_2-PIn composite (Mn-PIn), MnO_2-PPy composite (Mn-PPy), and MnO_2-PTh composite (Mn-PTh) indicates amorphous nature as there is no sharp peak. Table 1 shows the particle size estimated from XRD analysis.

Figure 2(a–i) shows the SEM images of (a) MnO_2, (b) PANi, (c) PTh, (d) PPy, (e) PIn, (f) MnO_2-PANi, (g) MnO_2-PTh, (h) MnO_2-PPy, and (i) MnO_2-PIn, respectively. SEM images shows the good quality information about the surface topography of as-prepared materials.

Raman spectra of MnO_2 clearly showing sharp peaks in the region between 500 and 700 cm^{-1}, which is characteristic peak of MnO_2 (Figure 3).[39] Raman spectra of PANi clearly indicate signal at 1140, 1230, 1500, and 1582 cm^{-1}. The 1100–1210 cm^{-1} region indicates C–H bending vibrations of benzene or quinone type rings. The 1210–1520 cm^{-1} region denotes C-N stretching

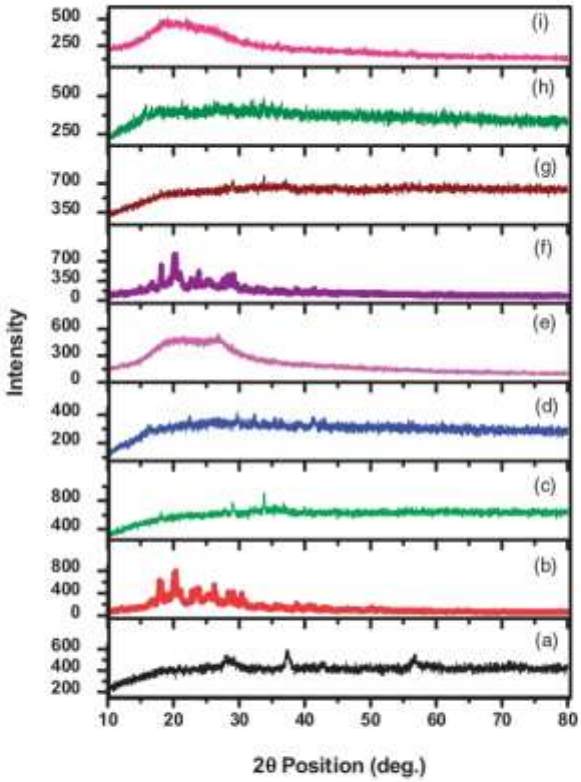

Figure 1. XRD patterns of (a) MnO_2, (b) PANi, (c) PTh, (d) PPy, (e) PIn, (f) MnO_2-PANi, (g) MnO_2-PTh, (h) MnO_2-PPy, and (i) MnO_2-PIn.

Table 1. Particle size of MnO_2, polymers, and their composites.

Compound	Estimated particle size by Scherrer equation D(nm)= $K\lambda/\beta\cos\theta$ (nm) [38]
MnO_2	61.32
Polyaniline (PANi)	84
Polythiophene (PTh)	108.51
Polypyrrole (PPy)	108.13
Polyindole (PIn)	10.28
MnO_2-polyaniline composite (Mn-PANi)	90.16
MnO_2-polythiophene composite (Mn-PTh)	132.87
MnO_2-polypyrrole composite (Mn-PPy)	91.23
MnO_2-polyindole composite (Mn-PIn).	7.20

vibrations and 1520–1650 cm^{-1} region represents C–C stretching vibration of benzene and quinone type rings.[40]

PTh shows sharp peak at 1209, 1379, and 1651 cm^{-1}. Signal near 1600 cm^{-1} shows unquestionably frequency dispersion with increasing chain length. Peak near1500 cm^{-1} is a common feature of/the Raman spectra of aromatic and heteroaromatic systems. It is always very strong and dominates the whole Raman spectrum. While it shifts to lower frequencies when chain length increases. It shows somewhat different frequencies from one chemical series to another within the class of oligo and PThs, but within each class it is almost invariably strong and unshifted. Some signals which appear at the lower frequency side shows intensity enhancement with increasing

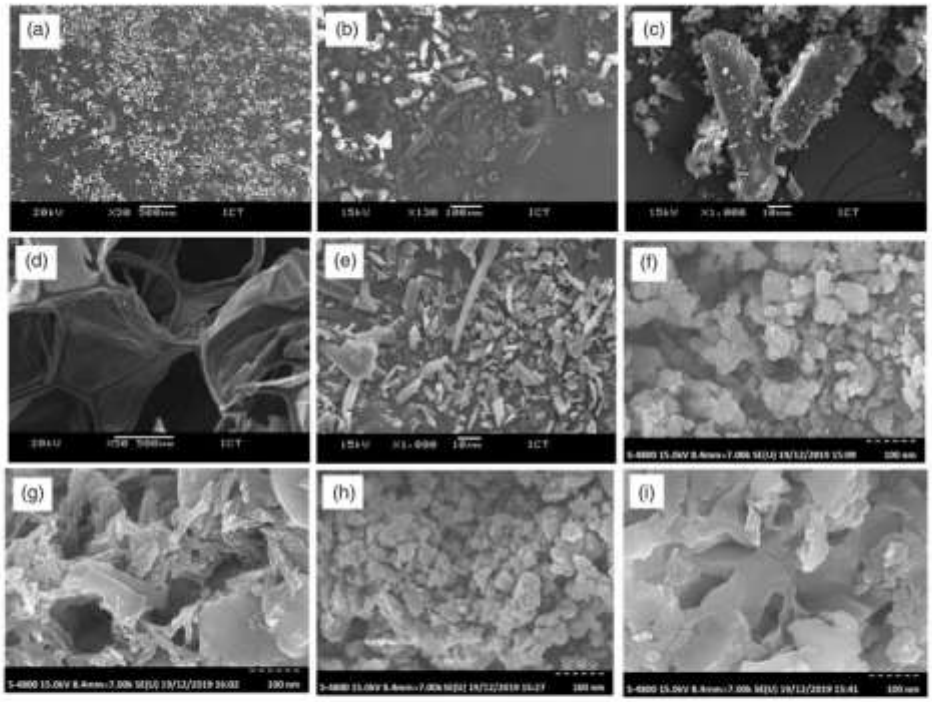

Figure 2. SEM images of (a) MnO_2, (b) PANi, (c) PTh, (d) PPy, (e) PIn, (f) MnO_2-PANi, (g) MnO_2-PTh, (h) MnO_2-PPy, and (i) MnO_2-PIn.

chain length.[41] PPy shows signal at 1330 cm^{-1} which corresponds to C–C stretching in ring and antisymmetric C–N stretching.[42] PIn shows signal 1102 due to out-of-plane as well as in-plane deformation of N-H, peak near 1594 corresponds to C = C backbone stretching and peak at 1414 due to ring stretching.[43,44]

In this work, UV–VIS technique was used to know the absorption wavelengths of materials and band gap (Figure 4). The energy band gap of sample can be calculated using relations: $E = hc/\lambda$,[45] where, Energy (E) = Band gap, Planks constant (h)=6.626×10^{-34} J s, Velocity of Light (c) = 2.99×10^{8} m/s, and Wavelength (λ) = Absorption peak value. 1 eV = 1.6×10^{-19} J (Conversion factor). Table 2 shows the band gap values of as-prepared materials.

In PL spectra, MnO_2 signal is found to in range of 300–800 nm (Figure 5). The spectrum exhibits prominent emission bands located in green–violet spectral region. A broad weak emission in the green region is observed at around 520 nm which can be ascribed to the surface defects or surface dangling bonds.[46–48] PANi shows peak at 367 nm, due to $\pi \rightarrow \pi^*$ transition.[49] PTh shows absorption near excitation wavelength 325 nm.[50] PL signal for PIn can be observed which comes from the recombination of electron in singly occupied oxygen vacancies with photo exited holes.[51–53] PPy shows PL emission peaks near 400 nm. However, agglomeration affects the PL intensity of the polymer.[51] This PL emission characteristics demonstrate the promise of the synthesized materials for practical applications in ultraviolet and visible light emission devices.

Figure 6 shows the cyclic voltammetric (CV) curves of MnO_2, PANi, PTh, PPy, PIn, Mn-PANi, MnO_2-PTh, MnO_2-PPy, and MnO_2-PIn recorded at a scan rate of 50 mV s^{-1}. The CV curves clearly shows that prepared composite has higher supercapacitive properties than sperate MnO_2, PANi, PTh, PPy, and PIn. The superior supercapacitive properties of composite attributed

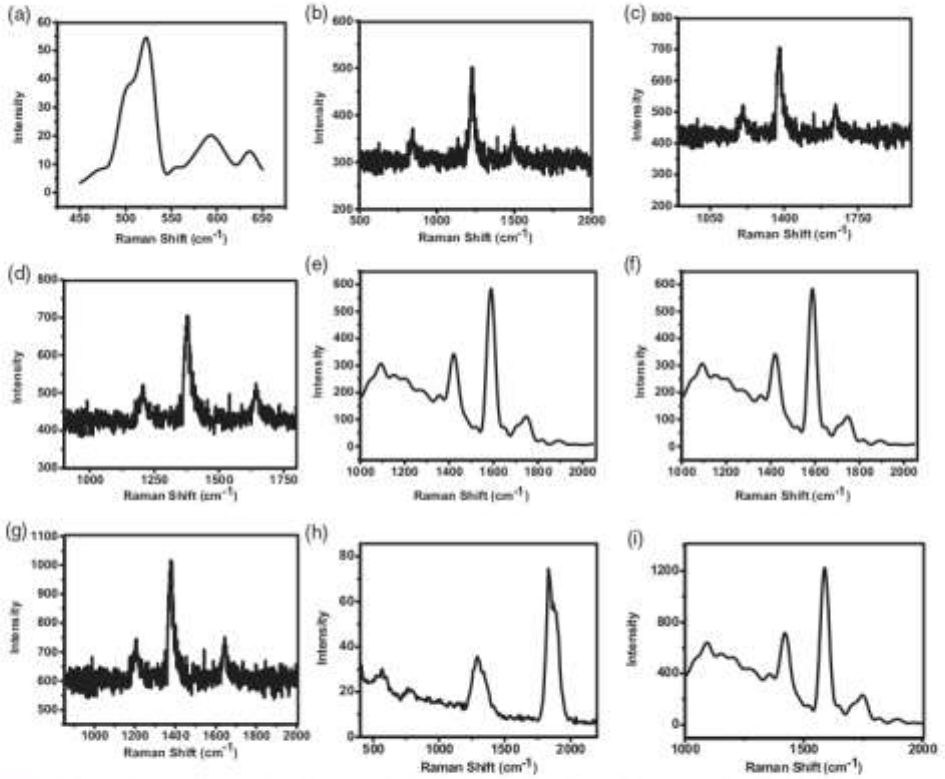

Figure 3. Raman Spectra of (a) MnO_2, (b) PANi, (c) PTh, (d) PPy, (e) PIn, (f) MnO_2-PANi, (g) MnO_2-PTh, (h) MnO_2-PPy, and (i) MnO_2-PIn.

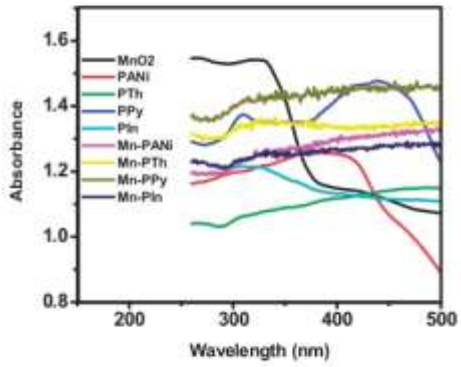

Figure 4. UV–VIS spectra of MnO_2, PANi, PTh, PPy, PIn, MnO_2-PANi, MnO_2-PTh, MnO_2-PPy, and MnO_2-PIn.

to synergetic effect between conducting polymers and MnO_2. Specific capacitance has been estimated using the relation (Equation (1))[45]

$$Cs = \frac{I}{m \times v}(Fg^{-1}) \quad (1)$$

Table 2. Band gap and Absorption peak values for MnO_2, Polymers and their composites.

Compound	Absorption peak value (nm)	Band gap (eV)
1. MnO_2	410	3.02
2. Polyaniline (PANi)	310	3.99
3. Polythiophene (PTh)	265	4.67
4. Polypyrrole (PPy)	440	2.82
5. Polyindole (PIn)	249	4.98
6. MnO_2-Polyaniline composite (Mn-PANi)	241	5.14
7. MnO_2-Polythiophene composite (Mn-PTh)	339	3.66
8. MnO_2-Polypyrrole composite (Mn-PPy)	394	3.15
9. MnO_2-Polyindole composite (Mn-PIn)	250	4.95

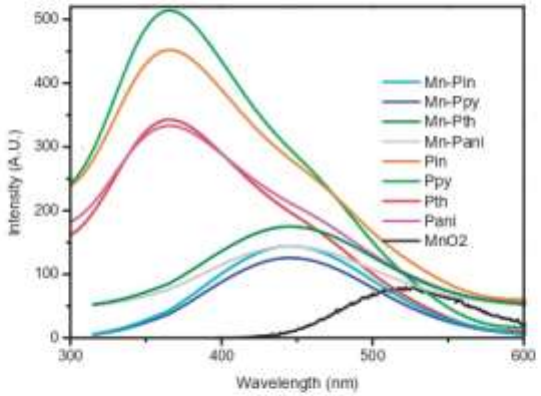

Figure 5. PL spectra of MnO_2, PANi, PTh, PPy, PIn, MnO_2-PANi, MnO_2-PTh, MnO_2-PPy, and MnO_2-PIn.

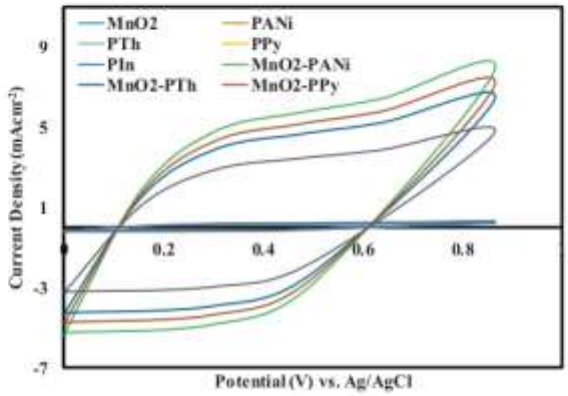

Figure 6. CV curves of MnO_2, PANi, PTh, PPy, PIn, MnO_2-PANi, MnO_2-PTh, MnO_2-PPy, and MnO_2-PIn recorded at a scan rate of 50 mV.s^{-1}.

where I is the average current during anodic and cathodic scan (A), m is the mass of the electrode (g), and v is the scan rate (V). In our case, the highest value of specific capacitance was associate with Mn-PANi composite, which was found to be 633.75 Fg^{-1} at a scan rate of 50 mV s^{-1}. The significant enhancement in electrochemical performance was attributed to improved carrier density, which results in good electrical conductivity.[54] Further study, confined about Mn-PANi composite, as it is optimized sample in this study.

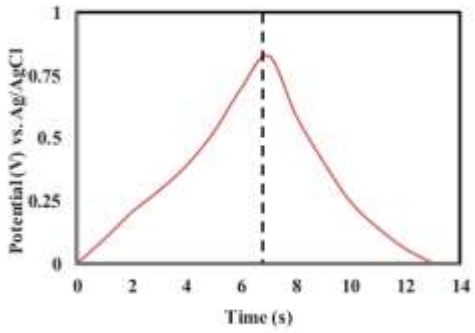

Figure 7. Galvanostatic charge/discharge curves of the MnO_2-PANi composite collected at a current density of 10 μAcm^{-2}.

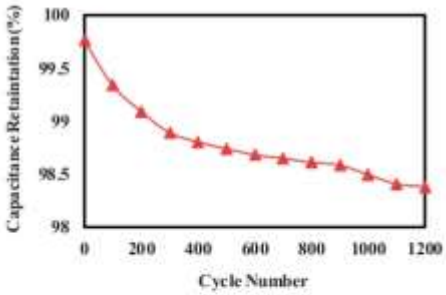

Figure 8. Cycle performance of the MnO_2-PANi composite measured at a scan rate of 50 mV s^{-1} for 1200 cycles.

Table 3. Comparison of present work with some recent reports on supercapacitive properties of MnO2-PANi composites.

Electrode material	Method	Specific capacitance (Fg^{-1})	References
Polyaniline–MnO_2 nanotube hybrid nanocomposite	*In situ* polymerization	626	[56]
MnO_2 nanorods intercalating graphene oxide/ polyaniline ternary composites	*Ex-situ* approach	512	[57]
Ultralong manganese dioxide/polyaniline coaxial nanowires	*Ex-situ* approach	346	[58]
MnO_2-PANi composite	*Ex-situ* approach	633.75	This work

Figure 7 shows the galvanostatic charge/discharge (GCD) curves of Mn-PANi composite. The GCD curves of Mn-PANi composite is nearly symmetric. As expected, Figure 7 shows that the Mn-PANi composite based electrode shows longer discharge time. It is due to the highest specific capacitance associated with Mn-PANi composite. Better electrochemical performance of Mn-PANi composite accredited to synergetic effect between MnO_2 and PANi.

Figure 8 depicts the capacitance drops in Mn-PANi composite. The Mn-PANi composite exhibits good stability with ~98.28% capacitance retention after 1200 cycles. Stable performance of Mn-PANi composite is ascribed to enhanced electrical conductivity and highly stable surface redox reaction.[55]

Table 3 shows the recent reports on supercapacitive properties of Mn-PANi composites and their comparison with findings of this work.

Conclusions

In this work, we successfully prepared the composites of MnO_2 and PANi, PTh, PPy, and PIn and mainly studied their supercapacitive properties. Similarly, the composites were characterized by XRD, SEM, Raman spectroscopy, UV–VIS spectroscopy, and PL. The highest value of specific capacitance was associate with Mn-PANi composite, which was found to be 633.75 Fg^{-1} at a scan rate of 50 $mV.s^{-1}$. The main accomplishment of this study is that MnO_2-PANi composite shows stable performance up to 1200 cycles.

Acknowledgments

The authors are very much thankful to Principal, Bajaj College of Science, Wardha, India for providing necessary facilities for the work.

References

[1] Chen, S. M., R. Ramachandran, V. Maniand, and R. Saraswathi. 2014. Recent advancements in electrode materials for the high-performance electrochemical supercapacitors: a review. *Int. J. Electrochem. Sci.* 9: 4072–4085.

[2] Chen, L., L. J. Sun, F. Luan, Y. Liang, Y. Li, and X. X. Liu. 2010. Synthesis and pseudocapacitive studies of composite films of polyaniline and manganese oxide nanoparticles. *J. Power Sources* 195:3742–3747. doi:10.1016/j.jpowsour.2009.12.036

[3] SimonandY. Gogotsi, P. 2010. Materials for electrochemical capacitors. *In Nanoscience and Technology: A Collection of Reviews from Nature Journals, pp.* 320–329. Singapore: World Scientific.

[4] Conwa, B. E . 1999. *Electrochemical Supercapacitors, Scientific Fundamentals and Technological Applications.* 2nd ed. New York, NY: Kluwer Academic/Plenum Press.

[5] Conwa, B. E. 2013. *Electrochemical Supercapacitors: Scientific Fundamentals and Technological Applications.* Berlin, Germany: Springer Science and Business Media.

[6] Miller, J. R., and P. Simon. 2008. Materials science. Electrochemical capacitors for energy management. *Science* 321:651–652. doi:10.1126/science.1158736

[7] Hu, C. C., K. H. Chang, M. C. Lin, and Y. T. Wu. 2006. Design and tailoring of the nanotubular arrayed architecture of hydrous RuO2 for next generation supercapacitors. *Nano Lett.* 6:2690–2695. doi:10.1021/nl061576a

[8] Yuan, C., X. Zhang, L. Su, B. Gao, and L. Shen. 2009. Facile synthesis and self-assembly of hierarchical porous NiO nano/micro spherical superstructures for high performance supercapacitors. *J. Mater. Chem.* 19: 5772–5777. doi:10.1039/b902221j

[9] Liu, K. C., and M. A. Anderson. 1996. Porous nickel oxide/nickel films for electrochemical capacitors. *J. Electrochem. Soc.* 143:124–130. doi:10.1149/1.1836396

[10] Sun, L. J., X. X. Liu, K. K. T. Lau, L. Chen, and W. M. Gu. 2008. Electrodeposited hybrid films of polyaniline and manganese oxide in nanofibrous structures for electrochemical supercapacitor. *Electrochim. Acta* 53:3036–3042. doi:10.1016/j.electacta.2007.11.034

[11] Beaudrouet, E., A. Le Gal La Salle, and D. Guyomard. 2009. Nanostructured manganese dioxides: synthesis and properties as supercapacitor electrode materials. *Electrochim. Acta* 54:1240–1248. doi:10.1016/j.electacta.2008.08.072

[12] Wang, Y. G., and Y. Y. Xia. 2006. Electrochemical capacitance characterization of NiO with ordered mesoporous structure synthesized by template SBA-15. *Electrochim. Acta* 51:3223–3227. doi:10.1016/j.electacta.2005.09.013

[13] Wei, T. Y., C. H. Chen, K. H. Chang, S. Y. Lu, and C. C. Hu. 2009. Cobalt oxide aerogels of ideal supercapacitive properties prepared with an epoxide synthetic route. *Chem. Mater.* 21:3228–3233. doi:10.1021/cm9007365

[14] Yu, P., X. Zhang, D. Wang, L. Wang, and Y. Ma. 2009. Shape-controlled synthesis of 3D hierarchical MnO2 nanostructures for electrochemical supercapacitors. *Cryst. Growth Des.* 9:528–533. doi:10.1021/cg800834g

[15] Zheng, J. P., and T. R. Jow. 1996. High energy and high-power density electrochemical capacitors. *J. Power Sources* 62:155–159. doi:10.1016/S0378-7753(96)02424-X

[16] Li, H., J. Wang, Q. Chu, Z. Wang, F. Zhang, and S. Wang. 2009. Theoretical and experimental specific capacitance of polyaniline in sulfuric acid. *J. Power Sources* 190:578–586. doi:10.1016/j.jpowsour.2009.01.052

[17] Yuan, A., and Q. Zhang. 2006. Novel hybrid manganese dioxide/activated carbon supercapacitor using lithium hydroxide electrolyte. *Electrochem. Commun.* 8:1173–1178. doi:10.1016/j.elecom.2006.05.018
[18] Bian, C., A. Yu, and H. Wu. 2009. Fibriform polyaniline/nano-TiO2 composite as an electrode material for aqueous redox supercapacitors. *Electrochem. Commun.* 11:266–269. doi:10.1016/j.elecom.2008.11.026
[19] Kim, J. H., A. K. Sharma, and Y. S. Lee. 2006. Synthesis of polypyrrole and carbon nano-fiber composite for the electrode of electrochemical capacitors. *Mater. Lett.* 60:1697–1701. doi:10.1016/j.matlet.2005.12.002
[20] Yan, J., Z. Fan, T. Wei, J. Cheng, B. Shao, K. Wang, L. Song, and M. Zhang. 2009. Carbon nanotube/MnO2 composites synthesized by microwave-assisted method for supercapacitors with high power and energy densities. *J. Power Sources* 194:1202–1207. doi:10.1016/j.jpowsour.2009.06.006
[21] Barpanda, P., Y. Li, F. Cosandey, S. Rangan, R. A. Bartynski, and G. G. Amatucci. 2009. Amatucci, fabrication, physical and electrochemical investigation of microporous carbon polyiodide nanocomposites. *J. Electrochem. Soc.* 156:A873–A885. doi:10.1149/1.3212851
[22] Zhu, S., W. Cen, L. Hao, J. Ma, L. Yu, H. Zheng, and Y. Zhang. 2014. Flower-like MnO2 decorated activated multihole carbon as high-performance asymmetric supercapacitor electrodes. *Mater. Lett.* 135:11–14. doi:10.1016/j.matlet.2014.07.120
[23] Yuan, C., L. Su, B. Gao, and X. Zhang. 2008. Enhanced electrochemical stability and charge storage of MnO2/carbon nanotubes composite modified by polyaniline coating layer in acidic electrolytes. *Electrochim. Acta* 53:7039–7047. doi:10.1016/j.electacta.2008.05.037
[24] Zhang, X., L. Ji, S. Zhang, and W. Yang. 2007. Synthesis of a novel polyaniline-intercalated layered manganese oxide nanocomposite as electrode material for electrochemical capacitor. *J. Power Sources* 173:1017–1023. doi:10.1016/j.jpowsour.2007.08.083
[25] Sun, L. J., and X. X. Liu. 2008. Electrodepositions and capacitive properties of hybrid films of polyaniline and manganese dioxide with fibrous morphologies. *Eur. Polym. J.* 44:219–224. doi:10.1016/j.eurpolymj.2007.10.017
[26] Liu, F. J., T. F. Hsu, and C. H. Yang. 2009. Construction of composite electrodes comprising manganese dioxide nanoparticles distributed in polyaniline–poly (4-styrene sulfonic acid-co-maleic acid) for electrochemical supercapacitor. *J. Power Sources* 191:678–683. doi:10.1016/j.jpowsour.2009.02.046
[27] Liu, F. J. 2008. Electrodeposition of manganese dioxide in three-dimensional poly (3, 4-ethylenedioxythiophene)–poly (styrene sulfonic acid)–polyaniline for supercapacitor. *J. Power Sources* 182:383–388. doi:10.1016/j.jpowsour.2008.04.008
[28] Prasad, K. R., and N. Miura. 2004. Polyaniline-MnO2 composite electrode for high energy density electrochemical capacitor. *Electrochem. Solid-State Lett.* 7:A425. doi:10.1149/1.1805504
[29] Jing, X., Y. Wang, D. Wu, and J. Qiang. 2007. Sonochemical synthesis of polyaniline nanofibers. *Ultrason. Sonochem.* 14:75–80. doi:10.1016/j.ultsonch.2006.02.001
[30] Vernitskaya, T. V., and O. N. Efimov. 1997. Polypyrrole: a conducting polymer; its synthesis, properties and applications. *Russ. Chem. Rev.* 66:443–457. doi:10.1070/RC1997v066n05ABEH000261
[31] Wadatkar, N. S., and S. A. Waghuley. 2015. Complex optical studies on conducting polyindole as-synthesized through chemical route. *Egyptian J. Basic Appl. Sci.* 2:19–24. doi:10.1016/j.ejbas.2014.12.006
[32] Wadatkar, N. S., and S. A. Waghuley. 2016. Studies on properties of as-synthesized conducting polythiophene through aqueous chemical route. *J. Mater. Sci. Mater. Electron.* 27:10573–10581. doi:10.1007/s10854-016-5152-7
[33] hi Hong hanhNguyen. 2017. Synthesis of MnO2 nanoparticle catalyst and application to treatment of organic compounds in agricultural processing villages- a case study in duong lieu village, ha noi Capital, Vietnam. *Int. J. Agric. Innov. Res.* 6:103–107.
[34] Nemade, K. R., and S. A. Waghuley. 2014. Preparation of MnO2 immobilized graphene nanocomposite by solid state diffusion route for LPG sensing. *J. Lumin.* 153:194–197. doi:10.1016/j.jlumin.2014.03.039
[35] Bhagwat, A. D., S. S. Sawantand and C. M. Mahajan. 2016. Facile rapid synthesis of polyaniline (PANI) nanofibers. *J. Nano- Electron. Phys.* 8: 01037.
[36] Sakthiveland, S., and A. Boopathi. 2014. Synthesis and preparation of polythiophene thin film by sPIn coating method. *Int. J. Sci. Res. sec* 141:97–100.
[37] Ma, C., P. Sg, G. Pr, and S. Shashwati. 2011. Synthesis and characterization of polypyrrole (PPy) thin films. *Soft Nanosci. Lett.* 1:6–10.
[38] Nemade, K. R., and S. A. Waghuley. 2014. Low temperature synthesis of semiconducting α-Al2O3 quantum dots. *Ceram. Int.* 40:6109–6113. doi:10.1016/j.ceramint.2013.11.062
[39] Wei, M., Y. Konishi, H. Zhou, H. Sugihara, and H. Arakawa. 2005. Synthesis of single-crystal manganese dioxide nanowires by a soft chemical process. *Nanotechnology* 16:245–249. doi:10.1088/0957-4484/16/2/011
[40] Mažeikienė, R., V. Tomkutė, Z. Kuodis, G. Niaura, and A. Malinauskas. 2007. Raman spectroelectrochemical study of polyaniline and sulfonated polyaniline in solutions of different pH. *Vib. Spectrosc.* 44:201–208. doi:10.1016/j.vibspec.2006.09.005

[41] Agosti, E., M. Rivola, V. Hernandez, M. Del Zoppo, and G. Zerbi. 1999. Electronic and dynamical effects from the unusual features of the raman spectra of oligo and polythiophenes. *Synth. Met.* 100:101–112. doi:10.1016/S0379-6779(98)00167-2

[42] Šetka, M., R. Calavia, L. Vojkůvka, E. Llobet, J. Drbohlavová, and S. Vallejos. 2019. Raman and XPS studies of ammonia sensitive polypyrrole nanorods and nanoparticles. *Sci. Rep.* 9:1–10. doi:10.1038/s41598-019-44900-1

[43] Raj, R. P., P. Ragupathy, and S. Mohan. 2015. Remarkable capacitive behavior of a Co 3 O 4–polyindole composite as electrode material for supercapacitor applications. *J. Mater. Chem. A.* 3:24338–24348. doi:10.1039/C5TA07046E

[44] Liu, Y. C., B. J. Hwang, W. J. Jian, and R. Santhanam. 2000. Santhanam, in situ cyclic voltammetry-surface-enhanced raman spectroscopy: studies on the doPIng–undoPIng of polypyrrole film. *Thin Solid Films* 374:85–91. doi:10.1016/S0040-6090(00)01061-0

[45] Nemade, K. R., and S. A. Waghuley. 2013. UV–VIS spectroscopic study of one pot synthesized strontium oxide quantum dots. *Results Phys.* 3:52–54. doi:10.1016/j.rinp.2013.03.001

[46] Toufiq, A. M., F. Wang, Q. U. A. Javed, Q. Li, and Y. A. N. Li. 2013. Photoluminescence spectra and magnetic properties of hydrothermally synthesized MnO 2 nanorods. *Mod. Phys. Lett. B.* 27:1350211. doi:10.1142/S0217984913502114

[47] Sherin, J. S., J. K. Thomas, and S. Manoj. 2015. Facile synthesis and characterization of pyrolusite, β-MnO2, nano crystal with magnetic studies. *Int. J. Sci. Eng. Appl.* 4:250–252. doi:10.7753/IJSEA0405.1003

[48] Toufiq, A. M., F. Wang, Q-U-A Javed, Q. Li, and Y. Li. 2014. Hydrothermal synthesis of MnO 2 nanowires: structural characterizations, optical and magnetic properties. *Appl. Phys. A.* 116:1127–1132. doi:10.1007/s00339-013-8195-0

[49] Chatterjee, M. J., A. Ghosh, A. Mondal, and D. Banerjee. 2017. Polyaniline–single walled carbon nanotube composite–a photocatalyst to degrade rose bengal and methyl orange dyes under visible-light illumination. *RSC Adv.* 7:36403–36415. doi:10.1039/C7RA03855K

[50] Tripathi, A., S. K. Mishra, I. Bahadur, and R. K. Shukla. 2015. Optical properties of regiorandom polythiophene/Al 2 O 3 nanocomposites and their application to ammonia gas sensing. *J. Mater. Sci: Mater. Electron.* 26:7421–7430. doi:10.1007/s10854-015-3373-9

[51] Vanheusden, K., W. L. Warren, C. H. Seager, D. R. Tallant, J. A. Voigt, and B. E. Gnade. 1996. Mechanisms behind green photoluminescence in ZnO phosphor powders. *J. Appl. Phys.* 79:7983–7990. doi:10.1063/1.362349

[52] Vanheusden, K., C. H. Seager, W. L. Warren, D. R. Tallant, and J. A. Voigt. 1996. Correlation between photoluminescence and oxygen vacancies in ZnO phosphors. *Appl. Phys. Lett.* 68:403–405. doi:10.1063/1.116699

[53] Dey, S., and A. Kumar Kar. 2019. Morphological and optical properties of polypyrrole nanoparticles synthesized by variation of monomer to oxidant ratio. *Mater. Today: Proc.* 18:1072–1076. doi:10.1016/j.matpr.2019.06.566

[54] Nemade, K., P. Dudhe, and P. Tekade. 2018. Enhancement of photovoltaic performance of polyaniline/graphene composite-based dye-sensitized solar cells by adding TiO2 nanoparticles. *Solid State Sci.* 83:99–106. doi:10.1016/j.solidstatesciences.2018.07.009

[55] Kaempgen, M., C. K. Chan, J. Ma, Y. Cui, and G. Gruner. 2009. Printable thin film supercapacitors using single-walled carbon nanotubes. *Nano Lett.* 9:1872–1876. doi:10.1021/nl8038579

[56] Jaidev , R. I. Jafri, A. K. Mishra, and S. Ramaprabhu. 2011. Polyaniline–MnO2nanotube hybrid nanocomposite as supercapacitor electrode material in acidic electrolyte. *J. Mater. Chem.* 21:17601–17605. doi:10.1039/c1jm13191e

[57] Han, G., Y. Liu, L. Zhang, E. Kan, S. Zhang, J. Tang, and W. Tang. 2014. MnO2 nanorods intercalating graphene oxide/polyaniline ternary composites for robust High-Performance supercapacitors. *Sci. Rep.* 4:4824–4830. doi:10.1038/srep04824

[58] Zhou, J., L. Yu, W. Liu, X. Zhang, W. Mu, X. Du, Z. Zhang, and Y. Deng. 2015. High performance all-solid supercapacitors based on the network of ultralong manganese dioxide/Polyaniline Coaxial Nanowires. *Sci. Rep.* 5:17858–17864. doi:10.1038/srep17858

11 Hawaman badal an jalstrot : ek Abhyas

MAHMUL/03051/2012
ISSN: 2319 9318
UGC Approved Sr.No.62759
Vidyawarta® | February 2018 Special Issue | 049

...जाण्याच्या लोकसंख्येला वेळीच आळा घालणे आवश्यक आहे.

६. पर्यावरणीय जनजागृती :

पर्यावरणाचा होणारा ऱ्हास थांबविण्या करिता आणि पर्यावरणीय संतुलन टिकविण्यासाठी मानवाची भूमिका अत्यंत मोलाची आहे. पर्यावरणाचे महत्व सर्वांना कळावे यासाठी जनजागृती करणे गरजेचे आहे. वृक्ष, हवा, पाणी, भूमि, प्राणी, खनिजे, ऊर्जा, प्राणी, खनिजे, ऊर्जा साधने, वन्यजीव, जलचर यांच्या संरक्षण संवर्धन कार्यक्रमाचा विस्तार करणे. शिकारी, मांस विक्री, प्रदुषण यावर कठोर कायदे करून अंमलबजावणी करणे. सरकारी संस्था, खाजगी संस्था, सुशिक्षित तरूणांनी वृत्तपत्रे, रेडीओ, टि.व्ही., सोशल मिडीया या माध्यमाद्वारे पर्यावरणीय घटकांचे महत्व सामान्य जनते पर्यंत पोहचविणे गरजेचे आहे. तसेच शालेय स्तरावर अभ्यासक्रमात पर्यावरण विषयांचा अभ्यास समाविष्ट करणे अनिवार्य असले पाहिजे.

निष्कर्ष :

१७ व्या शतकात जगतगुरू तुकाराम महाराजांनी वृक्ष वल्ली आम्हा सोयरे वनचरे ! असा अभंग लिहीला. छत्रपती शिवाजी महाराजांनी सुध्दा जनतेला आज्ञापत्रातून वृक्षांचे महत्व सांगितले २१ व्या शतकातील मानवाने मेट्रो ट्रेन, बुलेट ट्रेन, जेट विमाने, क्षेपणास्त्रे यांची निर्मिती केली. मानव चंद्रावर, मंगळावर व शुक्रावर पोहचला परंतु आर्थिक विकासा बरोबर पर्यावरणांचे मोल विसरला आर्थिक विकासा प्रमाणेच शाश्वत विकास सुध्दा झाला पाहिजे यावर मानवाने भर द्यावा. तरच वैश्विक विकास करता येईल.

संदर्भ

१. डॉ. घारपुरे विठ्ठल : "पर्यावरणशास्त्र", पिंपळापुरे अँण्ड कं. पब्लिशर्स, नागपूर, जून २००५

२. सवदी ए.बी. : "पर्यावरणशास्त्र", निराली प्रकाशन पुणे फेब्रुवारी २०१३

३. डॉ. चौरसिया राम आसरे : "पर्यावरण भूगोल", किताब महल एजन्सीज इलाहाबाद १९९८

४. प्रा.डॉ. घोलप टि.एन. "पर्यावरणशास्त्र" निशिकांत प्रकाशन पुणे, डिसेंबर २०००

५. विविध वृत्तपत्रे :

□□□

12

हवामानबदल आणि जलस्त्रोत : एक अभ्यास

प्रा. एन. व्ही. नरुले
भूगोल विभाग प्रमुख
इंदिरा महाविद्यालय, कळंब,जि.—यवतमाळ.

****

प्रस्तावना :—

मानवाने आपले जीवन सुखकर करण्यासाठी नैसर्गिक साधनांचा शोध घेवून उपयोग करुन घेतला. परंतु नैसर्गिक साधने मर्यादित असल्याने त्यांचा वापर काळजीपूर्वक केला पाहिजे. हल्ली काही नैसर्गिक साधनसंपत्तीचा क्षय होतांना दिसून येत आहे, त्यामुळेच त्याचा मानवी संस्कृतीवर प्रभाव पडत आहे. पर्यावरणाचे संतुलन बिघडून वैश्विक स्तरावर प्रदुषणाची समस्या निर्माण झाली आहे. पर्यावरणाचे संतुलन बिघडल्याने भारतात गेल्या तीन वर्षात काही राज्यात तसेच अनेक खेडयामध्ये अवर्षण व दुष्काळी स्थिती आहे. देशातील जवळपास २५६ जिल्हयामध्ये अधिकृतरित्या दुष्काळ जाहीर करण्यात आला आहे. महाराष्ट्रात विदर्भ, मराठवाडा, उत्तर प्रदेशात बुंदेलखंड, तेलगणा, आंध्रप्रदेश, कर्नाटक इत्यादी भागातील परिस्थिती गंभीर आहे. विहीरी, तलाव, धरणेही कोरडी पडलेली आहे. नदया सुकलेल्या अवस्थेत आहेत. आजच्या औद्योगिक युगात वाढत्या प्रदुषणामुळे आणि पर्यावरणीय संकटामुळे हवामानात मोठया प्रमाणावर बदल घडून येत आहे.

हवामान बदलाची कारणे:—

हवामान बदल हा पृथ्वीच्या अंतर्गत किंवा बाहय घटनांचा परिणाम असून त्यासाठी दोन बाहय घटक महत्वाचे मानले जाते. पृथ्वीच्या परिभ्रमणात हळूहळू बदल होत आहे. हा बदल अनेक ग्रहांच्या गुरुत्वाकर्षण शक्तीमुळे नसेल आकाशगंगेच्या मधात असलेल्या सौरप्रणालीमुळे झालेला आहे. दुसरे म्हणजे

पृथ्वीचे तापमान ही तीन प्रकारे होताना आढळून आले आहे. परंतु याचा सौरमंडळावर काहीही परिणाम झालेला नाही, मात्र अवकाश व येथील [illegible] बदल दिसून आलेला आहे. पृथ्वी गेल्या १६००० वर्षांपासून एका निश्चित [illegible] परिभ्रमण करीत आहे. जेव्हा पृथ्वीचा अक्ष सूर्याच्या अगदी जवळ असतो तेव्हा वातावरणात (हवामानात) बदल जाणवतो.

हरितगृहवायूंचा परिणाम :—

उष्णतेच्या सूर्याची लघुलहरी किरणे पृथ्वीच्या वातावरणात प्रवेश करतात त्यावेळी भिन्न प्रकारच्या वायूंची निर्मिती होते. ही किरणे पुन्हा अवकाशात [illegible] तेव्हा त्याचा काही भाग वातावरणात शोषला जातो. महत्त्वाचे म्हणजे पृथ्वीचा पृष्ठभाग अवकाशात किरणे सोडतात. त्यामुळे तयार झालेले काही वायू पुन्हा पृथ्वीवर येतात, त्यामुळे वातावरणात उष्णता निर्माण होऊन पृथ्वीचा समतोलपणा कायम राहतो. यालाच हरितगृह वायू म्हणतात. यात प्रामुख्याने कार्बन डाय ऑक्साईड, नायट्रस ऑक्साईड, मिथेन, बाष्प, क्लोरोफ्लुरोकार्बन्स, आणि ओझोन हे वायू आहेत. सूर्यप्रकाशाचा काही भाग शोषणाशिवाय वातावरणातून पृथ्वीवर येतो,

(१) शोषून त्याचे रूपांतर इन्फ्रारेड किरणांमध्ये होते. (उष्ण पृष्ठभाग), (२) वातावरणात इन्फ्रारेड किरणे परावर्तित जातात, त्यापैकी काही, (३) हरितगृह वायू शोषून घेतात आणि, (४) पुन्हा ते पृथ्वीच्या पृष्ठभागाकडे सोडतात, काही इन्फ्रारेड किरणे हरितगृह वायू मध्ये अडकून राहतात आणि, (५) काही अवकाशात जातात. मानवाच्या कृतीमधून वातावरणात अतिरिक्त हरितगृह वायू सोडले जातात. (६) अवकाशात पोहचण्यापूर्वी इन्फ्रारेड किरणांचे प्रमाण वाढून, यामुळेच हरितगृह वायू परिणाम होतो आणि पृथ्वीच्या तापमानात वाढ होते.

एकूणच पृथ्वीचे तापमान नियंत्रित ठेवण्यासाठी हरितगृहवायूंची भूमिका महत्त्वाची आहे. परंतु हरितगृह वायूंचे प्रमाण जास्त झाल्यास ते हानिकारक ठरून जागतिक हवामानात कमालीचा बदल होतो.

हवामान बदलाचे पुरावे :—

आयपीसीसी (२०१५) च्या पाचव्या मूल्यांकन अहवालानुसार जगात हवामानात बदल होत असल्याचे सिद्ध करणारे अनेक पुरावे उपलब्ध झालेले आहेत. अलीकडच्या काही दशकांमध्ये तापमानात [illegible] वाढ झालेली दिसून येत आहे. सन १८८० पासून पृथ्वीच्या तापमानात सतत वाढ होत आहे. आयपीसीसीच्या (२००८) नुसार १९८३ ते २०१२ ही ३० वर्षे कदाचित गेल्या १४०० वर्षांतील सर्वात उष्ण कालखंड आहे.

हवामानबदलाचा जलस्रोतांवर होणारा परिणाम अभ्यासण्याच्या पद्धती :—

जलस्रोतांवर होणाऱ्या हवामानबदलाचे परिणाम जाणून घेताना, हरितगृह वायूंचे प्रमाण वाढीव वातावरणातील बदल अभ्यासण्यासाठी ग्लोबल क्लायमेट मॉडेल्स (जीसीएम) ही पद्धत आहे, यामध्ये वातावरण, हिम, भूपृष्ठ, सागरी परिणामांचा अभ्यास करण्यात येतो. जीसीएम पद्धतीत पृथ्वीवर ग्रीड [illegible] वापर केला जातो.

हवामानबदल आणि उपाययोजना :—

आयपीसीसीच्या व्याख्येनुसार हवामानबदलाशी जुळवून घेण्याची प्रक्रिया ही नैसर्गिक आहे. परंतु जुळवून घेण्याच्या वेगवेगळ्या पद्धती आहे. हरितगृहवायूंचे उत्सर्जन कमी करण्यासाठी मानवाने केलेला हस्तक्षेप [illegible] उपाययोजना होय. शेती आणि वनीकरणाच्या माध्यमातून हरितगृहवायूंचे मोठ्याप्रमाणावर उपशमन करता येऊ शकते, जर उपशमन मोठ्याप्रमाणात झाले तर सामाजिक जीवनावर त्याचे परिणाम कमी होऊन लोकांना क्षती पोहचणार नाही. कमी उपशमन म्हणजेच व्यापक हवामानबदल, की ज्यास मोठ्या प्रमाणात समायोजनाची आवश्यकता असते. हरितगृह वायूंचे उत्सर्जन रोखण्यासाठी ही प्राथमिक गरज आहे.

विविध स्तरावर असलेले आर्थिक व्यवहार उदा. पर्यावरण— संवेदनशील स्थान, तसेच हे देश मर्यादित आर्थिक व्यवस्थेवर अवलंबून आहे. भारतातील शेतकरी शेतीवर आधारित अनेक उद्योगधंदे करू शकतो उदा. दुग्धव्यवसाय, मत्स्यपालन, फळसंवर्धन, पशुसंवर्धन इत्यादी. नवीकरणीय ऊर्जा म्हणजेच जलविद्युत हे पर्यावरणाचे संरक्षण करते, तसेच ऊर्जेची गरज भागवते. नवीकरणीय ऊर्जेचे कोणत्या प्रकारे हरितगृह वायूंची निर्मिती करत नाहीत.

जमिनीचा वापर आणि व्यवस्थापन :—

हवामान बदलाच्या उपशमनासाठी व्यवस्थापन पद्धती यांचाही जलस्रोतांवर परिणाम होतो. काही प्रक्रियांमध्ये मातीतील कार्बनचे प्रमाण वाढीस हातभार लावण्याचा सल्ला दिला जातो, वनस्पतींचे संरक्षण आच्छादन, बारमाही पिकांची लागवड, कमी प्रमाणात केलेली मशागत इत्यादी मुळे मातीची घुप होऊन पाण्याची गुणवत्ता सुधारते.

वृक्षारोपण किंवा वनीकरण :—

वृक्षारोपण किंवा वनिकरणाचे प्रमाण जास्त असलेल्या प्रदेशात हवामान बदलाचा कमी परिणाम दिसून येतो. कारण वृक्ष हे प्रकाशसंश्लेषण प्रक्रियेत कार्बन डाय ऑक्साईड शोषून घेतात. तसेच वनिकरणामुळे पर्यावरण चांगले राहते. जलीय चक्रासाठी वनांचे अनन्यसाधारण महत्व आहे.

नवीन लागवड करण्यात आलेले वृक्ष जास्त पाणी शोषून घेतात, म्हणून शुष्क कटीबंधीय प्रदेशात लावलेल्या वृक्षारोपणाचा भूपृष्ठीय जलावर आणि नदी प्रवाह प्रणालीचा गंभीर परिणाम होतो. म्हणजेच जमिनीची होणारी घुप थांबते, वाहणारे पाणी थांबते यामुळे झाडांचे वय वाढते. वनीकरण किंवा वृक्षारोपणाच्या माध्यमातून जलसंवर्धन होते, तसेच लहान प्रमाणात येणारे पूर थांबतात.

हवामानबदलाचा भारतीय जलस्त्रोतांवर होणारा परिणाम :—

बारमाही वाहणाऱ्या नद्या आणि मोठ्याप्रमाणात तलावांची संख्या यामुळे भारत हा जगातील एक आर्द्रता (ओलावा) असणारा प्रदेश आहे. गंगा, सिंधू, ब्रम्हपुत्रा या बारमाही वाहणाऱ्या मोठ्या नद्या पाण्याचे स्रोत आहेत. हा प्रवाह पाऊसमान नसणाऱ्या काळात कमी होतो. बारमाही वाहणाऱ्या नद्या मुख्यत्वे पावसाचे पाणी आणि जमिनीत पाण्याचे पुनर्भरण यावर अवलंबून असतात. तापमानात होणारे बदल, एकूण पर्जन्यमान इत्यादी गोष्टींचा नद्यांच्या प्रवाहावर नाबडतोब परिणाम होतो. भारताची अर्थव्यवस्था शेतीवर अवलंबून आहे, त्यामुळे हवामान बदलाचे भविष्यातील परिणाम भयंकर असणार आहेत. वाढती लोकसंख्या, त्याप्रमाणात लागणारे अन्न, पाणी आणि ऊर्जेची वाढत जाणारी मागणी यामुळे शेती प्रदेशात ताण पडणार आहे.

हिमालयीन प्रदेशातून वाहणाऱ्या तीन मोठ्या एकूण पाण्याच्या ६० टक्के गरज भागवत आहे, यावरून या नद्यांचे महत्व अधिक आहे. हिम आणि बर्फाचे वितळणे यावर यांचा प्रवाह अवलंबून आहे. त्यामुळेच या नद्यांवर जागतिक हवामान बदलाचा लक्षणीय परिणाम होतो हिमनगाच्या वितळण्याचे प्रमाण वाढते वाटत जाणार असून भारताला हवामान बदलाच्या फार मोठा धोका निर्माण होणार आहे. २१ व्या शतकात दुष्काळ आणि पुराचे वाढलेले प्रमाण आपल्याला यामुळेच दिसून येत आहेत. दुष्काळ आणि पुराचा फटका समाजातील सर्वच व्यक्तींना बसतो म्हणून आता दुष्काळ आणि पूर व्यवस्थापन हे हवामानबदल आणि जलस्रोत यांना समोर ठेवूनच करावे लागणार आहे. उन्ह दाणाऱ्या पूरामुळे जलसाठ्याच्या तलभागावर गाळ जमा होणे ही धोक्याची घंटा आहे.

भारतातील जलस्त्रोतांसंदर्भात हवामान बदलाच्या दृष्टिने करावयाच्या गोष्टी :—

१. हेरंबरेखांच्या दृष्टिने सुलभ असे जलविज्ञान प्रकल्पांचे जाळे जास्तीत जास्त प्रमाणात उभारावेत.

२. सद्य परिस्थितीत असलेल्या प्रत्येक खोऱ्यातील उपलब्ध जलसाठ्यांचे अद्ययावतीकरण करावे.

३. भविष्यातील हवामान बदलाचा पर्जन्यमानाची वारंवारिता आणि घनता यावर होणारा परिणाम हा सद्याच्या स्थितीतून अभ्यासावा.

४. प्रादेशिक व खोऱ्यांच्या पातळीवर फायदेशीर असा ऊर्ध्वगामी जीसीएम प्रकल्प उभारावा.

५. कार्बनचे उत्सर्जन व उपलब्ध जमिनीवरील पाणी यांचा एकमेकांशी असलेल्या संबंधाचा अभ्यास (विशेषत: सागरकिनारी प्रदेशासंबंधी) करावा.

६. जमिनीचा उपयोग आणि आच्छादन यावर कार्बन उत्सर्जनाचा 'परिणाम याचे मुल्यमापन करुन त्याचा जलस्रोतांवर होणाऱ्या परिणामाचा अभ्यास करावा.

७. कार्बनचे उत्सर्जनाचा शहरी भागातील पर्जन्य घनता, कालावधी, आणि वारंवारिता यांच्या संबंधावर अभ्यास करावा.

८. शेतीवरील हवामानविषयक व जलविज्ञान विषयक दुष्काळाचे प्रमाण, तीव्रता, वारंवारिता याचे मुल्यमापन करावे.

९. धरणे, नद्या, तलाव यांच्या तळाशी जमा होणारा गाळ आणि त्याचे व्यवस्थापन करावे.

१०. जलविद्युत प्रकल्पांचा आढावा, निर्मिती आणि संचलन हे बदलत्या परिस्थितीनुसार करावे.

११. अनेक ठिकाणची परिस्थिती लक्षात घेवून जलक्षेत्रात पर्याप्त अशा पायाभूत सुविधांची निर्मिती करावी.

१२. आकडेवारी गोळा करून एकात्मिक जलस्त्रोत व्यवस्थापन अमलात आणावे (IWRM) इत्यादी.

निष्कर्ष :—

एकूणच अलीकडच्या काही वर्षांमध्ये हवामान बदलाच्या कारणांचा शास्त्रीय पध्दतीने अभ्यास करण्याच्या पध्दतीत फार मोठा बदल झालेला दिसून येत आहे. नैसर्गिक विविधता हे पर्यावरणाचे मुख्य वैशिष्ट्ये आहे. भौतिक तत्वानुसार जगातील सागरावर उष्णता वाढलेली दिसून येत आहे. नैसर्गिक वाहस घटकात झालेले बदल हे काही वर्षांपासून झालेल्या हवामानबदलाचे कारण ठरलेले आहे. पृथ्वीचा पृष्ठभाग, सागरी भाग, वातावरण या सर्वांवर हवामानबदलाचा, वाढलेल्या उष्णतेचा परिणाम जाणवत आहे.

संदर्भ :—

१) पर्यावरणीय भूगोल — डॉ. यू. बी. सिंह

२) भारताचा समग्र भूगोल —ए. बी. सवदी व पी. एस. कोळेकर

३) योजना विशेषांक

❑❑❑

13

बुलडाणा जिल्हातील लोकसंख्येच्या घनतेचे अभिक्षेत्रीय व कालीक विश्लेषण.

डॉ. साधना सं. खंडार (भेंडकर)
वसंतराव नाईक शासकीय कला व समाजविज्ञान संस्था, नागपूर.

प्रा.संदिप रु. मसराम
वसंतराव नाईक शासकीय कला व समाजविज्ञान संस्था, नागपूर.

सारांश:

लोकसंख्येच्या अभ्यासात लोकसंख्येच्या घनतेला महत्त्व आहे. विशिष्ट क्षेत्रात किती लोकसंख्या सामावली आहे. याचे गुणोत्तर म्हणजे लोकसंख्येची घनता होय. प्रस्तुत संशोधनात बुलडाणा जिल्हातील ग्रामीण व शहरी घनतेचा तुलनात्मक अभ्यास करण्यात आलेला आहे. कोणत्याही प्रदेशाच्या विकासासाठी लोकसंख्येचा तपशिलवार अभ्यास करणे गरजेचे असते.

प्रस्तावना:

बुलडाणा जिल्हा हा विदर्भाचे प्रवेशद्वार म्हणुन ओळखले जाते. विदर्भाच्या पश्चिम दिशेला असलेला जिल्हा सांस्कृतिक दृष्टिनेही महत्त्वाचा आहे. लोकसंख्या शास्त्रीय घटकांचे विश्लेषण करण्याकरीता तेथील लोकसंख्येच्या घनतेचा अभ्यास केला जातो. लोकसंख्येची घनता ही एखाद्या प्रदेशातील दर चौ.कि.मी भागात राहणाऱ्या लोकांचे सरासरी प्रमाण दर्शविते. प्रस्तुत संशोधन पेपर मध्ये बुलडाणा जिल्हातील लोकसंख्येच्या एकूण, ग्रामीण, व शहरी घनतेचा १९९१, २००१ व २०११ यानुसार तालुकानिहाय अभ्यास करण्यात आला आहे.

12 Job Categories, Mental Health and Job satisfaction

VOLUME - IX, ISSUE - II - FEBRUARY - JULY - 2021
GENIUS - ISSN 2279 - 0489 - IMPACT FACTOR - 6.631 (www.sjifactor.com)

20. Job Categories, Mental Health and Job Satisfaction

Dr. P. B. Ingle
Assistant Professor, Department of Psychology, Indira Mahavidyalay, Kalamb, Dist. Yavatmal.

Abstract

Job has its own nature and its separate specific skills. And it is also a major source for earning wealth and health, for individuals and human resources development. We have some expectation form job like it should be given security of life, respect in society to us. If it fulfill our own needful criteria then it becomes suitable for the person otherwise not. Job also has expectation form the people that are skill oriented and interested person otherwise it becomes hectic for person. Several scientific studies on job and person relationship describe it as suitable job for suitable person. Present study focus on the job categories and its impact on mental health and job satisfaction score. Psychological standardized measure; Dr. Amar Singh and Dr. T. R. Sharma Job satisfaction scale and Employee's Mental Health Inventory by Jagdish were administered. Data collected form 20 subjects from two job categories teacher, clerk having 5 to 10 years' experience of job, at single job without any transfer were selected. - Collected data analyzed through descriptive statistical technique S. D. Mean and ANOV A. Result.

Keywords: Job Satisfaction, .Mental Health, Job Categories.

Introduction

Jon satisfaction is an aspect of functioning in any profession which is widely accepted. Hoppock (1935) bring this term into currency. He reviewed a little over 30 contemporary studies and concluded that though there was much opinion about job satisfaction yet there was not much factual work done in the field. The summum bonum of the opinion is that job satisfaction is favourableness with which workers view their job. It reflex when there is a fit between job requirements and wants and expectations of the employees. In other words, it expresses the extent of match between worker's expectation (also aspirations) and the rewards the job provides and values it creates and values it creates and gets cherished.

Recent years have witnessed a lot of conceptualization with regard to factors involving job satisfaction. The number of theories independent and interrelated, which explain, at least tend

doing so the different facets of Job satisfaction, which view this phenomena from different angles and endeavor to explore it in all its dimensions.

Performance Theory of Donald et al. 1970 explain employee's satisfaction connection with job performance; satisfaction leads to performance and performance to satisfaction and performance - satisfaction relationship is moderated by many variables link with man and his job. Brayfield and Grockett (1955) have reviewed 50 studies and provided a capstone to the satisfaction - performance relationship.

Schaffer (1953) has argued that job satisfaction will vary directly with the extent to which the need to an individual which can be satisfied, are actually satisfied.

Maslow (1954) proposes that people are continuously in motivational state, as one desire becomes satisfied another rises to take its place. He postulates, a hierarchy of human needs- physiological needs, safety needs, social needs, esteem status, self-actualization etc.

Mental Health

Health is defined as indispensable quality in human beings. It is said that no wealth without health. Sound health makes sound mind, adds to happiness of a person, and leads to a meaningful and active life.

"The preamble of the World Health Organization's charter defined health as a state of complete physical, mental and social well-being, not merely the absence of disease or infirmity" (Monopolis et. Al., 1977).

Bhatia (1982) Considered mental health as the ability to balance feelings, desires, ambitions and ideals in one's daily living

Objective

1. To study the Mental Health of the different job categories
2. To study Job Satisfaction among Teachers, Clerks.
3. To study the relationship between job satisfaction and Mental Health of the job categories.

Hypothesis

1. The teachers mental health will have significantly differ than the clerk's mental health.
2. Job satisfaction score will be different to the different job categories.
3. There will be positive relationship between job satisfaction and mental health of the teachers and clerk.

Methods & Sample

Independent Variable : Job Categories

A) Teaching

B) Clerical

Sample

There are 60 subjects were selected randomly from the two job category which teaching field and clerical field and same size into two category in this way 30 subjects from teaching field and 30 subjects form clerical field. Job experience 5-10 years was selecting criteria.

Tools & Techniques

1. Job Satisfaction Scale by Dr. Amar Sing & Dr. T.R. Sharma was used to measure job satisfaction of the employee. The test-retest reliability is 0.97 with N+52 and a gap of 25 days. The scale compares favourably with Muthayya's Job satisfaction questionnaire giving a validity coefficient of 0.74.

   Scoring: The positive statement carry a weightage of 4,3,2,1 and 0 and negative once a weightage of 0,1,2,3 and 4.

2. Employee's Mental Health Inventory (EMHI) constructed by Dr. Jagdish was applied to measure variable mental health. Test has the split-half reliability of the test was determined by computing the pearson's Product Moment coefficient of correlation .66 and index of reliability is .89 Inventory possesses content validity and Construct validity is determined by computing the coefficient of the correlation between the scores on EMHI and Mental Health Scale (Buck, 1972). The coefficient was found to be .74. It also validated by relationship with ' Personal Adjustment Scale' by Pestonjee (1973). The validity coefficient was found to be .57.

Techniques: Mean and S.D was calculated of each group and Student's t test is used to measure significant difference between means., product movement correlation was used to measure association between mental health and Job Satisfaction.

Result & Discussion

Table no.1 shows the statistics of mental Health of the Teachers and Clerk.

Variable	N	Mean	S.D.	T value	Sing.
Teachers	30	20.90	1.79	30.29	.05
Clerk	30	13.80	3.28		
Total	60	17.35	4.44		

Result was found that means of the Mental health of teachers 20.90, S.D. 1.79 and clerk 13.80, S.D. 3.28, t (59) = 30.29, $p<0.05$ it means that the hypothesis teachers mental health is greater than the clerk mental health is found significantly true.

Table no.2 shows the statistics of Job Satisfaction of the Teachers and Clerk.

Variable	N	Mean	S.D.	T value	Sing.
Teachers	30	79.97	11.90	40.11	.05
Clerk	30	60.80	6.64		
Total	60	70.38	13.59		

Result was found that means of the job satisfaction of teachers 79.90, S.D. 11.90 and clerk 6.80, S.D. 6.64, t (59) = 40.11, $p<0.05$ it means that the hypothesis teachers are high job satisfaction level than the clerk is found significantly true.

Table no.3 shows relationship between job satisfaction and mental health.

Variable	N	Job Satisfaction	Mental Health
Mental H	30	0.59	0.00
Job Satisfaction	30	0.00	0.59

Table no.3 shows the relationship between job satisfaction and mental health the person product movement correlation was sound .59 and positive direction. Hence it can be say that there is positive correlation, the hypothesis is accepted.

Conclusion

1. Teachers are better in mental health than the clerk.
2. Teacher have more satisfied in their job compare to clerk.
3. There is positive correlation between job satisfaction and mental health.

References

- Bhatia, B.D. (1982). Mental Hygiene in Education. In B. Kuppuswamy (Ed.) Advanced Educational Psychology. New Delhi: Sterling Publishers Pvt. Ltd.
- Monopolis, J., Kouvaris, M. and Galanopoulou, P (1977). Health as a human value. Transnational Mental Health. Research Newsletter, 19, (4), 5-9.
- Hoppock, R. (1935). Job-satisfaction, New York: National Occupational Conference, Harper & Row.

13 Preparation of spintronically active ferromagnetic contacts based on Fe, Co and Ni Graphene nanosheets for Spin-Field Effect Transistor

Materials Science & Engineering B 261 (2020) 114772

Contents lists available at ScienceDirect

Materials Science & Engineering B

journal homepage: www.elsevier.com/locate/mseb

Preparation of spintronically active ferromagnetic contacts based on Fe, Co and Ni Graphene nanosheets for Spin-Field Effect Transistor

Neetu Gyanchandani[a], Santosh Pawar[b], Prashant Maheshwary[a], Kailash Nemade[c,*]

[a] JD College of Engineering and Management, Nagpur 441501, India
[b] School of Engineering, Dr. A.P.J. Abdul Kalam University, Indore 452016, India
[c] Department of Physics, Indira Mahavidyalaya, Kalamb 445401, India

ARTICLE INFO

Keywords:
Ferromagnetic contacts
Spintronics
Graphene
Spin field effect transistor

ABSTRACT

Present experimentation reports the interaction between graphene and transition Metal (Fe, Co and Ni), in the context of ferromagnetism. Fe-Graphene, Co-Graphene and Ni-Gmphene samples were prepared by simple ex-situ approach followed by probe-sonication technique. The prepared samples were characterized by X-ray diffraction (XRD) technique and Scanning Electron Microscope (SEM) analysis. To study magnetic properties of prepared samples, few tests were performed namely Vibrating Sample Magnetometer (VSM) technique, Magnetoconductance Study, Temperature-dependent Magnetization Measurements and Large positive Magnetoresistance Study. Results obtained were analyzed specially in the context of Spin-Field Effect Transistor (s-FET) application.

1. Introduction

In scientific community, graphene is well accepted class of material which has important features as light weight, good transport properties and ease of synthesis. Spintronics is rapidly emerging area of research, which deals with the use of electron spin degree of freedom instead of/ in addition to electrical charge of electron. However, spin-polarization is very important condition for spintronics application which can easily be achieved by using ferromagnetic materials. The transition metals Fe ($3d^6s^2$), Co ($3d^7s^2$) and Ni ($3d^8s^2$) are partially filled d-block element and also well-known ferromagnets at room temperature. In metal spin relaxation time and length is very short, whereas it is long in semi-conductors [1].

Graphene-based spintronics is comparatively a new field of research and development. Recently, scientific community has seen noteworthy progress in spintronics technology. The graphene-based materials are the potential category of materials for spintronics application for the reasons mentioned below,

- Graphene based magnetic materials have long spin lifetime and diffusion length [2].
- Graphene is a very promising spin channel material, as it shows room temperature spin transport with long spin diffusion lengths up to several micrometers [3].
- Graphene has special motivating physical property i.e. tunable carrier concentration and high electronic mobility through Gate Voltage [4].
- Graphene has high electron mobility (about ten times higher) compared to commercial silicon wafers. It has long spin-relaxation length and ballistic transport characteristics (electrons can travel 300 nm or more without scattering) [5–9].
- Above characteristics of graphene facilitates huge scope to develop the spin-polarized devices, mainly spin-Field Effect Transistors. Therefore, scientists have concentrated on developing efficient magnetically active graphene based spintronics materials. Use of graphene based ferromagnetic materials for spintronics application needs an insight about the behavior of magnetic properties at the interfaces of graphene and Fe, Co and Ni nanocrystallite [10–12].

Therefore, in this primary research attempt of magnetic behavior of Fe, Co and Ni loaded Graphene nanosheets has been studied for future spintronics applications specially Spin-Field Effect Transistors. With this in mind, different tests as Vibrating Sample Magnetometer (VSM) Measurements, Magnetoconductance Study, Temperature dependent Magnetization Measurements, Large positive Magnetoresistance Study were performed and their results were studied to understand the ferromagnetic behavior of samples (Fe, Co, Ni – Graphene) for spintronics application.

* Corresponding author.
E-mail address: krnemade@gmail.com (K. Nemade).

https://doi.org/10.1016/j.mseb.2020.114772
Received 27 March 2020; Received in revised form 1 June 2020; Accepted 1 September 2020

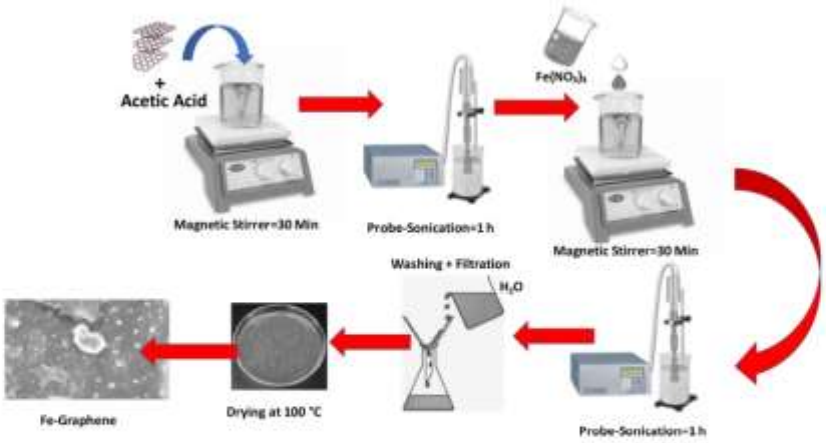

Fig. 1. Schematic synthesis process of Fe-Graphene nanosheets.

2. Experimentation

2.1. Synthesis of (Fe, Co & Ni-Graphene) nanosheets

Fig. 1 depicts the synthesis procedure of (Fe, Co & Ni-Graphene) nanosheets. Graphene used in this work is obtained by using previously reported method [13]. Firstly, to synthesize Fe-Graphene, 50 g of graphene sheets were dissolved in 100 ml acetic acid under magnetic stirring for 30 min. Secondly, the suspension of Fe-Graphene and acetic acid was subjected to probe-sonication for 1 h. Thirdly, 0.5 mg of Fe $(NO_3)_3$ was dissolved in 10 ml of acetic acid, which was added in former solution drop by drop under constant magnetic stirring for 30 min. The resultant suspension then was subjected to probe-sonication for 1 h. The final solution was then filtered and washed several times by deionized water to remove the impurities. Finally, black colored precipitate was collected and dried at 100 °C in oven.

The same procedure was adopted for the preparation of Co-Graphene and Ni-Graphene using precursors $Co(NO_3)_2$ and $Ni(NO_3)_2$, respectively. The schematic synthesis process of Fe-Graphene nanosheets shown in Fig. 1. Temperature conditioning was employed to all the three final products to form homogeneous magnetic system. The final product of all three samples were kept for heating in the temperature range of 100–500 °C in stepwise manner with an interval of 100 °C. At each fixed value of temperature, sample was heated for 60 min. Similarly, the sample was allowed to cool at 400, 300, 200 and 100 °C each for 60 min.

2.2. Characterization methods

The structural study of Fe-Graphene, Co-Graphene and Ni-Graphene nanosheets were executed using X-ray diffraction (XRD) analysis with Rigaku Miniflex XRD set up CuKα radiation (λ. = 1.5406 Å). Transmission electron microscopy with selected area diffraction pattern analysis was captured using TEM-Tecnai F-30107; Philips. The surface topography of Fe-Graphene, Co-Graphene and Ni-Graphene nanosheets was investigated by field emission scanning electron microscopy (FESEM) by using Scanning Electron Microscopy instrument, Model: ZEISS SIGMA operating at 5 kV ETH voltage. In addition to XRD and SEM analysis, elemental composition analysis was performed by using an energy dispersive X-ray analysis (EDAX) instrument, Model: EAG AN461.

To explore the ferromagnetic behavior of Fe-Graphene, Co-Graphene and Ni-Graphene nanosheets, Vibrating Sample Magnetometer (VSM) technique was employed at room temperature using VSM set up (Quantum Design Model- PAR 155) having specifications as Range: 0.00001 to 10,000 emu and Magnetic field: −10 to +10 kOe. To study ferromagnetic behavior in detail, the temperature dependent magnetization measurements with zero field cooled (ZFC) and field cooled (FC) condition were performed at 1000 Oe magnetic field strength using special Vibrating Sample Magnetometer (Lake Shore-7410) with temperature range −4.2 K to 1273 K. In the magnetoconductance measurement process, the material under study was mounted in cryostat-Janis CCS-350s, which was positioned between the pole pieces of an electromagnet (Lakeshore EM647). The magnetic field with the maximum strength of 20 kOe was applied and measured by Gauss Meter, Lakeshore 421 kept close to the material. The current–voltage characteristics was measured by a Keithley 2400 Source Meter and used further for the calculation of magnetoconductance.

Using Hall measurements, transport properties of samples were determined. The magnetoresistance (MR) was measured using direct current (Van der Pau method) at room temperature in the magnetic fields at around 0.5 T. For MR measurement, thin films of samples were prepared using spin coating technique with thickness ranging between 268 and 285 nm. MR is defined as, MR (%) = $[(R_B - R_0)/R_0] \times 100$ where R_0 is the initial sample resistance and R_B is its resistance in the magnetic field.

3. Results and discussion

3.1. Structural and morphological study of graphene

Fig. 2(a) depicts the XRD pattern of graphene, which comprises the signature peaks of graphene at 26.3° and 44.2° corresponds to plans (002) and (100), respectively. Whereas the inset of figure shows the Raman spectra of graphene. This spectrum also comprises the characteristics bands of graphene, D band (~1300 cm^{-1}), G band (~1580 cm^{-1}), and 2D band (~2720 cm^{-1}) [14]. Fig. 2(b) shows the TEM image of pure graphene with selected area diffraction pattern (inset). Inset shows a well-defined hexagonal array indicating structural purity of planes in graphene and also indicates graphene does not have a large number of sheets. The XRD, Raman and TEM analysis of graphene obtained in present study has structural purity.

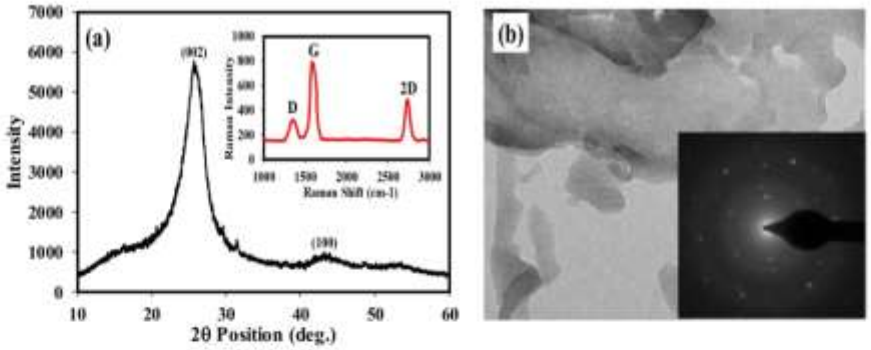

Fig. 2. (a) XRD pattern of pristine graphene. Inset of image shows Raman spectra of graphene. (b) TEM image of graphene and inset displays selected area diffraction pattern.

3.2. XRD analysis of composites

Fig. 3(a–c) shows the XRD pattern of Fe-Graphene, Co-Graphene and Ni-Graphene nanosheets, respectively. All three XRD patterns comprise two broad peaks, (002) and (100), which are signature peaks of graphene at 2θ positions of 26.3° and 44.2°. The corresponding peaks of graphene are in good agreement with recently reported work in literature [15,16]. No significant peak appears for the Fe, Co and Ni, which indicates that the orientation of graphene layers is not greatly influenced by nanocrystallites Fe, Co and Ni. The discernible peak at 26.42° in XRD of Fe-graphene composite as shoulder peak is the indication of formation of iron oxide nano-island. The previous report of Narayanaswamy et al demonstrated that the oxidation behavior of Fe can be controlled by the concentration of graphene in composite [17].

3.3. SEM study

Fig. 4(a–c) shows the SEM images and elemental X-ray mapping of (a) Fe-Graphene (b) Co-Graphene and (c) Ni-Graphene. The SEM image

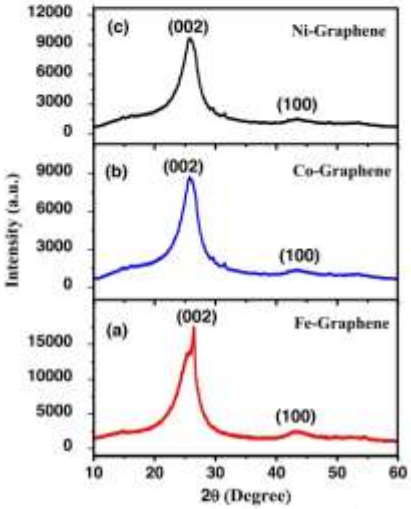

Fig. 3. XRD patterns of (a) Fe-Graphene, (b) Co-Graphene and (b) Ni-Graphene.

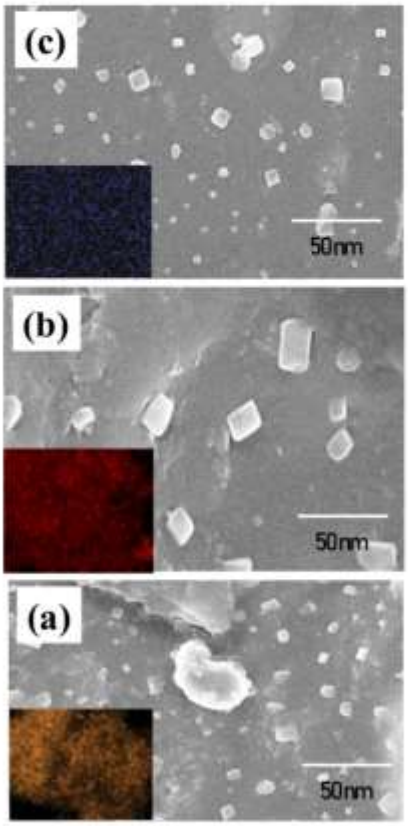

Fig. 4. SEM images and elemental X-ray mapping of (a) Fe-Graphene (b) Co-Graphene and (c) Ni-Graphene.

confirms that nanocrystallites Fe, Co and Ni are uniformly distributed over the graphene surface. No significant agglomeration observed in SEM micrographs. The elemental analysis was done using EDAX

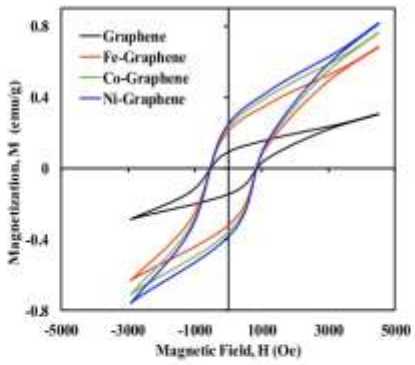

Fig. 5. VSM hysteresis loop of Fe-Graphene, Co-Graphene and Ni-Graphene nanosheets.

spectroscopy. The elemental analysis also confirms that nanocrystallites Fe, Co and Ni are distributed over the graphene surface. In present work, as the Fe, Co and Ni nanoparticles adsorbed by graphene results in formation of an electron transport channel between Fe, Co and Ni nanoparticles and graphene. In this type of materials, electron mobility proportional to surface electron concentration and the diameter of adsorbed atoms [18].

3.4. Magnetic characteristics

3.4.1. Vibrating sample magnetometer (VSM) measurements

Theoretically, the pristine graphene is diamagnetic in nature due to sp^2 hybridization. In the present study, obtained graphene synthesized using electrochemical exfoliation of graphite, which definitely comprises some defects, which imprint magnetic features into graphene [19]. Therefore, graphene used in present study shows weaken magnetic behavior. Fig. 5 shows the hysteresis loops of pristine graphene, Fe-Graphene, Co-Graphene and Ni-Graphene nanosheets, which were obtained at room temperature (298 K). The well-defined hysteresis curves indicate that good ferromagnetic ordering with considerably large coercivity was observed in Fe-Graphene, Co-Graphene and Ni-Graphene nanosheets. The values of coercivity, remanant magnetization and saturation magnetization estimated from hysteresis loops are presented in Table 1.

Fig. 4 and the values of coercivity (Hc), remanant magnetization (Mr) and saturation magnetization (Ms) listed in Table 1 for Fe-Graphene, Co-Graphene and Ni-Graphene nanosheets clearly indicates that synthesized materials exhibit ferromagnetic behavior. Actually, the presence of intrinsic magnetism in sp2 hybridized pure graphene has been a controversial topic [20]. In literature, few reports show that graphene exhibit uncommon magnetic properties including spin glass and magnetic switching application due the edge states arising from the nonbonding electrons [21,22]. The origin of magnetism in pristine graphene comes only due to the local states introduced by defects and molecular adsorption [23,24]. Kaur et al [25] and Wang et al. [26] studied that graphene may become magnetically active by removing the functional groups like –OH, –COOH, –O– and –C=O, which introduce the point defects and extended defects. In this way, graphene may become magnetically active.

Table 1
The measurement of coercivity (Hc), remanant magnetization (Mr) and saturation magnetization (Ms) of (a) Fe-Graphene, (b) Co-Graphene and (c) Ni-Graphene nanosheets.

Sample	Hc (Gauss)	Mr (emu/gm)	Ms (emu/gm)
Pristine Graphene	540	0.0754	0.306
Fe-Graphene	535	0.2002	0.682
Co-Graphene	537	0.2002	0.761
Ni-Graphene	534	0.2010	0.816

The presence of ferromagnetic behavior in nanosheets assigned to creation of more defective sites in graphene sheets due to addition of Fe, Co and Ni nanocrystallites. Due to the presence of Fe, Co and Ni clusters, nanosheets may exhibit the strong exchange interaction with ions and result in ferromagnetism. Abtew et al. [27] shows that spatial overlap, energy and symmetry matching between transition metals-dz^2 and C-pz orbitals results in good magnetic characteristics. In addition, the work of Abtew et al and co-worker demonstrated that charge transfer of 0.05e per C atom from Co to graphene and 0.07e per C atom from Ni to graphene induced ferromagnetism in graphene sheets.

The gradual increase in the values of remanant magnetization, saturation magnetization and area under the hysteresis loop of Fe-Graphene, Co-Graphene and Ni-Graphene nanosheets, clearly indicate that the ferromagnetism observed in samples was largely due to the outcome of charge transfer from Fe, Co and Ni to graphene and small due to intrinsic defects present in the graphene [28].

3.4.2. Magnetoconductance study

Fig. 6 depicts the magnetoconductance curve of Fe-Graphene, Co-Graphene and Ni-Graphene nanosheets as a function of the magnetic field at room temperature (298 K). The magnetoconductance is very important tool to identify microscopic behavior of ferromagnetic system. This parameter is used to identify the scattering centers present in the sample [28]. The magnetoconductance shows positive value on entire scale of magnetic field at room temperature (298 K). The magnetoconductance in Fe-Graphene, Co-Graphene and Ni-Graphene nanosheets is attributed to weak spin-orbit coupling. The magnetoconductance curve does not comprise any peak in low magnetic field [29,30], which indicates that the contribution of intrinsic impurities or defects present in the graphene in magnetoconductance are negligible. In this case, it is due to the interaction between conduction electrons and potential barrier at the graphene and Fe, Co, Ni interface. The magnetoconductance curve with no peak is an indication of good quality interface formed between graphene and Fe, Co, Ni nanocrystallite. As the concentration of Fe, Co, Ni nanocrystallite in graphene is very less, magnetoconduction has happened through graphene.

3.4.3. Temperature dependent magnetization Measurements

Fig. 7(a–c) depicts the temperature dependent magnetization data recorded under zero field cooled (ZFC) and field cooled (FC) conditions

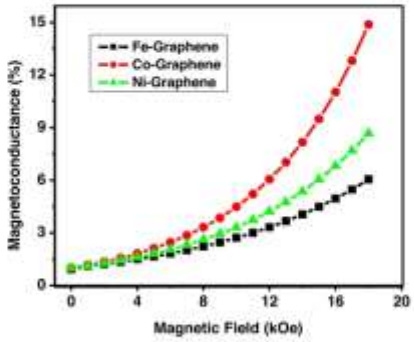

Fig. 6. Magnetoconductance curve of Fe-Graphene, Co-Graphene and Ni-Graphene nanosheets as a function of magnetic field at room temperature (298 K).

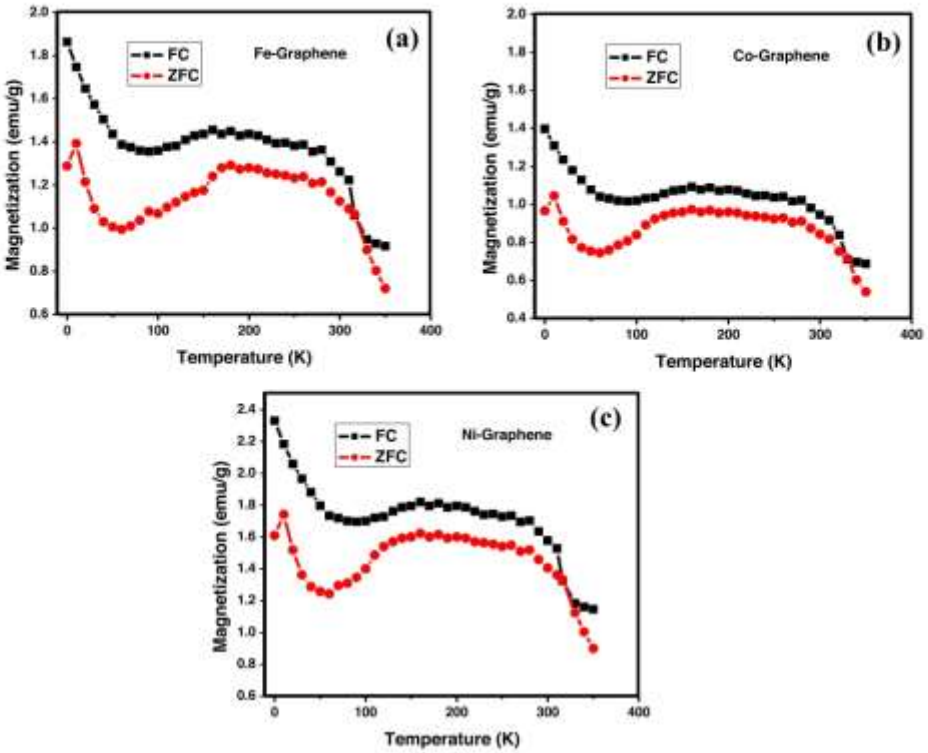

Fig. 7. Magnetization (Ms) as a function of temperature (a) Fe-Graphene, (b) Co-Graphene and (c) Ni-Graphene nanosheets measured under zero field cooled (ZFC) and field cooled (FC) condition under 1000 Oe magnetic field strength.

for external magnetic field 1000 Oe in the temperature range of 2–350 K for Fe-Graphene, Co-Graphene and Ni-Graphene nanosheets, respectively. In case of ZFC curve, Fe-Graphene, Co-Graphene and Ni-Graphene nanosheets show magnetization peaks at around 10 K. After 300 K, magnetization gradually drops up to 350 K. Similarly, FC curve shows no peak around 10 K with higher value of magnetization. The FC curve also shows gradual decrease in magnetization after 300 K. The slight difference in ZFC and FC data over the temperature range may be ascribed to the existence of small amount of magnetic inhomogeneous phase in prepared samples [31]. This type of behavior of samples is useful in spintronics and spin-glass application [32–35].

3.4.4. Large positive magnetoresistance study

Fig. 8 displays the magnetoresistance (MR) of Fe-Graphene, Co-Graphene and Ni-Graphene nanosheets versus magnetic field at a room temperature (298 K). The maximum value of MR around 94.87% was associated with Fe-Graphene sample, whereas minimum value of MR was 61.43% for Co-Graphene sample. All the measured MR values were positive, having quadratic magnetic field dependence behavior up to 0.05 T. Further, the MR values shows nearly linear dependence in the fields up to 0.5 T. The higher value of MR in Fe-Graphene sample is attributed to the process of hydrolysis of ferric nitrate, which produces islands of iron hydroxide and iron oxide on graphene surface [36]. These islands influenced the transport properties of graphene, similar to nanodiamonds work on graphene surface. These islands on graphene follow sp^3 configuration, which significantly alters the conductivity of sample [37]. In the present work, we conclude that ex-situ approach of

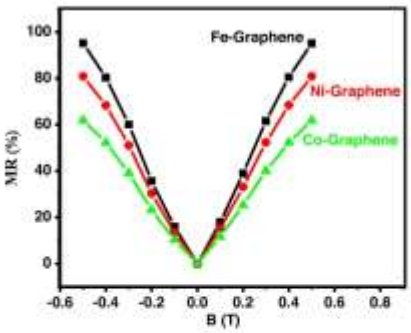

Fig. 8. The MR (%) of Fe-Graphene, Co-Graphene and Ni-Graphene nanosheets versus magnetic field at a room temperature.

Fe-Graphene, Co-Graphene and Ni-Graphene composite preparation create the islands of respective metal hydroxide and their oxide. Presently, we confirmed it from TEM and SEM images of pure graphene and composite. The comparative study of different ferromagnetic materials presented in Table 2, which are suitable for spintronic applications reported in the literature.

In the light of above discussion, it is observed that Co-Graphene is quite good material as ferromagnetic contacts in Spin-Field Effect

Table 2
Comparative study of different ferromagnetic materials, suitable for spintronic applications reported in the literature with regard to MR ratio.

Sample	Resistance type	Magneto-resistance	Ref.
α-Fe_2O_3 decorated graphene	Negative	32%	[38]
Graphene Oxide-Iron Oxide Nanocomposite	Positive	280%	[39]
Graphite intercalated with cobalt	Positive	148%	[40]
Co cluster decorated graphene	Negative	10%	[41]
Multilayer Graphene Grown on Nickel	Negative	10000%	[42]
Ni/graphene/Ni junctions	Positive	0.1%	[43]
Fe-Graphene	Positive	94.87%	This work
Co-Graphene	Positive	61.80%	This work
Ni-Graphene	Positive	80.89%	This work

Transistor (s-FET) application. Because, the origin of ferromagnetism between graphene and Co is due to electronic structure modifications. The US patent designed and published by Kelber et al shows that the charge current induces a spin current in the graphene, and it can be measured easily using spin selective cobalt electrodes. This work accomplishes that Graphene deposited over the Cobalt acts like efficient source and drain in field effect transistor. The fabricated spin- field effect transistor device shows durability, low power consumption, rapid switching action at room temperature [44].

In s-FET following three processes are extremely important,

Injection of spin polarized current of electron through the 2-dimentional electron gas channel from FM contacts (Source).
Transport of electrons through 2-dimentional electron gas channel without losing the spin direction
Detection of spin polarized current into FM contact (Drain).

In the working of s-FET, first and third process purely depends on quality of ferromagnetic materials, as it is used as ferromagnetic contacts (Source and Drain) in s-FET application. The 2-dimentional electron gas channel is heavily doped n-type silicon wafer, it has good compatibility with magnetically active Co-Graphene ferromagnetic material.

4. Conclusions

In summary, Fe, Co and Ni loaded Graphene explores the induced magnetism due to the charge transfer effect between graphene and Fe, Co, Ni interfaces. The VSM measurement shows that coercivity, remanant magnetization and saturation magnetization of Fe-Graphene, Co-Graphene and Ni-Graphene nanosheets show significant enhancement over the pure graphene. The magnetoconductance study discloses that the contribution of intrinsic impurities or defects present in the graphene in magnetoconductance is negligible. The ZFC and FC data shows that the small amount of magnetic inhomogeneous phase is present in prepared samples, which is useful in spintronics and spin-glass application. All samples show positive magnetoresistance having quadratic magnetic field dependence behavior up to 0.05 T and then linear dependence in the fields up to 0.5 T. The study reveals that Co-Graphene is quite good ferromagnetic material as Source and Drain contact application in s-FET.

Declaration of Competing Interest

The authors declare that they have no known competing financial interests or personal relationships that could have appeared to influence the work reported in this paper.

Acknowledgments

Prof. (Mrs.) Neetu Gyanchandani is very much thankful to Dr. S.R. Choudhary, Principal, JD College of Engineering and Management, Nagpur for providing necessary academic help.

Data availability

The raw/processed data required to reproduce these findings cannot be shared at this time as the data also forms part of an ongoing study.

References

[1] V. Shukla, Observation of critical magnetic behavior in 2D carbon-based composites, Nanoscale Adv. 2 (2020) 903–990.
[2] W. Han, K. Pi, K.M. McCreary, Y. Li, J.J.I. Wong, A.G. Swartz, R.K. Kawakami, Tunneling Spin Injection into Single Layer Graphene, Phys. Rev. Lett. 105 (2010) 167202.
[3] N. Tombros, C. Jozsa, M. Popinciuc, H.T. Jonkman, B.J. van Wees, Electronic spin transport and spin precession in single graphene layers at room temperature, Nature 448 (2007) 571–574.
[4] S.D. Sarma, S. Adam, E.H. Hwang, E. Rossi, Electronic transport in two-dimensional graphene, Rev. Mod. Phys. 83 (2011) 407.
[5] A.K. Geim, K.S. Novoselov, The rise of graphene, Nat. Mater. 6 (2007) 183–191.
[6] K.S. Novoselov, Z. Jiang, Y. Zhang, S.V. Morozov, H.L. Stormer, U. Zeitler, J.C. Maan, G.S. Boebinger, P. Kim, A.K. Geim, Science 315 (2007) 1379.
[7] K.S. Novoselov, A.K. Geim, S.V. Morozov, D. Jiang, M.I. Katsnelson, I.V. Grigorieva, S.V. Dubonos, A.A. Firsov, Two-dimensional gas of massless Dirac fermions in graphene, Nature 438 (2005) 197–200.
[8] P.B. Neetu Gyanchandani, P. Maheshwary, N. Nagrale, K. Indurkar, K.R.N. Jagtap, Recent advancements in the field of ballistic and non-ballistic spin-based field effect transistors, AIP Conf. Proc. 2104 (2019) 020016.
[9] T. Ohta, A. Bostwick, T. Seyller, K. Horn, E. Rotenberg, Controlling the electronic structure of bilayer graphene, Science 313 (2006) 951–954.
[10] Y.S. Dedkov, M. Fonin, C. Laubschat, A possible source of spin-polarized electrons: The inert graphene/Ni(111) system, Appl. Phys. Lett. 92 (2008) 052506.
[11] Y.S. Dedkov, M. Fonin, Electronic and magnetic properties of the graphene-ferromagnet interface, New J. Phys. 12 (2010) 125004.
[12] Y. Murata, V. Petrova, B.B. Kappes, A. Ebnonnasir, I. Petrov, Y.-H. Xie, C.V. Ciobanu, S. Kodambaka, Moiré superstructures of graphene on faceted nickel islands, ACS Nano 4 (2010) 6509–6514.
[13] E.B. Nemade, S.A. Waghuley, Chemiresistive gas sensing by few-layered graphene, J. Electron. Mater. 42 (2013) 2857–2866.
[14] Z. Ni, Y. Wang, T. Yu, Z. Shen, Raman spectroscopy and imaging of graphene, Nano Res. 1 (2008) 273–291.
[15] X. Wang, L. Zhang, Green and facile production of high-quality graphene from graphite by the combination of hydroxyl radicals and electrical exfoliation in different electrolyte systems, RSC Adv. 9 (2019) 3692–3703.
[16] Y. Zhao, X. Chen, B. Sun, D. Su, X. Huang, H. Liu, Y. Yan, K. Sun, G. Wang, Graphene/Co3O4 nanocomposite as electrocatalyst with high performance for oxygen evolution reaction, Sci. Rep. 5 (2015) 7628.
[17] V. Narayanaswamy, I.M. Obaidat, A.S. Kamzin, S. Lofland, S. Jain, H. Kumar, C. Srivastava, S. Alaabed, B. Issa, Synthesis of graphene oxide-Fe3O4 based nanocomposites using the mechanochemical method and in vitro magnetic hyperthermia, Int. J. Mol. Sci. 20 (2019) 3368–3375.
[18] X. Fang, X. Yu, H. Zheng, H. Jin, L. Wang, M. Cao, Temperature- and thickness-dependent electrical conductivity of few-layer graphene and graphene nanosheets, Phys. Lett. A 379 (2015) 2245–2251.
[19] J. Tuček, P. Błoński, J. Ugolotti, A.K. Swain, T. Enoki, R. Zbořil, Emerging chemical strategies for imprinting magnetism in graphene and related 2D materials for spintronic and biomedical applications, Chem. Soc. Rev. 47 (2018) 3899–3990.
[20] H.S.S. Ramakrishna Matte, K.S. Subrahmanyam, C.N.R. Rao, Novel magnetic properties of graphene: presence of both ferromagnetic and antiferromagnetic features and other aspects, J. Phys. Chem. C 113 (2009) 9982–9985.
[21] T. Enoki, Y. Kobayashi, K. Fukui, Electronic structures of graphene edges and nanographene, Int. Rev. Phys. Chem. 26 (2007) 609–645.
[22] T. Enoki, Y. Kobayashi, Magnetic nanographite: an approach to molecular magnetism, J. Mater. Chem. 15 (2005) 3999–4002.
[23] R. Saito, G. Dresselhaus, M.S. Dresselhaus, Physical Properties of Carbon Nanotubes, Imperial College Press (Knovel Library), London, 1998.

[24] V.W. Brar, R. Decker, H.M. Solowan, Y. Wang, L. Maserati, K.T. Chan, H. Lee, C.O. Gürü, A. Zettl, S.G. Louie, M.L. Cohen, M.F. Crommie, Gate-controlled ionization and screening of cobalt adatoms on a graphene surface, Nat. Phys. 7 (2011) 43–47.
[25] N. Kaur, R. Pal, Enhanced magnetic properties of cobalt-doped graphene nanoribbons, Appl. Phys. A 123 (2017) 259–266.
[26] Y. Wang, Y. Huang, Y. Song, X. Zhang, Y. Ma, J. Liang, Y. Chen, Room-temperature ferromagnetism of graphene, Nano Lett. 9 (2009) 220–224.
[27] T. Abtew, B. Shih, S. Banerjee, P. Zhang, Graphene–ferromagnet interfaces: hybridization, magnetization and charge transfer, Nanoscale 5 (2013) 1902–1909.
[28] P. Hota, A.J. Akhtar, S. Bhattacharya, M. Miah, S.K. Saha, Ferromagnetism in graphene due to charge transfer from atomic Co to graphene, Appl. Phys. Lett. 111 (2017) 042402.
[29] F.V. Tikhonenko, D.W. Horsell, R.V. Gorbachev, A.K. Savchenko, Weak localization in graphene flakes, Phys. Rev. Lett. 100 (2008) 056802.
[30] S.V. Morozov, K.S. Novoselov, M.I. Katsnelson, F. Schedin, L.A. Ponomarenko, D. Jiang, A.K. Geim, Strong suppression of weak localization in graphene, Phys. Rev. Lett. 97 (2006) 016801.
[31] R. Balaranjan, K. Kaleemullah, C. Krishnamoorthi, Structural and magnetic properties of NiO-MnO2 nanocomposites prepared by mechanical milling, J. Magnet. Magnet. Mater. 464 (2018) 36–43.
[32] A. Zeleňáková, J. Kovač, V. Zeleňák, Exchange bias in iron-oxide particles nanocasted in periodic porous silica, Acta Phys. Polon. Ser. A 115 (2009) 337–339.
[33] P. Mallick, C. Rath, A. Rath, A. Banerjee, N.C. Mishra, Antiferro to superparamagnetic transition on Mn doping in NiO, Solid State Commun. 150 (2010) 1342–1345.
[34] S.D. Tiwari, K.P. Rajeev, Signatures of spin-glass freezing in NiO nanoparticles, Phys. Rev. B 72 (2005) 104433.
[35] S. Lin, D.F. Shao, J.C. Lin, L. Ze, X.C. Kan, B.S. Wang, Y.N. Huang, W.H. Song, W.J. Lu, P. Tong, Y.P. Sun, Spin-glass behavior and zero-field-cooled exchange bias in a Cr-based antiperovskite compound $PdNCr_3$, J. Mater. Chem. C 3 (2015) 5683–5690.
[36] V.N. Matveev, V.I. Levashov, O.V. Kononenko, V.T. Volkov, Large positive magnetoresistance of graphene at room temperature in magnetic fields up to 0.5 T, Scrip. Mater. 147 (2018) 37–39.
[37] Y. Wang, M. Jaiswal, M. Lin, S. Saha, B. Özyilmaz, K.P. Loh, Electronic properties of nanodiamond decorated graphene, ACS Nano 6 (2012) 1018–1025.
[38] S. Bhattacharya, D. Dinda, E.M. Kumar, R. Thapa, S.K. Saha, Charge transfer induced ferromagnetism and anomalous temperature increment of coercivity in ultrathin α-Fe_2O_3 decorated graphene 2D nanostructures, J. Appl. Phys. 125 (2019) 213904.
[39] A.L. Lin, H. Peng, Z. Liu, T. Wu, C. Su, K.P. Loh, W. Ariando, A.T.S.W. Chen, Room Temperature magnetic graphene oxide–iron oxide nanocomposite based magnetoresistive random access memory devices via spin-dependent trapping of electrons, Small 10 (2014) 1949–1952.
[40] L. Ovsienko, L. Matzui, I. Berkutov, I. Mirzoiev, T. Len, Y. Prylutskyy, O. Prokopov, U. Ritter, Magnetoresistance of graphite intercalated with cobalt, J. Mater. Sci. 53 (2018) 716–726.
[41] C. Cai, J. Chen, Electronic transport properties of Co cluster decorated graphene, Chin. Phys. B 067304 (2018).
[42] S.C. Bodepudi, P. Singh, S. Pramanik, Giant current-perpendicular-to-plane magnetoresistance in multilayer graphene as grown on nickel, Nano Lett. 14 (2014) 2231–2241.
[43] Y. Hu, M. Ji, J. Peng, W. Qiu, M. Pan, J. Zhao, Y. Yao, C. Han, J. Hu, L. Pan, W. Tiana, D. Chen, Q. Zhang, P. Li, Anomalous temperature dependence of the magnetoresistance in vertical Ni/graphene/Ni junctions, J. Magnet. Magnet. Mater. 487 (2019) 165317.
[44] **J. Kelber, P. Dowben, Coherent Spin Field Effect Transistor, US. Patent, Patent No. US9,620,65482 (2017).**

14 Preparation of nanorefrigerants using mono-, bi-and tri-layer graphene nanosheets in R134a refrigerant

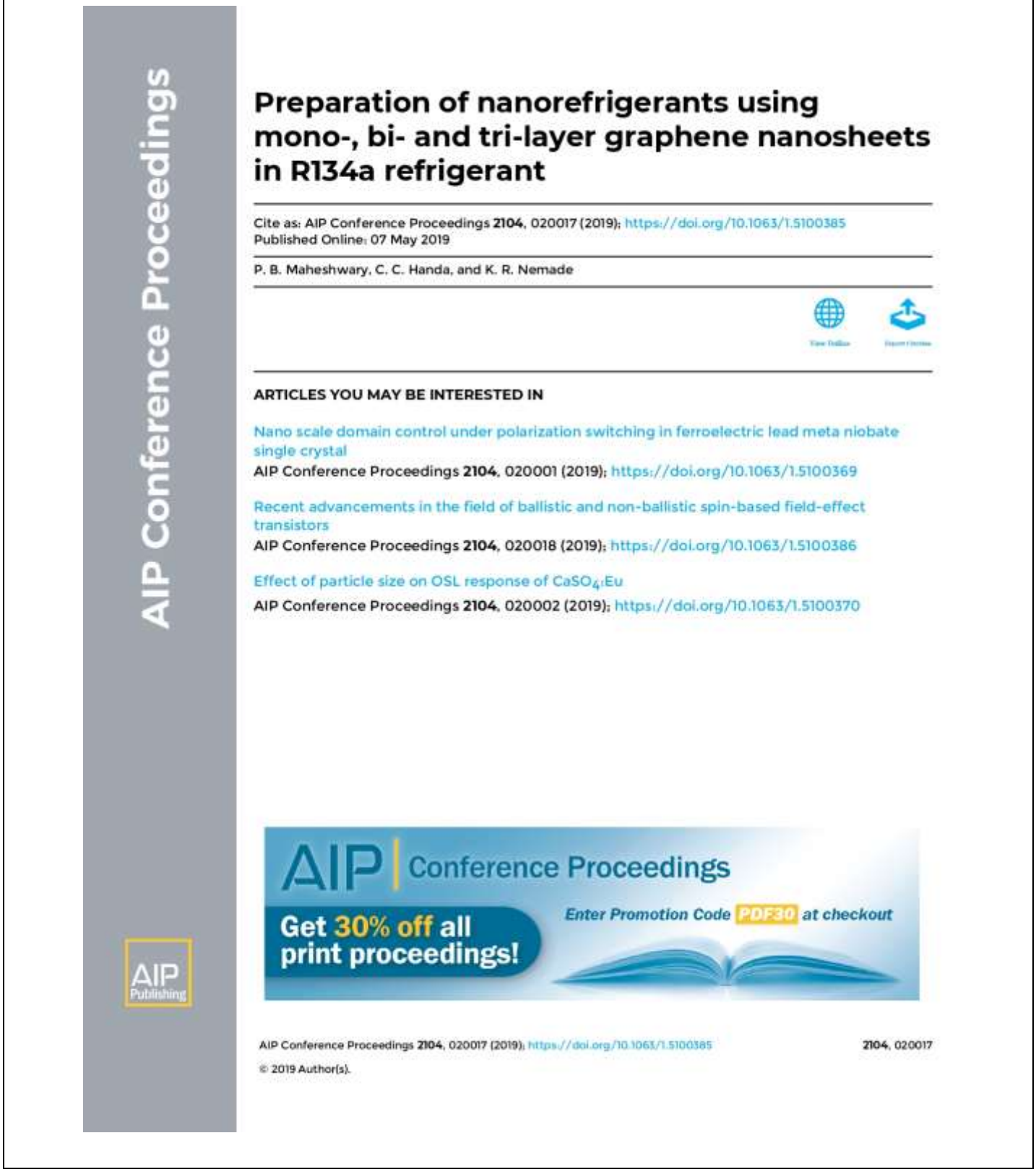

AIP Conference Proceedings

Preparation of nanorefrigerants using mono-, bi- and tri-layer graphene nanosheets in R134a refrigerant

Cite as: AIP Conference Proceedings **2104**, 020017 (2019); https://doi.org/10.1063/1.5100385
Published Online: 07 May 2019

P. B. Maheshwary, C. C. Handa, and K. R. Nemade

Preparation of Nanorefrigerants using Mono-, Bi- and Tri-layer Graphene Nanosheets in R134a Refrigerant

P.B. Maheshwary[1,a)], C.C. Handa[2,b)] and K.R. Nemade[3,c)]

[1]*Department of Mechanical Engineering, JD College of Engineering& Management, Nagpur 441 501, India.*
[2]*Department of Mechanical Engineering, KDK College of Engineering, Nagpur 400 049, India.*
[3]*Department of Physics, Indira Mahavidyalaya, Kalamb 445 401, India.*

[a)]Corresponding author: pbm51@rediffmail.com
[b)]chandrahashanda@rediffmail.com
[c)]krnemade@gmail.com

Abstract. Nano-refrigerants are a special class of nanofluids, prepared by addition of nanoscale impurity in refrigerants. The nano-refrigerants have a wide range of applications in many fields of thermal engineering including rapid refrigeration, air conditioning and heat pumps. In the present work, nanorefrigerants are prepared by forcefully dispersing Mono-, Bi- and Tri-layer graphene nanosheets in R134a refrigerant (as base fluid) at low temperature (278 K). To analyze the effect of number of layers of graphene, three types of graphene layers namely mono-, bi- and tri-layer graphene nanosheets are chosen. The result of the research work shows that thermophysical and heat transfer properties are strongly influenced by the number of layers of graphene. The nanorefrigerant prepared using mono-layer graphene shows outstanding heat transfer property in terms of ~96.14 % enhancement in thermal conductivity over the pure refrigerant.

INTRODUCTION

The cooling and heating in domestic and industrial applications mainly depends on the thermo–physical properties such as thermal conductivity, viscosity, specific heat and density of fluids which are used in system. Conventional fluids have poor heat transfer capacity due to low thermal conductivity. Hence, it consumes more energy, which indirectly results in the emission of large amount of CO_2. Therefore, the development of nanorefrigerants is very much necessary for the improvement in performance of refrigeration technology. The key advantages of nanorefrigerants are,

- Nanorefrigerants will lead to compact and lighter refrigeration systems.
- Nanorefigerant based refrigeration systems will consume low energy.
- Nanorefrigerants have virtue of low global warming and zero ozone depletion potential.

But the nanorefrigerant exhibits some unresolved issues such as particle clogging, large pressure drop, corrosion of components, still required to be addressed. Anand et al reviewed comprehensively the recent developments in the field of nanorefrigerants. The review is mainly focused on the domestic use of nanorefrigerants for improvement in coefficient of performance, energy saving and green environment. In the present work, after rigorous research authors have concluded that the refrigerant R134a has zero ozone depletion potential. During the experimentation with nanoparticles and lubricant mixture in refrigeration system, Anand et al demonstrated that the power consumption is significantly reduced [1]. Nair et al summarized the recent developments in the nanorefrigerants field in the context of its preparation, thermophysical properties and application. This study pointed out that the

International Conference on "Multidimensional Role of Basic Science in Advanced Technology" ICMBAT 2018
AIP Conf. Proc. 2104, 020017-1–020017-6; https://doi.org/10.1063/1.5100585
Published by AIP Publishing. 978-0-7354-1836-3/$30.00

research on the nanorefrigerant is slow and needs more attention of scientific community. In this review, many cases-studies are discussed, which shows that addition of nanoparticles in refrigerant improve performance of refrigeration system and energy efficiency [2].

Kumar et al reported the preparation of Al_2O_3-R134a nanorefrigerant to analyze the performance in refrigeration system. In this work, Al_2O_3 nanoparticles firstly mixed with poly alkylene glycol (PAG). Results of the investigation show that Al_2O_3nanorefrigerant performs efficiently in the refrigeration system. It is observed that refrigeration system performance is better than pure lubricant with R134a as working fluid. The use of nanorefrigerent reduces the energy consumption by 10.32% [3]. Kushwaha et al experimentally investigated the performance of (R134a + Al_2O_3) nanorefrigerent in refrigeration system. This study reports some motivating results, such as temperature drops significantly across the condenser for R134a+Al_2O_3nanorefrigerant and improvement in coefficient of performance. Work of Kushwaha et al proposed R134a+Al_2O_3nanorefrigerant for practical application in refrigeration system [4].

Ozturk et al formulated a new category of nanorefrigerants, which comprises graphene nanosheets. The graphene based nanorefrigerant shows outstanding thermal conductivity enhancements over carbon nanotube suspension with practical value of viscosity. The experimental study shows that graphene based nanorefrigerant is potential category of nonorefrigerant to achieve efficiency in many thermal management applications [5]. Fadhilah et al studied the thermophysical properties of CuO nanoparticle loaded nanorefrigerent through mathematical modelling. In this work, the physical properties of R-134a are used for mathematical modelling. The thermal conductivity, dynamic viscosity and heat transfer rate were the main parameters studied in this work. The mathematical modelling-based results show that nanorefrigerant will be the potential working fluid, which saves energy usage and environment [6].

Mahbubul et al investigated the heat transfer and pressure drop characteristics of Al_2O_3-R141b nanorefrigerant as a function of different volume concentrations. The results of the study show that heat transfer and pressure drop characteristics increased with the concentration of nanoparticle. The optimized nanorefrigerant improved the performance of cooling capacity of refrigeration system. This results in low energy consumption [7]. Ajayi et al studied the performance of 0.04%Ni/R134a nanorefrigerant as working fluid in refrigeration system. For the nanorefrigerant application, nanoparticles were prepared by one step method and dispersed into the mineral oil. The results of the study show that nanorefrigerant performed better with improved coefficient of performance of the order of 7.05% [8]. Mahbubul et al investigated the thermophysical properties of 5 vol.% Al_2O_3 nanoparticles loaded R-134a refrigerant and its effects on the coefficient of performance in the temperatures range 283–308 K. The result shows that thermal conductivity improved over pure refrigerant by 28.58%, whereas specific heat of nanorefrigerant is slightly reduced compare to R-134a [9]. Sanukrishna et al reported the thermophysical, heat transfer and pressure drop properties of TiO_2 nanoparticle loaded R134a nanorefrigerants. The results of study show that thermophysical and heat transfer characteristics improved due to the addition of nanoparticles in pure refrigerant. In this work, heat transfer coefficient got increased by 30.2% [10].

In the present work, it was planned to investigate the thermophysical characteristics of graphene/R134a nanorefrigerants. To analyze the effect of graphene and more importantly its layer number on performance of nanorefrigerants, Mono-, Bi- and Tri- layer graphene was used to prepare suspension. The thermo-physical characteristics like viscosity, density, specific heat and thermal conductivity were studied at low temperature.

EXPERIMENTAL

The graphene nanosheets required in this work were procured from Sigma-Aldrich. The procured graphene was characterized by X-ray diffraction (XRD) analysis and transmission electron microscopy (TEM). In the present work, Mono-, Bi- and Tri-layer graphene nanosheets were used for the preparation of nanorefrigerants. As the R134a refrigerant is highly unstable at room conditions, firstly the graphene sheets in three types namely Mono-, Bi- and Tri-layer added separately in lubricant of the compressor system. The preparation of mixture of nano-impurity and lubricant is very important step in the study of nanorefrigerant. The poly alkylene glycol (PAG) lubricant is used in this study, due to its wide acceptability in refrigeration technology and good physical properties. The nanosheets of graphene with the mass fraction of 1% were dispersed in lubricant. The graphene was forcefully dispersed into the lubricant using ultrasonic device for two hours at 150 W and 20 kHz to obtain well dispersed mixture. No surfactant was added in the preparation of graphene-lubricant mixture to avoid the effect of surfactant on heat transfer performance. To prepare nanorefrigerants, the mixture of lubricant and graphene was carefully injected to

the pure refrigerant. Three types of nanorefrigerants were prepared in this work using Mono-, Bi- and Tri-layer graphene.

The thermophysical and heat transfer properties of nanorefrigerant studied in the temperature range 283-307 K. The viscosity of nanorefrigerants was determined using AR-1000 Rheometer, TA Instrument. The specific heat and thermal conductivity measurements were carried out by using KD2 pro thermal analyzer (Decagon Devices).

RESULTS AND DISCUSSION

Figure 1 (a) shows the XRD pattern of graphene. The analysis of XRD pattern indicates the structural and phase purity of graphene. XRD pattern comprises two signature peaks of graphene, (002) and (100) at 26.3° and 44.2° respectively. Both these peaks indicate the highly organized structure of graphene. The topography of graphene under study is directly visualized by TEM as shown in Figure 1 (b). The nanosheets of grapheme were used for the preparation nanorefrigerants.

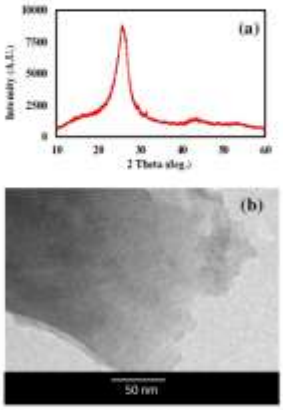

FIGURE 1. (a) XRD pattern and (b) TEM image of graphene.

Viscosity is a critical thermo-physical parameter in refrigeration system, which affects the performance of nanorefrigerant. Viscosity of nanofluids or nanorefrigerant normally increases with increase in concentration of nanoparticles and decreases with temperature. The viscosity of grapheme based R134a nanorefrigerants was studied using Brinkman model (Eq. 1) [11],

$$\mu_{nr} = \mu_r \frac{1}{(1-\phi)^{2.5}} \qquad \text{Eq. (1)}$$

where, μnr and μr is the effective viscosity of nanorefrigerant and pure refrigerant respectively.ϕ is particle volume fraction. The variation in viscosity of mono-, bi- and tri-layer graphenenanosheets based nanorefrigerants as a function of temperature is shown in Figure 2.The viscosity of nanorefrigerant decreases with increase in temperature. It is also observed from viscosity plot that trilayergraphene based nanorefrigerant has highest magnitude of viscosity and it decrease with temperature. Similarly, the monolayer graphene based nanorefrigerant has lower values of viscosity than tri- and bi-layer graphene. The decrease in viscosity as a function of temperature is justified as sub-micron dispersion behaves like a liquid. On other hand, decrease in viscosity with increasing temperature is result of diminishing adhesion forces between the particles and base fluid [12].

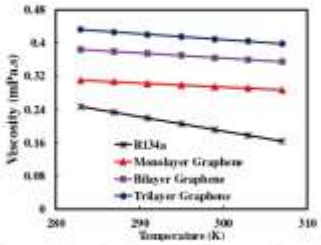

FIGURE 2. Variation in viscosity of mono-, bi- and tri-layer graphenenanosheets based nanorefrigerants as a function of temperature.

The variation in density of mono-, bi- and tri-layer graphenenanosheets based nanorefrigerants as a function of temperature is shown in Figure 3. The plot of density shows that with increase in temperature, density of nanorefrigerant decreases. Density is a function of mass and volume. Therefore, with increase in temperature the molecules of nanorefrigerant perform vibration, which ultimately increases volume [13]. Thus, the density of nanorefrigerant is decreases with temperature. The highest magnitude of density is associated with trilayergraphene based nanorefrigerant, whereas monolayer graphene based nanorefrigerant shows lowest magnitude.

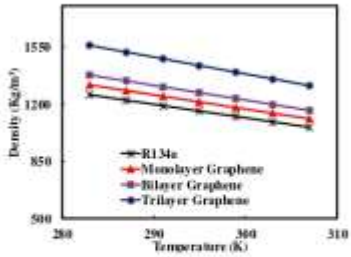

FIGURE 3. Variation in density of mono-, bi- and tri-layer graphenenanosheets based nanorefrigerants as a function of temperature.

Figure 4 shows the variation in specific heat of mono-, bi- and tri-layer graphenenanosheets based nanorefrigerants as a function of temperature. The specific heat of nanorefrigerant based on monolayer and bilayer graphene has much lower value than pure R-134a refrigerant. This lower value of specific heat of nanorefrigerant is result of lower specific heat of added particles.

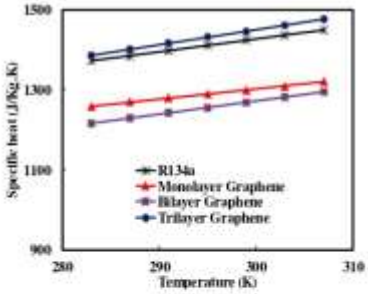

FIGURE 4. Variation in specific heat of mono-, bi- and tri-layer graphenenanosheets based nanorefrigerants as a function of temperature.

Graphene is a single layer of hybridized sp2 carbon atoms, which is the thinnest and thermally stable material in universe [14]. The graphene nanosheets exhibit the significant thermal conductivity value of the order 5000 W/m.K [15]. Hence, it is expected from graphene that it will display good thermal conductivity enhancement due to the outstanding properties [16].

Figure 5 shows the variation in thermal conductivity of mono-, bi- and tri-layer graphenenanosheets based nanorefrigerants as a function of temperature. From the plot of thermal conductivity, it is observed that thermal conductivity of R134a refrigerant decreases with increase in temperature. It may be due to the evaporation of refrigerant molecules. From plot, it is also observed that thermal conductivity of nanorefrigerants based on graphene shows increase in thermal conductivity as the temperature increases. This increase in thermal conductivity is assigned to the higher value of thermal conductivity of nanoimpurity that is graphene, in our case [17]. It is also observed that monolayer graphene based nanorefrigerant has highest value of thermal conductivity over the other nanorefrigerant samples. The manolayer based nanorefrigerant shows increase in thermal conductivity of the order 96.14 % over pure R134a refrigerant.

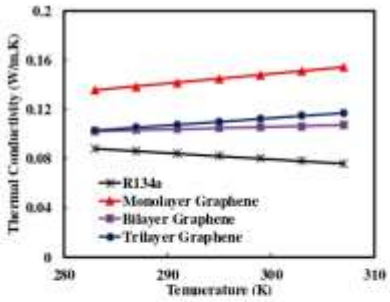

FIGURE 5. Variation in thermal conductivity of mono-, bi- and tri-layer graphenenanosheets based nanorefrigerants as a function of temperature.

CONCLUSIONS

In the present work, the mono-, bi- and tri-layer grapheme nanosheets based nanorefrigerants were successfully prepared and studied their thermophysical properties as a function of temperature. Following are the major concluding remarks made on the experimental investigation undertaken in the present work,

- Among mono-, bi- and tri-layer grapheme nanosheets based nanorefrigerants, it was observed that trilayergraphene based nanorefrigerant had highest magnitude of viscosity and it decreased with increase in temperature.
- The highest magnitude of density was associated with trilayergraphene based nanorefrigerant.
- The specific heat of nanorefrigerant was observed to be lower than the pure R134a refrigerant.
- The monolayer graphene based nanorefrigerant had highest value of thermal conductivity of the order of 96.14 % over the pure R134a refrigerant.

ACKNOWLEDGMENTS

The authors are very much thankful to Principal, KDK College of Engineering, Nagpur, India for providing necessary facilities for the work.

REFERENCES

1. N. Anand and M. Arya, International Journal of Science Technology & Engineering **2**, 488-490 (2016).
2. V. Nair, P.R. Tailor and A.D. Parekh, International Journal of Refrigeration**67**, 290-307 (2016).
3. D.S. Kumar and R. Elansezhian, International Journal of Modern Engineering Research**2**, 3927-3929 (2012).
4. P.K. Kushwaha, P. Shrivastava, A.K. Shrivastava, International Journal of Mechanical and Production Engineering**4**,90-95 (2016).
5. S. Ozturk, Yassin A. Hassanb and V.M. Ugaz, Nanoscale **5**,541-547 (2013).
6. S.A. Fadhilah, R.S. Marhamah and A.H.M. Izzat, Journal of Nanoparticles **2014**,1-5 (2014).
7. I.M. Mahbubul, R. Saidur and M.A. Amalina, Procedia Engineering **56**, 323-329 (2013).
8. O.O. Ajayi, O.O. Useh, S.O. Banjo, F.T. Oweoye, A. Attabo, M. Ogbonnaya, I.P. Okokpujie and Y. Salawu, IOP Conf. Series: Materials Science and Engineering **391**, 1-9 (2018).
9. I.M. Mahbubul, A. Saadah, R. Saidur, M.A. Khairul and A. Kamyar, International Journal of Heat and Mass Transfer **85**, 1034–1040 (2015).
10. S.S. Sanukrishna, N. Ajmal and M.J. Prakash, IOP Conf. Series: Journal of Physics: Conf. Series 969,1-7 (2018).
11. H. Brinkman, J. Chem. Phys. **20**,571-577 (1952).
12. C.T. Nguyen, F. Desgranges, G. Roy, N. Galanis, T. Mare, S. Boucher and H.A. Mintsa, Int J Heat Fluid Flow **28**,492–506 (2007).
13. P.B. Maheshwary, C.C. Handa and K.R. Nemade, Materials Today: Proceedings **5**,1635–1639 (2018).
14. K.S. Novoselov, A.K. Geim, S. Morozov, D. Jiang, Y. Zhang, S.A. Dubonos, I. Grigorieva and A. Firsov, Science **306**, 666–669 (2004).
15. M. Mehrali, E. Sadeghinezhad, M.A. Rosen, A.R. Akhiani, S. TahanLatibari, M. Mehrali and H.S.C. Metselaar, Int. Commun. Heat Mass Transf. **66**,23–31 (2015).
16. X. Fang, L.W. Fan, Q. Ding, X. Wang, X.L. Yao, J.-F. Hou, Z.T. Yu, G.H. Cheng, Y.C. Hu and K.F. Cen, Energy Fuel **27**,4041–4047 (2013).
17. P.B. Maheshwary, C.C. Handa and K.R. Nemade, Applied Thermal Engineering **119**, 79-88 (2017).

15 Recent advancements in the field of ballistic and non-ballistic spin-based field-effect transistors

AIP Conference Proceedings

Recent advancements in the field of ballistic and non-ballistic spin-based field-effect transistors

Cite as: AIP Conference Proceedings **2104**, 020018 (2019); https://doi.org/10.1063/1.5100386
Published Online: 07 May 2019

Neetu Gyanchandani, Prashant Maheshwary, Pragati Nagrale, Nehal Indurkar, Koumudi Jagane, and Kailash Nemade

Recent Advancements in the Field of Ballistic and Non-Ballistic Spin-Based Field-Effect Transistors

Neetu Gyanchandani[1,a)], Prashant Maheshwary[2,b)], Pragati Nagrale[3,c)], NehalIndurkar[4,d)], Koumudi Jagane[5,e)], Kailash Nemade[6,f)]

[1,3,4,5] *Department of Electronics Engineering, JD College of Engineering & Management, Nagpur 441501, India.*
[2] *Department of Mechanical Engineering, JD College of Engineering & Management, Nagpur 441501, India.*
[6] *Department of Physics, Indira Mahavidyalaya, Kalamb 445401, India.*

[a)]Corresponding author: gyanineetu@gmail.com
[b)] pbm51@rediffmail.com
[c)]pragatinagrale27@gmail.com
[d)]nehalindurkar78@gmail.com
[e)]jaganekoumudiu@gmail.com
[f)]krnemade@gmail.com

Abstract. The magnificent increase in the performance of integrated circuits is made possible by semiconductor Physics. Due to very large-scale integration, scaling has approached its fundamental limits, which is the biggest challenge for the semiconductor industry. Therefore, in the recent years researchers across the globe are focusing on emerging field of spintronics. In this thrust area of spintronics research, spin field effect transistor (s-FET) is an extensively studied device. In literature, researchers have studied and optimized two main types of spin field effect transistors namely Ballistic and Non-Ballistic spin-field effect transistors. This research paper has presented the recent developments in the field of Ballistic and Non-Ballistic spin-field effect transistors. This paper has briefly explained the approach to design, development and fabrication of s-FET by taking a case study. Firstly, the spin field effect transistor was proposed by Datta–Das, which has proved to be the milestone in the area of spintronic technology. Mainly, spin transistor is prepared using a ballistic semiconductor, sandwiched between ferromagnetic metallic source and drain contacts.

INTRODUCTION

In recent years, the functionality of data processing and information processing has improved due to spintronics by overcoming the serious limitations of conventional electronics. In this development, spin field effect transistor (s-FET) is the most studied device which is typically composed of a lateral semiconducting channel with two ferromagnetic contacts. s-FET is foundation of spintronics progress [1]. s-FET is working on the basic principle of modulation of resistance with control on the spin of the carriers by employing ferromagnetic contacts. Ferromagnetic contacts act as generator and detector of polarization [2]. In s-FET, spin transport is controlled through the gate voltage. The operation of spin transport phenomenon at nanoscale is useful for building spin-based quantum bits for processing quantum information [3].

During literature survey, it is observed that Datta-Das has firstly proposed s-FET which is applicable to non-ballistic semiconductor channel of two-dimensional electron gas (2DEG) system. But many researchers have studied s-FET with ballistic regime of 2DEG system. The present research paper in its brief review has tried to summarize the recent developments in

International Conference on "Multidimensional Role of Basic Science in Advanced Technology" ICMBAT 2018
AIP Conf. Proc. 2104, 020018-1–020018-4; https://doi.org/10.1063/1.5100586
Published by AIP Publishing. 978-0-7354-1836-3/$30.00

s-FET under two main categories that is ballistic and nonballistic type s-FET. The present manuscript is divided into three main sections, namely Ballistic s-FET, non-ballistic s-FET and challenges & future outlook associated with s-FET.

BALLISTIC s-FET

The ballistic s-FET is a rapidly growing side of spin transistors. In this section, the brief overview about the recent development in ballistic s-FET is summarized. The meaning of ballistic transport in the present work is to maintain spin direction in channel, without any scatterings. In other words, during the movement of electron from source to drain, the minimum number of scattering centers should come across the path. If the spin transport is affected by the presence of more scattering centers in the channel, it comes under the category of nonballistic s-FET.

Koo et al investigated the high mobility in s-FET based on InAsheterostructure. This also demonstrated the electrical injection and detection of ballistic spin-polarized electrons in s-FET. Further, it is observed that conduction of s-FET is a function of applied gate voltage [4]. Xiao et al studied the Ballistic transport in s-FET by focusing on the phenomenon such as, spin–orbit coupling, interfacial scattering and the different internal exchange energies for the ferromagnet regions. Griffith boundary conditions are used to analyze the transmission coefficients. The study concludes that transmission probability and conductance oscillation of the s-FET depend on device size, interfacial barriers and mainly on spin–orbit coupling precession [5]. Osintsev et al studied the properties of silicon Ballistic spin fin-based field-effect transistors using two ferromagnetic contacts having spin polarization $0 < P < 1$. The results of the study show that [100] and [110] orientated structures strongly influence to the conductance [6]. Osintsev et al investigated the transport properties of sFET at room temperature as a function of strength of the spin-orbit interaction using Schottky barriers created between the contacts and the channel. This concludes that silicon fins of the [100] orientation have the best performance and it is suitable for practical application of sFET [7]. Figure 1 shows the architecture of s-FET used by Osintsev et al.

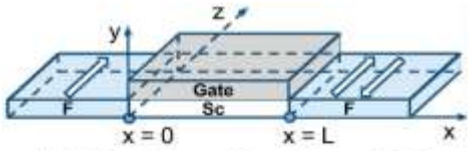

FIGURE 1. Architecture of sFET (Osintsev et al, 2013)

Gao et al demonstrated simulation of s-FET by considering the factors such as spin scattering, tunneling and self-consistent charge distribution. This work results in two solid outcomes, first one is to increase the energy of spin splitting in drain, raise potential barrier to block the drain leakage current and second is to introduce the spin-selective tunneling oxide layer between source and drain [8]. The s-FET architecture used by Gao et al is shown in Figure 2.

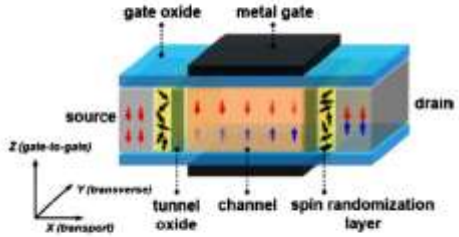

FIGURE 2. The s-FET architecture (used by Gao et al, 2010)

Jeong et al focused on the issue of multichannel effects in ballistic S-FET. The results of the study clearly show that when 2-dimentional electron gas is weakly diffusive, the fluctuation in modulation signal is observed and it depends on physical properties of sample [9]. Jiang et al studied the conductance properties in ballistic s-FET by considering Rashba effect, band mismatch, and spin polarization in ferromagnetic electrodes. This study shows that conductance of s-FET has prominent peaks for potential barriers at the contact/channel interfaces. Hence, switching action in ballistic s-FET is achieved by tuning band mismatch or direction of the magnetic field. The spin precession in channel of s-FET becomes noticeable as the spin polarization in the contacts increases [10]. Jiang et al verified the tunneling magnetoresistance properties of ballistic s-FET by considering the parameters Rashba spin–orbit coupling, presence of an in-plane magnetic field, band mismatch, and spin polarization in the ferromagnetic electrodes. Results of the present study show that as band mismatch is altered, the magnitude and sign of tunneling magnetoresistance is significantly modulated by Rashba spin–orbit coupling process. In study, it is also observed that variation in tunneling magnetoresistance is produced as a function of Rashba spin–orbit coupling strength and magnetic field [11]. Sherman et al studied the spin dynamics and relaxation in doped two-dimensional electron systems, dopants create the random fluctuations of the Rashba spin-orbit coupling. The random contribution to the spin-orbit coupling originates from random-spin precession, due to the presence of dopants. The randomness in spin precession is also important for device fabrication [12].

NON-BALLISTIC s-FET

This section deals with the non-ballistic s-FET and recent developments in it. It is observed that non-ballistic s-FET side of spin transistor is a less grown technology compared to ballistic s-FET.

Schliemann et al proposed s-FET based spin-orbit coupling of Rashba as well as the Dresselhaus types. In this work, spin transport through device is made tolerable for spin-independent scattering processes, to study s-FET in nonballistic mode. The ballistic transport s-FET proposed in this work has unique benefits of cancellation of Rashba and Dresselhaus effects, improve the performance of s-FET than ballistic s-FET [13]. Shafir et al investigated the spin polarization drag in an $Al_{0.3}Ga_{0.7}As/GaAs/Al_{0.3}Ga_{0.7}As$ heterostructure as a function of gate voltage. The focus of study is to analyze the role of Rashba and Dresselhaus spin-orbit interaction in the nonoballistic s-FET. In this work, actual parameters of materials were used for simulation of spin dynamics as a function of gate voltage. The estimated modulation in spin polarization was found to be in the range of 15–20 %. This result shows that practical application of s-FET with this range of spin polarization is not possible. But, this issue can be resolved by optical pulse-probe technique [14]. Ohno et al applied the semiempirical Monte Carlo simulation for spin transport in Datta-Das proposal for s-FET. This study gives interesting results such as spin helix state in two-dimensional electron gas system is adequately strong against D'yakonov-Perel' spin relaxation, which makes Datta-Das-type s-FET operable in the nonballistic transport regime. Also, it is marked that switching action on s-FET is achieved by creating a 180° phase difference in the spin precession motions, which is very much necessary for practical application [15]. Xu et al apply the lattice Green's function to study s-FET in one-dimensional case. The results of the study give outstanding coherent regime, which improve inelastic scattering and lateral confinement in the control of spins [16]. During study it is concluded that non-ballistic s-FET needs more study and research reports, which explore the anonymities associated with non-ballistic s-FET.

CHALLENGES AND FUTURE OUTLOOK

Spinvalve and s-FET are very important devices in the spintronics technology. Following are major challenges for the practical application of s-FET [17, 18],

- Injection of spin-polarized flow of electron in semiconducting channel.
- Control on Rashba spin-orbit coupling in the semiconducting channel through gate voltage.
- Serious fundamental challenges like the lowspin-injection efficiency, resistance mismatch, spin relaxation and the spread of spin precession angle are still not resolved entirely.

In conventional electronics, the operations like logic, communication and storage require separate device. But semiconductor spintronics has ability to perform all these three operations within single device by exploiting the spin coherence.

CONCLUSIONS

It is concluded that the study of s-FET in ballistic and non-ballistic regime is very much necessary for the deeper understanding of s-FET. Also, to reach a rigid conclusion about selection of ballistic and nonballistic s-FET, extensive study is required, as the study of s-FET is in early stages. The realization of more spintronics devices is an interesting and challenging task. It requires advanced technology for fabrication of device. To study s-FET, a sound understanding about materials science, semiconductor Physics and conventional electronics is very much essential.

ACKNOWLEDGMENTS

Prof. (Mrs.) Neetu Gyanchandani is very much thankful to Dr. S.R. Choudhary, Principal, JD College of Engineering and Management, Nagpur for providing necessary academic help.

REFERENCES

1. J. Wan, M. Cahay, and S. Bandyopadhyay, IEEE Trans. Nanotechnol 7, 34–39 (2008).
2. I. Zutic, J. Fabian and S.D. Sarma, Rev. Mod. Phys. **76**, 1–6 (2004).
3. T. Kontos and A. Cottet, Towards nanospintronics**38**, 28–30 (2007).
4. H.C. Koo, J.H. Kwon, J. Eom, J. Chang, S.H. Han and M. Johnson, Science **325**, 1515–1518 (2009).
5. Y. Xiao, R. Zhu and W. Deng, Solid State Communications **151**, 1214–1219 (2011).
6. D. Osintsev, V. Sverdlov, Z. Stanojevic, A. Makarov, J. Weinbub and S. Selberherr, ECS Transactions**35**, 277–282 (2011).
7. D. Osintsev, V. Sverdlov, A. Makarov and S. Selberherr, SainsMalaysiana**42**, 205–211 (2013).
8. Y. Gao, T. Low, M.S. Lundstrom and D.E. Nikonov, J. Appl. Phys. **108**, 83702–83708 (2010).
9. J. Jeong and H. Lee, Physical Review B**74**, 195311–195328 (2006).
10. K.M. Jiang, J. Yang, R. Zhang and H. Wang, J. Appl. Phys. **104**, 53722–53729 (2008).
11. K. Jiang, R. Zhang, J. Yang, C. Yue and Z. Sun, IEEE Transactions on Electron Devices**57**, 2005–2012 (2010).
12. E.Y. Sherman and J. Sinova, Phys. Rev. B, **72**, 75318–75324 (2005).
13. J. Schliemann, J. Carlos Egues and D. Loss, Phys. Review Letter**90**, 146801–146805 (2003).
14. E. Shafir, M. Shen and S. Saikin, Physical Review B **70**, 24130–24134 (2004).
15. M. Ohno and K. Yoh, Physical Review B77, 045323–45330 (2008).
16. L. Xu, X. Li and Q. Sun, Scientific Reporter **4**, 1–6 (2014).
17. A. Fert and H. Jaffre, Phys. Rev. B **64**, 184420–184426 (2001).
18. H. Kum, J. Heo, S. Jahangir, A. Banerjee, W. Guo and P. Bhattacharya, Appl. Phys. Lett. **100**, 182407–182412 (2012).

16 Role of nanoparticle shape in enhancing the thermal conductivity of nanofluids

Materials Today: Proceedings 28 (2020) 873–878

Contents lists available at ScienceDirect

Materials Today: Proceedings

journal homepage: www.elsevier.com/locate/matpr

Role of nanoparticle shape in enhancing the thermal conductivity of nanofluids

P.B. Maheshwary [a,*], C.C. Handa [b], K.R. Nemade [c], S.R. Chaudhary [d]

[a] Department of Mechanical Engineering, JD College of Engineering and Management, Nagpur 441 501, India
[b] Department of Mechanical Engineering, KDK College of Engineering, Nagpur 400 049, India
[c] Department of Physics, Indira Mahavidyalaya, Kalamb 445 401, India
[d] Department of Civil Engineering, JD College of Engineering and Management, Nagpur 441 501, India

ARTICLE INFO

Article history:
Received 25 September 2019
Received in revised form 9 November 2019
Accepted 26 December 2019
Available online 18 January 2020

Keywords:
Shape
Thermal conductivity
Nanofluids
Probe sonication

ABSTRACT

In present work, five different nanoparticles of three different shapes are used to study the enhancement in thermal conductivity, viscosity and stability of nanofluids. The main objective of present work is to analyze the effect of shape on thermo-physical properties of nanofluids. For this study, spherical, cubic and rod shaped nanoparticles are used. CuO, MgO, TiO_2, ZrO_2 and Al_2O_3 water based nanofluids are prepared by two step method using probe sonication technique. The effect of shape on thermal conductivity of nanofluids is analyzed experimentally by using hot-wire method set up. Results of this study reveal that the cubic shaped Al_2O_3 nanofluid (concentration 2.5 wt%) shows highest thermal conductivity over base fluid by 3.13 times. Effect of nanoparticle shape on the viscocity is also studied in the presnt work. Al_2O_3 nanofluid also has good stability amongst all nanofluids. Also, it is observed that in all five cases of nanofluid cubic shape nanoparticles enhance thermal conductivity at the highest rate than spherical and rod shape. Pumping power study shows that cubic shaped nanoparticles require higher pumping power than spherical and rod shaped nanoparticles.

Selection and peer-review under responsibility of the scientific committee of the 2nd International Conference on Recent Advances in Materials & Manufacturing Technologies.

1. Introduction

Research work done in the past suggests that nanofluids have the ability to be used for efficient heat transfer in thermal engineering applications [1]. For many industrial processes, heat transfer takes place through fluids as a medium. In many modern applications such as indoor ventilation with radiators, cooling of electrical components, and heat exchangers, quick heat transfer results in low energy consumption [2]. Due to this energy saving ability of nanofluids, variation in thermal conductivity of nanofluids because of change in shapof nanomaterial is investigated. Several research reports suggest that thermal conductivity of nanofluids is greatly influenced by shape of nanoparticle impurity used for the preparation of nanofluids. The outcome of this work indicates that spherical shaped solid nanoparticles enhance thermal conductivity of base fluid by a small magnitude, whereas non-spherical nanoparticles have higher ability to enhance thermal conductivity of nanofluid [3]. The heat transfer performance of an oscillating heat pipe is also investigated experimentally and it is concluded that alumina nanoparticle shape plays a very crucial role in enhancement of the heat transfer performance. In this work, it is also demonstrated that alumina nanofluid is not beneficial in laminar or turbulent flow mode [4]. The aggregation has positive effects on the thermal conductivity enhancement. It may be due to the fact that aggregated size offers fast heat transfer path for neighboring particles and it shows appreciable increase in the shape factor of the aggregate [5]. The comprehensive review made by Goharshadi et al considers several parameters, which influence thermal conductivity of nanofluids. Among these parameters, nanoparticle shape has considerable influence on enhancement of thermal conductivity [6,19].

To investigate the effect of shape on thermal conductivity, viscocity, stability and pumping power of nanofluid, five different nano-impurities (CuO, MgO, TiO_2, ZrO_2 and Al_2O_3) have been

* Corresponding author at: Department of Mechanical Engineering, JD College of Engineering and Management, Nagpur 441 501, India.
E-mail address: pbm51@rediffmail.com (P.B. Maheshwary).

https://doi.org/10.1016/j.matpr.2019.12.315
2214-7853/
Selection and peer-review under responsibility of the scientific committee of the 2nd International Conference on Recent Advances in Materials & Manufacturing Technologies.

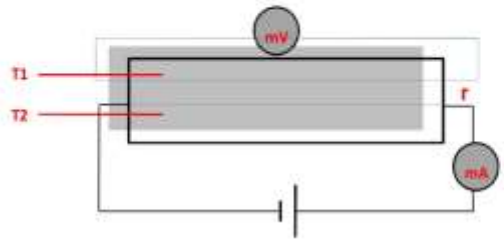

Fig. 1. Schematic sketch of two wire method based setup to determine thermal conductivity of nanofluid.

chosen for the preparation of nanofluids. Two step method is used for forceful dispersion of nanoparticles in base fluid (water) to prepare stable nanofluid.

2. Experimentation

A set up of hot-wire method is built to measure the thermal conductivity. The wire, which is immersed in the investigated sample is heated by passing a constant electrical current through it, and its temperature change ΔT, is measured as a function of time t, for several values of the current. The set up consists of chemically-inert cylindrical hallow tube of Teflon with special arrangement of wire and thermocouple. The schematic representation of set up is as shown in Fig. 1. The silver wire of 200 mm length and 2 mm diameter is used as the metal wire. Thermal conductivity of nanofluids was estimated by using relation

$$K = (q/4\pi K) \quad (1)$$

Where, K is Slope between ΔT and Time, k is thermal conductivity (W/m^0K)

q- Power generated by heating wire per unit length (W/m)

As the present work deals with the effect of nanoparticle shape on thermal conductivity of nanofluids, CuO, MgO, TiO_2, ZrO_2 and Al_2O_3 nanoparticles were procured in three different shapes i.e. spherical, cubic and rod from Sigma-Aldrich (AR-grade). Two step method is used to prepare nanofluids of CuO, MgO, TiO_2, ZrO_2 and Al_2O_3 nanoparticles. The water of electrical resistivity of the order of 18.2 MΩ.cm is used as base fluid. While preparing nanofluids concentration of nanofluids was kept constant (2.5 wt %) for three different shapes. In this way, three samples for every nanofluid were prepared for thermal conductivity investigation. For forceful dispersion, probe sonication technique was used to achieve stable nanofluids.

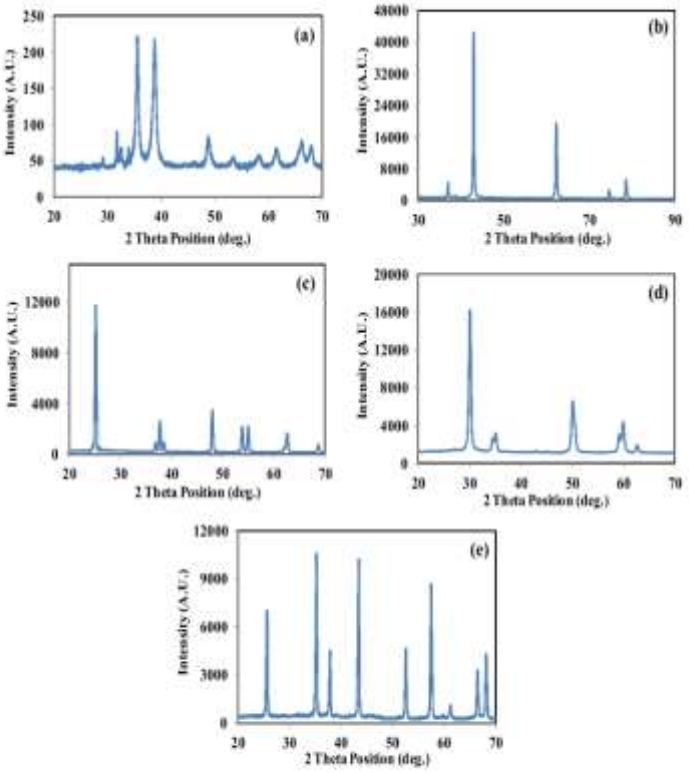

Fig. 2. XRD pattern of (a) CuO (b) MgO (c) TiO_2 (d) ZrO_2 and (e) Al_2O_3 nanoparticles.

X-Ray diffraction (XRD) analysis is used to ensure the structural purity of nanoparticles. For XRD analysis, related data was collected on Rigaku, Miniflex-II (Japan) X-ray diffractometer in the 2θ range 20-70° with step height of 0.02°. The present study deals with the effect of shape on thermal conductivity of nanofluids, morphology analysis plays a very important role. Therefore, morphology of all samples was confirmed using scanning electron microscopy (SEM) technique. SEM images of nanoparticles of different shapes were captured using JEOL JSM-7500F SEM.

The viscosity of nanofluids loaded with different shapes was analyzed by using AR-1000 Rheometer, TA Instrument. Thermal conductivity of nanofluids under investigation was measured using hot-wire method with the help of home built set up. All data related to viscosity and thermal conductivity was measured thrice to verify deviation in results. However no considerable deviation was observed in results. Stability of nanofluids is a crucial parameter which indicates quality of nanosuspension. This information of nanofluids was collected using dynamic light scattering technique (NanoZS, Malvern).

The experiments are repeated three times for each case and the average value is reported. No significant deviation is observed in the study.

3. Results and discussion

Fig. 2 (a) exhibits the pattern of XRD for CuO nanoparticles used for the preparation of nanofluids. Fig. 2 (a) shows the structural purity of CuO nanocrystals and it is in good agreement with JCPDS card No. 01-080-1268. The signature peaks mentioned in this card exactly match with XRD data of CuO nanocrystals. Fig. 1 (b) depicts XRD pattern of MgO nanoparticles, which represents that MgO has cubic phase with a lattice parameter of a = b = c = 4.213 Å and space group (Fm-3 m (2 2 5)). The XRD data of cubic MgO is in good agreement with JCPDS card No. 04-829. Fig. 2(c) shows the XRD pattern of TiO_2 nanocrystals, which exhibits anatase phase. All characteristic peaks of TiO_2 exactly with JCPDS card No. 21-1272 and no other impurity peak observed in XRD pattern. Fig. 2(d) shows the XRD patterns of ZrO_2 nanocrystals which exhibits tetragonal phase and is indexed to JCPDS card No. 79-1771. Fig. 1 (e) shows the XRD pattern of Al_2O_3 nanocrystals, which exhibits α-phase with no other impurity peak. The XRD data of Al_2O_3 nanocrystals shows good matching with JCPDS card No. 46-1212. All signature peaks and their marginal intensity are in good agreement with JCPDS card.

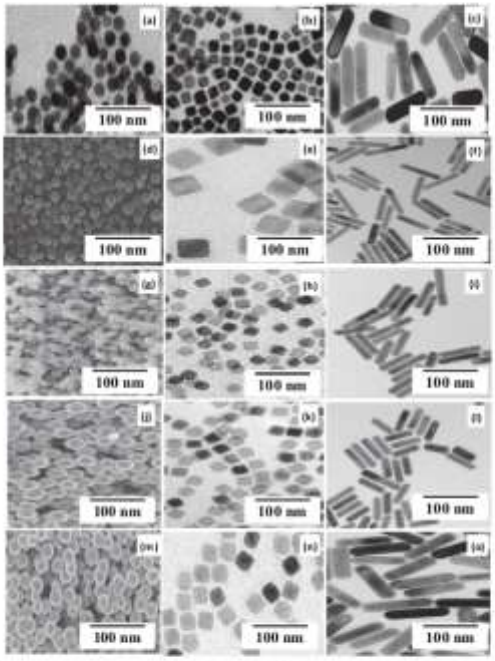

Fig. 3. SEM images of (a) spherical CuO, (b) cubic CuO, (c) rod CuO, (d) spherical MgO, (e) cubic MgO, (f) rod MgO, (g) spherical TiO_2, (h) cubic TiO_2, (i) rod TiO_2, (j) spherical ZrO_2, (k) cubic ZrO_2, (l) rod ZrO_2, (m) spherical Al_2O_3, (n) cubic Al_2O_3 and (o) rod Al_2O_3.

Present study deals with the effect of shape on thermal conductivity of nanofluids, three shapes i.e. spherical, cubic and rod shape have been chosen. To confirm the shape of nanoparticles, SEM analysis for all samples under investigation was performed. The SEM images of all samples were captured at same magnification (100 nm). Fig. 3(a–c) shows the SEM images of CuO nanoparticles of spherical, cubic and rod shape, respectively. Fig. 3(d–f) represents the SEM images of spherical, cubic and rod shape of MgO nanoparticle respectively. Fig. 3(g–i) depicts the SEM images of spherical, cubic and rod shape of TiO_2 nanoparticle respectively. Fig. 3 (j–l) shows the SEM images of spherical, cubic and rod shape of ZrO_2 nanoparticles respectively. Fig. 3 (m–o) shows the SEM images of spherical, cubic and rod shape of α-Al_2O_3 nanoparticles respectively. All SEM images of nanoparticles show that no agglomeration is presents between nanoparticles.

Fig. 4 (a–e) shows the variation of viscosity with temperature as a function of nanoparticle shape. All figures show that viscosity decreases with temperature due to lack of immobile fluid molecules [7]. It is also observed that cubic shaped nanoparticles of CuO (Fig. 3-a), MgO (Fig. 3-b), TiO_2 (Fig. 3-c), ZrO_2 (Fig. 3-d) and Al_2O_3 (Fig. 3-e) have higher magnitude of viscosity than spherical and rod shaped nanoparticle. This might happen due to the fact that cubic shaped nanoparticles are difficult to rotate given that they possess a higher surface area than rod and spherical shaped nanoparticles [8]. This result is in agreement with the investigation made by Gaganpreet et al which says that eccentricity of the particle increases relative viscosity [9,18]. According to the model proposed by Kreiger Dougherty, shape factor of nanoimpurity dispersed in base fluid has great influence on the viscosity [10,17].

A recent work published by Timofeeva et al established the relation between thermal conductivity of nanofluids and shape of nano-impurity and is given by (Eq. 1) [11,15].

$$\frac{k_{nf}}{k_e} = 1 + (C_k^{shape} + C_k^{surface}) \tag{2}$$

where, C_k^{shape} is thermal conductivity enhancement coefficient function of shape and $C_k^{surface}$ is thermal conductivity enhancement coefficient function of surface.

From Fig. 5 (a–e), thermal conductivity of nanofluids prepared by using cubic shaped nanoparticles has higher thermal conductivity than other shapes. The results obtained are having concurrence with Timofeeva et al The results obtained for thermal conductivity are supported by Jeong et al [Jeong] and Murshed et al [12,16] too.

Table 1 summarizes the stability data of CuO, MgO, TiO_2, ZrO_2 and Al_2O_3 nanofluids for different shape at room temperature (303 K). From Table 1, it is observed that settling velocity for cubic shaped nanoparticles is greater than that of spherical and rod

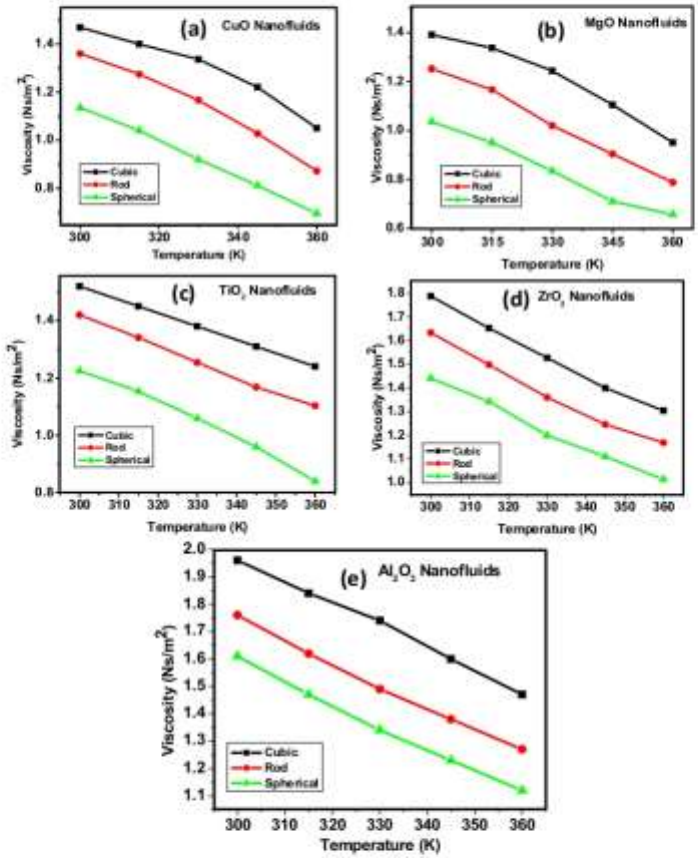

Fig. 4. Variation of viscosity with temperature for different shapes of (a) CuO, (b) MgO, (c) TiO_2, (d) ZrO_2 and (e) Al_2O_3 nanoparticles based nanofluids.

shaped nanoparticles. It also indicates that the base fluid loaded with cubic shaped nanoparticles has lower stability hence lower Brownian velocity. Cubic shaped Al_2O_3 nanofluid has more stability as compared to other cubic shaped nanofluids.

Table 2 shows the pumping power data of CuO, MgO, TiO_2, ZrO_2 and Al_2O_3 nanofluids for different shapes of nanoparticles at room temperature (303 K). It is observed that cubic shaped particles require higher pumping power than spherical and rod shaped nanoparticles. This higher pumping power for cubic shaped nanoparticles can be attributed to higher viscosity of nanofluids [13,14].

The data produced in this study was compared with the results of other reports available in the literature. It was observed that many parameters, such as particle concentration, size, shape, viscosity, environmental conditions, base fluid, and methods of nanofluid preparation influence to the measured results. As our study deals with effect of shape on thermal conductivity of nanofluids, no earlier similar reports are available in literature for comparison purpose.

4. Conclusion

The behavior of thermal conductivity, viscosity, stability and pumping power is investigated experimentally for five different nanofluids (CuO, MgO, TiO_2, ZrO_2, Al_2O_3) for three different shapes (spherical, cubic and rod). During this investigation results indicated that nanoparticles having cubic structure based nanofluids have higher viscosity and thermal conductivity compared to rod and spherical shape. The enhancement in viscosity and thermal conductivity is attributed to larger surface area of cubic shaped nanoparticles. However, stability data of CuO, MgO, TiO_2, ZrO_2 and Al_2O_3 nanofluids indicates that cubic shape nanoparticles based nanofluids have poor stability than spherical and rod shape. Similarly, cubic shape nanoparticle based CuO, MgO, TiO_2, ZrO_2 and Al_2O_3 nanofluids required higher pumping power. In this study cubic shaped Al_2O_3 nanofluid (concentration 2.5 wt%) has highest thermal conductivity in the order of 3.13 times that of base fluid. Practically, cubic shape nanoparticles based nanofluids are not used in thermal engineering applications due to blocking problem.

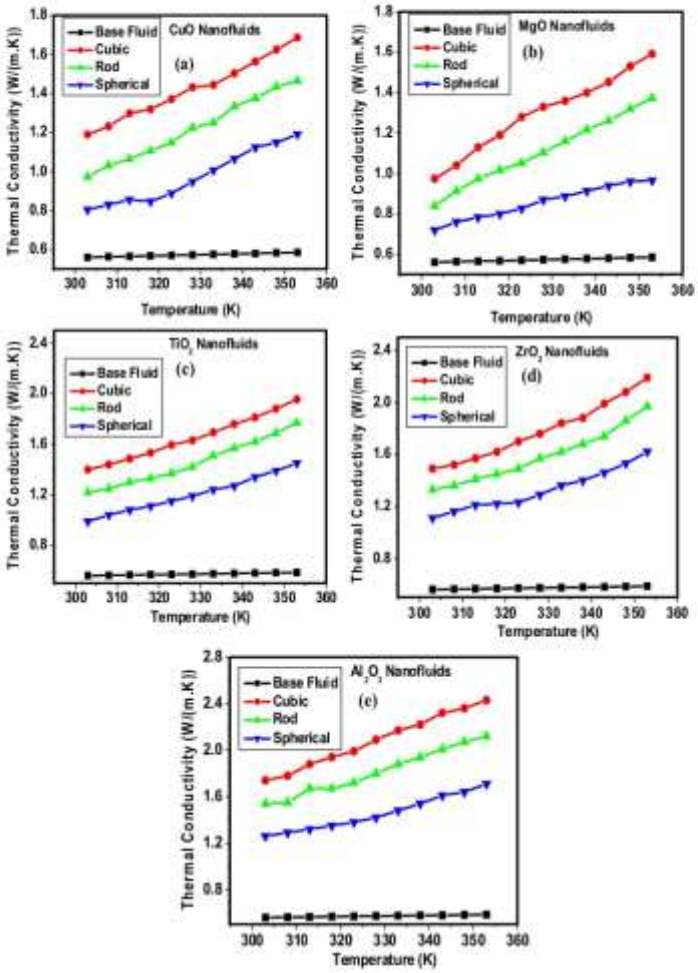

Fig. 5. Variation of thermal conductivity with temperature for different shape of (a) CuO, (b) MgO, (c) TiO_2, (d) ZrO_2 and (e) Al_2O_3 nanoparticles based nanofluids.

Table 1
Stability data of CuO, MgO, TiO_2, ZrO_2 and Al_2O_3 nanofluids for different shapes at room temperature.

Nanofluid	Shape	Settling velocity (m/s) × 10^{-10}	Brownian velocity (m/s) × 10^{-8}
CuO	Spherical	1.784	7.945
	Cubic	3.241	4.874
	Rod	2.784	6.914
MgO	Spherical	1.874	8.547
	Cubic	5.749	6.749
	Rod	4.412	8.471
TiO_2	Spherical	1.574	8.874
	Cubic	3.541	5.547
	Rod	2.914	7.496
ZrO_2	Spherical	1.418	9.412
	Cubic	2.874	6.324
	Rod	2.147	8.412
Al_2O_3	Spherical	1.342	9.645
	Cubic	2.987	7.145
	Rod	2.007	8.214

Table 2
Pumping power data of CuO, MgO, TiO_2, ZrO_2 and Al_2O_3 nanofluids for different shape at room temperature (303 K).

Nanofluid	Shape	Pumping power (W)
CuO	Spherical	9.21
	Cubic	10.25
	Rod	8.85
MgO	Spherical	8.84
	Cubic	11.89
	Rod	9.57
TiO_2	Spherical	8.14
	Cubic	11.37
	Rod	10.70
ZrO_2	Spherical	9.47
	Cubic	12.14
	Rod	11.74
Al_2O_3	Spherical	10.24
	Cubic	13.11
	Rod	9.57

17 Contribution of Psychology in Physical, Mental and Occupational Health.

VOLUME - VIII, ISSUE - I - JANUARY - MARCH - 2019
AJANTA - ISSN 2277 - 5730 - IMPACT FACTOR - 5.5 (www.sjifactor.com)

28. Contribution of Psychology in Physical, Mental and Occupational Health

P. B. Ingle
Research Scholar, Dr. Babasaheb Ambedkar Marathwada University, Aurangabad.
Dr. Tajne M. K.
Research Guide, Principal, Late Wamanrao Pitambare, Arts, Commers & Science College, Padegaon, Aurangabad.

Abstract

The main purpose of the paper is to describe the role of psychologist physical, mental and occupational health in the domain of work or organization. It was prove significantly, that physical health and psychological factors impact up on the life of individuals. There is not a single fix way to solve various behavioral problems, so the psychologist have major role to solve it by using various new strategies. It is necessary to understand the goal of the psychology Particularly, occupational health psychology, it has aims at improving the efficiency at organizational or group level and improving job satisfaction at the individual level (Milward,2008).

Keyword : Physiological health, Psychological health & Occupational health, contribution of psychologist.

Introduction

Occupational health psychology (OHP) is a marginal challenge and can be used successfully in developing a management strategy to lead to the production, development and implementation of healthy work environment in the organization. The term refer to physical and physiological symptoms in medical context (such as diseases diagnosis) applying it in the organizational context. The emphasis on physical and physiological indicators that are used to assess the health of employees. A psychologist specialized in health psychology should deal with issues related with organizational consulting, in particular with problem diagnosis, followed by design, implementation and evaluation of solutions leading to improvement of organization efficiency and increase the adaptability to change and develop of the organization. Further explanation about the role of psychology is as follows.

1) Ways of coping, different symptoms at individual level.

2) Job environment : work overload,

3) Organizational level : role conflicts and organizational unfairness,

4) External level : life events, home stress

Health and wellbeing in organization covers different perspectives on this issue : health(Cooper Kilkalzd and Brown, 1994), Psychological (cartwright and Cooper, 1993) and mental (Anderson and Grunert,1997) the board spectrum that range from these perspectives have generated a variety of definitions for organizational well-being and health.

Physical Health

According to Almedia (2005), Stress is emotional or physical response of an individual to stressor. He concludes that stress impact our body. Secondly, children are particularly vulnerable to stressors, and more current research indicates that that stress can have a major influence on their psychological and physical health status (e.g., Grant et al. 2003; Hostinar and Gunnar 2013; Miller et al. 2011). Most empirical work examining stress in children focuses on major life events, like divorce of parents, while fewer studies consider the role of daily stressors, or the routine challenges of day-to-day living. Existing work on children's daily stress is lacking such that it primarily: (1) focuses on children who are ill, disabled, or who face significant environmental risks, (2) relies on retrospective reports, (3) relies on parent or teacher reports of stressors experienced by children, or (4) does not comprehensively examine the role of stress on mood and health, (Margaret L, et.l.2017).

Mental Health

While employees' mental health is the focus of considerable attention from researchers, the public, and policymakers, leaders' mental health has almost escaped attention. We start by considering several reasons for this, followed by discussions of the effects of leaders' mental health on their own leadership behaviors, the emotional toll of high-quality leadership, and interventions to enhance leaders' mental health.

Occupational Health

Occupational health (OH) is the word more often than not used in the field of health care. But form 1950 it was defined in proper manner by two International authoritative bodies International Labor Office (ILO) and World Health Organization (WHO), that as "the promotion and maintenance of the highest degree of physical, mental and social well-being of workers in all occupation by preventing departures from health, controlling risk and the adoption of work by to

people and people to their job." Basically, occupational health objectives are as two prevention of the occupational disease or work-related health complaints and second one is prevention or mitigation of occupational disability resulting from the disease.

Researchers develop intervention strategies on the basis of these two objectives are the elimination or control of hazards at work. In organization related to health and disability, change in health and disability- related behavior and skills among workers; prevention or better treatment of diseases and related disabilities. In recent reviews on effectiveness of occupational hygiene strategies, studies were categorized according to the mean used to reduce exposure, referred as the "hierarchy of control".

To attain this goal the international contribution of the occupational health research data shows that highest rate of produce research papers in the area of U.S.A. by Mark Ferris (2015).

Conclusion

The result shows that the psychologist have major role in future in the domain of physical health, mental health, and occupational health. Ways of coping, different symptoms, individual level. Job environment: work overload, Organizational level : role conflicts and organizational unfairness, External level : life events, home stress occupational health is emerging newly strong field which contribute gather evidence on the effectiveness of occupational health interventions and stimulate systematic review.

References

- Anderson, R.C., Gurtnert, B. K. (1997). A cognitive behavioral approach to the treatment of post traumatic stress disorder after work related truma. Professional safety, 42 : 39-42.
- Barling, J., & Cloutier, A. (2017). Leaders' mental health at work: Empirical, methodological, and policy directions. *Journal of Occupational Health Psychology, 22*(3), 394-406.http://dx.doi.org/10.1037/ocp0000055
- Cartwright S. & Cooper C. L. (1993). The psychological impact of merger and aquisions on the individuals: A study of building society managers, Human relations, 46,327-347.
- Copper and kilkalz and Brown, (1994). A model of job stress and physical helath: the role of individual differences, personality and individual differences, 16 :653-655.

- Ferris, M., Hust A., Sanati N.A., Sanati K.A.(2015). The contribution of occupational health research. Scan J Work Environ Health; 41. (30) 294-298.
- International Labor Office (ILO). Technical and ethical guidelines for the worker's health surveillance. Geneva international labor office. 1997. OHS p. 21.(12).
- Margaret B. L., Melanie H. M., Katherine E. B.(2017). Daily reports of stress, Mood and physical health in midel childhood. https://mijn.bsl.nl/daily-reports-of-stress-mood-and-physical-health-in-middle-child/12067870.
- Milward, L. (2005). understanding occupational and organizational psychology. Thousand Oaks, CA : sage

18 Anna-dhanya Suraksha Yojanechya Amalbajavanitil Shasanachi Bhumika

अन्नधान्य सुरक्षा योजनेच्या अंमलबजावणीत शासनाची भूमिका

प्रा.श्रीमती रेखा मा. वाठ
वाणिज्य अधिव्याख्याता इंदिरा महाविद्यालय,
कळंब जि. यवतमाळ
rekhawath23@gmail.com

प्रस्तावना:

भारतासारख्या देशात अन्नधान्य समस्या स्वातंत्र्योत्तर काळात १९५१ नंतर अधिक तीव्रतेने भासत होती. या देशातील अन्न समस्येला संख्यात्मक व गुणात्मक अशा दोन बाजू आहे. वाढत्या लोकसंख्येवरोबर अन्नधान्याची मागणी दिवसेंदिवस वाढत आहे. त्याचप्रमाणे दुसरीकडे सशक्त व कार्यक्षम लोकसंख्या ही त्या लोकसंख्येला मिळणाऱ्या अन्नधान्याच्या गुणवत्तेवर अवलंबून आहे. भारतासारख्या विकसनशील देशात अद्यापी सुमारे ३५ टक्के लोक दारिद्र्य रेषेखाली जीवन जगत असल्याने त्यांना मिळणारे अन्नधान्य हे गुणवत्तेच्या दृष्टीने निकृष्ट असतेच आहेत. ही अन्नसमस्येची गुणात्मक बाजू होय. शाश्वत व सर्व समावेशक आर्थिक वृद्धिसाठी अशा लोकसंख्येस मिळणाऱ्या अन्नधान्याच्या उपलब्धतेचा व गुणवत्तेचा सांगोपांग विचार शासकीय पातळीवर व्हावयास पाहिजे. या दृष्टीने १९५० नंतर स्वतंत्र झालेल्या बहुसंख्य राष्ट्रांचा समावेश विकसनशील अवस्थेच्या राष्ट्रात केला जातो अशा राष्ट्रांनी देशातील लोकांच्या अन्नधान्य व आहारविषयक समस्या सोडविण्यासाठी गेल्या काही वर्षात विविध उपाययोजना केल्या आहे. त्या योजनाद्वारे विकसनशील अन्नधान्य व आहारविषयक सुरक्षा उपाययोजनांचे अध्ययन करणे आवश्यक आहे.

भारतात शासकीय पातळीवर अन्नधान्य समस्या सोडण्यासाठी अनेक उपाययोजना १९५१ नंतर करण्यात आलेल्या आहेत. या उपाययोजनांमध्ये प्रामुख्याने अन्नधान्याचे उत्पादन वाढवून संख्यात्मक उपाय योजिले आहेत. तर अन्नधान्यास पुरक अशा, फळे भाजीपाला अंडी, मांस इत्यादी पर्यायी उत्पादनाची मागणी वाढविण्यावर भर देण्यात आलेला आहे. भारतासारख्या विकसनशील देशात लोकसंख्यावाढीमुळेच अन्नधान्याची समस्या व अन्नसुरक्षेचा प्रश्न निर्माण झाल्यामुळे शासनातर्फे १२ सप्टेंबर २०१३ ला राष्ट्रीय अन्नसुरक्षा कायदा – २०१३ संमत करण्यात आला व ५ जुलै २०१३ पासून हा कायदा लागू करण्यात आला आहे. शासनाने देशात अन्नसुरक्षा कायम करण्यासाठी विविध प्रयत्न केले आहेत. शासनाच्या या भूमिकेचे अध्ययन करण्याच्या उद्देशाने मी संशोधनासाठी प्रस्तुत विषय निवडला आहे.

शोध निबंधासाठी वापरण्यात येणारी संशोधनाची पद्धती:

प्रस्तुत शोधनिबंधासाठी वापरण्यात येणारी माहिती व तथ्ये हे विषयाशी संबंधित विविध पुस्तके, मासिके, लेख, वर्तमानपत्र व सांकेतिक स्थळावरून संकलित करण्यात आले आहे.

संशोधनाचे उद्देश:

प्रस्तुत संशोधनाचे मुख्य उद्देश खालीलप्रमाणे आहे.

१) राष्ट्रीय अन्नसुरक्षा कायद्याची अन्नसुरक्षेत भूमिका जाणून घेणे.

२) शासनाची अन्नसुरक्षा व आहार विषयक सुरक्षेत भूमिका जाणून घेणे.

३) अन्नसुरक्षेसाठी त्या विविध योजना राबविण्यात आल्या आहेत. त्याचे अध्ययन करणे.

४) संशोधनाद्वारे निघणाऱ्या निष्कर्षाच्या आधारे योग्य उपाययोजना सूचविणे.

संशोधनाची गरज व महत्त्व:

अन्नधान्याच्या मागणीतील वृद्धिचे विश्लेषण करताना भारतातील स्थिती विचारात घेणे आवश्यक आहे. २० व्या शतकात आशियाई व आफ्रिका खंडातील विविध राष्ट्रांची लोकसंख्या वाढत गेली. त्यामुळे भारत, चीन, नेपाळ, बांग्ला देश व इतर आशियाई राष्ट्रात अन्नधान्याच्या संख्यात्मक मागणीत वाढ होत गेलेली दिसून येते. अन्नधान्याच्या मागणीतील वृद्धिवर अनेक घटक परिणाम

करीत आहेत. अन्नधान्याच्या किंमत व उत्पन्नपातळीत झालेला बदल हा प्रामुख्याने विकसित व विकसनशील देशात प्रभावी ठरत आहे. २०१० ते २०५० सालापर्यंत विकसित व विकसनशील देशातील अन्नधान्याच्या मागणीत होणारी संभाव्य वाढ विचारात घेता, जगातील सर्वच राष्ट्रांनी सुयोग्य अन्नधान्यविषयक धोरण राबवून अल्प व मध्यम उत्पन्न गटातील लोकांना पुरेशा प्रमाणात अन्नधान्य रास्त किंमतीत उपलब्ध करून देणे अन्नसुरक्षिततेच्या दृष्टीने अधिक महत्त्वाचे आहे. जागतिक भूक बळी निर्देशांकाचा विचार करताना, विकसनशील देशांची अन्नधान्य उत्पादनाची वाढती मागणी पूर्ण करण्यासाठी या देशांनी संख्यात्मक व गुणात्मक पातळीवर प्रयत्न करावयास हवेत. भारत सरकारने १९५१ नंतर या दृष्टीने पुरेसे प्रयत्न करण्यावर भर दिला आहे. तथापि त्याची व्याप्ती वाढविण्याची गरज आहे. म्हणून भारतातील अन्नधान्य सुरक्षेच्या विविध प्रयत्नांचे अध्ययन करण्याच्या हेतुने प्रस्तुत संशोधन महत्त्वाचे आहे.

अन्नधान्य सुरक्षिततेच्या व्याख्याः

जागतिक विकास अहवालानुसार १९८६ **(World Development Report 1986)** ''असुरक्षितता म्हणजे सर्व व्यक्तींना सर्वकाळी सक्रिय व आरोग्यप्रद जीवन कंठण्यासाठी आवश्यक अन्नधान्य मिळण्याची संधी होय.''

अन्न व कृषी संघटना १९८३ नुसार अन्न सुरक्षितता म्हणजे **(Food and Agriculture Organisation- FAO; 1983),** ''सर्व लोकांना सर्व वाबी मुलभूत अन्नाची शारीरिक व आर्थिक गरज भागण्याची संधी देण्याची हमी होय.''

अन्न सुरक्षा योजनेच्या अंमलबजावणीत शासनाची भूमिकाः

भारतीय नियोजनकारांनी सुरवातीपासून अन्नधान्याच्या स्वयंपूर्णतेला नियोजनाचे एक महत्त्वपूर्ण उद्दिष्ट मानले होते. सरकारलासुद्धा याचा अनुभव आला होता की अन्नधान्याच्या दृष्टीने अतिरिक्त असणारी राष्ट्रे, अन्नधान्य तुटीच्या देशांना आपल्या मागण्यापूर्ण करतांना कसे नमवितात.

या संदर्भात आपला अनुभव सांगतांना भारताचे प्रथम पंतप्रधान जवाहरलाल नेहरू यांनी एका प्रकरणात असे म्हटले आहे की, 'अमाची मदतीला जोडून काही अस्पष्टाचा राजकीय घटना टाळणे भारताला फार कठिण होते. परंतु त्यामुळे भारताच्या राष्ट्रीय अभिमान दुखावला गेला.' यावेळी राष्ट्राला उद्देशून केलेल्या भाषणात नेहरूंनी म्हटले होते की, ''आम्ही परकीय मदत घेवू व परिस्थितीच्या दबावाने घेत राहू. परंतु मला असे खात्रीलायकपणे वाटते की अन्नासारख्या प्राथमिक गरजेकरिता परकीय राष्ट्रावर अवलंबून असणे कसे धोकादायक आहे. जेव्हा आम्ही अन्नाच्या बाबतीत स्वयंपूर्ण होवू तेव्हाच आम्ही आपली प्रगती व विकास करू शकू. अन्यथा तेथे सतत परिस्थितीचा दबाव, चास संकटे व काही अवस्थेते अप्रतिष्ठा व मानखंडना सहन करावी लागते.''

पुढे इ.स. १९६५ व १९६६ मध्ये भारतात भयंकर दुष्काळाची परिस्थिती उद्‌भवली तेव्हा अमेरिकन अध्यक्ष जॉन लिंडन यांनी भारताला धडा शिकविण्याकरिता पी.एल. ४८० कार्यक्रमाअंतर्गत अन्न मदत मासिक आधारित निर्यातित केली होती. या मागील कारण म्हणजे भारताने व्हेटनॉम प्रकरणी अमेरिकेवर टिका करू नये. पंतप्रधान इंदिरा गांधीच्या सरकारने बीज-पाणी-खते धोरण अर्थात हरित क्रांतीचा स्वीकार करून १९७६ पर्यंत भारताला अन्नधान्याच्या बाबतीत स्वयंपूर्ण केले. त्यानंतर भारत अन्नधान्याची नाममात्र आयात करू लागला.

नवची पंचवार्षिक योजना (१९९७-२००२) म्हणते की, 'देशातील अन्नसुरक्षितता धोरण प्रभावीपणे कार्यान्वित करणे हे भारताचे प्रथम उद्दिष्ट असेल की ज्यामुळे देश दुष्काळी परिस्थितीच्या धमकीचा अधिक काळपर्यंत शिकार बनणार नाही.' गेल्या पाच दशकात देशाने दुष्काळ व भीषण उपोषणाला मोठ्या प्रमाणात अनुभवले नाही हा प्रयत्नांचा प्रभावी पुरावा म्हणावा लागेल.

अन्नधान्य विषयक प्रगती खाली विशद केली आहे.

१) १९५९-५१ ते २००१-२००२ (आणि २००३-२००४) मध्ये अन्नधान्याचे उत्पादन ५१ दशलक्ष टनावरून २१२ टनापर्यंत अर्थात चौपटीने वाढलेले आढळते. परंतु २००२-०३ मध्ये मात्र ह्यात ३८ दशलक्ष टनांची घट होवून ते केवळ १७४ दशलक्ष टन होते.

२) अन्नधान्यातील अनेक घटकांत अन्नाचे प्रतिशत १९५०-५१ मध्ये ८४ प्रतिशत होते. ते २००१-०२ मध्ये ९४ प्रतिशत पर्यंत वाढले होते. परंतु ह्याच वाढीचे कालावधीत उत्पादन १६ प्रतिशतने तर उपयुक्तचे उत्पादन ६ प्रतिशत घटलेले आढळते.

३) इ.स. १९५०-५१ मध्ये विशेषतः अन्नधान्यात तांदुळ व गव्हाचे उत्पादन ५३ प्रतिशत होते ते २००१-०२ मध्ये ७८ प्रतिशत पर्यंत वाढलेले आढळते. परंतु याच कालावधीत अन्य निम्न दर्जाच्या उत्पादन मात्र ३० प्रतिशत वरून १८ प्रतिशत पर्यंत घटलेले आहे. हे ह्या गोष्टीचे निर्देशक आहे की गरीब जनता सुद्धा निम्न दर्जाच्या अन्नधान्यापेक्षा तांदुळ व गहू यांना अधिक पसंत करतात.

इ.स. १९५०-५१ मध्ये भारताची अन्नधान्याची आयात ४.१ दशलक्ष टन होती. इ.स. १९६५ मध्ये ती १०.३ टनपर्यंत वाढलेली आढळते. इ.स. १९६६-१९७१ च्या दरम्यान अन्नधान्य उत्पादनात वार्षिक ६.४ दशलक्ष वाढ नोंदविली आहे. यानंतर आयातीत घट झालेली आढळते व १९७६ पासून अन्नधान्याची आयात नाममात्र होती. परंतु १९९५-९६ पासून भारत हा अन्नधान्याचा निर्यातक देश बनला. इ.स. २००१-०२ मध्ये भारताची अन्नधान्याची विक्रमी निर्यात ८.५ दशलक्ष टन होती.

अन्नधान्य व दाळींची प्रति व्यक्ती दिवस उपलब्धी १९५१ ते २००१ च्या दरम्यान ४१९ ग्रॅमवरून ४५१ ग्रॅमपर्यंत वाढली आहे. ह्या पन्नासवर्षात अन्नधान्याची प्रतिव्यक्ती उपलब्धी १५ प्रतिशतने वाढली आहे. अन्नधान्य व दाळी यांचा समावेश होतो. अन्नाच्या उपलब्धतेत ३५४ ग्रॅम वरून ३८५ ग्रॅमपर्यंत वाढ झाली आहे. अर्थात पन्नास वर्षांच्या कालावधीत प्रतिव्यक्ती अन्नधान्य उपलब्धता ९ प्रतिशत वाढली आहे. परंतु दाळींची प्रति व्यक्ती उपलब्धता १९५१-२००१ च्या दरम्यान ६५ ग्रॅमवरून घटून २९ ग्रॅमवर आलेली आहे. ही स्थिती दाळींची प्रतिव्यक्ती उपलब्धीत ५५ प्रतिशत घट दर्शविते.

तसेच इ.स. १९५०-५१ व १९९७-९८ च्या दरम्यान कनिष्ठ दर्जाच्या वस्तूंचा उपभोग सुद्धा प्रतिदिनी ११६ ग्रॅमवरून ९० ग्रॅमवर अर्थात २५ प्रतिशत घट दर्शवितो. या संबंधात नवल्या योजनेत, स्पष्टपणे म्हटले आहे की, कनिष्ठ दर्जाचे अन्न कमी किंमती असल्यामुळे ते स्वाभ खर्चात (किंमती वस्तूंची तुलनेत) अधिक उष्णता प्रदान करू शकतात. जर ह्या वस्तू सार्वजनिक वितरण प्रणालीने सवलती दरात उपलब्ध करविण्यात आले तर यामुळे उपभोगातील कॅलरीजची (उष्णता) संख्या वाढेल तसेच गरीब लोकांची भूक शमविण्यात मोलाची मदत होईल.

वरील विवेचनावरून स्पष्ट होते की जरी भारत अन्नधान्याचे उत्पादन वाढविण्यात यशस्वी झाला तरी दाळींच्या उत्पादनात अत्यंत अयशस्वी ठरला आहे.

यानंतर १२ सप्टेंबर २०१३ ला राष्ट्रीय अन्नसुरक्षा कायदा २०१३ (National Food Security Act) संमत करण्यात आला. ५ जुलै २०१३ पासून हा कायदा लागू करण्यात आला आहे. या कायद्यामुळे पोषण विषयक विविध योजनांना कायदेशीर अधिष्ठान प्राप्त झाले. तसेच सार्वजनिक वितरण व्यवस्थेत सुधारणा करण्यात आली. या शोषण योजनांतर्गत ६ ते ६२ महिन्यांच्या बालकांना अंगणवाडीत मोफत पूरक पोषण आहार, गरोदर व स्तनदा मातांना अंगणवाडीत पुरक पोषण आहार, ६ वर्षे ते १८ वर्षे वयोगटातील विद्यार्थ्यांना शाळेत पुरक पोषण आहार इत्यादी योजनांना कायदेशीर अधिष्ठान प्राप्त झाले आहे. इंदिरा गांधी मातृत्व सहयोग योजनेतर्गत गरोदर व स्तनदा मातांना आरोग्य व पोषणासाठी अनुदान दिले जाते. हे अनुदान थाटप या कायद्यान्वये कायदेशीर करण्यात आले आहे. आता ही योजना प्रधानमंत्री मातृ वंदना योजना' या नावाने कार्य करीत आहे.

राष्ट्रीय अन्नसुरक्षा कायद्याने अग्रक्रम कुटुंब आणि अंत्योदय असे अन्न योजनेचे लाभार्थी असे २ गट निर्धारित केले आहेत. देशातील कुटुंबापैकी किमान ग्रामिण क्षेत्रातील किमान ६५% कुटुंबे आणि शहरी क्षेत्रातील किमान ५०% कुटुंबे यांचा समावेश होता. ही अग्रक्रम कुटुंबे निवडण्याची जबाबदारी राज्यांवर टाकण्यात आली होती.

महाराष्ट्रात अंत्योदय रेशनकार्डधारक, पिवळे रेशनकार्डधारक आणि केसरी रेशनकार्डधारक कुटुंबाची बेरीज केली तर ती एकूण कुटुंबापैकी ९१.२ टक्के होती. अन्नसुरक्षा कायद्यानुसार ६७ टक्के कुटुंबांना लाभ द्यायचा होता. यासाठी केसरी रेशनकार्डधारकांचे आणखी २ गट करण्यात आले होते. ग्रामिण भागात १५००० रू ते ४४००० रू. वार्षिक उत्पन्न असणारे कुटुंब आणि शहरी भागात १५००० रूपये व ५२००० रूपये वार्षिक उत्पन्न असणारे कुटुंब अग्रक्रम कुटुंब (केसर कार्डधारक) म्हणून निवडले गेले. या कुटुंबांना पिवळ्या रेशनकार्डधारकांप्रमाणेच ३ रूपये प्रतिकिलो दराने तांदूळ, २ रूपये प्रतिकिलो दराने गहू आणि १ रूपया प्रतिकिलो दराने भरडधान्ये या दराने एकूण ५ कि.ग्रॅ. प्रतिव्यक्ती प्रतिमाह अन्नधान्य मिळत आहे.

महाराष्ट्रातील १४ दुष्काळग्रस्त जिल्हांमधील (औरंगाबाद, जालना, परभणी, हिंगोली, बीड, नांदेड, उस्मानाबाद, लातूर, अमरावती, अकोला, यवतमाळ आणि वर्धा) एपीएल शेतकरी कुटुंबांनादेखील वरील स्वस्त दराने अन्नधान्य पुरविले जात आहे ही योजना महाराष्ट्रामध्ये ऑगस्ट २०१५ पासून सुरू आहे. मात्र ही योजना महाराष्ट्र सरकार स्वतःच्या खर्चातून चालवते. कारण ही योजना राष्ट्रीय अन्नसुरक्षा कायद्याच्या कक्षेतील नाही.

आज सार्वजनिक वितरण व्यवस्थेचे संपूर्ण संगणकीकरण करण्यात आले आहे. यामुळे कामकाजात सुसूत्रता तर आली शिवाय राज्यातील सुमारे १० लक्ष शिधापत्रिका ह्या बोगस किंवा दुबारच्या आढळून आल्याने रद्द करण्यात आल्या आहेत. यामुळे अन्नधान्याची मोठ्या प्रमाणात बचत झाली. त्याशिवाय लाभार्थ्यांना आता नवीन प्रणालीमुळे दरमहा खात्रीशीर व योग्यदराने धान्य मिळण्याची हमी मिळाली आहे.

१ मे, २०१८ पासून-आधार आधारित सार्वजनिक वितरण सेवेचा वापर करून ई-पॉसद्वारे धान्य वितरण सुरू करण्यात आले आहे. या प्रणालीमुळे लाभार्थ्यांना कोणत्याही दुकानात धान्य घेण्याची सुविधा शक्य झाली आहे. ई-पॉस मशीनमधून धान्यवितरणामुळे एकूण धान्य उचलीमध्ये सुमारे ३६४-८०० मे. टन एवढी घट २०१६-१७ मध्ये झाली. ई-पॉसद्वारे केरोसीन व तुरडाळ विक्रीची सुविधा दिली जात आहे. या वर चालणारे विक्रीचे व्यवहार आता सामान्य जनतेला http://mahaepos.gov.in या संकेतस्थळावर बघता येतात त्यामुळे व्यवहारात पारदर्शकता निर्माण झाली आहे. अशाप्रकारे अन्नसुरक्षा योजनेच्या अंमलबजावणीत शासन महत्त्वाची भूमिका बजावित आहे.

निष्कर्ष:

भारतात पंचवार्षिक योजनेच्या काळापासून तर आतापर्यंत शासनाने देशात अन्न सुरक्षितता कायम करण्यासाठी अनेक प्रयत्न केले आहेत. त्यात विविध योजनांच्या माध्यमातून देशातील गरीब लोकांपर्यंत पौष्टीक आहार पोहचविण्याचे कार्य सरकारने केले आहे. या कार्यात सार्वजनिक वितरण व्यवस्थेने मोलाची भूमिका पार पाडली आहे, असे असले तरी देशात अन्नधान्य सुरक्षिततेला कायम करण्यासाठी कृषी क्षेत्राच्या विकासावर लक्ष देण्याची व शेतकऱ्यांची आर्थिक स्थिती सुधारण्याची गरज आहे.

सूचना:

१) अन्नधान्य उत्पादनात वाढ करण्यासाठी उपाययोजनांचा शोध घेऊन अंमलबजावणी करावी.

२) अन्नधान्याचा किमान आवश्यक राखीव साठा नियोजित करावा.

३) शेतकऱ्यांकडून किमान आधारभूत किंमतीला अन्नधान्याची खरेदी करून त्यांच्या हिताचे संरक्षण करावे.

४) लहान बालकांचे प्रमाण व पोषण आहार योजनेतर्गत मिळालेले लाभ यातील तफावत दूर करावे.

५) राष्ट्रीय स्तरावर शेती व्यवसायातील अस्थिरता कमी करून अन्नधान्याचे उत्पादन वाढविण्यासाठी व शाश्वत शेतीची संकल्पना अंमलात आणावी.

संदर्भ ग्रंथ सूची

१) भारतीय अर्थव्यवस्था, डॉ. घाटगे व बावरे, निराली प्रकाशन पुणे, जुलै, २०१०

२) स्पर्धा परिक्षा अर्थशास्त्र -२, आर्थिक व सामाजिक विकास, डॉ. किरण जी. देसले, दीपस्तंभ प्रकाशन, जळगाव, पाचवी आवृत्ती, जुलै २०१८

३) लोकराज्य, नोव्हेंबर २०१८, पान क्र. ४५

४) वर्तमानपत्र- नवभारत, लोकमत, टाईम्स ऑफ इंडिया

५) Indian Economy- Misra puri- Himalaua Publishing House, Mumbai 2010

६) https://mahaepos.gov.in/

७) https://maharastra.gov.on/

***

19 GST palanache tantradyan vastu v seva kar network: labh ani samasya

जीएसटी पालनाचे तंत्रज्ञान वस्तू व सेवा कर नेटवर्क (GSTN):

लाभ आणि समस्या

प्रा.श्रीमती रेखा मा. वाठ

वाणिज्य अधिव्याख्याता

इंदिरा महाविद्यालय कळंब जि. यवतमाळ

प्रस्तावना:

वस्तू व सेवा कर (जीएसटी) : भारतात एक जुलै २०१७ पासून वस्तू व सेवा कर (जीएसटी) हा एकच अप्रत्यक्ष कर लागू करण्यात आला. देशभरात एकसमान करप्रणाली असावी असा उद्देश यामागे होता. त्यानुसार केंद्र आणि राज्य सरकारद्वारे त्यापूर्वी लागू असलेले अनेक अप्रत्यक्ष कर रद्द करून ही करप्रणाली भारतात लागू करण्यात आली. जीएसटी लागू करण्यासाठी भारताच्या राज्यघटनेत दुरूस्ती करून नवीन कायदे करण्यात आले. गुड्स अॅन्ड सर्व्हिसेस काऊन्सिल ही मध्यवर्ती वैधानिक संस्था जीएसटीचे नियमन करते. केंद्रीय अर्थमंत्री हे या काऊन्सिलचे प्रमुख आहेत. जीएसटी लागू करण्यासाठी ३० जून २०१७ च्या रात्री संसदेचे विशेष अधिवेशन झाले. त्यात राष्ट्रपतींनी मध्यरात्रीच्या सुमारास जीएसटी लागू झाल्याची अधिकृत घोषणा केली. सर्व वस्तू आणि किंवा सेवा यांची विक्री, हस्तांतर, वस्तुविनिमय, भाड्याने देणे किंवा आयात व्यवहारांवर जीएसटी लागू झाले. जीएसटी अंतर्गत १ जुलै २०१७ पासून ० टक्के, ५ टक्के, १२ टक्के, १८टक्के व २८ टक्के असे कर दर ठरविण्यात आले आहेत.

वस्तू व सेवा कराच्या अंमलबजावणीसाठी माहिती तंत्रज्ञानाचे जाळे पसरविणे आवश्यक आहे. वस्तू व सेवा कराची आवश्यकता पूर्ण करण्यासाठी एक विशेष उद्देश वाहन म्हणून वस्तू व सेवा कराचे जाळे (जीएसटीएन) नावाची संकल्पना साकारण्यात आलेली आहे. जीएसटीएन कडून केंद्र आणि राज्य सरकारला माहिती तंत्रज्ञानाच्या पायाभूत सुविधा आणि सेवा पुरविण्यात येत आहेत. वस्तू व सेवा कराच्या अंमलबजावणीसाठी करदात्यास आणि इतर भागधारकांना देखील सादर सुविधा आणि सेवा पुरविण्यात आल्या आहेत. परंतु जीएसटीएनचे काही लाभ असले तरी त्यात काही समस्यांना करदात्यांना समोर जावे लागत आहे. त्यामुळे जरी जीएसटी तंत्रज्ञान खूप प्रगती पथावर असली तरी जीएसटी अंमलबजावणी आणि पालन योग्य तंत्रज्ञान विषयांवर अधिक लक्ष केंद्रीत करण्याची व समस्यांची पुनर्तपासणी करण्याची गरज निर्माण झाली आहे? सरकार आणि व्यवसाय दोन्हीच्या दृष्टीकोनातून तंत्रज्ञानाची भूमिका जीएसटी अंमलबजावणीत मोलाची आहे. म्हणून संशोधनासाठी "जीएसटी पालनाचे तंत्रज्ञान वस्तू व सेवा कर नेटवर्क (GSTN) –लाभ आणि समस्या" हा निवडला आहे.

शोध निबंधासाठी वापरण्यात येणारी संशोधनाची पद्धती:

प्रस्तुत शोधनिबंधासाठी लागणारी विषयसामग्री गोळा करण्याकरिता पुस्तके , मासिके, वर्तमानपत्रे, संशोधनपर लेख, वेबसाईट इत्यादी दुय्यम साधनांचा अवलंब करून निदानात्मक व वर्णनात्मक संशोधन आराखड्याचा वापर करण्यात आलेला आहे.

संशोधनाचे उद्देश:

प्रस्तुत संशोधनाचे मुख्य उद्देश खालीलप्रमाणे आहेत.

१) करदात्यांच्या सुलभेसाठी जीएसटीनची भूमिका हे जाणून घेणे.

२) जीएसटीन समोरील भविष्यातील विविध आव्हानांचा शोध घेणे.

३) तंत्रज्ञानाचा जीएसटीवर काय प्रभाव पडत आहे, याची माहिती प्राप्त करणे.

४) जीएसटीएनच्या विविध लाभाची व समस्येची माहिती प्राप्त करणे.

५) जीएसटीएनच्या कार्यप्रणालीचे अध्ययन करणे.

संशोधनाची गरज व महत्त्वः

जीएसटीन प्रणालीचा परिणाम जीएसटीवर आणि करदात्यावर काय होईल हे समजून घेणे आवश्यक आहे कारण जीएसटीएन प्रणालीच्या यशावरच संपूर्ण जीएसटी व्यवस्था अवलंबून आहे. करदाता आणि शासनाच्यामध्ये कर संकलन कार्यात मध्यस्थ म्हणून वस्तू व सेवा कर नेटवर्क मोलाची भूमिका बजावत आहे. परंतु जीएसटीन प्रणालीच्या विविध लाभासोबतच त्यात काही समस्या सुद्धा आहेत. त्याचा परिणाम करदात्याच्या कर भरणा कार्यावर पडत असून त्याला त्रास सहन करावा लागत आहे. या समस्यांकडे शासनाचे लक्ष वेधून वस्तू व सेवा कर नेटवर्कला अधिक मजबूत बनविता येवू शकते. म्हणून जीएसटीएनची जीएसटीमध्ये भूमिका जाणून घेण्याच्या उद्देशाने व जीएसटीएन समोरील समस्या व भविष्यातील आव्हानांचा शोध घेण्याच्या हेतूने संशोधनाचा हा विषय महत्वाचा आहे.

वस्तू व सेवा कर नेटवर्कची गरजः

जीएसटी प्रणाली एक वैशिष्ट्यपूर्ण आणि संकिर्ण किंवा सर्वसमावेशक माहिती तंत्रज्ञानाचा उपक्रम आहे. प्रथमच करदात्यासाठी नियमित संपर्क आणि माहिती तंत्रज्ञानाच्या समान आणि सामाईक पायाभूत सुविधा केंद्र शासन आणि राज्य शासन यामध्ये स्थापित करण्याचा प्रयत्न करणारा वैशिष्ट्यपूर्ण उपक्रम आहे. सद्यःस्थितीत, केंद्र शासन आणि राज्य शासन यांचे अप्रत्यक्ष कर प्रशासन भिन्न कायदे, अधिनियम, पद्धती आणि संरचना यांचा अवलंब करत आहे आणि परिणामतः माहिती तंत्रज्ञान प्रणाली देखील स्वतंत्रपणे कार्यरत आहे. या सर्वांना जीएसटीच्या अंमलबजावणीसाठी एकत्रित करणे क्लिष्ट होते. कारण सर्व कर प्रशासनांना (केंद्र, राज्य आणि केंद्रशासित प्रदेश) समान विहित नमुने आणि करदाते आणि इतर आर्थिक हितसंबंधी व्यक्ती यांच्याकरिता समान संपर्क साधने इत्यादींसह माहिती तंत्रज्ञानाच्या प्रगल्भतेच्या समान स्तरावर आणण्यासाठी संपूर्ण अप्रत्यक्ष कर इको-सिस्टम एकत्रित करावे लागले. याखेरीज, जीएसटी ''इच्छित स्थान/स्थळ'' आधारित करप्रणाली असल्याने, ''वस्तू/माल आणि सेवा यांचा आंतरराज्य व्यापार'' यासाठी राज्य शासनाने आणि केंद्र शासन यामध्ये सक्षम समेट किंवा समझोता यंत्रणा असणे आवश्यक अ हे. ही प्रक्रिया शक्य आहे जेव्हा माहिती तंत्रज्ञानाच्या पायाभूत सुविधा आणि सेवा यांचा आधारस्तंभ मजबूत असेल ज्यायोगे आर्थिक हितसंबंधी व्यक्ती (करदाते, राज्य शासने आणि केंद्रशासन, बँक आणि रिझर्व्ह बँक इत्यादी समाविष्ट) यांच्यात माहितीची देवाण-घेवाण, माहिती मिळविणे आणि प्रक्रिया करणे सुलभ होईल. सदर उद्दिष्ट्ये साध्य करण्यासाठी जीएसटीएनची निर्मिती केली गेली आहे.

करदात्यांच्या सोयीसाठी जीएसटीएनची भूमिकाः

''वस्तू/माल आणि सेवा कर नेटवर्क'' (जीएसटीएन) ''विना-नफा'' केंद्र सरकार आणि राज्य सरकारे यांचा संयुक्त पार्टिवा असलेली विन-सरकारी कंपनी आहे. सदर कंपनी केंद्र आणि राज्य सरकार/शासन या दोघांसह करदाते आणि इतर आर्थिक हितसंबंधी व्यक्ती यांना सामाईक माहिती तंत्रज्ञानाच्या पायाभूत सुविधा आणि सेवा उपलब्ध करून देत आहे. सर्व करदात्यांसाठी नोंदणी, विवरण आणि अधिदान इत्यादी दृश्यमान सेवा उपलब्ध करून देत आहे. सरकार आणि करदाते यामध्ये संपर्क दुव्याचे कार्य करीत आहेत.

जीएसटीएनच्या कार्यात पुढील बाबींचा समावेश आहे.

१) नोंदणी प्रक्रियेची सुविधा
२) भरणा केलेल्या कराचा तपशील बँक नेटवर्कशी जुळवणे
३) केंद्रीय आणि राज्य प्राधिकरणांना विवरण पत्रके पाठविणे
४) आयजीएसटी कराची संगणना करणे आणि समझोता करणे
५) करदात्यांच्या माहितीचे विश्लेषण उपलब्ध करून देणे.
६) करदात्यांच्या विवरण पत्रकांतील माहितीच्या आधारे केंद्र व राज्य शासनांना विविध एमआयएस अहवाल उपलब्ध करून देणे आणि
७) इनपूट टॅक्स क्रेडिटचा मेळ घालणे, परावर्तन करणे आणि पुनःप्राप्त करणे यासाठी सुसंगत आयोजन करणे.

जीएसटीएन हे नोंदणी, अभिदान/अदायगी, विवरण पत्रके आणि एमआयएस अहवाल इत्यादींसाठी एक सामाईक जीएसटी पोर्टल आणि ॲप्लिकेशन विकसित केले आहे. जीएसटीएन अस्तित्वात असलेल्या कर प्रशासन माहिती तंत्रज्ञान प्रणालीवरोवर सामाईक पोर्टल एकत्रित केले आहे आणि करदात्यांसाठी इंटरफेसेसची निर्मिती केली आहे. तसेच जीएसटीएन १९ राज्ये आणि

केंद्रशासित प्रदेश यांच्याकरिता एक निर्धारण, लेखापरिक्षण, परतावे, अपील इत्यादी बँक-एन्ड मॉड्युल्स विकसित केले आहे. सीबीईसी आणि मॉडेल १ राज्ये (१५ राज्ये) स्वतः त्यांचे जीएसटी बँक-एन्ड प्रणाली विकसित करीत आहेत. जीएसटी फ्रंट-एन्ड प्रणालीचे बँक-एन्ड प्रणाली बरोबर एकत्रिकरण पूर्ण करण्यात येईल आणि या प्रणालींचे सुरळीतपणे संक्रमण होण्यासाठी आधी चाचणी घेतली गेली आहे.

जीएसटी पोर्टलवर नोंदणीसाठी अर्ज ऑनलाईन दाखल करता येते. काही महत्त्वाची संगणकीय माहिती असे, PAN व्यापार/व्यवसाय घटना आधार क्रमांक, CIN/DIN (लागू असेल तसे) इत्यादी जीएसटी पोर्टलद्वारे CBDT, UID, MCA अशा संबंधित एजन्सी बरोबर ऑनलाईन प्रमाणित केले जाते. त्यायोगे कमीत कमी दस्तऐवज सादर करावे लागतात.

अर्जातील संगणकीय माहिती आधारभूत स्कॅन्ड दस्तऐवजासह जीएसटीएन राज्य शासने/केंद्र शासन यांना पाठवते. राज्य शासने/केंद्र शासन यानंतर अन्य काही शंका किंवा प्रश्न असल्यास किंवा मान्यतेच्या किंवा अमान्यतेच्या सूचना जीएसटीएनकडे अग्रेषित करते आणि डिजिटल स्वाक्षरी केलेली नोंदणी प्रमाणपत्रे सरतेशेवटी करदात्यांना डाऊनलोड करता यावे यासाठी पाठविते.

वस्तू व सेवा कर नेटवर्कद्वारे पुरविण्यात येणाऱ्या सेवाः

जीएसटीएन सामाईक पोर्टलद्वारे खालीलप्रमाणे सेवा पुरविण्यात येतात.

१) नोंदणी (विद्यमान करदाता स्थलांतर, प्रक्रिया ८ नोव्हेंबर, २०१६ रोजी सुरु झाली)

२) अधिदान व्यवस्थापनासह अधिदान सुविधा केंद्र आणि बँकिंग प्रणालीशी एकत्रिकरण.

३) विवरण दाखल करणे आणि विवरणाचे विश्लेषण करणे.

४) करदाता व्यवस्थापन यांच्यासह लेखा व्यवस्थापन, अधिसूचना निर्गमित करणे, माहिती उपलब्ध करणे आणि सद्यःस्थितीचा मागोवा घेणे

५) करप्राधिकरणाचे लेखे आणि खातेवही व्यवस्थापन

६) केंद्र शासन आणि राज्य शासनांमध्ये समेट/समझोत्याची संगणना करणे. आयजीएसटीसाठी क्लियरिंग हाऊसचे कार्य

७) आयातीवरील जीएसटी चे विश्लेषण करणे व जुळवणी करणे आणि सीमाशुल्काच्या इडीआय प्रणालीशी एकत्रिकरण

८) एमआयएस सहीत आवश्यकतेवर आधारित माहिती आणि व्यावसायिक बुद्धीमत्ता/माहिती.

९) मामाईइ जीएसटी पोर्टल आणि कर व्यवस्थापन प्रणाली मधील संपर्क साधने सुस्थितीत ठेवणे.

१०) आर्थिक हितसंबंधी व्यक्तींना प्रशिक्षण देणे.

११) कर प्राधिकाऱ्यांना विश्लेषणात्मक आणि व्यावसायिक माहिती/कौशल्य उपलब्ध करून देणे आणि;

१२) संशोधन करणे आणि उत्तम सरावांचा अभ्यास

वस्तू व सेवा कर नेटवर्क आणि राज्ये किंवा सी.बी.ई.सी. यामधील संपर्क प्रणालीः

जीएसटी करप्रणालीत, करदातादर्शी महत्त्वाच्या सेवा जसे नोंदणीसाठी अर्ज करणे, वीजक संगणकावर अपलोड करणे, विवरण दाखल करणे, कर भरणे इत्यादी सेवा, जीएसटी करप्रणालीद्वारे आयोजित केल्या. परंतु सर्व कायदेशीर कार्ये (जसे नोंदणीची मान्यता, विवरणाचे मूल्यांकन, चौकशीचे आयोजन, लेखापरीक्षण इत्यादी) राज्य शासन आणि केंद्र शासन यांची कर प्राधिकरणे आयोजित करते.

अशारितीने जीएसटीएन फ्रंट-एन्ड पद्धती (जीएसटी पोर्टल सेवा) उपलब्ध करून देते आणि बँक-एन्ड पद्धती राज्य शासने आणि केंद्र शासन स्वतः विकसित करीत आहेत. तथापि ,२४ राज्यांनी (मॉडेल -२ राज्ये म्हणून संज्ञा दिलेली) जीएसटीएनने त्याची बँक-एन्ड पद्धती विकसित केलेली आहे. राज्ये सीबीईसीसाठी करदात्यांनी सादर केलेली पूर्ण माहिती (नोंदणी, विवरण, अधिदान इत्यादी) त्यांना योग्य वाटेल तसे विश्लेषणाकरिता आणि माहितीकरिता, त्यांच्यावरोबर देवाण-घेवाण करीत आहेत.

अनुपालन प्रतवारी यंत्रणा (Compliance rating mechanism):

सीजीएसटी/एसजीएसटी अधिनियम कलम १४९ अनुसार, प्रत्येक नोंदणीकृत व्यक्तीला विवक्षित मापदंडाच्या अनुपालनाच्या कामगिरीवर आधारित अनुपालन प्रतवारी दिली जाते. सदर प्रतवारी सार्वजनिक क्षेत्रातही प्रदर्शिक केली जाते. भावी ग्राहकाला पुरवठाकर्त्यांची अनुपालन प्रतवारी ज्ञात होईल आणि त्या विशिष्ट पुरवठाकर्त्यांबरोबर व्यवहार करावा किंवा नाही याबाबत निर्णय घेता येते. यामुळे करपात्र व्यक्तींमध्ये निकोप स्पर्धा निर्माण होते.

करदात्यांच्या उपयोगितेसाठी जीएसटीएनद्वारे उपलब्ध करून देण्यात येणारी सामग्री:

जीएसटीएन संगणकावर आधारित प्रशिक्षण सामग्री तयार केली आहे. जीएसटी ज्यात पोर्टलद्वारे करण्यात येणाऱ्या प्रत्येक प्रक्रियेसंबंधीचे Videos अंतर्भूत केलेले आहेत. सदर सामग्री जीएसटी पोर्टलवर त्याचप्रमाणे सर्व कर प्राधिकरणांच्या वेबसाईटवर प्रदर्शित करण्यात आली आहे. सीबीटी खेरीज विविध वापरकर्त्यांसाठी माहितीपत्रके वारंवार विचारले जाणारे प्रश्न, करदात्यांच्या माहिती व जीएसटीचे आकलन होण्यासाठी जीएसटी पोर्टलवर ठेवण्यात आलेले आहेत. याखेरीज करदात्यांना ई-मेल किंवा दुरध्वनीद्वारे त्यांचा विशिष्ट क्रमांक देण्याकरिता मदतकक्षाची स्थापना केली आहे. नोंदणी प्रक्रियेसाठी सीबीटी, एफएओ आणि युझर्स मॅन्युअल्स पुढील वेबसाईटवर उपलब्ध आहेत- https:www.gst.gov.in/help. खातेवह्या आणि इतर लेखे पाहण्यासाठी मोबाईल आधारित ॲप्स उपलब्ध करून दिले आहे. जीएसटी पोर्टलची रचना अशाप्रकारे करण्यात आली आहे. ज्यामुळे पोर्टल कोणत्याही स्मार्ट मोबाईलवर पाहता येतो. त्यामुळे खातेवह्या जसे रोख खातेवही, दायित्व खातेवही, आयटीसी खातेवही इत्यादी सुसंगत मार्गनिर्देशक वापरून मोबाईलवर पाहता येते.

जीएसटीएन प्रणालीच्या सुरक्षिततेसाठी जीएसटीएनद्वारे योजण्यात आलेले उपाय:

जीएसटी प्रणाली प्रकल्पात माहिती आणि सेवा यांच्या सुरक्षेसाठी अत्याधुनिक सुरक्षा संरचनेचा अंतर्भाव केला आहे. याखेरीज उच्च प्रतीचे Firewalls, अवैध प्रवेश शोध, संचलित किंवा संचित माहिती सांकेतिकरित्या लिपीबद्ध करणे, लेखापरीक्षणाच्या पूर्णपणे मागोवा, अनधिकृत बदल न करता येण्याजोगी संचालन प्रणाली (OS), (Consistent hashing algorithms) and host hardening, etc. इत्यादी सुरक्षेचे उपायही योजण्यात आले आहेत. प्राथमिक आणि दुय्यम सुरक्षा कार्य उपविभाग आणि नियंत्रण केंद्र याची जीएसटीएनद्वारे स्थापना करण्यात येत आहे. Real time वेमिस अनुसार विद्वेषपूर्ण प्रयत्नांपासून जीएसटीएन यंत्रणेला स्वयंप्रेरितपणे नियंत्रण आणि सुरक्षा प्रदान करतील. जीएसटीएन त्यांच्या प्रणालीला ज्ञात आणि अज्ञात धोक्यांपासून संरक्षित करण्यासाठी स्रोत सांकेतिक लिपीच्या आणि जीएसटी प्रणालीत वापरल्या जाणाऱ्या अंकीय दस्तऐवजांच्या संग्रहाच्या सातत्याने केलेल्या छाननीद्वारे सुरक्षित सांकेतिक पद्धतीची खबरदारी आहे.

जीएसटी सामाईक पोर्टलवर करदात्यांनी सादर केलेल्या माहितीबाबत गुप्तता राखण्यासाठी जीएसटीएनद्वारे घेण्यात येणारी खबरदारी:

जीएटी सामाईल पोर्टलवर करदात्यांनी पाठविलेली व्यक्तिगत आणि व्यवसाय संबंधित असलेली माहिती बाबत गुप्तता राखण्यासाठी जीएसटीएनद्वारे सर्व खबरदारी घेण्यात आली आहे. यासाठी ''कार्य आधारित प्रवेश नियंत्रण '' यंत्रणा वापरली गेली आहे. आणि करदात्यांच्या महत्त्वाच्या माहितीचे संकलन किंवा संचय करताना ती माहिती सांकेतिक लिपीबद्ध केली गेली आहे याची पूर्ण खबरदारी घेण्यात आली आहे. केवळ प्राधिकृत कर प्राधिकरणांना ही माहिती पाहता किंवा वाचता येते.

जीएसटी सामाईक पोर्टलद्वारे करदात्याला करता येणारी कार्ये:

जीएसटी अंतर्गत करदात्यांसाठी जीएसटी सामाईक पोर्टल एकाच ठिकाणी सर्व आवश्यकतांची पूर्तता या विचाराने तयार करण्यात आलेले आहे. जीएसटीएन नियंत्रित करीत असलेल्या जीएसटी पोर्टलद्वारे करदात्यांना करता येणाऱ्या कार्यांची स्पष्टीकरणात्मक सूची खालीलप्रमाणे आहे.

१) नोंदणी अर्ज, तसेच नोंदणीमध्ये सुधारणा, नोंदणी रद्दबातल करणे आणि व्यक्तिगत माहितीचे व्यवस्थापन
२) भुर्दंड, दंड, व्याज इत्यादीसह कर अधिदान (चलन निर्मिती अनुसार बँकेच्या पोर्टलवर अधिदान केले जाईल किंवा प्रत्यक्ष बँकेत)
३) करदात्याच्या ''स्थितीत'' बदल-नियमित ते संयुक्त किंवा उलटपक्षी.
४) बीजकांचा तपशील अपलोड करणे आणि विविध कायदेशीर विवरणे आणि वार्षिक तक्ते दायल करणे.
५) जीएसटी पोर्टल निर्मित विशिष्ट Application Reference Number (ARN) वापरून विवरण/कर खातेवही/यांच्या सद्यःस्थितीचा मागोवा घेणे.

६) परताव्यासाठी अर्ज दाखल करणे.
७) विवरण/कर खातेवही/रोख खातेवही इत्यादींचे सद्यःस्थितीचे परीक्षण.

बीजकांची माहिती जीएसटी पोर्टलवर अपलोड करण्यासाठी उपलब्ध जीएसटीएन साधनेः

जीएसटीएन स्प्रेडशीट सारखी साधने विनाशुल्क करदात्याला उपलब्ध करून देण्यात आले आहे. ज्यामध्ये बीजकांची माहिती एकत्रित करणे आणि फाईल्स निर्माण करणे शक्य झाले आहे. नंतर सदर बीजकांची माहिती तात्काळ जीएसटी पोर्टलवर अपलोड करता येते. हे एक ऑफ-लाईन साधन आहे, ज्याचा वापर बीजकांची माहिती ऑन-लाईन वर न जाताही भरण्यासाठी/ मिळविण्यासाठी करता येते आणि त्यानंतर जीएसटी पोर्टलवर अपलोड करण्यासाठी सुसंगत नमुन्यात अंतिम फाईल्स निर्माण करता येते.

जीएसटीएनच्या समस्याः

१) जीएसटी रिटर्न भरताना करदात्यांना त्रास होत आहे. त्यामुळे सरकारला वारंवार जीएसटी रिटर्न भरण्याची शेवटची तारीख वारंवार वाढवावी लागते.
२) एचएसएन कोड भरण्याची समस्या
३) विजकांच्या जुळवणीतही अनेक समस्या निर्माण होत आहेत.
४) इंटरनेटर कनेक्टीव्हिटीची समस्या
५) ई-कॉमर्स कंपन्यांना थर्ड पार्टी सेलर्सद्वारे सोर्सवर गोळा केलेल्या टीसीएस टॅक्सच्या विवरणाला जीएसटीतून वर नोंदविण्यात अडचणी येत आहेत.
६) डेटा वघण्यासाठी वेळ लागतो.
७) इनपुट क्रेडिट सेट ऑफ प्रोसेस मध्ये वेळ लागते.
८) मोठी फाईल अपलोड करण्यात समस्या निर्माण होते.

निष्कर्षः

जीएसटीणनची जीएसटीच्या अंमलवजावणीत खूप महत्त्वाची भूमिका आहे. ही आधुनिक तंत्रज्ञानावर आधारित समन्वय तत्वावर आधारित कर संकलनासाठी उपयोगात येणारी अप्रतिम यंत्रणा आहे. यामुळे करदात्याला व सरकारला अनेक लाभ होत आहेत. जीएसटीएनच्या वरील काही समस्या आहेत परंतु या स्थायी समस्या नाहीत. योग्य उपाययोजना करून या समस्या दुरू करता येतील.

सूचनाः

करदात्यांनी जीएसटीएन प्रणालीशी पुरेसे संवाद साधण्यासाठी व तत्काळ, अचुक आणि विश्वसनीय मदत पाण्यासाठी अद्यावत सॉफ्टवेअर प्रस्थापित करणे आवश्यक आहे. बीजक जुळणी हि जीएसटीची एक अत्यंत गंभीर समस्या आहे. जीएसटीने एक स्पष्ट वेळ निर्धारित केल्या कारणाने पालन करणे हे महिना अखेर अथवा तिमाही अखेर कार्य राहिले नाही. त्यामुळे विजक जुळणी आणि इतर पालने ही निरंतर तंत्रज्ञान वापरून हे ध्येय गाठणे शक्य नाही. वेग आणि अचूकता हे दोन्ही महत्त्वाचे घटक आहेत.

व्यवसायांनी आता जीएसटी प्रणालीशी वारंवार संवाद साधावे लागणार आहे. यासाठी जीएसटीएनसाठी सक्षम व्यवसाय अनुप्रयोग सॉफ्टवेअरची गरज आहे. जेणेकरून जीएसटीशीसंबंधित कार्ये कार्यक्षम आणि एकसंध होतील. शासनाने जीएसटीचे कार्य सुरळीत चालावे यासाठी तज्ञांची चमू बनवून जीएसटीनचे वेळोवेळी मूल्यांकन करावे. व काही समस्या आल्यास त्वरीत तोडगा काढावा.

संदर्भ ग्रंथ सूची

१) प्रा. प्रविण घ.कामथे, प्रा. मेघना पाटील (मुदिराज), ''जी.एस.टी. वस्तू आणि सेवा कर कायदा- एक परिचय,'' साई ज्योती प्रकाशन, नागपूर.
२) महाराष्ट्र टाईम्स वृत्तपत्र नागपूर बुधवार दि. ६ डिसेंवर २०१७ मधील डॉ. अभिजीत फडवणीस यांच्या ''वाढत्या आर्थिक वाढीच्या सुखद खुणा'' हा लेख, पृ.६.
३) महाराष्ट्र टाईम्स वृत्तपत्र नागपूर मंगळवार दि. ३० मे २०१७ मधील श्री संजीव गोखले यांचा 'जीएसटी आणि सर्वसामान्य' हा लेख पृ. ९
४) https://www.cbec.gov.in
५) https://www.gst.gov.in/help.

***

20 Maharastra Rajyachya Arthasankalpat Mahilanvishayi Tartudi va yojan: Ek Drustikshep

महाराष्ट्र राज्याच्या अर्थसंकल्पात महिलांविषयक तरतुदी व योजना : एक दृष्टिक्षेप

प्रा. श्रीमती आर.एम. वाठ
वाणिज्य अधिव्याख्याता
इंदिरा महाविद्यालय, कळंब, जि. यवतमाळ

प्रस्तावना

देशाच्या विकासात स्त्रियांचे महत्त्व अतिशय जास्त आहे. स्त्रियांचा सर्वांगीण विकास व्हावा म्हणून भारतीय अर्थव्यवस्थेत लिंगावर आधारित बजेट ही संकल्पना पुढे आली. याद्वारे शासकीय विविध योजनांचा लाभ राष्ट्रात, राज्यात, समाजात आणि ग्रामीण भागातील स्त्रियांपर्यंत पोचावा आणि पुरुष व स्त्रियांची विषमतेचे असंतुलन दूर करता यावे यासाठी मुख्य बजेट मध्येच लिंगावर आधारित बजेटचे समायोजन करून बजेट प्रस्तुत करण्यात आले. सध्या भारतात कल्याणाची जागा सशक्तीकरणांनी घेतली असून लिंगावर आधारित बजेट वितरीत केले आहे. सर्वप्रथम लिंगावर आधारित बजेटची संकल्पना ऑस्ट्रेलियात १९८४ मध्ये मांडली. १९८९ मध्य ब्रिटीश वुमन बजेट ग्रुप या संघटनेचा वैचारिक दबावातून इंग्लंडमध्ये लिंगाधिरीत मूल्यमापनाची सुरुवात करण्यात आली. १९९३ मध्ये कॅनडा या देशात तर १९९५ मध्ये दक्षिण आफ्रिका या देशात लिंगावर आधारीत बजेट मांडल्या गेला. सध्या जगातील ७० देशात लिंग आधारित बजेटचा उपयोग केला जात आहे.

लिंगावर आधारित बजेट म्हणजे स्त्रियांकरिता वेगळे बजेट निर्माण करणे नसून मुख्य बजेटमध्येच समायोजन करून सामाजिक आणि लैंगिक विषमता दूर करणे होय. स्त्री भ्रुणहत्या समाज व्यवस्थेत स्त्रीला न मिळणारे फायदे त्यांचे शोषण, त्यांच्यावर होणारे अन्याय स्त्रियांचे अधिकार, साक्षरता इ. सर्व आकडेवारींचे अवलोकन करून महिलांना सशक्त करण्यासाठी त्यांना शिक्षण अधिकार वित्तीय सहायता आणि स्वयंनिर्भरतेची गरज आहे. भारतीय अर्थव्यवस्थेचा विचार करता आज लिंग आधारित बजेटची संकल्पना पुढे आलेली आहे. या सरकारी योजनेचा लाभ हा समाजातील प्रत्येक स्त्रीला मिळाला पाहिजे अशी राष्ट्र आणि राज्य यांचे प्रयत्न सुरू आहे.

महाराष्ट्र राज्याचा अर्थसंकल्प

२०१३–१४ अर्थसंकल्पातील महिला विषयक तरतुदी

सन २०१३–१४ च्या अर्थसंकल्पात महाराष्ट्र शासनाने महिला आणि लहान मुलांच्या आरोग्याची आणि सुरक्षिततेची विशेष दक्षता घेतली आहे. त्या योजना खालील प्रमाणे –

१. पोषण आहार कार्यक्रम – सन २०१३–१४ मध्ये १२९४ कोटी ७६ लाख रूपये गरोदर स्त्रिया, स्तनदा माता व ० ते ६ वयोगटातील मुलांमुलींच्या एकात्मीक बाल विकास योजनेअंतर्गत पोषण आहार कार्यक्रम राबविण्यात आला होता.

२. राजीव गांधी सबला योजना – या योजनेत २०१३–१४ साली केंद्र व राज्य शासनाचा ५०–५० टक्के वाटा होता. या योजनेचे बजेट ११० कोटी ७८ लाख रूप्ये अपेक्षित होते. महाराष्ट्र राज्यात बीड, नादेड, मुंबई, नाशिक, गडचिरोली, बुलडाण, कोल्हापूर, सातारा, अमरावती, नागपूर आणि गोंदिया या जिल्हयातील २०७ प्रकल्पात वर्षे ११ ते १८ या वयोगटातील किशोरवयीन मुलींच्या सक्षमीकरणासाठी राजीव गांधी सबल योजना सुरू करण्यात आली होती.

३. मुलींची वसतीगृहे– सन २०१३–१४ मध्ये १०० कोटी रूपये या योजनेसाठी होते यासाठी केंद्र शासनाचा ९० टक्के व राज्य शासनाचा १० टक्के हिस्सा होता. एक स्त्री शिकली तर संपूर्ण कुटुंब शिकते. स्त्रीयांचे समाजातील मागासलेपणा दूर करायचे असेल तर त्यांना शिक्षण देणे गरजेचे आहे. आजही आपल्याकडे शैक्षणिक गळतीमध्ये मुलींचे प्रमाण जास्त आहे. ते कमी करायचे असेल तर त्यांना शैक्षणिक सुविधा देणे त्यांना सुरक्षिततेच्या दृष्टिने वसतीगृहे बांधण्याची योजना होती.

अर्थ संकल्पातील महिला विषयक तरतुदी २०१४–२०१५

१. महिला बालसुरक्षेसाठी १०५ समुपदेशन केंद्र स्थापणार.
२. स्त्रीभ्रूणहत्या रोखण्यासाठी सुकन्या योजना.
३. मुलींसाठी सुकन्या योजना
४. लैंगिक अत्याचार रोखण्यासाठी १५ कोटी १० लाख ची तरतूद.
५. अंगणवाडी सेविकांच्या मानधनात वाढ.
६. अंगणवाडी सेविकांना निवृत्तीनंतर १ लाख रू.
७. ठेवी बुडालेल्या उपवर मुलींच्या पालकांना एक लाखाची मदत.

२०१५–२०१६ अर्थसंकल्पातील महिला विषयक तरतुदी

१. व्यवसाय कर – मासिक रुपये सात हजार पाचशे पेक्षा जास्त वेतन असणाऱ्या सर्व महिलांना व्यवसाय कर भरावा लागायचा. त्याची मर्यादा वाढवून दहा हजार रुपये करण्यात आली होती. दहा हजार रुपये पर्यंत मासिक वेतन असणाऱ्या महिलांना यापुढे व्यवसाय कर लागणार नाही. याचा जवळपास एक लाख पन्नास हजार नोकरदार महिलांना लाभ होईल असा अंदाज होता.

२. महिलांच्या पर्सेस व हॅण्डबॅग्ज वरील मूल्यवर्धित कराचा दर साडेबारा टक्क्यावरून पाच टक्के करण्यात आला.

३. मुलींसाठी वसतिगृह–माध्यमिक शाळेत दाखल होणाऱ्या मुलींचे गळतीचे प्रमाण कमी करण्याकरिता २०१४–१५ च्या आर्थिक बजेट पेक्षा दुप्पट म्हणजे ११२ कोटी ५२ लाख रू इतकी तरतूद मुलींच्या वसतीगृह बांधण्याची योजना होती.

४. मुलींच्या शासकीय वसतिगृहांना संरक्षक भित बांधणी. महाराष्ट्रातील सर्व मुलींच्या शासकीय वसतिगृहांना टप्याटप्यांनी संरक्षक भिंत बांधण्याचे शासनाने नियोजन असून सन २०१५–१६ मध्ये नियोजन विभागअंतर्गत अतिरिक्त नियम व्ययापैकी २५ पैकी रुपये आहे. येत्या तीन वर्षात राज्यातील सर्व वसतिगृहांना संरक्षक भिंती बांधण्याचा शासनाचा निर्धार आहे.

५. महिला बचत गटांचे सक्षमीकरण नारी शक्तीचा सन्मान व आदर करत महिलांचे सक्षमीकरण व त्यांना आत्मनिर्भर करण्यासाठी विविध योजना व या योजना राबविण्यात महिला वर्गास सूक्ष्म वित्तपुरवठा करण्याची शासनाचा मनोदय आहे.

६. पोषण आहार – पोषण आहारासाठी स्थानिक कृषी उत्पादनाच्या माध्यमातून चांगले तसेच दर्जेदार पोषण आहार उपलब्ध करून देण्याचा शासनाचा मानस आहे. हा पोषक आहार महिला बचत गटाच्या माध्यमातून उपलब्ध करून देण्यासाठी त्यांना यंत्रसामग्री खरेदीसाठी मदत करण्यात येईल. तसेच महिला बचत गटांनी उत्पादित केलेल्या वस्तुंच्या विक्रीसाठी जिल्हास्तरावर कायमस्वरूपी 'पुण्यश्लोक अहिल्याबाई होळकर बाजारपेठ' निर्माण करण्याचा शासनाचा मानस आहे. यासाठी नियोजन विभागांतर्गत अवितरीत नियतव्ययापैकी २०० कोटी रुपये नियत व्यय चिन्हांकित केला आहे.

७. अंगणवाडी सेविकांचे मानधन – अंगणवाडी सेविका, मिनी अंगणवाडी सेविका व मदतनीस यांच्या मानधनात केलेली वाढ दि. १ एप्रिल २०१५ पासुन लागू करण्यात येईल.

८. माझी कन्या भाग्यश्री – केंद्र सरकारच्या 'बेटी बचाओ बेटी पढाओ' या योजनेच्या धर्तीवर 'माझी कन्या भाग्यश्री' या नावाने नवीन योजना राज्यात सुरू करण्यात येत आहे. यासाठी सन २०१५–१६ मध्ये नियोजन विभागाअंतर्गत अवितरित नियतव्ययांपैकी २०० कोटी रूपये नियतव्यय चिन्हांकित केला आहे.

२०१६–१७ अर्थसंकल्पातील महिला विषयक तरतुदी

१. मुलीच्या वसतीगृहासाठी ५० कोटी रुपये इतका नियतव्यय आहे.

२. राज्यातील मुलींसाठी दि.१ एप्रिल २०१६ पासून 'माझी कन्या भाग्यश्री योजना राबविण्यात येणार असून त्यासाठी २५ कोटी रूपये इतका नियतव्यय आहे.

३. आदर्श अंगणवाडी कार्यक्रमांतर्गत १० हजार अंगणवाडया आदर्श करण्यासाठी १०० कोटी रुपये नियतव्यय आहे.

४. महिलांसाठी स्वतंत्र 'तेजस्विनी बस'

५. राज्य महामार्गावर महिलांसाठी स्वच्छतागृहे.

६. अंगणवाडी सेविका व मदतनिसांना विमा संरक्षण.
७. महिला बचत गटांना शून्य टक्के व्याजाने कर्ज
८. 'माझी कन्या भाग्यश्री योजना'
९. ब्रेस्ट कॅन्सरच्या पडताळणीसाठी वापरण्यात येत असलेल्या मॅमोग्राफी यंत्र करमाफ.
१०. कै. बाळासाहेब ठाकरे स्मृती मातोश्री ग्रामपंचायत व महिला सक्षमीकरण अभियान.

सारांश

महिला सक्षमीकरणाकरिता वरीलप्रमाणे विविध प्रकारच्या तरतुदी अणि योजना महिलांच्या आर्थिक आणि सामाजिक सुरक्षिततेकरिता तयार करण्यात आल्या. वास्तविक परिस्थिती अशी आहे की, या योजना ज्या महिलांसाठी तयार करण्यात आल्या, त्या महिलांपर्यंत पोचतच नाही प्रत्येक अर्थसंकल्पात मुलींच्या वसतिगृहाच्या तरतुदी आहेत. पण अजुनही काही शासकीय वसतीगृह आहे त्या परिस्थितीच आहे. अंगणवाडीच्या सेविका व मदतनीसांठी योजना आहेत. 'माझी कन्या भाग्यश्री' योजना मुलींसाठी आहेत. या योजना महिला आणि मुलींपर्यंत पोहचल्या पाहिजे तसेच महिलांना त्यांच्या हक्काची आणि अधिकाराची अजूनपर्यंत पूर्णपणे जाणीव झालेली नसल्याचे दिसून येते. अनेक अहवालावरून महिला हया आर्थिकदृष्ट्या सक्षम झाल्या असल्यातरी मानसीकदृष्टया त्या दबावात असल्याचे दिसून येते. जोपर्यंत महिला स्वत:हून मानसीक गुलामगिरीतून मुक्त होणार नाही, स्वत:वर निर्भर राहणार नाही, तोपर्यंत सरकारने कितीही योजना आखल्या तरी सर्वार्थिने महिलांचे सक्षमीकरण होणार नाही. महिलांना स्वत:चे सहकार्य आणि निर्धार अत्यंत महत्त्वाचे आहे.

निष्कर्ष

१. जास्तीत जास्त महिला व मुलींनी शिक्षण घेतले पाहिजे.
२. महिलांना अर्थसंकल्पातील तरतुदींची माहिती असली पाहिजे.
३. ज्या महिलासांठी या योजना तयार करण्यात येतात त्या त्यांच्या पर्यंत पोहचल्या पाहिजे व त्याचा फायदा त्यांना झाला पाहिजे.
४. समाजात महिलांना त्यांच्या हक्काची व अधिकाराची जाणीव करून देण्याची गरज आहे.
५. महिलांनी मानसिक गुलामगिरीतून मुक्त होवून आत्मनिर्भर व्हायला पाहिजे.

संदर्भ

1. www.maharastra gov.in/budget-2013-14
2. www.maharashtra gov.in/Budget-2014-15
3. www.maharashtra gov.in/Budget-2015-16
4. www.maharashtra gov.in/Budget-2016-17

❖❖❖

जंगलांचा विनाश आणि हवामानबदल : एक अभ्यास

प्रा. एन. व्ही. नरुले
(भूगोल विभाग प्रमुख)
इंदिरा महाविद्यालय, कळंब, जि. यवतमाळ

प्रस्तावना

भारतात गेल्या तीन वर्षात काही राज्यात तसेच अनेक खेड्यांमध्ये अवर्षण व दुष्काळी स्थिती आहे. देशातील जवळपास २५६ जिल्ह्यांमध्ये अधिकृतरित्या दुष्काळ जाहीर करण्यात आला आहे. महाराष्ट्रात विदर्भ, मराठवाडा, उत्तर प्रदेशात बुंदेलखंड, तेंलगणा, आंध्रप्रदेश, कर्नाटक इत्यादी भागातील परिस्थिती गंभीर आहे. विहिरी, तलाव, धरणेही कोरडी पडलेली आहे. नद्या सुकलेल्या अवस्थेत आहेत. आजच्या औद्योगिक युगात वाढत्या प्रदुषणामुळे आणि पर्यावरणीय संकटामुळे हवामानात मोठ्या प्रमाणावर बदल घडून येत आहे. याचसाठी आज जंगलाचे महत्त्व जाणवू लागले आहे. जंगले ही सदैव मनुष्यासाठी वरदान ठरलेली आहे. ती निसर्गाची सर्वात महत्त्वाची देणगी आहे.

सद्य:स्थिती

भारत हा कृषीप्रधान देश असून भारताची अर्थव्यवस्था ही कृषीप्रधान आहे. अशातच भारतात काही राज्यात तसेच अनेक खेड्यामध्ये अवर्षण व दुष्काळी स्थिती आहे. विहिरी, तलाव, धरणेही कोरडी पडलेली आहे. नद्या सुकलेल्या अवस्थेत आहेत. जंगलांचा विनाश मोठ्या प्रमाणावर करण्यात आला. गेली २० ते २५ वर्षे उत्पादन खर्च भरून निघत नसल्यामुळे कर्जफेड करू न शकलेले शेतकरी आत्महत्या करीत होते; परंतु गेल्या तीन वर्षापासून नापिकीमुळे अन्न उत्पादन होतच नसल्याने आत्महत्या होत आहेत. अवर्षण, अतिवृष्टी, महापूर, अवकाळी पाऊस, बर्फवृष्टी, घटते भूजल, उष्मांच्या लाटा, वादळे यांमुळे शेती पिकेल याची शाश्वती उरली नाही असे शेतकऱ्यांना वाटत आहे. जंगले कमी झाल्यामुळे प्राणी व पक्षी बाहेर पडून अन्नासाठी शेतात शिरून पिकांची नासधूस करीत आहे, त्यामुळे नवीन समस्या गेल्या काही वर्षात वाढताना दिसून येत आहे.

झाडे व जंगलाचा विनाश, वणवे वाईट परिणाम घडवित आहेत. ही गोष्ट मोठ्या प्रमाणावर लक्षात येत असूनही याबाबतचा अभ्यास कमी पडत आहे. तपमान वाढ आणि त्यास कारणीभूत ठरणाऱ्या कार्बनडॉयआक्साईड व यासारख्या वायूंच्या उत्सर्जनात होणारी वाढ यामुळे भयंकर परिणाम घडवून आणतील यांसाठी काही सृजन नागरिक आणि संस्था, संघटना वृक्षारोपणाचे कार्यक्रम पार पाडीत आहे. ही चांगली गोष्ट असली तरी समस्या मोठ्या असल्याने त्या कमी पडत आहे. मुळातच पृथ्वीवर माणसांनी झाडे लावली नव्हती तरी भारतात ५० ते ६० वर्षापूर्वी घनदाट जंगले अस्तित्वात होती. डोंगर व त्यावरील जंगलाचे आवरण भरपूर होते. नद्या हवा दुथडी भरून वाहत होत्या. वंदे मातरम गीतात "सुजलाम सुफलाम मलयज शीतलाम, सस्य शामलाम" अशा प्रकारे भारताचे वर्णन सांगितले आहे. ही स्थिती झपाट्याने बदलत आहे.

निसर्गातील काही क्षमतांना आपण जसे मधमाशा, भुंगे, पक्षी, फुलपाखरे इत्यादींना नामशेष करीत आहोत. ज्या ठिकाणी जंगले वाढावीत तेथील मातीचे आवरण व त्याखालील डोंगर आपण दिवसेंदिवस नष्ट करीत आहोत. आज कोणत्याही महामार्गाचे बांधकाम करण्यापूर्वीचे व त्या परिसराच्या विशाल भूभागाचे चित्र आणि बांधणीनंतरचे चित्र अवलोकन केले तर असे दिसून येते की रस्त्याच्या बांधणीनंतर काही काळात जवळपासचे जंगल नष्ट झालेले व डोंगर बोडखे झालेले दिसतात. औद्योगिकरणामुळे जंगले व समुद्रातील हरितद्रव्ये नष्ट होत आहे. वाढत्या लोकसंख्येच्या खाद्यान्नांसाठी जास्तीत जास्त जंगलाखालील जमीन नष्ट करण्यात आली.

भारतात १९४७ सालात स्वातंत्र्य प्राप्ती पर्यंत सुमारे ५० टक्के जमिनीवर घनदाट जंगले होती . आता केवळ सुमारे ५ टक्के क्षेत्रावर जंगल उरले आहे. वातावरणात, हवामानात होणारा बदल किंवा त्यामुळे भूपृष्ठावरील होणारी तापमान वाढ हे विनाशाशी संबधित आहे. भारताने जगाला चिरंजीव संस्कृतीचा मार्ग दहा हजार वर्षापूर्वी कृषीयुगाद्वारे दाखविला होता. हा मार्ग साधेपणा व संयमाचा होता. बाराशे वर्षाअगोदर आदी शंकराचार्य यानी "कपिल व कणादाच्या तंत्रबळाचा मार्ग योग्य नाही. तंत्रबळापेक्षा आत्मबल श्रेष्ठ आहे." असे म्हटले आहे.

महात्मा गांधी आपल्या हिंद स्वराज्य या ग्रंथात म्हणतात ''भारतीयांना यंत्र शोधता येत नव्हते असे नाही. त्यानी समजून उमजून शहाणपणाने ते टाळले.'' ते पुढे असेही म्हणतात, ''यंत्रामुळे युरोप उजाड झाला, हिंदुस्थानचेही तेच होईल, जर आपण यंत्र स्वीकारू.'' गांधीजींच्या मते भारतातील प्रत्येक शेत ही प्रयोगशाळा होती व प्रत्येक शेतकरी शास्त्रज्ञ होते.

ब्रिटीशांनी त्यांचे रासायनिक शेती तज्ञ डॉ. आल्बर्ट हॉवर्ड यांना सन १८९५ साली भारतीयांना शेती शिकविण्यासाठी भारतात पाठविले होते. त्यांनी पाच वर्ष भारतात फिरून भारतीय शेतीचा अभ्यास केला. त्यांनी त्यांच्या ''ॲन ॲग्रिकल्चर टेस्टामेंन्ट'' या ग्रंथात म्हटले आहे की ''एकाच खाचरात जमिनीचा कस जाऊ न देता शेती करणारे भारतीय शेतकरी माझे गुरू आहेत, त्यांच्याकडून मी शिकलो की, निसर्ग हा खरा शेतकरी आहे.'' ते असेही म्हणतात की ''रसायन हे पिकांचे अन्न नाही ते विष आहे.

वाढत्या औद्योगिकरणांमुळे जंगलाचा ऱ्हास होत आहे. जंगलात हजारो वर्षापासून राहणाऱ्या आदिवासींना जंगल सुरक्षित ठेवण्याच्या नावाखाली जंगलाबाहेर काढले जाते. 'अभयारण्य' असा दिशाभूल करणारा शब्दप्रयोग करण्यात येतो. शेतकऱ्यांनी हजारो वर्ष जंगलातील काडीकचरा, काटक्या जाळून चूली पेटविल्या, त्यांना दोष दिला जातो, की त्यांच्यामुळे वातावरण बदल होत आहे. आदिवासी काड्या तोडतात म्हणून शहरातील माणसे अस्वस्थ होतात; परंतु औद्योगिकरणासाठी व शहरीकरणासाठी अवैध वृक्ष व झाडे तोडली जातात, तेव्हा तो प्रतिष्ठेचा म्हणजेच कायदेशीर प्रश्न होऊन जातो.

डॉ. आल्बर्ट हॉवर्ड यांनी त्यांच्या १९३९ साली लिहिलेल्या ग्रंथात म्हटले की ''यंत्राची भूक पृथ्वी भागवू शकणार नाही.'' आता परिस्थिती बदलत चालली आहे, आपण यंत्राचे पूर्णपणे गुलाम झालेलो आहोत. यंत्रे ही कामे करण्यासाठी आहेत. पोकलेन हे यंत्र डोंगर तोडण्यासाठी, भूभाग सपाट करण्यासाठी, नद्यांची पात्रे रुंद व खोल करण्यासाठी वापरले जातात. ही यंत्रे चालू ठेवण्यासाठी डोंगर तोडले जातात. दरवर्षी भारतात उत्पादित होणारी एक लाख पोकलेन यंत्रे कोणते अपरिवर्तनीय विनाश घडवतील याची कल्पना करता येत नाही.

अलिकडेच युनेस्कोने पश्चिम घाटातील ३९ ठिकाणांना पर्यावरणदृष्ट्या संवेदनशील म्हणून संरक्षण दिल्याचे जाहीर केले आहे. म्हणजेच पश्चिम घाटातील संरक्षित भागात होणाऱ्या खाणी, नद्यांना अडविणारी धरणे, वीज निर्मिती केंद्रे, सोबतच इतर उद्योग यामुळे हा भाग आता उद्ध्वस्त होईल. हीच गोष्ट हिमालयात व ईशान्य भारतातील सदाहरित जंगलाबाबत घडत आहे.

जंगलांचा विनाश आणि हवामानबदल

१) पर्जन्यामध्ये घट :– वृक्षतोडीमुळे हवेचे तापमान वाढून हवेची आर्द्रता कमी होते आणि पर्जन्याच्या प्रमाणात लक्षणीय घट होते.

२) जागतिक तापमान वाढ :– निर्वनीकरणामुळे कार्बन डायऑक्साइड आणि हवेतील प्रदूषकांचे प्रमाण वाढून जागतिक तापमान वाढ होते. भारतात याचे दुष्परिणाम जाणवू लागले आहे.

३) अवर्षणाची वारंवारता आणि व्याप्ती :– वृक्षतोडीमुळे पावसाची कमतरता होऊन अवर्षणाची स्थिती निर्माण होते. मध्य महाराष्ट्रमध्ये अवर्षणाची वारंवारता वाढत आहे.

४) महापुराची शक्यता :– वनाच्छादन नष्ट झाल्यामुळे मुसळधार पावसाचे थेंब जोरात जमिनीवर येतात जमिनीत पाणी मुरत नाही, प्रसंगी पुराची स्थिती निर्माण होते.

५) वाळवंटीकरणाचा विस्तार :– वृक्षतोडीमुळे प्रदेश उजाड बनू लागतात, जोराच्या वाऱ्यामुळे खडकांचे बारीक कण वाहून नेऊन वालुकामय वाळवंटे निर्माण होतात. कमी पाऊस पडणाऱ्या प्रदेशात वाळवंटीकरणाची शक्यता असते.

६) भूमिगत पाण्याची पातळी खालावणे :– वृक्षतोड झाल्याने पावसाचे पाणी जमिनीत मुरण्यास पुरेसा अवधी मिळत नाही . पाणी वेगाने पुढे जाते. त्यामुळे भूमिगत पाण्याची पातळी खालावत जाते.

एकूणच औद्योगिकरण, शहरीकरण, हे एकाचवेळी कार्बनडॉयआक्साईड, इतर वातावरण बदल व तापमान वाढ घडविणाऱ्या वायुंची निर्मिती करते आणि जंगलाना नष्ट करते.

संदर्भ

१) पर्यावरणीय भूगोल – डॉ. यू. बी. सिंह
२) भारताचा समग्र भूगोल – ए. बी. सवदी व पी. एस. कोळेकर
३) योजना विशेषांक

❖❖❖

22 Vidyarthyanchi Sarvangin Surakhshata Palak va Shikshkachi Jababdari

विद्यार्थ्यांची सर्वांगीण सुरक्षितता पालक व शिक्षकाची जबाबदारी

प्रा. सरोज यादवराव लखदिवे
गृहअर्थशास्त्र विभाग प्रमुख
इंदिरा महाविद्यालय, कळंब, जि. यवतमाळ

सारांश

सध्या बालकांवर होणाऱ्या लैंगिक अत्याचाराबाबत सातत्याने प्रकरणे घडत आहे. शाळा आणि शाळाबाह्य अशा स्वरूपाची प्रकरणे समोर येत असल्याने बालकांचे लैंगिक शोषण होऊ नये, यास प्रतिबंध लागावा यासाठी प्रयत्न करणे गरजेचे आहे. पालकांमध्ये जागरूकता यासोबतच बालकांसाठी असलेले कायदे आणि त्यांना न्याय मिळवून देण्यासाठी पोलीस आणि कायद्याचे सहकार्य मिळावयास पाहिजे तसेच शाळेतपण त्यांना सुरक्षा मिळणे आवश्यक आहे. अत्याचार हा शाळेतच घडते असे नाही तर अत्याचाराच्या प्रकरणात जवळील व्यक्तींचे प्रमाण अधिक राहते, त्यामुळे बालक कुठे सुरक्षित आहे हेच कळत नाही. त्यामुळे बालकांवर होणारे अत्याचार आणि त्याबाबत असलेले कायदे, त्यांना लागणारी मदत याची माहिती समाजातील प्रत्येक घटकाला असणे आवश्यक आहे.

प्रस्तावना

मुलांना सुरक्षित वातावरण देण्याची जबाबदारी ही प्रत्येकाची आहे. मात्र प्रत्येकजण आपली जबाबदारी दुसऱ्यावर ढकलत आहे. हा प्रकार बंद होणे आवश्यक असून प्रत्येकाला आपल्या जबाबदारीची जाणीव असणे आणि त्याप्रमाणे वागणे गरजेचे आहे. अनेक कारणामुळे आज विद्यार्थी असुरक्षित झाले आहे. मुलांच्या कोवळ्या वयात त्यांच्यावर होणारे अत्याचार या समस्येने गंभीर रूप घेतले आहे. मुलांच्या सर्वांगिण विकासासाठी पालक, मुलांमध्ये जसा संवाद आवश्यक आहे तसाच शिक्षक व विद्यार्थी आणि शिक्षके व पालकांमध्ये देखिल संवादा झाला पाहिजे. पालक, शिक्षक व मुलांमध्ये खुला संवाद होणे आवश्यक आहे. मुलांना शरीराचे प्रायव्हेट पार्ट, त्यांच्यावर होणारे अत्याचार, तशा व्यक्तींचे हावभाव, त्यांची हालचाल अशा गोष्टींचे ज्ञान असणे आवश्यक आहे. घरातून मुल बाहेबर पडल्यापासून घरी परत येईपर्यंत प्रत्येक ठिकाणी मुलांची सुरक्षितता महत्वाची आहे. पालकांनी प्रत्यशेक टप्प्यांवर सतर्क असणे महत्वाचे आहे. शिक्षक आणि पालक हे मुलांचे खरे समुपदेशक आहे. परंतु प्रत्येकजण आपापली जबाबदारी एकमेकांवर ढकलतात. मुलांची जबाबदारी फक्त एका घटकावर टाकुन चालणार नाही तर सर्व समाजाने ती जबाबदारी सांभाळायला पाहिजे. शिक्षक, पालक व विद्यार्थ्यांमधील विसंवादामुळे ही असुरक्षितता निर्माण होत आहे.

बालकांचे पालकासोबत संबंध

बदलत्या काळानुसार पालक आणि मुलांचे संबंधही बदलत जातात. वडिलांनी हाक मारल्यावर थरथरणाऱ्या मुलामुलींचा काळ केव्हाच मागे पडला आहे. पूर्वी कुठल्याही गोष्टींची चर्चा मुलांसमोर केली जात नसे. वडील माणसे सांगतील ते ऐकायचे असेच होते. त्यामुळे मुलांनी आपले ऐकावे असे वाटणे साहजिकच होते. मुलांनी आपल्या वस्तू नेहमीच्या जागी ठेवाव्या, मैदानी खेळ खेळावे, टीव्ही, कॉम्प्युटर कमी वापरावा असे पालकांना वाटते परंतु यातले काहीच होत नाही. या गोष्टींशिवाय मुलांचे पानही हालत नाही. या गोष्टींच्या आहारी मुलांनी जाऊ नये असे पालकांना वाटते. पालक उपदेश करतात हेच मुलांना आवडत नाही. सतत ओरडणे, मुलांना रागावणे या गोष्टींशिवाय केव्हा तरी मुलांचे सर्वांसमोर कौतुक करायला हवे, त्यांच्याशी मायेने बोलायला हवे.

आपण कितीही वेळा सांगितले तरी पण मुले आपल्या मनाप्रमाणेच करतात अशा वेळी त्रागा न करता मुलांशी संवाद साधण्याचा प्रयत्न केला पाहिजे. मुलांसोबत जास्तीत जास्त वेळ घालविला पाहिजे. पालकांसोबतच राहून मुले अनेक गोष्टी शिकत असतात व मग आपणे म्हणणे हळूहळू ऐकायला लागतात. सुसवांद हा

महत्त्वाचा असतो. पालक, बालक संबंधांमध्ये प्रेम, जिव्हाळा मिळत असेल तर मुले समायोजित व समाजमान्य असे वर्तन करू लागतात. आनंदी वातावरणामुळे मुलांमध्ये आत्मविश्वास निर्माण होतो. उलट जे पालक मुलांना रागावतात, मुलांना कडक शिक्षा करतात अशा मुलांचा समाजविरोधी कृत्यांकडे असतो.

पालक बालक संबंध मैत्रीपूर्ण असल्याची गरज सध्याच्या वातावरणात आवश्यक आहे. बाहेर मुलामुलींसोबत काय घडत आहे हे पालकांना माहीत असणे आवश्यक आहे. मुलांनापण एवढा विश्वास आईवडिलांवर असणे आवश्यक आहे, की आईवडील माझ्यावर विश्वास ठेवतात व प्रत्येक गोष्टीत मार्गदर्शन करतात. मुलांमध्ये काही बदल जाणवत असल्यास पालकांनी लगेच त्याबद्दल चौकशी करायला पाहिजे. आपल्या घरात कोण येते, त्यांची मुलांसोबत वागणूक कशी आहे या गोष्टींची काळजी घ्यायला पाहिजे. शिवाय पालकांनी मुलांनी मानसिकता समजून घेणे आवश्यक आहे. मुलांशी प्रेमपूर्वक वागणूक अर्थपूर्ण व विश्वासपूर्ण संवाद साधल्यास तितक्याच विश्वासाने बालक आपल्या समस्या आवडीनिवडी, इच्छा पालकांना सहज सांगतात म्हणून त्यांचे मित्र बनून नेहमी मदतीचा हात द्यावा आवश्यक तिथे धोक्याचे सूचना सांगाव्या. मुलांशी संवाद सकारात्मक दृष्टीने साधावा.

बालकांचे शिक्षकासोबत संबंध

मूल घरच्यापेक्षा जास्त वेळ शाळेत शिक्षकाचा सान्निध्यात असतात. त्यामुळे शिक्षक व विद्यार्थ्यांचे सबंध चांगले असणे आवश्यक आहे. मुलांना शिक्षकाप्रती आदर असावा. धाक किंवा भीती असू नये. विद्यार्थ्यासोबत शिक्षकाचे मैत्रीचे नाते असते तेव्हाच मूल त्यांच्यासोबत चुकीचे वर्तन घडल्यास शिक्षकांना सांगू शकेल. मुलांचे आयुष्य पालटून टाकण्याचे कसब शिक्षकांकडे असते. मुलांना बोलके करण्याचे काम शिक्षक करत असतात. शिक्षण घेत असताना काही मुले जी संवाद साधण्यात कमजोर पडतात, आपले म्हणणे त्यांना मांडावयाचे असते; परंतु घाबरल्यामुळे ती आपले म्हणणे व्यक्त करू शकत नाही अशा मुलांना धीर देणे गरजेचे असते, त्याला कुठल्यातरी त्याच्या आवडीच्या विषयांवर बोलायला लावलं पाहिजे. शिक्षकाने विद्यार्थ्याला 'तुला हे करताच येत नाही' असे न म्हणता 'तू ते व्यवस्थित करू शकतोस' अशाच शब्दांनी त्याचा आत्मविश्वास वाढविणे महत्त्वाचे असते. मुलींच्या शाळेत स्त्री शिक्षकांची नेमणूक करणे आवश्यक आहे. त्यांनी विद्यार्थिनींना शारीरिक वाढीसंबंधी पूर्णत: जाणीव करून द्यावी. शिक्षक व विद्यार्थी यांच्यात मैत्रीचे नाते असणे आवश्यक आहे. विद्यार्थी मुक्तपणे आपल्या मनातील गोष्टी उघड करतील.

विद्यार्थ्यांच्या सर्वांगीण विकासासाठी उपाययोजना

जिह्यात बालकांवर होणारे लैंगिक अत्याचाराबाबत सातत्याने प्रकरणे घडत आहे. शाळा आणि शाळाबाहेरही अशा प्रकारची प्रकरणे समोर येत आहे. अशा प्रकारची कृत्ये घडू नये यासाठी शाळांमधून बालकांसाठी असलेल्या हेल्प लाईनची माहिती, तक्रारकर्त्यांचे नाव गोपनिय ठेवण्याची व्यवस्था आदी बाबी या उपक्रमात प्रामुख्याने घ्याव्यात. शाळा हा केंदबिंदू असल्याने शाळांच्या व्यवथापनाला विश्वासात घेऊन ही जाणीव जागरूकता राबवावी. बालके ही प्रामुख्याने शाळेत जात असल्यामुळे त्याठिकाणी त्यांना सुरक्षा मिळणे गरजेचे आहे. बालकावर अत्याचार होणार नाही यासाठी बालक, पालक आणि शिक्षकांमध्ये आपसी सामंजस्य असणे आवश्यक आहे. शाळेला पालकांनी भेटी द्याव्यात, विद्यार्थ्यांशी हितगुज करून त्यांच्या अडचणी जाणून घ्याव्यात. समाजानेही अशा घटना दिसत असल्यास एक जबाबदार घटक म्हणून पुढे यावे. बालकांच्या वर्तनात काही फरक आढळल्यास बारकाईने चौकशी करावी. बालकांना त्यांच्या शरिराला होत असलेल्या स्पर्शाबाबत माहिती द्यावी, असे वर्तन होत असल्यास पालकांना माहिती देण्यास सांगावे. शाळेत बालकांसाठी असलेल्या इल्पलाईनचे बोर्ड लावावे जेणेकरून ते त्याच्यासमोर कायम राहिल्यास अशा प्रकारचे वर्तन झाल्यास त्याबाबत ते तक्रार करू शकतील. अशी तक्रार करण्यासाठी बालकांना त्याच्या पालकांसोबतच शिक्षकांची भूमिका महत्त्वाची असते. बालकांसाठी असलेल्या कायद्याची त्यांना माहिती द्यावी.

निष्कर्ष

जिल्ह्यामध्ये सातत्याने बालकांवर लैंगिक अत्याचाराची प्रकरणे समोर येत आहे. मुलांच्या कोवळ्या मनावर झालेला आघात कधीही भरून निघू शकत नाही. मुलांचे मानसिक आरोग्य बिघडल्यास त्यांचे संपूर्ण

23 Samajik shastra Sanshodhanat Shaikshnik granthalaychi Bhumika

सामाजिक शास्त्र संशोधनात शैक्षणिक ग्रंथालयाची भूमिका

डॉ. जी.पी. उरकुंदे
ग्रंथपाल
इंदिरा महाविद्यालय, कळंब, जि. यवतमाळ

प्रस्तावना

सामाजिक संशोधन ही बौद्धिक प्रकिया आहे. संशोधनामुळे उपलब्ध असलेल्या ज्ञानाचा शोध घेऊन ज्ञानामध्ये भर टाकली जाते. उपलब्ध असलेल्या ज्ञानाचे पुन:परीक्षण केले जाते. आणि साहित्याची समीक्षा करून ज्ञानात भर टाकली जाते. संशोधन ही सतत चालणारी प्रकिया आहे. संशोधनाच्या संदर्भात Systematized effort to gain New Knowledge असे म्हटले जाते.

☐ शिक्षणाचा प्रसार आणि संशोधनामुळेच समाज, राष्ट्र आणि मानवाचा विकास होण्यास मदत होते. सुसंस्कृत समाज निर्मितीसाठी शिक्षण आणि संशोधन या गोष्टी दोन्ही आवश्यक आहेत.

☐ शिक्षण आणि संशोधनाचे कार्य सफल होण्यासाठी वाचनीय साहित्य उपलब्ध होणे गरजेचे आहे. या गरजेतूनच ग्रंथालय आणि संशोधनाची निर्मिती झाली आहे. गरज ही शोधाची जननी होय. असे म्हटल्यास वावगे ठरणार नाही. ग्रंथालये ही वाचनीय साहित्य उपलब्ध करून देशाबरोबरच ज्ञानाचे ग्रंथरूपाने जतन करत असतात. संशोधकाला संशोधन कार्यात मदत करणारी यंत्रणा म्हणून ग्रंथालये ही आधुनिक स्वरूपात कार्य करीत आहेत.

माहिती व तंत्रज्ञानाच्या क्षेत्रात बदलत्या घडामोडींचे आधुनिक तंत्रज्ञान संशोधकांना पुरविण्यासाठी ग्रंथालये सज्ज आहेत. सामाजिक संशोधनाद्वारे आधुनिक परिस्थतीची व संस्थेची परिपूर्ण ओळख करून देण्यासाठी ग्रंथालये ही समाजाभिमुख झाल्याचे दिसून येत आहे.

सामाजिक शास्त्र संशोधनाची व्याख्या

सामाजिक संशोधन म्हणजे सामाजिक संशोधनाबाबत नवीन माहिती शोधण्यासाठी किवा जुन्या माहितीचे परीक्षण करण्यासाठी त्या ज्ञानातील अनुक्रम, परस्पर संबंध, कार्यकारण संबंध याविषयी स्पष्टीकरण व सामान्यीकरण प्रस्थापित करण्याची प्रक्रिया होय. – पी.व्ही.चंग

सामाजिक संशोधन ही सामाजिक जीवनाचे अध्ययन, विश्लेषण आणि संकल्पनी करण्याची एक पद्धत आहे. ज्यामुळे ज्ञानाची वृध्दी शुद्धीकरण किंवा पुनर्परीक्षण होऊ शकेल. मग ते ज्ञान एका सिद्धांतांची रचना करण्यास किंवा एका कलेस व्यवहारात करण्यास सहाय्यक ठरू शकेल. – स्लेसिंजट व स्टिफेनसन.

सामाजिक संशोधनाचे उद्देश (Objectives of Social Science Research)

सामाजिक संशोधनाचा हेतू किंवा उद्देश, मानवी समाज मानवाचे समाजजीवन, त्यावर प्रभाव टाकणोरे घटक आणि परिणाम यांच्याशी संबंधित असतो. सामाजिक संशोधनातून वेगवेगळ्या समस्यांचा अभ्यास केला जातो.

१. सामाजिक घटकांचा अभ्यास.
२. परस्पर संबंधाची उकल करणे.
३. नवनवीन ज्ञानाचा शोध घेणे.
४. जुन्या ज्ञानाची पुनर्मांडणी करणे.
५. सामाजिक जीवनकाळात नविन दृष्टिकोन अंगीकारणे.
६. सामाजिक नियंत्रण.

सामाजिक संबंध आणि प्रक्रिया, क्रिया आणि प्रतिक्रिया आणि विघटन प्रकृतीबाबत माहिती गोळा करणे, विश्लेषण करणे, प्रभावी उपाययोजना करणे आणि त्याद्वारे सामाजिक नियंत्रण प्रस्थावीत करण्यासाठी सामाजिक संशोधन उपयुक्त ठरते.

संशोधन प्रक्रिया

संशोधन हे वेगवेगळया विषयाअंतर्गत चालू असणोरे कार्य आहे. संशोधन हे शास्त्रीय पध्दतीने पूर्ण करण्यासाठी आणि संशोधनाचे निष्कर्ष हे संशोधनाच्या चौकटीतच राहण्यासाठी संशोधकाने संशोधन कार्य सरू करण्यापूर्वी संशोधन प्रक्रियेचा आराखडा तयार करणे आवश्यक आहे.

संशोधनामध्ये Design या शब्दाचा अर्थ Drawing an outline or planning or arranging details असा घेतला जातो तर Research Design चा अर्थ **Planning a strategy of conducting research** असा आहे. संशोधन आराखडयामुळे संशोधनात सुसूत्रता निर्माण होते आणि संशोधन प्रक्रियेत गती प्राप्त होते. यासाठी संशोधन प्रक्रियेला महत्व प्राप्त झाले आहे.

संशोधन प्रक्रियेतील महत्वाचे घटक

संशोधन ही अनेक टप्पे असणारी प्रक्रिया आहे. यामध्ये पुढील बाबीचा प्रामुख्याने समावेश करावा लागतो.

१. संशोधनाचा विषय
२. संशोधन संस्थेची निवड
३. संशोधनाची पार्श्वभूमी
४. संशोधनाचे उद्देश
५. संशोधनाची गृहितके
६. माहितीचे संकलन आणि विश्लेषण करणे.
७. अहवाल लिहिणे.

संशोधनात ग्रंथालयाची भूमिका

आजच्या आधुनिक युगात सामाजिक संशोधनामध्ये संशोधन करीत असताना नवनवीन तंत्रज्ञानाचा वापर अत्यंत गरजेचा झाला आहे. कठीण प्रश्नाची सोडवणूक करण्यासाठी आधुनिक तंत्रज्ञानाचा उपयोग संशोधकांनी करणे आवश्यक आहे. संगणकाचा वापर करून बऱ्याच माहिती व आकडेवारीचे वर्गीकरण, सारणीकरण करून विश्लेषण करावे लागते.

आजच्या आधुनिकतेच्या युगात ग्रंथालये व माहिती केंद्रे ही वाचनीय साहित्य विकसित करीत असतात. ग्रंथालये ही वाचन साहित्याच्या रूपाने संशोधकाना तसेच उपभोक्त्यांना गरजांची पूर्ती होईल अशी माहिती पुरवित असतात. ग्रंथालये ही संशोधकांना गुणवत्तापूर्ण वाचनीय साहित्याचा पुरवठा करत असतात. ग्रंथालयातील सेवा अधिक परिणामकारकपणे होण्यासाठी विविध स्तरावरील शैक्षणिक ग्रंथालये, उदा. महाविद्यालयीन ग्रंथालये, विद्यापीठ स्तरावरील ग्रंथालये, विशेष ग्रंथालये परिपूर्ण माहितीने सज्ज झालेली आहेत. ग्रंथालयात येणारा वाचक, संशोधक हा ग्रंथालयातून हवी असलेली माहिती मिळावी या अपेक्षेने येत असतो. यासाठी आधुनिक काळातील ग्रंथालयीन माहितीची साठवणूक करून संशोधकांना माहिती पुरविण्यासाठी सज्ज असली पाहिजेत. संशोधन हे कोणत्याही प्रकारचे असो त्या संशोधकांना उपयुक्त असलेली माहिती देणे हे ग्रंथालयाचे आद्यकर्तव्य आहे.

संशोधनामध्ये ग्रंथालयाची भूमिका ही महत्त्वपूर्ण आहे. संशोधक हा माहिती शोधण्यासाठी ग्रंथालयावरच अवलंबून असतो, त्यासाठी ग्रंथालयानी वाचनीय साहित्याचे वर्गीकरण करून वाचकांना/संशोधकांना माहिती उपलब्ध करून दिली जातात.

सामाजिक शास्त्र संशोधनात उपभोक्त्यांना परिणामकारकपणे सेवा देण्यासाठी ग्रंथालयात ई–बुक्स ही जर्नल, विश्वकोष, संदर्भ ग्रंथ इत्यादी माध्यमाचा समावेश असणे गरजेचे आहे. ग्रंथालयात कोणकोणत्या स्वरूपाची नियतकालीके आहेत, वर्तमानपत्रे आहेत, कॉन्फरन्स प्रोसिडींग आहेत याची संशोधकांना जाणीव करून देणे गरजेचे आहे. ग्रंथालयाने ग्रंथालयात असणारी सामाजिक शास्त्राविषयीची साधने संशोधकांना उपलब्ध करून देणे गरजेचे आहे. पुढील बाबीसाठी ग्रंथालयात संशोधन करण्यासाठी आवश्यकता आहे.

१. माहितीची साधने विकसित करण्यासाठी.
२. संशोधकांना /उपभोक्त्याला परिपूर्ण माहिती मिळवून देण्यासाठी.
३. सिद्धंत तत्त्वे विकसित करण्यासाठी.

४. येणाऱ्या बदलास सामोरे जाण्यासाठी.

५. संशोधकात/उपभोक्त्यास असणारे नेतृत्व गुण विकसित करण्यासाठी.

निष्कर्ष

सामाजिक संशोधन हे सामाजिक विकासाचे प्रेरणास्थान आहे. अज्ञान दूर करण्यासाठी, सामाजिक प्रगतीसाठी, सामाजिक कल्याणाकरीता, सामाजिक नियोजन व नियंत्रण प्रस्थापित करण्यासाठी सामाजिक संशोधन अतिशय महत्त्वाचे आहे. सध्याच्या युगात शैक्षणिक ग्रंथालये संशोधकांना विविध स्वरूपाची माहिती पटवून संशोधनाच्या कार्यात सतत मदत करीत आहेत. सामाजिक संशोधनात माहिती पुरवित असताना विविध माध्यमाचा वापर करून संशोधकांना, समाजात माहिती सेवा देण्याचे कार्य ग्रंथपालास करावे लागते. ग्रंथालयामध्ये माहिती साक्षरता सारखे अभियान राबवून वाचकांना, संशोधकाला माहिती पुरविण्याचे कार्य ग्रंथालये करीत आहेत. त्यामुळेचे सामाजिक शास्त्रासारख्या विस्तृत विषयात ग्रंथालयाची भूमिका फार महत्त्वपूर्ण आहे.

संदर्भ सूची

1. Information competency standards for Higher education : Association of collage and Research Librarian 2000 Chicago

२. बोधनकर, सुधीर आणि अलोणी विवेक, सामाजिक संशोधन पद्धती, साईनाथ प्रकाशन, नागपूर,–१३

३. कायंदे पाटील गंगाधर, संशोधन पध्दती, चैतन्य पब्लिकेशन, नाशिक–१३

४. कुमार राजेंद्र, ग्रंथालय आणि माहितीशास्त्र संशोधन, युनिव्हर्सल प्रकाशन, पुणे–२०१३.

❖❖❖

स्त्रीजाणिवेचा हुंकार : कमल देसाई आणि विजया राजाध्यक्ष

प्रा.डॉ.सौ. वीरा मांडवकर
एम.ए. मराठी, इतिहास, बी.एड., पीएच.डी., सेट
सहा. प्राध्यापक, मराठी विभाग
इंदिरा महाविद्यालय, कळंब, जि. यवतमाळ ४४५४०१
Û³ ¿'æ¿³¿²³ ¿³½¿³µ¿ß §¿ ±±ð±³ भ्रमणध्वनी ९४०३०१४८८५

प्रस्तावना

कथा, गोष्ट हा प्रकार लहानांपासून मोठ्यांपर्यंत सर्वांनाच भावणारा आहे. लहानपणी तर गोष्टींनी विशेष वेड लावलेले असते. अशा वेळी लहान मुलांना वळण लावताना आईने या छोट्या छोट्या गोष्टींचाच आधार घेतलेला असतो. त्यातून संस्काराचे बीज पद्धतशीरपणे ती आपल्या मुलांच्या मनात पेरत असते. आपल्या प्रत्येकाच्या बालमनातल्या आतल्या कप्प्यात या गोष्टी आपली जागा ठेवून असतात. म्हणूनच हे मूल मोठे झाले तरी त्याच्या मनातील गोष्टींचे आकर्षण लोप पावलेले नसते. 'आई साऱ्या मानवजातीसाठी आद्य कथनकर्ता असते. या अर्थाने या सृष्टीचक्रात जेव्हा केव्हा पहिल्यांदा गोष्ट सांगितली गेली असेल, तेव्हा ती स्त्रीनंच सांगितली असेल, पुरुषानं नव्हे. म्हणजेच कल्पित सृष्टीची आद्य रचनाकर्ता एखादी आईच असेल आणि ही गोष्ट अर्थातच मौखिक परंपरेतील असेल.' [१]

बीजशब्द : स्त्री, कथा, पुरुष, मराठी, आशय, लेखन, परिस्थिती, मर्यादा, तत्त्वज्ञान

विषय विवेचन

स्त्री ही पहिली कथाकार असूनही संपूर्ण मराठी कथावाङ्मयाचा आढावा घेतला तर पुरुष कथाकारांच्या तुलनेत स्त्री कथाकारांचे लेखन मर्यादित स्वरूपाचे आहे. ही मर्यादा संख्यात्मक, गुणात्मक, विषयात्मक अभ्यासात्मक अशा सर्वच दृष्टींनी आहे. याचे कारण भारतातली स्त्री पुरुषांच्या जडणघडणीतली तफावत होय. पुरुषाचे लेखक असणे हा त्याचा विशेष गुण म्हणून गणला जातो. लेखन करताना तशी विशेष वागणूक त्याला मिळते. खोलीचे दार बंद करून तो निःशंकपणे लेखनकार्यात गढून जाऊ शकतो. स्त्रियांना मात्र घरातील सर्व जबाबदाऱ्या पार पाडून आपल्या लेखनकार्याला वेळ द्यावा लागतो. त्यामुळे बरेच सुंदर विचार घरातल्या जबाबदाऱ्यांमध्ये वाहून जातात. अशा प्रतिकूल परिस्थितीत प्रतिकूल प्रतिक्रियांना तोंड देत स्त्रियांचे लिखाण होत असते. त्यामुळे स्त्रियांच्या लेखनातील विषयांना गुणवत्तेला मर्यादा पडणे स्वाभाविक आहे.

अशा कारणांमुळे सुरुवातीला लेखन क्षेत्र म्हणजे पुरुषांची मक्तेदारी होती. 'स्त्रीच्या भोवतालचे सामाजिक, सांस्कृतिक, पर्यावरण जसजसे बदलत गेले, शिक्षणविषयक सुविधा, संधी उपलब्ध होत गेल्या. विविध वाङ्मयप्रकारांमध्ये स्त्रियांनी लिहिलेलं साहित्य स्त्रीवादी दृष्टिकोनामुळे लक्षवेधक ठरले. साहित्य क्षेत्रात बहुसंख्य स्त्रियांनी स्वतःचे अस्तित्व सिद्ध केले. आणि स्त्रीवादी साहित्याचा नवा प्रवाह निर्माण झाला. त्यातून स्त्रीच्या बदललेल्या आयुष्याचा वेध घेतला जाऊ लागला.' [२] या पार्श्वभूमीवर मराठी कथासाहित्यात अशा अनेक स्त्री कथाकार होवून गेल्या आहेत. त्यांचा उल्लेख साहित्यात पुरुषी सत्तेला आव्हान देणाऱ्या कथालेखिका असा करावा लागेल. या कथालेखिकांनी आपल्या स्त्रीसुलभ मर्यादांवर मात करून जीवनाचा व्यापक आशय आपल्या कथांमधून मांडला आहे. गुणात्मकदृष्ट्या या स्त्रियांच्या कथा अत्यंत दर्जेदार होत्या. आशय अभिव्यक्तीच्या बाबतीत त्यांची क्षितिजे विस्तारलेली दिसतात. अशाच साहित्यक्षेत्रात पुरुषी वर्चस्वाला आव्हान देणाऱ्या दोन कथालेखिका म्हणजे कमल देसाई आणि विजया राजाध्यक्ष होय.

कमल देसाई

कमल देसाई या मराठी साहित्यातल्या एक ज्येष्ठ लेखिका. अत्यंत व्यासंगी असणाऱ्या कमलताईंचे तत्त्वज्ञानावर विशेष प्रभुत्व होते. कमल देसाई या महाराष्ट्र – कर्नाटक सीमेवर बेळगाव आणि धारवाड गावाकडच्या. बालपण, शालेय शिक्षण येथेच झाले. कथा, नाटके, कविता, अनुवाद असे विविधांगी लेखन त्यांनी

केले. त्यांची कथा विशिष्ट साच्याने बनलेली नाही. त्या पूर्णत: भारतीय असल्या, भारतीय संस्कृतीशी त्यांचे जवळचे नाते असले तरीही स्वातंत्र्य, बंडखोरी, प्रयोगशीलता, आधुनिकता अशा वैशिष्ट्यांनी परिपूर्ण कथा त्या लिहितात. भारतीय स्त्रियांच्या अनुभवविश्वाच्या मर्यादा कमल देसाईंच्या बाबतीत दृष्यमान होत नाहीत, याचे कारण कुठेतरी त्यांच्या वैयक्तिक आवडीनिवडीत लपलेले असावे. त्यांना तत्त्वज्ञानात जितका रस होता तितकाच सौंदर्यशास्त्र, हास्यकला, सामाजिक शास्त्राचे चित्रपट, नाटके, या विषयाचे चौफेर ज्ञान त्यांना होते. भारतीय संस्कृती आणि पाश्चात्य परंपरा यांचा सुरेख मेळ त्यांच्या कथांमध्ये दिसतो. 'मानवी जीवनाच्या प्रातातच विणले गेलेले आध्यात्मिक आणि अधिभौतिक प्रश्न हाताळणाऱ्या फँटसी, स्वप्ने आणि जाणीव–नेणीव यांच्या खेळातून आणि स्वत:च्या प्रतिमेचा शोध घेणाऱ्या एकमेव लेखिका म्हणून कमल देसाईंचा निर्देश करावा लागेल.'[3] कमल देसाई यांचा कथेविषयीचा दृष्टिकोन स्पष्ट आहे. त्यांच्या मते, गोष्ट कुठेही घडते आणि कशीही घडते. प्रत्येक क्षण हा तुमच्या मनात एक गोष्ट घडवित असतो. अशी कथेविषयीची त्यांची संकल्पना असल्यामुळे कथाविष्कार त्यांना सहज साधा सोपा वाटतो. म्हणूनच मोठमोठं तत्त्वज्ञान आपण कथेच्या माध्यमातून रसिकांपर्यंत सहजपणे पोचवू शकातो. असा त्यांना विश्वास आहे. आणि त्यांच्या कथा पाहिल्या तर हा विश्वास अनाठायी नाही हेही लक्षात येते.

कमल देसाई यांच्या अनेक कथाचा आढावा घेतला तर त्यानी सखोल असे तत्त्वज्ञान आपल्या दृष्टीकोनातून मांडून वाचकाला नवी दिशा दिली आहे. उदा 'मोडका बाजार', या कथेत जो त्यांनी सजीव निर्जीवातला भेद नष्ट करून त्यांच्यात अंतरक्रिया घडवून आणली आहे. त्यातून सृष्टीबददलचं सम्यक ज्ञान त्या हळुवारपणे उलगडतात. 'रंगत्रयी' कथेत कलाकाराचा कलाविष्कार आणि त्यांचा स्वशोध ही प्रक्रिया पाहावयास मिळते. मानवी अस्तित्व, जाणीव–नेणिवेतले हिंदोळे, स्वप्न, फँटसी हे सगळे विशेष त्यांच्या 'तिळाबंद' या कथेत दिसतात. 'महादेववाडी' कथेतील प्रयोगशीलता म्हणजे मुख्य कथनकर्त्याऐवजी अन्य पात्रांकरवी विविध पातळ्यांवर कथा फुलविणे. 'प्लास्टीकचे विश्व' या कथेतून त्याचा मिथकांबद्दलची आस्था पहावयास मिळते. मिथकीय व्यक्तिरेखा त्यातील कथासूत्रे यांच्याशी एकात्म स्वरूपाचा सहबंध प्रस्थापित करून त्यांना विस्तारित अवकाश प्राप्त करून देण्याचा प्रयत्न कमल देसाई या कथेतून करतात. कमल देसाई यांची 'श्रादध' ही कथा कुटुंबकथेचा चेहरा घेऊन अवतरलेली असली तरीही माणसाच्या आयुष्यातील अनेक विरोधात्म पैलू दर्शविणारी आहे. 'आठ वर्ष', 'आत्मा विकणे आहे', 'माणसाची गोष्ट', 'हॅट घालणारी बाई', 'भेट' अशा अनेक कथांनी इतके विविध विषय आणि दृष्टिकोन कमल देसाई यांनी पुढे आणले की, त्यावरून त्यांची जीवन जाणीव किती व्यापक, प्रगल्भ होती हे लक्षात येईल.

विजया राजाध्यक्ष

पन्नास वर्षांच्या वर सातत्याने लेखन करणाऱ्या विजया राजाध्यक्ष म्हणजे कथाक्षेत्रातलं एक महत्त्वपूर्ण नाव. प्रामुख्याने स्त्रियांचे विश्व निर्माण करून कथाविश्वाला समृद्धी आणणारया विजयाताई कथालेखिका म्हणून बहुरंगी बहुढंगी आहेत. बरीच वर्षे लेखनक्षेत्रात राहिल्यामुळे त्यांच्या लिखाणातून विविध कालखंडात झालेली स्त्रीजीवनातील विविध स्थित्यंतरे अत्यंत समर्पकपणे प्रगटतात. वेगवेगळ्या वयाच्या निरनिराळ्या भूमिकांमधून वावरणाऱ्या, सामाजिक, सांस्कृतिक पार्श्वभूमी असलेल्या स्त्रिया रेखाटून त्यांनी स्त्रियांची प्रत्येक बाजू आपल्या लेखनात उजळ केली आहे. विजया राजाध्यक्षांनी कधी कोणत्याही एका विचारप्रणालीचा आधार घेतला नाही. त्यांची लेखणी विविध विचारतरंगातून विहरत राहिली.

स्त्रीचे मुख्य वेगळेपण म्हणजे तिची निर्मितीक्षमता यांचे कुतूहल आदिम काळापासून मानवाला आहे. अनेक संशोधनानंतरही अनेक अज्ञात रहस्ये दडलेली आहे. याच रहस्यांचे आकर्षण विजयाताईंना वाटत आले आहे. त्यांच्या कथांमधील रूपबंधातून त्यांचे हे आकर्षण बरेचदा डोकावते. मानवाच्या जन्मासोबतच मृत्यू, वृद्धत्व, एकाकीपण यांचा शोधही त्यांना सातत्याने घ्यावासा वाटतो. पन्नास वर्षांपासून मध्यमवर्गीय जीवनाचा एक सामाजिक, सांस्कृतिक लेखाजोखा विजया राजाध्यक्ष यांच्या कथांतून मांडलेला आहे.

विजया राजाध्यक्षांच्या कथांचा आढावा घेतला तरीही त्यातून त्यांच्या विषयांची विविधता लक्षात येते. स्त्रियांचेच अनुभवविश्व साकारत असतानाही त्यांची चाकोरीबाहेरची वाट चोखाळली होती. 'विदेही'सारखी कथा वाचली तरी विजयाताईंच्या लेखनाची गहनता लक्षात येते. 'विदेही ही आशयघन, लालित्यपूर्ण, व सखोल अशी कथा आहे. लेखिका सुबक, रेखीव शैलीतून प्रकृती पुरुष नात्याची अथांगता, कलात्मकता, ताटस्थ्याने चित्रीत करीत जाते. कथा वाचून संपविल्यावर प्रश्न पडतो, ही कथा कोणाची? स्त्रीची की पुरुषाची? ही कथा किंवा पुरुष

कोणाही एकाची नसून दोघांचीही आहे. आलेल्या अनुभूतीचे मुक्त चिंतन एका कलात्मक पातळीवर कथारूप धारण करते. कथेतील व्यक्तींना कोणतेही विशिष्ट लिंग ठरविता येत नाही. किंबहुना तसा शोध घेणेही गौण आहे.[४] 'कमळ' यासारख्या कथा यांतून स्त्रियांचे नावीन्यपूर्ण भावविश्व त्यांनी निर्माण केले. पूर्वसूरींपेक्षा धीट अभिवृत्ती त्यानी कथांतून साकारल्यावर पुढच्या स्त्रीसाहित्याच्या पांथस्थांसाठी एक पायवाट निर्माण केली. लैंगिक सुखाचा टप्पा ओलांडल्यानंतर ज्या रहस्याचे आकर्षण विजयाताईंना आहे, त्या मातृत्वाच्या अनुभवाला सामोरी जाणारी स्त्री मातृत्वाच्या आपल्या देहाकडे निर्मितीसाठीचे साधनरूप म्हणून बघताना सखोलतेने तिच्या मनातील विचारलहरी त्या अचूकपणे मांडतात. विजयाताईंना स्त्रीविचारांबरोबरच परंपरेचेही आकर्षण आहे. भारतीय संस्कृती, संस्कार त्यातील एकत्र कुटुंबव्यवस्था, या कुटुंबव्यवस्थेतील स्त्रीचे स्थान अशा विविध अंगांनी त्या परंपरांचा विचार करतात. म्हणुनच पारंपरिक कौटुंबिक परिघात राहूनही त्या बंधनामध्ये मानवी नात्यांचे सौंदर्य कसे उजळून निघते हे त्यांच्या 'वर्तमान' आणि 'निर्वाण कथेतून आपल्याला जाणवते. परंपरांचा मनावर खोल पगडा असल्यामुळे १९६७ साली 'सत्यकथा'मध्ये प्रकाशित झालेली 'जेहत्ते कालाचे ठायी' ही कथा पारंपरिक हरदासी आख्यानाचा फॉर्म त्या आधुनिक रूपात मांडतात. 'संधिकाल' या कथेतून 'स्त्री–पुरुषांच्या सहजीवनाचे आधुनिक रूप दाखवितानाच, त्यातील कंगोरे, चढउतार, परस्परांमधील नाते समजून घेण्याची ओढ आणि मग स्वच्छपणे जाणवलेले सत्य स्वीकारण्याची तयारी याचा मनोज्ञ आलेख मांडते.[५] 'अंधाराचा अर्थ', 'अनपढ', 'कमळ', 'नकोच', 'जानकी देसाईचे प्रश्न', 'षोडशी', 'भास', ' कडा', 'पश्चिम' अशा अनेक कथा विजयाताईंचे लेखनाचे विविध पैलू दर्शवितात.

तुलना

कमल देसाई आणि विजया राजाध्यक्ष हया दोघीही मराठी कथा साहित्य विश्वातील एक वेगळी विचारधारा घेऊन अवतरलेल्या लेखिका होत. कमलताईंच्या मते कथालेखन ही एक सहजपणे घडणारी प्रक्रिया आहे. म्हणजे कथा ही आपल्या आजूबाजूला सतत घडत असते. प्रत्येक क्षण आपल्या मनात सतत कथा घडवत असतो. तो क्षण पकडणं हे प्रत्येकाला शक्य होत नाही. पण एखादे संवेदनशील मन हे क्षण लेखणीत कैद करतात, आणि कथेचा जन्म होतो. विजयाताईंना कथा लिहिताना विविध विचारतरंग प्रवृत्त करतात. वेगवेगळ्या वयाच्या निरनिराळ्या भूमिकांमध्ये वावरणाऱ्या स्त्रिया या विजयाताईंच्या कथा लिखाणाचे मुख्य केंद्रबिंदू होय.

या कथासृष्टीत जेव्हा केव्हा पहिल्यांदा कथा सांगितली गेली असेल ती एखाद्या स्त्रीनेच सांगितली असेल असे म्हटले जाते. या अर्थाने स्त्री ही आद्य रचनाकर्ती आहे. कमल देसाईंच्या लिखाणात हा आद्य रचनाकर्तीचा सूर दिसतो. म्हणजेच ही कथा आपल्या मानव इतिहासाच्या जवळ जाणारी आहे. विजयाताईंचे लिखाण हे स्त्रीजीवनातील विविध रहस्ये उलगडण्यात गुंतलेली आहेत. धीट अभिव्यक्तीसाठी विजयाताईंनी विदेही कमळ यांसारख्या कथा लिहिल्या असल्या तरीही त्यांचे मूळ मातृत्वाचे लेखन करण्यासाठी आसुसलेले होते. लैंगिक सुख आणि मातृत्व यांचा परस्पर संबंध असला तरी स्त्रीच्या मनातील या दोन्हींविषयीचे वेगळे संदर्भ याचे विजयाताईंना आकर्षण वाटते.

कमल देसाई यांना तत्त्वज्ञानाची फार आवड होती. त्यांच्या कथांना एक सहजतेचे प्रवाहीपण असले तरी त्याला आतून अविरतपणे तत्त्वज्ञानाचा पाझर फुटलेला होता. त्यांच्या अनेक कथांमधून हा ओढा व्यक्त होतो. विजयाताईंचे लेखन तत्त्वज्ञानापेक्षा आत्मशोधकेंद्रित दिसते. हा आत्मशोध विशेषत: स्त्रीच्या आत्मभानाशी निगडित आहे. विजयाताई स्वत: स्त्री असल्याने तिच्या वेदना, मर्यादा, गरजा, सामर्थ्य, संवेदनशीलता, आत्मसन्मान याअंगाने त्यांची कथा फुलते.

कमलताई आणि विजयाताई यांच्या कथांची काही बाबतीत साम्यस्थळे दिसतात. कमलताई यांची 'तिळाबंद' ही कथा आणि जानकी देसाईचे प्रश्न ही विजया राजाध्यक्षांची कथा स्त्रीच्या 'स्व'त्वाशी निगडित अनुभव मांडणाऱ्या आहेत. कमलताई यांची 'श्राद्ध' ही कथा आणि संधिकाल ही विजया राजाध्यक्ष यांची कथा पुरुषकेंद्री धर्मव्यवस्था– समाजव्यवस्था दर्शविणाऱ्या आहेत. कमल देसाई यांची अर्थ आणि विजया राजाध्यक्ष यांची वर्तमान या कथा स्त्रीचे द्वंद्वात्मक अनुभव मांडणाऱ्या आहेत. अशी अनेक उदाहरणे या दोन्ही कथालेखिकांच्या बाबतीत देता येतील जेथे त्यांचे मूळ विचार पातळी समांतर असल्याचे जाणवते.

सिमोन द बोव्हुआर यांच्या 'द सेकंड सेक्स' या पुस्तकात निष्कर्षरूपात एक महत्त्वाचे विधान आहे. 'स्त्रीला मुक्त करणे याचा अर्थ तिला पुरुषाबरोबर एकाच नात्यात जखडून न ठेवता तिला बहुरंगी नाती प्रस्थापित करण्याचे स्वातंत्र्य देणे. स्त्रीला तिचे स्वतंत्र अस्तित्त्व मिळू द्या. तसे झाल्यास ती स्वत:साठी तर जगेलच, पण

पुरुषासाठीही जगणे बंद करणार नाही. स्त्री पुरुष दोघेही एकमेकांना क्रियाशील अस्तित्व मानू लागतील व त्याच वेळी एकमेकांसाठीही उरतील."[६] अशा प्रकारचे विचार दोन्ही कथालेखिकांच्या कथांमधून स्वबलेले आढळतात.

निष्कर्ष

१. कल्पित सृष्टीची आद्य रचनाकर्ता एखादी आईच असेल आणि ही गोष्ट अर्थातच मौखिक परंपरेतील असेल.

२. स्त्री ही पहिली कथाकार असूनही संपूर्ण मराठी कथावाङ्मयाचा आढावा घेतला तर पुरुष कथाकारांच्या तुलनेत स्त्री कथाकारांचे लेखन मर्यादित स्वरूपाचे आहे.

३. या पार्श्वभूमीवर मराठी कथासाहित्यात अशा अनेक स्त्री कथाकार होऊन गेल्या आहेत. त्यांचा उल्लेख साहित्यात पुरुषी सत्तेला आव्हान देणाऱ्या कथालेखिका असा करावा लागेल. उदा. कमल देसाई आणि विजया राजाध्यक्ष.

४. कमल देसाई यांना तत्त्वज्ञानात जितका रस होता तितकाच सौंदर्यशास्त्र, हास्यकल्प, सामाजिक शास्त्राचे चित्रपट, नाटके, या विषयाचे चौफेर ज्ञान त्यांना होते. भारतीय संस्कृती आणि पाश्चात्य परंपरा यांचा सुरेख मेळ त्यांच्या कथांमध्ये दिसतो.

५. कमल देसाई यांच्या अनेक कथांचा आढावा घेतला तर त्यांनी सखोल असे तत्त्वज्ञान आपल्या दृष्टीकोनातून मांडून वाचकाला नवी दिशा दिली आहे.

६. 'मोडका बाजार', 'रंगत्रयी', 'तिळबंद', महादेववाडी', 'प्लास्टीकचे विश्व श्रादूष', 'आठ वर्ष', 'आत्मा विकणे आहे', 'माणसाची गोष्ट' 'हॅट घालणारी बाई,' 'भेट' अशा अनेक कथांनी इतके विविध विषय आणि दृष्टिकोन कमल देसाई यांनी पुढे आणले की, त्यावरून त्यांची जीवन जाणीव किती व्यापक, प्रगल्भ होती हे लक्षात येईल.

७. पन्नास वर्षांच्या वर सातत्याने लेखन करणाऱ्या विजया राजाध्यक्ष म्हणजे कथाक्षेत्रातलं एक महत्त्वपूर्ण नाव. प्रामुख्याने स्त्रियांचे विश्व निर्माण करून कथाविश्वाला समृद्धी आणणाऱ्या विजयाताई कथालेखिका म्हणून बहुरंगी बहुढंगी आहेत.

८. भारतीय संस्कृती, संस्कार त्यातील एकत्र कुटुंबव्यवस्था, या कुटुंबव्यवस्थेतील स्त्रीचे स्थान अशा विविध अंगांनी विजयाताई परंपरांचा विचार करतात. म्हणूनच पारंपरिक कौटुंबिक परिघात राहूनही त्या बंधनामध्ये मानवी नात्यांचे सौंदर्य कसे उजळून निघते याचे त्या यथार्थ वर्णन करतात.

९. कमलताई आणि विजयाताई यांच्या कथांची काही बाबतीत साम्यस्थळे दिसतात. कमलताई व विजयाताईच्या कथांमध्ये स्त्रीच्या 'स्व'त्वाशी निगडित अनुभव मांडणारे, पुरुषकेंद्री धर्मव्यवस्था– समाजव्यवस्था दर्शविणारे स्त्रीचे द्वंद्वात्मक अनुभव मांडणारे अनेक प्रसंग दिसतात. अशी अनेक उदाहरणे या दोन्ही कथालेखिकांच्या बाबतीत देता येतील जेथे त्यांचे मूळ विचार पातळी समांतर असल्याचे जाणवते.

संदर्भ

१. आर्वीकर, संजय, 'सहा दशकांच्या समृद्धीची गोष्ट', स्त्री–लिखित मराठी कथा (१९५० ते २०१०) संपा. अरुणा ढेरे, पद्मगंधा प्रकाशन, २०१४ पुणे, प्रथमावृत्ती, पृ. बारा.

२. देवरी, प्रा. डॉ. लीलावती, 'मराठी साहित्यात महिला स्त्रीवादी दृष्टीने एक आकलन', स्त्री अभ्यासाच्या दिशा, संपा. – डॉ. सुनंदा अहिरे, प्रा.डॉ. उषा य. साळुंके, अथर्व पब्लिकेशन्स, धुळे, २०१२, पृ. ९८

३. ढेरे, अरूणा (संपा.), 'कमल देसाई', स्त्री–लिखित मराठी कथा (१९५० ते २०१०), पद्मगंधा प्रकाशन, पुणे, २०१४, पृ. ६३

४. चवरे, डॉ. रा.गो., 'नवकथेचा मध्यान्ह', मराठी कथा : प्रवृत्ती आणि प्रवाह, सुयश प्रकाशन, पुणे, २००३, पृ. १९०

५. आर्वीकर, संजय, 'सहा दशकांच्या समृद्धीची गोष्ट', उनि. पृ. २०.

६. सिमोन द बोव्हुआर, द सेकंड सेक्स, अनुवाद : करुणा गोखले, पद्मगंधा प्रकाशन, पुणे, प्रथमावृत्ती, २०१०, पृ ५५८.

संदर्भग्रंथ

१. अदवंत, म.ना., मराठीतले काही कथाकार, अनमोल प्रकाशन, पुणे, प्रथमावृत्ती, १९७०
२. धोंगडे, अश्विनी, स्त्रीवादी साहित्य व समीक्षा, महाराष्ट्र साहित्य पत्रिका, जुलै– सप्टें. अंक २५८
३. पुरोहित, के. ज. (संपा.), सुधा जोशी, 'मराठी कथा : विसावे शतक', मॅजेस्टिक प्रकाशन, मुंबई, २००४
४. फडके, डॉ. भालचंद्र, मराठी लेखिका–चिंता आणि चिंतन, श्रीविद्या प्रकाशन, पुणे, प्रथमावृत्ती, १९८०
५. वरखेडे, मंगला, स्त्रियांचे कथालेखन : नवी दृष्टी, नवी शैली, साकेत प्रकाशन, औरंगाबाद, प्रथमावृत्ती, २००५
६. शेवडे, डॉ. इंदुमती, मराठी कथा उगम आणि विकास, सोमैया, मुबई, प्र. आ., १९७३
७. साळुंखे, आ.ह., हिंदू संस्कृती आणि स्त्री, लोकवाङ्मय गृह, मुंबई, दहावी आवृत्ती, २०११

❖❖❖

25 Swatantryottar Sathpurva Vaidharbiya kadambaritil Samajik Janiva

स्वातंत्र्योत्तर साठपूर्व वैदर्भीय कादंबरीतील सामाजिक जाणिवा

डॉ. पवन मांडवकर
प्राचार्य, इंदिरा महाविद्यालय, कळंब, जि. यवतमाळ ४४५४०१
अध्यक्ष, संत गाडगे बाबा अमरावती विद्यापीठ मराठी प्राध्यापक परिषद
E mail: pavanmandavkar@hotmail.com भ्रमणध्वनी ९४२२८६७६५८

सारांश

बा.सं. गडकरी यांनी १९०९ मध्ये 'सुधारणेचा मध्यकाल' ही सामाजिक कादंबरी लिहून खऱ्या अर्थाने वैदर्भीय मराठी कादंबरीची सुरुवात केली. स्वातंत्र्योत्तर साठपूर्व कालखंडात ना.रा. शेंडे, भाऊ मांडवकर, ग.त्र्यं. मांडखोलकर, पु.भा. भावे, पु.य. देशपांडे, वरखेडकर, मुक्तिबोध, उद्धव शेळके, दिनकर देशपांडे, महाजन, भोळे, टोंगो अशा अनेक नामवंतांनी सामाजिक जाणिवांनी परिपूर्ण कादंबरीलेखन केले. ना.रा. शेंडे यांची 'काजळी रात्र', 'तांबडा दगड', भाऊ मांडवकरांची 'माझी चाळीस भावंडं', पु.भा. भावे यांची 'अकुलिना', ग.त्र्यं. मांडखोलकरांची 'अनघा', शरच्चंद्र मुक्तिबोधांची 'शिप्रा', उद्धव शेळक्यांची 'धग' आणि 'नांदते घर' अशा काही सामाजिक जाणिवांच्या कादंबऱ्यांचा उल्लेख अपरिहार्यपणे करावा लागतो. स्वातंत्र्योत्तर साठपूर्व या तपात आलेल्या वैदर्भीय कादंबऱ्यांचे विषय स्वातंत्र्य चळवळीच्या आणि घडून गेलेल्या महायुद्धाच्या पार्श्वभूमीवर होते. एकीकडे गांधीवाद, मार्क्सवाद आणि कौटुंबिक, सामाजिक जीवनावर होत गेलेले विविध प्रभाव आणि अशा अनेक समस्यांपासून दूर जाऊन रंजनवादाकडे लेखण्या वळल्या. त्यातूनच अनेक कादंबऱ्यांमध्ये कमीअधिक प्रमाणात सामाजिक जाणिवा प्रगट होत गेल्या. या सामाजिक कादंबऱ्यांच्या पुनर्अध्ययनाची गरज आज निर्माण झाली आहे.

बीजशब्द

वैदर्भीय, सामाजिक, जाणिवा, स्वातंत्र्योत्तर, साठपूर्व

प्रस्तावना

साधारण: इ.स. १९०० नंतर वैदर्भीय कादंबरीक्षेत्रात आशावादी व चैतन्यमय चित्र दिसू लागले. विदर्भाचे ह.ना. आपटे म्हणून ओळखले जाणाऱ्या बा.सं. गडकरी यांनी १९०९ मध्ये 'सुधारणेचा मध्यकाल' ही सामाजिक कादंबरी लिहून खऱ्या अर्थाने वैदर्भीय मराठी कादंबरीची सुरुवात केली. पुढे त्यांनी 'दुर्दैवी प्रेमयोग', 'पातितेचे हृदय', 'पुष्पमाला', 'विद्वान सोबती की कुशल गृहिणी' अशा अनेक कादंबऱ्या लिहिल्या. विशिष्ट सामाजिक समस्यांची मांडणी, त्यातून आदर्श मार्ग काढणे ही त्यांची पद्धत होती. विदर्भाने मराठी साहित्याला अनेक मोहरे दिले. काही खूप गाजले, काही कमी गाजले. कै.ग.त्र्यं. मांडखोलकर व कवी अनिल या दोन वैदर्भीय लेखकांना सबंध महाराष्ट्राने डोक्यावर घेतले. वीर वामनराव जोशींचे नाव घेतले तरी आज महाराष्ट्र नतमस्तक होतो. वामन मल्हार जोशींचा 'सुशीलेचा देव' व 'इंदू काळे सरला भोळे' या कादंबऱ्या आज मराठी साहित्यात दृढ स्थानावर आहेत.[1]

स्वातंत्र्योत्तर साठपूर्व कालखंडातील विविध प्रकारच्या कादंबऱ्यांमध्ये ना.रा. शेंडे, भाऊ मांडवकर, ग.त्र्यं. मांडखोलकर, पु.भा. भावे, पु.य. देशपांडे, वरखेडकर, मुक्तिबोध, उद्धव शेळके, दिनकर देशपांडे, महाजन, भोळे, टोंगो अशा अनेक नामवंतांनी कादंबरीलेखन केले आहे. यामध्ये सामाजिक जाणिवा व्यक्त करणाऱ्या कादंबऱ्यांचा भरणा अधिक आहे.

विषय विवेचन

स्वातंत्र्योत्तर साठपूर्व कालखंडातील कादंबऱ्यांनी करमणुकीवर अधिक जोर दिला असला तरी त्यातूनही सामाजिक आशयप्रधान कादंबऱ्या दुर्लक्षून चालत नाही. वि.ल. भावे, ना.रा. शेंडे आणि डॉ. भाऊ

मांडवकरांसारख्या कादंबरीकारांनी सामाजिक कादंबऱ्यांची उल्लेखनीय निर्मिती केली. समाजातील विविध समस्यांना वाचा फोडताना त्यांनी समाजाचे ज्ञात–अज्ञात कोपरे धुंडाळून वस्तुनिष्ठ संशोधन करून साहित्यनिर्मिती केल्याचे निदर्शनास येते. प्रत्येक साहित्यिकाच्या आविष्कारांचे स्वरूप भिन्न आहे. अगदी घनदाट अरण्यांमध्ये जगापासून दूर वास्तव्य करणाऱ्या आदिम जमातींपासून तर अनाथालयात वाढणाऱ्या समाजघटकांच्या प्रश्नांना वाचा फोडण्याचे काम या कादंबऱ्यांनी केले.

ना.रा. शेंडे यांनी ग्रामीण जीवनावर आधारित असलेली 'काजळी रात्र' ही कादंबरी लिहिली. या कादंबरीतील कथानकाचा कालखंड १९४२ ते १९४७ असा आहे. अस्पृश्यांवर होणाऱ्या अन्यायाचे भेसूर चित्र लेखकापुढे तरळत असावे आणि त्यातूनच या कादंबरीचा जन्म झाला. माणसांमधील विषमता नष्ट होऊन समता प्रस्थापित व्हावी, जातिभेद नष्ट व्हावा, दारिद्र्यात होरपळणाऱ्या तळागाळातील लोकांची उन्नती व्हावी अशा विचारांतून ही निर्मिती झाली. ब्राम्हण, ब्राम्हणेतर आणि दलितांनी एकत्र येऊन भावनिक एकता निर्माण व्हावी, ही इच्छा या कादंबरी लिहिण्यामागची आहे, हे जाणवते. या कादंबरीत मोहन गडकरी हे अस्पृश्य पात्र, चित्रा सरंजामे ब्राम्हणवर्गीय, सरू हे ब्राम्हणेतर पात्र आणि मिस आर्कनी ख्रिस्ती अशा विभिन्न जातीपंथाची पात्रे आणि त्याबरोबरच समाजोन्नतीसाठी कराव्या लागणाऱ्या कार्याची दिशा लेखकाने दाखवून दिली आहे. श्रीमंतांना लुटून गरिबांना मदत करणारे शेष महाराज, अस्पृश्यता नष्ट होऊन ब्राम्हण, महार एक व्हावेत अशी इच्छा बाळगणारी चित्रा सरंजामे, समाजोन्नतीसाठी झटणारे, स्वत:ची विहीर आणि देऊळ अस्पृश्यांसाठी खुले करणारे दयाळबाबा, दु:खीकष्टी लोकांचे जीवन फुलवून समतेसाठी प्राणपणाने झुंज देणारा अज्ञात इसम अशी ही पात्रे आणि प्रसंग लेखकाने चित्रित केली आहेत. तसेच चित्रा आणि मोहन यांच्या प्रेमातून लेखकाने समाजातील बदलाची दिशाही सूचित केली आहे.

अशीच सामाजिक दृष्टी ना.रा. शेंडे यांच्या 'तांबडा दगड' या कादंबरीतही आहे. ही कादंबरी आदिवासींच्या जीवनावर आधारित आहे. दलितोद्धार आणि भारताच्या प्राचीन संस्कृतीचे वारसदार असलेल्या आदिवासींचा विकास हाच विषय या कादंबरीचा आहे. ही एक वास्तवदर्शी कलाकृती आहे. त्यातून पळसवनातील दोन गावांच्या सुधारणेसाठी काही निस्वार्थी कार्यकर्त्यांनी केलेले प्रयत्न, परिणामी द्वेषबुद्धी नाहीशी होऊन समाजसुधारणेचा पाया घातला जाणे असे मनोज्ञ दर्शन या कादंबरीतून होते. शहरापासून दूर अशा अरण्यात राहणाऱ्या आदिवासींना विश्वासात घेत त्यांच्या कलेने वागून त्यांना मुख्य प्रवाहात आणताना सुधारणाभिमुख करता येते, याची प्रचिती या कथानकात येते. त्यांच्या अंधश्रद्धा, चुकीच्या चालीरीती, अज्ञान नाहीसे करून त्यांना स्वत:च्या स्थितीसंबंधी विचारप्रवृत्त करणे हे काम कादंबरीतील रायभान, धोंडबा ही पात्रे करतात. 'तांबडा दगड' हा मुळातच लालसा, दुष्ट भावना आणि आसुरी वृत्तीचा प्रतीक आहे. तांबड्या दगडाच्या ठिकऱ्या उडवून त्याच ठिकाणी आदिवासींच्या सेवेसाठी शुश्रूषागृह उघडले जाते. आदिवासी सेवा संघाची एक भव्य इमारत निर्माण होऊन दोन्ही गावांचा विकास साधला जातो. योग्य मार्गदर्शन मिळाले तर परिवर्तन घडते असा संदेश लेखक देतात.

डॉ. भाऊ मांडवकरांनी 'माझी चाळीस भावंडं' या आपल्या पहिल्याच कादंबरीतून समाजाच्या सहानुभूतीला पारखे झालेल्या उपेक्षितांचे दु:ख मांडले आहे. समाजाचा दंभस्फोट करणारी कादंबरी म्हणून ती ओळखली जाते. अनाथांच्या जीवनाला आणि त्यांच्या अनाकलनीय अंतरंगाला प्रकट करणारी ही कादंबरी. वास्तव वर्णनात रमलेली आणि अनाथालयांमधील भ्रष्ट यंत्रणा वर्णन करताना लेखकाच्या लेखणीची ताकद येथे जाणवते. 'माझी चाळीस भावंडं' ही कलाकृती अनन्यसाधारण आहे. अनुभूतीच्या भक्कम खडकावर ही वास्तवपूर्ण कथा उभी आहे. ही कादंबरी लिहिण्यापूर्वी लेखकाने अनेक आश्रम फार जवळून पाहिले आहेत. त्या आश्रमातील अनाथांशी त्यांचा घनिष्ट परिचय आहे. त्यांची सुखदु:खे त्याने ऐकली आहेत, उघड्या डोळ्यांनी पाहिली आहेत. 'लेखकाने या कादंबरीतील काही व्यक्ती समाजात पाहिलेल्या आहेत. त्यांच्या वृत्तीचे सूक्ष्म अध्ययन करून त्योन त्याला कलेचा साज चढवला आहे.'[२]

अनाथांना विकणारी दुकाने असे रूप असणारी अनाथालये, तिथले गैरव्यवहार, समाजात प्रतिष्ठित म्हणून लौकिकप्राप्त व्यक्तींचे हिडीस आंतरिक जीवन या सगळ्यांचा जीवन आलेख या कादंबरीत आत्मनिवेदनपर प्रयोगाद्वारे मांडला आहे. समाजावर प्रचंड चिडलेली नायिका येथे वर्णन केली आहे. संधी मिळताच ती समाजावर व समाजकंटकांवर तुटून पडते. अनाथपण तिच्यावर लादले गेले आहे. तिच्या जीवनाचे सतत धिंडवडे निघतात आणि त्यामुळे तिचे संघर्षशील मन पेटून उठते. समाजातील तथाकथित प्रतिष्ठितांचे बुरखे फाडून त्यांचे वास्तव ती पुढे आणते. 'आश्रमातल्या मुली म्हणजे माळरानावरची माती. ती कुणीही उखरावी, कुणीही उधळावी, कुणीही

न्यावी, कुणीही तुडवावी! रानातील पाचोळा वारा आला की उडत जाणार! कुठंतरी पडणार! वाऱ्याच्या गतीबरोबरच पाचोळ्याचं भवितव्य ठरतं!'[३] असं हृदयविदारक वर्णन या कादंबरीत येतं.

पु.भा. भावे यांनी समाजातील विविध पातळीवरच्या वेगळ्या आणि हृदयभेदक प्रश्नांना आपल्या कादंबऱ्यांतून वाट मोकळी करून दिली. अकुलीनांच्या व्यथा, अपौरुषांच्या पत्नीची जीवघेणी कहाणी, तिची तडफड त्यांनी वर्णन केली. समाजात अगतिक झालेल्या व्यक्तींचा संघर्ष त्यांनी मांडला. समकालीन सामाजिक समस्या आणि पूर्वीपासून चालत आलेल्या सामाजिक समस्या या दोन्हींना समर्थपणे मांडण्यात भावे यशस्वी झाले आहेत. त्यांचे विषय नवे नव्हते; परंतु अनुभव घेण्याची आणि वाचकांपर्यंत पोचविण्याची त्यांची संपन्न हातोटी वाचकांची मने सुन्न करून टाकणारी ठरली. १९५१ मधील 'अकुलीना' या कादंबरीसाठी त्यांनी वेश्याकन्येविषयी आत्मीयता हा विषय निवडला होता. पत्रपद्धतीचा वापर करून कथानायकाने आपली संपूर्ण कहाणी मित्राला कळविली, ही पद्धत किंवा रचना या कादंबरीची आहे. ल.ग. जोग यांच्या मते, ' 'अकुलिना' हा वाचकाला अमर्याद अस्वस्थ करून सोडणारा अनुभव आहे. ही दुसरी मनोवस्था प्रभावी होत जाते त्यामुळ कादंबरीचा दर्जा एकदम उंचावतो.....एखाद्या नायकाने वा वक्त्याने आपल्या कलेची कमाल उंची गाठून एकदम थांबावे म्हणजे जसा अनुभव येतो, तसा येथेही येतो.'[४]

ग.त्र्यं. मांडखोलकरांच्या कादंबऱ्या राजकीय पटलावरील असल्या तरी त्यातही काही सामाजिक जाणिवा उमटलेल्या दिसतात. वैवाहिक समस्यांवरील विवेचन त्यांच्या 'अनघा'मध्ये आढळते. 'स्त्रीजीवनाची सफलता, प्रौढ विवाहातील नाजूक गुंतागुंती, विज्ञान आणि नवी नीती यांच्यामुळे पातिव्रत्याविषयीच्या कल्पनांमध्ये झालेले बदल, कुटुंबसंस्थेचा होत असलेला ऱ्हास'[५] या प्रश्नांचा विचार या कादंबरीत केलेला आहे. माडखोलकर पत्रकारही असल्यामुळे समाजातील सर्व थरातील जीवनाचे अवलोकन करण्याची संधी त्यांना मिळाली. परिणामी त्यांच्या कादंबऱ्यांमध्ये समाजजाणिवांना महत्त्व दिलेले आहे.

कुठल्याही व्यक्तीची जडणघडण ही समाजातच होते. त्याच्या व्यक्तिमत्त्वाला समाज जबाबदार असतो. शरच्चंद्र मुक्तिबोधांची 'शिप्रा' ही कांदबरी याच कालखंडातील. एका कनिष्ठ मध्यमवर्गीय कुटुंबाचा, स्वार्थी, लोभी, दांभिक जगात स्वत:च्या अस्तित्वाकरिता सुरू असलेला संघर्ष या कादंबरीत आहे. अनेक अभ्यासक या कादंबरीला व्यक्तिप्रधान कलाकृती मानतात. मात्र स्वत: लेखकाच्या मते, 'व्यक्तिमन ससंदर्भच आकळावे लागते. ते तसे आकळले गेले तरच त्याला अर्थ प्राप्त होऊ शकतो. मुळात व्यक्त म्हणजे काही सुप्त शक्तींचा एक पिंडच असतो व समाजात राहू लागल्यावर त्याला बरेवाईट व्यक्तित्व प्राप्त होत असते. समाजाबाहेत त्या व्यक्ती अव्यक्तच राहतात. तेव्हा व्यक्ती म्हणजे सामाजिक प्रक्रियांमधून आकाराला आलेले व्यक्तिमत्त्व असते.'[६] व्यक्ती आणि समाजाचे नाते उलगडवणारी ही कादंबरी.

वैदर्भीयच काय तर मराठी कादंबरीक्षेत्रात ज्यांचे नाव अपरिहार्यपणे व आदराने घ्यावे लागते त्या उद्धव शेळक्यांनी 'मागणी तसा पुरवठा' या न्यायाने अनेक कादंबऱ्या लिहिल्या. लिखाणात सातत्य टिकविणारे शेळके यांनी ग्रामीण, प्रादेशिक कादंबऱ्यांमधून निवडलेले विषय हे सामाजिकच होते. 'नांदते घर' ही त्यांची नागरजीवनावरील पहिली कादंबरी. अमरावती शहरातील मध्यमवर्गीय कुटुंबातील मोजक्या कालावधीमधील सुखदु:खाच्या चढउताराचा आलेख काढणारी ही कादंबरी. 'बाईविना बुवा' या कादंबरीत शेळके यांनी वेगळाच विषयाला हात घातला. बायकोने टाकून दिल्यावर स्त्री–समागमासाठी हपापलेल्या दुबळ्या नवऱ्याला योग्य मार्ग न सापडल्याने क्रमाक्रमाने त्याची होत जाणारी अध:पतित अवस्था लेखकाने अत्यंत संयमाने आणि ताकदीने चित्रित केली आहे. बायकोने टाकणे या अपमानास्पद भावनेने समाजात जगणाऱ्यांची मनोवस्था, त्यांना लुबाडणारा समाज आणि अशा व्यक्तींचे होणारे अध:पतन लेखकाने वर्णन केले आहे.

प्रादेशिक कादंबरी म्हणून गणल्या गेलेल्या शेळक्यांच्या 'धग'ने तर अनेक विक्रम मोडले. ग्रामीण भागातील एका जिद्दी आणि कर्तृत्ववान नायिकेच्या लढ्याची करुण कहाणी म्हणजे 'धग'. कामचुकार नवरा नशिबी आल्याने लेकराबाळांसाठी स्त्रीला किती कष्ट करावे लागतात, अनेक आघातांना तोड देत समाजात कसे जगावे लागते किंवा जगण्यासाठी कशी केविलवाणी धडपड करावी लागते याचे वर्णन येथे आहे. वैदर्भीय म्हणी, वाक्प्रचार आणि संवाद यांची रेलचेल असलेली ही सामाजिक विषयाला स्पर्श करणारी कादंबरी मराठी कादंबरीक्षेत्रात मानाचे पान मिळवून गेली.

दिनकर देशपांडे यांची 'तपझिरा' (१९६०), ना.के. महाजन यांच्या 'विनाश' भाग १ आणि भाग २ (१९४७–१९४८), 'चारुता' (१९५३), मा.ना. भोळे यांची 'दुनिया', श्रीकांत राय यांची 'वीस दिवस' (लघुकादंबरी) (१९५३) अशा काही कादंबऱ्यांमधून सामाजिक विषयांना हात घालण्यात आला आहे.

स्वातंत्र्योत्तर साठपूर्व या तपात वैदर्भीय कादंबऱ्या विपुल प्रमाणात आल्या. अनेकांचे विषय स्वातंत्र्य चळवळीच्या आणि घडून गेलेल्या महायुद्धाच्या पार्श्वभूमीवर होते, हे मान्य करावे लागते. त्याच काळात समाजातील विविध समस्यांनी तोंड वर काढले होते. एकीकडे गांधीवाद, मार्क्सवाद आणि कौटुंबिक, सामाजिक जीवनावर होत गेलेले विविध प्रभाव आणि अशा अनेक समस्यांपासून दूर जाऊन रंजनवादाकडे वळलेल्या लेखण्या या सर्वांचा विचार करता अनेक कादंबऱ्यांमध्ये कमीअधिक प्रमाणात सामाजिक जाणिवा प्रगट होत गेल्या. त्या कादंबऱ्यांनी जे मराठी साहित्यविश्वाला दिले, त्याला तोड नाही. त्याच्या पुनर्अध्ययनाची गरज मात्र आहे.

निष्कर्ष

१. इ.स. १९०० नंतर वैदर्भीय कादंबरीक्षेत्रात दिसू लागलेल्या आशावादी व चैतन्यमय चित्रात बा.सं. गडकरी यांनी १९०९ मध्ये 'सुधारणेचा मध्यकाल' ही सामाजिक कादंबरी लिहून खऱ्या अर्थाने वैदर्भीय मराठी कादंबरीची सुरुवात केली.

२. वि.ल. भावे, ना.रा. शेंडे आणि डॉ. भाऊ मांडवकरांसारख्या कादंबरीकारांनी सामाजिक कादंबऱ्यांची उल्लेखनीय निर्मिती केली.

३. समाजातील विविध समस्यांना वाचा फोडताना विविध कादंबरीकारांनी समाजाचे ज्ञात–अज्ञात कोपरे धुंडाळून वस्तुनिष्ठ संशोधन करून साहित्यनिर्मिती केली.

४. गांधीवाद, मार्क्सवादाचा प्रभाव पाडणारा काळ आणि कौटुंबिक, सामाजिक जीवनावर होत गेलेले आघात त्यामुळे समस्यांपासून दूर जाऊन रंजनवादाकडे वळलेल्या लेखण्यांनी सामाजिक जाणिवांना तितक्याच कसदारपणे सादर केलेला हा वैदर्भीय कादंबरीचा कालखंड आहे.

संदर्भ

१. गडकरी, माधव, साहित्यातील हिरे आणि मोती, उत्कर्ष प्रकाशन, पुणे, प्रथमावृत्ती, १९८४, पृ. १०१–१०२

२. कळणावत, शरद, अभिप्राय, माझी चाळीस भावंडं, भाऊ मांडवकर, सेवा प्रकाशन, अमरावती, पाचवी आवृत्ती, २००९, पृ. १६७

३. मांडवकर भाऊ, माझी चाळीस भावंडं, सेवा प्रकाशन, अमरावती, पाचवी आवृत्ती, २००९, पृ. २३

४. जोग, ल.ग., कादंबरी, चिरंजीव ग्रंथ प्रकाशन, पुणे, प्रथमावृत्ती, १९६३, पृ. १४७–१४८

५. माडखोलकर, ग.त्र्यं., निवेदन, अनघा, मॅजेस्टिक बुक स्टॉल, मुंबई, प्रथमावृत्ती, १९५०

६. मुक्तिबोध, शरच्चंद्र, माझ्या कादंबरी लेखनाच्या प्रेरणा, प्रतिष्ठान, फेब्रु–मार्च–एप्रिल, १९६४, पृ. ३२

❖❖❖

26 Teaching Methodology in Geography at College level

MAH MUL/03051/2012
ISSN : 2319 9318
UGC Approved Sr. No. 62759
Vidyawarta®
March 2018 Special Issue
105

35

Teaching Methodology in Geography at College Level

Asst. Prof. N. V. Narule
Indira Mahavidylaya, Kalamb, Distt.- Yavatmal

Introduction : -

Teaching is one of the main components in educational planning which is a key factor in conducting educational plans. Despite the importanceof good teaching, the outcomes are far fromideal.

Successful teachers always keep in view that teaching must "be dynamic, challenging and in accordance with the learner's comprehension. He does not depend on any single method for making his teaching interesting, inspirational and effective"

Regarding the importance of Methodology it may be said that a Methodologist, like any other scholar will be required to carry on his self-education throughout his life because a well trained Methodologist will confront new developments in his science, judge their merits, relate them to past trends and make a reasoned choice as to what he wants to integrate into his own thinking.'

Now a days gengraphy is considered as a part of the composite science of Human Society. Its purpose is to study the structure and behavior of human society. Therefore, it is one of the social sciences. Though all the social sciences have common purpose i.e. the study of man, yet each presents unique point of view and each has evolved its own technique of studying human affairs and solving social problems.

Objectives : -

- To familiarize the student teacher with different methods of teaching geography in classroom.
- To develop an understanding the role of a teacher for application of methods in classroom.
- To develop an understanding of the merit and limitations of various methods.

Acquisition of permanent knowledge and skill in Geography teaching methodology at college.

Methods : -

It may also be printed out that a meaningful solution of the problem depends on the methods which are available. In other words, it means that if a problem has been unsuccessfully examined at an earlier stage of discipline's evolution, it should be repeatedly attempted till a synthetic approach has been achieved. With this end in view we should talk about new Methodology in Geography in the field of teaching methods.

The instinct of curiosity is the master instinct among students. Students, experience proves, are curious to see things for themselves Their environment is full of things and object about which students want to know everything They have questions of which they want answers. The geography theacher exploits this instinct to make the teaching of geography interesting and meaningful.

A) Observation Method :-

The principles aspects of observation method are 1) To observe, 2) To record, 3) To interpret. The technique of obtaining geographical information by direct observation is

basis to the subject.

Observation method for teaching geography may be used inside the class room as well as outside the class-room.

Inside the class room the following aids help observation:

i) **Globe :** Globe is a useful aid by observation, students can develops such concepts as longitude, latitude, meridian etc.

ii) **Charts :** Charts prepared by students themselves or those commercially produced also enhance students obse-rvation.

iii) **Models :** Students observe things and they can convertthe results of their observation into models.

Outside the Class-room:

The teacher can enrich students observation by adopting certain modes outside the class room. The teacher may use the following modes for this purpose Geography is essentially an observational science. Within the four walls of the class room, the teaching of geography is limited to the globe, maps and the text-book . The real geography exists outside the class room. The students should be made to observe geography facts like the temperature, pressure, direction and velocity of the wind, clouds, lakes and mountains. The first hand experience about these phenomena of nature gives clear understanding of natural happenings.

Outside the class room , there are fields, crops, soil etc. which also froms part of geographical content. On the spot observation of these entities followed by discussion in the classes enriches students knowledge of geographical facts. The teacher of geography would like to make students study the surrounding environment, the landscape and what it offers to man to make his living meaningful.

a) Field Trips : Field trips help in exploring the environment. Students may be taken out into the larger landscape to oserve geographical objects, prepare brief notes, and collect specimens and so on.

b) Excursion : Excursions educate as well as entertain. Students learn by interacting with the environment. Excursions to hill stations, to geographical monuments help students to understand certain phenomena.

Merits of Observation method:

1. Trains the pupils to observe and reason about the fact they observe. This method brings the students of geography into direct relationship with the environment.

2. By this method we interpret the unknown in terms of the known–the known by observation and experience. It is essentially an outdoor work. Nothing should be allowed to take the place of direct observation whenever this is possible. So this is direct method of gaining geographic knowledge.

3. The merit of this method lies in the work and not in the results. It is training in intelligent observation and no in collecting the data.

4. This method develops the habit of accurate thought and investigation.

It is based on the finding of psychology i.e. there is instinct of curiosity in every human being which prompts every human being to know.

Limitations of Oservation Methods:

Observational study makes a big demand on the out-of-class time of teachers and the students, which the time-table of the college does not permit in Indian college.

1. Method is suitable for lower classes as the observation made by young students are necessarily limited.

2. Sometimes the observational study may degenerate into aimless wandering, wastage of much time and energy because of lack of understanding and direct action from the teacher. To let the students observe things without proper guidance and the knowledge may not be profitable at all. There must be proper guidance and the knowledge gained by observation must not be supplemented through methods as actual observation of student is always limited.

8)Laboratory Method :-

A geography Laboratory may be difined as a room in which are contained all written, audio and visual materials pertinent to geographic instructions. The class room itself may be converted into a laboratory if it is relatively self – contained and has within it most of the materialsthat the teacher and the students will normally be utilizing. The physical arrangement of a class room thus made is such that book cases, magazine racks, newspaper holders and equipment almirahs surround the room.

i) The laboratory method of instruction, usrd so successfully in the natural sciences, has been adopted for application to geography with equal success.

ii) This method seems to have grown out of the directed study. The laboratory method places primary emphasis upon equipment and its use.

iii) So this method presupposes a well equipped room in which the students have access to books, magazines, maps, pictures, drawing and construction material and other type of material which will promote better work. In those situations a special room is not available, the teacher of geography can place these instruments in an ordinary class-room.

iv) The procedure of the laboratory method is similar to that of problem solving appeoach or a completion of a project or preparation of charts, models, and maps or conducting of experiment to arrive at a general principle.

v) The teacher and the pupils both perform certain experiments based on scientific principles to make certain concept of geography clear. The students either individually or in groups make use of the material" for solving different problems in geography.

vi) Practical work in geography constitutes the laboratory work.

vii) The data collected in the field or a from the statistical reports are transformed into maps and diagrams in the laboratory. After the field observation, the need of laboratory is felt to give concrete shape to the ideas.

Project Method Discussed :

Among all the methods of teaching geography, Project method is the most important which is frequently applicable to teaching-learning process. It is a method which stands against the traditional method of teaching where the theoretical knowledge from the book is accepted 01 received by the students. In propagating this method, American educationist John Dewey did much work.

Prof. Kilpatrick defined a project as " a purposeful activity which proceeds in a social environment."

Dr. J.A. Stevenson who perfected it as a method of teaching said " it is a problematic act carried to completion in its natural setting."

C. V. Good according to " A project is a significant unit of activity, having educational value and aimed at one or more definite goals of understanding." It involves investigation and solution of problems and frequently the use and manipulate of physical materials. It is planned and carried to completion.

completion by the pupils and the teacher in a natural life-like manner.

Project may be individual or co-operative, large or small. It may be employed according the mental age of the pupils. But that must be done under the guidance of an expert.

Psychologically, the project method is based on the principles of learning by doing encourages maximum amount of purposefully activity on the part of the pupils. Adopting method, the heart, head and hand are to be functional. That means both the physical and also the mental powers of the students are to be exercised or utilized.

Basic Principles of Project Method :

1) The project must be based on activity-mental or motor.

2) It must be purposeful in its action.

3) Under the project, the students must accumulate experience-manipulative, concrete or mental.

4) It must provide real experience.

5) It must be useful in nature.

The Role of the Teacher :

i) In this method the role of the teacher is that of a guide and helper than that of task master.

ii) Before performing the expenments in the class the teacher should test the apparatus by performing the experiments himself and if the experiment is successful only then he should perfrom the same experiment, to the students beforehand. The students should be encouraged to arrive at the results themselves.

Conclusion :

It may, however not be understood that all method intends to minimize the importance of teaching methodology in Geography. In spite of these limitations, all method is a very useful and effective for teaching in Gegraphy.

References :

- Dr. S. Harichandan, Dr. Asam Shaik - Methods of teaching Geography.

K.Prabhakaran, E-research Methodology.

36

अध्ययन, अध्यापन पध्दतीत शिक्षक व विद्यार्थ्यांचा सहभाग

प्रा.डॉ. विलास माहुलकर

कला व वाणिज्य महाविद्यालय,चोरी अरब

प्रस्तावना :

शिक्षणाच्या आंतरराष्ट्रीय स्पर्धेत आपल्याला टिकायचे असेल तर पहिल्यांदा आपल्याला शैक्षणिक दर्जा व गुणवत्ता सिध्द करावी लागेल. यासाठी शैक्षणिक धोरणामध्ये नाविन्यपूर्ण बदल करुन अध्यापन पध्दतीतही नाविन्यपुर्ण तंत्र, कौशल्यांचा स्विकार सर्वच विद्या-शाखांमध्ये कराया लागणार आहे. यामध्ये शिक्षकांच्या बरोबरच विद्यार्थ्यांच्या सहभागाचीही अत्यंत महत्वाची भुमिका असणार आहे.कारण सद्यस्थितीत भारतातील उच्च शिक्षण क्षेत्रात धोक्याची घंटा वाजत आहे. अपु-या शैक्षिक सुविधा, फीस मधील भरमसाट वाढ, नोकरीचे व रोजगाराचे कुठलीही हमी नसणे, बेरोजगारीतली प्रचंड वाढ, महागाई, न्युनगंड, गैरसमज, आदी कारणांमुळे विद्यार्थी, पालक व समाज उच्च शिक्षणाकडे नकारात्मक दृष्टीने पाहत असुन उच्च शिक्षणापासून कोसो दुर राहुन अलिप्त राहू पाहत आहे व जे विद्यार्थी उच्च शिक्षण घेत आहेत. यातील विशेश करुन कला, विज्ञान, वाणिज्य, शिक्षण व विधी विद्याशाखांच्या प्रवेशित विद्यार्थ्यांची सातत्याने वर्गातील व महाविद्यालयातील उपस्थिती अत्यंत नगण्य असुन चिंतेचा विशय ठरली आहे. नाविन्यपुर्ण अध्यापन पध्दतीमुळे उच्च शिक्षणात विद्यार्थ्यांचा सहभाग निश्चितपणे मोठ्या प्रमाणात वाढेल व यातून कुशल मनुश्यबळ निर्माण होऊन साश्वत, चिरंतन व सर्वांगिण विकासासाठी राष्ट्रिय अधिक गतिमान होईल.

उद्देश :-

प्रस्तुत संशोधन लेखाचे उद्दिश्टये खालील प्रमाणे मांडता येतील.

1.उच्च शिक्षणातील विद्यार्थ्यांच्या गळतीचा अभ्यास करुन ती रोकण्यासाठीचे उपाय शोधने.

2.नाविण्यपुर्ण अध्यापन पध्दती, तंत्र व साधनांकडे शिक्षक व विद्यार्थ्यांचे लक्ष वेधून घेणे.

3.उच्च शिक्षणातील नाविन्यपूर्ण अध्यापन पध्दतीत शिक्षकांच्या बरोबरच विद्यार्थ्यांचा सहभाग व सकारात्मक भुमिका वृध्दींगत करणे.

4.पारंपारिक व नाविन्यापूर्ण अध्यापन पध्दतीची चर्चा होणे.

5.शिक्षण क्षेत्रातल्या सद्यस्थितीकडे अभ्यासकांचे, शिक्षक, विद्यार्थी व शिक्षण प्रेमींचे लक्ष वेधून घेणे.

27 Jagtik Tpman Ani Prayawarn Pradushan: ek abhyas

MAH MUL/03051/2012 ISSN: 2319 9318 UGC Approved Sr.No.62759 Vidyawarta® March 2018 Special Issue-06 063

14

जागतिक तापमान वाढ आणि पर्यावरणीय प्रदुषण : एक अभ्यास

प्रा. एन. व्ही. नरले
भूगोल विभाग प्रमुख

सारांश :—

जागतिक तापमान वाढ आणि त्याला अनुसरुन होणारे पर्यावरणीय बदल, त्याबद्दल निर्माण होणाऱ्या समस्या संपूर्ण जगाला भेडसावीत आहे. देशाच्या आर्थिक विकासासाठी ऊर्जासाधनांचा अविवेकी वापर हा तापमान वाढीच्या समस्येला उग्र रुप देत आहे. पृथ्वीवरील तापमानाची स्थिती आता वेगाने बदलू लागली आहे. याकरणपणे ही वाढ ०.५ अंश सेंग्रे. इतकी आहे. आणि २०५० पर्यंत ही वाढ ३ अंश सेंग्रे. इतकी होईल असे शास्त्रज्ञ म्हणत आहेत. भारतातील सरासरी तापमान १.५ अंश से ग्रे नी वाढलेले आहे. १९९८ हे वर्ष सर्वाधिक उष्ण वर्ष ठरले. २००१ पासून ही वाढ कायम आहे, ही वाढ अशीच होत राहिली तर पृथ्वीवरील सजीवसृष्टी या उच्च तापमानात जगू शकणार नाही. त्यामुळे वेळीच जागृत होण्याची गरज आहे.

प्रस्तावना :—

मानवी संस्कृतीच्या विकासाबरोबरच हे सिद्ध होत आले की, मनुष्य व निसर्ग हे एका व्यवस्थेवर अवलंबून आहे. या व्यवस्थेतील हवा, पाणी, जमीन, वनस्पती व जीवजंतू हे पाच घटक एकमेकांवर अवलंबून असतात. ज्यातून एक निसर्गचक्र तयार होत. परंतु निसर्गाची पूजा करणारा मानव कालांतराने पृथ्वीवरील वनस्पतींची तोड करुन शेती, उद्योग व वसाहती निर्माण करताना. नैसर्गिक साधनसंपत्तीचा दुरुपयोग करु लागल्याने मानवाच्या सभोवतालची परिस्थिती म्हणजेच पर्यावरण प्रदुषित होऊ लागल्याने पर्यावरणीय धोक्यांची मालिका सुरु झाली आहे.

विषय विवेचन :—

पृथ्वीच्या सरासरी तापमानातील अलिकडच्या दशकातील वाढ आणि भविष्यात होणारी वाढ ही म्हणजे जागतिक तापमान वाढ (Global warming) व मानवी संबंध स्पष्ट करते. पृथ्वीच्या भूपृष्ठाचे व सागराचे सरासरी तापमान नजिकच्या काळात झपाट्याने वाढत आहे. १९०५ ते २००५ या कालावधीत पृथ्वीची सरासरी तापमानवाढ ०.७४ से १.३३ फॅ. इतकी राहीली आहे व त्याचे प्रमुख कारण म्हणजे हरितगृह वायुत झालेली वाढ होय. पृथ्वीच्या तापमान वाढीसाठी काही नैसर्गिक कारणेही जबाबदार असले तरी मानवाची कृती हे तापमान वाढीचे मुख्य कारण होय. वातावरणातील कर्बवायुच्या वाढीमुळे सुर्याची उष्णता पृथ्वी पृष्ठाकडे मोठ्या प्रमाणात परावर्तित होत नाही. हरितगृहा मधून मोठ्याप्रमाणात कार्बन डाय ऑक्साईड वातावरणात सोडला जातो. याबरोबरच इंधनाचे ज्वलन, कोळशाचे ज्वलन या क्रियातूनही कर्बन डाय ऑक्साईड वायू वातावरणात सोडल्या जातो. ज्यामुळे वैश्विक तापमान वाढ झालेली आहे. तापमानातील वाढ जर याच प्रमाणात होत राहीली तर सागराच्या हालचाली, रोगप्रसार, शेतीची नाविकी या समस्या अधिक प्रमाणात उद्भवतील.

Global warming is nothing but it is a greatest start of atmospheric changes which directly effects on human lifestyles as well as every living thing and name carbon dia oxide will de stroy earth without taking space or any sympathy with livinghood.

जगतिक तापमान वाढ :—

जीन फोरियरने १०० वर्षापूर्वी ग्रीन हाउस इफेक्ट या शब्दाचा प्रयोग केला. हरितगृह परिणामामुळे पृथ्वीचे तापमान (१५ अंश सेंग्रे.) ठराविक मर्यादेत कायम राहते. परंतु कार्बन डाय ऑक्साईड, मिथेन, क्लोरोफल्युरोकार्बन, नायट्रस आक्साईड सारख्या वायूने वातावरणातील प्रमाण वाढले तर पृथ्वीला सुर्याकडून मिळालेली उष्णता वातावरणाच्या बरच्या घरात जाऊ

शकत नाही. जमीन पृष्ठीवरील वातावरणात तापमान वाढते. हेच तापमान वाढ म्हणून ओळखले जाते. वाहतूक, खाणी, व व्यवसायासाठी इंधनाचे ज्वलन होत असताना अधिक प्रमाणात वातावरणात कार्बन डायऑक्साईड वायूची निर्मिती होते. या वायूचा वातावरणातील वाढता प्रभाव हाच आपल्या चिंतनाचा विषय आहे. ही कोणतीही नैसर्गिक आपत्ती नसून मनुष्याच्या आधुनिक जीवनशैलीचा परिणाम आहे.

हरितगृह वायू :—

औद्योगिक क्रांतीनंतर सुरुवात झाल्यापासून वातावरणातील या वायूचे प्रमाण दिवसेंदिवस वाढत आहे. या हरितगृह वायूत क्लोरोफ्लूरोकार्बन, हायड्रोफ्लुरो कार्बन, हायड्रोक्लोरोफ्लूरोकार्बन, परफ्लुरोकार्बन, आणि हायपाफ्लूराईड्स हे सर्व मानव निर्मित हरितगृह वायू आहेत.

हरितगृह वायूचे परिणाम :—

१. ध्रुवीय प्रदेशातील व उंच प्रदेशातील बर्फ वितळू लागले आहे.

२. उंच हिमाच्छादीत पर्वतात उगम पावणाऱ्या नद्यांचे बर्फ वितळून नद्यांना महापूर येत आहेत. त्यामुळे नदीकाठच्या व मुखाशी असणाऱ्या प्रदेशांचा हानी होते.

३. पृथ्वीवरील हिमसाठे वितळल्यामुळे समुद्राच्या पातळीत १५ ते ९० से.मी. ने वाढ होईल अशा वर्तवेस उत्तर व वायव्य युरोप भूमध्य समुद्रकिनारी प्रदेश, प्रशांतदेश, उत्तर कॅनडा, सैबेरिया इत्यादी प्रदेश पुराखाली येतील.

४. बर्फ वितळल्यामुळे हिमप्रदेशाची उष्णता परिवर्तिनता कमी होऊन पृथ्वीच्या उष्णता ग्रहणात वाढ होईल.

५. तापमान वाढीमुळे भूप्रदेशाची शुष्कता वाढून पर्जन्याचे प्रमाण कमी होईल. शेतीक्षेत्र ओसाड पडण्याचा धोका संभवतो.

६. कार्बनडाय ऑक्साईडच्या प्रमाणात वाढ झाल्याने वन परिसंस्था परिवर्तन घडेल.

७. तापमान वाढीमुळे प्राण्यांच्या स्थलांतर बदल घडून काही जीवजातींचे लुप्तीकरण होईल तर काही नवीन जाती निर्माण होतील.

८. प्रतीय तापमान वाढीमुळे पृथ्वीवरील वातावरण बदलून, पर्जन्य चक्रामध्ये बदल होऊन हवामानात परिवर्तन होईल.

पर्यावरणीय प्रदूषण :—

पृथ्वीच्या पृष्ठभागा दरम्यान सजीवसृष्टीसाठी कार्बनडाय ऑक्साईड अल्प प्रमाणात असणे आवश्यक आहे. मात्र त्याचेप्रमाण मर्यादेपेक्षा जास्त झाल्याने जागतिक उष्णतेची पट्टा वाढायला सुरुवात झाली आहे. त्यातून उद्भवणारे धोके पुढीलप्रमाणे आहेत.

१. **ओझोनचा क्षय :**

ऑक्सीजन सोबत सूर्यप्रकाशाची अभिक्रिया होऊन ओझोन वायू तयार होतो. पृथ्वीच्या वातावरणात २० ते ५० कि.मी.उंचीवर हा थर अस्तित्वात आहे. या थरामुळे पृथ्वीकडे येणारी अतिनिल किरणे जोपर्यंत येतली जात असल्याने हा थर पृथ्वीची संरक्षक छत्री म्हणून काम करतो. मात्र १९८० च्या दशकात या थराची जाडी कमी झाल्याचे तर काही थराला छिद्रे पडल्याचे लक्षात आले. ओझोन थराच्या नाशामुळे पृथ्वीकडे येणारे अतिनिल सूर्यकिरणे आपला प्रभाव सजीव सृष्टीवर पाडू लागले. त्वचेचे कर्करोग, मोतिबिंदूचा विकार बळावू लागले. शेतातील पिके व एकपेशीय शजीवांना धोका पोहोचला त्यामुळे नैसर्गिक अन्नसाखळ्यावर परिणाम होऊन वनस्पतींची तोड झाल्याने वातावरणातील कर्बनडाय ऑक्साईडचे प्रमाण वाढले.

२. **वातावरणातील बदल :**

विज्ञान व तंत्रज्ञानाच्या बळावर मानवाने निसर्गावर स्वामित्व मिळविण्याचा प्रयत्न सुरू ठेवला आहे. यासाठी औद्योगिकरणाचा आधार घेतला. उद्योगामधून बाहेर पडणारे दूषित वायू वातावरणात कमालीचे बदल घडवून आणत आहेत. मानवाने नैसर्गिक संसाधनाची केलेली लूट, जंगलाची बेछूट कत्तल, दगडी कोळसा, पेट्रोलियम यासारख्या इंधनाचा अमर्याद वापरामुळे कार्बनडाय ऑक्साईड ४९ टक्के, मिथेन १८ टक्के, क्लोरोफ्लुरो कार्बन १४ टक्के, नायट्रस ऑक्साईड ६ टक्के हे सर्व हरितगृह वायू या टक्केवारीने तापमान वाढ घडवून आणत आहेत.

जपानमध्ये नाशी पर्जन्यमान ५०मी.मी.ने वाढल्याचा लावला आहे. जपानमध्ये १९९७ साली

सरासरी पाऊस ३३४३ मि.मी. इतका पडला. त्याचे जगाचे सरासरी जागतिक तापमान याहे होय होते. जगातील अनेक देशांनी २०व्या शतकातील जागतिक उष्मान्या अहवाल वेळून कार्यवाही सुरू केली आहे. उदा. मलेशियाने कोलालपूरची राजधानी पुत्रजयाला हलवली. जपानने किनाऱ्यालगतची शहरे टप्प्याटप्प्याने हलवायला सुरुवात केली आहे. सिंगापूरसारख्या शहराला हलवण्याची गरज प्रसंगास काय करावे लागेल यासाठी योजना तयार केली जात आहे. अमेरिका, ऑस्ट्रेलिया, युरोप येथे या नोंदीचे पुनरुपातळीवर नियोजन सुरू आहे.

३. वादळे व चक्रिवादळे :

तापमान वाढीने सागरी वादळांची संख्या वाढत आहे. त्यामुळे भरतीच्या लाटा अधिक वेगाने किनाऱ्यावर धडकतात. जगातल्या अनेक किनाऱ्यावर समुद्राने अतिक्रमण केल्याचे उपग्रहीय फोटोमधून दिसून येते. बंगालच्या उपसागरातून आंध्र, ओरिसाला येणारी चक्रीवादळे, अरबी समुद्रातून गुजरात, महाराष्ट्रावर येणारी मुंबई वादळे हिंदी महासागरातील सुनामि परिवर्तीत होणारी वादळे इत्यादीचा अप्रत्यक्षरित्या ग्लोबल वार्मिंगशी संबंध सांगितला जातो.?

४. सागरपातळीत वाढ :

सद्यस्थितीत महासागराच्या पातळीत लक्षणीय वाढ होत आहे. इ.स.२१००पर्यंत सागराची सरासरी पातळी ९.८८ से.मी. वाढण्याची शक्यता दर्शविण्यात येत आहे. ज्याचा परिणाम सागराचे खारे पाणी जमिनीवर पसरण्याने अनेक पर्यावरणीय समस्यांचा सामना करावा लागेल. इजिप्तमधील नाईल नदीचे खोरे, बांग्लादेशमध्ये गंगा—ब्रम्हपुत्रेचे खोरे, मालदीव बेट, मार्शल द्विपसमुह यांना या समस्येचा अधिक धोका असल्याचे जागतिक आरोग्य संघटना २००१ च्या अहवालात म्हटले आहे. गेल्या दशकात सागरी पातळी १ इंचाने वर आली. २०५० पर्यंत ती १ इंचाने वाढलेली असेल. त्यामुळे किनाऱ्या लगतची शहरे जसे गाने २० इंचाने पाण्याखाली गेलेली.

वातावरणातील सर्वसाधारण वायुंचे जे मिश्रण आहे त्यात कार्बनडाय ऑक्साईडचे प्रमाण ०.०३ टक्के आहे. या प्रमाणात वाढ होत असल्याने मार्च १९९५ मध्ये अंटार्क्टिका खंडातील हिमनगाचा ७० किमी लांब व १०० मिटर खोल असा प्रचंड खंड पडला. त्यामुळे २०००० वर्षांपासून बर्फाखाली राहिलेला काही भूभाग उघडा पडला आहे. त्यामुळे बर्फ वितळून सागरी पाण्याची पातळी वाढत आहे.

५. मानवी आरोग्य :

उष्मावृध्दीचा धोका मानवी आरोग्यालाही आहे. सामान्यत: समाजाचे स्वास्थ, पिण्याचे पाणी, पोष्टीक अन्न, योग्य निवारा हे सर्व घटक वातावरणातील बदलानुसार प्रभावित होतात. त्यामुळे पिण्याच्या पाण्याची समस्या गंभीर होत चालली आहे.

६. एल निनो :

पॅसिफिक महासागरातील प्रवाहामध्ये काही ठराविक कालावधीनंतर होणाऱ्या बदलाशी एल निनो संबंधीत आहे. पॅसिफिक महासागरात दर तीन ते सहा वर्षांनी याचा प्रभाव जाणवतो. महासागराच्या वाढत्या तापमानामुळे १९९७ साली पॅसिफिक महासागरातील प्रवाळ खडकाचे अतोनात नुकसान झाले. ऑस्ट्रेलियातील टाऊन्सविले येथील जागतिक प्रवाळ खडक नियंत्रण संस्थेद्वारे इ.स.२०५० पर्यंत पृथ्वीवरील सर्व प्रवाळ खडक नष्ट होण्याची भिती व्यक्त करण्यात येत आहे.

७. पूर :

गेल्या १०० वर्षात पृथ्वीचे तापमान ०.५ अंश. से ने वाढले आहे. हिमाचे आवरण कमी होत आहे. हिमाच्या वितळल्यामुळे गंगा, ब्रम्हपुत्रा इ. नद्यांना पूर येण्याचा धोका उत्तर भारत व बांग्लादेशाला आहे. पूर परिस्थितीचा तडाखा बसलेल्या प्रदेशात अन्नधान्याचे उत्पादन कमी होते. रोगराई व किडींचा प्रादूर्भाव वाढतो. अन्नधान्य तुटवडा उग्र रूप धारण करतो.

८. जैवविविधतेचा ऱ्हास :

पृथ्वीवरील वाढत्या तापमानामुळे वनस्पती व प्राण्यांच्या काही प्रजाती नष्ट झाल्या आहेत तर अनेक प्रजाती नष्ट होण्याचा धोका निर्माण झाला आहे. त्यामुळे अन्नसाखळ्यामध्ये विघाड निर्माण होत आहे. सजीव सृष्टीसाठी जैवविविधतेचा ऱ्हास फार मोठा धोका आहे.

९. बाळबंटीकरण :

अपुऱ्या पर्जन्याने वनस्पती उभी पिके आणि जंगल संपत्तीवर विपरीत परिणाम होतात.

जमिनीमधील आम्लाचे प्रमाण वाढल्यामुळे कॅल्शियमचे प्रमाण कमी होऊन जमिनीचा कस जातो. असे भाग उष्ण वाळवंटात रूपांतरीत होण्याचा धोका निर्माण झाला आहे.

१०. जिवीत हानी :

जागतिक उष्मात कमालीची वाढ झाल्याने पाण्याचे बाष्पीभवन होऊन जमिनीतील ओलावा नाहिसा होईल. नद्या आणि सरोवरे यातील जलपातळी खाली जावून कृषि उत्पन्नावर त्याचा परिणाम संभव आहे. अमेरिकेत शिकागोमध्ये १९९५ साली ७३० माणसे उष्माघातामुळे मरण पावली. ऑगस्ट २००३ च्या युरोपियन उष्म्याच्या लाटेने ३५००० माणसे दगावली. फ्रान्समध्ये तापमान ४० अं.से.च्या वर गेल्याने १५००० माणसे मृत्यू झाली.

११. लोकसंख्या विस्फोट :

जगाची लोकसंख्या प्रतिवर्षी १० द.ल.एवढया प्रचंड वेगाने वाढत आहे. इ.स.२०१५ मध्ये जगाची लोकसंख्या ७.२७ अब्ज असेल. वाढत्या लोकसंख्येच्या नैसर्गिक संसाधनावर ताण पडून त्याचा ऱ्हास होत जातो. त्यामुळे पर्यावरणाशी निगडीत अनेक समस्या निर्माण होत आहेत.

नियंत्रणात्मक उपाययोजना :—

१. वृक्ष पुर्नलागवड करणे.

२. उर्जा वापरासंबंधी नव तंत्रज्ञान विकसित करण्याची गरज.

३. क्षय पावणाऱ्या उर्जा साधनांवर मात करण्यासाठी अक्षय उर्जा साधनांचा शोध घेणे.

४. पृथ्वीवर अस्तित्वात असलेली उर्जा साधने संरक्षित केली पाहिजेत.

५. इंधनातून बाहेर पडणाऱ्या ऑक्सीजनचे प्रमाण कमी केल्यास हरितगृह परिणाम कमी होईल.

६. मोठया प्रमाणावर वेतले जाणारे सी.एफ. सी. व हॅलोजन्सचे उत्पादन मर्यादीत करण्याची आवश्यकता आहे.

७. ओझोन थराचे संरक्षणासाठी रासायनिक द्रव्यांचे उत्पादन व वापर कमी करणे.

८. सुपरसॉनिक विमानांच्या वापरावर मर्यादा आणणे.

९. युरोपिय व अमेरिकी प्रगत राष्ट्रांनी रेफ्रिजरेटर्स, एरोसोल्स, अग्निशामके इत्यादींचा वापर टाळला पाहिजे. त्यानंतरचे विकसनशील राष्ट्रांनी अशा वस्तू वापरू नयेत.

संदर्भ सूची :—

१. पर्यावरणशास्त्र — ए.भरूचा, ओरिएंट लॉंगमन

२. पर्यावरणशास्त्र—प्रा.डॉ.सुर्यवंशी, श्री विद्या प्रकाशन, पुणे.

३. पर्यावरणशास्त्र—रमेश उमाठे, रेखा ठाकरे, विसा बुक्स, नागपूर.

४. पर्यावरण शिक्षण — प्रा.नीलम पाथरे, चैतन्य प्रकाशन, कोल्हापूर.

५. पर्यावरण समस्या — डॉ.श्रीकांत कार्लेकर, डायमंड पब्लिकेशन, पुणे.

६. वायुप्रदूषण — डॉ.किशोर पवार, सौ.नलिनी पवार, मेहता पब्लिशिंग हाऊस,पुणे.

७. पर्यावरण अभ्यास— डॉ.सुरेखा फुले, विद्याभारती प्रकाशन,लातूर.

८. पर्यावरणशास्त्र, डॉ.सुरेखा पंडित, श्री साईनाथ प्रकाशन, नागपूर.

९. पर्यावरणशास्त्र—डॉ.विठ्ठल धापुरे, पिंपळापुरे पब्लिशर्स,नागपूर.

❑❑❑

28 A chief, industrial waste, activated red mud for subtraction of methylene blue dye from environment

Materials Today: Proceedings 29 (2020) 822–827

Contents lists available at ScienceDirect

Materials Today: Proceedings

journal homepage: www.elsevier.com/locate/matpr

A chief, industrial waste, activated red mud for subtraction of methylene blue dye from environment

Sanjay R. Thakare [a,*], Jyoti Thakare [b], P.T. Kosankar [c], Mangala R. Pal [d]

[a] Department of Chemistry, Government Institute of Forensic Science, Nagpur 400 001, India
[b] Departments of Chemistry, St. Vincent Pallotti College of Engineering and Technology, Nagpur, India
[c] Yashwant Rao Chauhan College of Engineering and Technology, Nagpur, India
[d] Chemistry Department, Pandav College of Engineering and Technology, Nagpur, India

ARTICLE INFO

Article history:
Received 22 March 2020
Received in revised form 24 April 2020
Accepted 25 April 2020
Available online 6 May 2020

Keywords:
Activated Red Mud
Adsorbent
Dyes
Methylene Blue
Industrial waste

ABSTRACT

Dyes are used as a colored compound and considered as a highly toxic to biological species in water medium. Adsorption is most comprehensively used technology because of simple, low cost and effective for pollutant removal. Red mud activated by acid followed by heat treatments (ARM) was used as an adsorbent. 80% dye removal within 75 min observed when adsorbent dose was 100 mg and initial dye concentration 10 ppm having solution pH 10. The R^2 value was to be 0.991 at temperature 308 K which fits with Langmuir isotherm model. The process is exothermic in nature was confirmed by thermodynamic parameters.

Selection and Peer-review under responsibility of the scientific committee of the 11th National Conference on Solid State Chemistry and Allied Areas.

1. Introduction

The heavy toxic metal ions, various types of dyes, drugs, various phenolic compounds, pest and insect controlling chemicals, house hold products and wide spectrum of aromatics are a common pollutants present in a water [1–2]. The presence of pollutants in water makes water highly toxic to the aquatic life and changing the water potable to the non potable. A number of processes are available for the treatment of water to make water potable having some advantages and disadvantages [3]. Adsorption of various pollutants from the water and waste water is more superior process among the different treatment processes. It is well known that solid waste materials (byproducts) generated from various industrial activities poses one of most vexing problems of society. Cities of developing countries have no adequate treatments for solid waste generated by houses and industries and are a major challenge to solve. Solid waste generated form houses and industries were used as adsorbents for the treatment of water and waste water is an interesting and beneficial alternative. If it is, reduces the volume of solid waste and reduces the pollution at reasonable cost.

Adsorption of different types of pollutants from solution is a superior choice and many advantages over the other processes. For the adsorption process, adsorbents material with specific properties was essential. Oxides and hydroxides of metal, biomaterial, synthetic resins, polymer, porous materials and industrial waste were reported as adsorbents for the elimination of pollutants from solution [4–7]. Industrial waste from thermal power station, metallurgical processes and others industrial waste can be a smart choice over the others due to advantages was reported [8]. In aluminum metallurgical processes, the bauxite ores was leach with alkali and red mud, an industrial waste product was generated. Globally 90 millions tones red mud was produced each year [9–10]. Size and worth of red mud generated in alumina process obtained from one location was not similar from other location.

Red mud is a highly alkaline waste material due to use of sodium hydroxide solution during metallurgical process. Fine particles of red mud containing oxides and hydroxides of aluminum, iron, silicon and titanium metal mainly. Red mud containing 60% mass of oxidized iron and hence the color becomes red. High alkali content, chemical species and a noteworthy impact on environment make red mud problematic and hence its dumping is a big challenge where alumina industries are installed. Alkaline nature of red mud makes is harmful material and is big hurdle using this material as an adsorbent [11–13].

* Corresponding author.
E-mail address: sanjaythakare@yahoo.co.uk (S.R. Thakare).

https://doi.org/10.1016/j.matpr.2020.04.759
2214-7853/
Selection and Peer-review under responsibility of the scientific committee of the 11th National Conference on Solid State Chemistry and Allied Areas.

Dyes are used as a colored compound and considered as a highly toxic to biological species in water medium in a different ways. Due to presence of dyes in water several common problem was observed in human such as allergic symptoms, skin related problem, leads to cancer and mutation in genetic material [14–15].

The elimination of chemicals having serious impact on environment using different industrial waste reported in the literature. The removal of dyes from water using red mud was also reported [16]. The procion orange dye removal from water by red mud was reported in a literature. It is observed that it is act as an adsorbent and its efficiency was not only affected by initial dye concentrations but also by agitation time, adsorbent dosage and pH [17]. Acid violet dye, can be eliminated from the environment using red mud was reported [18]. Red mud for the elimination of dyes from the environment has less effectiveness been reported as an adsorbent. Hence in order to explore more applicability and excellent effectiveness on the removal of different classes of dyes using red mud as adsorbent more emphasis is required.

2. Experimental

Red mud used in the present experiments was supplied from (Jawaharlal Nehru Aluminum Research Design and Development Centre) JNARDDC, Nagpur, Maharashtra. It has the following average chemical composition (%): Al_2O_3, 19.88; Fe_2O_3, 36.47; CaO, 2.33; SiO_2, 15.95; Na_2O, 10.03; TiO_2, 4.97; CO_2, 2.48; S, 0.09; V_2O_5, 0.074; P_2O_5, 0.041 and loss on ignition is 8.04%. Red mud was first air dried and sieved by 200 mesh steal sieve. Sieved red-mud was stored in a laboratory under atmospheric conditions before activation processes. 10 g of red mud and 190 mL of Millipore water was introduced in a beaker and stirred to form slurry. Further 18 mL of 31% HCl was introduced in a beaker and resulting solution was heated at 60 °C for 20 min and diluted with water to make total volume of 800 cm^3 with constant stirring. Liquor ammonia was added drop wise with constant stirring till the pH of solution become 8. The precipitate obtained was further heated at 50 °C for 10 min with constant stirring. The whole solution was cooled and precipitate has been separated using Whatmann filter paper. After filtration, precipitate wash with Millipore water several times and dried in oven at 110 °C and finally calcined at 700 °C for 2 h. The resultant material place in a desiccators and finally grind in a fine powder and here after is called as an activated red mud (ARM). 0.1–1.0 mm diameter red mud particles were used for all characterization and dye adsorption study.

X-ray diffraction (XRD) patterns were collected on a Philips PANalytical Diffractometer with standard protocol. Fourier transform infrared spectroscopy (FT-IR) spectra were measured on a Bruker alpha model. SEM images was recorded by JEOL Model JSM – 6390 LV field-emission instrument, Nitrogen adsorption–desorption isotherms were determined on a Micromeritics ASAP 2420 analyzer and data analyse by software.

100 ppm methylene blue (s.d fine Chemicals) stock solution was used. Methylene blue solution having concentrations ranging between 5 ppm and 50 ppm of MB were prepared using stock solution. All experiments were measured at room temperature (25 °C) and the initial pH of the solution was adjusted by NH_4OH (0.1 M) and HCl (0.1 M) solution. The amount of MB dye was calculated spectrophotometrically (Shimadzu UV-1800 model) using wavelength of maximum 663 nm.

3. Results and discussion

The X-ray diffraction pattern of red mud and activated red mud is represented in Fig. 1.

Fig. 1 shows that, the raw red mud having calcite phase had been disappears after acid treatment. This is may be due to decomposition of goethite phase and formation of new magnetite phase after acid-thermal treatment. The dominant phase in activated red mud is hematite and its peak intensity significantly enhance. SEM pictures provide morphology of surface of red mud before activation of sample at micro-scale and after activation was represented in a Fig. 2. Fig. 2 shows that there is a mark difference in a surface morphology of red mud before acid activation and red mud after acid activation. SEM images of red mud after acid activation shows illustrative proof for the enhancement of surface area by acid followed by thermal treatment. The red mud after acid treatments has many cavities probably due to removal of some acid-soluble salts. After heat treatment, Activated Red Mud exhibits flake like morphology with additional porosity.

The EDS spectrum of Activated Red Mud clearly provides the obvious highest content of aluminum as shown in Fig. 3(A). The presence of iron with traces of oxygen and silicon content was also observed. These may be attributed towards reactive component as a result of activation of red mud with Acid treatment.

Fig. 3 (B & C) represented the FT-IR spectra of red mud before activation (B) and after activation(C). Both the samples show two peaks at 3450 cm^{-1} which one is very broad and another one at 1643 cm^{-1} corresponding to the stretching vibration of hydroxyl. The presence of water molecule or hydroxyl group in the samples was confirmed by these two peaks. The peak at 1470 cm^{-1} and 1400 cm^{-1} was observed in the red mud sample before the activation corresponding to the presence of CO_3^{2-} indicating the presence of a large amount of carbonate in the sample. However, these two bands was not observed in red mud after activation, owing to the fact that the carbonates are reacted with HCl and decomposed after thermal treatments. The peaks at 591 cm^{-1} and 546 cm^{-1} in both the sample were attributed to the stretching vibration of Fe–O, indicating the existence of Fe compounds. The peak at 1002 cm^{-1} corresponding to Si–O stretching vibrations was observed for the red mud before activation which was noticeably absent in the red mud after activation. This indicated that that the silicate groups may be remove during the activation process. The peak at 617 cm^{-1} correspond to Al–O band was observed in both the sample. The results observed are well match with reported literature [19].

The surface areas of red mud before activation and red mud after activation were evaluated by BET method and results are represented in Table 1. The surface area of red mud before activation is low than red mud after activation. This change of specific surface area will be an advantage to use red mud as an adsorbent after activation. During the activation process the metal ions present in red mud may react with acid molecules and assemble in such a manner so the diameter of internal pore increases which leads to increase of surface area.

Activated red mud (ARM) was use as a adsorbent for the removal of methylene blue. To analyse the efficiency of ARM as a adsorbent the influence factors including adsorbent dosage, contact time, pH, and initial concentration was studied and result are represented in Fig. 4. The amount of ARM dose was investigated to analyze the maximum dose of ARM for MB dye removal. To analyze it, 10 ppm initial concentration and 100 mL volume of MB dye solution was used for all experiments. The results are depicted in Fig. 4(A), show that as an amount of ARM was increases the subtraction efficiency of MB dye also increases. It shows that removal efficiency was 50% when the amount was 40 mg. For 50 mg, it was 60% and 85% for 100 mg. The increase of removal efficiency with increase of ARM amount is may be due to increase of number of sites available for adsorption. Therefore, removal efficiency reached in equilibrium with the amount of 100 mg of ARM and is sufficient for 85% MB dye removal from 10 ppm solu-

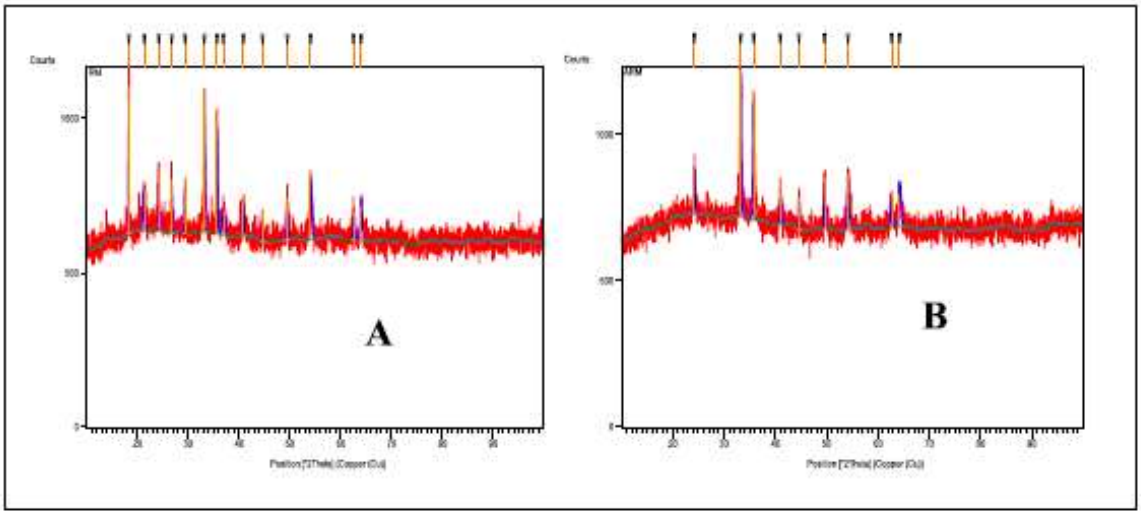

Fig. 1. X-ray diffraction spectra for (A) Red Mud and (B) Activated Red Mud. (For interpretation of the references to color in this figure legend, the reader is referred to the web version of this article.)

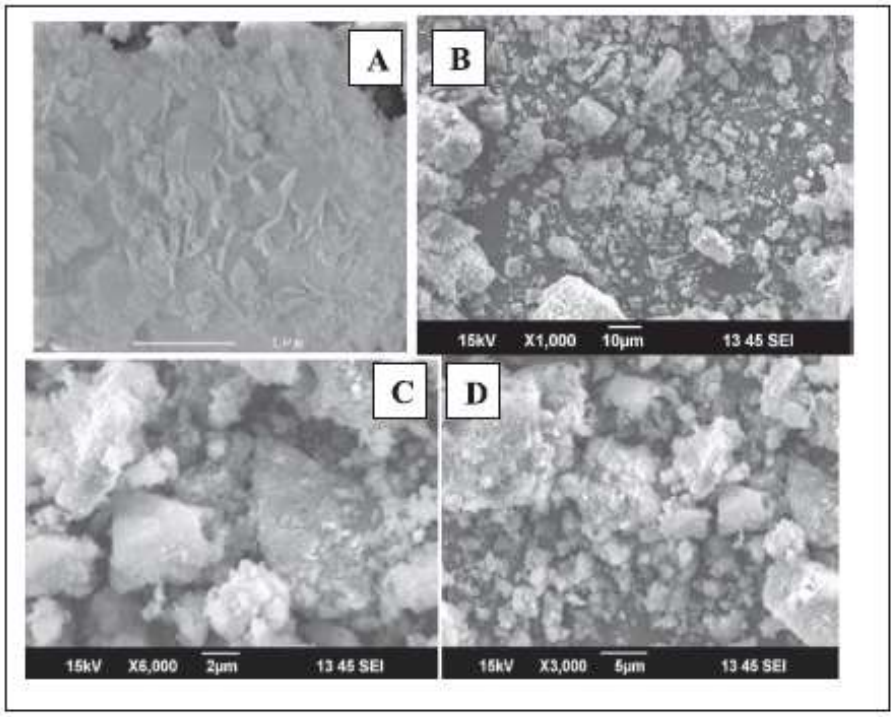

Fig. 2. SEM images of Red Mud before activation (A) and Activated Red Mud (B, C, D).

tion. The higher dose of adsorbent seems not to be required in all concentration ranges suggesting the effective use of ARM for efficient MB dye removal from water. The highly competent adsorption property may be ascribed due to the porous and crystalline layered structure formation of ARM.

The pH of solution is critical factor and to analyze the pH of solution on the subtraction efficiency of MB dye was studied in a solution pH of 2–12 using volume of solution 100 mL with 10 ppm MB concentrations. Fig. 4(B) indicates the outcome of pH on the removal of MB dye in the presence of ARM. When initial pH of the dye solution was increased from 3 to 11, the percentage removal increased from lower to higher. The subtraction tendency of methylene blue increases with increasing the solution pH is dependent on the environment of the adsorbent. At lower pH, the percentage of the removal of MB dye was 40%. Interestingly, at higher pH, the trend of the removal was increased. Fig. 4(B) sug-

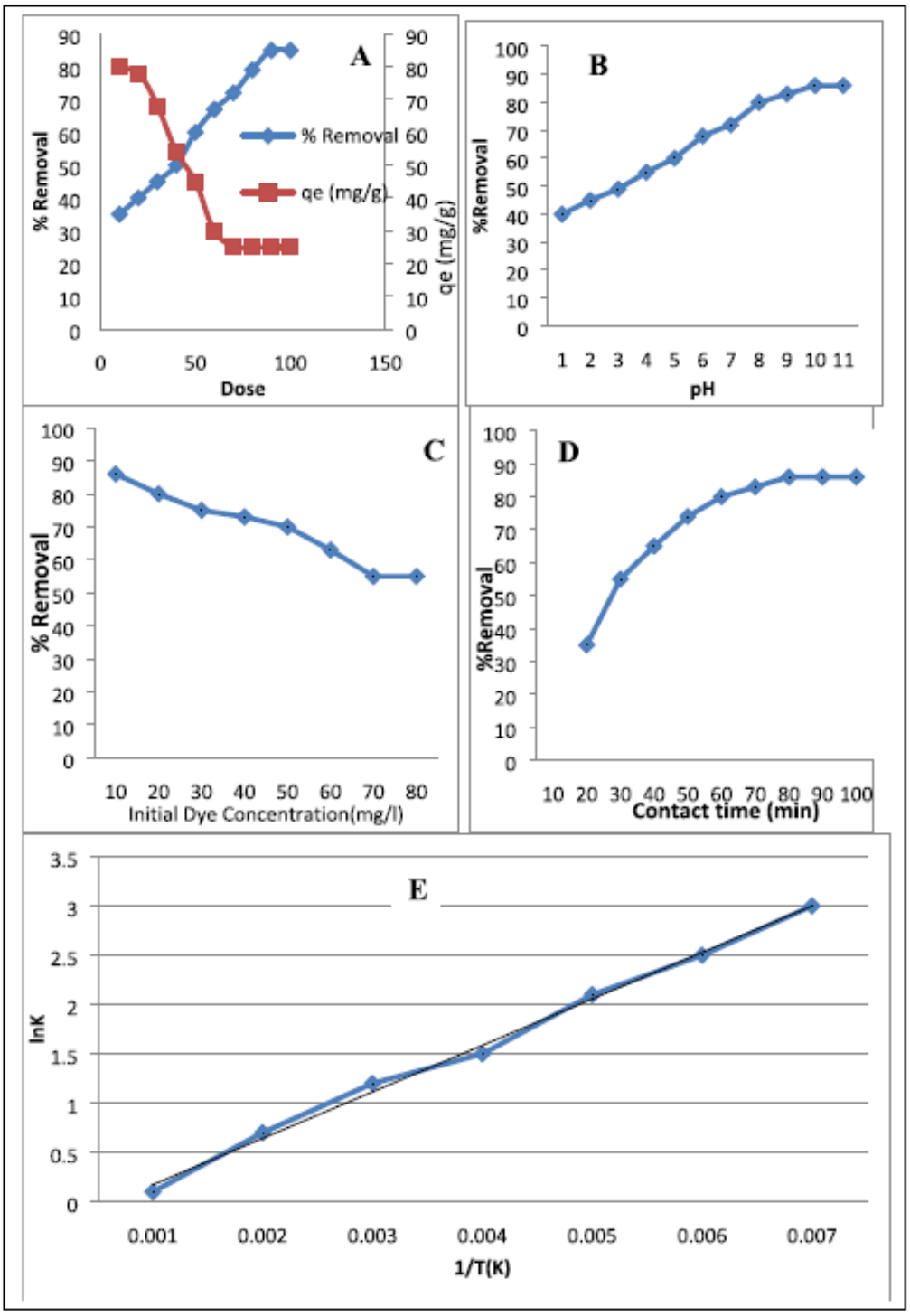

Fig. 4. Removal efficiency of MB Dye by activated red mud A-Dose of ARM; B-pH effect; C-Dye concentration; D-Contact time; E- Van't Hoff plot. (For interpretation of the references to color in this figure legend, the reader is referred to the web version of this article.)

4. Conclusion

Activation of red mud is a important tool for using this industrial waste as a adsorbent for environmental purification. Activation of red mud induced the formation of new magnetite phase and decomposition of calcite and goethite phase was confirmed by XRD analysis.

Surface morphology of ARM is porous while red mud before activation is not porous was confirmed by SEM analysis. It is

assume that during the activation process the carbonate and silicate are removed from the material induces the porosity. This was confirmed by FTIR analysis. The inducement of porosity to the material may be a reason of increase of surface area of red mud after activation than red mud before activation. From the result it was concluded that red mud which is a waste was successfully utilized for the removal of methylene blue from water.

Authors contributions

All authors are equally contributed for materials Synthesis, characterizations, experimental and writing of manuscript.

Declaration of Competing Interest

The authors declare that they have no known competing financial interests or personal relationships that could have appeared to influence the work reported in this paper.

References.

[1] A. Bhatnagar, A.K. Jain, J. Colloid Interface Sci. 281 (2005) 49–55.
[2] G.E. Walsh, L.H. Bahner, W.B. Horning, Environ. Pollut. A. 21 (2013) 169–179.
[3] P.Rajasulochana, V.Preethy, Resource: Efficient Tech. 2(2016) 175-184.
[4] R.G. Chaudhary, V. Sonkusare, G. Bhusari, A. Mondal, D. Shaik, H. Juneja, Res. Chem. Intermed. 44 (2017) 2039–2060.
[5] V.N. Sonkusare, R.G. Chaudhary, G.S. Bhusari, A. Mondal, A.K. Potbhare, R. Kumar Mishra, A.A. Abdala, H.D.Juneja, ACS Omega. 5 (2020) 7823-7835.
[6] R. Bagade, V. Sonkusare, A. Potbhare, R. Chaudhary, R. Husain, H. Juneja, Mater. Today: Procs. 15 (2019).
[7] V. Sonkusare, R.G. Chaudhary, G. Bhusari, A. Rai, H. Juneja, Nano-Struct. Nano-Objets. 13 (2018) 121–131.
[8] M. Ahmaruzzam, Adv. Colloid Interface Sci. 166 (2011) 36–58.
[9] A. Bhatnagar, V. Vilar, C. Botelho, R. Boaventura, Environ Technol. 32 (2011) 231–249.
[10] Y. Zhou, R. J. Haynes. Critical Reviews in Environ. Sci. Technol. 40 (2010) 909-977.
[11] H. Nath, A. Sahoo, Mater. Today: Procs. 5 (2018) 2207–2215.
[12] G. Collin, V. Krishnan, G. Puma, Environ. Eng. Res. 25 (2020) 795–806.
[13] H. Nath, P. Sahoo, A. Sahoo, Powder Technol. 269 (2015) 233–239.
[14] B. Lellis, C.Z. Favaro-Polonio, J. Alencar, P. Julio, C. Polonio, Biotech. Res. Innov. 3 (2019) 275–290.
[15] M. Berradi, R. Hsissou, M. Khudhair, M. Assouag, O. Cherkaoui, A. Bachiri, A. Harfi, Heliyon 5 (2019) e0276.
[16] C.P. Costa de Jesus, M.L. Antunes, G.B. Navarro, R.B. Moruzzi, Desalin. Water Treat. 55 (2015) 1040–1047.
[17] C. Namasivayam, R.T. Yamuna, D. Arasi, Sci. Technol. 37 (2002) 2421–2431.
[18] C. Namasivayam, R.T. Yamuna, D. Arasi, Environ. Geol. 41 (2001) 269–273.
[19] S. Sushil, V.S. Batra, J. Hazard. Mater. 203 (2012) 264–273.
[20] S. Ozcan, A. Tor, M.E. Aydin, Clean- Soil Air Water. 39(2011) 972-979.
[21] Q. Wang, Z. Luan, N. Wei, J. Hazard. Mater. 170 (2009) 690–698.

29 Strengthening of photovoltaic and supercapacitive properties of graphene oxide-polyaniline composite by dispersion of α-Al2O3 nanoparticles

Chemical Physics Letters 706 (2018) 647–651

Contents lists available at ScienceDirect

Chemical Physics Letters

journal homepage: www.elsevier.com/locate/cplett

Research paper

Strengthening of photovoltaic and supercapacitive properties of graphene oxide-polyaniline composite by dispersion of α-Al_2O_3 nanoparticles

Kailash Nemade [a,*], Pradip Tekade [b], Priyanka Dudhe [b]

[a] Department of Physics, Indira Mahavidyalaya, Kalamb 445 401, India
[b] Department of Chemistry, Jankidevi Bajaj College of Science, Wardha 442 001, India

ARTICLE INFO

Article history:
Received 3 May 2018
In final form 8 July 2018
Available online 10 July 2018

Keywords:
Graphene oxide
Polyaniline
Photovoltaic
Supercapacitive properties

ABSTRACT

It is demonstrated that the dispersion of α-Al_2O_3 nanoparticles in graphene oxide (GO)-polyaniline (PANi) composite results in significant enhancement of photovoltaic and supercapacitive properties. In order to improve PV and SC properties of GO-PANi composite, 0.5 wt% of α-Al_2O_3 nanoparticles were added in composite. Both PV and SC properties of composites becomes strengthen by addition of 0.5 wt% of α-Al_2O_3 nanoparticles. The GO-PANi/α-Al_2O_3 composite shows power conversion efficiency (%η) 9.31%, which is significantly higher than pure α-Al_2O_3 nanoparticles and GO-PANi composite. The GO-PANi/α-Al_2O_3 composite achieve considerable specific capacitance of the order 715.5 Fg^{-1} at scan rate of 2 $mV\,s^{-1}$.

1. Introduction

The widespread use of inorganic photovoltaic cell is still limited because of complications in modification of band gap of inorganic materials and high processing costs [1]. Different approaches using organic or polymer materials such as conducting polymer, graphene and metal oxides have received considerable attention because of their low cost, light weight and flexibility [2]. Whereas supercapacitor is a new class of device, which comes under the category of energy storage devices, and fulfill the technological gap between conventional capacitor and battery. Supercapacitor has some outstanding features like power density, rapid store/release of energy, good charge/discharge life cycles, and Eco friendliness. For supercapacitor application, carbon nanomaterials such as carbon nanotubes and graphene are extensively used, due to their high specific surface area and good electrical conductivity [3].

The use of carbon nanostructures with the conducting polymer is also investigated as supercapacitive material extensively. Yu et al investigated the polyaniline/graphene composite as electrode material for supercapacitors. The electrochemical capacitance of composite has value 596.2 Fg^{-1} and after 1500 cycles at a current density of 2 Ag^{-1}, only 16.3% drop in the initial capacitance is observed [4]. Wang et al synthesized PANi with different morphologies and combined with graphene to use as electrode materials of supercapacitors. The result of the study shows that sheet-like Graphene/PANi composites can deliver specific capacitances of 532.3–304.9 Fg^{-1} at scan rates of 2–50 mV/s [5]. Wu et al prepared the Polyaniline/graphene hydrogel composites for supercapacitor application with macroscopically phase-separated structure, which exhibits the high specific capacitance and excellent rate performance. This work concludes the PANi is mainly outside the graphene hydrogel matrix, can enhance the rate performance of the composites [6]. Cong et al prepared the graphene–PANi paper and employed for the supercapacitor application. The composite paper has considerable specific capacitance (763 Fg^{-1}) and good cycling stability [7]. Moussa et al reviewed comprehensively the recent developments in polyaniline/graphene nanocomposites as supercapacitor electrodes. This work underlined the polyaniline/graphene nanocomposites have great potential in electrochemical energy storage applications, especially supercapacitors [8]. Theophile et al reported the successful preparation of Poly(vinyl alcohol)-graphene oxide and Poly(vinyl alcohol)-reduced graphene oxide composite for supercapacitor application. The results of the study indicates that Poly(vinyl alcohol)-reduced graphene oxide composite (190 Fg^{-1}) deliver good supercapacitive properties than Poly(vinyl alcohol)-graphene oxide (13 Fg^{-1}) composite [9]. Loeblein et al a novel material having oxidized-three-dimensional-graphene, with a band gap of 0.2 eV. This material found suitable for electrode application in dye-sensitized solar cells where electrode has stringent work-function requirements [10]. Li et al successfully

* Corresponding author.
E-mail address: knemade@gmail.com (K. Nemade).

https://doi.org/10.1016/j.cplett.2018.07.018
0009-2614/

fabricated the PANi nanotubes-based supercapacitors having maximum areal capacitance of 237.5 mF cm^{-2} (scan rate = 10 mVs^{-1}) with maximum energy density of 24.31 mW h cm^{-2} (power density = 2.74 mW cm^{-2}). Under bending condition, supercapacitor shows excellent performance. After 2000 cycles, the capacitor maintains 95.2% of the initial capacitive value [11].

Feng et al prepared the graphene/polyaniline nanocomposites by using one-step hydrothermal method. The graphene/PANi nanowire composites exhibit the excellent electrochemical properties having specific capacitance 724.6 F/g higher than the graphene/PANi nanocomposite (602.5 F/g). This study demonstrated that morphology of materials also plays key role in optimization of electrochemical properties [12]. Zhou et al reported the effect of morphology on electrochemical properties using materials system nanoflake-like and nanobelt-like α-MoO_3/graphene nanocomposites. The results of the investigation demonstrated that α-MoO_3 nanoflakes/graphene exhibited better supercapacitive (up to 360 Fg^{-1}) performances than α-MoO_3 nanobelts/graphene [13].

In the light of above discussion, we planned to investigate the photovoltaic and primary electrochemical properties of α-Al_2O_3/PANi-GO composite. In this work, we studied the PV cell properties such as fill factor and power conversion efficiency and supercapacitive properties such, cyclic voltammetry (CV) curve, areal capacitance and cycle stability performance of composite materials. The main accomplishment of present work is that we achieved considerable value of power conversion efficiency and specific capacitance for α-Al_2O_3/PANi-GO composite.

2. Experimental

2.1. Materials preparation and characterization

In the present study, all AR-grade (SD Fine, India) chemicals were used for the preparation materials without further purification. The chemical oxidative polymerization was adopted for the preparation of Polyaniline (PANi). The method of preparation of PANi is reported previously [14]. In this process, aniline monomer and ammonium persulphate were used with molar ratio 1:1 M for preparation of PANi in aqueous media. The addition of aniline monomer in oxidant under constant magnetic stirring results in dark greenish precipitated. As obtained precipitated was washed two times with distilled water and dried in oven for overnight. The fine powder of PANi was used for the preparation of composites. The graphene oxide (GO) used in this work was prepared by previously reported method [15]. The ex-situ approach was adopted for the preparation of composites. The GO loaded PANi composite was prepared by taking equal wt.% of both contents. Whereas, α-Al_2O_3 loaded-GO/PANi composite was prepared by taking 0.5 wt% concentration of α-Al_2O_3 nanoparticles. Both the composites prepared in organic media (Acetone).

The X-ray diffraction (XRD) patterns of as-prepared materials were recorded on Rigaku Miniflex-II using CuK_α radiation (λ = 1.54 Å). The morphology of samples was investigated using scanning electron microscope (SEM) images obtained from JEOL JSM-7500F.

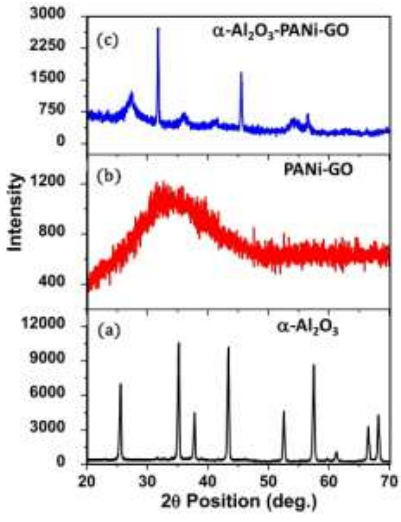

Fig. 1. XRD pattern of α-Al_2O_3 nanoparticle, PANi-GO and α-Al_2O_3/PANi-GO composite.

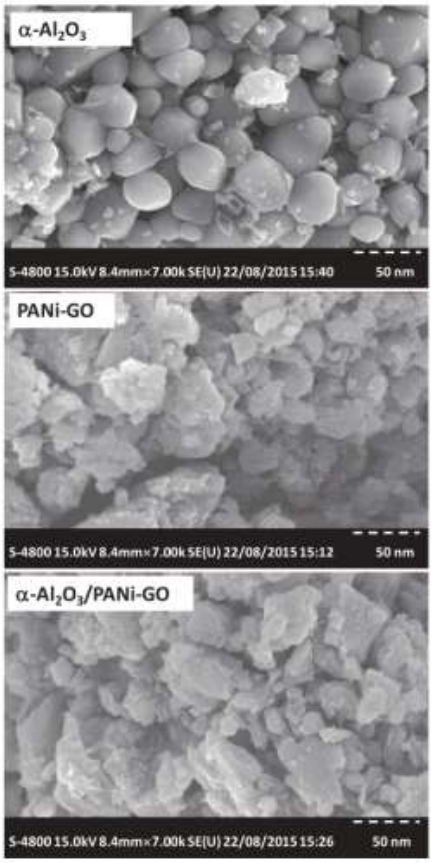

Fig. 2. FE-SEM images of α-Al_2O_3, PANi-GO and α-Al_2O_3/PANi-GO composite.

2.2. Supercapacitive study

Electrochemical measurements such as cyclic voltammetry (CV), areal capacitance and capacitance retention analysis were carried out using three-electrode cell systems (CHI 660 D, CH Instruments). As-prepared materials were used as the working electrode, platinum wire as counter electrode and Ag/AgCl as the reference electrode.

2.3. Photovoltaic (PV) study

PV cell required for testing was prepared by doctor blade technique. During the fabrication of PV cell, indium tin oxide (ITO) coated glass plate were used as transparent electrode and aluminum as metallic electrode. The photovoltaic properties of as-fabricated PV cell such as fill factor (FF) and power conversion efficiency (%η) confirmed by measuring short circuit current (Isc), open circuit voltage (Voc) and I_{max} and V_{max} from IV characteristics of PV cells.

3. Results and discussion

3.1. Characterization of materials

Fig. 1(a) shows the XRD pattern of α-Al_2O_3 nanoparticles, which is in good agreement with PDF Card No-01-081-1667. No other peaks for impurities were detected in pattern. The average crystallite size was computed by considering all prominent diffraction peaks using the Debye-Scherrer equation, which found to be 37.3 nm [16]. Fig. 1(b) depicts the XRD pattern of PANi-GO composite. The XRD pattern shows noisy behavior of diffraction peaks, which confirms the composite exhibited amorphous nature. In addition to this composite comprises broad hump between 2θ-range 20–30°. Fig. 1(c) shows the XRD pattern of α-Al_2O_3 nanoparticles loaded PANi-GO composite. Pattern clearly indicates the presence of signature peaks of α-Al_2O_3 and GO. This indicates the nice incorporation of α-Al_2O_3 in PANi-GO composite.

Fig. 2 represents the SEM images of α-Al_2O_3, PANi-GO and α-Al_2O_3/PANi-GO composite. SEM image of α-Al_2O_3 shows the nanoparticles have irregular shape with well separated boundaries. The average crystallite size estimated using XRD analysis is in good agreement with SEM study. The SEM images of PANi-GO and α-Al_2O_3/PANi-GO composite have almost identical morphology like petals or sheets structure.

3.2. PV study of materials

Fig. 3(a–c) shows IV characteristics of PV cell fabricated using the active PV material, α-Al_2O_3, PANi-GO and α-Al_2O_3/PANi-GO composite respectively and the PV parameters reflected by materials are listed in Table 1. From results, it is concluded that α-Al_2O_3 loaded PANi-GO composite achieve higher short circuit current (I_{sc}) than pure α-Al_2O_3 and PANi-GO. This might be attributed to the good dispersion of α-Al_2O_3 in PANi-GO composite and good charge–transfer process within composite, which is evident in the higher value of Isc [17]. There is a significant enhancement in

Table 1
PV parameters of α-Al_2O_3, PANi-GO and α-Al_2O_3/PANi-GO composite.

Material	I_{max} (mA)	V_{max} (V)	I_{SC} (mA)	V_{OC} (V)	FF	%η
α-Al_2O_3	23.8	0.2	23.8	0.7	0.285	1.61
PANi-GO	86	0.2	86	0.7	0.285	5.81
α-Al_2O_3/PANi-GO	137.7	0.2	137.7	0.8	0.25	9.31

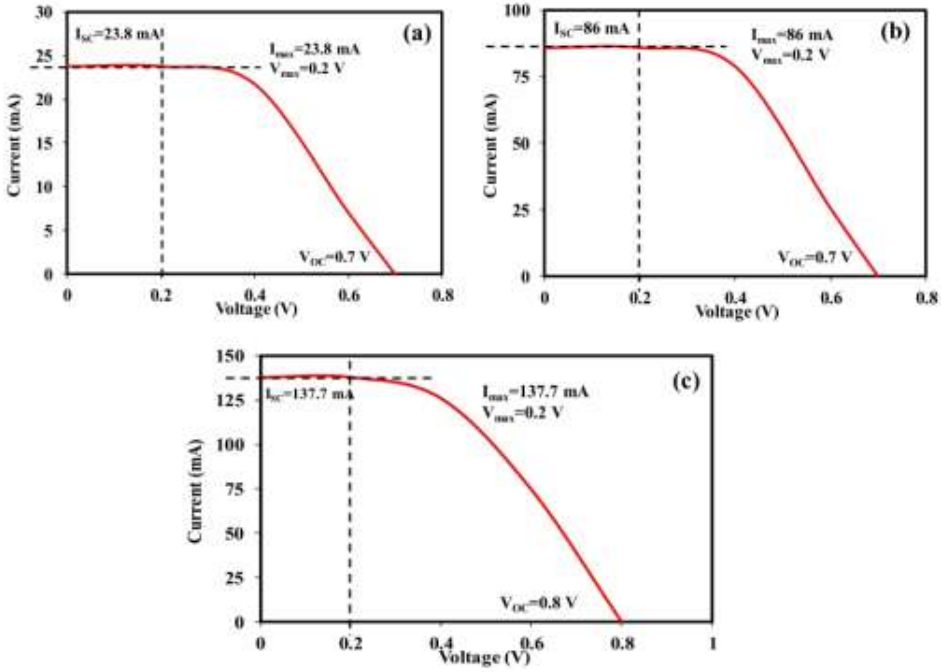

Fig. 3. PV response of (a) α-Al_2O_3, (b) PANi-GO (c) α-Al_2O_3/PANi-GO composite.

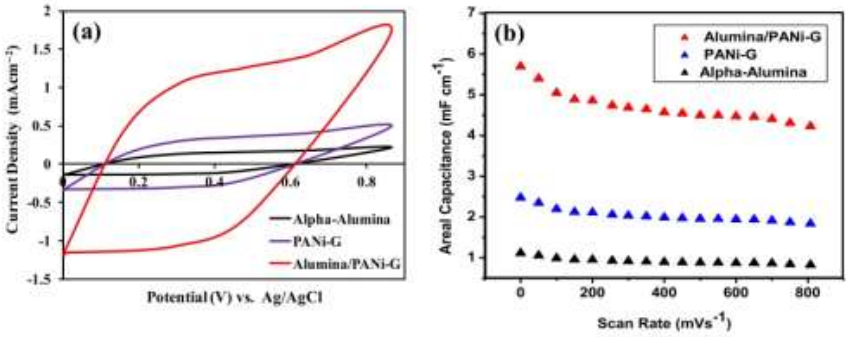

Fig. 4. (a) CV curves and (b) Areal capacitance as a function of scan rate of the α-Al_2O_3, PANi-GO and α-Al_2O_3/PANi-GO recorded at a scan rate of 2 mV s^{-1}.

%η resulted due to the addition of α-Al_2O_3 in PANi-GO composite. The highest value of %η is 9.31% for α-Al_2O_3/PANi-GO composite, whereas %η is 5.81% for PANi-GO composite and 1.61% for α-Al_2O_3.

3.3. Supercapacitive study of materials

Fig. 3a shows the cyclic voltammetric (CV) curves of α-Al_2O_3, PANi-GO and α-Al_2O_3/PANi-GO recorded at a scan rate of 2 mV s^{-1}. The CV curves clearly shows the α-Al_2O_3/PANi-GO composite have superior supercapacitive properties over pristine α-Al_2O_3, PANi-GO composite. The superior supercapacitive properties of α-Al_2O_3/PANi-GO composite can be attributed to oxidation/reduction of surface hydroxyl groups [18]. Specific capacitance has been estimated using the relation (Eq. (1)) [19],

$$Cs = \frac{I}{m \times v}(Fg^{-1}) \quad (1)$$

where I is the average current during anodic and cathodic scan (A), m is the mass of the electrode (g) and v is the scan rate (V). In our case, the highest value of specific capacitance was found to be 715.5 Fg^{-1} at a scan rate of 2 mV s^{-1} for α-Al_2O_3/PANi-GO composite.

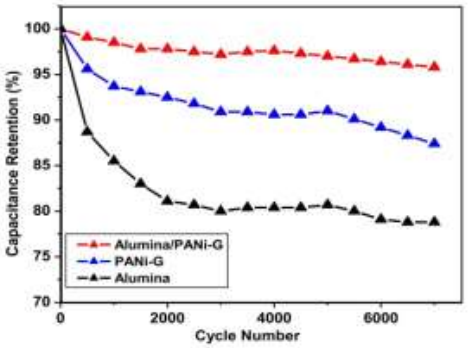

Fig. 5. Cycle performance of the alpha-Al_2O_3, PANi-GO and α-Al_2O_3/PANi-GO composite measured at a scan rate of 2 mV s^{-1} for 7000 cycles.

Fig. 3b shows the variation of calculated areal capacitance of the α-Al_2O_3, PANi-GO and α-Al_2O_3/PANi-GO composite as a function of scan rate. Here also plot clearly depicts that α-Al_2O_3/PANi-GO composite has several fold higher capacitance over the pristine α-Al_2O_3, PANi-GO composite. The significant enhancement in electrochemical performance was attributed to two main processes occurring in the composite. First is that composite possesses improved carrier density, which results in good electrical conductivity. Second is the increase of density of hydroxyl groups on α-Al_2O_3/PANi-GO composite [20]. The absence of redox peak indicates that capacitance was mainly contributed by non-faradaic redox reactions.

As shown in Fig. 4, the capacitance drops in pristine α-Al_2O_3 and PANi-GO composite is significantly more than α-Al_2O_3/PANi-GO composite. The α-Al_2O_3/PANi-GO composite electrode exhibits an excellent long-term stability with 95.83% capacitance retention after 7000 cycles. The good capacitance ability of α-Al_2O_3/PANi-GO composite is ascribed to enhanced electrical conductivity and highly stable surface redox reaction [21] (see Fig. 5).

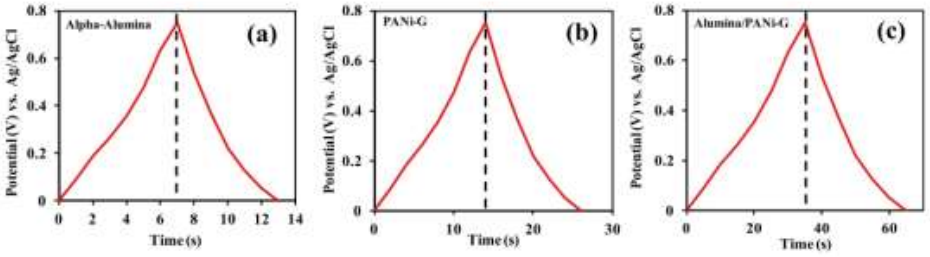

Fig. 6. Galvanostatic charge/discharge curves of the (a) alpha-Al_2O_3, (b) PANi-GO and (c) Al_2O_3/PANi-GO collected at a current density of 10 μAcm^{-2}.

Electrochemical study of alpha-Al_2O_3, PANi-GO and Al_2O_3/PANi-GO samples were extended by measuring charge/discharge measurements. Fig. 6(a–c) shows the galvanostatic charge/discharge (GCD) curves of alpha-Al_2O_3, PANi-GO and Al_2O_3/PANi-GO samples, respectively. The GCD curves of Al_2O_3/PANi-GO sample is nearly symmetric and significantly lengthy than alpha-Al_2O_3 and PANi-GO. This indicates capacitive properties of Al_2O_3/PANi-GO sample superior than alpha-Al_2O_3 and PANi-GO. Improved performance of Al_2O_3/PANi-GO attributed to synergetic state between alpha-Al_2O_3 and PANi-GO.

4. Conclusions

In summary, we have successfully demonstrated that the photovoltaic and supercapacitive performance of GO-PANi/α-Al_2O_3 composite is superior over the α-Al_2O_3 and PANi-GO composite. GO-PANi/α-Al_2O_3 composite based PV cell shows significant power conversion efficiency of the order of 9.31%, which much higher than α-Al_2O_3 and PANi-GO composite. The GO-PANi/α-Al_2O_3 composite exhibits the considerable specific capacitance of the order 715.5 Fg^{-1}. The GO-PANi/α-Al_2O_3 composite retain 95.83% capacitance after 7000 cycles, which shows the good cycling stability of composites. The GCD characteristics of Al_2O_3/PANi-GO sample improved due to synergetic effect between α-Al_2O_3 and PANi-GO composite. At present work is underway for the optimization of the electrochemical performance GO-PANi/α-Al_2O_3 composite.

Acknowledgment

The authors appreciate the help of Dr. S.K. Omanwar Head, Department of Physics, Sant Gadge Baba Amravati University, Amravati for providing necessary facilities for the work.

References

[1] R.M. Swanson, Progress in Photovolt.: Res. Appl. (Special Issue) 14 (2006) 443–453.
[2] N.S. Sariciftci, S.S. Sun, Organic Photovoltaics: Mechanism, Materials, and Devices, Taylor & Francis, New York, 2005.
[3] M.F. El-Kady, V. Strong, S. Dubin, R.B. Kaner, Laser scribing of high-performance and flexible graphene-based electrochemical capacitors, Science 335 (2012) 1326–1330.
[4] T. Yu, P. Zhu, Y. Xiong, H. Chen, S. Kang, H. Luo, S. Guan, Synthesis of microspherical polyaniline/graphene composites and their application in supercapacitors, Electrochim. Acta 222 (2016) 12–19.
[5] R. Wang, M. Han, Q. Zhao, Z. Ren, X. Guo, C. Xu, N. Hu, L. Lu, Hydrothermal synthesis of nanostructured graphene/polyaniline composites as high-capacitance electrode materials for supercapacitors, Scientific Reports 7 (2017), Article number: 44562.
[6] J. Wu, Q. Zhang, A. Zhou, Z. Huang, H. Bai, L. Li, Phase-separated polyaniline/graphene composite electrodes for high-rate electrochemical supercapacitors, Adv. Mater. 28 (2016) 10211–10216.
[7] H. Cong, X. Ren, P. Wang, S. Yu, Flexible graphene–polyaniline composite paper for high-performance supercapacitor, Energy Environ. Sci. 6 (2013) 1185–1191.
[8] M. Moussa, M. El-Kady, Z. Zhao, P. Majewski, J. Ma, Recent progress and performance evaluation for polyaniline/graphene nanocomposites as supercapacitor electrodes, Nanotechnology 27 (2016) 395201.
[9] N. Theophile, H.K. Jeong, Electrochemical properties of poly(vinyl alcohol) and graphene oxide composite for supercapacitor applications, Chem. Phys. Lett. 669 (2017) 125–129.
[10] M. Loeblein, A. Bruno, G.C. Loh, A. Bolkere, C. Saguy, L. Antila, S.H. Tsang, E.H.T. Teo, Investigation of electronic band structure and charge transfer mechanism of oxidized three-dimensional graphene as metal-free anodes material for dye sensitized solar cell application, Chem. Phys. Lett. 685 (2017) 442–450.
[11] H. Li, J. Song, L. Wang, X. Feng, R. Liu, W. Zeng, Z. Huang, Y. Ma, L. Wang, Flexible all-solid-state supercapacitors based on polyaniline orderly nanotubes array, Nanoscale 9 (2017) 193–200.
[12] X. Feng, N. Chen, J. Zhou, Y. Li, Z. Huang, L. Zhang, Y. Ma, L. Wang, X. Yan, Facile synthesis of shape-controlled graphene–polyaniline composites for high performance supercapacitor electrode materials, New J. Chem. 39 (2015) 2261–2268.
[13] J. Zhou, J. Song, H. Li, X. Feng, Z. Huang, S. Chen, Y. Ma, L. Wang, X. Yan, The synthesis of shape-controlled α-MoO_3/graphene nanocomposites for high performance supercapacitors, New J. Chem. 39 (2015) 8780–8786.
[14] K.R. Nemade, Chemically synthesized Sn doped polyaniline hydrochloride for carbon dioxide gas sensing, Sensors Transducers 135 (2011) 110–117.
[15] K.R. Nemade, S.A. Waghuley, Chemiresistive gas sensing by few-layered graphene, J. Electron. Mater. 42 (2013) 2857–2866.
[16] K.R. Nemade, S.A. Waghuley, Preparation of MnO2 immobilized graphene nanocomposite by solid state diffusion route for LPG sensing, J. Lumin. 153 (2014) 194–197.
[17] B. He, Q. Tang, M. Wang, H. Chen, S. Yuan, Robust polyaniline-graphene complex counter electrodes for efficient dye-sensitized solar cells, ACS Appl. Mater. Interfaces 6 (2014) 8230–8236.
[18] D. Choi, G.E. Blomgren, P.N. Kumta, Fast and reversible surface redox reaction in nanocrystalline vanadium nitride supercapacitors, Adv. Mater. 18 (2006) 1178–1182.
[19] B. Sethuraman, K.K. Purushothaman, G. Muralidharan, Synthesis of mesh-like Fe2O3/C nanocomposite via greener route for high performance supercapacitors, RSC Adv. 4 (2014) 4631–4636.
[20] X. Lu, G. Wang, T. Zhai, M. Yu, J. Gan, Y. Tong, Y. Li, Hydrogenated TiO_2 nanotube arrays for supercapacitors, Nano Lett. 12 (2012) 1690–1696.
[21] M. Kaempgen, C.K. Chan, J. Ma, Y. Cui, G. Gruner, Printable thin film supercapacitors using single-walled carbon nanotubes, Nano Lett. 9 (2009) 1872–1876.

30 Effect of Shape on Thermophysical and Heat Transfer Properties of ZnO/R-134a Nanorefrigerant

Available online at www.sciencedirect.com

ScienceDirect

Materials Today: Proceedings 5 (2018) 1635–1639

materialstoday: PROCEEDINGS

www.materialstoday.com/proceedings

PMME 2016

Effect of Shape on Thermophysical and Heat Transfer Properties of ZnO/R-134a Nanorefrigerant *

P.B. Maheshwary[a], C.C. Handa[b], K.R. Nemade[c]*

[a]Department of Mechanical Engineering, JD College of Engineering and Management, Nagpur 441 501, India.
[b]Department of Mechanical Engineering, KDK College of Engineering, Nagpur 400 049, India.
[c]Department of Physics, Indira Mahavidyalaya, Kalamb 445 401, India.

Abstract

Presently, nanorefrigerant becoming the important class of nanofluids due to its heat transfer performances of refrigeration and air-conditioning systems. In the present study, we analyze the effect of shape on the thermophysical and heat transfer properties of ZnO/R-134a nanorefrigerant. The spherical and cubic shape ZnO nanoparticles used in this study for addition in refrigerant. The results of study indicate that the thermophysical and heat transfer properties significantly affected by shape of ZnO nanoparticles. In case of cubic ZnO nanoparticles, 42.5 % of increment observed over the pure refrigerant. This preliminary study about the effect of shape on thermophysical and heat transfer properties shows that ZnO/R-134a nanorefrigerant suitable for refrigeration and air-conditioning systems.

Selection and Peer-review under responsibility of International Conference on Processing of Materials, Minerals and Energy (July 29th – 30th) 2016, Ongole, Andhra Pradesh, India.

Keywords: thermophysical properties; heat transfer; nanorefrigerant; R-134a refrigerant

1. Introduction

Nanorefrigerant is adulterate suspension of solid particles and refrigerant as base fluid. Nanorefrigerants have been found great application in the field of refrigeration and air-conditioning systems because of tunable thermal

* Corresponding author. K.R. Nemade, Tel.: +091-9049703051
E-mail address: krnemade@gmail.com

Selection and Peer-review under responsibility of International Conference on Processing of Materials, Minerals and Energy (July 29th – 30th) 2016, Ongole, Andhra Pradesh, India.

conductivity of refrigerants by addition of nanoparticles. Higher thermal conductivity of nanorefrigerants can extract maximum output from the refrigeration and air-conditioning systems [1]. Addition of metal oxide nanoparticle as an impurity significantly enhances the thermal conductivity of nanorefrigerant [2].

Mahbubul et al analyzed the volumetric effects of thermal conductivity, viscosity and density of Al_2O_3/R141b. The results of this study show that an optimum concentration of nanoparticles in refrigerant can enhance the performance of a refrigeration system [3]. Bi et al investigated the performance of TiO_2-R600a nano-refrigerants in a domestic refrigerator without any system reconstruction. The refrigerator performance was analyzed by using energy consumption test and freeze capacity test. The results of this study show that 9.6% less energy used with 0.5 g/L TiO_2-R600a nano-refrigerant [4]. Sarkar et al reported the thermodynamic properties and optimization cascade system with different natural refrigerants. Their study gives two selection charts along with tables one for higher coefficient of performance and the other for highest volumetric capacity [5]. Jiang et al study shows that the thermal conductivities of carbon nanotube based nanorefrigerants are much higher than those of carbon nanotube -water Nanofluids or spherical nanoparticle-R113 nanorefrigerants [6].

In light of above discussion, it is observed that most of the researchers analyzed the effect of concentration on performance of nanorefrigerants. Thus, in the present study effect of nanoparticle shape on thermal conductivity of nanorefrigerants studied for spherical and cubic shape ZnO nanoparticles loaded R-134a refrigerant. The main accomplishment of the present work is that thermal conductivity of R-134a refrigerant increase by 42.5 % for cubic shape ZnO nanoparticles.

2. Experimental

In the present work, ZnO/R-134a nanorefrigerant was prepared by two step method. In this method, 0.1 (10 %) volume fraction of ZnO added in pure R-134a refrigerant and kept for 2 h under probe sonication process for forceful dispersion of ZnO nanoparticles. All thermophysical and heat transfer properties of ZnO/R-134a nanorefrigerant measured in the temperature range 283-307 K. The viscosity of nanorefrigerant of different particle shape was determined using AR-1000 Rheometer, TA Instrument. The thermal conductivity and specific heat measurements were carried out by using KD2 pro thermal analyzer (Decagon Devices).

3. Results and Discussion

Figure 1(a) shows the SEM image of spherical ZnO nanoparticles. SEM image revealed that ZnO used for the dispersion in R-134a refrigerant is nearly spherical. The average particle size of spherical ZnO nanoparticles estimated using the SEM images was found to be 29.1 nm. Figure 1 (b) represents the SEM image of cubic shape ZnO nanoparticles dispersed in R-134a refrigerant. The average particle size of cubic ZnO nanoparticles was found to be 21.4 nm. Figure 1 (c) depicts the XRD pattern of ZnO nanoparticles. The diffraction peaks position in XRD pattern of ZnO reflects the crystalline purity of used ZnO nanoparticles. The peak position in XRD pattern of ZnO nanoparticles shows excellent agreement with JCPDS file no.36-1451. The JCPDS data card shows that ZnO has hexagonal wurtzite structure. The lattice parameters of ZnO nanoparticles are with a = 3.25 Å and c = 5.2 Å and its ratio is c/a ~ 1.60. The data card also shows that ZnO nanoparticles belongs to space group C6mc. The average particle size was computed using Debye-Scherrer equation. The average crystallite size for ZnO nanoparticles estimated using this information was found to be 25.7 nm.

The viscosity of ZnO nanoparticles dispersed refrigerant was calculated using Brinkman model [7],

$$\mu_{nr} = \mu_r \frac{1}{(1-\phi)^{2.5}}$$

where, μnr and μr are the effective viscosity of ZnO nanoparticles dispersed refrigerant and pure refrigerant, respectively. ϕ is the particle volume fraction which is 0.1 (10 %) in present study. Figure 2 depicts the variation of viscosity with temperature for pure R-134a refrigerant, spherical and cubic ZnO loaded R-134a nanorefrigerant. The spherical and cubic ZnO loaded R-134a nanorefrigerant shows typical behavior.

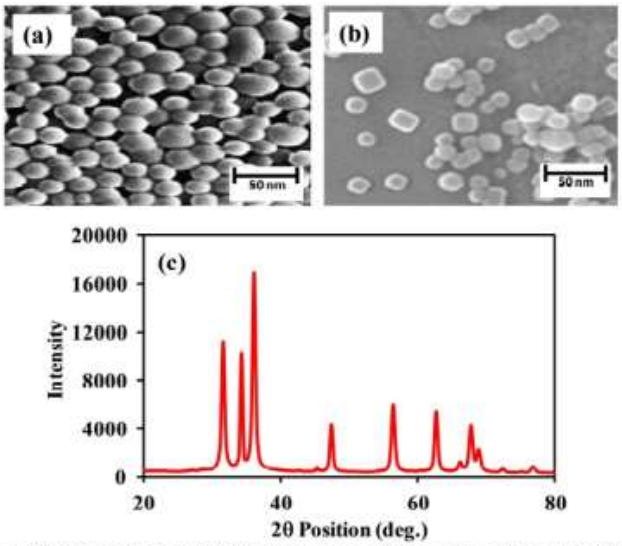

Figure 1. SEM images of (a) Spherical and (b) Cubic shape ZnO nanoparticles and (c) XRD pattern of ZnO nanoparticles.

The viscosity of nanorefrigerant decreases with increase in temperature for systems that is spherical and cubic ZnO loaded R-134a nanorefrigerant. This decrease in viscosity assigned to the sub-micron dispersion behaves like a liquid. The obtained results in our case as a function of temperature is parallel to results reported by Mahbubul et al [8]. Another possible reason for decrease in viscosity with increasing temperature is weakening of adhesion forces among the particles and base fluid molecules [9]. From Figure 2, it is also observed that cubic shape ZnO nanoparticles loaded R-134a nanorefrigerant has higher viscosity value than spherical shape ZnO nanoparticles. The higher value of viscosity in case of cubic shape nanoparticles may be due to cubic shape nanoparticles are difficult to rotate. The difficulty in the rotation increases the viscosity of nanorefrigerant.

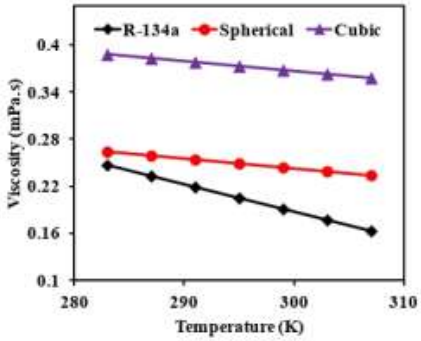

Figure 2. Influence of spherical and cubic shape ZnO nanoparticles on viscosity of R-134a refrigerant.

The variation of density with respect to temperature of pure refrigerant and spherical and cubic ZnO loaded R-134a nanorefrigerant has been shown in Figure 3. The plot shows that density of pure refrigerant and spherical and cubic ZnO loaded R-134a nanorefrigerant decreases moderately with the increase of temperature. The value of density found higher for cubic shape ZnO loaded R-134a nanorefrigerant. All samples show the typical behavior as

a function of temperature. At 283 K, cubic shape ZnO loaded R-134a nanorefrigerant show enhancement in density of the order of 22.62 % over pure R-134a refrigerant.

Density is mass and volume based parameter. With increase in temperature, molecules of refrigerant undergoes to vibration which increases volume. Hence the density of refrigerant was decrease monotonically with temperature. The density of solid particles is much greater than liquid or gases. Therefore, spherical and cubic ZnO loaded R-134a nanorefrigerants have higher density than pure R-134a refrigerant. The optimized value of cubic shape ZnO loaded R-134a nanorefrigerants attributed to the higher volume of cubic shape object.

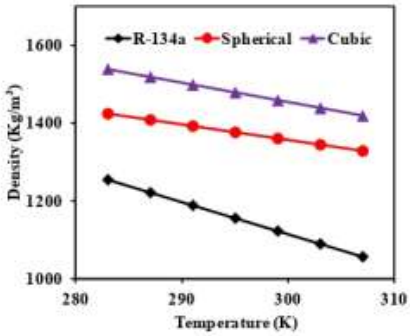

Figure 3. Influence of spherical and cubic shape ZnO nanoparticles on density of R-134a refrigerant.

The specific heat of pure R-134a refrigerant, spherical and cubic ZnO nanoparticle loaded R-134a refrigerant linearly increase with the temperature as shown in Figure 4. For fixed value of concentration of nanoparticles, specific heat of nanorefrigerant decreases than pure R-134a refrigerant. This decrease in specific heat with the addition of nanoparticles is attributed to the lower specific heat of added particles. The increasing temperature results in the fluctuation of refrigerant molecules about their equilibrium value to a higher extent, which increases heat capacity. The increases in heat capacity increases internal energy of the system. The result obtained in our case is parallel with most of the researchers [10].

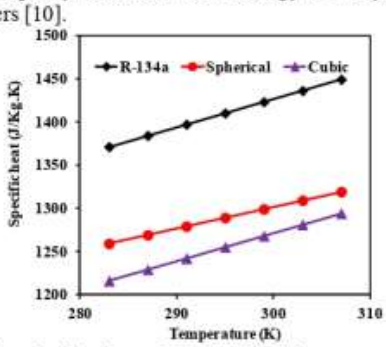

Figure 4. Influence of spherical and cubic shape ZnO nanoparticles on specific heat of R-134a refrigerant.

Figure 5 depicts the variation of thermal conductivity of pure refrigerant and nanorefrigerant with temperature. It can be observed in Figure 1, the thermal conductivity of nanorefrigerant was increases linearly with temperature. The thermal conductivity of pure R-134a refrigerant decreases linearly with increasing temperature. The increase in thermal conductivity of nanorefrigerant is attributed to the higher thermal conductivity of ZnO nanoparticles. The decreases in thermal conductivity of pure R-134a refrigerant may be due to the evaporation of refrigerant molecules. The increment in thermal conductivity due to addition of spherical and cubic ZnO nanoparticles over pure R-134a refrigerant is 25.26% and 42.5 %, respectively.

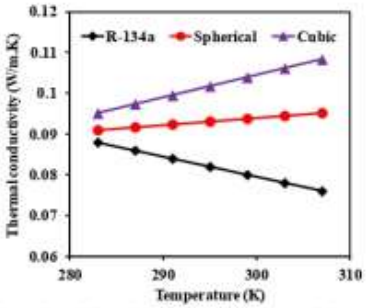

Figure 5. Influence of spherical and cubic shape ZnO nanoparticles on thermal conductivity of R-134a refrigerant.

4. Conclusions

In the summary of present work, thermophysical and heat transfer properties of ZnO/R-134a nanorefrigerant analyzed for two different shapes of ZnO nanoparticles with respect to temperature. The major outcomes of this study could be drawn as follows,

- The addition of spherical and cubic shape ZnO nanoparticles in R-134a refrigerant increases viscosity of nanorefrigerant. Cubic ZnO loaded nanorefrigerant has higher value of viscosity.
- Similar observation is made for density of spherical and cubic shape ZnO nanoparticles loaded in R-134a refrigerant.
- Specific heat of ZnO nanoparticles loaded nanorefrigerant found to be lower than pure R-134a refrigerant.
- The significant enhancement in the thermal conductivity of spherical and cubic shape ZnO nanoparticles in R-134a refrigerant observed of the order of 25.26% and 42.5 % respectively.

Acknowledgements

The authors very much thankful to Principal, KDK College of Engineering, Nagpur, India for providing necessary facilities for the work.

References

[1] I.M. Mahbubul, et al., Int. J. Heat Mass Transfer 57 (2013) 100–108.
[2] R. Saidur, et al., Renew. Sustain. Energy Rev. 15 (2011) 310–323.
[3] I.M. Mahbubul, et al., Procedia Engineering, 56 (2013) 310-315.
[4] S. Bi, et al., Energy Conversion and Management 52 (2011) 733–737.
[5] J. Sarkar, et al., Proceedings of the Institution of Mechanical Engineers Part A: Journal of Power and Energy, 227 (2013) 612-622.
[6] W. Jiang, et al., Int. J. Thermal Sciences, 48 (2009) 1108-1115.
[7] H. Brinkman, et al., J. Chem. Phys. 20 (1952) 571-577.
[8] I.M. Mahbubul, et al., International Journal of Heat and Mass Transfer 85 (2015) 1034–1040.
[9] C.T. Nguyen, et al., Int J Heat Fluid Flow, 28 (2007)492–506.
[10] I.M. Shahrul, et al., Renew. Sustain. Energy Rev. 38 (2014) 88–98.

31 Mindfulness and Life satisfaction: A review

VOLUME - VII, ISSUE - IV OCTOBER - DECEMBER - 2015
AJANTA - ISSN 2277 - 5730 - IMPACT FACTOR - 5.5 (www.sjifactor.com)

4. Mindfulness and Life satisfaction: A Review

Dr. Madhukar K. Tajne
Research Guide, Late Wamanrao Pitambare Arts, Commerece, Sience and Management College
Padegaon, Aurangabad.
P. B. Ingle
Research Scholar.

Abstract

The purpose of this review was to understand the association between mindfulness and life satisfaction and contribution to current knowledge in the domain of life satisfaction and mindfulness. Second aim was to investigate the impact of mindfulness as an intervention on low life satisfactions; more one was to verify findings for future research. A review was conducted through various database like e-list.inflibnet, Googel Scholar, result of this paper shows that mindfulness and life satisfaction is positively associated with each other.

Keywords: mindfulness, life satisfaction, Happiness, Well-being review.

Introduction

Life Satisfaction

Every person has desire to 'ive happy his or her life. This concept is defined largely in the past literature. It is a state of mind, it tends to remove the negative thoughts and replace it rather than positivity. it is the path upon that people show their self mood, feeling, emotions and evaluate their life future direction and options. There are several factors which effect life satisfaction like personality, self – esteem, age, value, culture, family, life events and it was see. scientifically determined. Several studies show that Big Five Factor Model is one more concept of personality. This model consisted with openness to experience, consciousness, extraversion agreeableness and neuroticism. Costeve and Cooper (1998) analyzed several studies with certain personality tests are linked with subjective well being and personality measures. They found that neuroticism was major role in predicting life satisfaction and linked with those people who have suffering from mental illness. The openness to experience is the factor positively correlated with life satisfaction. Apartform this the Big Five Model; the trait prototype shows the relationship with life satisfaction. Morning-oriented people (larks) show higher life satisfaction than the evening- oriented (Owls) Hoyelt, A. J., Dopko, R. L., Passmore, H. A., & Buro, K.(2011). Self-

esteem plays an important role to define influencing life satisfaction. Previous modeling shows that positive views and life satisfaction determined completely by self esteem Cummins, Robert (2002). According to Bailey, T., Eng, W., Frisch, M. & Snyder, C. R. (2007), A Person's perception toward stimuli (life) and emotion have great impact on life satisfaction. There are two kind of emotions that influence on life satisfaction they are Hope and Optimism. It consists of cognitive process emphasis on the perception of goals. Optimism is associated with higher life satisfaction and pessimism is related to the depression (Chang, E. C., & Sanna, L. J. (2001). Furthermore, Seligman (2012), reported that the happier people focus on the negative aspects of their lives and they like other people, which promotes a happier environment. This correlates to a higher level of the person's satisfaction with his or her life, because of the notion that constructiveness with others can positively influence life satisfaction. It is indentified that age is one of the most important aspect of the life satisfaction (Pelgi, Y. Shmotkin, D. (2010). the experiment on how life satisfaction grows as people become older because they become wiser and more knowledge, so they being to see that life will be better as they grow older and understand the important things in life more. Also it was found that life satisfaction in term of sexuality comes in to increase. This is because at this age many adolescents reach sexual maturation, which can encourage them to find verification and satisfaction in the idea of sexual partnership (Goldbeck, Lutz, Schmitz, Tim, G. Besier Tanja, Herschbach.Peter, Henrich, Gerhard , 2007). It was found that value of materiality impact higher on the life satisfaction of the person than the person who has not give the important of materiality, Keng, Ah, Kwon, Jung, Jochen, Wirtz, (2000). Communication in family member is very essential process because research found that life satisfaction is depend on communication of family member Hubbard, A. (2018).

Mindfulness

Mindfulness is the phenomenon in mind which indicated how the person or object is aware about awareness of self. It is a mental process, it can been measured today by modern techniques like psychological Questionnaires; based on self-reporting of trait; Mindfulness Attention Awareness Scale(MAAS), Freiburg Mindfulness Inventory (FMI), Kentucky Inventory of Mindfulness Skills (KIMS), Cognitive and Affective Mindfulness Scale (CAMS), Mindfulness Questionnaire (MQ), Revised Cognitive and Affective Mindfulness Scale(CAMS-R) and so on., Many studies shows the data bout mindfulness in the setting of medical

perspectives. A group of psychiatric at Melbourne, reviewed previous meta -analytical studies and present background to the practice of Mindfulness-based therapies as relevant to the general professional reader. They have addressed the empirical evidence for these therapies, the principles through which they might be operate some practical questions facing those wishing to commence practice in this area or send patients into mindfulness-based. They have some considerations relevant to the conduct and interpretation of research into the therapeutic application of mindfulness.

Methods

Procedure of search: a literature was collected by using electronic database PsyINFO, n-list,inflibnet, Google Scholar. First set the concept life satisfaction in google scholar and select review which are more relevant to the research topic. Life satisfaction 'AND' Then word well-being was searched on academic journals only. Second set the word Mindful, Mindfulness etc. and collect the information from the site.

Result

After the previous research is verified form 2010 to till date, it is identified that new trend in the applied psychology is applied to this concepts for various perspectives.

Meditation is one then clinical field as well as positive psychological based application.

It is also seen that mindfulness and life satisfaction is positively correlated with each others. Life satisfaction is depend on various angle of the life of the individual.

Limitation of review

This review papers cover the literature a little more than 10 years back so that there is not sufficient work for generalize the result of the above stated problem of the papers.

Implication and future research

Mindfulness and Life satisfaction research may be applied in the various field of psychology to the understanding the various perspectives related with this concepts and knowledge to how to solve the problems regarding depression, anxiety, and personality related disorders as well as this review can be helpful to the other researchers, psychologist, counselor, teachers to extend their experience and good result in their work. There is some suggestion for the future research in taking into consideration of the limitation of this review article. It is seen that in previous research there is lack of randomized techniques so there should be use randomized sample.

Conclusion

The purpose of this review article was to focus the previous literature in order to understand mindfulness and life satisfaction relationship. There was criteria to review the literature that back ten years from till. This review article shows that life satisfaction is observed by researchers to identify the core aspect of life such family, environment, workplace, clinical and values etc. Mindfulness is mental process can be useful to determine the characteristics of the individual who have the ability to live satisfied in his life.

References

1) Academic Mindfulness Interest Group, M., & Academic Mindfulness Interest Group, M. (2006). Mindfulness-based psychotherapies: a review of conceptual foundations, empirical evidence and practical considerations. *Australian and New Zealand Journal of Psychiatry*, *40*(4), 285-294.

2) Bailey, T., Eng, W., Frisch, M. & Snyder, C. R. (2007). Hope and Optimism as related to life satisfaction. *Journal of Positive Psychology*, 2(3), page 168-69.

3) Chang, E. C., & Sanna, L. J. (2001). Optimism, pessimism, and positive and negative affectivity in middle-aged adults: a test of a cognitive-affective model of psychological adjustment. *Psychology and Aging*, 16 (3), 524-531.

4) Cummins, Robert (2002). *Normative Life Satisfaction: Measurement Issues and a Homeostatic Model* (PDF) (Report). Retrieved 15 Oct. 2018.

5) Deneve, K. M. & Cooper H. (1998). The happy personality: A meta-analysis of 137 personality trait and subjective well-being. *Psychological Bulletin* 124, 197-229.

6) Goldbeck, Lutz, Schmitz, Tim, G. Besier, Tanja, Herschbach, Peter, Henrich, Gerhard. (2007). Life satisfaction decreases during adolescence. *Quality of Life Research*. 16 (6): 969-979.

7) Howell, A. J. Dopko, R. L. Passmore, H. A. & Buro, K. (2011). Nature connectedness: Associations with well-being and mindfulness. Personality and Individual differences, 51,(2), 166-171.

8) Hubbard, A. (2018). Evaluating Relational Factors as Possible Protective Factors for Work–Life Balance via a Linear Mixed Effects Model. In *The Work-Family Interface: Spillover, Complications, and Challenges* (pp. 349-364). Emerald Publishing Limited.

32 Enhancement of photovoltaic performance of polyaniline/graphene composite-based dye-sensitized solar cells by adding TiO2 nanoparticles

Solid State Sciences 83 (2018) 99–106

Contents lists available at ScienceDirect

Solid State Sciences

journal homepage: www.elsevier.com/locate/ssscie

Enhancement of photovoltaic performance of polyaniline/graphene composite-based dye-sensitized solar cells by adding TiO_2 nanoparticles

Kailash Nemade[a,*], Priyanka Dudhe[b], Pradip Tekade[b]

[a] Department of Physics, Indira Mahavidyalaya, Kalamb 445 401, India
[b] Department of Chemistry, Jankidevi Bajaj College of Science, Wardha 442 001, India

ARTICLE INFO

Keywords:
Photovoltaic
Polyaniline
Graphene
TiO_2

ABSTRACT

Polyaniline (PANi)-graphene composites and polyaniline-graphene/TiO_2 composites were prepared by ex-situ approach. Systematic investigation was carried out to explore photovoltaic (PV) properties of PANi-graphene and PANi-graphene/TiO_2 composite. The prepared composites were characterized using X-ray diffraction (XRD), Scanning Electron Microscope (SEM), Raman Spectroscopy and Ultraviolet–Visible (UV–Vis) Spectroscopy. The PV properties of dye-sensitized solar cells (DSSCs) prepared composites investigated by assembling materials in ITO/PANi-graphene/Al and ITO/PANi-graphene/TiO_2/Al architecture. Different PV parameters such as short circuit current, open circuit voltage, fill factor and power conversion efficiency were determined from the (Current-Voltage) IV characteristics of PV cell. The 15 wt% PANi loaded graphene composite based PV cell shows optimized power conversion efficiency of the order 6.47%. The main accomplishment of present work is that efficiency associated with 15 wt% PANi loaded graphene composite, improved further by addition of TiO_2 nanoparticles. The composite system between PANi-graphene/TiO_2 for 1 wt% of TiO_2 nanoparticles shows optimized power conversion efficiency of the order 8.63%.

1. Introduction

Global demand of energy rising gradually, due to heavy industrialization and urbanization. Developed countries have huge demands of energy while demand is going on increasing in developing countries. The International Energy Agency states that energy needs are projected to expand by 55% till 2030 [1]. But unfortunately, the complete demand of energy is satisfied through non-renewable energy sources such as coal, petroleum, and natural gas. The exploitation of non-renewable energy sources results in range of adverse effects like air and water pollution, damage to public health, global warming and unnecessary atmospheric changes. Key solution for this issue is to use renewable energy sources such as hydropower, geothermal, wind and solar energy instead of non-renewable energy sources. Among these renewable energy sources, solar energy is best option due to outstanding characteristics such as the most abundant, inexhaustible and clean of all the renewable energy resources till date.

Across the globe researchers takes great interest in identification of alternative materials to silicon. The downside associated with silicon-based photovoltaic (PV) cell technology is their manufacturing requires costly ultra-high-purity silicon. Also, this process of manufacturing of PV cell results in significant carbon emission. Organic materials are considered as close competitive and alternative to the standard silicon-based PV cell technology. The main causes behind the development of organic PV cell technology are less expensive, thinner, more flexible, and amenable to a wide range of lighting conditions. Another interesting reason is low material consumption results in a high absorption coefficient [2]. Some other advantages of organic PV cells are low specific weight, mechanical flexibility, tunable material properties and high transparency [3].

During literature survey on organic PV materials, we come across three efficient materials which exhibits outstanding PV properties. These three materials are polyaniline, graphene and TiO_2 nanoparticles. Among the conducting polymers such as polyaniline (PANi), polypyrrole (PPy) and polythiophene (PTh), PANi has been extensively studied by researchers.

Conducting polymer is the class of materials, which is fit for photovoltaic application and device fabrication. This is because of outstanding characteristics such as intrinsically stable photoexcitation with visible light, high photon harvesting efficiency, tunable band gap engineering on the entire visible spectral range and large charge generation when mixed with electron acceptor materials [4].

PANi display good electron conducting behaviors, interesting redox behavior, high environmental stability and controllable electrical and

* Corresponding author.
E-mail address: krnemade@gmail.com (K. Nemade).

https://doi.org/10.1016/j.solidstatesciences.2018.07.009
Received 9 May 2018; Received in revised form 14 July 2018; Accepted 16 July 2018
Available online 17 July 2018
1293-2558/

optical properties [5–7]. All these outstanding features of PANi attributed to the delocalized π-electron structure. The optical absorption coefficient of organic molecules specially in case of PANi is very high. Therefore, large amount of light can be trap by an insignificant amount of materials [8].

Graphene possesses a substantial number of wonderful optical and electronic properties, such as zero band-gap, semi-conducting with a high carrier mobility and high optical transparency, which generally not observed in other materials [9]. It is well accepted principle for organic PV cells that optimization of both charge transport and optical properties are necessary for good performance.

Out of many semiconducting metal oxides, TiO_2 has some attractive features for PV cell application. TiO_2 nanomaterial suitable for PV cell application due to its high chemical and optical stability, non-toxicity, low cost, corrosion resistance and ease of synthesis [10,11]. Many reports show that graphene–TiO2 nanocomposites possess superior photovoltaic properties than pristine TiO_2 [12].

The composite preparation using organic and inorganic constituent's results in improved electronic properties. It is well known principle of materials science that in synergetic state, physical and chemical properties of most of the composite improves. Therefore, in this section it is analyzed using some reports on PV properties of PANi-Metal Oxide composite. The addition of metal oxides impurity in PANi enhance the PV properties and increase the efficiency of solar cells.

Ameen et al. fabricated TiO_2/PANi and dye absorbed TiO_2/PANi electrodes by plasma polymerization for solar cells application. The results of the study indicate that dye absorbed TiO_2/PANi electrode based DSSCs have high charge carrier transportation between the TiO_2 and PANi layer. This rapid charge transportation in dye absorbed TiO_2/PANi electrode improves the performance of solar cell than the TiO_2/PANi electrode [13]. Shen et al. architecture PV cell with layers ITO/nano-crystalline TiO_2/PANi/Aluminum. This shows largest open voltage of 0.397 V and short current density of 65.9 μA/cm^2 under simulated solar radiation. Using current-voltage characteristics, the formation of p-n junction between nano-crystalline TiO_2 and PANi interface is also verified [14]. Yang et al. synthesized grafted aniline on aminobenzoate monolayer to adsorbed TiO_2 nanocrystal to fabricate a uniform core/shell structured TiO_2/PANi nanocomposite. The DSSC fabricated with an electrode of TiO_2/PANi film have considerably high short circuit current density of 0.19 mA/cm^2 and an open circuit voltage of 0.35 V [15]. Zhu et al. adopted the two-step process to prepared PANi hybridized ZnO photoanode on FTO substrate. The results of the study show that light-conversion efficiency of PANi hybridized ZnO nanograss improves by 60% than pure ZnO nanograss photoanode [16]. Momeni et al. studied the dye-sensitized solar cell based on TiO_2 nanotube arrays. In this work, TiO_2 nanotubes were prepared by two different approaches namely one-step and two-step process. This work concludes that TiO_2 nanotubes prepared using two-step process shows higher efficiency [17]. Bahramian et al. prepared in situ PANi-based counter electrode and coral-likeTiO_2 to assemble DSSC with transparent PANi films as counter electrode. This bifacial DSSC have power conversion efficiency of 8.22%, which is assigned to excellent light scattering by the coral-like TiO_2 and high specific surface area of PANi nanofibers [18]. Duan et al. fabricated the DSSC with PANi incorporated TiO_2 anodes, PANi counter electrodes, and iodide doped PANi solid-state electrolytes. The results of the study show that DSSC with proper assembly process and iodide dosage provides good PV performances with power conversion efficiency of 3.1% [19].

The humankind has been gifted by many brilliant materials by nature, one of those is Graphene. Graphene possess noticeable enigmatic optical and electronic properties such as zero band gap, high carrier mobility, high optical transparency. The synergetic phase of graphene with PANi, also results in efficient PV materials. Some reports on PANi-Graphene composite have been reviewed in this section.

Wang et al. prepared graphene/PANi nanocomposite by polymerization of aniline monomer in situ method. In DSSC, graphene/PANi nanocomposite deposited on FTO, which gives power conversion efficiency of 6.09% compared to 6.88% of efficiency for PV cell with expensive Pt counter electrode under similar experimental conditions [20]. Liu et al. designed DSSC by coating a nanocomposite thin film of graphene/PANi on FTO glass by electro-polymerization method. In comparison, graphene/PANi based electrode has power conversion efficiency of 7.17%, which is close to 7.24% of a DSSC with a Pt counter electrode. This study shows that graphene/PANi electrode has potential to replace conventional Pt counter electrode in DSSC [21]. Dinari et al. designed the Pt free DSSC using PANi-Graphene quantum dots by in situ electrochemical polymerization on FTO coated glass. The synergistic effect between PANi and graphene quantum dots provides higher electrochemical catalytic activity which resulted into improved PV performance with power conversion efficiency of 1.6% [22].

Loryuenyong et al. fabricated DSSCs with counter electrode based on PANi-graphene hybrid material. The counter electrode was prepared by depositing material on FTO by drop casting method. The PANi/graphene hybrid counter electrode exhibits superior PV performance with open circuit voltage of 0.57 V, Short Circuit Current of 5.15 mA cm^{-2}, fill factor of 0.40 and power conversion efficiency of 1.16% which results in improved PV performance than DSSC based on Pt electrode [23]. Yang et al. synthesized multilayer counter electrodes from positively charged PANi-graphene complex and negatively charged platinum nanoparticles with different number of layers and different concentration of graphene in PANi-graphene complex. This work concludes that the electron migration from graphene to PANi helped in good charge transfer. This multilayer interface based DSSC has power conversion efficiency of 7.45%. This work also pointed that multi-interfacial counter electrodes are suitable for robust DSSC [24].

During literature survey, it is observed that PANi, TiO_2 nanoparticles and Graphene have much potential to improve their PV properties. The necessity of development of new kinds of PV materials with improved power conversation efficiencies is being touched by different research groups across the globe. Therefore, the problem is identified on the basis of following remarks:

- During study, it is observed that concentration of impurity in composite has play crucial role. Therefore, in this work it planned to investigate optimized composition of PV material based on PANi and graphene.
- In second step, after successful finding of optimized composition, another impurity that is TiO_2 used for further enhancement of PV properties of PANi-graphene composite.

Therefore, the objectives of present work are to prepare and optimized PV properties of PANi-graphene composite. Then prepare and optimized TiO_2 nanoparticles loaded PANi-graphene composite for PV application.

2. Experimentation

2.1. Preparation of materials

2.1.1. Preparation of PANi

In the present work, PANi was synthesized by using chemical oxidative method. In this method, ammonium persulfate was used as an oxidizing agent. All chemicals required for the preparation of PANi procured from SD fine, India of AR grade and used without further purification. In the process of preparation of PANi, following steps were executed,

- During the synthesis of PANi, one condition is imposed on molar ratio between ammonium persulfate to aniline monomer should not exceed the ratio ≤1.15. The reason behind this condition is to obtain high conductivity and yield [25].
- With this condition, both aniline monomer and ammonium

persulfate dissolve separately in aqueous (100 ml) medium.

- Subsequent to this step, the solution of aniline monomer was added in ammonium persulfate solution in dropwise manner under magnetic stirring.
- The greenish-black precipitate was observed in beaker with increase in temperature.
- This precipitate was kept for overnight (24 h) for good quality polymerization.
- On next day, precipitate was washed three times with distilled water to remove un-reacted contents in product.
- The obtained product was dried at 50 °C and used for further process.

2.1.2. Preparation of PANi/Graphene composites

The *ex-situ* approach was adopted for the preparation of PANi/Graphene composite. The graphene required for the composite preparation was prepared by previously reported method [26]. The weight % (wt.%) stoichiometry was adopted for the preparation of composites. The wt.% stoichiometry was calculated using relation (Eq. (3.1)),

$$wt.\ \% = \frac{A}{(A+B)} \times 100 \tag{3.1}$$

where A and B are constituents of composite.

In our case, the content of PANi in composite was varied for 5–20 wt % by an interval of 5 wt%. In this way, four samples were obtained. During preparation of composite, both constituents of composite was added in 25 ml acetone under magnetic stirring at room temperature.

2.1.3. Preparation of PANi/graphene-TiO_2 composites

PANi/Graphene-TiO_2 composites was also prepared by ex-situ approach. In this process, TiO_2 was directly procured from SD fine, India of high purity. This TiO_2 was probe sonicated using sonicator (PCi, 750-F, PCI Analytics Pvt Ltd). This process of probe sonication, splits the TiO_2 particles up to the nano-dimensions. As-obtained TiO_2 nanoparticles, was used for the preparation of composites. By adopting wt.% stoichiometry, four samples of PANi/Graphene-TiO_2 composites were prepared by varying content of TiO_2 nanoparticles in composite from 0.5 to 2 wt% by an interval of 0.5 wt%. The optimized stoichiometry between PANi and graphene were used further for addition of TiO_2 nanoparticles, to improve PV properties. Here also, acetone was used as an organic media for the preparation of composites. For dye sensitization process, Ru-based N719 dye was used by preparing media of 0.25 mM ethanolic solution of dye N719.

2.2. Fabrication of photovoltaic cell

The doctor blade technique was used to fabricate the PV cells. During this process, the composites was sandwiched between cleaned ITO plate as transparent electrode and Aluminum electrode. The aluminum foil was used as metallic electrode for the PV cell. ITO plate (Dimension: 25 mm × 25 mm) used in this work was procured from Techinstro (ITO-SE-011), India. With the help of temporary binder (based on 3% ethyl cellulose and 97% butyl digol), composite was deposited on ITO electrode and then Aluminum electrode was deposited. This fabricated cell allows to dry at 40 °C for 3 h for evaporation of volatile organic compounds. The thickness of deposited layer controlled by thickness of transparency used during doctor blade technique. In this way, PV cells were fabricated for further study. The side face of fabricated PV cell is depicted in Fig. 1.

2.3. Measurements of photovoltaic characteristics

The current-voltage (IV) characteristics of PV cell collected under incandescent light bulb of power 0.2956 Watt/m^2. The separation between incandescent light source and PV cell was about 15 cm. The important diode parameters like open circuit voltage (V_{OC}), short circuit current (I_{SC}), fill factor (FF), and power conversion efficiency (η) were measured under these conditions, which reproduced without any considerable deviation. The FF of PV cell computed using relation Eq. [1] [27]:

Fig. 1. Side face of fabricated PV cell.

$$FF = \frac{I_{MAX} \times V_{MAX}}{I_{SC} \times V_{OC}} \tag{1}$$

Whereas, power conversion efficiency (%η) of PV cell estimated using the relation Eq. [2]. [28],

$$\%\eta = \left(\frac{I_{SC} \times V_{OC} \times FF}{P_{in}}\right) \times 100 \tag{2}$$

The FF and %η are the crucial parameters for any PV cell. On the basis of these parameters, it is possible to discriminate any PV cell and its performance.

3. Results and discussion

3.1. Materials characterization and PV properties of PANi/Graphene

3.1.1. XRD analysis

Fig. 2 (a) shows the XRD pattern of pure PANi synthesized by chemical oxidative method. The XRD pattern of pure PANi comprises only one broad peak around 26°, which indicates the poor crystallinity phase of PANi. This broad peak is also assigned to the scattering from the PANi chains at inter planar spacing [29]. Fig. 2 (b) depicts XRD pattern of graphene, which has well structural, and phase purity. The XRD of graphene possesses two signature peaks at 26.3° (002) and 44.2° (100). The peak at 2θ = 26.3° indicates well organized structure of graphene with an interlayer spacing of 0.339 nm. This layer spacing is

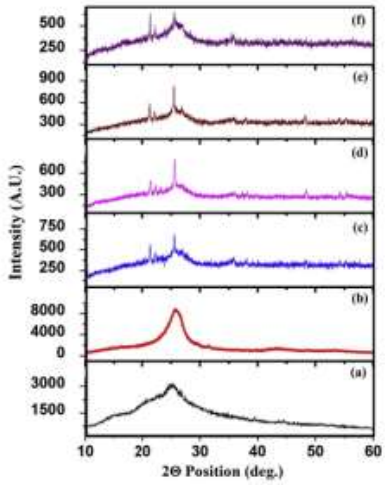

Fig. 2. XRD pattern of pure (a) PANi, (b) graphene and (c) 5 wt%, (d) 10 wt%, (e) 15 wt%, (f) 20 wt% PANi loaded graphene composites.

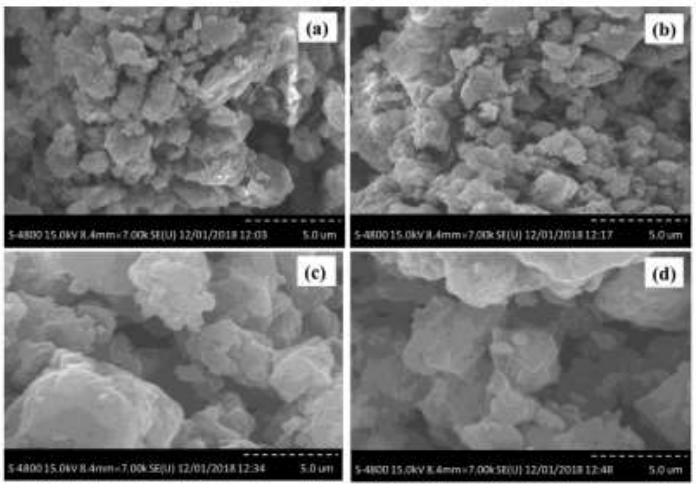

Fig. 3. SEM images of (a) 5 wt%, (b) 10 wt%, (c) 15 wt% and (d) 20 wt% PANi loaded graphene composites.

in agreement with spacing in graphite. The broad peak at $2\theta = 44.2^{\circ}$ is attributed to presence of some defects [30]. Fig. 2 (c, d, e and f) shows the XRD pattern of 5 wt%, 10 wt%, 15 wt% and 20 wt% PANi loaded graphene composites, respectively. XRD pattern shows that with an increase in PANi content in composites, noisy behavior of pattern increases. This indicates that crystalline nature of composites decreases. Sharp peaks appear between 20 and 26° is attributed to the presence of smaller crystalline regimes in composites. The decrease in peak height intensity of composites than graphene and PANi, justify the formation of composites.

3.1.2. Morphology study

Fig. 3 shows the SEM images of (a) 5 wt%, (b) 10 wt%, (c) 15 wt% and (d) 20 wt% PANi loaded graphene composites prepared by ex-situ approach. In all cases, graphene sheets are homogeneously dispersed in PANi. At fixed resolution, one thing is observed from SEM images that agglomeration phenomenon increases with wt.% of PANi. All composite samples have irregular shape.

3.1.3. Raman Spectroscopy

Fig. 4 depicts the Raman spectra of 15 wt% PANi loaded graphene composite, which is optimized sample in PV study. The C – N stretching vibration from benzenoid structure appears through band 1548 cm^{-1}. The semi-benzenoid polaronic band of C–N^{+} appears at 1318 cm^{-1} and plane bending vibration of CH is appears at 1200 cm^{-1}. The Raman spectrum comprises clear band D (1325 cm^{-1}) [31], G (1598 cm^{-1}), and 2D (2695 cm^{-1}), which are signature band of graphene [32–34]. The shift in band position is observed, which is attributed to the structural changes in resultant composite. The quinoid rings in the PANi have a similar atomic structure with the C6 rings of graphene. This situation in both constituents allow for a strong π -π stacking interaction and beneficial for electronic transmission [35].

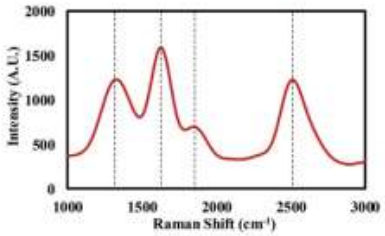

Fig. 4. Raman spectrum of 15 wt% PANi loaded graphene composite.

3.1.4. Optical properties

In PV technology, optical properties of PV materials play crucial role. Therefore, in our case it is studied using UV-VIS spectroscopy. In PV cell technology, both types of band gap materials that is low-band gap and high-band gap materials have their own importance. Therefore, by combining appropriate materials to obtain band gap which efficiently used available solar radiations is necessary. This is necessary, if the band gap is very small than incident photon energy, then considerable photon energy converted in heat energy, which raise the temperature of PV materials. On other hand, if the band gap is very large, it restricts the transition between valance band to conduction band [36].

Fig. 5 shows the UV-VIS spectrum of 5 wt%, 10 wt%, 15 wt% and 20 wt% PANi loaded graphene composites. From plot, it is clearly

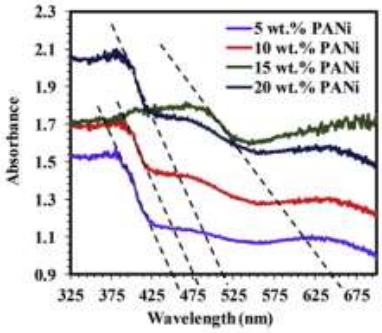

Fig. 5. UV-VIS spectrum of 5 wt%, 10 wt%, 15 wt% and 20 wt% PANi loaded graphene composites.

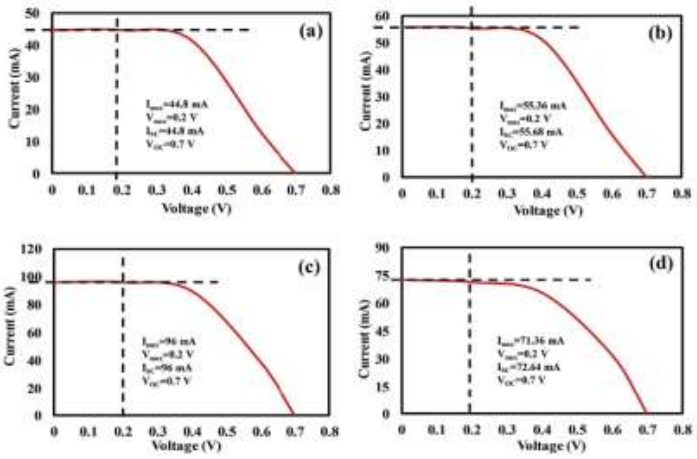

Fig. 6. PV response of (a) 5 wt%, (b) 10 wt%, (c) 15 wt% and (d) 15 wt% PANi loaded graphene composite.

observed that the samples 5 wt%, 10 wt% and 20 wt% PANi loaded graphene composites have absorption tail at lower wavelength than 15 wt% PANi loaded graphene composites. The band gap values for as-prepared composite samples (estimated using frequency-wavelength relation) ranges between 2.73 and 1.92 eV. The lowest value of band gap is associated with 15 wt% PANi loaded graphene composite.

3.1.5. PV performance

Fig. 6 shows the PV response of (a) 5 wt%, (b) 10 wt%, (c) 15 wt% and (d) 15 wt% PANi loaded graphene composite based DSSCs. All diode parameters like I_{max}, V_{max}, I_{SC}, V_{OC}, FF and %η are provided in Table 1. Among all PV cells, the response of 15 wt% PANi loaded graphene composite has highest power conversion efficiency of order 6.479% (FF = 0.285). The highest power conversion efficiency was attributed to lower band gap value (1.92 eV) of 15 wt% PANi loaded graphene composite. All samples have stable diode parameters and reproducible results.

Fig. 7 shows the variation of FF and %η as a function wt.% of PANi in composite. Plot shows that 15 wt% PANi loaded graphene composite has highest power conversion efficiency. The possible reason for highest power conversion efficiency may be

Table 1
PV parameters of TiO_2 nanoparticles loaded PANi-graphene composites and PANi loaded graphene composites.

TiO_2 nanoparticles loaded PANi-graphene composite						
Wt.% of TiO_2 nanoparticles	I_{max} (mA)	V_{max} (V)	I_{SC} (mA)	V_{OC} (V)	FF	%η
0.5 wt%	95.17	0.2	95.23	0.8	0.2499	6.43
1 wt%	127.71	0.2	127.79	0.8	0.2498	8.63
1.5 wt%	106.59	0.2	106.65	0.8	0.2498	7.21
2.0 wt%	105.73	0.2	105.8	0.8	0.2498	7.15
PANi loaded graphene composite						
Wt.% of PANi	**I_{max} (mA)**	**V_{max} (V)**	**I_{SC} (mA)**	**V_{OC} (V)**	**FF**	**%η**
5 wt%	44.8	0.2	44.8	0.7	0.285	3.068
10 wt%	55.36	0.2	55.68	0.7	0.284	3.741
15 wt%	96	0.2	96	0.7	0.285	6.479
20 wt%	71.36	0.2	72.64	0.7	0.280	4.816

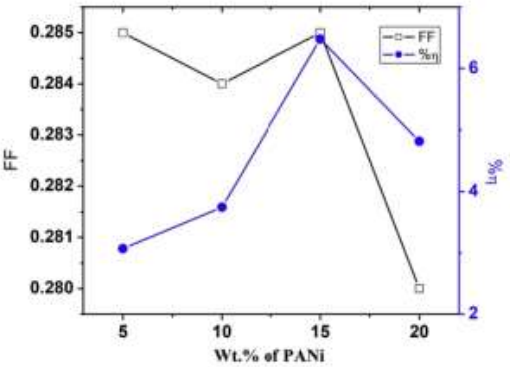

Fig. 7. Variation of FF and %η as a function wt.% of PANi in composite.

- the homogeneous presence of PANi and graphene in composite, can reduce the interfacial resistance between the graphene and the PANi. This homogeneity in composite results in better electron transfer.
- The presence of high electrical conductive graphene in composite and agglomerated nature of composite reduce inter-domain resistance.
- Lower band gap (1.92 eV) value of 15 wt% PANi loaded graphene composite.

3.2. Improvement in PV performance by addition of TiO_2 nanoparticles

3.2.1. XRD analysis

Fig. 8 (a) shows the XRD pattern of anatase phase TiO_2 nanoparticles. The strong signature peaks at 25° and 48° confirms the anatase phase. All remaining peaks position and marginal intensity data are in good agreement with standard spectrum (JCPDS card No. 84–1286) [37]. The average crystallite size of TiO_2 nanoparticles was estimated using Scherrer equation [38], $D = (K\lambda/\beta\cos\theta)$, where D is average crystallite size (nm), k is a shapes factor (K = 0.89), λ is the wavelength of X-ray source equals 1.540 Å, β is the full width at half maxima, and θ is the diffraction peak angle. The average crystallite size of TiO_2

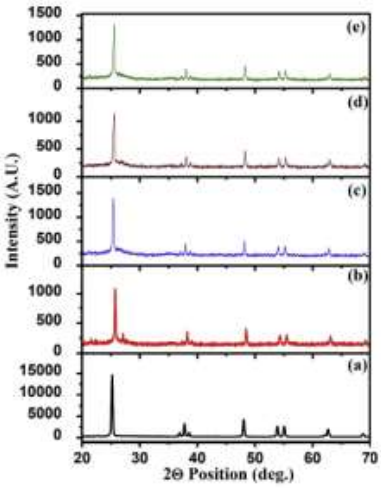

Fig. 8. XRD pattern of pure (a) TiO_2 nanoparticles and (b) 0.5 wt%, (c) 1 wt%, (d) 1.5 wt% and (e) 2 wt% TiO_2 nanoparticles loaded PANi-graphene composites.

nanoparticles was found to be 51.27 nm. Fig. 8 (b, c, d and e) depicts the XRD pattern of 0.5 wt%, 1 wt%, 1.5 wt% and 2 wt% TiO_2 nanoparticles loaded PANi-graphene composites, respectively. The addition of TiO_2 nanoparticles in PANi-graphene composites results in interesting results. The XRD pattern clearly shows the composite exhibits the crystalline phase with shape peaks. As discussed in section 4.1.1, the PANi-graphene composites have amorphous phase, which was diminish by addition of TiO_2 nanoparticles.

3.2.2. Morphology study

Fig. 9 represents the SEM images of (a) 0.5 wt%, (b) 1 wt%, (c) 1.5 wt% and (d) 2 wt% TiO_2 nanoparticles loaded PANi-graphene composites. Here also, TiO_2 nanoparticles nicely dispersed in PANi-graphene composites. The addition of TiO_2 in PANi-graphene results in improvement of crystallinity. In all SEM images, well defined crystalline boundaries are observed. The crystallinity of all composite samples reflects also from XRD analysis. The irregular particle size distribution observed in all regions of SEM.

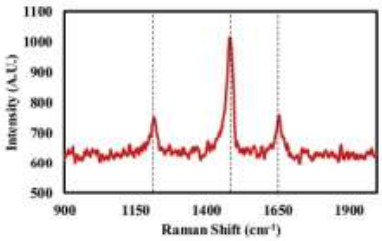

Fig. 10. Raman spectrum of 1 wt% TiO_2 nanoparticles loaded PANi-graphene composite.

3.2.3. Raman Spectroscopy

Fig. 10 shows the Raman spectrum of 1 wt% TiO_2 loaded PANi-Graphene composite. This spectrum also comprises the C – N stretching vibration from benzenoid, which appears around 1548 cm^{-1}. Similarly, semi-benzenoid polaronic band of $C–N^+$ appears around 1318 cm^{-1} and plane bending vibration of C-H is appears around 1200 cm^{-1}. No significant peaks were associated with TiO_2 nanoparticles in spectrum.

3.2.4. Optical properties

Fig. 11 shows the UV-VIS spectrum of 0.5 wt%, 1 wt%, 1.5 wt% and 2 wt% TiO_2 nanoparticles loaded PANi-graphene composites. From the plot, it is clear that absorption tail of 1 wt% TiO_2 nanoparticles loaded PANi-graphene composite has higher value than other three samples. The band gap values of 0.5 wt%, 1 wt%, 1.5 wt% and 2 wt% TiO_2 nanoparticles loaded PANi-graphene composites ranges between 3.02 and 2.53 eV. The lowest value of band gap is associated with 1 wt% TiO_2 nanoparticles loaded PANi-graphene composite.

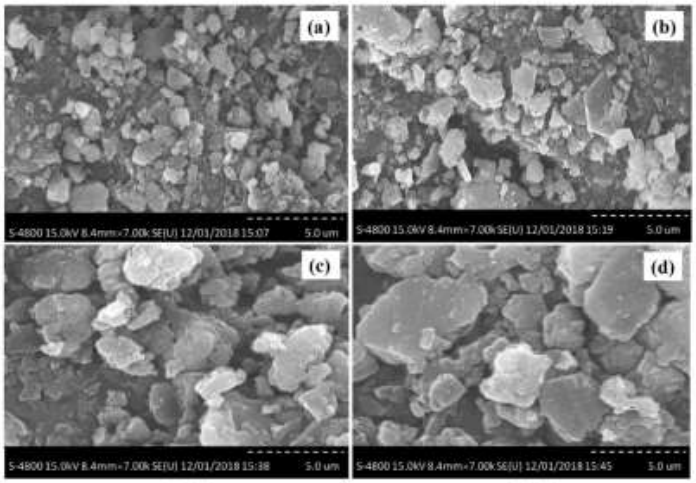

Fig. 9. SEM images of (a) 0.5 wt%, (b) 1 wt%, (c) 1.5 wt% and (d) 2 wt% TiO_2 nanoparticles loaded PANi-graphene composites.

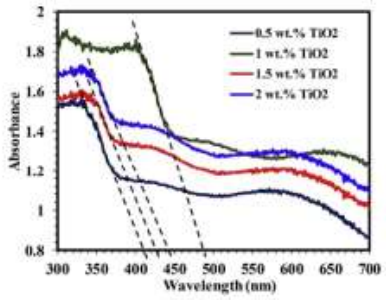

Fig. 11. UV-VIS spectrum of 0.5 wt%, 1 wt%, 1.5 wt% and 2 wt% TiO_2 nanoparticles loaded PANi-graphene composites.

3.2.5. PV performance

Fig. 12 shows the PV response of (a) 0.5 wt%, (b) 1 wt%, (c) 1.5 wt% and (d) 2 wt% TiO_2 nanoparticles loaded PANi-graphene composites based DSSCs and all diode parameters listed in Table 1. In PANi-graphene/TiO_2 composite, stable diode parameters observed. From Table 1, it is observed that 1 wt% TiO_2 nanoparticles loaded PANi-graphene composite has highest power conversion efficiency. The highest power conversion efficiency was attributed to good optical properties and lower band gap (2.53 eV) value.

Fig. 13 depicts the variation of FF and %η as a function wt.% of TiO_2 nanoparticles in PANi-graphene composites. The highest power conversion efficiency was associated with 1 wt% of TiO_2 nanoparticles in PANi-graphene composite. The possible reasons for the highest power conversion are,

- The addition of TiO_2 nanoparticles in PANi-graphene composite, results in increase of both photocurrent density and open circuit voltage.
- The presence of graphene sheets in composite reduces charge recombination and increasing open circuit voltage as a result of high electron [39,40].

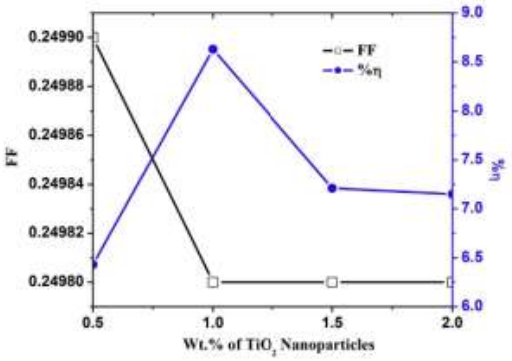

Fig. 13. Variation of FF and %η as a function wt.% of TiO_2 nanoparticles in composites.

4. Conclusions

During the study, two material systems that is PANi-graphene composite and PANi-graphene/TiO_2 composites based DSSCs were successfully prepared by ex-situ approach. The structural, morphological and optical study of both systems were carried out to understand physical properties of materials. To analyze the PV performance of PANi-graphene composite and PANi-Graphene/TiO_2 composites, PV cells were fabricated using doctor blead technique in architecture ITO/PV materials/Aluminum.

The PANi required for composite preparation was synthesized by using chemical oxidative route successfully. During composite preparation wt.% of PANi varied in graphene, to analyze effect of PANi on PV properties of composite. In this study, 15 wt% PANi loaded graphene composite shows optimized power conversion efficiency of order 6.47% with I_{sc} = 96 mA. The highest power conversation efficiency of this sample attributed to reduction in the interfacial resistance between the graphene and the PANi, lower inter-domain resistance and lower band gap of 15 wt% PANi loaded graphene composite than other samples.

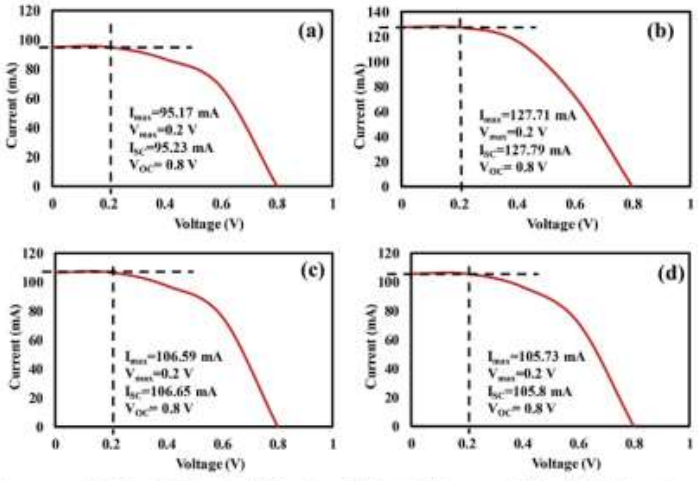

Fig. 12. PV response of (a) 0.5 wt%, (b) 1 wt%, (c) 1.5 wt% and (d) 2 wt% TiO_2 nanoparticles loaded PANi-graphene composites.

In order to improve further the power conversion efficiency of 15 wt % PANi loaded graphene composite, TiO_2 nanoparticles were added in this composite. To obtain again optimized sample with outstanding PV properties, the content of TiO_2 nanoparticles were varied with 0.5–2 wt % by an interval of 0.5 wt%. In this study, 1 wt% TiO_2 nanoparticles loaded PANi-graphene composite shows optimized PV properties. The power conversion efficiency was successfully improved and its value was found to be 8.63%. This is the main accomplishment of present work. In this complete, it is also observed that diode parameters have stable value.

In the concluding remark of this work, it is underlined that concentration of impurity in composite play very important role. Similarly, band gap engineering is also necessary to fabricate more efficient PV cells.

Data availability

The datasets generated during the current study are available from the corresponding author on reasonable request.

Acknowledgements

Authors are very much thankful to Dr. S.K. Omanwar, Head, Department of Physics, Sant Gadge Baba Amravati University, Amravati for providing the facility of Probe Sonicator. Authors are also grateful to Dr. Om Mahodaya, Principal, Jankidevi Bajaj College of Science, Wardha for providing necessary facilities for this work.

Appendix A. Supplementary data

Supplementary data related to this article can be found at https://doi.org/10.1016/j.solidstatesciences.2018.07.009.

References

[1] https://www.bbc.co.uk/education/guides/zpmnmp3/revision.
[2] Y. Liu, X. Wan, F. Wang, J. Zhou, G. Long, J. Tian, J. You, Y. Yang, Y. Chen, Advanced Energy Materials 1 (2011) 771–775.
[3] G. Dennler, M.C. Schaefer, C.J. Brabec, Adv. Mater. 21 (2009) 1323–1338.
[4] H.S. Nalwa, Handbook of Organic Conductive Molecules and Polymers, John Wiley & Sons, Chichester, UK, 1997.
[5] E.W. Paul, A.J. Ricco, M.S. Wrighton, J. Phys. Chem. 89 (1985) 1441–1447.
[6] C.R. Kagan, D.B. Mitzi, C.D. Dimitrakopoulos, Science 286 (1999) 945–947.
[7] S.A. Chen, Y. Fang, Synth. Met. 60 (1993) 215–222.
[8] L.D. Pulfry, Photovoltaic Power Generation, Van Nostrand Reinhold Co., New York, 1978.
[9] H.K. Bisoyi, S. Kumar, Liq. Cryst. 38 (2011) 1427–1449.
[10] O. Carp, C.L. Huisman, A. Reller, Prog. Solid State Chem. 32 (2004) 33–177.
[11] D. Dambournet, I. Belharouak, K. Amine, Chem. Mater. 22 (2010) 1173–1179.
[12] E. Singh, H.S. Nalwa, Sci. Adv. Mater. 7 (2015) 1863–1912.
[13] S. Ameen, M.S. Akhtar, G. Kim, Y.S. Kim, O. Yang, H. Shin, J. Alloy. Comp. 487 (2009) 382–386.
[14] L. Shen, W. Guo, H. Xue, Z. Liu, J. Zhou, C. Liu, W. Chen, Proceedings of the 3rd IEEE Int. Conf. on Nano/Micro Engineered and Molecular Systems, January 6-9, (2008) (Sanya, China).
[15] S. Yang, Y. Ishikawa, H. Itoh, Q. Feng, J. Colloid Interface Sci. 356 (2011) 734–740.
[16] S. Zhu, W. Wei, X. Chen, M. Jiang, Z. Zhou, J. Solid State Chem. 190 (2012) 174–179.
[17] M.M. Momeni, M.G. Hosseini, J Mater Sci, Mater Electron 25 (2014) 5027–5034.
[18] A. Bahramian, D. Vashaee, Sol. Energy Mater. Sol. Cells 143 (2015) 284–295.
[19] Y. Duan, Y. Chen, Q. Tang, Z. Zhao, M. Hou, R. Li, B. He, L. Yu, P. Yang, Z. Zhang, J. Power Sources 284 (2015) 178–185.
[20] G. Wang, S. Zhuo, W. Xing, Mater. Lett. 69 (2012) 27–29.
[21] C. Liu, K. Huang, P. Chung, C. Wang, C. Chen, R. Vittal, C. Wu, W. Chiu, K. Ho, J. Power Sources 217 (2012) 153–157.
[22] M. Dinari, M.M. Momeni, M. Goudarzirad, J. Mater. Sci. 51 (2016) 2964–2971.
[23] V. Locyuenyong, S. Yaotrakoo, P. Prathumtrd, J. Lertsiri, A. Buasri, Micro & Nano Lett. 11 (2016) 77–80.
[24] P. Yang, J. Duan, D. Liu, Q. Tang, B. He, Electrochim. Acta 173 (2015) 331–337.
[25] A.A. Syed, M.K. Dinesan, Talanta 38 (1991) 815–837.
[26] K.R. Nemade, S.A. Waghuley, J. Electron. Mater. 42 (2013) 2857–2866.
[27] T. Salmi, M. Bouguenda, A. Gastli, A. Masmoudi, Int. J. Renew. Energy Resour. 2 (2012) 213–219.
[28] M. Seifi, A. Sah, N. Izzrih, A. Wahab, M.K.B. Hassan, International Journal of Electrical, Robotics, Electronics Communication Engineering 7 (2013) 97–103.
[29] W. Feng, E. Sun, W.A. Fujii, H.C. Niihara, K. Yoshino, Bull. Chem. Soc. Jpn. 73 (2000) 2627–2632.
[30] Y. Wu, B. Wang, Y. Ma, Y. Huang, N. Li, F. Zhang, Y. Chen, Nano Research 3 (2010) 661–669.
[31] A. Ferrari, J. Robertson, Phys. Rev. B 61 (2000) 14095–14099.
[32] L. Cancado, M. Pimenta, B. Neves, M. Dantas, A. Jorio, Phys. Rev. Lett. 93 (2004) 247401–247405.
[33] A.C. Ferrari, Solid State Commun. 143 (2007) 47–57.
[34] A.C. Ferrari, J. Robertson, Phys. Rev. B 61 (2000) 14095–14107.
[35] R. Wang, Y. Wang, C. Xu, J. Sun, L. Gao, RSC Adv. 3 (2013) 1194–1200.
[36] https://www.e-education.psu.edu/ems812/node/534.
[37] K. Thamaphat, P. Limsuwan, B. Ngotawornchai, J. Kasetsart, Nat. Sci. 42 (2008) 357–361.
[38] K.R. Nemade, S.A. Waghuley, AIP Conference Series 1536 (2013) 1258–1259.
[39] L. Yang, W.W.F. Leung, Adv. Mater. 25 (2013) 1792–1795.
[40] A. Kongkanand, R.M. Dominguez, P.V. Kamat, Nano Lett. 7 (2007) 676–680.

33 Synthesis and charctrerization of cycloruthenation of cycloruthenated complexes

Synthesis and Characterization of Cycloruthenation of Cycloruthenated Complexes

[1]S.R. Khandekar [2]K.P. Suradkar

[1] Department Of Chemistry, Indira Mahavidyalaya, Kalamb, Dist.Yavatmal, M.S.

[2] Department Of Botany, Indira Mahavidyalaya, Kalamb, Dist.Yavatmal, M.S.

Corresponding author: kishorsu5@gmail.com

ABSTRACT:

Cycloruthenated (II) complexes offer several favorable properties suited for anticancer drug design, which provide a new class of compounds for clinical uses as an alternative to platinum antitumor drugs for the treatment of cancer. In the present work various precursors and ligand were synthesized such as $[Ru(bpy)_2Cl_2].2H_2O$, $[Ru(phen)_2Cl_2].2H_2O$ and 2-phenyl imidazoline respectively for the production of Cycloruthenated (II) complexes like $[Ru(bpy)_2(2PZ\text{-}L)]PF_6$(2) and $[Ru(phen)_2(2PZ\text{-}L)]PF_6$(3). During the study different physical methods have been used ie. Nuclear magnetic resonance(NMR); Infrared spectroscopy (IR); UV-Visible spectroscopy for characterization. These complexes have anticancerous as well as great antimicrobial properties

INTRODUCTION:

Reaction of a series of nitrogen donar ligands with metals salts gave complexes where ortho Metalation had occurred resulting in bidentate binding to the metal centers through N and C atoms are the cyclometalated complex.[2]

Cyclometalation was discovered in the early 1960s providing a straightforward entry to organometallic compounds that feature a metal-carbon σ-bond. Cyclometalation generally supports highly susceptible M-C bond and forms highly stable organometallic compounds.[4] Cyclometalation reaction represents probably the mildest route for activating strong C-H and C-R bonds. Because of these capability they have been employed in various application, for example as active units in sensors, in anticancer agents, as photophysical in organometallic light emitting diodes , for light harvesting and energy transfer such as in photovoltaic cells, as gelators and birefringents in liquid crystalline materials and as molecular or crystalline switches.

Imidazoles and benzimidazoles are present in various bioactive compounds possessing antiviral and anticanceral properties. The invention of Cisplatin – $[Pt[NH_3]_2Cl_2]$ has motivated us to search for alternative transition metal complexes with improved pharmacological properties. During this cycloruthenated complexes are coming out as an better option as it possesses several favorable properties suited to reasonable anticancer drug design. In the present study we synthesized and characterized the cycloruthenated complexes which having anticancerous and antiviral properties.

EXPERIMENTAL METHODS:

Chemicals:

All chemicals used in this work were of analytical grade. $RuCl_3.3H_2O$, 2,2'-bipyridine(bpy), 1,10-phenanthrolinemonohydrate, benzaldehyde, ethyleneiamine, KI (potassium iodide), potassium carbonate, iodine, potassium hexafluoro phosphate, methanol, ethanol, acetonitrile, DMF, DMSO, chloroform, DCM, acetone, ethyl acetate, hexane and diethyl ether.

b)[Ru(phen)$_2$(2PZ-L)]PF$_6$(2):

The ligand 2-phenylimidazoline (25.72 mg ,0.1759 mmol),cis-[Ru(phen)$_2$Cl$_2$].2H$_2$O (100 mg, 0.1759 mmol) and triethylamine5mL was added to ethanol-water (20 mL ,V$_{ethanol}$:V$_{water}$=2:1) solvent .Then reaction mixture was magnetically stirred and refluxed for 12 hours under nitrogen atmosphere.The reaction mixture was concentrated by rotary evaporator and a saturated KPF$_6$ aqueous solution was added to give precipitate. The precipitate was filtered and was with water and dried. Product was purified by column chromatography using acetonitrile as an eluent.

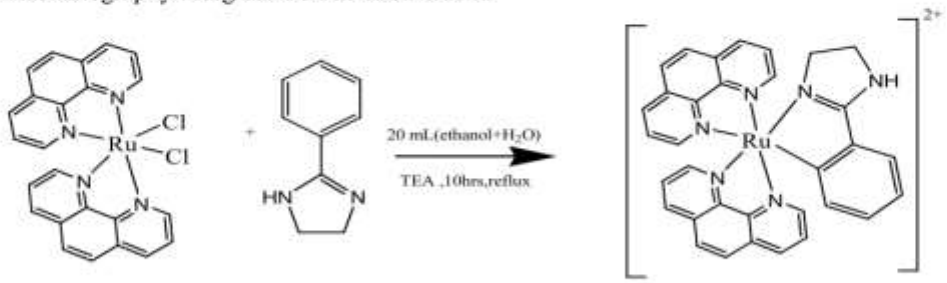

Figure 5: Synthetic scheme of complex **2**

Characterization:

UV-Visible Spectroscopy:-

The complexes [Ru(bpy)$_2$(2PZL)]PF$_6$, [Ru(phen)$_2$(2PZL)]PF$_6$ exhibits the absorption bands at 500-800 nm in visible region due to d-d transition and ligand based π-π^* transition occurs in the UV region of 210-350 nm.The molar extinction coefficient (ε_{max}) value for the complexes were 10^3-10^4 mol^{-1}cm^{-1}in visible region.

Photophysical data of UV-Visible Spectroscopy.

Table 1

COMPLEXES	ABSORBANCE λ_{max}/ε(M^{-1}cm^{-1})			
	Acetonitrile		Dimethylformamide	
	Ligand transition	MLCT	Ligand transition	MLCT
[Ru(bpy)$_2$(2PZ-L)]PF$_6$	**4410**/5855.05 **18292**/24627.65 **9245**/10514.85	**3486**/4067.5	**7350**/8456.3 **28094**/36958.25	**6492**/7189.2
[Ru(phen)$_2$(2PZ-L)]PF$_6$	**36264**/41800.45 **33223**/41880	**8469**/9742.7		**7490**/8240

Fluorescence Spectroscopy:-

The fluorescence spectroscopic data for the complexes [Ru(bpy)$_2$(2PZ-L)]PF$_6$ and [Ru(phen)$_2$(2PZ-L)]PF$_6$ in Acetonitrile and Dimethylformamide solvent are as follows:

Fluorescence data : Intensity and λ_{em} in different solvent

Table 2

Sr. No.	Complexes	Acetonitrile	Dimethylformamide
1	[Ru(bpy)$_2$(2PZ-L)]PF$_6$	355/485	260/492
2	[Ru(phen)$_2$(2PZ-L)]PF$_6$	389/469	320/490

IR Spectroscopy:

The solid IR spectrum of the ligand and their complexes have corresponding stretching frequency as given below:

the dark brownish product was obtained by filtering it. IR was taken in KBr ,which gives the different values as 3047 cm^{-1}(=C-H);1672 cm^{-1}.

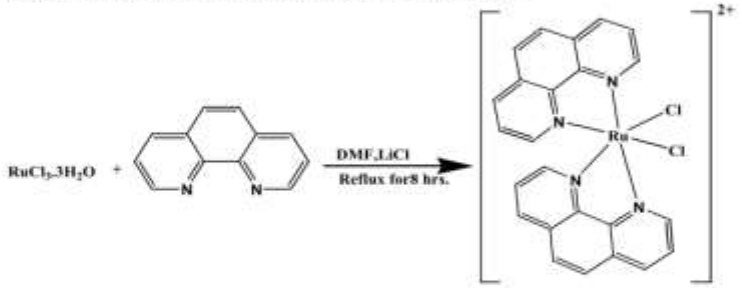

Figure 3: Synthetic scheme of P2

Physical methods:

The ligands and complexes synthesized during the study have beencharacterized by Nuclear magnetic resonance(NMR); Infrared spectroscopy(IR); UV-Visible spectroscopy. These methods are briefly outlined as follows:

1.Infrared spectroscopy (IR):

The spectra of solid samples were recorded by using KBr pellets as in theso called Shimadzu FTIR-8400 spectrophotometer at department of thechemistry, University of Pune.

2.UV-Visible spectroscopy:

UV-visible absorption measurements were carried on JASCO V-630 Spectrophotometer using matched pair of 1 cm quartz cells at Department of chemistry,University of Pune.

3. NMR spectroscopy:

^{1}H NMR spectra of the ligands and the complexes were measured on a Varian-Mercury 300 MHz spectrometer with $CDCl_3$,DMSO-d_6 as solvent at room temperature and all the chemical shifts are given relative to tetramethylsilane (TMS) as the internal standard at Department of chemistry, University of Pune and National Chemical Laboratory (NCL).

RESULTS AND DISCUSSION:

Synthesis Of Complexes:

a)[Ru(bpy)$_2$(2PZ-L)]PF_6(1):-

The ligand 2-phenylimidazoline (28.0958 mg ,0.1921 mmol) cis-[Ru(bpy)$_2$$Cl_2$].2$H_2O$ (100 mg, 0.1921 mmol)and triethylamine 5mL was added to ethanol-water (20 mL,$V_{ethanol}$:V_{water}=2:1) solvent .The reaction mixture was magnetically stirred and refluxed for 12 hours under nitrogen atmosphere.The reaction mixture was concentrated by rotary evaporator and a saturated KPF_6 aqueous solution was added to give precipitate.The precipitate was filtered and was with water and dried.After drying the precipitate was collected by using acetonitrile.

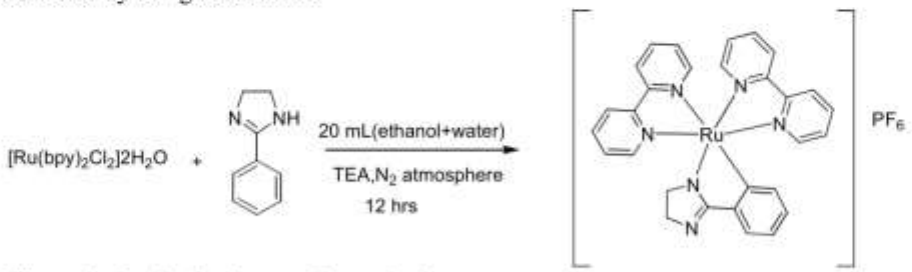

Figure 4: Synthetic scheme of complex **1**

Preparation of of ligand

2-phenyl imidazole:

In a typical procedure,aldehyde (1.0 mmol) and diamine (1.2 mmol) in water (10 ml), were stirred for 20 min, potassium carbonate (1.5 mmol), iodine (1 mmol) and potassium iodide (25 mol %) were then added consecutively and the mixture kept at 90°C with stirring for 30–50 min. After work-up, the corresponding imidazoline or benzimidazole was obtained in good to excellent yield .The condensation of aldehydes with diamines occurs without any catalyst,and the addition of molecular iodine as an oxidant in the presence of potassium iodide and base, smoothly oxidized the condensed products of aldehydes and diamines to imidazolines/benzimidazole.

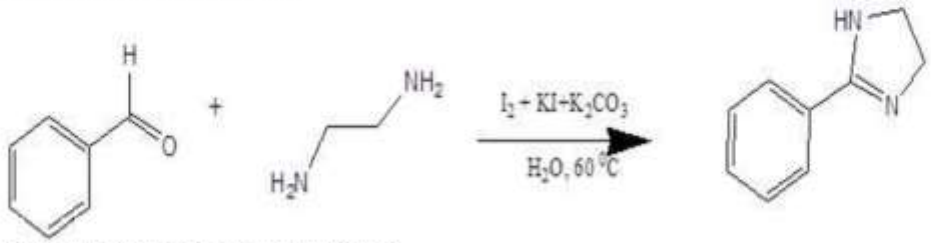

Figure 1 : Synthetic scheme of ligand

Preparation of the Precursor Complexes:

a)[Ru(bpy)$_2$Cl$_2$].2H$_2$O (P1):

The mixture of RuCl$_3$.H$_2$O(250 mg,0.9 mmol),LiCl (405 mg, 9.5mmol), 2,2'-bipyridyl (298 mg, 1.9mmol) were heated at reflux in grade dimethyl formamide (15 mL) for 8 hour. After the reaction mixture was cooled to room temperature, 50 mL of reagent grade acetone was added and the resultant solution cooled at 0°C overnight. Filtering yielded a red to red-violet solution and a dark-green-black microcrystalline product .The solid was washed three times with 25 mL portions of water followed by three 25 mL portions of diethyl ether, and then it was dried by suction.Finally the black colour product was obtained by filtering it.IR was taken in KBr ,which gives the different values as 3066 cm^{-1} (=C-H); 1672 cm^{-1}(-C=N) ; 1460 cm^{-1}, 1417 cm^{-1} (-C=C-) ; and 3497 cm^{-1}.

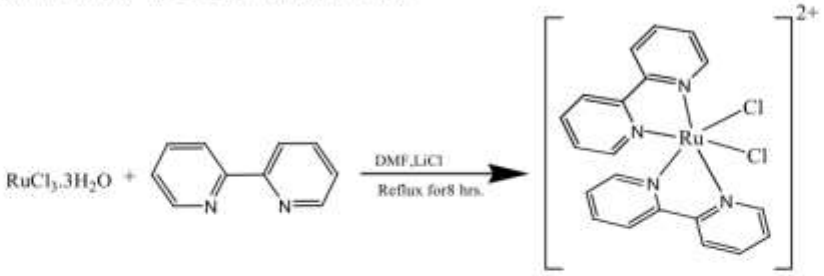

Figure 2: Synthetic scheme of P1

b)[Ru(phen)$_2$Cl$_2$].2H$_2$O (P2):

The mixture of RuCl$_3$.H$_2$O (250 mg,0.9 mmol),LiCl (405 mg, 9.5 mmol), 1,10-phenanthroline monohydrate (379 mg,1.9 mmol) were heated at reflux in grade dimethyl formamide (15 mL) for 8 hour. After the reaction mixture was cooled to room temperature, 50 mL of reagent grade acetone was added and the resultant solution cooled at 0°C overnight. Filtering yielded a red to red-violet solution and a dark-green-black microcrystalline product .The solid was washed three times with 25 mL portions of water followed by three 25 mL portions of diethyl ether, and then it was dried by suction.Finally

References:

1. Sharma, R. P., **'Western Political Thought'** (Plato to Hugo Grotius) Sterling Publishers private limited, New Delhi
2. Gyanender Singh, '**Western Political Thinkers** Omega Publications, New Delhi, first published : 2008, ISBN: 978-818455-051-1
3. Gyanender Singh '**Western Political Thinkers'** Omega Publications, New Delhi, first published : 2008, ISBN: 978-818455-051-1
4. Dhawan, M. L., **पाश्चात्य राजनितीक विचारक,** Arjun Publishing house, , New Delhi
5. Sreedathan, G., **'Western Political thought and Theories'** Deep & Deep Publication PVT. LTD, New Delhi
6. Sharma, Raj, **'Western Political Thinkers'**, Srishti book distributors, New Delhi
7. Translated by Benjamin Jowett, With the Jowett Notes and Marginalia. **'Plato The Republic'**, The world Publishing Company, Cleveland and New York
8. Bhandari, D.R., J.N.V. University, **'Plato's Concept Of Justice: An Analysis'**, www.bu.edu/wcp/Papers/Anci/AnciBhan.htm
9. Janusz Symonides, **'Human Right concept and Standards'**, Rawat Publications, Jaipur and New Delhi

❖❖❖

IR spectral data:

Table 3

Complexes/ligand	-C=C-	-C=N	-C-H	-N-H	-S-CH_3	-S=O
$[Ru(bpy)_2(2PZ\text{-}L)]PF_6$	1453	1633	3076	-	-	-
$[Ru(phen)_2(2PZ\text{-}L)]PF_6$	1417	1621	3067	-	-	-

CONCLUSION:

In the present investigation Cycloruthenated (II) complexes were synthesized and characterized by spectroscopic analysis. Spectroscopical and theoretical data of these complexes were compared. On the basis of this comparison it is concluded that the Cycloruthenated (II) complexes possesses anticancerous and enormous antimicrobial properties.

REFERENCES:

(1) Jiang-Yang Shao, Jiannian Yao and Yu-Wu Zhong, *Organometallics* 2012, *31*, 4302−4308.

(2) Kiyoshi C. D. Robson, AswaniYella, BarboraSporinova, Mohammad K. Nazeeruddin, Thomas Baumgartner, Michael Grϵatzel, and Curtis P. Berlinguette,*Inorg. Chem.* 2011, *50*, 5494–5508.

(3) Kiyoshi C. D. Robson, AswaniYella , Thomas Baumgartner, Michael Grϵatzel, and Curtis P. Berlinguette, *Inorg. Chem.*2011, *50*, 5494–5508.

(4) Jiang-Yang Shao,JiannianYao,and Yu-Wu Zhong,*Organometallics*2012, *31*, 4302−4308

(5) Sumanta KumarPadhi,Ryoichi Fukuda,Masahiro Ehara,and Koji Tanaka *Inorg. Chem.*2012, *51*, 5386−5392.

(6) Wen-Wen YangJiannian Yao,and Yu-Wu Zhong, *Organometallics*, 2012, *31*, 8577−8583.

(7) Myung-Jong Ju,HongSeok Kang, Moon-Sung Kang, and JaejungKo, *Inorg. Chem.,* 2011, *50*, 11340–11347

(8) PranjalGogoi and DilipKonwar ,*Tetrahedron Letters,* 47, (2006) 79–82.

(9) Kumar Vikrant, MamgainRitu and Singh Neha, *Research Journal of Chemical Sciences,* 2, (2012) 18-23.

(10) Tarighi S., Abbasi A., *JSUT, 33, (2007) 19-21.*

(11) Jennifer L. Kisko and Jacqueline K. Barton, *Inorg. Chem., 39, (*2000), 4942-4949.

(12) Takashi Funaki,Hiromi Funakoshi, Osamu Kitao, Nobuko Onozawa- Komatsuzaki, Kazuyuki Kasuga, Kazuhiro Sayama, and Hideki Sugihara *Angew. Chem. Int. Ed.* 51, (2012), 7528 –7531.

❖❖❖

34 Inferiority of Women in Shashi Deshpande's Novel the binding wine

Inferiority of women in Shashi Deshpande's novel *The Binding Vine*

Prof.Prashant S. Jawade

Indira Mahavidyalaya Kalamb

Email-id:-bhaktijawade@gmail.com

Abstract

In recent times the status and position of women is changing. Particularly in developing country like India, The women are shifting themselves towards autonomy self realization and need of independence etc. In Indo English novels the traditional images of women are portrayed they are shown as devoted wife devoted mother, sister daughter etc .The women writers changed the attitude of women towards women and society. The writings are not only depicted the external affairs but also the internal journey of feelings, psychological, stress and distress and feminine sensibilities also. A few women writers like Manju Kapur, Shashi Deshpande ,Anita Desai are very much concerns about the psyche, inner feelings of their women characters that makes infected on account of tensions generated by surroundings. They trying to do good way to present Indian women in their novels with their pen and finds women's need for self independence, individuality. This paper aims to deal with inferiority of women, the theme of alienation, helplessness which are somewhat created by surroundings/society.

Introduction

The Indian fiction is enriched with the writings of women's who paved the way for struggles, conflicts and empowered the position of women in contemporary India which was not suitable in the history of Indian society. We found the reflection in the writings of women's writers trying to explore the psychic moral political social liberations/rights from the existed patriachrial system governed over them. To establish new harmony required changes within relationships and with surrounding. The women writers displayed the domestic social frames with social, cultural modes responsibilities and values which created the images of in Indian society and handover their devoted role to shoulder the more responsibilities duties morally towards every factor which is associated with her. In short stereotyped image changes simultaneously modern, educated self thinking.

Shashi Deshpande is the major voice in the writings of women writers who discarded the traditional ways of describing the events/ stories etc. provided less importance to external life of human being. She has appreciative style of most of the novels are mind provoking she has great art of dealing with women world. In her characters she brings out the feelings of loneliness victims of depression and exploitation and subjection etc. They have subaltern role in the novels she chooses the Indian women of different fields like educational economic etc. Her novels deal with recognisation of individuality and realization of freedom. The endings of the novels are linking to revolutionary changes made by characters and joined a

courage to identify wrong and right. Firm decisions are occurred to find out solutions on their own problems. Though some women characters are pictured as well educated modern most striking point is that they are shown weak in their understanding/ handling situations, searching for sympathy but affected restricted from patriarchal dominations and power. They wanted to arise with their potential/ caliber etc. to joint their wrist against social systems/ orders. Her Protagonist are educated well qualified, modern belongs to middle class families. They are isolated and in alienation and stricken to their destiny from male domination and emotionally they are suppressed. Shashi Deshpande did not blaming the male power or their domination, the slavery of women is responsible to ruin themselves and they found refusing to change not so dared to protest against which are becoming obstacles in their way.

About *The Binding Vine (1993)*

In novel The Binding Vine (1993) Shashi Deshpande presented middle class female protagonist which has not voice in the male dominated world . It is the story of three/ four sufferings women, which are existed in three different age and time. They are Kalpana , Mira, Urmila ,Akka etc. Kalpana is shown as little bit conscious, Mira has level of dead and Urmi IS full of Spirit a Searching for the meaning of life through the other characters like Mira and Kalpana. Only the difference is that the Kalpana is raped by her own relative and Mira is by her own husband. No doubt the novel is full of women characters having their own meanings/ perceptions of their lives. It made the reasons of their miserable conditions. In the end of novel Inni took the incidents in flashback. She had been come with Urmi as a honest, trusted male servent. Urmi father knew that the girl was accompanied with male servent and had lines of anger on his forehead. After that he sent Urmi to his mother without consulting it with his cruel power of male dominance, that suffered her mother become helpless, victim. Urmi made aware about the pain of separation in which Inni suffered and she bravely faced it for couple of years without single of complaint. She is very upset about her mother and extremely sorry for her mother which was helpless women in powerful male dominated society

Portrayal Of women In *the Binding Vine (1993)*

The novel Binding Vine -The five women are presented with different characteristic and generations but all are subjected, exploited with different circumstances. They are Akka, Mira Shakutai Kalpana and Sullu etc. Akka is woman who suffers from her husband. Her husband did not pay much more attention towards his wife as wife. She has impact of Indian tradition /customs; she has no option/ choice and remains silent. She was deprived from her basic right and unable to speak about it. She spent her life like thing put into house and not as human being.

Second woman is Mira an educated upper class middle class woman Mira has to become victim of unnatural uncalled circumstances and her husband love is only physical, nothing to do with emotions affections and care etc. Because of over thinking and with depressed soul her mind developed a fear and she becomes unconscious even in odd times. She suffers in breathless silence, she wrote poems and maintain diaries as an account of life she recorded facts happened with her. She knows English little bit her poems are in Kannada. She does not have a liberty to write specially in language of her own choices from the character of Mira Shashi's characters/ protagonists are passionate about writings which is a matter of self-expression and symbol of liberation . In second category there is Shakutai Kalpana Sullu.

Kalpana sweet girl was brutally raped. After this inhumanly incident, she was not dare to go to police and demand the justice also request the doctor not to disclose it to police or other agencies etc. The criminal of this worse did none other than Prabhakar who is relative of her mother. He is husband of Sullu the Kalpana's view about this terrible matter upset her, but she leaves the decision to Kalpana.

Shakutai is sufferings come with her marriage as her husband was not properly employed. Automatically she becomes bread earner of her family and shouldering the responsibility of two daughters and a son. She is also fearful about her sister Sullu who is not blessed by child after marriage, her husband is drunkard. Shashi Deshpande presented Urmi a caring in nature towards women very conscious about life. She is happy and satisfied in her life. A sudden death of her baby girl not break her courage. She also suffers with helplessness created by her own luck/destiny. But she is very concerns about womens problems .She pours her sympathy towards Shakutai and also for her own mother- in -law Mira who has raped by her husband in nights. Later she published the poems of Mira. She was ready to fight for Kalpana and supported her for his medical treatment. And Kalpana raised her voice against injustice done by her own relative and took support of media like TV channels and printed media. As she adviced by Urmi. In this way Urmi strengthen the women like Mira, Shakutai, and Kalpana against wrong unsuitable conditions which are they facing from ages.

Conclusion –

The Shashi Deshpande's women characters are faced subjection by social disorders. The women have positive attitude towards life through surroundings is not suitable for them. Though world is uncaring towards the women, the characters are full of strengths and weaknesses. They learn the harsh realities of life from their own experiences about life. The women characters are depicted with sorrows, sufferings and miserable conditions and part of subjugation. From the writings of Shashi Deshpande's we found that she believes that women should educate and make themselves self reliance and more creative to contribute in the power of

liberty to women. The Deshpande's novels show women's world is more important as they are real founder of society's moral values.

References:

Agrawal Malti- New Perspectives On Indian English Writings

The Binding Vine –Critical

A handbook of critical approaches to literature

Prasad Amarnath- New Lights On Indian Women Novelists In English

35 Prakrutik Sansadhno ke Sanrkashan me Vyakti ki Bhumika

प्राकृतिक संसाधनों के संरक्षण मे व्यक्ति की भूमिका

(Role of an Individual in Conservation of Natural Resources)

प्रा. एन. व्ही. नरुले
भूगोल विभाग प्रमुख, इंदिरा महाविद्यालय, कळंब, जि. यवतमाळ
भ्रमणध्वनी ९९२३९०९२९६ E mail: narulenilkanth3@gmail.com

संसाधन का अर्थ :

वह तत्त्व या स्रोत जो मानवीय उद्देशों तथा आवश्यकताओं की पूर्ति करने मे सक्षम है, संसाधन कहलाता है। संसाधन मनुष्य के लिए उपयोगी होता है और मानवीय उपयोगिता ही संसाधन का विशिष्ट गुण है। वास्तव मे कोई भी वस्तु या तत्व अपने आप में संसाधन नही है, बल्कि मनुष्य के लिए उसकी उपयोगिता ही उसे संसाधन बना देती है।

सामान्य अर्थ में संसाधन का अभिप्राय केवल मूर्त या गोचर पदार्थों से लगाया जाता है किन्तु अनेक अमूर्त तत्त्व जो मनुष्य की आवश्यकताओं की पूर्ती करते है, संसाधन की श्रेणी के अंतर्गत आतें है। मूर्त (दृश्य) तत्त्वों में भूमि, जल, वन, मिट्टी, खनिज पदार्थ, कृषि उपजें, औद्योगिक उत्पादन, कारखाने, भवन, सडकें आदि प्रमुख है।

प्राकृतिक संसाधन :

प्रकृति द्वारा उत्पन्न वे समस्त तत्व या तत्व समूह जो मनुष्य के लिए उपयोगी है, वह प्राकृतिक संसाधन कहलाते है। भूमि, जल, मिट्टी, खनिज, शैले, उर्जा, प्राकृतिक वनस्पती, पशु तथा आक्सीजन आदी प्राकृतिक संसाधन के उदाहरण है। प्राकृतिक संसाधन किसी देश-काल में मानव सभ्यता की प्रगती की आधारशिला होते है। किसी भी देश के प्राकृतिक संसाधन उसकी आर्थिक धुरी होते है।

प्राकृतिक संसाधनों के (दोहन) अपव्यय :

'संसाधन संरक्षण' संसाधन प्रबंध का एक अंग है। संसाधन प्रबंध किसी संसाधन के कुशल नियंत्रण तथा व्यवस्थापन से सम्बंधित होता है जो वर्तमान सामाजिक आर्थिक आवश्यकताओं, उपलब्ध प्रौद्योगिकी, भावी उपयोगिता, पर्यावरण संरक्षण आदी को ध्यान में रखते हुए संचालित होता हैं। संसाधन संरक्षण का सिद्धांत किसी देश काल मे विद्यमान प्राकृतिक संसाधन आधार और जनसंख्या के मध्य संतुलन का प्रतिपादन करता है। जिसमे वर्तमान सामाजिक आर्थिक प्रगती के लिए विद्यमान संसाधनो के उचित तथा सर्वोत्तम उपयोग के साथ ही उन संसाधनो की सतत आपूर्ति भविष्य में भी बनाये रखने की दृष्टि से इस बात पर ध्यान दिया जाता है कि वर्तमान उपयोग में उनका दुरुपयोग, अपशिष्टीकरण तथा अनावश्यक शोषण या विदोहन न्युनतम हो। इस प्रकार संसाधन संरक्षण का अर्थ संसाधनो के अनुकूलतम या अभीष्टतम उपयोग (optimum use) से है। भविष्य में भी संसाधन का उपयोग सातत्य और सुनिश्चित हो। संसाधन संरक्षण का उद्देश्य अनावश्यक तथा अंधाधुंध प्रयोग अथवा अवांछित दुरुपयोग को कम करके उसके समुचित उपयोग से है जिससे वर्तमान के साथ ही भविष्य में भी उसका प्रयोग सतत बना रह सके।

बीसवीं शताब्दी के उत्तरार्ध से अंतिम तीन दशकों से संसाधन संरक्षण की समस्या गंभीर हो गयी है। जनसंख्या में तिव्र वृध्दि, प्राद्योगिकीय क्रांती, औद्योगीकरण, भौतिकवादी अर्थप्रधान जीवन दर्शन तथा उच्च जीवन स्तर के प्रती लोलुपतामें तिव्र वृध्दि आदी के कारण प्राकृतिक संसाधनो का अंधाधुंध शोषण किया गया है, जिससे असंख्य जैव,अजैव संसाधन या तो सदा के लिए विनष्ट हो गये है। प्राकृतिक संसाधनों का अतिशोषण तथा विनाश और पर्यावरण प्रदूषण सम्बधी समस्याओंने भंयकर रुप धारण कर लिया है जो सम्पूर्ण मानव जाति के अस्तित्व के लिए खतरा तथा चुनौती बन गयी है।

मनुष्य में भौतिकवादी दृष्टिकोण तथा विश्वव्यापी आर्थिक लूट (economic plunder) के चलते अनेक वन्य जन्तु मानव का शिकार बनते जा रहे हैं। पौधों तथा पशु-पक्षियों की कितनी प्रजातीयां विलुप्त हो चुकी है और कितनी विलुप्त होने के कगार पर हैं। औद्योगिक कच्चे माल तथा शक्ति संसाधन की प्राप्ती के लिए कई खनिज एवं शक्ति संसाधनो का अंधाधुंध खनन किया गया जिससे अनेक खनिज भंडार या तो समाप्त हो गये हैं या कुछ ही वर्षों में समाप्त होने वाले है।

वर्तमान परिस्थितियों में प्राकृतिक संसाधनों के अपव्यय, अतिशोषण तथा पर्यावरण प्रदूषण को रोकने, संसाधनो के समुचित तथा अनुकूलतम उपयोग और भविष्य में भी संसाधनो की आपूर्ती बनाये रखने आदी उद्देश्यों से संसाधनो का संरक्षण आधुनिक मानव समाज की अनिवार्य आवश्यकता है। इसके माध्यम से वर्तमान मानव जीवन के साथ ही भविष्य को भी संवारा जा सकता है और संसाधन अभाव तथा पर्यावरण अवनयन या परिस्थितिकीय असंतुलन से उत्पन्न होने वाली त्रासदी से मानव जाती को बचाया जा सकता है। संसाधन संरक्षण में सरकारी एजेन्सियों तथा गैर सरकारी संगठनों के साथ ही व्यक्ति की महत्वपूर्ण भूमिका हो सकती है।

प्राकृतिक संसाधनों के संरक्षण में व्यक्ति की भूमिका :

1) जानकार व्यक्ति पर्यावरण के महत्व, पर्यावरण प्रदूषण तथा वन विनाश आदी से होने वाली हानियों से अपने संपर्क में आने वाले लोंगो तथा समाज को अवगत कराये और पर्यावरण संरक्षण के प्रति जन जागरुकता उत्पन्न करने का यथा संभव प्रयत्न करें।

2) संसाधन संरक्षण के लिए बनाये गये कानूनों तथा नियमों का उल्लंघन करने वाले व्यक्तियों या संस्थाओं के विषय में संम्बधित विभाग या पुलिस को सुचित करना चाहिए जिससे उन्हें दण्डित किया जा सके।

3) कृषक मृदा अपरदन को रोकने के लिए वृक्षारोपन, मेंडबंदी करने, परती भूमी पर घास लगाने, समोच्चरेखी जुताई करने और अतिचारण को रोकने जैसे विधियों को अपना सकता है।

4) प्रत्येक व्यक्ति अपनें घरों, व्यावसायिक दूकानों तथा कार्यालयों में बिजली का उपयोग आवश्यकतानुसार ही करे । दिन में बल्ब न जलाये और रात में भी बल्ब की जगह ट्यूब लाइट जलाये क्योंकि बिजली की बचत ही बिजली का उत्पादन मानी जाती है।

5) नगरों में जलापूर्ति की समस्या निरन्तर विकट होती जा रही है। व्यक्ति का कर्तव्य है की वह जल को बेकार न बहाये और पेयजल का उपयोग बगीचे आदी की सिंचाई के लिए कम से कम अथवा न करे। नल की टोटीयों से जल रिसाव को रोकना तथा जल के व्यर्थ बहाव को रोकना व्यक्ति का परम कर्तव्य है।

6) व्यक्ति को चाहीए कि वह बाजार से सामान लाने के लिए पालीथिन के थैलियों के स्थान पर कागज के थैलों तथा कपडे या जूट के बने थैलों का उपयोग करे । दूकानदार भी पालीथिन के स्थान पर कागज के थैलों का उपयोग करें।

7) व्यक्ति वन्य पशुओं या पक्षियों विशेषरुप से संरक्षित प्रजाती के प्राणियों का शिकार कदापि न करे क्योंकी उनके विलुप्त होने का खतरा है।

8) प्रत्येक व्यक्ति को चाहिए कि वह अपने घर के आगे-पीछे या अन्य खाली पडी भूमी पर उपयोगी वृक्ष (पौध) लगाये और कभी भी हरे वृक्षों को न काटे।

9) वर्षा जल के संचय के लिए घर के छत पर एकत्रित जल को पाइप द्वारा नीचे लाकर भूमि में निर्मित जलभण्डार या सोखते में गिराया जा सकता है। इससे भौम जल स्तर ऊपर उठेगा।

10) भोजन पकाने के लिए प्रेशर कुकर का प्रयोग करने से 75 प्रतिशत तक ऊर्जा की बचत की जा सकती है। भोजन पकाने के लिए गैर परम्परागत ऊर्जा स्त्रोंतो जैसे बायोगैस, सौर ऊर्जा (सोलर कुकर) आदी का प्रयोग ऊर्जा संरक्षण में सहायक है।

संदर्भ :

१. पर्यावरण अध्ययन – डॉ. एस. डी. मौर्य / श्रीमती शालिनी, प्रयाग पुस्तक भवन, इलाहाबाद
२. पर्यावरण भूगोल – प्रो. सविन्द्र सिंह / प्रयाग पुस्तक भवन, इलाहाबाद
३. पर्यावरण और पारिस्थितिकी – डॉ. बी. पी. राव/ डॉ. वी. के. श्रीवास्तव, वसुंधरा प्रकाशन, गोरखपुर
4. The Nature of Environment -- Basic Blackwell Publisher Ltd., 1984

❖❖❖

मोगलकालीन भारताचा जमा खर्च

प्रा. एन. आर. ठवळे
इंदिरा महाविद्यालय, कळंब, जि. यवतमाळ
मो.नं. ९४२०६८३११६ E mail: n.r_thawale@rediffmail.com

सरकारी आवक :

देशाचा कारभार चालवण्यासाठी शासकाला मोठा पैसा गोळा करावा लागतो व तो कर रुपाने गोळा केला जातो. भारतात प्राचीन काळापासून राजाला प्रजा कर देत असे. त्या मोबदल्यात राजा प्रजेचे संरक्षण करीत असे. कल्याणकारी कामे करीत असे. आपल्या प्रदेशाचे संरक्षण करीत असे. मध्ययुगात कराचे विविध प्रकार होते. त्यात जमीन महसूल, सिमा कर, वहातूक कर, इत्यादी महत्त्वाचे मानले जात. सर्वात मोठे उत्पन्न देणारे कर म्हणजे जमीन महसूल होय. हा कर प्राचीन काळात सुद्धा वसूल केला जाई. वैदिक काळात उत्पन्नाच्या १/१० तर सम्राट हर्षाच्या काळात १/६ वसूल केला जाई. सूलतान शाही काळात वेगवेगळ्या सूलतानांनी कमी जास्त वसूल केलेला दिसतो. त्यात कुमूबद्दीन ऐवकाने १/५ तर अल्लाउद्दीन खिल्जीने १/२ एवढा वसूल केला. मोगल सम्राट बाबरचे संपूर्ण आयुष्य युद्धाच्या धामधूमीत गेले. त्याला महसूल व्यवस्था स्थिरस्थावर करण्यात फारसे यश मिळाले नाही. हुमायूचे ही आयुष्य धावपळीतच गेले. परंतु अकबराने उत्पन्नाच्या १/३ महसूल वसूल करणे सूरु केले. १५४० ते १५४५ या काळात दिल्लीवर सूर वंशाच्या शेरशहा नावाच्या शासकाचे राज्य होते. भुमी सुधारणेसाठी तो प्रसिद्ध होता. दोरीच्या सहाय्याने जमीनीची मोजणी करुन १/३ जमीन महसूल आकारला होता. त्यातील दोष दूर करुन सम्राट अकबरने जमीन महसूल वसूल करणे सुरु केला. तो नगदी स्वरुपात वसूल अकबराचा महसूल मंत्री राजा तोरडमलने दोरीने जमीन मोजणी बंद केली. त्यासाठी बांबू किंवा लोखंडी साखळीचा वापर सुरु केला. जमीनीच्या उत्पादन क्षमतेच्या आधारावर जमीनीची पतवार केली आणि शेतसारा वूसलीसाठी राजस्व अधिकारी नेमले. परगण्यात अमलगुजार हा प्रमुख अधिकारी होता. त्याच्या हाताखाली वितकची, फोतदार, कानूनगो, मुकद्दम आणि पटवारी काम करीत असे. त्यामुळे महसूल वसुलीत सुसूत्रता आली आणि मागल बादशहाला जमीन महसूलापासून मोठे उत्पन्न केंद्रीय तिजोरीत गोळा होवू लागले. सिमा शुल्क हा एक महत्त्वाचा कर मोगल काळात वसूल केला जात असे. मालाची आयात निर्यात होत असतांना बंदरात व सिमेवर हा कर वसूल केला जात असे. गांधार कडून येणाऱ्या मालावर लाहोरमध्ये सीमाशुल्क वसूल केले जाई. तर नेपाळकडून येणाऱ्या मालावर गोरखपूरमध्ये सीमाशुल्क वसूल केला जाई. याशिवाय वेगवेगळ्या बंदरामध्येसुद्धा मोठ्या प्रमाणात हा कर वसूल केल्या जात असे. हा कर वस्तूंच्या किंमतीवर प्रती शेकडा आकारला जात असे. अकबर काळात तो २ $^{1}/_{२}$ रु. शेकडा आकारला जाई. सोन्या चांदीवर शेकडा २ टक्के आकारला जाई. सूरत लुटीनंतर औरंगजेबने सूरत शहरात एका वर्षासाठी सीमाशुल्कात वसुली थांबवली होती. एकट्या इस्ट इंडिया कंपनीकडून सूरत बंदरातून कमी अधिक २०००० /— रु. सीमाशुल्क भारताला मिळत असे. याशिवाय फ्रेंच, डच, पोर्तुगिज इत्यादी व्यापारी कंपनीकडूनही मोठा सीमाकर भारताला प्राप्त होत असे.

पथकर (चुंगीकर) (Toll Tax) हा कर सुद्धा प्राचीन काळापासून वसूल केला जाई. सुलतान काळातही तो अस्तित्वात होता. मोगल शासकांनीही तो कायम ठेवला होता. त्यातूनही भारताला मोठा पैसा प्राप्त होत असे. माल एका ठिकाणाहून दुसऱ्या ठिकाणी नेण्यासाठी हा कर लावत जाई. रस्तेबांधणीसाठी हा कर वसूल केल्या जाई. अकबराने पथकर बंद करण्याचा आदेश दिला होता. परंतु देशातत्याची योग्य अंमलबजावणी होत जात नव्हती. जहांगीर, शहाजहान यांच्या काळात अधिकारी वर्ग व्यापाऱ्यांना जास्तीत जास्त लुबाडण्याचा प्रयत्न करित असे. ही वार्ता औरंगजेबाच्या कानी पडताच त्याने १६६७ मध्ये एक आदेश काढला होता की, सूरत बंदरात येणाऱ्या मालाला कोणत्याही अधिकाऱ्याने अडवू नये. तरीही तो प्रकार थांबला नव्हता. औरंगजेबाच्या काळात कर वसुलीत मोठा भेदभाव केला जाई. हिंदू व्यापाऱ्याकडून ५ टक्के वसुली केली जात. युरोपियन व्यापाऱ्यांकडून २ टक्के वसूल केला जाई. तसेच युरोपियन व्यापाऱ्यांना हिंदू व्यापाऱ्यांपेक्षा अधिक सोई सुविधा दिल्या जाई.

युद्धात विजय प्राप्त झाल्यावर पराजीत राजाची सेना राजधानी सोडून निघून जाते किंवा पळून गेल्यावर त्या शहरात विजयी झालेल्या राजाची फौज लूट करते. शहरातील संपूर्ण धन संपत्ती लुटून गोळा केली जाते. त्यात मुस्लीम परंपरेनुसार १/५ भाग सैनिकांनी सरकारला द्यावा लागत असे व ४/५ ज्या सैनिकाने लूट केली त्याला प्राप्त होत असे. अकबर त्याच्या काळात सरकारी वाटा जास्त घेत असे. जर एखाद्या सैनिकाने लुटीतील वाटा सरकार जमा केला नाही तर त्यांना कठोर शिक्षा दिली जाई. सम्राट अकबराने आधमखानला याबद्दल कठोर शिक्षा दिली होती. सहाजिकच अशा भीतीपोटी प्रत्येक सैनिक लुटीतील ठरलेला वाटा सरकार जमा करीत असल्यामुळे सरकारात मोठी रक्कम गोळा होत असे. सरकारी न्यायालयाद्वारे प्राप्त होणारी फी व गुन्हेगाराकडून वसूल होणारा दंड हे सुद्धा सरकारात गोळा होणारी मोठी रक्कम होती. बंडखोरी करणाऱ्या सरदारांनाही मोठा दंड आकारला जात असे. कधी कधी त्यांची संपूर्ण संपत्ती सरकार जमा केली जाई. राजकीय कैद्यांकडूनही मोठा दंड वसुल केला जाई. लग्नप्रसंगात नोंदणी शुल्कही मोगल काळात वसुल केला जात. हा कमीत कमी १ दाम पासून १० मोहर पर्यंत विवाह करणाऱ्याच्या ऐपतीप्रमाणे वसूल केला जाई. एखाद्या व्यक्तीचा उत्तराधिकारी नसेल तर त्याची संपूर्ण संपत्ती सरकार जमा केली जात. मध्ययुगात शरण आलेल्या राजांकडून सम्राटाला दरवर्षी ठरलेली खंडणी प्राप्त होत असे. सम्राटाच्या वाढदिवशी बादशहाला मोठ्या प्रमाणात अमुल्य असा उपहार आमीर, उमराव, सरदार व मांडलीक राजांपासून प्राप्त होत असे. हा सर्व पैसा व संपत्ती सरकारला प्राप्त होत असे. मोगल साम्राज्यात मनसबदाराच्या मृत्यू झाल्यास त्याची सर्व संपत्ती सरकार जमा होत असे. ती संपत्ती त्याच्या वारसांना प्राप्त होत नसे. नूरजहॉचा भाऊ आसफखॉची संपूर्ण संपत्ती २ $^{१}/_{२}$ करोड सरकार जमा केल्याची नोंद इतिहासात आहे. मृत्यूनंतर सर्व संपत्ती सरकार जमा होईल यामुळे मनसबदार आपल्या संपूर्ण आयुष्यात संपत्तीची मोठी उधळपट्टी करीत असे. आपले संपूर्ण आयुष्य चैन आणि विलासात घालवत असे. याशिवाय मनसबदारांच्या वेतनातून १० ते २५ टक्के पैसा सरकार जमा होत असे. आजच्या इनकम टॅक्स सारखा हा प्रकार होता. त्यातून फार मोठा पैसा सरकारी तिजोरीत गोळा होत असे. देशात विविध व्यवसाय करणारे जे व्यवसायिक होते. त्यांच्या जवळून व्यवसाय कर वसूल केला जाई. शाही कारखान्यात तयार होणारा माल राजघराणे, सरदार, सरंजामदार इत्यादींना विकला जात. त्यातूनही केंद्रीय तिजोरीत पैसा गोळा होत असे. उरलेला माल सार्वजनिक बाजारपेठेत विकून पैसा सरकार जमा होत असे. मोगल सम्राटांनी मुसलमान सोडून इतर समाजावर जिजिया कर लावला होता. अकबरने कलांतराने तो कर बंद केला. पण औरंगजेबाने पुन्हा तो कर सुरू केला. हिंदूवर तीर्थयात्रा कर लावला. अकबरने तो बंद केला. पण औरंगजेबने तो पुन्हा लावला. मुसलमानांवर जकात हा कर लावला. मात्र गरीब मुसलमानांना त्यात सूट मिळत असे. असे हिंदू बाबत होत नसे. धार्मिक करांपासून केंद्रीय तिजोरीत मोठा पैसा गोळा होत असे. याशिवाय जंगल, खनिज पदार्थ, मीठ इत्यादींपासून सरकारला कर मिळत होता. जहाजबांधनी, इमारत व राजवाडे बांधन्यासाठी लाकूड लागत असे. त्याच्या पैसा सरकारला प्राप्त होई. मीठ उत्पादन मात्र सरकारच्या मालकीचे होते. राजस्थान मधील सॉभर तलाव व पंजाब प्रांतातील मिठाची टेकडी येथून मीठ प्राप्त होई व ते देशभर विकल्या जाई. त्यातून सरकारला मोठा फायदा मिळत असे. सम्राट अकबराच्या केंद्रीय तिजोरीत १३२१३६८२१ रु. वर्षाला गोळा होत असे, असे इतिहासकार अबुल फजलने, सम्राट शहाजहानच्या केंद्रीय तिजोरीत २२५०००००० रु. वर्षाला गोळा होत असे, असे अब्दुल हमिद लाहोरीने, औरंगजेबाच्या केंद्रीय तिजोरीत ३८६८१६५८४ रु. गोळा होत असे, असे सुजनराय नावाच्या लेखकाने लिहून ठेवले आहे.

सरकारी जावक :

मध्ययुगात लष्करी प्रशासनावर मोठा खर्च होत असे. त्यात सैनिक व सैनिकी अधिकऱ्याचे भत्ते, तोफा, बारुद, तोफगोळे, सैनिकांना मिळणारे घोडे, बैल, बैलगाड्या, हत्ती, उंट तसेच ह्या प्राण्यांना देखरेखीसाठी मोठा कर्मचार वर्ग नेमला जाई.

उत्तम दर्जाचे घोडे अरबस्तानातून आयात केले जाई. त्यावर मोठी रक्कम खर्च होई. नागरी प्रशासन चालवण्यासाठी जो खर्च सरकारला करावा लागे. राजघराण्यावर, दरबारावर सुद्धा मोठा खर्च होत असे. बादशहाच्या जनानखान्याचा स्वतंत्र खर्च होता. जनानखान्यात हजारो स्त्रीया राहत असे. अकबराकडे ५००० पेक्षा जास्त स्त्रिया होत्या. त्यांच्या देखरेखीसाठी, मोठा नोकरवर्ग होता, दासदासीवर, शाही स्वयंपाकगृहावर मोठा खर्ज होत असे कारण हजारो लोकांचे जेवण तेथे तयार होत असे. शाही कारखान्यात काम करणाऱ्या हजारो

कामगारांचा पगार केंद्रीय तिजोरीतून होत असे. त्याशिवाय मोगल बादशहा चैनी व विलासी होते. त्याच्यासाठी उच्च दर्जाच्या विदेशी वस्तू परदेशातून बोलावल्या जाई. त्यावरही मोठा खर्च होत असे. मोगल काळात हा लोककल्याणाचा काळ नव्हता. बादशहाला सर्व सामान्य लोकांचे फारसे घेणे देणे नव्हते. लोकांनाही आपला बादशहा कोण आहे हे माहित नव्हते. स्थानिक सरंजामदार, मनसबदारांनाच आपला स्वामी समजत असे. असे असले तरी बादशहा भारभर वाहतूक व प्रवासासाठी रस्ते तयार करीत असे. रस्त्याच्या कडेला झाडे लावणे, विहीरी बांधणे, धर्मशाळा बांधणे इत्यादी कामे मोगल बादशहा स्थानिक प्रशासना मार्फत करीत असे. ओलीतासाठी तलाव खोदले जाई. नद्यांवर पुल बांधले जाई. या शिवाय देशभरातील वार्ता, बातम्या बादशहाला कळाव्या म्हणून डाकव्यवस्था चालविली जात. ही व्यवस्था धावक, उंट, घोडे इत्यादी मार्फत होत असे. त्यावरही मोठा खर्च होत असे. मोगल बादशहांना बांधकामाची मोठी आवड होती, हे आजही दिल्ली व उत्तर भारतातील बांधकाम पाहिल्यानंतर लक्षात येईल. येथे किल्ले, महाल, मकबरे, मशिदी इत्यादींवर मोठा खर्च होत असे. मोगल बादशहाच्या दरबारात अनेक विद्वान लोकांना आश्रय दिला जाई. मक्का व मदिना येथेही बादशहा पैसा पाठवित असे, याशिवाय सार्वजनिक दवाखाने, औषधालय, अनाथ लोकांना मदत, निर्धन लोकांचे विवाह, दुष्काळात होणारा खर्च, बाग बगीचे निर्माण इत्यादींवर मोठा खर्च होत असे.

संदर्भ ग्रंथ सूची :

१) हमारे पुराने नगर,	लेखक डॉ. उदयनारायण राय
२) दिल्ली और उसका आंचल,	लेखक वाय. डी. शर्मा
३) मध्यकालीन भारत,	लेखक प्रा. ठवळे, बारगळ
४) भारताचा इतिहास,	लेखक डॉ. नि. सी. दिक्षीत
५) मध्ययुगीन भारताचा इतिहास,	लेखक प्रा. मा. म. देशमुख
६) भारतका आर्थिक इतिहास,	लेखक डॉ. ओमप्रकाश सिंह
७) ऐतिहासिक मानचित्रावली	लेखक सुश्मिता राणी, अखिलेश झा
८) Our Pasts-II	N.C.E.R.T.
९) इतिहास विश्वकोश	लेखक डॉ. राजेशकुमार

❖❖❖

महाविद्यालयीन ग्रंथालय आणि माहिती साक्षरता

(College Library & Information Literacy)

डॉ. जी.पी. उरकुंदे
ग्रंथपाल, इंदिरा महाविद्यालय, कळंब, जि. यवतमाळ
भ्रमणध्वनी ९७६५०३४०९७ E mail: dr.urkunde@gmail.com

प्रस्तावना :–

एकविसावे शतक हे माहितीचे ज्ञान युग आहे. या ज्ञान युगामध्ये माहितीवर आधारित ग्रंथालय व्यवसायाला अधिकच महत्त्व प्राप्त झाले आहे. ग्रंथालयामध्ये माहिती तंत्रज्ञानाचा वापर फार मोठ्या प्रमाणात केला जात आहे. माहिती ग्रहण करण्याच्या जुन्या पद्धती कालबाह्य झालेल्या आहेत, त्यामुळे नव्याने भर पडणाऱ्या माहितीचा मागोवा घेणे, त्या माहितीचे उपयुक्त ज्ञानात रूपांतर करणे आणि त्या ज्ञानाच्या आधारे समाजाच्या उत्पादकतेत भर घालून मूल्यवृद्धी करणे हे आजच्या युगात आपल्यापुढे फार मोठे आव्हान आहे. आज जगातल्या जवळपास सर्वच देशामध्ये माहिती तंत्रज्ञानाच्या उपयोगामुळे सर्वच क्षेत्रात महत्त्वपूर्ण क्रांती घडून आलेली आहे. माहिती तंत्रज्ञानाच्या उपयोगामध्ये भारताचा ४० वा क्रमांक लागतो.

महिती साक्षरता खरे तर आयुष्यभरातील निरंतर शिक्षणाचे मूळ आहे. ते सर्व क्षेत्रासाठी सर्व शैक्षणिक वातावरणामध्ये तसेच शिक्षणाच्या सर्व स्तरासाठी सारखेच आहे. माहिती साक्षरतेमुळे विद्यार्थ्याला माहितीच्या आशयावर (Contents) प्रभुत्व मिळते. शिवाय स्वत:ला संशोधनात निर्देश करण्याचे सामर्थ्य येते. माहिती साक्षरता ही संकल्पना सर्वप्रथम १९७४ मध्ये पॉल जी. झुरकोस्की यांनी मांडली. सध्या माहिती ही ग्रंथ, नियतकालिके,शोधनिबंध, ई–बुक्स, सी.डी., इंटरनेट अशा वेगवेगळया माध्यमातून प्रकाशीत होत आहे. आपणाला हवी असेलेली माहिती ही कोणत्या साधनामध्ये आहे, उपयोग कसा करावा, हे आव्हान आपल्या सगळ्यांच्या समोर आहे. त्यासाठी विशेष कौशल्याची गरज भासते. त्यासाठीच माहिती साक्षरता ही संकल्पना पुढे आलेली आहे.

महिती साक्षरता (Information Literacy) :–

अमेरिकन लायब्ररी असोशिएशनने १९८९ मध्ये केलेली व्याख्या खालीलप्रमाणे –

"माहिती साक्षरता म्हणजेच अशा विविध क्षमतांचा समूह की, ज्यामध्ये व्यक्ती आपणस हव्या असणाऱ्या माहितीची गरज ओळखू शकतो, तसेच अशी आवश्यक माहिती शोधण्याची, तिचे मूल्यमापन करण्याची आणि ती परिणामकारकपणे वापरण्याची क्षमता प्राप्त करू शकतो."

बर्चिनल यांनी खालीलप्रमाणे माहिती साक्षरतेची व्याख्या केलेली आहे –

"माहिती साक्षर होण्याकरिता नवकौशल्यांचा संच आवश्यक असतो. यामध्ये समस्या सोडविण्यासाठी तसेच कार्यक्षमपणे आणि प्रभावीपणे निर्णय घेण्याकरिता माहितीचा शोध आणि वापर याचा समावेश होतो.

Association of college and Research libraries (ACRL) has defined the "Information Literacy as the set of skill needed to find, retrieve, analyze and use information".

माहिती साक्षरता म्हणजे एक अशी कला की, ज्यात संगणकाचा वापर कसा करावा आणि त्या माध्यमातून माहितचे वेगवेगळे पैलू तांत्रिक, सामाजिक, सांस्कृतिक, तात्त्विक आणि त्याचा प्रभाव जाणणे म्हणजेच माहिती साक्षरता होय. कोणत्याही ग्रंथालयात माहिती साक्षरता कार्यक्रम राबविण्यापूर्वी त्यांची माहितीची गरज समजावून घेणे महत्त्वाचे ठरते.

महाविद्यालयीन ग्रंथालयात माहिती साक्षरतेची गरज :–

२१ व्या शतकामध्ये प्रचंड प्रमाणात माहितीचा विस्फोट झालेला आहे. अशी माहिती विविध साधनांमध्ये दृकश्राव्य स्वरूपात प्रकाशित होत आहे. त्यातच माहिती तंत्रज्ञानामध्ये प्रचंड प्रमाणात वाढ होताना दिसते आहे.

आजचे तंत्रज्ञान उद्या कालबाह्य होत आहे. पारंपारिक स्वरूपाच्या ग्रंथालयांमध्ये बदल होऊन इलेक्ट्रॉनिक ग्रंथालये, डिजीटल ग्रंथालये असे आधुनिक स्वरूप प्राप्त झाले आहे. त्यातच सध्या आंतरशाखीय संशोधन होत असून एखाद्या विषयावरील संशोधनपद्धती, तंत्रे दुसऱ्या विषयामध्ये वापरली जात आहेत. या सर्व प्रश्नांमुळे माहितीचा वापर करणाऱ्या संशोधनामध्ये संभ्रमावस्था निर्माण झालेली आहे. त्यामुळेच माहिती साक्षरतेला महत्त्व प्राप्त झाले आहे.

महाविद्यालयीन ग्रंथालयात विद्यार्थी, प्राध्यापक आणि वेगवेगळ्या विषयावर संशोधन करणारे संशोधक हे महत्त्वाचे वाचक असतात. त्या घटकांना वेगवेगळ्या विषयावरची पुस्तके तसेच माहिती हवी असते. शिक्षकांना शिकविण्यासाठी वेगवेगळ्या नवनवीन वाचन साहित्याची गरज भासते. ती गरज ग्रंथालयामधून पूर्ण व्हावी अशी वाचकांची अपेक्षा असते. यासाठी माहिती साक्षरतेच्या खालील घटकांना महत्त्व प्राप्त झाले आहे.

१. माहितीची गरज
२. माहितीची साधने
३. रोजच्या घडमोडींची माहिती
४. बैठका आणि कार्यशाळेत सहभाग
५. विकासाच्या वेगवेगळ्या संधीची गरज
६. नवीन माहितीची निर्मिती करणे
७. माहितीचे मूल्यमापन

माहिती साक्षरता आणि महाविद्यालयीन ग्रंथालये :–

ग्रंथालयामध्ये येणाऱ्या नवीन वाचकांना ग्रंथांबद्दल सविस्तर माहिती देऊन त्यांच्यामध्ये वाचनाची गोडी तयार करण्याशिवाय ग्रंथालयांना तरणोपाय नाही. महाविद्यालयीन तसेच विद्यापीठ ग्रंथालयामध्ये कोणकोणती माहिती उपलब्ध आहे व ती माहिती कोणकोणत्या स्वरूपात आहे. त्या माहितीचा शोध कसा घ्यावा याची माहिती वाचकांना देणे आवश्यक आहे. आजचे युग हे इंटरनेटचे युग आहे. इंटरनेटद्वारे नवनवीन माहिती वाचकांना हवी असते. ती सेवा देण्याकरिता तयार असणे अशी भूमिका ग्रंथालयांची असली पाहिजे.

महाविद्यालयीन ग्रंथालयातील वाचक हा मोठ्या संख्येने विद्यार्थी असतो. त्यांना माहितीच्या संदर्भात साक्षर करण्यासाठी ग्रंथपालांनी वेगवेगळे उपक्रम राबविले पाहिजे. आजच्या माहिती तंत्रज्ञानाच्या युगात माहिती ही प्रचंड प्रमाणात दररोज प्रकाशित होत असल्यामुळे ती ग्रंथालयात वेगवेगळ्या स्वरूपात साठवून ठेवल्या जाते. या साधनाची विद्यार्थ्यांला माहिती नसते. अशावेळी ग्रंथालयासंबंधी माहिती देणे हे महाविद्यालयीन ग्रंथपालाचे आद्य कर्तव्य असते.

माहिती साक्षरतेचे विविध पैलू :–

ग्रंथालयात माहिती साक्षरता उपक्रम राबवित असताना पुढील घटकांचा समावेश करणे आवश्यक असते.

१. विद्यार्थ्यांना ग्रंथालयाबद्दल ग्रंथालय सेवांची तसेच ग्रंथालयाच्या विविध उपक्रमाची माहिती देणे.
२. वाचक उदबोधन वर्ग चालविणे.
३. प्रत्येक विषयातील नवनवीन माहिती, संदर्भग्रंथातील माहितीचा उपयोग कशा पद्धतीने करावा यांचे मार्गदर्शन करणे.
४. ग्रंथ प्रदर्शन भरवून विद्यार्थ्यांना नवनवीन ग्रंथाची माहिती देणे.
५. विद्यार्थ्यांसाठी स्पर्धा परीक्षा, नोकरीविषयक माहिती, स्वयंरोजगाराविषयी माहिती उपलब्ध करून देणे.
६. वाचन संस्कृती आणि लेखन संस्कृती विषयी महत्त्व विशद करणे.
७. विद्यार्थ्यांना भावी जीवनातील जबाबदाऱ्या समर्थपणे पेलण्यासाठी मार्गदर्शन करणे.
८. चालू घडामोडींचे ज्ञान प्राप्त करून देणे.
९. इंटरनेटचा वापर कसा करावा व इंटरनेटवरून माहिती कशी मिळवावी याचे मार्गदर्शन करणे.
१०. ग्रंथालयातील बहि:शाल योजनांची माहिती देणे.

माहिती साक्षरता उपक्रमाचे फायदे :–

आजच्या जागतिकीकरणामुळे परदेशी विद्यापीठे आपल्या देशात स्वत:चे स्थान निर्माण करण्यासाठी उत्सुक आहेत व त्या दिशेने त्यांची वाटचाल सुरू आहे. या विदेशी शिक्षण संस्थांची स्पर्धा करण्यासाठी आपला विद्यार्थी शैक्षणिकदृष्टया सक्षम असणे आवश्यक आहे.

१. ग्रंथालयाची विद्यार्थ्यांचा सतत संपर्क राहत असल्यामुळे वाचन संस्कृती विकसित होईल.
२. विद्यार्थ्यांच्या ज्ञानाच्या कक्षा रूंदावण्यास मदत होईल.
३. संशोधनासाठी ग्रंथालयाचा अधिकाधिक उपयोग होईल.
४. विद्यार्थ्यांमध्ये स्वयंअध्ययनाची सवय लागेल.
५. महाविद्यालयीन ग्रंथालयाचा उपयोग जास्तीत जास्त प्रमाणात होईल.

समारोप :–

भारतातील उच्च शिक्षणामध्ये दर्जा वाढविण्यासाठी ज्या गोष्टीची आवश्यकता आहे. त्यासाठी महाविद्यालयीन ग्रंथालयांमध्ये माहिती साक्षरता उपक्रम राबविणे क्रमप्राप्त आहे. त्यामुळे विद्यार्थ्यांमध्ये आत्मनिर्भरता निर्माण होऊ शकेल. महाविद्यालयीन ग्रंथालयामध्ये माहिती साक्षरता उपक्रम मांडताना उच्च शिक्षणातील घटक, विद्यापीठ, महाविद्यालयाचे व्यवस्थापक, प्राचार्य व प्राध्यापक यांचेही मत जाणून घेणे आवश्यक आहे. ग्रंथालयात ग्रंथपाल व काम करणारे कर्मचारी यांच्या संयुक्त प्रयत्नाने माहिती साक्षरता उपक्रम प्रभावीपणे राबविता येऊ शकतो.

माहिती साक्षरता ही खरोखरच आयुष्यभरातील निरंतर शिक्षणाचे मूळ आहे. इंटरनेटच्या उपलब्धतेमुळे माहिती साक्षरतेस आणखी महत्त्व प्राप्त झाले आहे. आजच्या स्पर्धेच्या युगात प्रवाहाबरोबर चालणे फार गरजेचे आहे. जो थांबला तो संपला या करिता माहिती साक्षरतेची अतिशय आवश्यकता आहे.

संदर्भ ग्रंथसूची

१. Deshmukh Prashant : An Analytical study of literature on Information literacy, library Herald, vol. 49(4) Dec. 2011.
२. बाहेती एस.आर., 'महाविद्यालयीन ग्रंथालयात माहिती साक्षरता कार्यक्रम, ज्ञानगंगोत्री २००७.
३. खेरडे मोहन, 'महाविद्यालयीन ग्रंथालयात माहिती साक्षरता, ज्ञानगंगोत्री, ऑगस्ट २००७.
४. वीर डी.के.(संपा), 'ग्रंथपरिवार परभणी : मराठवाडा ग्रंथालय संघ २००५ संपादकीय सप्टें–आक्टों. २००५.

❖❖❖

श्रमयोगी बाबा आमटे

प्रा. रा.तु. आदे
मराठी विभाग, इंदिरा महाविद्यालय, कळंब, जि. यवतमाळ
भ्रमणध्वनी ९४२२६०८७१५ E mail: rajuade2512@gmail.com

''शृंखला पायी असू दे, मी गतीचे गीत गाई
दु:ख उधळायास आता, आसवांना वेळ नाही''

दु:खावर मात करून गतीचे गीत गाण्याची अभिलाषा बाळगणाऱ्या मुरलीधर देविदास आमटे यांचा जन्म २६ डिसेंबर १९१४ रोजी 'हिंगणघाट' येथे झाला. अत्यंत संपन्न वारसा लाभलेल्या मालगुजार–जमीनदार कुटुंबात जन्माला आलेल्या आमटेंची वडिलोपार्जित शेकडो एकर शेती वरोऱ्याजवळील 'गोरज' या ठिकाणी आहे. वडील सरकारी अधिकारी. त्यामुळे सर्वार्थाने सुखवस्तू असलेल्या कुटुंबात मुरलीधर आमटेंचा जन्म हा 'चांदीचा चमचा तोंडात घेऊन जन्माला यावे' अशा घराण्यात झाला होता. एम.ए.,एल.एल.बी.पर्यंतचे शिक्षण घेतल्यानंतर त्यांनी वकिलीस प्रारंभ केला. वकिली व्यवसायात सफाईदारपणे खोटं बोलता येणे आवश्यक आणि यांना खोटं बोलता येत नसे. तसेच काबाडकष्ट करणाऱ्यापेक्षा कमी श्रमात अधिक मोबदला ही विषमताही त्यांना अमान्य होती. या कारणास्तव त्यांनी अल्पावधीतच वकिली सोडली.

समाजकार्याची–लोकसेवेची आवड त्यांना आधीपासूनच होती. वकिली करत असताना अनेक अडल्या–नडल्यांची कामे त्यांनी नि:शुल्क करून दिली होती. गोरगरिबांविषयी त्यांच्या मनात कणव होती. त्यातूनच समाजाप्रती त्यांच्या मनात आपुलकी निर्माण झाली त्याचाच परिपाक म्हणजे राजकारणात त्यांनी केलेला प्रवेश हा होय! वरोरा नगरपालिकेचे उपाध्यक्ष म्हणून त्यांनी सूत्रे स्वीकारली व समाजकार्यात ते समरस झाले. भंगी युनियनचे अध्यक्ष म्हणून त्यांची निवड झाली. एकदा भंग्यांनी कामबंद आंदोलन पुकारले, तेव्हा डोक्यावरून मैला वाहून नेण्याचे कार्य त्यांनी केले. अशाच एका पावसाळी रात्री 'तुळशीराम' नामक कुष्ठरोग्याला त्यांनी अत्यंत कुरूप अवस्थेत पाहिले. भीती, जुगुप्सा, किळस, कारुण्य या भावनांनी त्यांच्या मनाभोवती थैमान घातले. कंठातून शब्द फुटेनासा झाला. पण काही वेळाने जुगुप्सेची जागा करुणेने घेतली. त्यांनी कुष्ठरोग्यांची सेवा हेच जीवित ध्येय ठरविले व तिथूनच मुरलीधर देविदास आमटे हे 'बाबा आमटे' म्हणून प्रसिद्ध झाले. एका समाजसेवकाच्या आयुष्याला अशाप्रकारे सुरुवात झाली.

समाजाने टाकलेल्या, झिडकारलेल्या कुष्ठरोग्यांना हक्काचे घर मिळवून देण्याचे कार्य त्यांनी केले. ६ कुष्ठरोगी, लंगडी गाय व १४ रु. इतके भांडवल घेऊन ते दोन मुले व साधनाताईसमवेत आनंदवनाच्या जंगलात आले. पाच कुष्ठरोगी मनोहर दिवाणांना मागितले. त्यात शंकरराव देव हे पहिले होत. अशाप्रकारे समाजाने दूर लोटलेल्या, व्याधीग्रस्त, निराश, जगण्याची उमेद गमावून बसलेल्या, हातापायांची बोटे झडलेल्या, कुष्ठरोग्यांना सन्मानाने जीवन प्रदान करण्यासाठी बाबांचे प्रयत्न सुरू झाले. कुणाचा बाप, कुणाचा भाऊ, कुणाचा मुलगा अशा नातेबंधनात अडकलेल्या माणसाला या रोगानी परस्परांपासून दूर केले. म.गांधी म्हणत, ''शरीराला जडलेला महारोग हा औषधाने बरा होऊ शकतो पण मनाला जडलेला महारोग दुर्धर आहे.''[१] माणसाविषयीचे प्रेम, जिव्हाळा, आपुलकी या रोगामुळे पार आटून जाते. व्याधीग्रस्त माणसे असहाय, दुबळी, परावलंबी, कर्तव्यशून्य, बनतात. अशा माणसांमध्ये जगण्याची नवी उमेद निर्माण करण्याचे कार्य बाबा आमटेंनी केले. 'दान नादान करते, काम उभारते' हे तत्त्व उराशी बाळगून थापे झालेल्या हातांकडून त्यांनी श्रमाची कामे करवून घेतली व श्रमाची महती त्यांच्या मनात रुजविली. जगण्याचा आत्मविश्वास त्यांच्यामध्ये निर्माण केला, स्वावलंबी बनविले. महात्मा गांधीची प्रेरणा त्यांना या कामी उपयुक्त ठरली.

बाबा आमटेंनी सुरू केलेले कुष्ठरोगासंबंधीचे कार्य 'रिलिफ वर्क' नव्हे, फक्त पुनर्वसन नव्हे तर निराशेचे आशेत रूपांतर करण्याचे ते अभियान आहे. आपल्या पायाखालची जमीन ही आपली नाही, असे वाटणाऱ्या माणसांना मजबूतपणे पाय रोवून स्वबळावर उभे करणारा तो 'यज्ञ' आहे. पारशी भाषेत देवाची प्रार्थना करतांना तीन प्रतिकांचा उल्लेख करतात. ''तू आमचा रहीम आहेस! तू आमचा हकीम आहेस! तू आमचा वकील आहेस! करुणा करतो तो रहीम, दु:ख मिटवतो तो हकीम तर अन्यायापासून संरक्षण करतो तो वकील''[१] ही

वेदशास्त्रसंपन्न घुलेशास्त्री यांच्या इंदू नामक मुलीशी बाबा आमटे १८ डिसेंबर १९४६ साली प्रेमविवाहबद्ध झाले. कट्टर सोवळे–ओवळे पाळणाऱ्या इंदूताई, आवडीने गोड खाणाऱ्या असूनही येथील परिस्थिती बघितल्यानंतर त्यांनी गोड खाणे बंद केले. पूजा–अर्चा, व्रतवैकल्ये, कर्मकांड, पोथ्या–पारायणे यात रमणाऱ्या साधनाताई, बाबांना या सर्व गोष्टींची नावड. त्यामुळे अशा विरूद्ध मनोवस्था असणाऱ्या व्यक्तीसोबत संसार करण्याचा खरा प्रश्न होता. मात्र, उभयतांनी सामंजस्याने त्यातून मार्ग काढला.

''नवरा ज्वालामुखी, मी बर्फाचा पर्वत झाले
समिधाच सख्या या, यात कुठे ओलावा!
तव आंतर अग्नि क्षणभर तरी फुलवावा''

अशा पद्धतीने प्रेमाने बाबांच्या रागाची तीव्रता शमविण्याची कला साधनाताईंना गवसली व उभयतांचे जगणे व जीवन जाणिवा एकरूप झाल्या. स्वत:साठी सगळेच जगतात पण दुसऱ्यांसाठी जगायला व सोसायला मनाचा मोठेपणा असावा लागतो, तो या दाम्पत्यात पुरतेपणे वसत होता. कुष्ठरोग्यांना बाबा नेहमी सांगत, ''जे हरपले, जे नाही त्याचा शोक करीत आयुष्य वाया घालवू नका! जे नाही त्याने, जे आहे त्याचा अवमान करू नका, जे आहे ते जास्तीत जास्त सार्थकी लावण्याचा प्रयत्न करा. त्यातूनच तुमच्या जीवनात आनंद निर्माण होईल.''[५] आयुष्याकडे बघण्याचा हा नवा दृष्टिकोण कुष्ठरोग्यांमध्ये आमूलाग्र बदल घडवू लागला. बाबा आमटेंविषयी एस.एम. जोशी म्हणाले होते ''बाबांचे जीवन म्हणजे शाश्वत सत्याचा शोध घेणारी एक चालती बोलती प्रयोगशाळा आहे. त्यासाठी त्यांनी आपला पुरुषार्थ ओतला आहे आणि त्यातून 'आनंदवना'ची निर्मिती झाली.''[६] निर्मितीतले सौंदर्य आणि श्रमातले संगीत यांचा शोध घेण्याचा प्रयत्न येथे केला जात आहे.

श्री.राहुल बारपुते मित्रमेळाव्याची महती विषद करताना म्हणतात,''संपूर्ण जीवन काळवंडल्या अवस्थेत असताना, माणसांचा उबग आलेला असताना आनंदवनाची ओढ लागते. बाबा व त्यांच्या सारखी माणुसकीवर श्रद्धा ठेवून जीवनाच्या वेगवेगळया क्षेत्रात नि:स्वार्थ बुध्दीने काम करणारी माणसे भेटतात, बोलतात. अनुभवांची देवाण–घेवाण होते, विचारांचे आदानप्रदान होते आणि मनाची उमेद जागी होते. माणसाची माणुसकीवरील श्रध्दा दृढ होते. जीवनात दुसऱ्यांसाठी सर्वस्वाचा होम करून जगणारी माणसे इथे पाहिली की मन उजळून निघते.''[७] मित्रमेळाव्यातून निघालेला निष्कर्षच त्यांनी त्यातून विषद केला आहे. ''समतेसाठी स्वत: वेडे होऊन दुसऱ्यांना वेड लावणारी काही माणसे आहेत. त्यामध्ये बाबा आमटे यांचा पहिला नंबर लावावा लागेल.''[८]

वकील, नगराध्यक्ष, समाजसेवक, लेखक, कवी, वक्ता, समीक्षक अशा नानाविध भूमिका सहजगत्या पार पाडणारे बाबा अत्यंत दूरदर्शी, कल्पक, व्यवहारी व चोख हिशेबी आहेत. ते विज्ञान योगी असून लोक–संग्राहक आहेत, संघटक आहेत त्याचबरोबर गुणग्राहकही आहेत. ते काय–काय आहेत ते शब्दात सांगणे अवघड आहे.

त्यांनी केलेल्या कामांची नुसती नामावली जरी पाहिली तरी सामान्य माणसाची छाती दडपून जाते. आनंदवन, सोमनाथ प्रकल्प, लोकबिरादरी प्रकल्प, भामरागड, 'भारत जोडो' अभियान, अशोकवन, हेमलकसा प्रकल्प, पंजाब शांतता यात्रा, मुक्तांगण, स्वरानंदनवन, नर्मदा बचाओ आंदोलन, इ. प्रकल्पांमध्ये आणि आंदोलनांमध्ये ते सतत कार्यमग्न राहत असत. त्यामुळे त्यांच्या वर्तनात एक प्रकारची निश्चयात्मकता आली होती. श्रमाची संस्कृती निर्माण करण्याची एक अभिनव कल्पना त्यांनी प्रत्यक्षात साकार केली.

''आर्थर तोरनोस्की हा पोलीश काऊंट, वयाच्या २८ व्या वर्षी त्याला पोलिओ झाला. इंग्लंडमध्ये स्थायिक झालेल्या या लेखकाला जगभर हिंडायचे होते. 'रिडर्स डायजेस्ट ग्रुप ऑफ अमेरिका यांनी त्यांची भ्रमणयात्रा आयोजित केली. जिथे आजवर कुणी गेले नाही तिथे तो जाऊन आला. त्याचे त्याने एक पुस्तक लिहिले 'आमटेज मिरॅकल' या नावाची दोन प्रकरणे त्यात होती. त्याला लेखनासाठी कॉपीराईटचे दीड लाख रुपये मिळाले. त्या पैशातून त्यांनी बाबा आमटे यांच्या 'संधीनिकेतन' साठी मदत केली व प्रकल्प सुरू झाला.''[९] अंध, अपंग, दुर्बलमनस्क, मूक–बधीर असे सारे लोक एकत्र 'संधीनिकेतन' मध्ये काम करत आहे, असे उदाहरण जगात नाही. कुष्ठरोग बरा झाल्यानंतर त्यांना यात संधी मिळते. सुतारकाम, लोहारकाम, प्लंबिंग, प्रिंटींग, शिवणकला, गालीचा बनविणे, खादीचे कापड तयार करणे, चित्रकला, पोस्टर, ग्रिटींग कार्डस् इ. वस्तू तयार करण्याचे काम येथे केले जाते. यामुळे स्वाभिमानाने जीवन जगण्याची संधी त्यांना मिळते. 'तुम मुझे पसीना दो। मै तुम्हे जिंदगी दूँगा।। असे म्हणत बाबांनी त्यांच्यासाठी जगण्याच्या नव्या वाटा उघडल्या.

तिन्ही रूपे बाबांमध्ये पहावयास मिळतात. वेदनांच्या जखमा घेवून जगणारा माणूस म्हणजे बाबा आमटे! येशू ख्रिस्त, म.गांधी, विनोबा भावे, साने गुरूजी, मनोहर दिवाण यांच्या सेवाकार्यातून प्रेरणा घेऊन बाबा आमटेंनी कार्यारंभ केला. समाजाने 'मृत' म्हणून जाहीर केलेल्या रुग्णातून जिवंत मानव उभा करणे हे त्यांनी स्वत:चे कर्तव्य मानले.

ज्यांच्या हातापायांची बोटे झडली आहेत, ज्यांच्या संवेदना बधीर झाल्या आहेत, ज्यांची दृष्टी गेली आहे, ज्यांना धड ताठ उभे राहता येत नाही, नीट चालता येत नाही अशा रुग्णांच्या परिश्रमातून आनंदवनाचे सौंदर्य, वैभव, निर्मलता व आनंद उभा राहिला आहे व आनंदवनाचे नावही सार्थक करतो आहे. बाबा आमटे यांनी वयाच्या ३३ व्या वर्षापासून समाजसेवेला आरंभ केला. मातीतून मोती पिकविण्याची प्रेरणा त्यांनी कुष्ठरोग्यांना दिली. समाजाने किंवा नियतीने ज्यांना अखंड उपेक्षाच दिली. अशा कुष्ठरोग्यांसाठी, अंध–अपंगांसाठी, मूक–बधिरांसाठी त्यांनी स्वत:चे आयुष्य खर्ची घातले. स्वत:चे व्यक्तिमत्त्व त्यांच्यात विलीन करून टाकले. 'मी एका वेडश्या आईचा मुलगा' असे ते संबोधत. हे संबोधन सानेगुरुजींसाठी आलेले होते. सेवेचा धर्म त्यांनी गुरूजींपासूनच आत्मसात केला. साने गुरुजी म्हणजे सौंदर्य आणि शुचिता याचा मनोज्ञ संगम' मांगल्याच्या ध्यासाचा नाजूक बळी. बाबा आमटे यांनी 'गर्भवती मातेचे प्रतीक' साने गुरूजींना मानले होते.

ज्याकाळी कुष्ठरोग हा महारोग समजला जात असे, पूर्वजन्माच्या पापाचे फळ म्हणून कुष्ठरोग होतो, अशी समाजाची धारणा होती आणि औषधोपचारही उपलब्ध नव्हते, अशा काळात बाबा आमटेंनी अतिशय समर्पित भावनेने व मिशनरी वृत्तीने कुष्ठरोग्यांच्या पुनर्वसनाचे कार्य केले. त्यांच्या या कामगिरीचा समाजमनावर खोल ठसा उमटला आणि कुष्ठरोगाकडे पाहण्याची दृष्टी आमूलाग्र बदलली.

तत्कालीन आरोग्यमंत्री श्री. बळीराम हिरे यांना लिहिलेल्या पत्रात बाबा आमटे लिहितात, ''आनंदवनासारख्या संस्था ही समाजाच्या मानसिक आरोग्याची प्रतिके नव्हेत. सामाजिक अनारोग्याचीच ती लक्षणे आहेत. या संस्थांचे स्वरूप कायम वसाहतीचे नाही व असू नये... कुष्ठ पीडितांचा प्रश्न हा समाजाचा प्रश्न असून त्याचा समाजनिरपेक्ष विचारच करता येणार नाही, हे लक्षात घेतले तर कुष्ठरोग्यांच्या स्वतंत्र वसाहतीतून एक नवा जातीयवाद जन्माला येईल आणि समाजाची कायम उपेक्षा त्यांच्या वाटयाला येईल.''[३] यामधून बाबांनी या समस्येकडे किती आस्थेवाईकपणे पाहिले व द्रष्टेपणाने यावर विचार केला हे लक्षात येते.

देशभरातील तरुणांना आत्मसपर्णाची दिलेली हाक, त्यांना सुसंस्कारित करण्यासाठी घेतलेले सतीचे वाण व त्यांच्या सामूहिक पुरुषार्थातून त्यांनी उभारलेली आनंदवनाची नवी सृष्टी ह्यामध्ये समर्थ रामदासांचे 'आनंदवनभुवन' व आमटयांचे 'आनंदवन' यात साम्य आहे. बाबा आमटे यांनी तरुणांना व समाजाला कोणीतरी व्हा! कशावर तरी श्रद्धा ठेवा! काही तरी करा!'' अशा प्रकारे कर्तव्यासाठी मनाची तयारी असणे व निष्ठेने काम करणे गरजेचे असते असे सांगितले. श्रमानीच माणसे मोठी होतात. काम में ही राम है! ही भावना त्यांनी कुष्ठरोग्यांमध्ये निर्माण केली.

''पांगळयांच्या सोबतीला, येऊ द्या बलदंड बाहू
निर्मितीच्या स्वेदगंगा, द्या इथे मातीत वाहू''[४]

श्रमाने नवनिर्मितीची संकल्पना प्रत्यक्षात उतरू शकते यावर बाबांचा विश्वास होता. श्रम हाच श्रीराम! असे मानून त्यांनी सोमनाथ येथे श्रमिक विद्यापीठाच्या स्थापनेची कल्पना मांडली व पूर्णत्वास नेली. कुष्ठरोग्यांना समाजात मानाने जगता यावे, मैत्रीचे संबंध निर्माण व्हावे, पूर्वग्रहाचे निराकरण व्हावे म्हणून १९६१ पासून आनंदवनात 'मित्र मेळावा' भरू लागला. पु.ल. देशपांडे, वसंतराव देशपांडे, राम शेवाळकर, दादा धर्माधिकारी अशा प्राध्यापक, डॉक्टर, लेखक, कलावंत, न्यायाधीश, समाजसेवक आदि मान्यवरांनी या मेळाव्यास आपली हजेरी लावली होती. व्याधीग्रस्त माणसाच्या मनावर मायेची फुंकर घालण्याची गरज असते,स्नेह सावलीची गरज असते. तेच काम या मेळाव्याने केले.

१९५० साली 'महारोगी सेवा समिती, वरोरा' ही संस्था पंजीबद्ध झाली. त्यानंतर दुसऱ्यास वर्षी १९५१ मध्ये 'आनंदवन' या संस्थेची स्थापना झाली. या संस्थेच्या निर्मितीपूर्वी १९४९ मध्ये कलकत्त्याला जाऊन'स्कुल ऑफ ट्रापिकल डिसीझेज' चे प्रशिक्षण त्यांनी घेतले. त्यावेळी 'मायक्रोबॅक्टेरियम लेप्री' या जंतूमुळे हा रोग होतो, हे त्यांना कळले. आनंदवनाकरिता कोल्हापूरच्या कोरगांवकर ट्रस्टकडून प्रतिमाह २०० रु. देणगी मिळते. दातृत्त्व जागी असणारी माणसेच दु:खी माणसांचे दु:ख जाणू शकतात, हेच त्यांच्या कृतीतून लक्षात येते.

बाबांनी आनंदवनात अंधांसाठी 'आनंद बुनियादी प्राथमिक शाळा', रोगमुक्त मुलांसाठी 'गोकुळ' ही स्वतंत्र शाळा, 'मुक्तिसदन' व 'सुखसदन' ही कुष्ठरोगातून मुक्त झालेल्या पण समाजाने न स्वीकारलेल्या वा ज्यांना स्वेच्छेने तेथे रहावयाचे आहे अशांसाठी त्यांनी स्वत:च निर्माण केलेली सुंदर वास्तू आहे. अनुभव–ज्ञानाने परिपक्व वयोवृद्धांसाठी बाबांनी 'उत्तरायण' आश्रम काढला. अशा प्रकारे दु:खितांचे अश्रू पुसून त्यांच्या आयुष्यात नवसंजीवनी निर्माण करण्याचे कार्य बाबा आमटेंनी केले. त्यांच्या या लोकविलक्षण कार्याचा गौरव म्हणूनच त्यांना पद्मश्री, राष्ट्रभूषण, डी.लिट्., कृषिरत्न, मेगॅसेसे अवॉर्ड पद्मविभूषण, सामाजिक न्याय पुरस्कार अशा अनेकविध पुरस्कारांनी गौरविले गेले. अमेरिकेतील कुष्ठरोगी सेवासंस्थेच्या वतीने त्यांना 'डेनियन डेरेन पारितोषिक' देऊन गौरविले गेले.

म. गांधींनी बाबांच्या कार्याचा गौरव 'अभय साधक' अशा सार्थ शब्दात केला आहे तर कविवर्य कुसुमाग्रजांनी त्यांच्याविषयी 'मातीची मागणी आकाशापर्यंत पोहचविणारा महामानव' असे प्रशंसोद्गार काढले. नरहर कुरुंदकर देखील त्यांना 'महाकवी' मानतात. एकूणच कवी, समाजसुधारक, तत्त्वज्ञ, विचारवंत, समीक्षक या साऱ्या भूमिका एकाचवेळी समर्थपणे पेलणारे बाबा आमटे हे चतुरस्र व्यक्तित्व होय. बाबा आमटे या कवीवर त्यांच्यातील समाजसेवकाने मात केलेली आहे,[१०] हे नरहर कुरूंदकरांचे मत लक्षणीय आहे.

संदर्भसूची :

१. चंद्रशेखर धर्माधिकारी, बाबा आमटे : व्यक्ती आणि कार्य–भ.ग.बापट, लोकमत, रविवार साहित्य जत्रा, ११ जाने. १९९८ पृ. ७
२. तत्रैव, पृ. ७
३. अविनाश पितळे, आनंदवनीचा श्रमयोगी, प्रथमावृत्ती, कॉन्टिनेन्टल प्रकाशन, १९८५, प्रका. अ.अ. कुळकर्णी, विजयानगर, पुणे पृ. ३०
४. बाबा आमटे, ज्वाला आणि फुले, १९६४.
५. मालती देशपांडे, 'बाबा आमटे आणि आनंदवन' लोकराज्य, व ३३,अंक९, १६ सप्टेंबर १९८३, पृ. ८.
६. उनि, अविनाश पितळे, पृ.८८.
७. उनि, अविनाश पितळे, पृ.४२.
८. 'समाजसेवकांचे साहित्य' प्रा.श्रीकांत पाटील, आमची श्रीवाणी, वर्ष १५, अंक १, आक्टोंबर २००७ ते २००८,पृ.४१
९. उनि, अविनाश पितळे, पृ.२४–२५
१०. उनि, श्रीकांत पाटील, पृ.४६

❖❖❖

39 Kishor Awastet mahiti wa tantradhyananacha Honara Parinam ek manasshastriy abbhyas

किशोरावस्थेत माहिती व तंत्रज्ञानाचा होणारा परिणाम एक मानसशास्त्रीय अभ्यास

प्रा. पी.बी. इंगळे
राज्यशास्त्र विभाग, इंदिरा महाविद्यालय, कळंब, जिल्हा यवतमाळ
भ्रमणध्वनी ९१५८६८६०६६ E mail: pandurangingle@gmail.com

सारांश

माहिती व तंत्रज्ञान हा आजच्या युगातील एक महत्त्वाचा आणि जीवनोपयोगी विषय आहे; शिक्षण क्षेत्र, वैद्यकीय क्षेत्र, व्यावसायिक क्षेत्र, अशा अनेक मानवी जीवनातील कार्यक्षेत्रांमध्ये हा विषय अपरिहार्य बनला आहे. शिक्षण क्षेत्रात तीनही प्रकारच्या विद्याशाखेत माहिती व तंत्रज्ञानाने प्रगती केली आहे. आज शिक्षणक्षेत्रात माहिती तंत्रज्ञानाने मोठी क्रांती घडून आणली आहे. 'व्हर्चुअल क्लास रूम' ही संकल्पना याच तंत्रज्ञानाचा एक पैलू आहे. डिजिटलायझेशनच्या माध्यमातून शालेय जीवनाचे स्वरूप हे पूर्णत: बदलेले आहे. पूर्वी शालेय जीवनात विद्यार्थी वह्या, पुस्तके, पाटी, पेन्सिल, खडू, लेखणी, इत्यादी शालेय साहित्याचा वापर करत असत. परंतु डिजिटलायझेशनमुळे या साहित्याची जागा एलसीडी प्रोजेक्टर, टॅब, कॉम्प्युटर, मोबाईल यांनी घेतली आहे. यामुळे विषयाचे स्वरूप कितीही अवघड असले तरी आकृती, चित्रांचा हुबेहूब वापर करण्यास, हे तंत्रज्ञान विषय समजावून देण्यासाठी शिक्षकासाठी व विद्यार्थ्यांसाठी विषयाचे आकलन करण्यास खूपच उपयोगी पडतो.

प्रस्तुत संशोधनाचा मुख्य उद्देश हा किशोरावस्थेत माहिती व तंत्रज्ञानाचा भावनिक बुद्धिमत्तेवर होणारा परिणाम याचा अभ्यास करण्याचा आहे. यासाठी संशोधकाने शालेय विद्यार्थ्यांचे दोन गट निवडले. त्यात व्हर्च्युअल क्लास मधील २० मुले पारंपारिक वर्गातील २० मुले असा तयार केला. दोन्ही गटाला डॉ. एन. के. चंदा यांची सामाजिक बुद्धिमत्ता चाचणी दिली. मिळालेल्या प्रदत्त घेऊन संख्या विश्लेषणातून सार्थक परिणाम दिसून आले. ज्या मुलांची भावनिक बुद्धिमत्ता अधिक होती, ती कम्प्युटरचा अधिक वापर करणारी दिसून आली.

प्रस्तावना

वैकासिक मानसशास्त्रात किशोरांच्या बद्दल, त्यांच्या व्यक्तिमत्त्व विकासावर, वाढ आणि विकासावर भरपूर संशोधन झाले आहे. किशोरावस्था याला इंग्रजीत 'ॲडोलेसेन्स' असे म्हणतात. हा शब्द लॅटिन क्रियापदापासून तयार झाला आहे. परिपक्वता लाभणे असा याचा अर्थ आहे. प्रस्तुत संशोधन हे किशोरांच्या भावनिक विकासावर माहिती व तंत्रज्ञाना काय परिणाम होतो या संदर्भात केले आहे. आधुनिक युगात संगणकाचा वापर हा विविध क्षेत्रात वाढत आहे. या संगणाचे मानवी जीवनात अनेक चांगले परिणाम झाले. त्या संदर्भात अनेक संशोधने झाली आहेत. तसेच संगणकाच्या वापरामुळे मानवी आरोग्यावर विपरित परिणाम होतात. या बाबतही अनेक निष्कर्ष मांडले आहेत.

भावना विकास

व्यक्तीच्या मनाच्या आंतरिक अवस्थेला भावना, इमोशन असे म्हणतात. व्यक्तीचा जीवन अनुभव जसा जसा वाढत जातो तसतसे व्यक्तीच्या अंतरंगातील अवस्थेचा म्हणजे भावनेचा विकास होतो. बाल्यावस्थेत होणारी जडणघडण हा मुख्य पाया समजला जातो. बाल्यावस्थेत भावनेचे स्वरूप हे खूपच मर्यादित असते जसे की लहान मूल प्राथमिक गरजा पूर्ण झाल्या तर आंनदी, समाधानी असते. जर प्राथमिक गरजा पूर्ण झाल्या नाही तर दु:खी होते, कधी भुकेसाठी तर कधी झोपेसाठी रडते. वाढत्या वयानुसार भावनेचा विकास होत जातो. मग शारीरिक गरजांपलीकडे जाऊन मनाविरुद्ध झाले म्हणून राग येणे, जे वाटते ते इतरांना नीट न समजल्यामुळे मनाची होणारी चिडचीड, नंतर निराशा, खिन्नपणा अशा दु:खाच्या वेगवेगळ्या छटा तयार होतात. पुढे जाऊन मान, अपमान, राग, संताप असे भावनेतील फरक जाणवायला लागतात. प्रेमाचे माणूस कोणते आणि अनोळखी कोण हा फरक कळायला लागतो. एरिक एरिकसन यांनी असे म्हटले की, तान्हेपणी विश्वाचे नाते निर्माण होणे किंवा न होणे यावर पुढील आयुष्यात होणारी व्यक्तिमत्त्वाची जडणघडण अवलंबून असते.

भावना देहबोलीतून व्यक्त होतात. लहानपणापासून इतरांच्या भावना ओळखून स्वत:ला जे वाटते ते प्रकट करणे याला सुरुवात होत असते. स्वत:च्या भावना जाणणे, इतरांच्या भावना ओळखणे हे औपचारिक अभ्यासापेक्षा वेगळे आहे. बुद्धीचाच एक पैलू 'भावनिक बुद्धिमत्ता' आहे. भावनिक बुद्धिमत्तेशी निगडित आणखी एक पैलू म्हणजे सामाजिक बुद्धिमत्ता होय.

समस्या : किशोरावस्थेतील मुलामुलींच्या भावनिक बुद्धिमत्तेवर होणारा माहिती व तंत्रज्ञानाचा परिणामाचा अभ्यास.

उद्देश : किशोरावस्थेतील मुलामुलींच्या भावनिक विकासावर माहिती व तंत्रज्ञानाचा होणारा परिणाम अभ्यासणे.

गृहितके : १. किशोरावस्थेतील मुलामुलींमधील भावनिक बुद्धिमत्तेत माहिती व तंत्रज्ञानाचा सार्थक परिणाम दिसून येईल.
२. माहिती तंत्रज्ञानाचा अधिक वापर करणाऱ्या मुलींचा भावनिक विकास हा इतर मुलांच्या तुलनेत अधिक असेल.

संशोधन साहित्य : डॉ. एन.के. चंदा यांची समाजिक बुद्धिमत्ता चाचणी.

संशोधन आराखडा :

प्रस्तुत परिणामाचा अभ्यास करण्यासाठी खालील संशोधन आराखडा उपयोगात आणला.

२ × २ घटकात्मक संशोधन आराखडा

लिंग	गट	
	व्हर्च्युअल क्लास	परंपारिक क्लास
मुले	२०	२०
मुली	२०	२०
एकूण	४०	४०

एकूण ८० प्रयुक्तांची अनियत पद्धतीने प्रयुक्तांची निवड केली.

परिवर्त्य :

स्वतंत्र परिवर्त्य : अ. निवासाचे क्षेत्र
१. व्हर्च्युअल क्लास २. पारंपारिक क्लास
ब. लिंग
१. मुले २. मुली

परतंत्र परिवर्त्य :
भावनिक बुद्धिमत्ता

परिणामाचा तक्ता :

किशोर अवस्थेतील माहिती व तंत्रज्ञानाचा परिणाम दर्शवणारे मध्यमान व प्रमाण विचलनाचा तक्ता.

लिंग		क्लासरूमचे प्रकार		टी गुणांक
		व्हर्च्युअल	पारंपारिक	
मुले	मध्यमान	०८	०७	१.८८
	प्रमाण विचलन	२.३०	२.००	
मुली	मध्यमान	१०	०८	२.९८
	प्रमाण विचलन	३.६४	२.८८	

P<0.01 level.

या तक्त्यात दर्शविल्या प्रमाणे मुलांचे मध्यमान व प्रमाण विचलन अनुक्रमे ८ व २.३० आणि मुलीचे मध्यमान व प्रमाण विचलन ($p<0.01$ df =79,80) १० व ३.६४ हे ०.०१ स्तरावर सार्थक दिसून आले.

चर्चा :

व्यक्तीच्या मनाच्या आंतरिक अवस्थेला भावना, इमोशन असे म्हणतात. व्यक्तीचा जीवन अनुभव जसा जसा वाढत जातो तसतसे व्यक्तीच्या अंतरंगातील अवस्थेचा म्हणजे भावनेचा विकास होतो. सोशल वेबसाईट मुलांना एकमेकांमध्ये गुंतून ठेवणारा एक दुवा आहे. त्यामुळे त्यांच्यात भावनिक विचारांची देवाणघेवाण होते, असे मत इल्टो २००८. , सोशल साईटचा वापर मुले सल्ला मिळवण्यासाठी मोठ्या प्रमाणावर करतात नेल्सन २००९. प्रस्तुत अभ्यासामध्ये माहिती तंत्रज्ञानाचा भावनिक विकासावर परिणाम दिसून आला.

निष्कर्ष :

संशोधनात दिसून आलेली परिणाम लक्षात घेता असा निष्कर्ष काढता येईल की माहिती तंत्रज्ञानाचा वापर करुन भावनिक बुद्धिमत्ता वाढवता येऊ शकते.

संदर्भ :

१. वैकासिक मानसशास्त्र: डॉ. रा. र. बोरुडे, मेघा कुमठेकर, डॉ. भरत देसाई, सौ. शीला गाळविलकर, पुणे विद्यार्थी गृह प्रकाशन.
२. विद्या गोखले, मुलांचा भावनिक विकास, साप्ताहिक सकाळ, फेब्रुवारी २०१०.
३. वैकासिक मानसशास्त्र: प्रा. हिरवे, प्रा. तडसरे, फडके प्रकाशन कोल्हापूर.
४. जरनल ऑफ अॅडोलेन्स डेव्हलपमेंन्ट.
५. Impact of social media on Adolescent's behavioral health in colifornia,*www.phi.org./g9g6xbfghdxoe3yytmc1rfvvm8lt1ly9sr3j369pstkojdly1...*

❖❖❖

40 Strengthening of photovoltaic and supercapacitive properties of graphene oxide-polyaniline composite by dispersion of a-Al2O3 nanoparticles

Chemical Physics Letters 706 (2018) 647–651

Contents lists available at ScienceDirect

Chemical Physics Letters

journal homepage: www.elsevier.com/locate/cplett

Research paper

Strengthening of photovoltaic and supercapacitive properties of graphene oxide-polyaniline composite by dispersion of α-Al_2O_3 nanoparticles

Kailash Nemade [a,*], Pradip Tekade [b], Priyanka Dudhe [b]

[a] Department of Physics, Indira Mahavidyalaya, Kalamb 445 401, India
[b] Department of Chemistry, Jankidevi Bajaj College of Science, Wardha 442 001, India

ARTICLE INFO

Article history:
Received 3 May 2018
In final form 8 July 2018
Available online 10 July 2018

Keywords:
Graphene oxide
Polyaniline
Photovoltaic
Supercapacitive properties

ABSTRACT

It is demonstrated that the dispersion of α-Al_2O_3 nanoparticles in graphene oxide (GO)-polyaniline (PANi) composite results in significant enhancement of photovoltaic and supercapacitive properties. In order to improve PV and SC properties of GO-PANi composite, 0.5 wt% of α-Al_2O_3 nanoparticles were added in composite. Both PV and SC properties of composites becomes strengthen by addition of 0.5 wt% of α-Al_2O_3 nanoparticles. The GO-PANi/α-Al_2O_3 composite shows power conversion efficiency (%η) 9.31%, which is significantly higher than pure α-Al_2O_3 nanoparticles and GO-PANi composite. The GO-PANi/α-Al_2O_3 composite achieve considerable specific capacitance of the order 715.5 Fg^{-1} at scan rate of 2 $mV\,s^{-1}$.

1. Introduction

The widespread use of inorganic photovoltaic cell is still limited because of complications in modification of band gap of inorganic materials and high processing costs [1]. Different approaches using organic or polymer materials such as conducting polymer, graphene and metal oxides have received considerable attention because of their low cost, light weight and flexibility [2]. Whereas supercapacitor is a new class of device, which comes under the category of energy storage devices, and fulfill the technological gap between conventional capacitor and battery. Supercapacitor has some outstanding features like power density, rapid store/release of energy, good charge/discharge life cycles, and Eco friendliness. For supercapacitor application, carbon nanomaterials such as carbon nanotubes and graphene are extensively used, due to their high specific surface area and good electrical conductivity [3].

The use of carbon nanostructures with the conducting polymer is also investigated as supercapacitive material extensively. Yu et al investigated the polyaniline/graphene composite as electrode material for supercapacitors. The electrochemical capacitance of composite has value 596.2 Fg^{-1} and after 1500 cycles at a current density of 2 Ag^{-1}, only 16.3% drop in the initial capacitance is observed [4]. Wang et al synthesized PANi with different morphologies and combined with graphene to use as electrode materials of supercapacitors. The result of the study shows that sheet-like Graphene/PANi composites can deliver specific capacitances of 532.3–304.9 Fg^{-1} at scan rates of 2–50 mV/s [5]. Wu et al prepared the Polyaniline/graphene hydrogel composites for supercapacitor application with macroscopically phase-separated structure, which exhibits the high specific capacitance and excellent rate performance. This work concludes the PANi is mainly outside the graphene hydrogel matrix, can enhance the rate performance of the composites [6]. Cong et al prepared the graphene–PANi paper and employed for the supercapacitor application. The composite paper has considerable specific capacitance (763 Fg^{-1}) and good cycling stability [7]. Moussa et al reviewed comprehensively the recent developments in polyaniline/graphene nanocomposites as supercapacitor electrodes. This work underlined the polyaniline/graphene nanocomposites have great potential in electrochemical energy storage applications, especially supercapacitors [8]. Theophile et al reported the successful preparation of Poly(vinyl alcohol)-graphene oxide and Poly(vinyl alcohol)-reduced graphene oxide composite for supercapacitor application. The results of the study indicates that Poly(vinyl alcohol)-reduced graphene oxide composite (190 Fg^{-1}) deliver good supercapacitive properties than Poly(vinyl alcohol)-graphene oxide (13 Fg^{-1}) composite [9]. Loeblein et al a novel material having oxidized-three-dimensional-graphene, with a band gap of 0.2 eV. This material found suitable for electrode application in dye-sensitized solar cells where electrode has stringent work-function requirements [10]. Li et al successfully

* Corresponding author.
E-mail address: knemade@gmail.com (K. Nemade).

https://doi.org/10.1016/j.cplett.2018.07.018
0009-2614/

fabricated the PANi nanotubes-based supercapacitors having maximum areal capacitance of 237.5 mF cm^{-2} (scan rate = 10 mVs^{-1}) with maximum energy density of 24.31 mW h cm^{-2} (power density = 2.74 mW cm^{-2}). Under bending condition, supercapacitor shows excellent performance. After 2000 cycles, the capacitor maintains 95.2% of the initial capacitive value [11].

Feng et al prepared the graphene/polyaniline nanocomposites by using one-step hydrothermal method. The graphene/PANi nanowire composites exhibit the excellent electrochemical properties having specific capacitance 724.6 F/g higher than the graphene/PANi nanocomposite (602.5 F/g). This study demonstrated that morphology of materials also plays key role in optimization of electrochemical properties [12]. Zhou et al reported the effect of morphology on electrochemical properties using materials system nanoflake-like and nanobelt-like α-MoO_3/graphene nanocomposites. The results of the investigation demonstrated that α-MoO_3 nanoflakes/graphene exhibited better supercapacitive (up to 360 Fg^{-1}) performances than α-MoO_3 nanobelts/graphene [13].

In the light of above discussion, we planned to investigate the photovoltaic and primary electrochemical properties of α-Al_2O_3/PANi-GO composite. In this work, we studied the PV cell properties such as fill factor and power conversion efficiency and supercapacitive properties such, cyclic voltammetry (CV) curve, areal capacitance and cycle stability performance of composite materials. The main accomplishment of present work is that we achieved considerable value of power conversion efficiency and specific capacitance for α-Al_2O_3/PANi-GO composite.

2. Experimental

2.1. Materials preparation and characterization

In the present study, all AR-grade (SD Fine, India) chemicals were used for the preparation materials without further purification. The chemical oxidative polymerization was adopted for the preparation of Polyaniline (PANi). The method of preparation of PANi is reported previously [14]. In this process, aniline monomer and ammonium persulphate were used with molar ratio 1:1 M for preparation of PANi in aqueous media. The addition of aniline monomer in oxidant under constant magnetic stirring results in dark greenish precipitated. As obtained precipitated was washed two times with distilled water and dried in oven for overnight. The fine powder of PANi was used for the preparation of composites. The graphene oxide (GO) used in this work was prepared by previously reported method [15]. The ex-situ approach was adopted for the preparation of composites. The GO loaded PANi composite was prepared by taking equal wt.% of both contents. Whereas, α-Al_2O_3 loaded-GO/PANi composite was prepared by taking 0.5 wt% concentration of α-Al_2O_3 nanoparticles. Both the composites prepared in organic media (Acetone).

The X-ray diffraction (XRD) patterns of as-prepared materials were recorded on Rigaku Miniflex-II using CuK_α radiation (λ = 1.54 Å). The morphology of samples was investigated using scanning electron microscope (SEM) images obtained from JEOL JSM-7500F.

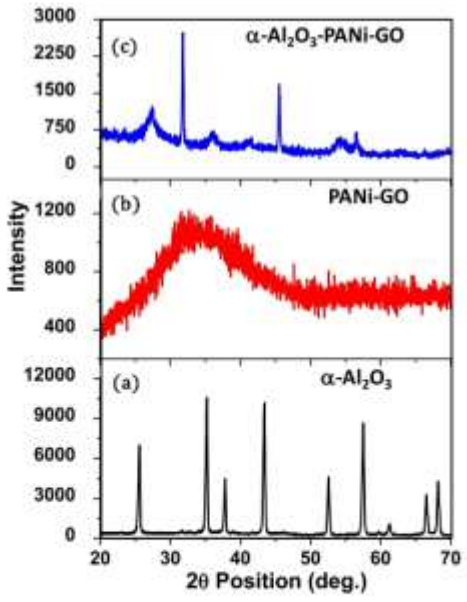

Fig. 1. XRD pattern of α-Al_2O_3 nanoparticle, PANi-GO and α-Al_2O_3/PANi-GO composite.

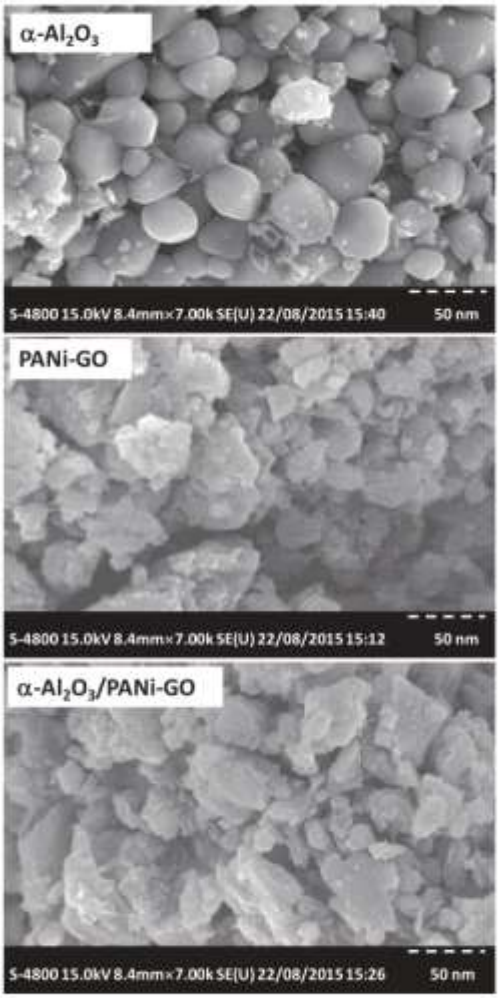

Fig. 2. FE-SEM images of α-Al_2O_3, PANi-GO and α-Al_2O_3/PANi-GO composite.

2.2. Supercapacitive study

Electrochemical measurements such as cyclic voltammetry (CV), areal capacitance and capacitance retention analysis were carried out using three-electrode cell systems (CHI 660 D, CH Instruments). As-prepared materials were used as the working electrode, platinum wire as counter electrode and Ag/AgCl as the reference electrode.

2.3. Photovoltaic (PV) study

PV cell required for testing was prepared by doctor blade technique. During the fabrication of PV cell, indium tin oxide (ITO) coated glass plate were used as transparent electrode and aluminum as metallic electrode. The photovoltaic properties of as-fabricated PV cell such as fill factor (FF) and power conversion efficiency (%η) confirmed by measuring short circuit current (Isc), open circuit voltage (Voc) and I_{max} and V_{max} from IV characteristics of PV cells.

3. Results and discussion

3.1. Characterization of materials

Fig. 1(a) shows the XRD pattern of α-Al_2O_3 nanoparticles, which is in good agreement with PDF Card No-01-081-1667. No other peaks for impurities were detected in pattern. The average crystallite size was computed by considering all prominent diffraction peaks using the Debye-Scherrer equation, which found to be 37.3 nm [16]. Fig. 1(b) depicts the XRD pattern of PANi-GO composite. The XRD pattern shows noisy behavior of diffraction peaks, which confirms the composite exhibited amorphous nature. In addition to this composite comprises broad hump between 2θ-range 20–30°. Fig. 1(c) shows the XRD pattern of α-Al_2O_3 nanoparticles loaded PANi-GO composite. Pattern clearly indicates the presence of signature peaks of α-Al_2O_3 and GO. This indicates the nice incorporation of α-Al_2O_3 in PANi-GO composite.

Fig. 2 represents the SEM images of α-Al_2O_3, PANi-GO and α-Al_2O_3/PANi-GO composite. SEM image of α-Al_2O_3 shows the nanoparticles have irregular shape with well separated boundaries. The average crystallite size estimated using XRD analysis is in good agreement with SEM study. The SEM images of PANi-GO and α-Al_2O_3/PANi-GO composite have almost identical morphology like petals or sheets structure.

3.2. PV study of materials

Fig. 3(a–c) shows IV characteristics of PV cell fabricated using the active PV material, α-Al_2O_3, PANi-GO and α-Al_2O_3/PANi-GO composite respectively and the PV parameters reflected by materials are listed in Table 1. From results, it is concluded that α-Al_2O_3 loaded PANi-GO composite achieve higher short circuit current (I_{sc}) than pure α-Al_2O_3 and PANi-GO. This might be attributed to the good dispersion of α-Al_2O_3 in PANi-GO composite and good charge–transfer process within composite, which is evident in the higher value of Isc [17]. There is a significant enhancement in

Table 1
PV parameters of α-Al_2O_3, PANi-GO and α-Al_2O_3/PANi-GO composite.

Material	I_{max} (mA)	V_{max} (V)	I_{SC} (mA)	V_{OC} (V)	FF	%η
α-Al_2O_3	23.8	0.2	23.8	0.7	0.285	1.61
PANi-GO	86	0.2	86	0.7	0.285	5.81
α-Al_2O_3/PANi-GO	137.7	0.2	137.7	0.8	0.25	9.31

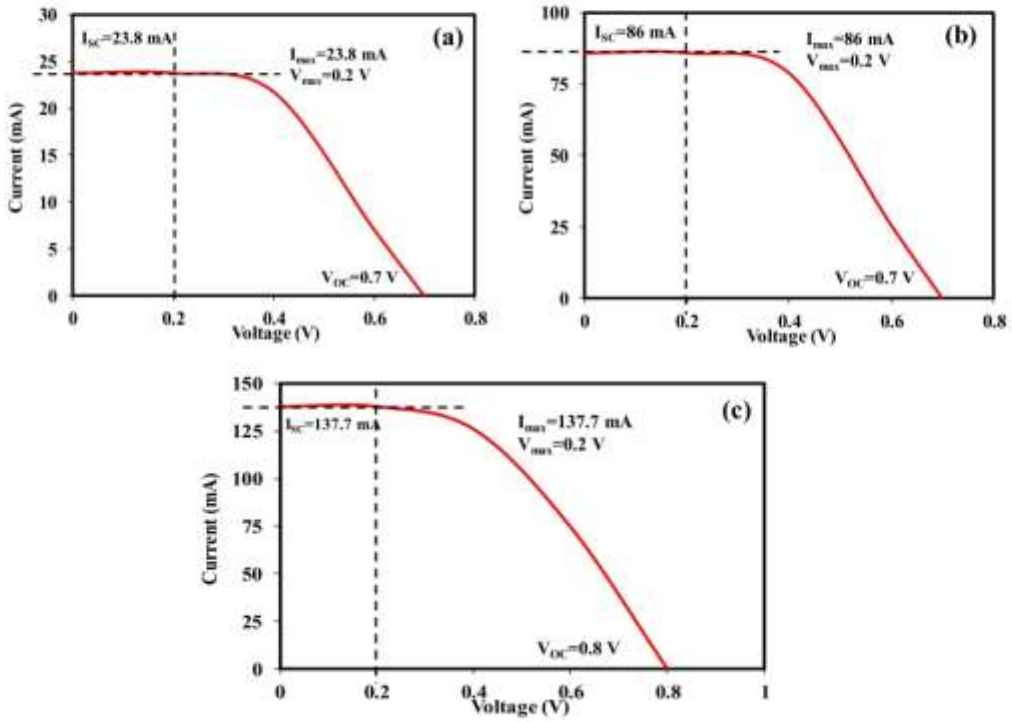

Fig. 3. PV response of (a) α-Al_2O_3, (b) PANi-GO (c) α-Al_2O_3/PANi-GO composite.

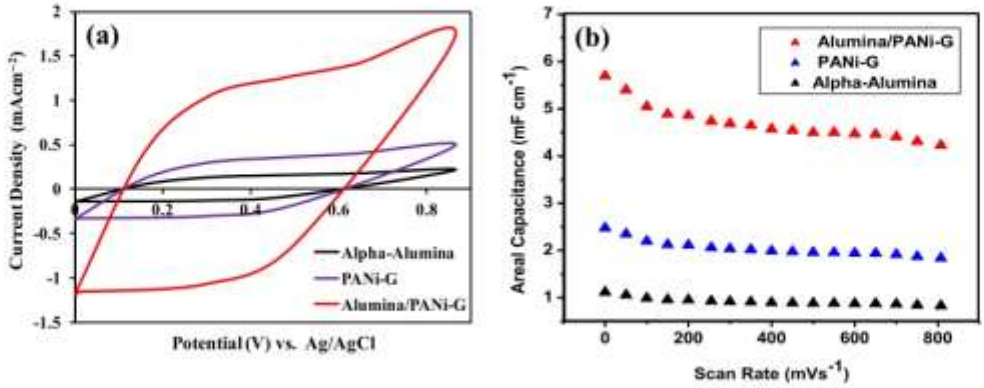

Fig. 4. (a) CV curves and (b) Areal capacitance as a function of scan rate of the α-Al_2O_3, PANi-GO and α-Al_2O_3/PANi-GO recorded at a scan rate of 2 mV s^{-1}.

%η resulted due to the addition of α-Al_2O_3 in PANi-GO composite. The highest value of %η is 9.31% for α-Al_2O_3/PANi-GO composite, whereas %η is 5.81% for PANi-GO composite and 1.61% for α-Al_2O_3.

3.3. Supercapacitive study of materials

Fig. 3a shows the cyclic voltammetric (CV) curves of α-Al_2O_3, PANi-GO and α-Al_2O_3/PANi-GO recorded at a scan rate of 2 mV s^{-1}. The CV curves clearly shows the α-Al_2O_3/PANi-GO composite have superior supercapacitive properties over pristine α-Al_2O_3, PANi-GO composite. The superior supercapacitive properties of α-Al_2O_3/PANi-GO composite can be attributed to oxidation/reduction of surface hydroxyl groups [18]. Specific capacitance has been estimated using the relation (Eq. (1)) [19],

$$Cs = \frac{I}{m \times v} (Fg^{-1}) \quad (1)$$

where I is the average current during anodic and cathodic scan (A), m is the mass of the electrode (g) and v is the scan rate (V). In our case, the highest value of specific capacitance was found to be 715.5 Fg^{-1} at a scan rate of 2 mV s^{-1} for α-Al_2O_3/PANi-GO composite.

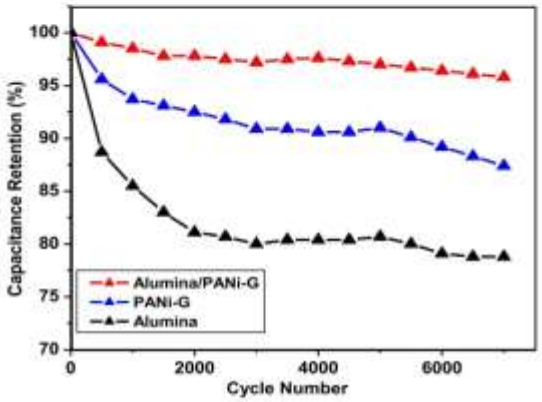

Fig. 5. Cycle performance of the alpha-Al_2O_3, PANi-GO and α-Al_2O_3/PANi-GO composite measured at a scan rate of 2 mV s^{-1} for 7000 cycles.

Fig. 3b shows the variation of calculated areal capacitance of the α-Al_2O_3, PANi-GO and α-Al_2O_3/PANi-GO composite as a function of scan rate. Here also plot clearly depicts that α-Al_2O_3/PANi-GO composite has several fold higher capacitance over the pristine α-Al_2O_3, PANi-GO composite. The significant enhancement in electrochemical performance was attributed to two main processes occurring in the composite. First is that composite possesses improved carrier density, which results in good electrical conductivity. Second is the increase of density of hydroxyl groups on α-Al_2O_3/PANi-GO composite [20]. The absence of redox peak indicates that capacitance was mainly contributed by non-faradaic redox reactions.

As shown in Fig. 4, the capacitance drops in pristine α-Al_2O_3 and PANi-GO composite is significantly more than α-Al_2O_3/PANi-GO composite. The α-Al_2O_3/PANi-GO composite electrode exhibits an excellent long-term stability with 95.83% capacitance retention after 7000 cycles. The good capacitance ability of α-Al_2O_3/PANi-GO composite is ascribed to enhanced electrical conductivity and highly stable surface redox reaction [21] (see Fig. 5).

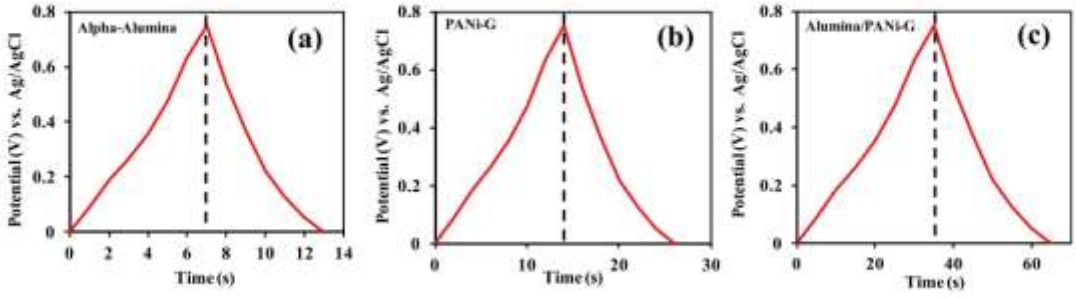

Fig. 6. Galvanostatic charge/discharge curves of the (a) alpha-Al_2O_3, (b) PANi-GO and (c) Al_2O_3/PANi-GO collected at a current density of 10 μAcm^{-2}.

Electrochemical study of alpha-Al_2O_3, PANi-GO and Al_2O_3/PANi-GO samples were extended by measuring charge/discharge measurements. Fig. 6(a–c) shows the galvanostatic charge/discharge (GCD) curves of alpha-Al_2O_3, PANi-GO and Al_2O_3/PANi-GO samples, respectively. The GCD curves of Al_2O_3/PANi-GO sample is nearly symmetric and significantly lengthy than alpha-Al_2O_3 and PANi-GO. This indicates capacitive properties of Al_2O_3/PANi-GO sample superior than alpha-Al_2O_3 and PANi-GO. Improved performance of Al_2O_3/PANi-GO attributed to synergetic state between alpha-Al_2O_3 and PANi-GO.

4. Conclusions

In summary, we have successfully demonstrated that the photovoltaic and supercapacitive performance of GO-PANi/α-Al_2O_3 composite is superior over the α-Al_2O_3 and PANi-GO composite. GO-PANi/α-Al_2O_3 composite based PV cell shows significant power conversion efficiency of the order of 9.31%, which much higher than α-Al_2O_3 and PANi-GO composite. The GO-PANi/α-Al_2O_3 composite exhibits the considerable specific capacitance of the order 715.5 Fg^{-1}. The GO-PANi/α-Al_2O_3 composite retain 95.83% capacitance after 7000 cycles, which shows the good cycling stability of composites. The GCD characteristics of Al_2O_3/PANi-GO sample improved due to synergetic effect between α-Al_2O_3 and PANi-GO composite. At present work is underway for the optimization of the electrochemical performance GO-PANi/α-Al_2O_3 composite.

Acknowledgment

The authors appreciate the help of Dr. S.K. Omanwar Head, Department of Physics, Sant Gadge Baba Amravati University, Amravati for providing necessary facilities for the work.

References

[1] R.M. Swanson, Progress in Photovolt.: Res. Appl. (Special Issue) 14 (2006) 443–453.
[2] N.S. Sariciftci, S.S. Sun, Organic Photovoltaics: Mechanism, Materials, and Devices, Taylor & Francis, New York, 2005.
[3] M.F. El-Kady, V. Strong, S. Dubin, R.B. Kaner, Laser scribing of high-performance and flexible graphene-based electrochemical capacitors, Science 335 (2012) 1326–1330.
[4] T. Yu, P. Zhu, Y. Xiong, H. Chen, S. Kang, H. Luo, S. Guan, Synthesis of microspherical polyaniline/graphene composites and their application in supercapacitors, Electrochim. Acta 222 (2016) 12–19.
[5] R. Wang, M. Han, Q. Zhao, Z. Ren, X. Guo, C. Xu, N. Hu, L. Lu, Hydrothermal synthesis of nanostructured graphene/polyaniline composites as high-capacitance electrode materials for supercapacitors, Scientific Reports 7 (2017), Article number: 44562.
[6] J. Wu, Q. Zhang, A. Zhou, Z. Huang, H. Bai, L. Li, Phase-separated polyaniline/graphene composite electrodes for high-rate electrochemical supercapacitors, Adv. Mater. 28 (2016) 10211–10216.
[7] H. Cong, X. Ren, P. Wang, S. Yu, Flexible graphene–polyaniline composite paper for high-performance supercapacitor, Energy Environ. Sci. 6 (2013) 1185–1191.
[8] M. Moussa, M. El-Kady, Z. Zhao, P. Majewski, J. Ma, Recent progress and performance evaluation for polyaniline/graphene nanocomposites as supercapacitor electrodes, Nanotechnology 27 (2016) 395201.
[9] N. Theophile, H.K. Jeong, Electrochemical properties of poly(vinyl alcohol) and graphene oxide composite for supercapacitor applications, Chem. Phys. Lett. 669 (2017) 125–129.
[10] M. Loeblein, A. Bruno, G.C. Loh, A. Bolkere, C. Saguy, L. Antila, S.H. Tsang, E.H.T. Teo, Investigation of electronic band structure and charge transfer mechanism of oxidized three-dimensional graphene as metal-free anodes material for dye sensitized solar cell application, Chem. Phys. Lett. 685 (2017) 442–450.
[11] H. Li, J. Song, L. Wang, X. Feng, R. Liu, W. Zeng, Z. Huang, Y. Ma, L. Wang, Flexible all-solid-state supercapacitors based on polyaniline orderly nanotubes array, Nanoscale 9 (2017) 193–200.
[12] X. Feng, N. Chen, J. Zhou, Y. Li, Z. Huang, L. Zhang, Y. Ma, L. Wang, X. Yan, Facile synthesis of shape-controlled graphene–polyaniline composites for high performance supercapacitor electrode materials, New J. Chem. 39 (2015) 2261–2268.
[13] J. Zhou, J. Song, H. Li, X. Feng, Z. Huang, S. Chen, Y. Ma, L. Wang, X. Yan, The synthesis of shape-controlled α-MoO_3/graphene nanocomposites for high performance supercapacitors, New J. Chem. 39 (2015) 8780–8786.
[14] K.R. Nemade, Chemically synthesized Sn doped polyaniline hydrochloride for carbon dioxide gas sensing, Sensors Transducers 135 (2011) 110–117.
[15] K.R. Nemade, S.A. Waghuley, Chemiresistive gas sensing by few-layered graphene, J. Electron. Mater. 42 (2013) 2857–2866.
[16] K.R. Nemade, S.A. Waghuley, Preparation of MnO2 immobilized graphene nanocomposite by solid state diffusion route for LPG sensing, J. Lumin. 153 (2014) 194–197.
[17] B. He, Q. Tang, M. Wang, H. Chen, S. Yuan, Robust polyaniline-graphene complex counter electrodes for efficient dye-sensitized solar cells, ACS Appl. Mater. Interfaces 6 (2014) 8230–8236.
[18] D. Choi, G.E. Blomgren, P.N. Kumta, Fast and reversible surface redox reaction in nanocrystalline vanadium nitride supercapacitors, Adv. Mater. 18 (2006) 1178–1182.
[19] B. Sethuraman, K.K. Purushothaman, G. Muralidharan, Synthesis of mesh-like Fe2O3/C nanocomposite via greener route for high performance supercapacitors, RSC Adv. 4 (2014) 4631–4636.
[20] X. Lu, G. Wang, T. Zhai, M. Yu, J. Gan, Y. Tong, Y. Li, Hydrogenated TiO_2 nanotube arrays for supercapacitors, Nano Lett. 12 (2012) 1690–1696.
[21] M. Kaempgen, C.K. Chan, J. Ma, Y. Cui, G. Gruner, Printable thin film supercapacitors using single-walled carbon nanotubes, Nano Lett. 9 (2009) 1872–1876.

41 Enhancement of photovoltaic performance of polyaniline/graphene composite-based dye-sensitized solar cells by adding TiO2 nanoparticles

Solid State Sciences 83 (2018) 99–106

Contents lists available at ScienceDirect

Solid State Sciences

journal homepage: www.elsevier.com/locate/ssscie

Enhancement of photovoltaic performance of polyaniline/graphene composite-based dye-sensitized solar cells by adding TiO_2 nanoparticles

Kailash Nemade[a,*], Priyanka Dudhe[b], Pradip Tekade[b]

[a] Department of Physics, Indira Mahavidyalaya, Kalamb 445 401, India
[b] Department of Chemistry, Jankidevi Bajaj College of Science, Wardha 442 001, India

ARTICLE INFO

Keywords:
Photovoltaic
Polyaniline
Graphene
TiO_2

ABSTRACT

Polyaniline (PANi)-graphene composites and polyaniline-graphene/TiO_2 composites were prepared by ex-situ approach. Systematic investigation was carried out to explore photovoltaic (PV) properties of PANi-graphene and PANi-graphene/TiO_2 composite. The prepared composites were characterized using X-ray diffraction (XRD), Scanning Electron Microscope (SEM), Raman Spectroscopy and Ultraviolet–Visible (UV–Vis) Spectroscopy. The PV properties of dye-sensitized solar cells (DSSCs) prepared composites investigated by assembling materials in ITO/PANi-graphene/Al and ITO/PANi-graphene/TiO_2/Al architecture. Different PV parameters such as short circuit current, open circuit voltage, fill factor and power conversion efficiency were determined from the (Current-Voltage) IV characteristics of PV cell. The 15 wt% PANi loaded graphene composite based PV cell shows optimized power conversion efficiency of the order 6.47%. The main accomplishment of present work is that efficiency associated with 15 wt% PANi loaded graphene composite, improved further by addition of TiO_2 nanoparticles. The composite system between PANi-graphene/TiO_2 for 1 wt% of TiO_2 nanoparticles shows optimized power conversion efficiency of the order 8.63%.

1. Introduction

Global demand of energy rising gradually, due to heavy industrialization and urbanization. Developed countries have huge demands of energy while demand is going on increasing in developing countries. The International Energy Agency states that energy needs are projected to expand by 55% till 2030 [1]. But unfortunately, the complete demand of energy is satisfied through non-renewable energy sources such as coal, petroleum, and natural gas. The exploitation of non-renewable energy sources results in range of adverse effects like air and water pollution, damage to public health, global warming and unnecessary atmospheric changes. Key solution for this issue is to use renewable energy sources such as hydropower, geothermal, wind and solar energy instead of non-renewable energy sources. Among these renewable energy sources, solar energy is best option due to outstanding characteristics such as the most abundant, inexhaustible and clean of all the renewable energy resources till date.

Across the globe researchers takes great interest in identification of alternative materials to silicon. The downside associated with silicon-based photovoltaic (PV) cell technology is their manufacturing requires costly ultra-high-purity silicon. Also, this process of manufacturing of PV cell results in significant carbon emission. Organic materials are considered as close competitive and alternative to the standard silicon-based PV cell technology. The main causes behind the development of organic PV cell technology are less expensive, thinner, more flexible, and amenable to a wide range of lighting conditions. Another interesting reason is low material consumption results in a high absorption coefficient [2]. Some other advantages of organic PV cells are low specific weight, mechanical flexibility, tunable material properties and high transparency [3].

During literature survey on organic PV materials, we come across three efficient materials which exhibits outstanding PV properties. These three materials are polyaniline, graphene and TiO_2 nanoparticles. Among the conducting polymers such as polyaniline (PANi), polypyrrole (PPy) and polythiophene (PTh), PANi has been extensively studied by researchers.

Conducting polymer is the class of materials, which is fit for photovoltaic application and device fabrication. This is because of outstanding characteristics such as intrinsically stable photoexcitation with visible light, high photon harvesting efficiency, tunable band gap engineering on the entire visible spectral range and large charge generation when mixed with electron acceptor materials [4].

PANi display good electron conducting behaviors, interesting redox behavior, high environmental stability and controllable electrical and

* Corresponding author.
E-mail address: krnemade@gmail.com (K. Nemade).

https://doi.org/10.1016/j.solidstatesciences.2018.07.009
Received 9 May 2018; Received in revised form 14 July 2018; Accepted 16 July 2018
Available online 17 July 2018
1293-2558/

optical properties [5–7]. All these outstanding features of PANi attributed to the delocalized π-electron structure. The optical absorption coefficient of organic molecules specially in case of PANi is very high. Therefore, large amount of light can be trap by an insignificant amount of materials [8].

Graphene possesses a substantial number of wonderful optical and electronic properties, such as zero band-gap, semi-conducting with a high carrier mobility and high optical transparency, which generally not observed in other materials [9]. It is well accepted principle for organic PV cells that optimization of both charge transport and optical properties are necessary for good performance.

Out of many semiconducting metal oxides, TiO_2 has some attractive features for PV cell application. TiO_2 nanomaterial suitable for PV cell application due to its high chemical and optical stability, non-toxicity, low cost, corrosion resistance and ease of synthesis [10,11]. Many reports show that graphene–TiO2 nanocomposites possess superior photovoltaic properties than pristine TiO_2 [12].

The composite preparation using organic and inorganic constituent's results in improved electronic properties. It is well known principle of materials science that in synergetic state, physical and chemical properties of most of the composite improves. Therefore, in this section it is analyzed using some reports on PV properties of PANi-Metal Oxide composite. The addition of metal oxides impurity in PANi enhance the PV properties and increase the efficiency of solar cells.

Ameen et al. fabricated TiO_2/PANi and dye absorbed TiO_2/PANi electrodes by plasma polymerization for solar cells application. The results of the study indicate that dye absorbed TiO_2/PANi electrode based DSSCs have high charge carrier transportation between the TiO_2 and PANi layer. This rapid charge transportation in dye absorbed TiO_2/PANi electrode improves the performance of solar cell than the TiO_2/PANi electrode [13]. Shen et al. architecture PV cell with layers ITO/nano-crystalline TiO_2/PANi/Aluminum. This shows largest open voltage of 0.397 V and short current density of 65.9 μA/cm^2 under simulated solar radiation. Using current-voltage characteristics, the formation of p-n junction between nano-crystalline TiO_2 and PANi interface is also verified [14]. Yang et al. synthesized grafted aniline on aminobenzoate monolayer to adsorbed TiO_2 nanocrystal to fabricate a uniform core/shell structured TiO_2/PANi nanocomposite. The DSSC fabricated with an electrode of TiO_2/PANi film have considerably high short circuit current density of 0.19 mA/cm^2 and an open circuit voltage of 0.35 V [15]. Zhu et al. adopted the two-step process to prepared PANi hybridized ZnO photoanode on FTO substrate. The results of the study show that light-conversion efficiency of PANi hybridized ZnO nanograss improves by 60% than pure ZnO nanograss photoanode [16]. Momeni et al. studied the dye-sensitized solar cell based on TiO_2 nanotube arrays. In this work, TiO_2 nanotubes were prepared by two different approaches namely one-step and two-step process. This work concludes that TiO_2 nanotubes prepared using two-step process shows higher efficiency [17]. Bahramian et al. prepared in situ PANi-based counter electrode and coral-likeTiO_2 to assemble DSSC with transparent PANi films as counter electrode. This bifacial DSSC have power conversion efficiency of 8.22%, which is assigned to excellent light scattering by the coral-like TiO_2 and high specific surface area of PANi nanofibers [18]. Duan et al. fabricated the DSSC with PANi incorporated TiO_2 anodes, PANi counter electrodes, and iodide doped PANi solid-state electrolytes. The results of the study show that DSSC with proper assembly process and iodide dosage provides good PV performances with power conversion efficiency of 3.1% [19].

The humankind has been gifted by many brilliant materials by nature, one of those is Graphene. Graphene possess noticeable enigmatic optical and electronic properties such as zero band gap, high carrier mobility, high optical transparency. The synergetic phase of graphene with PANi, also results in efficient PV materials. Some reports on PANi-Graphene composite have been reviewed in this section.

Wang et al. prepared graphene/PANi nanocomposite by polymerization of aniline monomer in situ method. In DSSC, graphene/PANi nanocomposite deposited on FTO, which gives power conversion efficiency of 6.09% compared to 6.88% of efficiency for PV cell with expensive Pt counter electrode under similar experimental conditions [20]. Liu et al. designed DSSC by coating a nanocomposite thin film of graphene/PANi on FTO glass by electro-polymerization method. In comparison, graphene/PANi based electrode has power conversion efficiency of 7.17%, which is close to 7.24% of a DSSC with a Pt counter electrode. This study shows that graphene/PANi electrode has potential to replace conventional Pt counter electrode in DSSC [21]. Dinari et al. designed the Pt free DSSC using PANi-Graphene quantum dots by in situ electrochemical polymerization on FTO coated glass. The synergistic effect between PANi and graphene quantum dots provides higher electrochemical catalytic activity which resulted into improved PV performance with power conversion efficiency of 1.6% [22].

Loryuenyong et al. fabricated DSSCs with counter electrode based on PANi-graphene hybrid material. The counter electrode was prepared by depositing material on FTO by drop casting method. The PANi/graphene hybrid counter electrode exhibits superior PV performance with open circuit voltage of 0.57 V, Short Circuit Current of 5.15 mA cm^{-2}, fill factor of 0.40 and power conversion efficiency of 1.16% which results in improved PV performance than DSSC based on Pt electrode [23]. Yang et al. synthesized multilayer counter electrodes from positively charged PANi-graphene complex and negatively charged platinum nanoparticles with different number of layers and different concentration of graphene in PANi-graphene complex. This work concludes that the electron migration from graphene to PANi helped in good charge transfer. This multilayer interface based DSSC has power conversion efficiency of 7.45%. This work also pointed that multi-interfacial counter electrodes are suitable for robust DSSC [24].

During literature survey, it is observed that PANi, TiO_2 nanoparticles and Graphene have much potential to improve their PV properties. The necessity of development of new kinds of PV materials with improved power conversation efficiencies is being touched by different research groups across the globe. Therefore, the problem is identified on the basis of following remarks:

- During study, it is observed that concentration of impurity in composite has play crucial role. Therefore, in this work it planned to investigate optimized composition of PV material based on PANi and graphene.
- In second step, after successful finding of optimized composition, another impurity that is TiO_2 used for further enhancement of PV properties of PANi-graphene composite.

Therefore, the objectives of present work are to prepare and optimized PV properties of PANi-graphene composite. Then prepare and optimized TiO_2 nanoparticles loaded PANi-graphene composite for PV application.

2. Experimentation

2.1. Preparation of materials

2.1.1. Preparation of PANi

In the present work, PANi was synthesized by using chemical oxidative method. In this method, ammonium persulfate was used as an oxidizing agent. All chemicals required for the preparation of PANi procured from SD fine, India of AR grade and used without further purification. In the process of preparation of PANi, following steps were executed,

- During the synthesis of PANi, one condition is imposed on molar ratio between ammonium persulfate to aniline monomer should not exceed the ratio ≤1.15. The reason behind this condition is to obtain high conductivity and yield [25].
- With this condition, both aniline monomer and ammonium

persulfate dissolve separately in aqueous (100 ml) medium.
- Subsequent to this step, the solution of aniline monomer was added in ammonium persulfate solution in dropwise manner under magnetic stirring.
- The greenish-black precipitate was observed in beaker with increase in temperature.
- This precipitate was kept for overnight (24 h) for good quality polymerization.
- On next day, precipitate was washed three times with distilled water to remove un-reacted contents in product.
- The obtained product was dried at 50 °C and used for further process.

2.1.2. Preparation of PANi/Graphene composites

The *ex-situ* approach was adopted for the preparation of PANi/Graphene composite. The graphene required for the composite preparation was prepared by previously reported method [26]. The weight % (wt.%) stoichiometry was adopted for the preparation of composites. The wt.% stoichiometry was calculated using relation (Eq. (3.1)),

$$wt.\ \% = \frac{A}{(A+B)} \times 100 \tag{3.1}$$

where A and B are constituents of composite.

In our case, the content of PANi in composite was varied for 5–20 wt % by an interval of 5 wt%. In this way, four samples were obtained. During preparation of composite, both constituents of composite was added in 25 ml acetone under magnetic stirring at room temperature.

2.1.3. Preparation of PANi/graphene-TiO_2 composites

PANi/Graphene-TiO_2 composites was also prepared by ex-situ approach. In this process, TiO_2 was directly procured from SD fine, India of high purity. This TiO_2 was probe sonicated using sonicator (PCi, 750-F, PCI Analytics Pvt Ltd). This process of probe sonication, splits the TiO_2 particles up to the nano-dimensions. As-obtained TiO_2 nanoparticles, was used for the preparation of composites. By adopting wt.% stoichiometry, four samples of PANi/Graphene-TiO_2 composites were prepared by varying content of TiO_2 nanoparticles in composite from 0.5 to 2 wt% by an interval of 0.5 wt%. The optimized stoichiometry between PANi and graphene were used further for addition of TiO_2 nanoparticles, to improve PV properties. Here also, acetone was used as an organic media for the preparation of composites. For dye sensitization process, Ru-based N719 dye was used by preparing media of 0.25 mM ethanolic solution of dye N719.

2.2. Fabrication of photovoltaic cell

The doctor blade technique was used to fabricate the PV cells. During this process, the composites was sandwiched between cleaned ITO plate as transparent electrode and Aluminum electrode. The aluminum foil was used as metallic electrode for the PV cell. ITO plate (Dimension: 25 mm × 25 mm) used in this work was procured from Techinstro (ITO-SE-011), India. With the help of temporary binder (based on 3% ethyl cellulose and 97% butyl digol), composite was deposited on ITO electrode and then Aluminum electrode was deposited. This fabricated cell allows to dry at 40 °C for 3 h for evaporation of volatile organic compounds. The thickness of deposited layer controlled by thickness of transparency used during doctor blade technique. In this way, PV cells were fabricated for further study. The side face of fabricated PV cell is depicted in Fig. 1.

2.3. Measurements of photovoltaic characteristics

The current-voltage (IV) characteristics of PV cell collected under incandescent light bulb of power 0.2956 Watt/m^2. The separation between incandescent light source and PV cell was about 15 cm. The important diode parameters like open circuit voltage (V_{OC}), short circuit current (I_{SC}), fill factor (FF), and power conversion efficiency (η) were measured under these conditions, which reproduced without any considerable deviation. The FF of PV cell computed using relation Eq. [1] [27]:

Fig. 1. Side face of fabricated PV cell.

$$FF = \frac{I_{MAX} \times V_{MAX}}{I_{SC} \times V_{OC}} \tag{1}$$

Whereas, power conversion efficiency (%η) of PV cell estimated using the relation Eq. [2]. [28],

$$\%\eta = \left(\frac{I_{SC} \times V_{OC} \times FF}{P_{in}}\right) \times 100 \tag{2}$$

The FF and %η are the crucial parameters for any PV cell. On the basis of these parameters, it is possible to discriminate any PV cell and its performance.

3. Results and discussion

3.1. Materials characterization and PV properties of PANi/Graphene

3.1.1. XRD analysis

Fig. 2 (a) shows the XRD pattern of pure PANi synthesized by chemical oxidative method. The XRD pattern of pure PANi comprises only one broad peak around 26°, which indicates the poor crystallinity phase of PANi. This broad peak is also assigned to the scattering from the PANi chains at inter planar spacing [29]. Fig. 2 (b) depicts XRD pattern of graphene, which has well structural, and phase purity. The XRD of graphene possesses two signature peaks at 26.3° (002) and 44.2° (100). The peak at 2θ = 26.3° indicates well organized structure of graphene with an interlayer spacing of 0.339 nm. This layer spacing is

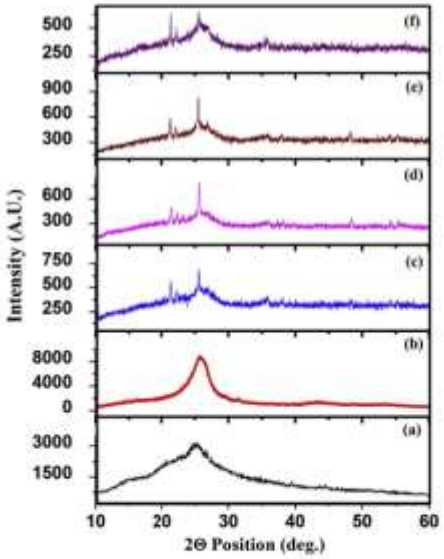

Fig. 2. XRD pattern of pure (a) PANi, (b) graphene and (c) 5 wt%, (d) 10 wt%, (e) 15 wt%, (f) 20 wt% PANi loaded graphene composites.

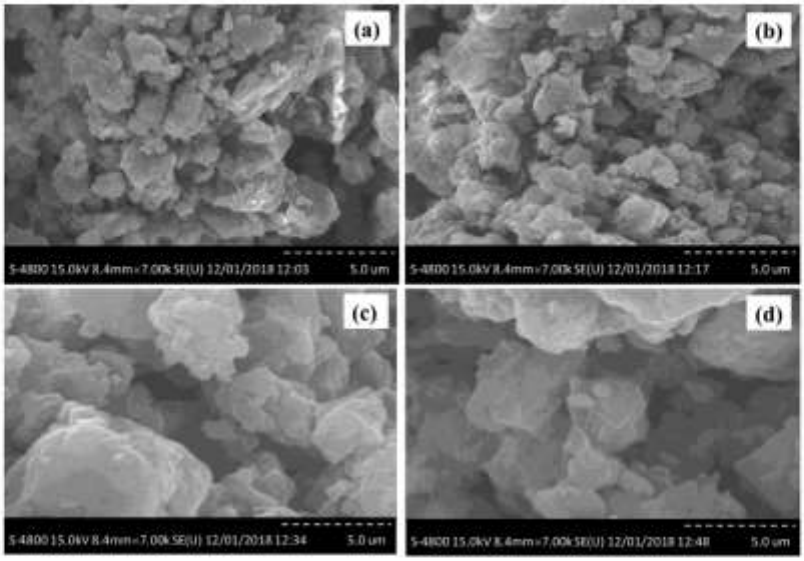

Fig. 3. SEM images of (a) 5 wt%, (b) 10 wt%, (c) 15 wt% and (d) 20 wt% PANi loaded graphene composites.

in agreement with spacing in graphite. The broad peak at $2\theta = 44.2°$ is attributed to presence of some defects [30]. Fig. 2 (c, d, e and f) shows the XRD pattern of 5 wt%, 10 wt%, 15 wt% and 20 wt% PANi loaded graphene composites, respectively. XRD pattern shows that with an increase in PANi content in composites, noisy behavior of pattern increases. This indicates that crystalline nature of composites decreases. Sharp peaks appear between 20 and 26° is attributed to the presence of smaller crystalline regimes in composites. The decrease in peak height intensity of composites than graphene and PANi, justify the formation of composites.

3.1.2. Morphology study

Fig. 3 shows the SEM images of (a) 5 wt%, (b) 10 wt%, (c) 15 wt% and (d) 20 wt% PANi loaded graphene composites prepared by ex-situ approach. In all cases, graphene sheets are homogeneously dispersed in PANi. At fixed resolution, one thing is observed from SEM images that agglomeration phenomenon increases with wt.% of PANi. All composite samples have irregular shape.

3.1.3. Raman Spectroscopy

Fig. 4 depicts the Raman spectra of 15 wt% PANi loaded graphene composite, which is optimized sample in PV study. The C−N stretching vibration from benzenoid structure appears through band 1548 cm^{-1}. The semi-benzenoid polaronic band of C–N^+ appears at 1318 cm^{-1} and plane bending vibration of CH is appears at 1200 cm^{-1}. The Raman spectrum comprises clear band D (1325 cm^{-1}) [31], G (1598 cm^{-1}), and 2D (2695 cm^{-1}), which are signature band of graphene [32–34]. The shift in band position is observed, which is attributed to the structural changes in resultant composite. The quinoid rings in the PANi have a similar atomic structure with the C6 rings of graphene. This situation in both constituents allow for a strong π -π stacking interaction and beneficial for electronic transmission [35].

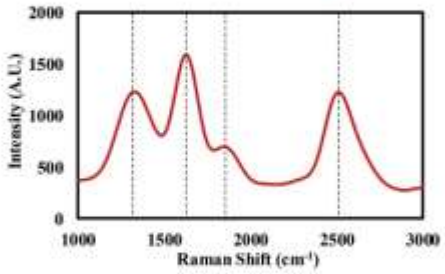

Fig. 4. Raman spectrum of 15 wt% PANi loaded graphene composite.

3.1.4. Optical properties

In PV technology, optical properties of PV materials play crucial role. Therefore, in our case it is studied using UV-VIS spectroscopy. In PV cell technology, both types of band gap materials that is low-band gap and high-band gap materials have their own importance. Therefore, by combining appropriate materials to obtain band gap which efficiently used available solar radiations is necessary. This is necessary, if the band gap is very small than incident photon energy, then considerable photon energy converted in heat energy, which raise the temperature of PV materials. On other hand, if the band gap is very large, it restricts the transition between valance band to conduction band [36].

Fig. 5 shows the UV-VIS spectrum of 5 wt%, 10 wt%, 15 wt% and 20 wt% PANi loaded graphene composites. From plot, it is clearly

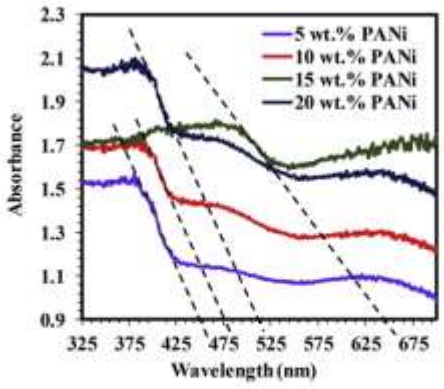

Fig. 5. UV-VIS spectrum of 5 wt%, 10 wt%, 15 wt% and 20 wt% PANi loaded graphene composites.

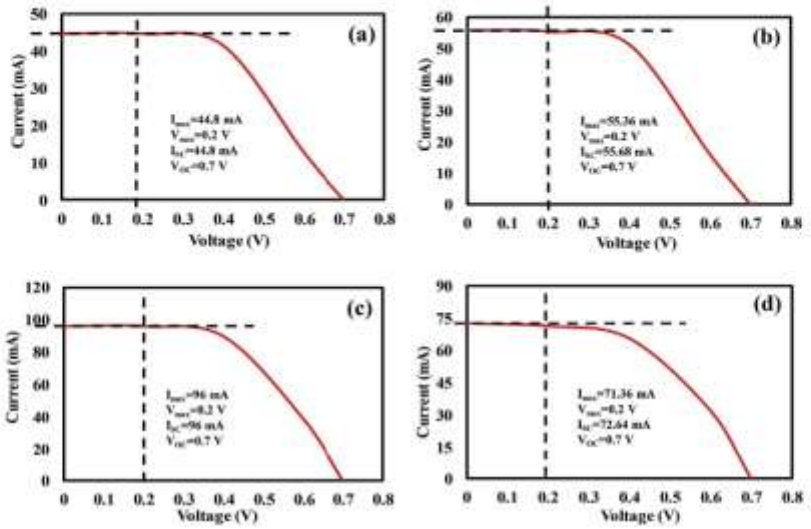

Fig. 6. PV response of (a) 5 wt%, (b) 10 wt%, (c) 15 wt% and (d) 15 wt% PANi loaded graphene composite.

observed that the samples 5 wt%, 10 wt% and 20 wt% PANi loaded graphene composites have absorption tail at lower wavelength than 15 wt% PANi loaded graphene composites. The band gap values for as-prepared composite samples (estimated using frequency-wavelength relation) ranges between 2.73 and 1.92 eV. The lowest value of band gap is associated with 15 wt% PANi loaded graphene composite.

3.1.5. PV performance

Fig. 6 shows the PV response of (a) 5 wt%, (b) 10 wt%, (c) 15 wt% and (d) 15 wt% PANi loaded graphene composite based DSSCs. All diode parameters like I_{max}, V_{max}, I_{SC}, V_{OC}, FF and %η are provided in Table 1. Among all PV cells, the response of 15 wt% PANi loaded graphene composite has highest power conversion efficiency of order 6.479% (FF = 0.285). The highest power conversion efficiency was attributed to lower band gap value (1.92 eV) of 15 wt% PANi loaded graphene composite. All samples have stable diode parameters and reproducible results.

Fig. 7 shows the variation of FF and %η as a function wt.% of PANi in composite. Plot shows that 15 wt% PANi loaded graphene composite has highest power conversion efficiency. The possible reason for highest power conversion efficiency may be

Table 1
PV parameters of TiO_2 nanoparticles loaded PANi-graphene composites and PANi loaded graphene composites.

TiO_2 nanoparticles loaded PANi-graphene composite						
Wt.% of TiO_2 nanoparticles	I_{max} (mA)	V_{max} (V)	I_{SC} (mA)	V_{OC} (V)	FF	%η
0.5 wt%	95.17	0.2	95.23	0.8	0.2499	6.43
1 wt%	127.71	0.2	127.79	0.8	0.2498	8.63
1.5 wt%	106.59	0.2	106.65	0.8	0.2498	7.21
2.0 wt%	105.73	0.2	105.8	0.8	0.2498	7.15
PANi loaded graphene composite						
Wt.% of PANi	**I_{max} (mA)**	**V_{max} (V)**	**I_{SC} (mA)**	**V_{OC} (V)**	**FF**	**%η**
5 wt%	44.8	0.2	44.8	0.7	0.285	3.068
10 wt%	55.36	0.2	55.68	0.7	0.284	3.741
15 wt%	96	0.2	96	0.7	0.285	6.479
20 wt%	71.36	0.2	72.64	0.7	0.280	4.816

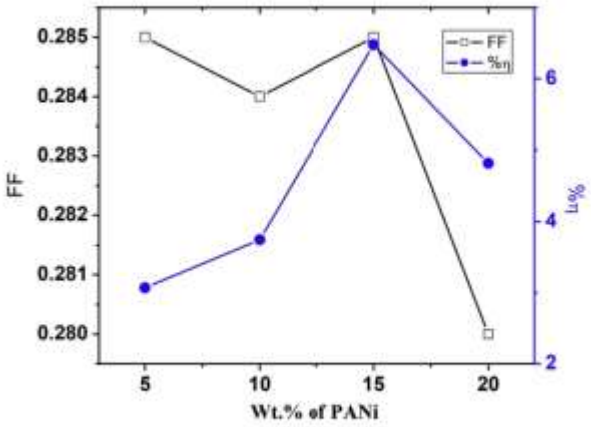

Fig. 7. Variation of FF and %η as a function wt.% of PANi in composite.

- the homogeneous presence of PANi and graphene in composite, can reduce the interfacial resistance between the graphene and the PANi. This homogeneity in composite results in better electron transfer.
- The presence of high electrical conductive graphene in composite and agglomerated nature of composite reduce inter-domain resistance.
- Lower band gap (1.92 eV) value of 15 wt% PANi loaded graphene composite.

3.2. Improvement in PV performance by addition of TiO_2 nanoparticles

3.2.1. XRD analysis

Fig. 8 (a) shows the XRD pattern of anatase phase TiO_2 nanoparticles. The strong signature peaks at 25° and 48° confirms the anatase phase. All remaining peaks position and marginal intensity data are in good agreement with standard spectrum (JCPDS card No. 84–1286) [37]. The average crystallite size of TiO_2 nanoparticles was estimated using Scherrer equation [38], $D=(K\lambda/\beta\cos\theta)$, where D is average crystallite size (nm), k is a shapes factor (K = 0.89), λ is the wavelength of X-ray source equals 1.540 Å, β is the full width at half maxima, and θ is the diffraction peak angle. The average crystallite size of TiO_2

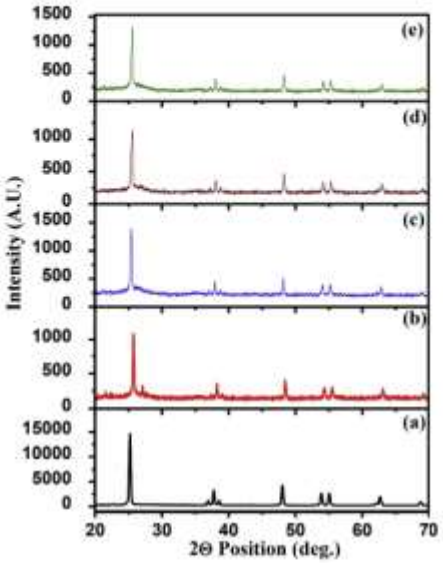

Fig. 8. XRD pattern of pure (a) TiO_2 nanoparticles and (b) 0.5 wt%, (c) 1 wt%, (d) 1.5 wt% and (e) 2 wt% TiO_2 nanoparticles loaded PANi-graphene composites.

nanoparticles was found to be 51.27 nm. Fig. 8 (b, c, d and e) depicts the XRD pattern of 0.5 wt%, 1 wt%, 1.5 wt% and 2 wt% TiO_2 nanoparticles loaded PANi-graphene composites, respectively. The addition of TiO_2 nanoparticles in PANi-graphene composites results in interesting results. The XRD pattern clearly shows the composite exhibits the crystalline phase with shape peaks. As discussed in section 4.1.1, the PANi-graphene composites have amorphous phase, which was diminish by addition of TiO_2 nanoparticles.

3.2.2. Morphology study

Fig. 9 represents the SEM images of (a) 0.5 wt%, (b) 1 wt%, (c) 1.5 wt% and (d) 2 wt% TiO_2 nanoparticles loaded PANi-graphene composites. Here also, TiO_2 nanoparticles nicely dispersed in PANi-graphene composites. The addition of TiO_2 in PANi-graphene results in improvement of crystallinity. In all SEM images, well defined crystalline boundaries are observed. The crystallinity of all composite samples reflects also from XRD analysis. The irregular particle size distribution observed in all regions of SEM.

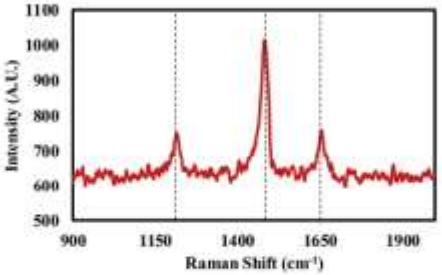

Fig. 10. Raman spectrum of 1 wt% TiO_2 nanoparticles loaded PANi-graphene composite.

3.2.3. Raman Spectroscopy

Fig. 10 shows the Raman spectrum of 1 wt% TiO_2 loaded PANi-Graphene composite. This spectrum also comprises the C−N stretching vibration from benzenoid, which appears around 1548 cm^{-1}. Similarly, semi-benzenoid polaronic band of $C–N^+$ appears around 1318 cm^{-1} and plane bending vibration of C-H is appears around 1200 cm^{-1}. No significant peaks were associated with TiO_2 nanoparticles in spectrum.

3.2.4. Optical properties

Fig. 11 shows the UV-VIS spectrum of 0.5 wt%, 1 wt%, 1.5 wt% and 2 wt% TiO_2 nanoparticles loaded PANi-graphene composites. From the plot, it is clear that absorption tail of 1 wt% TiO_2 nanoparticles loaded PANi-graphene composite has higher value than other three samples. The band gap values of 0.5 wt%, 1 wt%, 1.5 wt% and 2 wt% TiO_2 nanoparticles loaded PANi-graphene composites ranges between 3.02 and 2.53 eV. The lowest value of band gap is associated with 1 wt% TiO_2 nanoparticles loaded PANi-graphene composite.

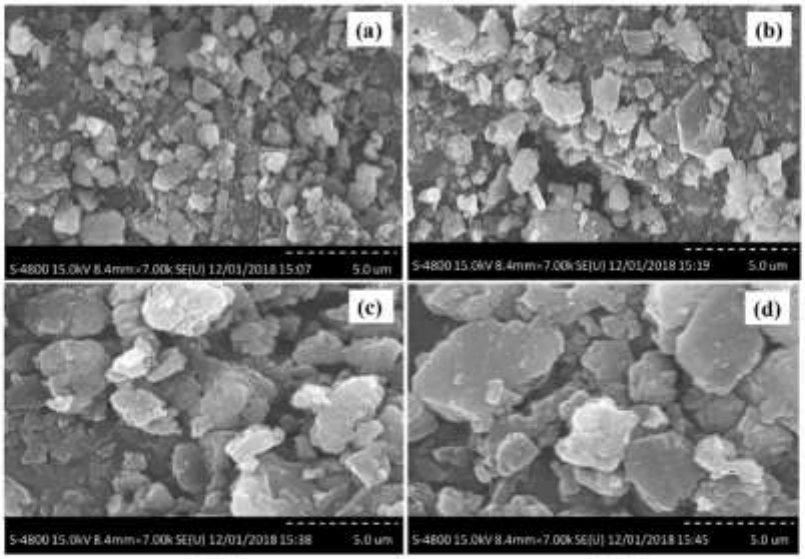

Fig. 9. SEM images of (a) 0.5 wt%, (b) 1 wt%, (c) 1.5 wt% and (d) 2 wt% TiO_2 nanoparticles loaded PANi-graphene composites.

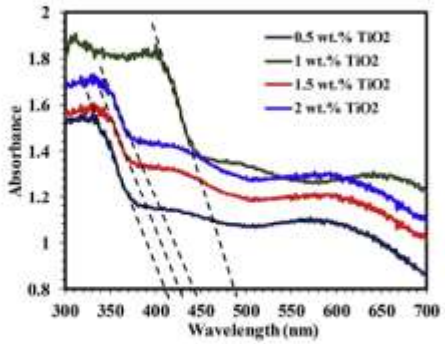

Fig. 11. UV-VIS spectrum of 0.5 wt%, 1 wt%, 1.5 wt% and 2 wt% TiO_2 nanoparticles loaded PANi-graphene composites.

3.2.5. PV performance

Fig. 12 shows the PV response of (a) 0.5 wt%, (b) 1 wt%, (c) 1.5 wt% and (d) 2 wt% TiO_2 nanoparticles loaded PANi-graphene composites based DSSCs and all diode parameters listed in Table 1. In PANi-graphene/TiO_2 composite, stable diode parameters observed. From Table 1, it is observed that 1 wt% TiO_2 nanoparticles loaded PANi-graphene composite has highest power conversion efficiency. The highest power conversion efficiency was attributed to good optical properties and lower band gap (2.53 eV) value.

Fig. 13 depicts the variation of FF and %η as a function wt.% of TiO_2 nanoparticles in PANi-graphene composites. The highest power conversion efficiency was associated with 1 wt% of TiO_2 nanoparticles in PANi-graphene composite. The possible reasons for the highest power conversion are,

- The addition of TiO_2 nanoparticles in PANi-graphene composite, results in increase of both photocurrent density and open circuit voltage.
- The presence of graphene sheets in composite reduces charge recombination and increasing open circuit voltage as a result of high electron [39,40].

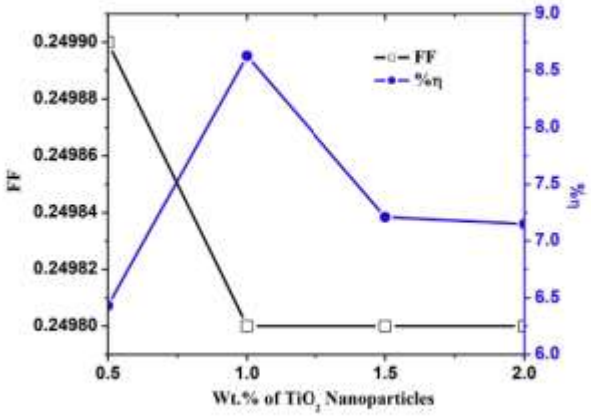

Fig. 13. Variation of FF and %η as a function wt.% of TiO_2 nanoparticles in composites.

4. Conclusions

During the study, two material systems that is PANi-graphene composite and PANi-graphene/TiO_2 composites based DSSCs were successfully prepared by ex-situ approach. The structural, morphological and optical study of both systems were carried out to understand physical properties of materials. To analyze the PV performance of PANi-graphene composite and PANi-Graphene/TiO_2 composites, PV cells were fabricated using doctor blead technique in architecture ITO/PV materials/Aluminum.

The PANi required for composite preparation was synthesized by using chemical oxidative route successfully. During composite preparation wt.% of PANi varied in graphene, to analyze effect of PANi on PV properties of composite. In this study, 15 wt% PANi loaded graphene composite shows optimized power conversion efficiency of order 6.47% with I_{sc} = 96 mA. The highest power conversation efficiency of this sample attributed to reduction in the interfacial resistance between the graphene and the PANi, lower inter-domain resistance and lower band gap of 15 wt% PANi loaded graphene composite than other samples.

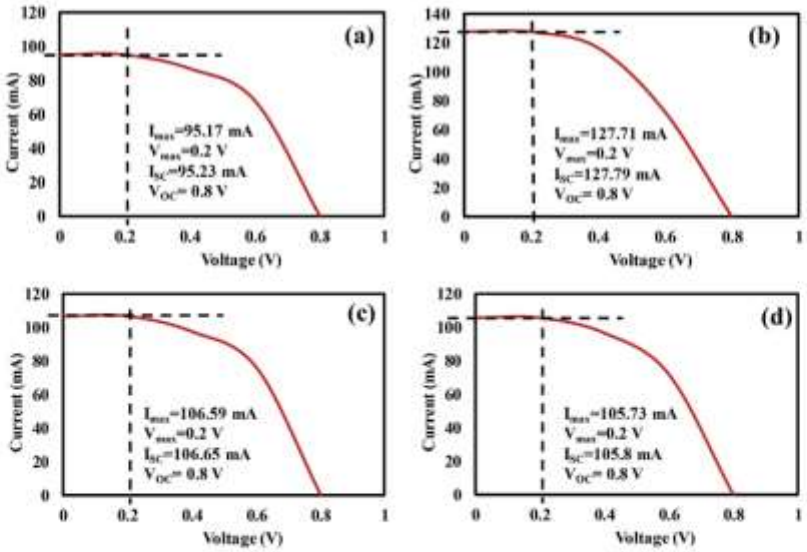

Fig. 12. PV response of (a) 0.5 wt%, (b) 1 wt%, (c) 1.5 wt% and (d) 2 wt% TiO_2 nanoparticles loaded PANi-graphene composites.

In order to improve further the power conversion efficiency of 15 wt % PANi loaded graphene composite, TiO_2 nanoparticles were added in this composite. To obtain again optimized sample with outstanding PV properties, the content of TiO_2 nanoparticles were varied with 0.5–2 wt % by an interval of 0.5 wt%. In this study, 1 wt% TiO_2 nanoparticles loaded PANi-graphene composite shows optimized PV properties. The power conversion efficiency was successfully improved and its value was found to be 8.63%. This is the main accomplishment of present work. In this complete, it is also observed that diode parameters have stable value.

In the concluding remark of this work, it is underlined that concentration of impurity in composite play very important role. Similarly, band gap engineering is also necessary to fabricate more efficient PV cells.

Data availability

The datasets generated during the current study are available from the corresponding author on reasonable request.

Acknowledgements

Authors are very much thankful to Dr. S.K. Omanwar, Head, Department of Physics, Sant Gadge Baba Amravati University, Amravati for providing the facility of Probe Sonicator. Authors are also grateful to Dr. Om Mahodaya, Principal, Jankidevi Bajaj College of Science, Wardha for providing necessary facilities for this work.

Appendix A. Supplementary data

Supplementary data related to this article can be found at https://doi.org/10.1016/j.solidstatesciences.2018.07.009.

References

[1] https://www.bbc.co.uk/education/guides/zpmmmg3/revision.
[2] Y. Liu, X. Wan, F. Wang, J. Zhou, G. Long, J. Tian, J. You, Y. Yang, Y. Chen, Advanced Energy Materials 1 (2011) 771–775.
[3] G. Dennler, M.C. Schasfter, C.J. Brabec, Adv. Mater. 21 (2009) 1323–1338.
[4] H.S. Nalwa, Handbook of Organic Conductive Molecules and Polymers, John Wiley & Sons, Chichester, UK, 1997.
[5] E.W. Paul, A.J. Ricco, M.S. Wrighton, J. Phys. Chem. 89 (1985) 1441–1447.
[6] C.R. Kagan, D.B. Mitzi, C.D. Dimitrakopoulos, Science 286 (1999) 945–947.
[7] S.A. Chen, Y. Fang, Synth. Met. 60 (1993) 215–222.
[8] L.D. Pulfry, Photovoltaic Power Generation, Van Nostrand Reinhold Co., New York, 1978.
[9] H.K. Bisoyi, S. Kumar, Liq. Cryst. 38 (2011) 1427–1449.
[10] O. Carp, C.L. Huisman, A. Reller, Prog. Solid State Chem. 32 (2004) 33–177.
[11] D. Dambournet, I. Belharouak, K. Amine, Chem. Mater. 22 (2010) 1173–1179.
[12] E. Singh, H.S. Nalwa, Sci. Adv. Mater. 7 (2015) 1863–1912.
[13] S. Ameen, M.S. Akhtar, G. Kim, Y.S. Kim, O. Yang, H. Shin, J. Alloy. Comp. 487 (2009) 382–386.
[14] L. Shen, W. Guo, H. Xue, Z. Liu, J. Zhou, C. Liu, W. Chen, Proceedings of the 3rd IEEE Int. Conf. on Nano/Micro Engineered and Molecular Systems, January 6-9, (2008) (Sanya, China).
[15] S. Yang, Y. Ishikawa, H. Linh, Q. Feng, J. Colloid Interface Sci. 356 (2011) 734–740.
[16] S. Zhu, W. Wei, X. Chen, M. Jiang, Z. Zhou, J. Solid State Chem. 190 (2012) 174–179.
[17] M.M. Momeni, M.G. Hosseini, J Mater Sci, Mater Electron 25 (2014) 5027–5034.
[18] A. Bahramian, D. Vashaee, Sol. Energy Mater. Sol. Cells 143 (2015) 284–295.
[19] Y. Duan, Y. Chen, Q. Tang, Z. Zhao, M. Hou, R. Li, B. He, L. Yu, P. Yang, Z. Zhang, J. Power Sources 284 (2015) 178–185.
[20] G. Wang, S. Zhuo, W. Xing, Mater. Lett. 69 (2012) 27–29.
[21] C. Liu, K. Huang, P. Chung, C. Wang, C. Chen, R. Vittal, C. Wu, W. Chiu, K. Ho, J. Power Sources 217 (2012) 153–157.
[22] M. Dinari, M.M. Momeni, M. Goudarzirad, J. Mater. Sci. 51 (2016) 2964–2971.
[23] V. Locyuenyong, S. Yaotrakoo, P. Prathumtrd, J. Lertsiri, A. Buaari, Micro & Nano Lett. 11 (2016) 77–80.
[24] P. Yang, J. Duan, D. Liu, Q. Tang, B. He, Electrochim. Acta 173 (2015) 331–337.
[25] A.A. Syed, M.K. Dinesan, Talanta 38 (1991) 815–837.
[26] K.R. Nemade, S.A. Waghuley, J. Electron. Mater. 42 (2013) 2857–2866.
[27] T. Salmi, M. Bouroumba, A. Gastli, A. Mahmoudi, Int. J. Renew. Energy Resour. 2 (2012) 213–219.
[28] M. Seifi, A. Soh, N. Izzrih, A. Wahab, M.K.B. Hassan, International Journal of Electrical, Robotics, Electronics Communication Engineering 7 (2013) 97–103.
[29] W. Feng, E. Sun, W.A. Fujii, H.C. Niihara, K. Yoshino, Bull. Chem. Soc. Jpn. 73 (2000) 2627–2632.
[30] Y. Wu, B. Wang, Y. Ma, Y. Huang, N. Li, F. Zhang, Y. Chen, Nano Research 3 (2010) 661–669.
[31] A. Ferrari, J. Robertson, Phys. Rev. B 61 (2000) 14095–14099.
[32] L. Cancado, M. Pimenta, B. Neves, M. Dantas, A. Jorio, Phys. Rev. Lett. 93 (2004) 247401–247405.
[33] A.C. Ferrari, Solid State Commun. 143 (2007) 47–57.
[34] A.C. Ferrari, J. Robertson, Phys. Rev. B 61 (2000) 14095–14107.
[35] B. Wang, Y. Wang, C. Xu, J. Sun, L. Gao, RSC Adv. 3 (2013) 1194–1200.
[36] https://www.e-education.psu.edu/emc812/node/534.
[37] K. Thamaphat, P. Limsuwan, B. Ngotawornchai, J. Kaewtart, Nat. Sci. 42 (2008) 357–361.
[38] K.R. Nemade, S.A. Waghuley, AIP Conference Series 1536 (2013) 1258–1259.
[39] L. Yang, W.W.F. Leung, Adv. Mater. 25 (2013) 1792–1795.
[40] A. Kongkanand, R.M. Domingurz, P.V. Kamat, Nano Lett. 7 (2007) 676–680.

42 Effect of Shape on Thermophysical and Heat Transfer Properties of ZnO/R-134a Nanorefrigerant

Available online at www.sciencedirect.com

ScienceDirect

Materials Today: Proceedings 5 (2018) 1635–1639

materialstoday: PROCEEDINGS

www.materialstoday.com/proceedings

PMME 2016

Effect of Shape on Thermophysical and Heat Transfer Properties of ZnO/R-134a Nanorefrigerant *

P.B. Maheshwary[a], C.C. Handa[b], K.R. Nemade[c]*

[a]Department of Mechanical Engineering, JD College of Engineering and Management, Nagpur 441 501, India.
[b]Department of Mechanical Engineering, KDK College of Engineering, Nagpur 400 049, India.
[c]Department of Physics, Indira Mahavidyalaya, Kalamb 445 401, India.

Abstract

Presently, nanorefrigerant becoming the important class of nanofluids due to its heat transfer performances of refrigeration and air-conditioning systems. In the present study, we analyze the effect of shape on the thermophysical and heat transfer properties of ZnO/R-134a nanorefrigerant. The spherical and cubic shape ZnO nanoparticles used in this study for addition in refrigerant. The results of study indicate that the thermophysical and heat transfer properties significantly affected by shape of ZnO nanoparticles. In case of cubic ZnO nanoparticles, 42.5 % of increment observed over the pure refrigerant. This preliminary study about the effect of shape on thermophysical and heat transfer properties shows that ZnO/R-134a nanorefrigerant suitable for refrigeration and air-conditioning systems.

Selection and Peer-review under responsibility of International Conference on Processing of Materials, Minerals and Energy (July 29th – 30th) 2016, Ongole, Andhra Pradesh, India.

Keywords: thermophysical properties; heat transfer; nanorefrigerant; R-134a refrigerant

1. Introduction

Nanorefrigerant is adulterate suspension of solid particles and refrigerant as base fluid. Nanorefrigerants have been found great application in the field of refrigeration and air-conditioning systems because of tunable thermal

* Corresponding author. K.R. Nemade, Tel.: +091-9049703051
E-mail address: krnemade@gmail.com

Selection and Peer-review under responsibility of International Conference on Processing of Materials, Minerals and Energy (July 29th – 30th) 2016, Ongole, Andhra Pradesh, India.

conductivity of refrigerants by addition of nanoparticles. Higher thermal conductivity of nanorefrigerants can extract maximum output from the refrigeration and air-conditioning systems [1]. Addition of metal oxide nanoparticle as an impurity significantly enhances the thermal conductivity of nanorefrigerant [2].

Mahbubul et al analyzed the volumetric effects of thermal conductivity, viscosity and density of Al_2O_3/R141b. The results of this study show that an optimum concentration of nanoparticles in refrigerant can enhance the performance of a refrigeration system [3]. Bi et al investigated the performance of TiO_2-R600a nano-refrigerants in a domestic refrigerator without any system reconstruction. The refrigerator performance was analyzed by using energy consumption test and freeze capacity test. The results of this study show that 9.6% less energy used with 0.5 g/L TiO_2-R600a nano-refrigerant [4]. Sarkar et al reported the thermodynamic properties and optimization cascade system with different natural refrigerants. Their study gives two selection charts along with tables one for higher coefficient of performance and the other for highest volumetric capacity [5]. Jiang et al study shows that the thermal conductivities of carbon nanotube based nanorefrigerants are much higher than those of carbon nanotube -water Nanofluids or spherical nanoparticle-R113 nanorefrigerants [6].

In light of above discussion, it is observed that most of the researchers analyzed the effect of concentration on performance of nanorefrigerants. Thus, in the present study effect of nanoparticle shape on thermal conductivity of nanorefrigerants studied for spherical and cubic shape ZnO nanoparticles loaded R-134a refrigerant. The main accomplishment of the present work is that thermal conductivity of R-134a refrigerant increase by 42.5 % for cubic shape ZnO nanoparticles.

2. Experimental

In the present work, ZnO/R-134a nanorefrigerant was prepared by two step method. In this method, 0.1 (10 %) volume fraction of ZnO added in pure R-134a refrigerant and kept for 2 h under probe sonication process for forceful dispersion of ZnO nanoparticles. All thermophysical and heat transfer properties of ZnO/R-134a nanorefrigerant measured in the temperature range 283-307 K. The viscosity of nanorefrigerant of different particle shape was determined using AR-1000 Rheometer, TA Instrument. The thermal conductivity and specific heat measurements were carried out by using KD2 pro thermal analyzer (Decagon Devices).

3. Results and Discussion

Figure 1(a) shows the SEM image of spherical ZnO nanoparticles. SEM image revealed that ZnO used for the dispersion in R-134a refrigerant is nearly spherical. The average particle size of spherical ZnO nanoparticles estimated using the SEM images was found to be 29.1 nm. Figure 1 (b) represents the SEM image of cubic shape ZnO nanoparticles dispersed in R-134a refrigerant. The average particle size of cubic ZnO nanoparticles was found to be 21.4 nm. Figure 1 (c) depicts the XRD pattern of ZnO nanoparticles. The diffraction peaks position in XRD pattern of ZnO reflects the crystalline purity of used ZnO nanoparticles. The peak position in XRD pattern of ZnO nanoparticles shows excellent agreement with JCPDS file no.36-1451. The JCPDS data card shows that ZnO has hexagonal wurtzite structure. The lattice parameters of ZnO nanoparticles are with a = 3.25 Å and c = 5.2 Å and its ratio is c/a ~ 1.60. The data card also shows that ZnO nanoparticles belongs to space group C6mc. The average particle size was computed using Debye-Scherrer equation. The average crystallite size for ZnO nanoparticles estimated using this information was found to be 25.7 nm.

The viscosity of ZnO nanoparticles dispersed refrigerant was calculated using Brinkman model [7],

$$\mu_{nr} = \mu_r \frac{1}{(1-\phi)^{2.5}}$$

where, μnr and μr are the effective viscosity of ZnO nanoparticles dispersed refrigerant and pure refrigerant, respectively. ϕ is the particle volume fraction which is 0.1 (10 %) in present study. Figure 2 depicts the variation of viscosity with temperature for pure R-134a refrigerant, spherical and cubic ZnO loaded R-134a nanorefrigerant. The spherical and cubic ZnO loaded R-134a nanorefrigerant shows typical behavior.

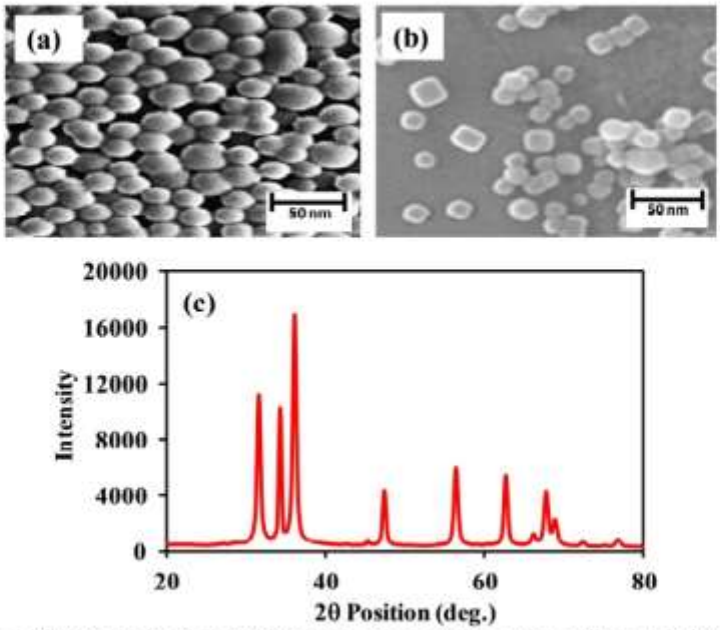

Figure 1. SEM images of (a) Spherical and (b) Cubic shape ZnO nanoparticles and (c) XRD pattern of ZnO nanoparticles.

The viscosity of nanorefrigerant decreases with increase in temperature for systems that is spherical and cubic ZnO loaded R-134a nanorefrigerant. This decrease in viscosity assigned to the sub-micron dispersion behaves like a liquid. The obtained results in our case as a function of temperature is parallel to results reported by Mahbubul et al [8]. Another possible reason for decrease in viscosity with increasing temperature is weakening of adhesion forces among the particles and base fluid molecules [9]. From Figure 2, it is also observed that cubic shape ZnO nanoparticles loaded R-134a nanorefrigerant has higher viscosity value than spherical shape ZnO nanoparticles. The higher value of viscosity in case of cubic shape nanoparticles may be due to cubic shape nanoparticles are difficult to rotate. The difficulty in the rotation increases the viscosity of nanorefrigerant.

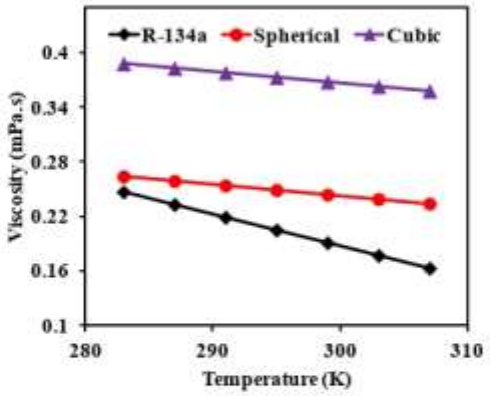

Figure 2. Influence of spherical and cubic shape ZnO nanoparticles on viscosity of R-134a refrigerant.

The variation of density with respect to temperature of pure refrigerant and spherical and cubic ZnO loaded R-134a nanorefrigerant has been shown in Figure 3. The plot shows that density of pure refrigerant and spherical and cubic ZnO loaded R-134a nanorefrigerant decreases moderately with the increase of temperature. The value of density found higher for cubic shape ZnO loaded R-134a nanorefrigerant. All samples show the typical behavior as

a function of temperature. At 283 K, cubic shape ZnO loaded R-134a nanorefrigerant show enhancement in density of the order of 22.62 % over pure R-134a refrigerant.

Density is mass and volume based parameter. With increase in temperature, molecules of refrigerant undergoes to vibration which increases volume. Hence the density of refrigerant was decrease monotonically with temperature. The density of solid particles is much greater than liquid or gases. Therefore, spherical and cubic ZnO loaded R-134a nanorefrigerants have higher density than pure R-134a refrigerant. The optimized value of cubic shape ZnO loaded R-134a nanorefrigerants attributed to the higher volume of cubic shape object.

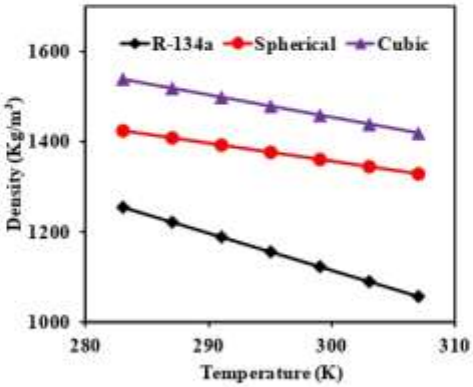

Figure 3. Influence of spherical and cubic shape ZnO nanoparticles on density of R-134a refrigerant.

The specific heat of pure R-134a refrigerant, spherical and cubic ZnO nanoparticle loaded R-134a refrigerant linearly increase with the temperature as shown in Figure 4. For fixed value of concentration of nanoparticles, specific heat of nanorefrigerant decreases than pure R-134a refrigerant. This decrease in specific heat with the addition of nanoparticles is attributed to the lower specific heat of added particles. The increasing temperature results in the fluctuation of refrigerant molecules about their equilibrium value to a higher extent, which increases heat capacity. The increases in heat capacity increases internal energy of the system. The result obtained in our case is parallel with most of the researchers [10].

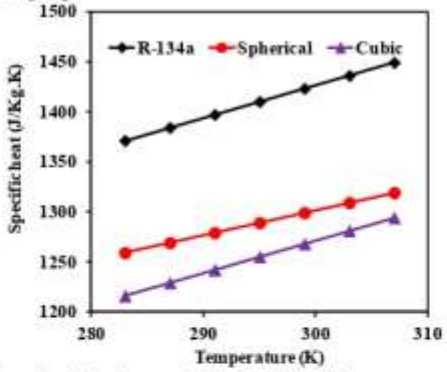

Figure 4. Influence of spherical and cubic shape ZnO nanoparticles on specific heat of R-134a refrigerant.

Figure 5 depicts the variation of thermal conductivity of pure refrigerant and nanorefrigerant with temperature. It can be observed in Figure 1, the thermal conductivity of nanorefrigerant was increases linearly with temperature. The thermal conductivity of pure R-134a refrigerant decreases linearly with increasing temperature. The increase in thermal conductivity of nanorefrigerant is attributed to the higher thermal conductivity of ZnO nanoparticles. The decreases in thermal conductivity of pure R-134a refrigerant may be due to the evaporation of refrigerant molecules. The increment in thermal conductivity due to addition of spherical and cubic ZnO nanoparticles over pure R-134a refrigerant is 25.26% and 42.5 %, respectively.

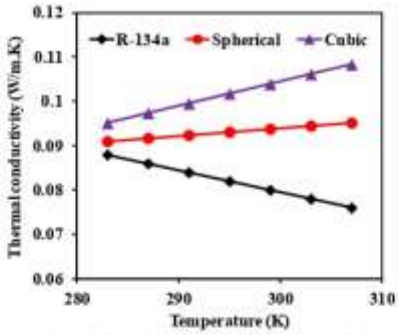

Figure 5. Influence of spherical and cubic shape ZnO nanoparticles on thermal conductivity of R-134a refrigerant.

4. Conclusions

In the summary of present work, thermophysical and heat transfer properties of ZnO/R-134a nanorefrigerant analyzed for two different shapes of ZnO nanoparticles with respect to temperature. The major outcomes of this study could be drawn as follows,

- The addition of spherical and cubic shape ZnO nanoparticles in R-134a refrigerant increases viscosity of nanorefrigerant. Cubic ZnO loaded nanorefrigerant has higher value of viscosity.
- Similar observation is made for density of spherical and cubic shape ZnO nanoparticles loaded in R-134a refrigerant.
- Specific heat of ZnO nanoparticles loaded nanorefrigerant found to be lower than pure R-134a refrigerant.
- The significant enhancement in the thermal conductivity of spherical and cubic shape ZnO nanoparticles in R-134a refrigerant observed of the order of 25.26% and 42.5 % respectively.

Acknowledgements

The authors very much thankful to Principal, KDK College of Engineering, Nagpur, India for providing necessary facilities for the work.

References

[1] I.M. Mahbubul, et al., Int. J. Heat Mass Transfer 57 (2013) 100–108.
[2] R. Saidur, et al., Renew. Sustain. Energy Rev. 15 (2011) 310–323.
[3] I.M. Mahbubul, et al., Procedia Engineering, 56 (2013) 310-315.
[4] S. Bi, et al., Energy Conversion and Management 52 (2011) 733–737.
[5] J. Sarkar, et al., Proceedings of the Institution of Mechanical Engineers Part A: Journal of Power and Energy, 227 (2013) 612-622.
[6] W. Jiang, et al., Int. J. Thermal Sciences, 48 (2009) 1108-1115.
[7] H. Brinkman, et al., J. Chem. Phys. 20 (1952) 571-577.
[8] I.M. Mahbubul, et al., International Journal of Heat and Mass Transfer 85 (2015) 1034–1040.
[9] C.T. Nguyen, et al., Int J Heat Fluid Flow, 28 (2007)492–506.
[10] I.M. Shahrul, et al., Renew. Sustain. Energy Rev. 38 (2014) 88–98.